SEPTEMBER · 1954

roceedings of the I·R·E

Journal of Communications and Electronic Engineering

Illinois U Library

"RATE-GROWN" GERMANIUM INGOT

Volume 42 Number 9

General Electric Company

"rate-grown" process of producing germanium makes it possible to
large quantities of uniform transistor elements with pre-specified operat-
aracteristics. The ingot shown above takes only two hours to produce
ill supply material for 2000 transistors.

IN THIS ISSUE

The Tacitron, A Low Noise Thyratron
IRE Standards on Interference Output of TV Receivers
Water Adsorption on Germanium *N-P* Junctions
Surface Conduction Channel Phenomena in Germanium
Channels and Excess Reverse Current in *P-N* Junction Diodes
Significance of Receiver Errors to Color Reproduction
Coupling of Modes in Helixes
Detection of TV Signals in Thermal Noise
Ground Conductivity Map for U. S.
Minimum Range for Radiation Patterns
Automatic Impedance Recorder for *X*-Band
Performance of Space-Charge Deflection Tubes
Coding for Constant-Data-Rate Systems
RC Filter with Bilinear Element
Optical Automatic Ranging
Abstracts of *Transactions*
Abstracts and References

TABLE OF CONTENTS INDICATED BY BLACK-AND-WHITE MARGIN, FOLLOWS PAGE 80A

IRE Standards on TV Receiver Interference appear in this issue.

The Institute of Radio Engineers

for SPECIALIZED FILTERS

Decades of experience in the design and production of specialized filters have resulted in UTC being a first source for difficult filters. Fifteen years ago UTC was already the largest user of permalloy dust toroids in the world (exclusive of the telephone system). Present designs include a wide variety of core materials, structures, and winding methods to provide maximum performance in electrical requirements and stability. Illustrated below are a few of the thousands of special filter designs in present production.

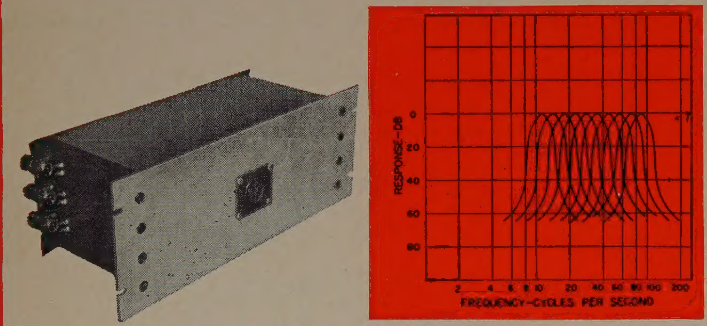

These low frequency band pass filters are held to 1 DB tolerance at the 3 DB crossover...600 ohm...4 filters per 7½" rack panel.

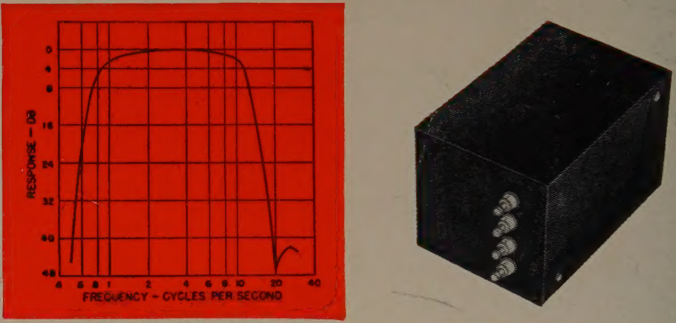

This ultra low frequency filter has a band pass range of one cycle to 10 cycles...50,000 ohms...700 cubic inches.

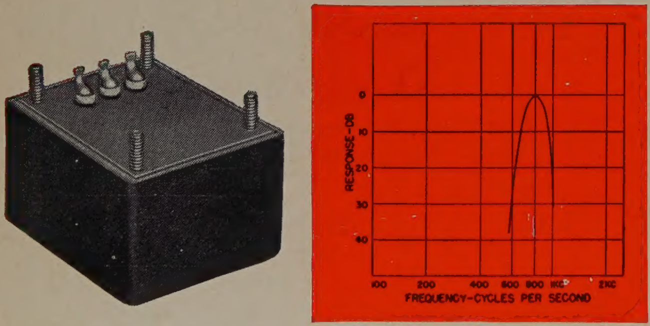

This 600 ohm miniaturized 1 KC band pass filter is housed in a case only 1" x 1¾" x 2½".

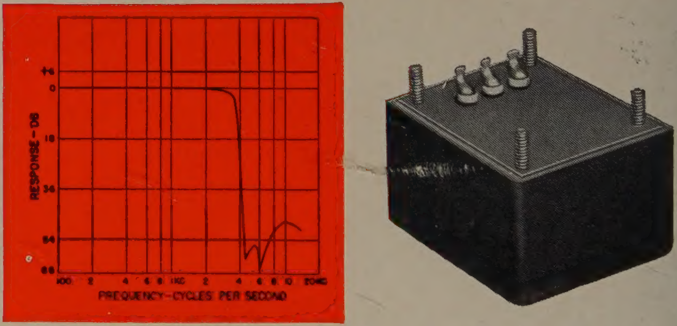

This 600 ohm miniaturized low pass filter is housed in a case only 1" x 1¾" x 2½".

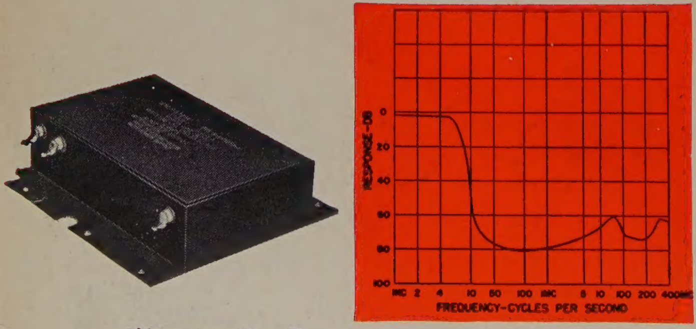

This power line filter provides correct output voltages from sources of 50 to 400 cycles...noise attenuation is from 14 KC to 400 MC...29 cubic inches.

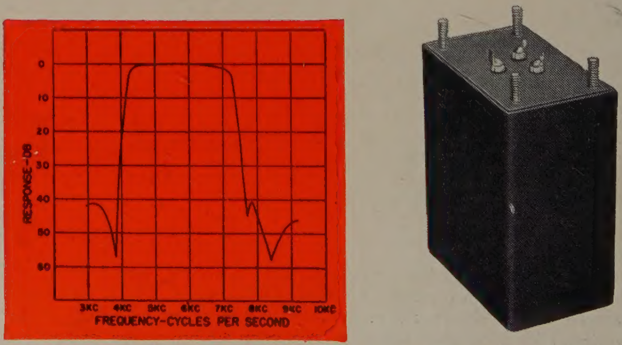

This band pass filter is designed for sharp cut-off at both ends of the range...10,000 ohms...case dimensions 1⅝" x 2½" x 3¼".

United Transformer Co.

150 VARICK STREET NEW YORK 13, N. Y.

FIRST to the electronics industry

NEW DRAWN-RECTANGULAR CAPACITORS

★ Solderless, double-rolled cover seam

★ Seamless case with standard dimensions

To answer the needs of the electronics industry, General Electric's capacitor engineers have developed a fixed paper-dielectric capacitor in a seamless, solderless case with standard dimensions. Because these new capacitors are the same sizes and have the same mounting dimensions as fabricated units, they can be applied to existing electronic equipment without changing component layouts.

Drawn construction offers the user important advantages. The seamless case is virtually leakproof. There is no dependence on solder for mechanical strength and effective sealing. The double-rolled seam between case and cover further assures a true hermetic seal.

G-E Drawn-rectangular capacitors can be supplied with suitable bushings for a wide range of voltage ratings or special applications. The new units comply with or exceed MIL specifications.

Proof of the dependability of the rugged construction of these new drawn-rectangular capacitors can be found in another General Electric pioneered development, the drawn-oval capacitor, of which there are more than 55 million being used in electrical and electronic equipment today.

For further information contact your nearest G-E Apparatus Sales Office. *General Electric Company, Schenectady 5, New York.* 442-23

* Reg. trade-mark of General Electric Co.

Progress Is Our Most Important Product

GENERAL ELECTRIC

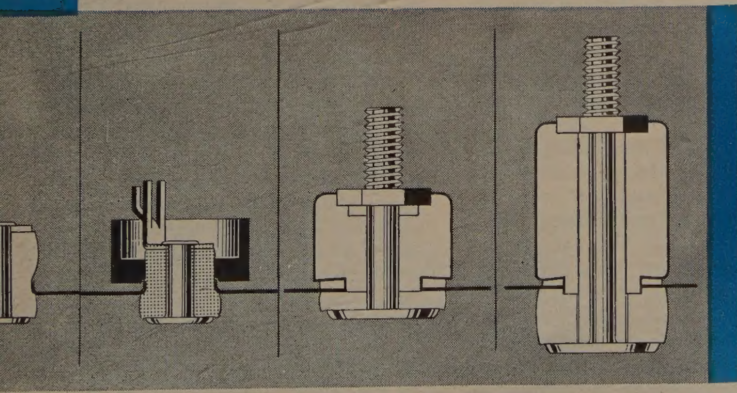

UR BUSHING STYLES can be furnished, depending on rating and applica-
n requirements. All bushings are designed to provide a liquid-tight seal
ng with generous air-strike and creepage distance.

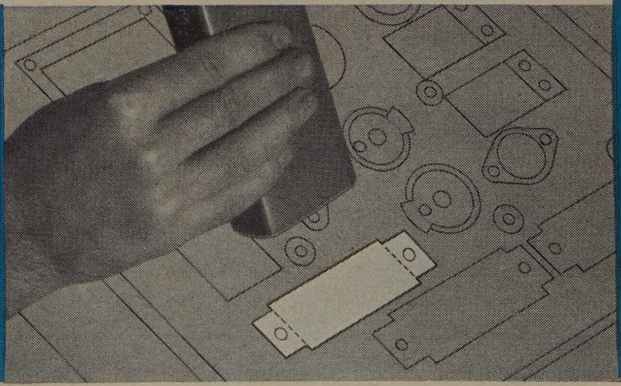

STANDARD CASE SIZES of G-E Drawn-rectangular capacitors are interchangeable with existing fabricated styles. This makes it unnecessary to change drawings or circuit layouts.

NEWS and NEW PRODUCTS

September 1954

Computation Center

A Computation Center, available to industry on a rental basis, was opened July 14th near Princeton, New Jersey, by **Electronic Associates, Inc.,** Long Branch, N. J., to meet the demand for an Eastern headquarters where members of industry may rapidly solve complex problems in Management Operations Control, Dynamic Systems Analysis, and Applications Engineering. The Center is equipped with Electronic analog computer equipment, and will be staffed with scientists experienced in the use and applications of analog computers. These specialists will be available to industry and business to help solve the problems submitted.

The Center is equipped with a dual control console and related equipment. This permits the simultaneous solution of two problems or the use of the entire facility to solve more complicated problems.

To each problem, the Center will assign scientists, engineers or mathematicians. When individual situations require specialized aid, the staff will be augmented by additional scientists from various research institutions and universities in the area and from Electronic Associates.

Customers may set up their problems themselves, either at their own plant or at the Center, by using the special problem boards available for that purpose.

Pulse and Square Wave Oscillator

The Rutherford Electronics Co., 3707 S. Robertson Blvd., Culver City, Calif., has a new square-wave oscillator which is a source of pulses and square waves with accurate, continuously variable repetition rates.

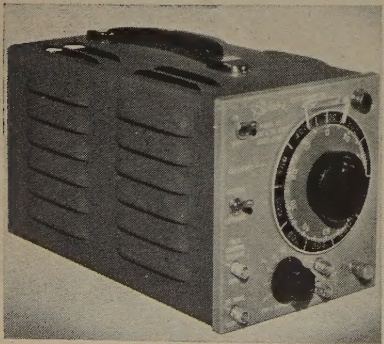

These manufacturers have invited PROCEEDINGS readers to write for literature and further technical information. Please mention your I.R.E. affiliation.

The Model G-1 offers repetition rates variable from 1 to 100,000 pps in five decade ranges. These repetition rates may be controlled by the main dial or by an external control voltage to an accuracy of 1 per cent.

Three outputs are available. Positive and negative pulses of 0.2 microsecond width and 30 volts amplitude are simultaneously available, together with a square wave of 75 volts amplitude.

The Model G-1 can be used as a variable frequency master timing oscillator in laboratory experiments; for the determination of operating rate limits of equipment under test; and, as a frequency modulated oscillator in data transmission systems. This instrument measures 7½×7½×13 inches over-all, and weighs 15 pounds.

Megacycle Preset Interval Generator

A new Model 564 Preset Interval Generator designed for testing and calibrating systems that rely on precise time measurements for their operation is announced by **Potter Instrument Co., Inc.,** 115 Cutter Mill Rd., Great Neck, L. I., N. Y.

Time intervals and delays from 1 microsecond to 1 second may be generated or measured. In generating an interval or delay, the desired number of microseconds is selected by means of six 10-position switches, one for each digit of the delay in microseconds. To measure an existing time interval, the instrument counts the exact number of pulses produced by a 1-mc crystal-controlled oscillator during the interval.

Particularly new is the ability of the instrument to produce delays as small as 1 microsecond. Intervals of the order of seconds are generated with better than 0.0001 per cent accuracy. Manual or automatic reset may be used; with automatic resetting, the instrument recycles itself to produce trains of accurately-spaced pulses.

A separate amplifier and shaper unit is provided for applications where an external time-base source is used for simulating target delays selectable directly in feet or yards.

Optical Test Bench

The Hugo Meyer Universal Instrument Bench, an apparatus designed to prove out and test instrumentation systems in the optical, electronic, electromechanical, industrial photography, physics, and allied fields, is available from **Meyer-Opticraft Co.,** 39 W. 60th St., New York 23, N. Y.

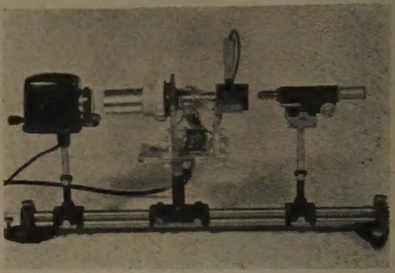

A number of instrumentation set-ups can be made by choosing from over 50 available components and assembling them in various combinations. The instrument bench can be utilized in the laboratory, the production line, in assembly and inspection, and for industrial photography for 30× enlargements.

The photograph shows a set-up for testing the image quality of an electron tube. With a few substitutions, the bench can be converted into a set-up to test the optical properties of a lens, either internally or fully assembled.

A 20-page catalog describes the apparatus.

Report on Meeting and Symposium of Cleveland Electronic Show

The Cleveland Electronic Show was held in Case Institute's Tomlinson Hall on Wednesday, February 24, 1954. This was the first attempt at bringing the various Cleveland manufacturers together to pool their products for display purposes and discuss ways that Cleveland and Ohio could increase electronic manufacturing activity. Mr. Joseph Keithley was Chairman and Show Manager. Show hours were from 10 a.m. to 7 p.m. and over a 1000 registration cards were filled out indicating interest in the IRE and The Professional Group on Audio which is just getting underway at the Cleveland Section.

Fifteen exhibitors displayed their products and found considerable activity throughout the show hours. At the close of the show, Dr. S. J. Begun, Vice President and Director of Advance Development at Clevite Brush Development Company, Cleveland, Ohio, held an introductory session of all the exhibitors at which time the problems of establishment and growth of the various concerns was discussed by the company representatives. The future plans of each of these exhibitors were also made known.

Dr. Begun pointed up the fact that by using the manufacture of vacuum tubes as

(Continued on page 20A)

Spotlighting Standardization!

E-I hermetically-sealed terminations and miniature closures*

- **MULTIPLE HEADERS** — Strain-free, vacuum tight headers featuring cushioned glass construction. Silicone treated for maximum dielectric strength and tin dipped for easy soldering.
- **SEALED TERMINALS** — These E-I terminals offer high thermal shock resistance and feature cushioned glass construction. Available in many economical preferred types and special designs.
- **OCTAL HEADERS** — Both plug-in and multiple types feature a new principle of hermetic sealing. Solid metal blanks afford maximum rigidity and mechanical strength.
- **E-I END SEALS** — Completely strain-free. Provide a permanent hermetic seal. For condensers, resistors and other tubular-type components. Available in many standard types.
- **COMPRESSION TYPE HEADERS** — Super rugged, practically indestructible and absolutely rigid. Exclusive E-I process affords increased resistance to shock and vibration.
- **LUG-TYPE, LEAD-THRU INSULATORS** — Compression sealed, super rugged. For applications requiring voltage ratings from 2000 to 4000 (rms.) — transformers, "bath-tub" condensers, etc.
- **MINIATURE CLOSURES** — For transistors and other components requiring hermetic sealing. Square, rectangular and round cases. Supplied in E-I standard types or custom designs to specifications.
- **COLOR-CODED TERMINALS** — Featuring glass inserts with permanent coloring in the glass. All types offered in standard, easily-identified RMA color codes.

*PATENT PENDING
ALL RIGHTS RESERVED

AVAILABLE IN A WIDE RANGE OF STANDARD TYPES TO ECONOMICALLY MEET SPECIAL REQUIREMENTS!

Economical E-I standardized hermetically-sealed terminals and miniature closures are available to meet almost any electronic application. Samples and recommendations on your particular needs will be supplied promptly on receipt of your data. Call or write for complete E-I catalogs, today!

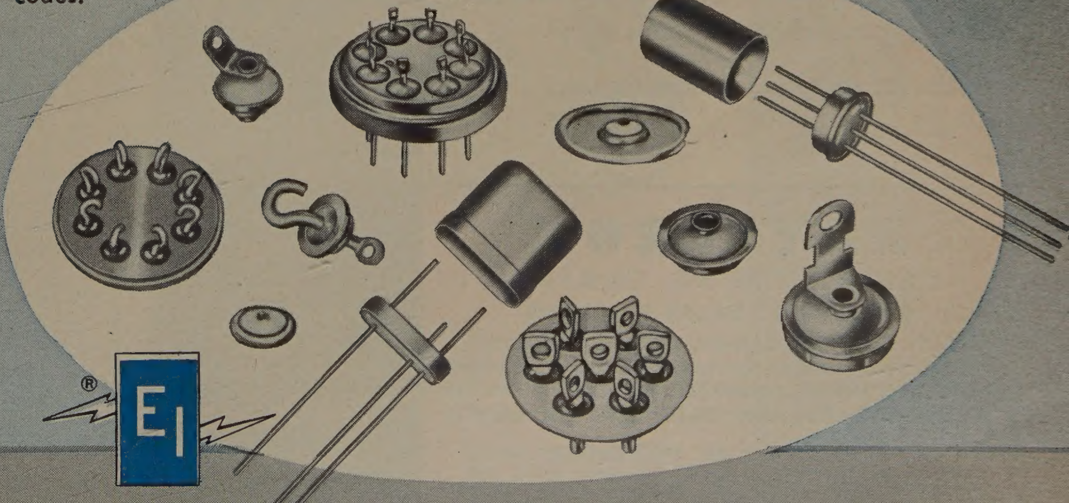

® E I

ELECTRICAL INDUSTRIES

44 SUMMER AVENUE, NEWARK 4, NEW JERSEY

DIVISION OF AMPEREX ELECTRONIC CORP.

Hermetically Sealed... No Increase In Size

RAYTHEON

MOLDED TRANSFORMERS

Raytheon, leaders in custom transformer design, offers the electronics industry custom built transformers with all the advantages of hermetic sealing — *without increase in size over conventional open types.*

Encapsulated and sealed with Acme molding compound, these transformers fill a definite need on MIL-T-27 applications where space limitations are critical.

Write for complete information.

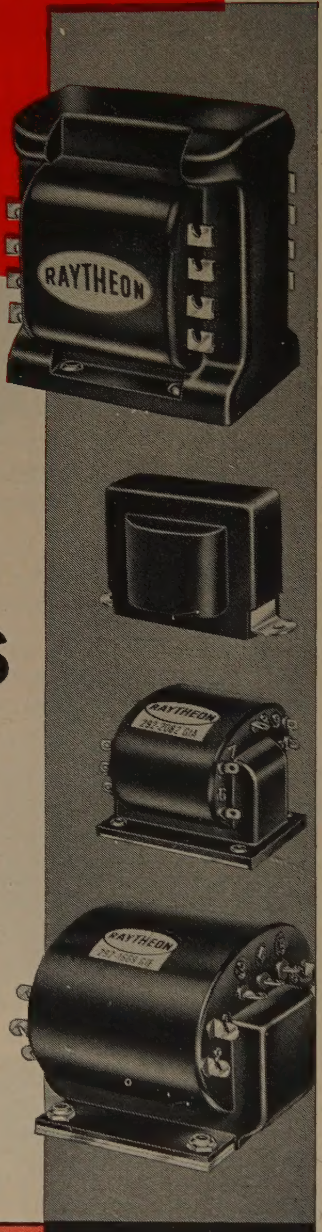

RAYTHEON
MANUFACTURING COMPANY
EQUIPMENT SALES DIVISION
DEPT. 6120-P WALTHAM 54, MASSACHUSETTS
DISTRICT OFFICES: BOSTON, NEW YORK, CLEVELAND, CHICAGO, NEW ORLEANS, LOS ANGELES (WILMINGTON), SAN FRANCISCO, SEATTLE
INTERNATIONAL OPERATIONS: 589 FIFTH AVE., NEW YORK CITY

RAYTHEON PRODUCTS INCLUDE: WELDPOWER* welders; Voltage stabilizers (regulators); Transformers; Sonic oscillators for laboratory research; Standard control knobs; Electronic calculators and computers; Radio, television, subminiature and special purpose tubes and other electronic equipment. *Reg. U. S. Pat. Off.

BUILD
RAYTHEON
Excellence in Electronics
DEPENDABILITY
INTO YOUR
PRODUCTS

News—New Products

These manufacturers have invited PROCEEDINGS readers to write for literature and further technical information. Please mention your I.R.E. affiliation.

Report on Meeting and Symposium of Cleveland Electronic Show

(Continued from page 16A)

a standard the electronic field has grown from a consumption of 100 million tubes in 1930 to approximately 800 million in 1953–54. Also, whereas Cleveland has approximately 2% of the total manufacturers of electronic equipment, the Cleveland manufacturers account for 5% of the nationwide business.

Dr. Begun had as his guest Mr. Newell Sanders, Chief of the Physics Division of NACA in Cleveland. Mr. Sanders brought out the important part that electronics plays in the production of jet aircraft parts, particularly, how milling machines regulated by an electronic signal can manufacture exacting parts with high production. Mr. Sanders pointed out that we are aware that electronic equipment can receive signals but now we have advanced to a point where a machine can receive, digest and act electronically.

#1. **BIRD ELECTRONIC CORP.,** Cleveland; in attendance, H. E. Stevens, Engr., H. H. Heller, Engr.

Products on display: Wattmeters to measure high frequency power above 100 mc, VHF and UHF coaxial line filters, coaxial selector switches, coaxial load resistors.

History: Started in 1942 to aid military in measuring radar jamming transmitters in 100 mc band. Bird manufactures a wide variety of 100 mc measuring equipment in small quantities all designed by J. R. Bird. This experience enabled Bird to apply research to TV transmitting measuring equipment.

#2. **ROLA CORPORATION,** Cleveland; in attendance, John Adams, Asst. S.M., Earl Wilks, Sales.

Products on display: Color TV deflecting yokes, loudspeakers, monochrome deflecting yokes and the JETEC deflecting yoke. The JETEC (Joint Electron Tube Engineering Council) Yoke is the first adapted standard yoke in use by 14 tube manufacturers. These tube manufacturers have agreed to use this standard that was designed and built by Rola in order to have a traceable standard with which reference checking points could be determined. It is the only such standard in TV at present.

History: Founded in 1924. Produce speakers for TV and radio manufacturers solely. Employ approximately 1200 people at peak. After death of Ben Engholm, one of the founders, Rola sold controlling interest to Muter Corporation and Larry King was made President and General Manager.

#3. **THOMPSON PRODUCTS,** Cleveland; in attendance, Fred Weihmiller, S.M., Dale A. Schonmeyer, Sales.

Products on display: 6–60 cm wavemeter, lobing switches, rf coaxial attenuator, rotary selector switches, special test equipment for antenna model pattern measuring range systems.

(Continued on page 24A)

RESISTORS...FOR EVERY NEED

Meets JAN-R-94
type RV3

1/2 watt 1-1/8″ diameter variable composition resistor. Also available with other special military features not covered by JAN-R-94.

TYPE 35

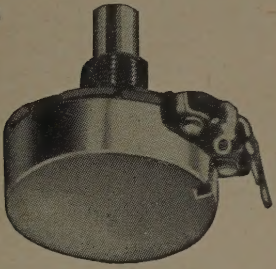

TYPE GC-35
With Switch

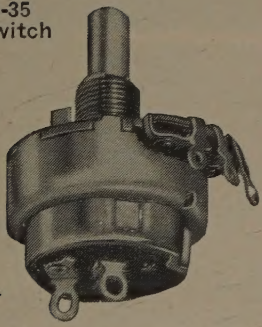

TYPE C2-35
Tandem

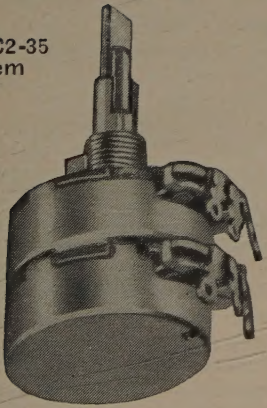

Meets JAN-R-94
type RV2

1/4 watt 15/16″ diameter variable composition resistor. Also available with other special military features not covered by JAN-R-94.

TYPE 45

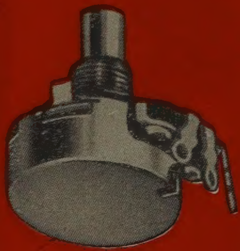

TYPE GC-45
With Switch

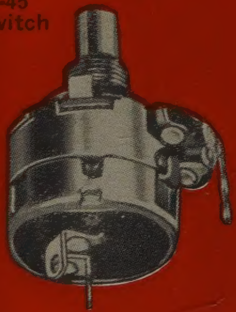

TYPE C2-45
Tandem

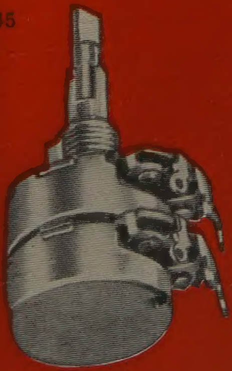

Meets JAN-R-19
types RA25 and RA30

4 watt 1-17/32″ diameter variable wirewound resistor. Also available with other special military features not covered by JAN-R-19.

TYPE 25

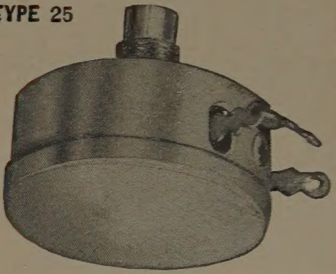

TYPE GC-25
With Switch

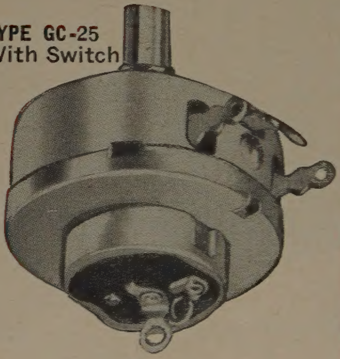

TYPE C2-25
Tandem

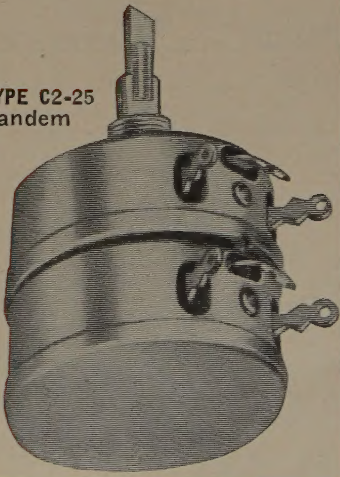

Meets JAN-R-19
type RA20

2 watt 1-17/64″ diameter variable wirewound resistor. Also available with other special military features not covered by JAN-R-19.

TYPE 252

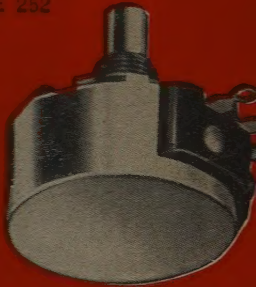

TYPE GC-252
With Switch

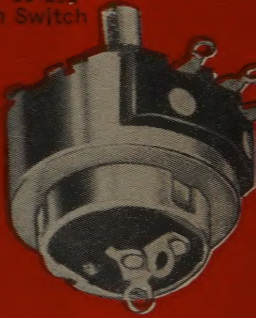

TYPE C2-252
Tandem

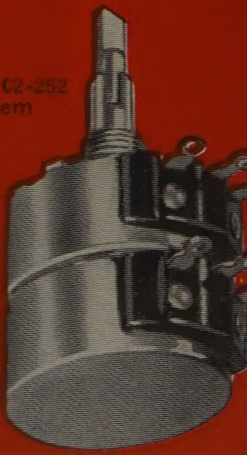

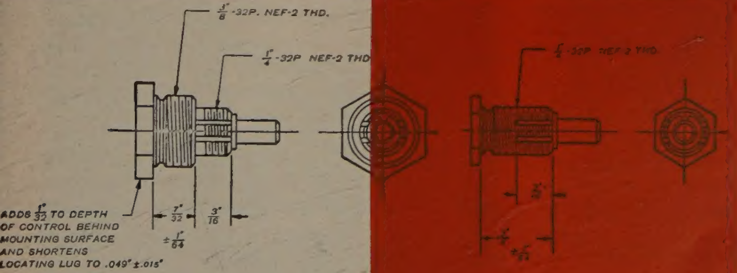

3/8″-32P. NEF-2 THD.
1/4″-32P NEF-2 THD
ADDS 1/32″ TO DEPTH OF CONTROL BEHIND MOUNTING SURFACE AND SHORTENS LOCATING LUG TO .049″±.015″
7/32″
3/16″
±1/64″
1/4″-32P NEF-2 THD.

LOCKING BUSHINGS FOR TYPE 65 CONTROL.

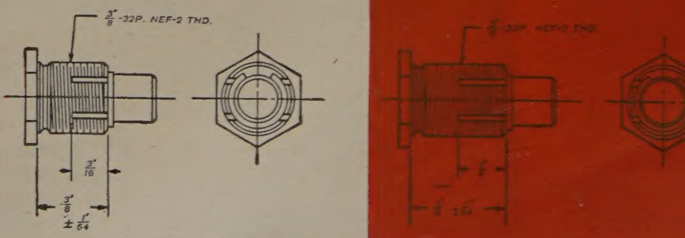

3/8″-32P. NEF-2 THD.
3/16″
3/8″
±1/64″

LOCKING BUSHINGS FOR CONTROL TYPES 25, 252, 95, 35, 90, 45.

Specialists in Precision Mass Production of Variable Resistors • Founded 1896

LAB PULSESCOPE

by Waterman

MODEL S-5-A

Size: 13" x 16½" x 14⅛"

ANOTHER EXAMPLE OF Waterman PIONEERING...

The LAB PULSESCOPE, model S-5-A, is a JANized (Gov't Model No. OS-26) compact, wide band laboratory oscilloscope for the study of all attributes of complex waveforms. The video amplifier response is up to 11 MC and provides an equivalent pulse rise time of 0.035 microseconds. Its 0.1 volt p to p/inch sensitivity and 0.55 microsecond fixed delay assure portrayal of the leading edge when the sweep is triggered by the displayed signal. An adjustable precision calibration voltage is incorporated. The sweep may be operated in either triggered or repetitive modes from 1.2 to 120,000 microseconds. Optional sweep expansion of 10 to 1 and built-in markers of 0.2, 1, 10, 100, and 500 microseconds, which are automatically synchronized with the sweep, extend time interpretations to a new dimension. Either polarity of the internally generated trigger voltage is available for synchronizing any associated test apparatus. Operation from 50 to 400 cps at 115 volts widens the field application of the unit. These and countless additional features of the LAB PULSESCOPE make it a MUST for every electronic laboratory.

WATERMAN PRODUCTS CO., INC.
PHILADELPHIA 25, PA.
CABLE ADDRESS: POKETSCOPE

MEMO... Write for details today!

WATERMAN PRODUCTS INCLUDE
S-4-C SAR PULSESCOPE®
S-5-A LAB PULSESCOPE
S-6-A BROADBAND PULSESCOPE
S-11-A INDUSTRIAL POCKETSCOPE®
S-12-B JANized RAKSCOPE®
S-14-A HIGH GAIN POCKETSCOPE
S-14-B WIDE BAND POCKETSCOPE
S-15-A TWIN TUBE POCKETSCOPE
RAYONIC® Cathode Ray Tubes
and Other Associated Equipment

WATERMAN PRODUCTS

News—New Products

These manufacturers have invited PROCEEDINGS readers to write for literature and further technical information. Please mention your I.R.E. affiliation.

Report on Meeting and Symposium of Cleveland Electronic Show

(Continued from page 24A)

History: In 1950 and 1951 Thompson Products Electronic Division was in business on paper only. October of 1951 Thompson bought out Antenna Research Laboratories and later Bell Sound Systems in Columbus. These acquisitions will enable Thompson to enter into the electronic field through the high frequency interest and through stereophonic sound and tape recording interests. Mr. Weihmiller indicated that Thompson is looking to the consumer market also with the eventual development of a UHF tuner.

#4. **ASSEMBLY PRODUCTS,** Chagrin Falls; in attendance, Paul Saint-Amour, Sales Engr., Robert Pugsley, Sales.

Products on display: SimPlyTrol Indicating and Controlling Pyrometers, Contact meter-relays with electro magnetic locking, Meter-relays of the plug-in hermetically sealed type (a new development) that has been ruggedized and conforms to the MIL-M 10304 meter spec and MIL-M 5757B relay spec.

History: Founded in 1945 by 6 men. Made successful contact meters despite difficulty of making and breaking contacts with a sensitive D'Arsonval movement. Accomplished this by augmenting standard coil with another coil to assist in making and breaking contact in meter case. Future developments will include automatic testing devices and automatic adjustment of auto horns and automation controls.

#5. **BRUSH ELECTRONIC CORP.,** Cleveland; in attendance, E. M. Hensley, Sales, A. Novak, S.M.

Products on display: Brush Oscillographs, Amplifiers, Surface Analyzer.

History: Founded in 1921 as research organization. Developed a high-speed pen motor in 1936. In 1940 Dr. Begun came

(Continued on page 34A)

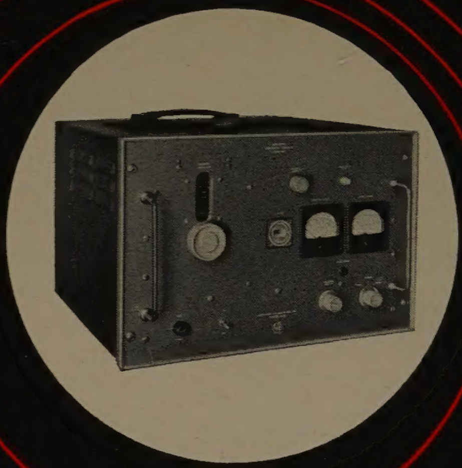

Ultra-stable Microwave Oscillator

LFE Model 804 X-band Microwave Oscillator holds frequency to 1 part in 100,000,000, giving you *real* stability. It is the oscillator you need for VSWR or Q measurements, general narrow band design work, or any application where a high degree of stability is required.

This same stability is available in C-band as well as X-band oscillators and in other microwave frequencies to meet your specifications.

SPECIFICATIONS: *(Model 804)*

Frequency Coverage
8,500 — 10,000 Mc-X-Band

Dial Calibration
Calibrated directly in frequency — 1 Mc per division

Frequency Stability
Short Term Deviation — less than one part in 10^8
Long Term Drift — negligible after complete warm-up

Modulation
Can be modulated 25% when stabilized; 100% modulation possible when stabilization is removed

Power Output
80 — 100 milliwatts
Output flange — UG 40/U

Power Consumption
160 watts

Size
$12\frac{7}{32}''$ x 19" front panel, $19\frac{1}{4}''$ deep, cabinet or rack mounting

Weight
100 lbs.

®

LABORATORY for ELECTRONICS, INC.
75 Pitts Street • Boston 14, Mass.

PRECISION ELECTRONIC EQUIPMENT • OSCILLOSCOPES • NUMAR CHEMICAL SPECTROMETER • COMPUTERS • SOLID DELAY LINES

it's VARIAN...
for top performance in every KLYSTRON application

System designers and equipment buyers specify Varian klystrons for optimum performance because they know that **only** Varian klystrons combine extreme ruggedness and reliability with excellent frequency stability and ample power. Designed and built by the acknowledged leader in klystron development, Varian klystrons offer outstanding performance advantages in these and many other applications:

- Microwave relay transmitters and receivers
- Telemetering systems
- UHF television transmitters
- Radar receivers—local oscillators
- Coherent and pulsed radar transmitters
- Guided missile applications
- Microwave test equipment
- Particle accelerators—power tubes

COMPARE THESE FEATURES

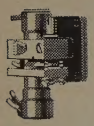

FOR RADARS AND BEACONS
Unmatched high altitude performance **without** pressurization—excellent frequency stability — low noise — rapid warm-up — rugged — reliable.

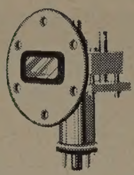

FOR MICROWAVE RELAY SYSTEMS
Ample power to override noise—excellent frequency stability—economy of operation—long life.

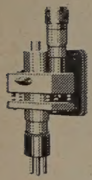

FOR LABORATORY TESTING
Smooth, single-shaft tuning over a wide range—matched waveguide output—excellent microphonic characteristics—linear reflector tracking.

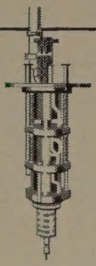

FOR UHF TELEVISION
Integral cavity construction for economical operation and simple installation—wide band-width for color TV—high power gain—long life.

VARIAN HAS A PRODUCTION KLYSTRON...
that meets the requirements of these typical applications:

APPLICATION	FREQUENCY RANGE (Megacycles)	POWER RANGE	TUBE TYPES
Radar & Beacon Local Oscillators	8500 — 10,500	25 — 140 mw	V-270, V-290, V-151, V-153, V-155
Radar Transmitters	8500 — 11,000	100 W — 9 KW	V-23, V-63, V-27, V-82, V-45
Beacon Transmitters	9100 — 12,200	450 mw — 9 KW	V-54, V-63, V-27, V-82, V-45
Relay Local Oscillators & Transmitters	5100 — 7500	30 mw — 1 W	X-26B, X-26D, X-26E, X-26F
UHF Television	470 — 890	15 KW	VA-6237, 38, 39, 40, 41 and 42
Laboratory Testing	8200 — 12,400	450 mw — 8 W	X-13, V-21, V-27, V-54, V-58

FOR COMPLETE SPECIFICATIONS
and technical data on these outstanding Varian klystrons, and for information about special purpose klystron engineering—write to the VARIAN Application Engineering Department today.

IN KLYSTRONS, THE MARK OF LEADERSHIP IS
VARIAN associates
PALO ALTO 2, CALIFORNIA

News—New Products

These manufacturers have invited PROCEEDINGS readers to write for literature and further technical information. Please mention your I.R.E. affiliation.

Report on Meeting and Symposium of Cleveland Electronic Show

(Continued from page 24A)

with company and assisted in magnetic recording. Company is now split up into Brush Beryllium, Brush Development, Brush Electronics. Merged with Cleveland Graphite about a year and a half ago. Brush equipment is used in textile industry to measure uniformity of fibers.

#6. **DESIGNERS FOR INDUSTRY,** Cleveland; in attendance, M. Snedeker, Proj. Engr., Eugene Gibbons, Publ. Rel. Dir.

Products on display: New UHF-VHF Signal Generator covering 54 to 330 mc in UHF band and 300 to 950 mc in UHF band. Accuracy is ±2% on the two RF ranges.

History: Formed in 1935 as an industrial designing service; 1945, entered the electronic field employing 180 people. Company offers four services: technical survey, research development, product design and product engineering. Utilizes an experimental manufacturing installation to assist realization of engineering developments. Future developments will be in the automatic control field such as automatic honing controlled by electronics.

#7. **CLEVELAND CONTAINER,** Cleveland; in attendance, R. P. Summerville, Chem. Engr., L. C. Hoaglund, Plant Sales, Jay Sebesky, S.M.

Products on display: Completed coil forms made of laminated phenolic tubing, samples of available forms showing punching, threading, grooving and grinding facilities available at Cleveland Container Company.

(Continued on page 115A)

3 Low Cost VARIABLE RESISTORS for COMPACT CIRCUITS

COST-CUTTING TAB-MOUNTING CONTROL

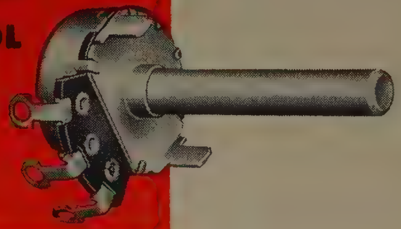

0.5 watt metal shaft type for TV picture adjustment, pre-set gain controls, etc. Tab-mounting cuts mounting time, eliminates hardware. Nine different Stackpole line switches available for this control. *Send for specifications on Type LR-5.*

TAB-MOUNTING "DOUBLE-ENDER"

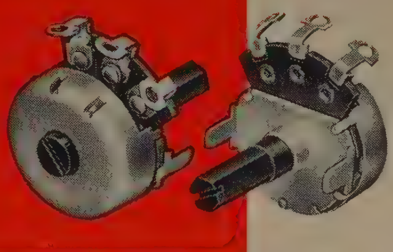

Just right for rear-of-chassis or concealed front panel controls in TV receivers . . . especially in high voltage circuits. Bakelite shaft can easily be adjusted from either side of control. Measures only .894″ in diameter, yet handles a full .5-watt. *Write for data on Stackpole Type LR-6.*

MINIATURE TONE CONTROL with SPECIAL DP-DT SWITCH

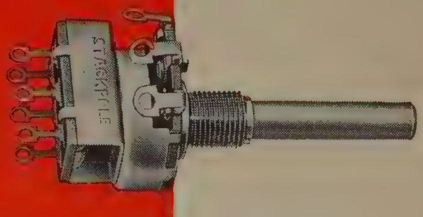

A really versatile space-saver for midget radios, combination receivers, or amplifiers. Helps reduce the number of controls on complicated sets. U.L. Approved .5 amp., switch throws at opposite ends of control rotation—maintains full 270° shaft motion in either position. Ideal for band changing, input or bandwidth switching. *Write for details on Stackpole Type LRSS-150.*

Electronic Components Division
STACKPOLE CARBON COMPANY
St. Marys, Pa.

STACKPOLE

In Canada: Canadian Stackpole Ltd., 550 Evans Avenue, Etobicoke, Toronto 14, Ontario

VHF

. . . Very High Frequencies

RADIO INTERFERENCE and FIELD INTENSITY* measuring equipment

Stoddart NM-30A • 20mc to 400mc

Commercial Equivalent of AN/URM-47

PRINTED CIRCUITRY . . . Modern printed circuits offer many advantages over conventional wiring, lighter weight, more compact units and freedom from many of the troubles normally encountered in conventionally-wired electronic equipment. Vibration becomes even less of a problem with printed circuits, adding to the many portable features already available with Stoddart equipment.

ADVANCED DESIGN . . . Specialized engineering and modern production techniques have produced one of the most advanced instruments for the accurate measurement, analysis and interpretation of radiated and conducted radio-frequency signals and interference ever manufactured. Designed to laboratory standards, rugged, and with matchless performance, the versatile NM-30A is an outstanding example of modern instrumentation. Its frequency range includes FM and TV bands.

SMALLER SIZE . . . A wider frequency range and higher standard of performance is incorporated into an equipment whose size is one-third that of any similar equipment ever manufactured.

SENSITIVITY . . . Sensitivity ranges from one to ten microvolts-per-meter, depending upon frequency and antenna in use.

APPLICATIONS . . . Field intensity surveys, antenna radiation pattern studies, interference location and measurement for checking radiation from virtually any mechanical or electrical device capable of generating or radiating radio-frequency signals or interference.

Stoddart RI-FI* Meters cover the frequency range 14kc to 1000mc

VLF
NM-10A, 14kc to 250kc
Commercial Equivalent of AN/URM-6B. Very low frequencies.

HF NM-20B, 150kc to 25mc
Commercial Equivalent of AN/PRM-1A. Self-contained batteries. A.C. supply optional. Includes standard broadcast band, radio range, WWV, and communications frequencies. Has BFO.

UHF
NM-50A, 375mc to 1000mc
Commercial Equivalent of AN/URM-17. Frequency range includes Citizens band and UHF color TV band.

STODDART AIRCRAFT RADIO Co., Inc.
6644-C Santa Monica Blvd., Hollywood 38, California • Hollywood 4-9294

Contributors

M. Balser, whose paper appears on page 1428 of this issue, is currently affiliated with the Lincoln Laboratory, Massachusetts Institute of Technology, where he is working on problems in radio wave propagation and communication theory.

M. Balser

Dr. Balser was born in Brooklyn, N. Y., on May 23, 1927. He served in the Army from 1945 to 1947. He received a B.S. degree, summa cum laude, from Brooklyn College in 1948, an M.A. in 1949 and a Ph.D. in theoretical physics in 1953, both from Harvard. He was a Teaching Fellow at Harvard from 1950 to 1952.

He is a member of Pi Mu Epsilon and Sigma Xi.

❖

V. W. Bolie (M'54) joined the engineering staff of Collins Radio Co. in March, 1952. His work has consisted of theoretical research in the various phases of communication engineering, performing services as consulting mathematician, and teaching courses in advanced mathematics and electromagnetic theory. His paper appears on page 1435 of this issue.

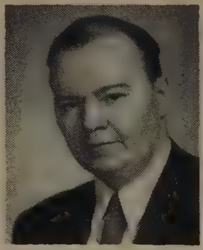

V. W. Bolie

Dr. Bolie was born on July 23, 1924, in Silverton, Ore. He received the B.S. degree in physics in 1949, the M.S. degree in mathematics in 1950, and the Ph.D. degree in applied mathematics in 1952, from Iowa State College.

From 1942 through 1944 he attended numerous CPT and AAF pilot training schools. Following USAF commission, from 1945 to 1947, he attended B-17 and B-29 transition training schools, served as single- and multi-engine pilot instructor, and administrated public relations, and information and education duties in the United States and Pacific. While studying for an advanced degree at Iowa State College, he taught various college mathematics courses.

He is a member of Pi Mu Epsilon, Sigma Xi, and the American Mathematics Society.

(Continued on page 64A)

New Towers in the Sky!

Research information readily exchanged between engineers and scientists has been the forerunner of every radio-electronic advance. This is the priceless service to all of "Proceedings of the I.R.E."

ECLIPSE-PIONEER AUTOMATIC PILOT *equipped with A-B resistors* ... brings plane down safely and automatically on glide path

The plane in this picture is automatically controlled to the glide path by computer signals fed to the Automatic Pilot. As may be seen by the sweep of the windshield wipers, rain is coming down heavily, obscuring the runway which is dimly visible through the left windshield.

Despite these adverse landing conditions, the human pilot . . . with the plane only a few hundred feet above the runway . . . displayed his complete confidence in the Automatic Pilot by stepping aside during its descent to permit the photographer to snap this remarkable action shot.

Such precision and accuracy call for QUALITY electronic components, like the Bradleyometers used for adjustable resistance controls and Bradleyunits used for fixed step resistors.

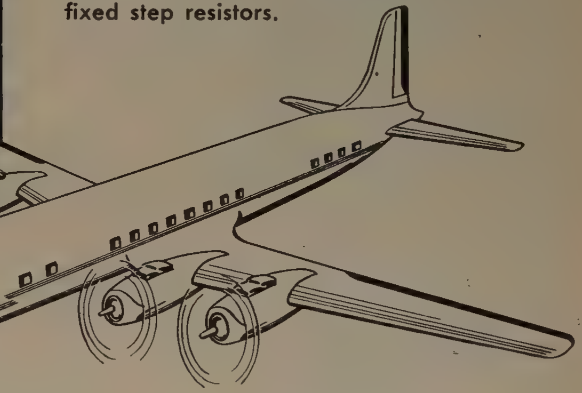

Each computer, located in the rear of the pilot-copilot area, and not visible in the above photograph, has six Bradleyometers and 130 Bradleyunits. For critical applications, where accuracy and permanence of resistor values and ratings are of vital importance, Allen-Bradley fixed and adjustable resistors are the logical choice of experienced radio and electronic engineers.

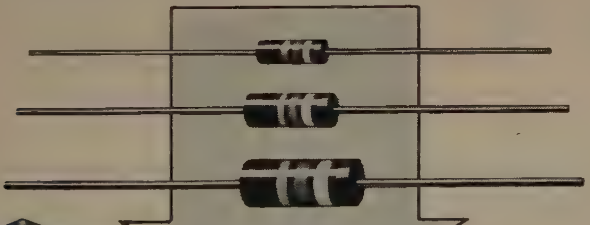

BRADLEYUNITS

BRADLEYUNIT FIXED RESISTORS ½, 1, 2 WATT

Their world-wide reputation for high quality is due to the fact that Bradleyunits are rated at 70C ambient . . . not 40C. When used according to published ratings, Bradleyunits will not open circuit nor exhibit large erratic changes of resistance. Standard RETMA values in ½, 1, and 2 watt ratings.

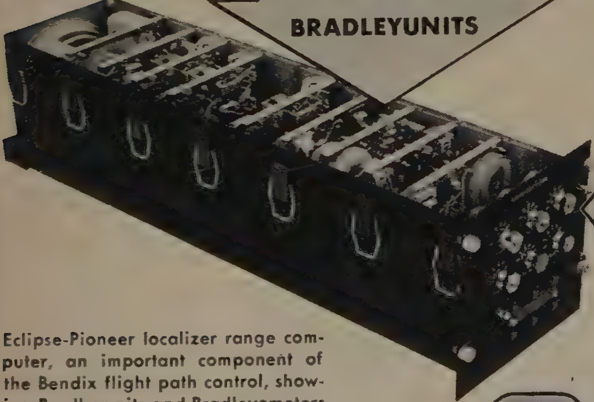

Eclipse-Pioneer localizer range computer, an important component of the Bendix flight path control, showing Bradleyunits and Bradleyometers on cards and in end of coupler case.

TYPE J BRADLEYOMETER

The stability of Bradleyometer resistance is due to the solid, circular resistor that is molded to produce any resistance-rotation curve. Not affected by temperature or humidity. Made in ⅓ and 2 watt sizes.

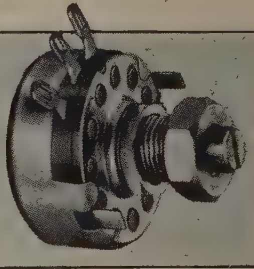

Allen-Bradley Co.
114 W. Greenfield Ave., Milwaukee 4, Wis.

In Canada—Allen-Bradley Canada Limited, Galt, Ont.

A-B Quality

ALLEN-BRADLEY

FIXED & ADJUSTABLE RADIO RESISTORS

QUALITY

Sold exclusively to manufacturers of radio and electronic equipment

A NEW SUB-MINIATURE PRECISION QUARTZ CRYSTAL THAT USES ONLY 1/5th THE SPACE FORMERLY REQUIRED

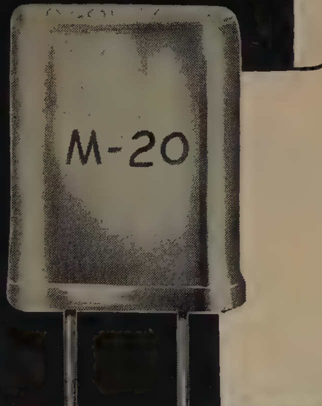

The McCoy M-20 "McMite" has a frequency range of 5.0 mc. to 110 mc. It's a sub-miniature hermetically sealed unit, adaptable to multi-channel design for communications and frequency control equipment. Can be plugged into a sub-miniature tube socket, wired into miniature selector switch assembly or can be soldered to a printed circuit terminal board. Meets Military Specification requirements for fundamental operation above 5 mc. and overtone operation above 15 mc. The "McMite" does not sacrifice stability or dependability but meets same characteristics and performance requirements as larger crystal units used by the Military.

Send for FREE catalog today on the McCoy line of high quality, precision made quartz crystals.

McCoy ELECTRONICS CO.
MT. HOLLY SPRINGS PENNSYLVANIA

McCoy M-20 "McMite"

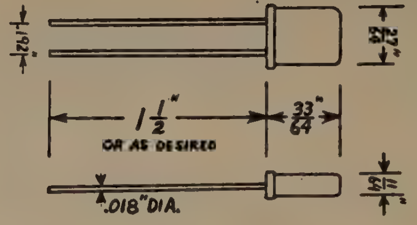

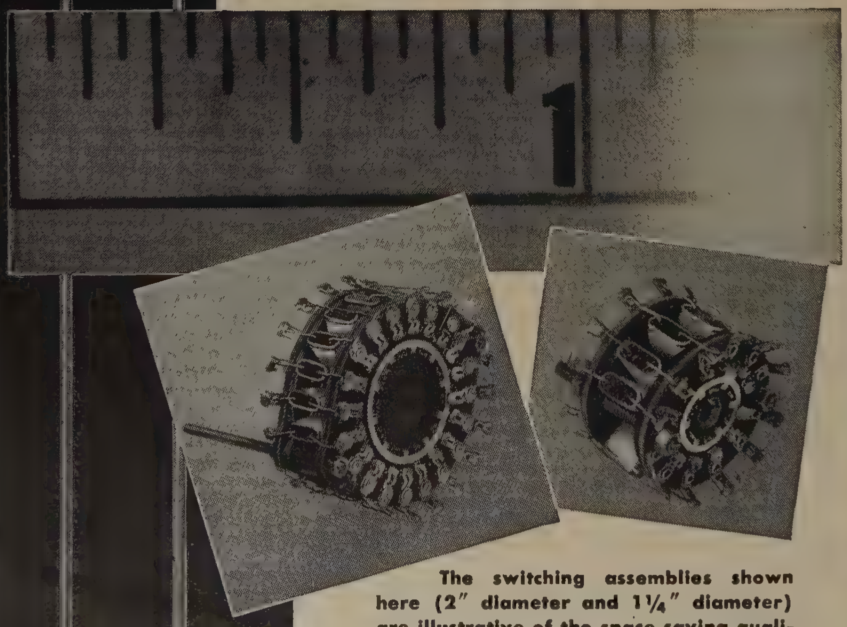

The switching assemblies shown here (2" diameter and 1¼" diameter) are illustrative of the space saving qualities of our M-20 "McMite" crystals.

Contributors

(Continued from page 62A)

J. E. Bridges, whose paper appears on page 1396 of this issue, has been engaged as a research engineer by the Zenith Radio Corporation since 1949. Prior to that, he taught electrical engineering at Iowa State College from 1947 to 1948.

J. E. Bridges

Mr. Bridges was born in Denver, Colorado on January 6, 1925. He received his B.S. degree with honors in Electrical Engineering from the University of Colorado. After completion of active duty with the U. S. Navy he obtained his M.S. degree from the University of Colorado in 1947.

He is a member of Tau Beta Pi and Eta Kappa Nu.

❖

H. Christensen, whose paper appears on page 1371 of this issue, has been a member of the Technical Staff of Bell Telephone Laboratories since 1930. His first assignment was in the Submarine Cable Research Department. In 1937 he took up semiconductor material research work which he later used in the development of the thermistor bolometer. From the beginning of World War II until 1950, Mr. Christensen worked on NDRC and Navy Contracts. Since then he has been engaged in investigation of germanium material processing and surface phenomena related to photocell performance.

H. Christensen

Mr. Christensen was born in Manti, Utah on August 29, 1908. He received a B.S. degree from Brigham Young University in 1930 and an M.A. degree from Columbia University in 1935.

He is a member of the American Physical Society and a former member of the AIEE.

❖

H. Fine (A'50), whose paper appears on page 1405 of this issue, is Chief of the Applied Propagation Branch, Technical Research Division of the Federal Communications Commission, Washington, D. C. He has been associated with them since 1940, first as a Radio Inspector and Intercept Officer at Boston from 1940–45, then with the Technical Research Division in Wash-

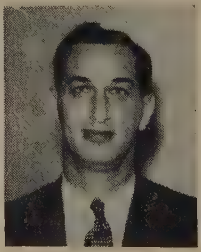

H. Fine

(Continued from page 68A)

SPECIFY THEM FOR CRITICAL APPLICATIONS!

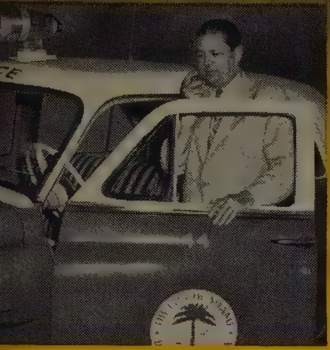
. . for 2-way radio emergency communications.

. . . for radar installations.

. . . for remote-controlled transmitters and unattended relays.

. . . for studio and transmitter equipment in AM-FM-TV broadcasting.

SPECIALLY MANUFACTURED!

Utmost care in manufacture follows. G-E 5-Star Tubes are built to only one standard of quality . . . the highest!

INCREASED reliability brought about by special tube design, is further accented by pre-assembly inspection of individual parts, painstaking manufacture, and thorough testing.

5-Star Tubes are built in separate G-E factory areas, by selected operators whose output features quality, not quantity. Advanced optical equipment is used to magnify parts and to check measurements. Many such inspections involve every 5-Star Tube.

The industry's strictest quality-control standards are observed. Final tube tests are comprehensive and exacting. All G-E 5-Star Tubes receive a final 46-hour "burn-in" before shipment.

Design, manufacture, testing—all focussed on dependability—join to make G-E 5-Star Tubes the best and most reliable you can install! *Tube Dept., General Electric Company, Schenectady 5, N. Y.*

- 5-Star Tube parts are individually inspected by microscope. Grids are micrometer-gaged for accurate dimensions. These are pre-assembly checks with every G-E 5-Star Tube.

- During rigid short-circuit tests, 5-Star Tubes are tapped with a cork mallet. A single flicker of the short test indicator brings immediate tube rejection.

★ ★ ★ ★ ★

ATTENTION: EQUIPMENT DESIGNERS!

33 G-E 5-Star Tubes—19 miniatures, 1 glass octal-base, 2 metal, 11 subminiatures—give you a wide choice, enabling you to put high reliability in virtually every socket. Ask for *new* Bulletin ETD-548C, with full tube listing and application data!

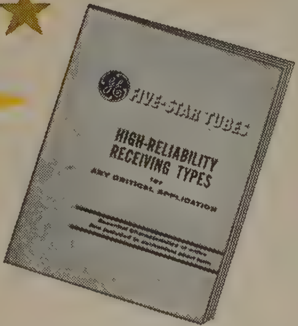

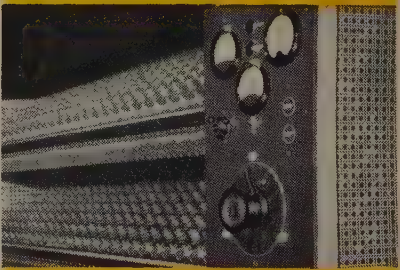
- Every 5-Star Tube receives a 46-hour "burn-in" under Class A conditions. This avoids early life failures, and assures stable electrical performance.

Progress Is Our Most Important Product

GENERAL ELECTRIC

162-1B10

Maxson Engineering
develops
and
manufactures
gyros
for military applications.
Eighteen years' experience, and 3000 employees can augment your facilities.
What are your requirements?
THE W. L. MAXSON CORPORATION
460 West 34th Street, New York 1, New York
Plants at Long Island City, N. Y. and Old Forge, Pennsylvania
MAXSON

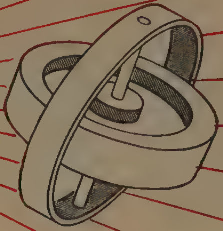

plan your production with **KAHLE** machinery
built specifically for your operation...

Industry leaders in electronics, glass, and allied fields have continuously keyed their operations to KAHLE Machines for over a quarter of a century. *Your* production rate, *your* specifications, *your* requirements—are "planned-in" KAHLE Machines.

Call KAHLE for "machines that think for you!"

Kahle
ENGINEERING COMPANY
1314 SEVENTH STREET
NORTH BERGEN, N. J.

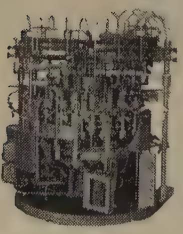

Contributors

(*Continued from page 64A*)

ington since 1945. Prior to that, he was an engineer with the Submarine Signal Co., Boston, Mass. from 1935–40.

Mr. Fine was born on November 27, 1912. He attended the Massachusetts Institute of Technology receiving the B.S. degree in 1934 and the M.S. degree in 1935.

He holds a professional engineering license for the District of Columbia.

❖

W. F. Gabriel (S'45–A'46) is now engaged in research and development work on rapid scanning antennas, waveguide components, and special instrumentation, for the Microwave Antennas and Components Branch at the Naval Research Laboratory in Washington, D.C. His paper appears on page 1410 of this issue.

Dr. Gabriel was born in Sault Ste. Marie, Mich., on October 17, 1925. He received the B.S. degree in electrical engineering from the University of Wisconsin in 1945. After one year of active duty in the U. S. Naval Reserve, he returned to the University of Wisconsin for graduate work in electrical engineering in the communications department, receiving the M.S. degree in 1948, and the Ph.D. degree in 1950.

He is a member of Sigma Xi, Tau Beta Pi, and Eta Kappa Nu.

❖

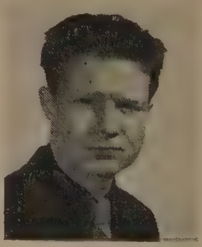

E. O. Johnson

E. O. Johnson (S'46–A'49–M'52) whose paper appears on page 1350 of this issue joined the RCA Laboratories Division, Princeton, N. J. in 1948. He has been engaged in work on gaseous electronics. He is also a part time student in the graduate school at Princeton University.

Mr. Johnson was born in Hartford, Conn. in 1919. He received the B.S. degree in Electrical Engineering in 1948 from the Pratt Institute in Brooklyn. From 1941–1945 he served as chief aircraft electronics technician in the U. S. Navy.

He received honorable mention in the Eta Kappa Nu recognition for 1952 and, along with Dr. W. M. Webster, received the 1953 IRE Editors Award. He is a member of Sigma Xi and Tau Beta Pi.

❖

H. E. Kallmann (A'38–M'41–SM'43), since 1939, has been a consulting engineer in New York, N. Y., except for the period

(*Continued on page 70A*)

REED MAGNETIC AMPLIFIERS

Series MAFS

Designed for high-performance control systems

TWO CYCLE RESPONSE TIME — DRIFT-FREE

The Freed MAFS series of Magnetic Amplifiers is characterized by

- FAST RESPONSE — 2 cycles of power frequency delay for 100% response to step input signal.
- PHASE REVERSIBLE A.C. OUTPUT WITH ZERO DRIFT OF NULL POINT

The MAFS series includes the units described below. Engineering and development facilities are available for the design and development of Magnetic Amplifiers having special performance characteristics.

FAST-RESPONSE MAGNETIC AMPLIFIERS — DRIFT-FREE

1φ Supply Voltage and Frequency	Full Power Output	Max. Voltage Output	Signal Req. for full output	Max. Power Gain	Typical Motor Load Mfr. and Type No.	Stall Torque	No Load Speed	FREED Type No.
115V., 60	15 watts	115V. AC phase reversible	.1V. AC (10,000 ohms input impedance)	1.5 x 10^7	Diehl FPE 25-11	5.5 in-oz	3500 RPM	MAFS-1
115V., 400	5	57.5V. AC phase reversible	.1V. AC (10,000 ohms input impedance)	5 x 10^6	Kearfott R 110-2	1.5	5300	MAFS-2
115V., 400	10	57.5V. AC phase reversible	.1V. AC (10,000 ohms input impedance)	1 x 10^7	Kearfott R 111-2	2.4	5300	MAFS-3
115V., 400	50	115V. AC phase reversible	.1V. AC (10,000 ohms input impedance)	5 x 10^7	Bendix CK-3000	14	3700	MAFS-4

SEND FOR LATEST DETAILED BULLETINS AND CATALOGS

FREED RESEARCH, Engineering and Production Facilities Combine to Produce Transformers and Instruments of Top Performance.

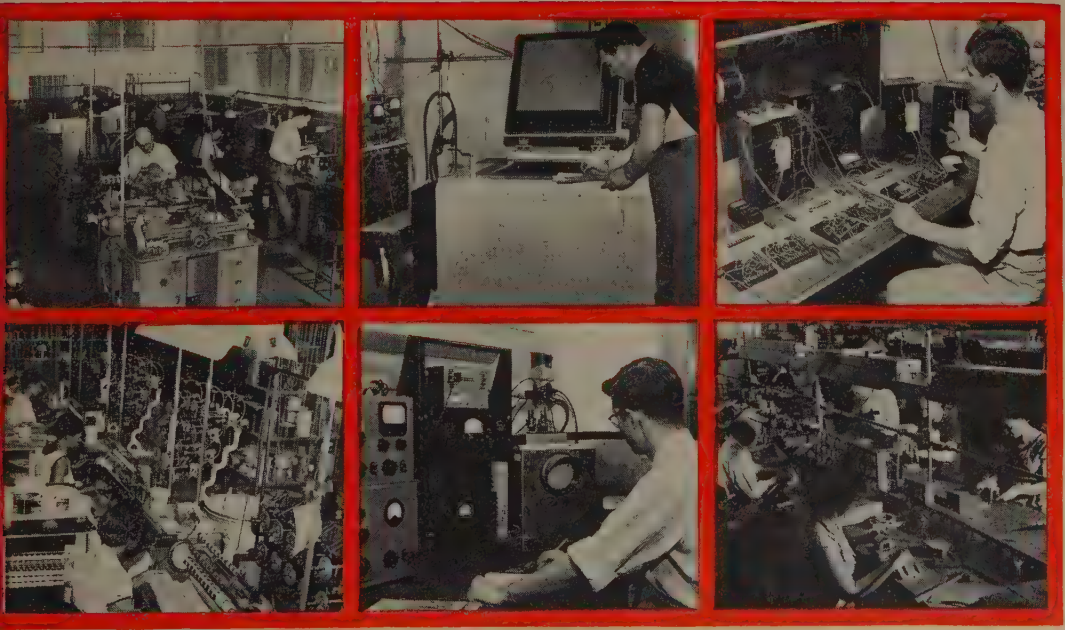

FREED TRANSFORMER CO., INC.

1720 WEIRFIELD ST., BROOKLYN (RIDGEWOOD) 27, N. Y.

Freed Magnetic Amplifiers, Saturable Transformers and Reactors are designed for efficient operation and long life. They can be used wherever reliable, rugged and maintenance free systems are required.

The types of amplifiers listed are designed to control AC servomotors.

Development facilities are available for the design of magnetic amplifiers to meet specific requirements.

All standard units are hermetically sealed and meet MIL-T-27 Specifications.

SATURABLE TRANSFORMERS — Controlled with dual triode; plate supply can be either DC or AC; no rectifiers; AC or DC control signals.

PUSH-PULL MAGNETIC AMPLIFIERS — AC or DC control signals; high gain; may be used with magnetic or vacuum tube preamplifiers if needed.

FAST-RESPONSE MAGNETIC AMPLIFIERS — High gain; half-cycle per stage response time; AC or DC control signals; RC feedback networks for control system stabilization can be used directly; preamplifier not needed.

HIGH TEMPERATURE MAGNETIC AMPLIFIERS — Designed to operate in ambient temperatures as high as 200° C.; AC or DC control signals.

DRIFT-FREE MAGNETIC AMPLIFIERS — For rigid drift-free requirements of control systems; designed to meet specific requirements.

OTHER FREED PRODUCTS
TRANSFORMERS

- High Fidelity
- High Level Pulse
- High Q Toroids
- Power
- Slug-Tuned
- Hermetically Sealed
- Step-down
- Miniature
- Transistor
- High Q Reactors
- High Temperature
- Miniature Audio
- Charging Reactors
- Sub-miniature
- Precision Reactors
- Precision Filters

INSTRUMENTS

- Comparison and Limit Bridges
- Low frequency "Q" Indicators
- Incremental Inductance Bridges
- Universal Bridges
- Null Detectors and V.T. Voltmeters
- Power Supplies
- A.C. Bridges and Accessories
- Differential Voltmeters
- Harmonic Distortion Meters
- Wide Band Amplifiers
- Decade Amplifiers
- Decade Inductors
- Decade Capacitors
- Megohmmeters
- Filters
- Magnetic Voltage Regulators

Another **NEW** Fairchild Precision Potentiometer

TYPE
910
Rectilinear

The basic Type 910 rectilinear potentiometer is flexible in design to accommodate dual resistance elements, various stroke lengths, double shaft extensions, external fixed resistors, various methods of actuating, and a broad range of shaft speeds. It meets or exceeds military specifications for vibration and high and low temperature exposure. A mandrel resistance element of all-welded construction, aged and stabilized for accuracy and long life, provides small diameter, uniform cross section and a smooth operating surface for the new one-piece wiper design. Rigid mechanical construction maintains initially-tight electrical tolerances throughout stringent environmental and performance conditions.

Another reason why **Fairchild can supply ALL your precision potentiometer needs**

Fairchild makes a complete line of precision potentiometers to fill all your needs—linear and nonlinear potentiometers, singly or in ganged combinations . . . single-turn, helical and linear motion . . . and with resistance elements to meet your requirements.

Fairchild guarantees accuracy of ±1% or better in nonlinear types and ±0.5% or better in linear types. Highly accurate production methods and close mechanical tolerances, plus thorough type-testing and quality control, provide high resolution, long life, low torque and low electrical noise level in every Fairchild potentiometer. For more information, or for help in meeting your potentiometer problems, call on Fairchild Camera and Instrument Corporation, Potentiometer Division, 225 Park Avenue, Hicksville, L. I., N. Y., Department 140-57H.

FAIRCHILD
PRECISION POTENTIOMETERS

Contributors

(Continued from page 68A)

H. E. KALLMANN

from 1943 to 1945, when he joined the Radiation Laboratory of the Massachusetts Institute of Technology, Cambridge, Mass. His paper appears on page 1438 of this issue.

Dr. Kallmann was born on March 10, 1904, in Berlin, Germany. He received the Ph.D. degree in physics from the University in Goettingen in 1929. From 1929 to 1934, he was a research engineer in the laboratories of the C. Lorenz A.G., Berlin, concerned with the development of rf test equipment, ultra-short-wave receivers for communications, wideband television, and television development.

From 1934 to 1939 he was a television engineer with Electric and Musical Industries, Ltd., Hayes, England, doing research and advanced circuit development.

He is a member of the APS and has served on various RMA committees on uhf and color television systems.

❖

For a photograph and biography of R. H. Kingston, see page 863 of the May, 1954 issue of the PROCEEDINGS OF THE I.R.E. His paper appears on page 1376 of this issue.

❖

J. T. Law, whose paper appears on page 1367 of this issue, became a member of the Technical Staff of Bell Telephone Laboratories in 1952. Since that time he has been engaged in semi-conductor surface studies.

J.T. LAW

He was born in Christchurch, New Zealand in 1926. He attended the University of New Zealand, receiving the B.Sc. degree in chemistry in 1945, the M.Sc. in physical chemistry in 1946, and the Ph.D. in physical chemistry in 1949. From 1949 to 1951 he was a Beit Memorial Fellow at London University. In 1952 he came to the United States as a research associate at Pennsylvania State College.

❖

A. L. McWhorter (S'51) is presently working on noise in junction diodes and transistors in the Research Laboratory of

(Continued on page 72A)

AUTOMATIC
AUTOMATIC
AUTOMATIC

Superior Design

+ Mass Production

= Low Cost

TV TUNERS,
YOKES and
FLYBACKS

BY
AUTOMATIC

AUTOMATIC
MANUFACTURING
CORPORATION
GOUVERNEUR ST., NEWARK 4, N. J.

MASS PRODUCERS OF
ELECTRONIC COMPONENTS

K-CAP
100
T.C.
AUTOMATIC
K-TRAN
K-CAP®
K-TRAN®

The BALLANTINE SENSITIVE INVERTER

for the precise measurement of small DC potentials

from

10μv—100v

Threshold Sensitivity

1 μv

FOR USE WITH

Vacuum Tube Voltmeters

Oscilloscopes

Voltage Amplifiers

Multimeters

Servo-Amplifiers

AC OUTPUT
BALLANTINE LABORATORIES, INC.
BOONTON, NEW JERSEY
SENSITIVE INVERTER
ON
OFF
POLARITY
VOLTAGE RATIO
DC TO AC RMS
1:100
10:1
CAL STD
DC INPUT

MODEL 700

FEATURES

- Built-in Calibrator
- High Sensitivity
- High Input Resistance
- Distortion-free Output
- Low Noise Level
- Accurate for 50-70 cps Line Frequencies
- Polarity Sensing
- Immune to 60 cps Stray Magnetic Fields

SPECIFICATIONS—MODEL 700

INPUT VOLTAGE RANGE	10 μv—100 v DC (Sensitive to 1 μv)
VOLTAGE RATIOS (DC input to AC RMS output)	1:100 & 10:1
INVERSION STABILITY (>100 μv input)	1%
CALIBRATOR ACCURACY	0.25%
DC INPUT RESISTANCE	10 meg for 1:100; 50 meg for 10:1
AC INPUT IMPEDANCE	>200k
INPUT NOISE LEVEL	Approx. 3 μv
AC OUTPUT FREQUENCY	Line Frequency
MAX AC OUTPUT LEVEL	10 v RMS
TOTAL DISTORTION IN OUTPUT WAVE FORM	<2%
RESPONSE TIME (90% of Final Amplitude)	0.25 sec
POWER REQUIREMENTS	105-125 v; 50-70 cps; 15 watts

BALLANTINE LABORATORIES, INC.

102 Fanny Road, Boonton, New Jersey

Contributors

(*Continued from page 70A*)

A. L. McWhorter

Electronics and Lincoln Laboratory at the Massachusetts Institute of Technology. His previous work at Lincoln Laboratory also includes the microwave application of ferrites. His paper appears on page 1376 of this issue.

Mr. McWhorter was born in Crowley, La., on August 25, 1930. He received the B.S. degree in electrical engineering from the University of Illinois in 1951, and since then has been studying for an Sc.D. degree in electrical engineering at M.I.T. During the summer of 1953 he worked in the solid-state physics section of the Philips Research Laboratory in Eindhoven, Holland, on an M.I.T. Overseas Summer Fellowship.

He is a member of Tau Beta Pi and Eta Kappa Nu.

❖

J. A. Olmstead

J. A. Olmstead whose paper appears on page 1350 of this issue joined the Radio Corporation of America in 1952. He is a member of the research staff of the RCA Laboratories Division in Princeton, N. J. He has been engaged in the manufacturing process and development of the gas tube.

Mr. Olmstead was born in Buffalo, New York in 1930. He attended the University of Buffalo receiving the B.S. degree in Electrical Engineering in 1952.

❖

For a photograph and biography of J. R. Pierce, see page 512 of the March, 1954 issue of the Proceedings of the I.R.E. His paper appears on page 1389 of this issue.

❖

D. R. Rhodes

D. R. Rhodes, whose paper appears on page 1408 of this issue, is a Research Electrical Engineer in the Tactical Air Group at Cornell Aeronautical Laboratory, Buffalo, N. Y. Until this year he was associated with the Ohio State University Research Foundation as a Research Associate. He was engaged in research on microwave antennas and radar cross-section studies. While at

(*Continued on page 82A*)

PROCEEDINGS OF THE I-R-E®

Published Monthly by

The Institute of Radio Engineers, Inc.

VOLUME 42 — *September, 1954* — NUMBER 9

BOARD OF DIRECTORS, 1954

William R. Hewlett
President

M. J. H. Ponte
Vice-President

W. R. G. Baker
Treasurer

Haraden Pratt
Secretary

John R. Pierce
Editor

D. B. Sinclair
Senior Past President

J. W. McRae
Junior Past President

1954
A. N. Goldsmith
J. T. Henderson (R8)
A. V. Loughren
C. A. Priest (R4)
J. R. Ragazzini (R2)
J. D. Ryder
A. W. Straiton (R6)
J. A. Stratton
Ernst Weber

1954–1955
S. L. Bailey
C. J. Marshall (R5)
L. E. Packard (R1)
J. M. Pettit (R7)
B. E. Shackelford
H. W. Wells (R3)

1954–1956
A. G. Jensen
George Rappaport

●

George W. Bailey
Executive Secretary

●

John B. Buckley
Chief Accountant

Laurence G. Cumming
Technical Secretary

Evelyn Davis
Assistant to the Executive Secretary

Emily Sirjane
Office Manager

Responsibility for the contents of papers published in the PROCEEDINGS OF THE I.R.E. rests upon the authors. Statements made in papers are not binding on the Institute or its members.

PROCEEDINGS OF THE I-R-E

Joseph M. Pettit, Director, 1954–1955 1348
The Need for a New Type of Frequency and Time Standard . . . . . W. D. George 1349
5036. The Tacitron, A Low Noise Thyratron Capable of Current Interruption by Grid Action . . . . . E. O. Johnson, J. Olmstead, and W. M. Webster 1350
5037. **IRE Standards on Receivers: Methods of Measurement of Interference Output of Television Receivers in the Range of 300 to 10,000 KC, 1954** 1363
5038. A Mechanism for Water Induced Excess Reverse Dark Current on Grown Germanium *N-P* Junctions . . . . . J. T. Law 1367
5039. Surface Conduction Channel Phenomena in Germanium . . . . . H. Christensen 1371
5040. Channels and Excess Reverse Current in Grown Germanium *P-N* Junction Diodes . . . . . A. L. McWhorter and R. H. Kingston 1376
5041. Significance of Some Receiver Errors to Color Reproduction . . . . . Harold Weiss 1380
5042. Coupling of Modes in Helixes . . . . . J. R. Pierce and P. K. Tien 1389
5043. Detection of Television Signals in Thermal Noise . . . . . J. E. Bridges 1396
5044. An Effective Ground Conductivity Map for Continental United States . . . . . Harry Fine 1405
5045. On Minimum Range for Radiation Patterns . . . . . D. R. Rhodes 1408
5046. An Automatic Impedance Recorder for X-Band . . . . . William F. Gabriel 1410
5047. An Investigation of the Ultimate Performance of Space-Charge Deflection Tubes . . . . . J. T. Wallmark 1422
5048. Coding for Constant-Data-Rate Systems—Part I. A New Error-Correcting Code . . . . . R. A. Silverman and Martin Balser 1428
5049. Analysis of a Special Purpose RC Filter Incorporating a Periodically Conducting Bilinear Element . . . . . Victor W. Bolie 1435
5050. Optar, a Method of Optical Automatic Ranging, as Applied to a Guidance Device for the Blind . . . . . Heinz E. Kallmann 1438
Correspondence:
5051. "Comment on 'A Simple Graphical Analysis of a Two-Port Waveguide Junction' " . . . . . L. B. Felsen and A. A. Oliner 1447
5052. "Rebuttal" . . . . . S. Stein, L. S. Sheingold and J. E. Storer 1447
5053. "Further Comment" . . . . . L. B. Felsen and A. A. Oliner 1448
5054. "Comment on 'Developments in Sintered Magnetic Materials' " . . . . . T. Powell 1448
5055. "Rebuttal" . . . . . J. L. Salpeter 1449
5056. "Comment on 'Wien Bridge Oscillator Design' " . . . . . J. M. Diamond 1449
5057. "Waveguides with Nonhomogenous Dielectric" . . . . . Dario Graffi 1449
5058. "A Method of Broadbanding Waveguide Windows" . . . . . H. G. Hereward 1450
5059. "Relationship between the Bott-Duffin and Pantell Impedance Synthesis" . . . . . James E. Storer 1451
5060. "Rhombic Antenna Design" . . . . . H. T. Friis 1451
5061. "Bits and Binits" . . . . . M. J. E. Golay 1452
5062. "High Frequency Crystal Units for Primary Frequency Standards" . . . . . A. W. Warner 1452
5063. "A Note on the Transfer Voltage Ratio of Passive RLC Networks" . . . . . F. M. Reza 1452

IRE NEWS AND RADIO NOTES SECTION

Joint Computer Conference Scheduled 1453
Technical Committee Notes 1454
Professional Group News 1456
Obituaries 1456
5064. Abstracts of TRANSACTIONS OF THE I.R.E. 1456
Professional Groups and Sections 1457
5065. Abstracts and References 1460
Meetings with Exhibits 2A
News—New Products 16A
Contributors in This Issue 62A
Section Meetings 86A
IRE People 90A
Professional Group Meetings 95A
Membership 103A
Positions Open 128A
Positions Wanted 136A

EDITORIAL DEPARTMENT

Alfred N. Goldsmith
Editor Emeritus

John R. Pierce
Editor

E. K. Gannett
Managing Editor

Marita D. Sands
Assistant Editor

●

ADVERTISING DEPARTMENT

William C. Copp
Advertising Manager

Lillian Petranek
Assistant Advertising Manager

●

EDITORIAL BOARD

John R. Pierce, *Chairman*
D. G. Fink
E. K. Gannett
T. A. Hunter
J. W. McRae
J. A. Stratton
W. N. Tuttle

Changes of address (with advance notice of fifteen days) and communications regarding subscriptions and payments should be mailed to the Secretary of the Institute, at 450 Ahnaip St., Menasha, Wisconsin, or 1 East 79 Street, New York 21, N. Y.

All rights of publication, including translation into foreign languages, are reserved by the Institute. Abstracts of papers with mention of their source may be printed. Requests for republication privileges should be addressed to The Institute of Radio Engineers.

Copyright 1954, by the Institute of Radio Engineers, Inc.

Joseph M. Pettit

DIRECTOR, 1954–1955

Joseph M. Pettit was born on July 15, 1916 in Rochester, Minnesota. He attended the University of California at Berkeley, receiving his B.S. degree in 1938. In 1940 he received the degree of Engineering from Stanford University, and the Ph.D. degree in 1942 from the same institution.

From 1938 to 1940 Dr. Pettit was a teaching and research assistant in electrical engineering at Stanford; from 1940–1942 he was a research associate there, and an instructor in electrical engineering at the University of California. During World War II he was engaged first in radar countermeasures work on the staff of the Radio Research Laboratory, then in sevice as a technical observer with the Air Force in India and China, and finally as associate technical director of ABL-15, a laboratory associated with the Radio Research Laboratory. In 1945, he became supervising engineer with the Airborne Instruments Laboratory, Inc., Mineola, N. Y., in charge of receiver development. Since January, 1947, he has been at Stanford University where he is now professor of electrical engineering.

Dr. Pettit became a Student member of the IRE in 1939, an Associate in 1940, a Member in 1945, and a Senior Member in 1946. In 1954 he received the Fellow Award "for his outstanding work as engineer and educator in the field of high-frequency and microwave communications." He has been active on several IRE committees, and was Institute Representative at Stanford University from 1948–1951. In 1952 he received the Region 7 Electronics Achievement Award, and was elected Director of the IRE from Region 7 for the term 1954–1955.

Dr. Pettit is a member of the American Institute of Electrical Engineers, Sigma Xi, Tau Beta Pi, and Eta Kappa Nu.

The Need for a New Type of Frequency and Time Standard*

W. D. GEORGE, VOTING ASSOCIATE, IRE

National Bureau of Standards, Washington, D. C.

The measurement of a physical quantity requires first, a unit in terms of which to make the measurement, and second, an operation by means of which the standard and the unknown may be compared. Although the details of defining both the standard and the operation vary widely for measurements of different types, the two factors can always be observed in any physical measuring process. For example, the determination of a length consists first of defining a unit of length which may be a light year or a kilometer or a yard or an x-unit and then comparing the length of the standard with that of the unknown by direct comparison, triangulation, or some other method.

The establishment of a standard having all the possible desirable characteristics is not a simple matter. The ideal standard should be indestructible, simple, invariable, independent of any and all external influences, reproducible, and readily accessible. No known standard meets all of these conditions. It is also desirable to distinguish between operational standards and defining standards since few, if any, standards meet the requirements for both. An operational standard is one which is used in making measurements: for example, a liter measure. A defining standard is one used in setting forth the definition of a unit: for example, the wavelength of the light of a certain spectral line. In some cases a defining standard may also be an operational standard, as the spectral definition of length.

The measurement of time, time-interval and frequency is no exception. It is first necessary to have a standard in terms of which to define the unit of time, and second it is necessary to have an operation by means of which time intervals can be compared with this standard. For immediate use without prolonged waiting the standard of time is a provisional standard defined as a certain fraction of the average period of the rotation of the earth. Another and more uniform standard is defined with reference to long-term observations of celestial bodies and their motions. Unfortunately, the period of rotation of the earth is not constant over long periods of time and it is erratic over short periods of time and no adequate and satisfactory means exists for interpolating the standard for comparison with the periods of high frequency oscillations.

Years ago it was realized that the wave-length of the light in a spectral line of an atom is an excellent length standard. The fact that even this is not an ideal standard because of the effect of the uncertainty principle need not be discussed here. Such a standard does satisfy the requirements of permanence, invariance, and reproducibility. It is not, however, convenient, and it is, therefore, used as a defining standard, rarely as an operating standard.

There is at present no perfect time standard. The second, which is defined as 1/86,400 part of a mean solar day, is not invariant over periods of the order of a century, nor is it constant over periods of the order of a day. Astronomers have defined a more nearly uniform time as the sidereal year at 1,900.0 and designated it ephemeris time. No satisfactory operational means for employing this definition is known.

Despite the fact that time is inseparably involved in most of the other physical constants and relationships and in many engineering and scientific principles, the common unit of time is far from being readily available with high accuracy at the time it is needed.

An immediate problem is that of providing time (frequency) standards of adequate accuracy for use in communication and navigation devices and scientific work. Precisions approaching one part in 10^9 over long intervals (days) are now being approached and will soon be achieved. In order to produce and calibrate such devices and monitor them it is essential that the unit of time be quickly available with an accuracy of one part in 10^9 and that transfer standards be devised with which to compare the defined standard with the operating device.

The above statement may be clarified by consideration of the process by means of which the standard meter is defined. The unit of length is that of the wave-length of the red line of cadmium (the work of Meggers and others shows that better standards could now be chosen). By means of an interferometer, the distance between two indicating marks on a suitable bar is compared with the wavelength of the chosen light. The bar then becomes the operational standard. If lost or damaged, a new one, as good as or better than the original can be made quickly to replace it. It can be quicly recalibrated at intervals in case of suspicion of variance. The length of the meter is defined as being equal to a certain number multiplied by the wavelength of the light in the selected spectral line. This is the defining standard even though it is inconvenient or even impractical to use it as an operational standard.

The present state of physical knowledge suggests only one source of a satisfactory time standard, namely the period of molecular, atomic, or nuclear vibrations. Such a time standard would meet the requirements of permanence, reproducibility, invariance and ready access without prolonged waiting and expense.

It is possible today to define the unit of time in terms of the period of vibration of a chosen molecular resonance. A reproducibility to one part in 10^7 has been obtained using molecular and atomic clocks. A number of atomic clocks of the most promising type should be built and observed. Effort should be concentrated on obtaining agreement and reproducibility to one part in 10^9 or better between independent units.

To put such an atomic time standard into operation requires the following steps: (1) Investigation of the most nearly ideal molecular, atomic or nuclear vibration to be used as the defining standard; (2) Development of suitable apparatus reproducible to one part in 10^9 or better for correlation of an operating standard to the defining standard; (3) Legislation and/or agreement designed to implement the new standard in practice.

Of course, formidable difficulties lie in the way of each of these steps, but the importance of the measurement of time, time-interval, and frequency in both applied and pure research make it imperative that this work be started at once and actively carried to completion.

---

* RDB Subpanel on Frequency Control Devices, W. D. George, Chairman.

The Tacitron, A Low Noise Thyratron Capable of Current Interruption by Grid Action*

E. O. JOHNSON†, MEMBER, IRE, J. OLMSTEAD†, AND W. M. WEBSTER†, ASSOCIATE, IRE

Summary—**Two thyratron considerations are (1) spurious noise output, and (2) speed and ease with which the anode current can be tuned on and off. The spurious noise output of conventional thyratrons often is such that they cannot be operated close to sensitive communications equipment. In addition, while the anode current can be established in a fraction of a microsecond, current interruption often requires times of the order of 100 microseconds. During this time one is confronted with the additional disadvantage of having to remove the anode voltage.**

The tacitron, a new thyratron whose construction and operation are herein described and analyzed, is so quiet in operation that it can be operated in close proximity to sensitive communications equipment without noticeable interference. Furthermore, its anode current can be switched on or off in about one microsecond without the necessity of anode voltage removal. With respect to arc drop, over-all efficiency, tube construction, and other salient characteristics the tube is similar to conventional ones. The tacitron owes its unusual capabilities mainly to a grid design that insures tube operation in a unique discharge mode where in ion generation takes place solely in the grid-anode region.

Besides being useful in applications in which conventional thyratrons are now used, this new tube offers the possibility of use in many new applications presently denied conventional thyratrons, either because of noise or recovery time considerations. This includes computers and all sorts of pulse circuits.

INTRODUCTION

A THYRATRON is essentially a triode-vacuum tube which has been filled with some gas such as xenon, argon, hydrogen, or mercury. Electrons en route from the cathode to the anode create ions which serve to neutralize the electron-space charge. This makes possible the passage of large electron currents at low-anode voltages, allowing the tube to operate with high efficiency. This important characteristic combined with simplicity, ruggedness, and high power sensitivity has made the thyratron a popular device for diverse switching applications.

The thyratron has, however, serious disadvantages. Two very important ones are: (a) the tube is often noisy,[1] and (b) once the anode current has started to flow it cannot be turned off by the grid. The latter difficulty has had to be surmounted by the troublesome expedient of first removing the anode voltage and then waiting for the tube to totally, or at least partly, deionize. This complicates the attendant circuitry and restricts the thyratron to relatively low frequency applications.

Fundamental studies of externally-heated hot-cathode discharges[2–4] have illuminated the way to a tube design that overcomes these two difficulties. This design insures operation in a unique discharge mode wherein ion generation occurs solely in the grid-anode region. This mode is stable, noiseless,[1] and allows positive ion sheaths from a negative grid to span the grid holes and choke off tube current. In practice this mode of discharge is achieved by proper selection of the size of the grid openings, gas, gas pressure, and over-all tube geometry. Aside from having a relatively opaque grid the tube is very similar to conventional ones with respect to geometry, efficiency, and operating conditions.

It is fairly well known that thyratron current can be interrupted by application of a reasonably small grid bias, providing that the tube current is very small, i.e., one per cent, or so, of the rated current. It has also been known[5] that there are certain conditions under which current cutoff with much larger currents can be achieved These conditions have to do with gas, gas pressure, and grid geometry. As will be seen, these conditions are included in a set of broader conditions that include overall tube geometry. In particular, it will be shown that the conditions for practical current cutoff are synonymous with those for noise free operation.

In brief, current cutoff cannot be generally achieved in a conventional thyratron with any reasonable grid bias because the action of an increasing grid bias in expanding positive ion sheaths around the grid wires is largely cancelled by a feedback process that tends to decrease the size of the grid sheaths by causing an increase in the positive ion current to the grid wires. In the tube to be described this effect is minimized by restricting the site of ion generation to the grid-anode region.

DESCRIPTION OF TYPICAL EXPERIMENTAL TUBE AND ITS OPERATING CHARACTERISTICS

A photograph of a tube of the 100 milliampere size is shown in Fig. 1. In this photograph the top end mica has been removed and a portion of the shield electrode has been peeled back. In the shield compartment at the right of the photograph can be seen the 50-mil diameter oxide-coated cathode. Directly to the left of this is a grid mesh composed of 50 openings per linear inch. In this particu-

---

* Decimal classification: R337.12. Original manuscript received by the IRE, April 15, 1954; revised manuscript received, May 24, 1954. Presented at 1954 IRE National Convention, March 22–25, New York, N. Y.

† RCA Laboratories Div., Princeton, N. J.

[1] Throughout this paper the word "noise" will be taken to mean the coherent and incoherent anode voltage fluctuations, in the frequency range between several kilocycles and about 100 kilocycles, that are commonly found in hot cathode gas tubes. These fluctuations often produce interference at several hundred megacycles.

[2] L. Malter, F. O. Johnson, and W. M. Webster, "Studies of externally heated hot cathode arcs, I—modes of the discharge," *RCA Review*, vol. XII, pp. 415–435; September, 1951.

[3] W. M. Webster, F. O. Johnson, and L. Malter, "Studies of externally heated hot cathode arcs, II—the anode glow mode," *RCA Review*, vol. XIII, pp. 163–182; June, 1952.

[4] M. J. Druyvesteyn and F. M. Penning, "Electrical discharges in gases," *Rev. Mod. Physics*, vol. 12, pp. 148–150; April, 1940.

[5] H. Fetz, "On the control of a mercury arc by means of a grid in the plasma," *Ann. der Phys.*, vol. 37, pp. 1–40; January, 1940.

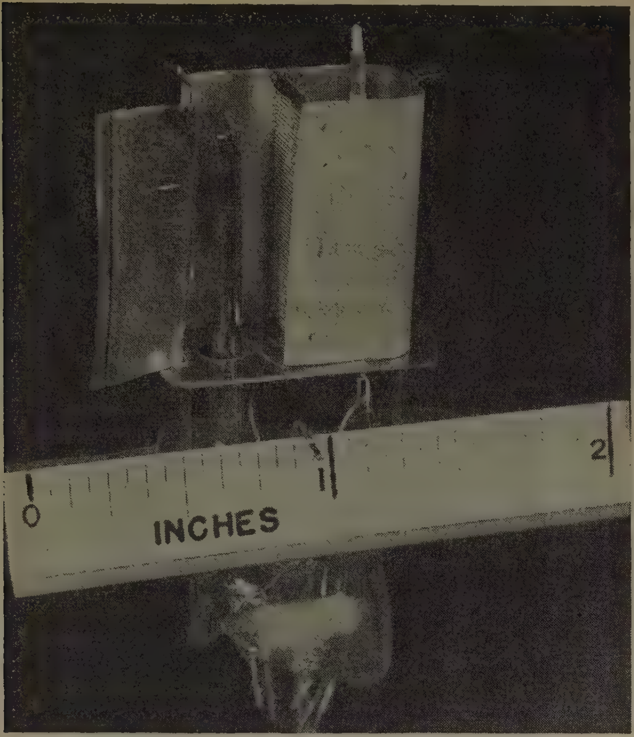

Fig. 1—Experimental tacitron. A section of the grid shield has been peeled back to expose the internal geometry.

lar tube this mesh is electrically tied to the shield electrode. Facing this mesh, with a lead that comes from the stem through a glass insulator, is the anode.

A crosssection of the tube along with the basic operating circuit is shown in Fig. 2. The supply potential V and the resistor R limit the anode current to the value I. The grid is connected to a bias potential V_g.

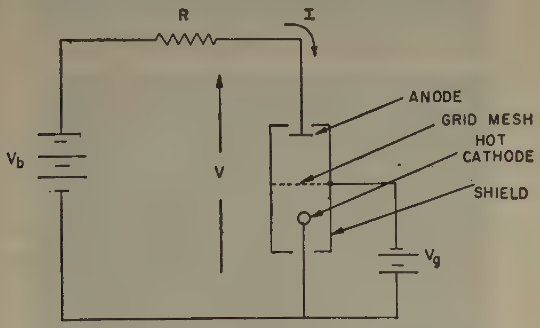

Fig. 2—Cross section of experimental tacitron, together with test circuit.

The volt-ampere characteristic of the tube, as traced out by the usual 60-cycle sweep technique, is shown in the lower half of the photograph in Fig. 3. Here the anode potential is measured horizontally and the anode current vertically. The origin on the voltage axis is marked by a short vertical line. The scale can be judged from the fact that the onset of anode current starts at about 13v and the maximum anode current has a value of 400 ma. It is seen that the anode voltage remains almost constant as the current increases smoothly up to a value close to the maximum. Beyond this value the discharge becomes unstable and gives rise to the voltage fluctuations evidenced by the broadening of the top portion of the characteristic. For comparison, the volt-ampere characteristic of a comparable commercial tube is shown in the upper portion of the same photograph along with the same current and voltage scales. It is seen that in the latter case the anode-voltage fluctuations have a value of about 10 v. It is just this sort of voltage fluctuation that gives rise to the troublesome noise and interference which commonly emanates from hot cathode gas tubes. For example, when a tube having this noisy sort of volt-ampere characteristic is operated as a half-wave, 60-cycle, rectifier-near-a-television-receiver, the picture is often badly disrupted. On the other hand, a tacitron, even when its anode lead is wrapped around the antenna terminals of the receiver, causes no noticeable interference.

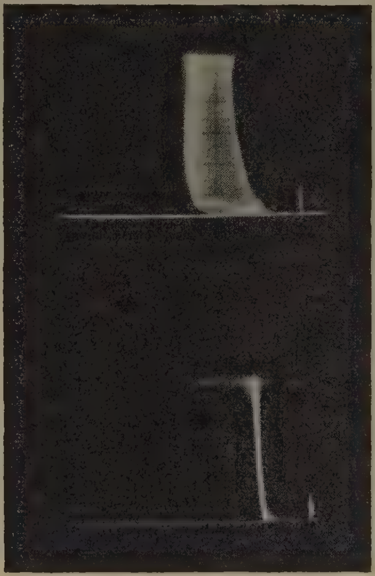

Fig. 3—Oscilloscope trace showing volt-ampere characteristics of conventional thyratron (above) and tacitron (below).

In Fig. 4, following page, is plotted the combined firing and cutoff characteristics of a typical experimental tube such as the one shown in Fig. 1. The circuit from which these characteristics were obtained is the same as the one shown in Fig. 2. The solid curve on the extreme right represents the conventional control characteristic, or firing curve: the other solid curves to the left of this comprise the current-cutoff characteristic. The dashed curves are the grid current characteristics which will be discussed later. To illustrate the use of the combined firing and cutoff curves let us suppose that the unfired tube has grid and anode voltages represented by point x on Fig. 4. Now, with the supply voltage held constant, suppose that the bias is reduced from its value at point x to a new value indicated by point y. As with conventional tubes the tube will have fired when the control characteristic was crossed. If we now wish to cut off a tube current of say, 50 μA, we need only increase the grid bias until some point z, located to the left of the 50-μA curve, is reached. The current-cutoff characteristic is independent of the rapidity of application of the grid bias.

The wavy lines on the extremities of the cutoff characteristics indicate the presence of noise, such as that shown on the top of the volt-ampere characteristic of the lower curve in Fig. 3. As is apparent from the accompanying saturation in the cutoff characteristics, the presence of this noise is accompanied by an abrupt increase in the difficulty of achieving current cutoff. Practical operation of this tube is, therefore, limited to grid bias values which are smaller than about 15v.

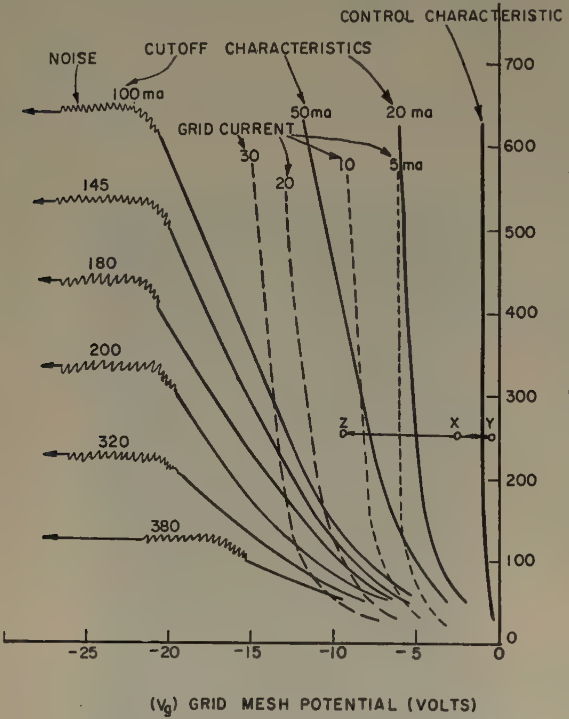

Fig. 4—Firing and cut-off characteristics of experimental tacitron of form shown in Fig. 1.

The dashed lines in Fig. 4 are lines of constant-grid current. These currents were measured when the tube was on the verge of cutoff. For example, when $V_b = 300$v and the anode current is 50 μA, the grid bias voltage required for cutoff is 8.3v. The corresponding grid current is 10 μA. The grid currents noted in the figure are reduced by a factor of three to five if the grid mesh is not connected to the shield electrode, and the latter is connected to the cathode.

The top photograph in Fig. 5 gives a more direct illustration of the cutoff action. The top half of this photograph is an oscilloscope picture of the grid voltage V_g in the circuit of Fig. 2. Here, a switch operating at a 60-cycle rate is arranged so that the grid has a 15v bias[6] for half of the 60-cycle period, and then a positive bias of about 3v for the other half of the cycle. The unbroken horizontal line represents zero, or cathode potential. In the lower half of the same photograph is shown the simultaneous course of the tube's anode potential. The unbroken horizontal line again represents cathode potential. It is seen that the anode potential is low when the grid is positive, and high when the grid is negative. In the first instance, the anode potential has a value of about 13v and the tube is passing a current of 100 μA. In the second instance, the anode is at the 200v supply potential and the anode current is zero.

No detailed studies have been made of the speed of cutoff other than noting, in cases such as described above, that the anode potential rises from the 13 to the 200v level in about half a microsecond. This time is tied up with circuit constants as well as with the dynamics of the ion sheaths which accomplish the current cutoff. There seems to be no reason why the propagation of these ion sheaths, and hence the actual cutoff, cannot be

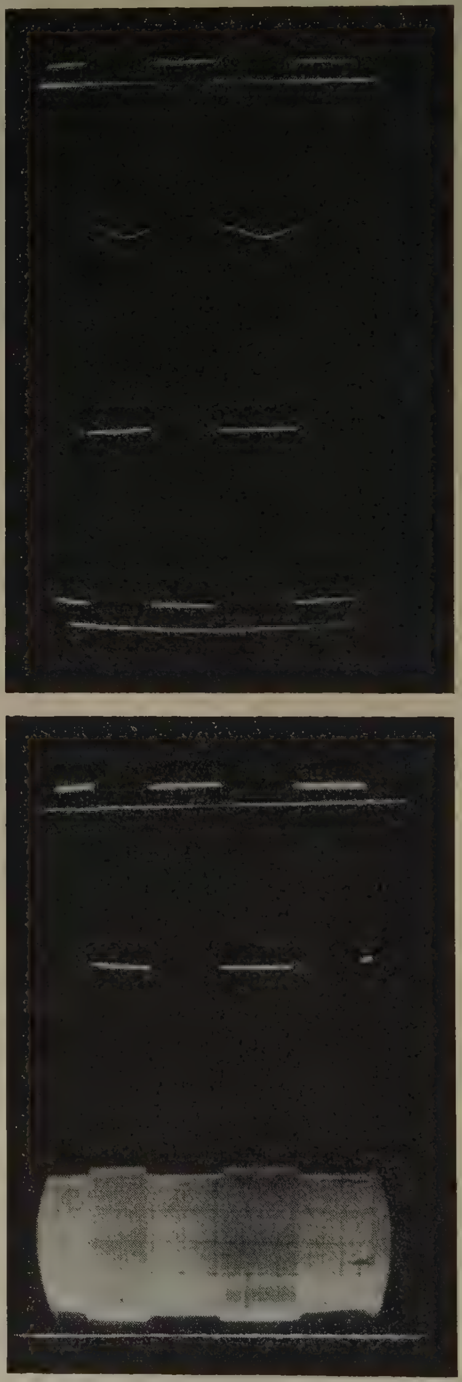

Fig. 5—(Top) Grid and anode potential traces of tacitron. Grid potential is alternated between minus 15 and minus 3 volts. (Bottom) Same traces but for standard thyratron

made to proceed arbitrarily fast, depending on how large and fast a grid bias one is willing to apply.

---

[6] The wavy character of the 15-v grid bias is caused by ripple in the grid-voltage supply.

The photograph in the lower half of Fig. 5 is included to show what happens when cutoff of anode current is attempted with the thyratron which yielded the volt-ampere characteristic in the upper half of Fig. 3. Here the grid voltage scale is the same as in the preceding case and the amount of expansion of the anode voltage scale can be judged with reference to the 28v peak of the anode-voltage fluctuations. The only effect that the application of bias has is the slight change in the fluctuation amplitude. In fact, this is all that happens even with a grid bias of 100 to 200v.

With respect to such things as heater power, peak inverse voltage, firing conditions, and life, the tube does not appear to differ in any essential way from a comparable conventional tube. Tube life, as with other thyratrons, depends upon tube currents, the applied voltages, and the frequency of operation. These parameters are paramount in determining the severity of such deteriorating agents as sputtering and gas cleanup. A typical experimental tube of the sort previously described can be expected to have a life of about 800 hours when subjected to 420 cps operation with the waveforms and also the current and voltage values associated with the top photograph in Fig. 5. The failure in this case is caused by sputtered material from the grid landing on the cathode surface.[7] Tube deterioration inevitably shows up as an increasing tube drop and a decreasing value of the peak noiseless current. Along with these symptoms there is a slow drift in the cutoff and control characteristics to lower grid bias values.

Whereas a tube of the 100 to 200 milliampere size has been described, experimental tubes of both larger and smaller sizes have also been successfully operated. For example, tubes have been constructed to handle an average current of about a quarter of an ampere. These tubes interrupt peak currents of about half an ampere in a circuit where the post-conduction anode potential was several kilovolts. The principles of operation thus appear to be applicable to tubes of a wide range of size.

THEORY

1. Noiseless Operation

Studies[2–4] of the discharge mechanism in hot-cathode gas diodes have defined four distinctly different modes in which the discharge may operate. Each of these is distinguished by the pattern of the observable glow and the interelectrode space potential. Generally, as the current in a hot-cathode gas diode is increased, the discharge will operate in one mode after the other in the idealized volt-ampere sequence illustrated in the top of Fig. 6. The basic circuit for obtaining this sequence is shown at the bottom of the same figure. This idealized sequence of modes is not usually observed in practice but, rather, has been pieced together from observations made on many tubes of different geometries, pressures, and noble gas fillings. Briefly, the different modes noted in the figure can be described as follows: (a) the "anode glow" mode, as the name implies, is visually characterized by a glow which exists only immediately adjacent to the anode surface; (b) The "ball of fire mode," as the name implies, is readily recognized by the presence of a sphere of luminosity, whose size is roughly inversely proportional to the gas pressure; (c) The "Langmuir'' mode exists when the whole interelectrode space is suffused with luminosity except for a thin region immediately in front of the cathode surface; (d) The "temperature-limited" mode exists when the glow fills the entire interelectrode space and, as implied by the name, the cathode current is temperature limited. Since the last two modes are of no interest in this paper, it may simply be noted that (a) the onset of the Langmuir mode occurs when the circuit current is roughly one-half of the free field emission of the hot cathode and (b) in both the Langmuir and temperature-limited modes the space potential close to the cathode surface is approximately equal to the tube drop.

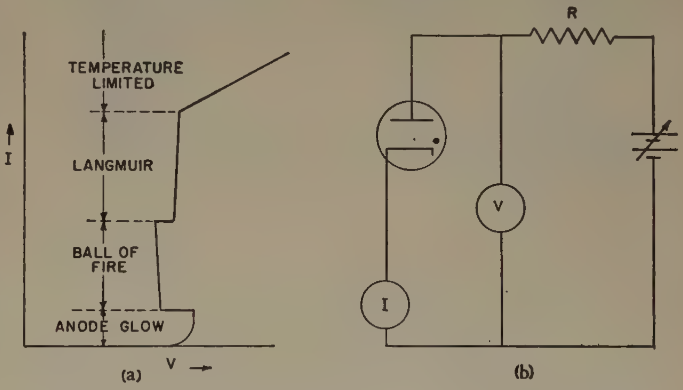

Fig. 6—(a) Volt-ampere characteristic of indirectly-heated hot-cathode-arc diode. (b) Circuit used in obtaining experimental characteristic of Fig. 6 (a).

It seems quite certain that commercial hot-cathode gas tubes normally operate in some combination of the first three modes, particularly the ball of fire and Langmuir, since the anode-glow mode is usually not found when the tube current is greater than several per cent of the rated current. This is unfortunate because the anode glow mode is the only one that can be relied upon for noiseless operation: the other modes are almost inevitably noisy and so unstable that the discharge usually jumps erratically from one to the other. Thus, the problem in getting noiseless hot cathode gas tube operation becomes one of finding how to make the tube remain in the anode glow mode up to appreciable currents. Before discussing the practical solutions to this problem it is expedient to treat the anode glow mode in somewhat more detail.

In Fig. 7 is shown the potential distribution between the cathode and anode of a tube operating in the anode-glow mode. The main volume of the interelectrode space contains a plasma, and is characterized by very small electric fields. Nearly all of the applied voltage appears across the sheath, or high-field region, which separates the plasma from the anode. Only here do electrons attain sufficient energy to ionize and excite gas atoms, the latter phenomenon producing the characteristic glow pattern from which the name of the mode was derived. It is to be noted in the figure that the anode potential V is somewhat greater than the ionization potential. The ions generated in the sheath fall back into the plasma and sustain it against diffusion losses[8] of the ions to the end micas and other insulating surfaces where surface recombination takes place. The ions are trapped between the cathode and anode by the positive potential barriers at these electrodes. However, certain portions[3] of an oxide-cathode surface do not have the potential barrier shown in the figure and so can provide a surface for recombination. As will be pointed out, this factor plays an important role in the operation of the tube, particularly at higher anode currents. Electrons from the hot cathode enter the plasma against the retarding potential indicated in the left of the figure. This potential is necessary if the current demanded by the circuit is less than the emission capability of the cathode. The cathode electrons diffuse through the plasma to the edge of the sheath where they are "pulled" toward the anode. Since the cathode electrons enter the plasma against a retarding potential they arrive in the plasma with a temperature corresponding to that of the cathode. With no significant energy sources or sinks in the plasma, the plasma electrons remain in thermal equilibrium with the cathode. Consequently, it is not unexpected that this plasma is stable and free from the oscillations that are often generated[9] when a stream of energetic electrons is fired into a plasma as is the case with both the ball of fire and Langmuir modes. A detailed analysis[3] of the anode glow mode shows that it has the electrical characteristics of a nonlinear positive resistance with no obvious tendency for instability.

---

[7] See following section.

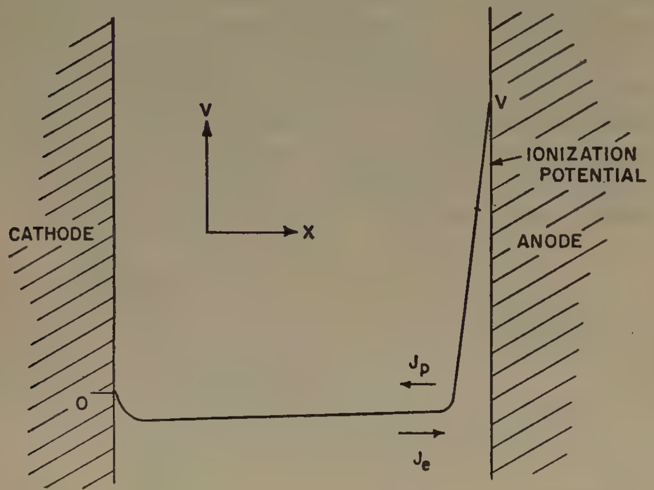

Fig. 7—Potential distribution between hot cathode and anode of diode gas discharge operating in anode glow mode.

From both analysis and experiment it appears that there are four conditions that must be satisfied if the anode-glow mode is to exist.[10] The first two of these set upper-and-lower gas pressure limits. These limits are very wide and include the usual pressures used with hot-cathode gas tubes. The third limit requires that the saturated-cathode emission current be at least twice the circuit current. This, too, is easily satisfied in practice. The fourth condition is really the crucial one. It states that the ratio of ion to electron current densities at the anode edge of the plasma must always be less than either of two quantities described by the relations[10]

$$\frac{J_p}{J_e} < \frac{\mu_p}{\mu_e} F, \tag{1}$$

$$\frac{J_p}{J_e} < S\sqrt{\frac{m}{M}}\,. \tag{2}$$

Here, J_p is the ion current density flowing out of the electron sheath at the anode, J_e is the electron-current density flowing into this sheath from the plasma, μ_p is the ion mobility in the plasma, and μ_e is the electron mobility in the plasma, F is dimensionless factor involving plasma geometry and the mean free paths of the plasma electrons, m and M are the electron and ion masses, resp., and S is a factor involving anode sheath geometry. The first relation arises from a lack of capacity of the plasma in the vicinity of the anode to carry the required electron current: the second arises because of space-charge considerations within the anode sheath. If either of these relations is violated the electron sheath will move away from the anode toward the cathode, and the discharge will shift to the ball of fire mode. In that case a plasma, which is a virtual anode, bridges the gap between the new location of the sheath and the anode surface. For infinite plane-parallel structures $F=1$, for a cylindrical case with an inner hot cathode surrounded by an anode $F<1$, and for the reverse cylindrical case $F>1$: the same can be said for the factor S. The mobilities are functions of gas pressure, but the ratio is not, having an essentially constant value for a given gas. Practically all of the electron current is carried through the tube by electrons, so that J_e is equal to the circuit current divided by the anode area. Thus, since the mobility and mass ratios are fixed, the only way to insure satisfying both relations (1) and (2)[11] is to make F and S as large as possible and the current ratio as small as possible.

To minimize the current ratio the ion current density, J_p and hence the ion losses in the tube, should be minimized. This can be realized in a "trapped" structure wherein negative electrodes, micas, and any other surfaces that can accept an ion current are eliminated. A working realization of this goal consists of the cylindrical diode shown in Fig. 8. Here, because of the anode end plates, the ion losses are cut to zero[8] except for the stray losses to the oxide cathode mentioned earlier. An experimental tube of this sort passed well over an ampere of anode glow current. With the end plates made several volts negative, to insure ion losses at these electrodes, the maximum anode glow current was only 10 μA. This approach to noiseless operation is not particularly practical because of the sensitivity to cathode quality. A slight deterioration in cathode uniformity, as inevitably occurs during life, causes a large relative increase in ion loss and so causes a significant reduction in the maximum noiseless current.

---

[8] Under the conditions of these experiments volume recombination losses are negligible.

[9] G. Wehner, "Plasma oscillator," *Jour. Appl. Physics*, vol. 21, pp. 62–63; January, 1950.

[10] These will be treated in more detail in a forthcoming paper.

[11] Since the right-hand members of these relations are roughly equal, it is not possible to say which relation is the more critical.

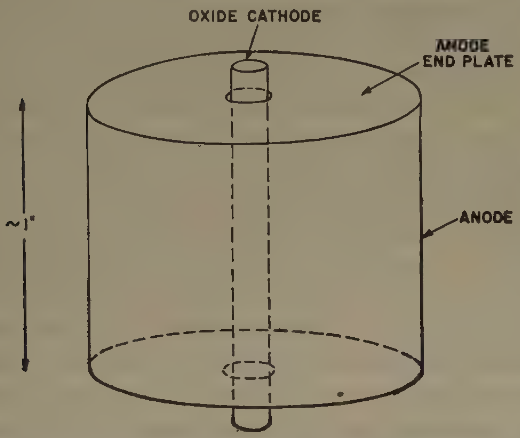

Fig. 8—Experimental gas diode with metal end plates connected to the anode to achieve effective ion trapping. This insures operation in the anode glow mode up to high current values.

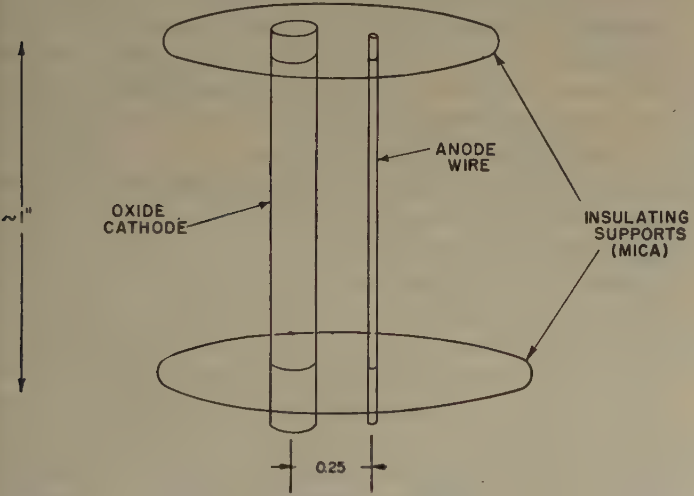

Fig. 9—Experimental gas diode with wire anode to effect anode-glow operation up to high currents.

Another approach to the construction of noiseless gas diodes is the use of a geometry which makes the factors *F* and *S* large. This is most practically accomplished by a tube of the sort shown in Fig. 9, where a wire of about 20 mils diameter replaces the usual cylindrical anode which surrounds the cathode. The use of the fine wire anode is, mathematically speaking, an approach to the case where a cylindrical cathode surrounds a coaxial-cylindrical anode. Noiseless anode-glow currents of an ampere or so are readily obtained with the structure shown in the figure. Visually, the anode glow mode in these tubes is manifested by a glow which closely hugs the anode wire.

We now come to the more important problem of achieving noiseless operation with a three-element gas tube, such as the thyratron. This is a more complicated problem than with the diode. Studies of thyratron discharges show, however, the existence of modes comparable to the anode glow and ball of fire modes in the diode. Further, the mode which compares to the anode-glow mode is noise-free and allows the grid to interrupt the tube current: the mode which can be compared to the ball of fire mode is noisy and very difficult to cut off by grid action. In the anode-glow mode analog of the thyratron, ionization and excitation take place solely in the region between the grid and anode. Visually, this is evidenced by the uniform glow which fills the grid-anode region and the absence of glow in the cathode-grid region. This glow pattern is exemplified by the sketch shown in the left of Fig. 10. In the right of the same figure is shown the ball of fire analog, wherein a ball of luminosity protrudes through a grid opening into the cathode space. Severe fluctuations of the anode potential always attend the appearance of this luminous protuberance. The presence of this phenomenon is indicated in Fig. 4 by the wavy lines.

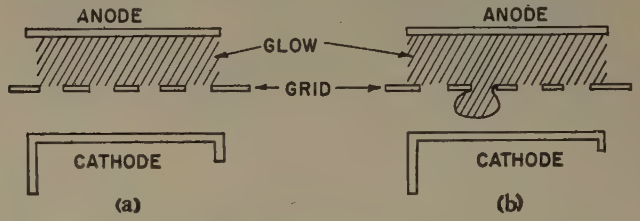

Fig. 10—(a) Gas discharge glow pattern in case of triode operating in analog to ball-of-fire mode. (b) Gas discharge glow pattern in case of triode operating in analog to ball-of-fire mode.

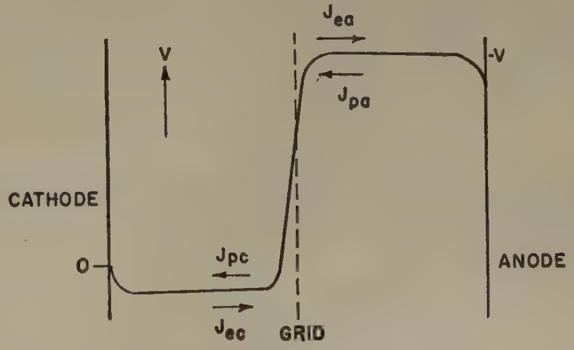

Fig. 11—Potential distribution in triode operating in analog to anode-glow mode.

The potential diagram in Fig. 11 corresponds to the anode glow, or quiet, mode which will hereafter be referred to as the "tacitron" mode to avoid confusion with the anode glow mode in diodes. There are two regions of plasma in this discharge. The one in the cathode region has a potential slightly negative with respect to that of the cathode; the one in the anode region has a potential about equal to that of the anode. The conditions in the cathode-grid plasma are identical to those in the anode glow plasma of the diode. The ions which supply this plasma are generated in the grid-anode region and fall through the double sheath[12] which exists in the plane of the grid wires.

In an ordinary thyratron, the grid generally has one or a few large apertures and the discharge will operate in the tacitron mode for currents which are only a few per cent of the rated current. If, however, the grid is made to have a large number of small holes, whose size is properly related to the gas, gas pressure, and over-all tube geometry, noise-free conduction in the tacitron mode can be obtained up to much larger currents and, in addition, the grid cutoff action at substantial values of plate current is possible.

Although the details of the discharge phenomena in the three element tubes are difficult to deal with, the over-all picture is fairly well understood and capable of treatment in terms of the diode operation. As with the diode the ratio of ion to electron current density is of cardinal importance and, as implied in Fig. 11, these densities have different values on either side of the grid. These differences arise because the grid intercepts or blocks some of the charged particles flowing from one plasma to the other. If ϕ_p is defined as the effective transparency of the grid to ions and ϕ_e as the effective transparency to electrons, then

$$J_{pc} = \phi_p J_{pa}, \tag{3}$$

and

$$J_{ea} = \phi_e J_{ec}. \tag{4}$$

Here, J_{pc} is the ion current density entering the cathode plasma, J_{ec} is the electron-current density leaving this plasma, J_{ea} is the electron-current density entering the anode plasma, and J_{pa} is the ion-current density leaving the anode plasma. On the cathode side of the grid conditions are identical with those in the diode case so that for tacitron operation it is necessary that:

$$\frac{J_{pc}}{J_{ec}} < \frac{\mu_p}{\mu_e} F_c. \tag{5}$$

On the anode side of the grid, the plasma boundary conditions are inverted and, therefore, the inverse of (5) must hold:

$$\frac{J_{pa}}{J_{ea}} > \frac{\mu_p}{\mu_e} F_a. \tag{6}$$

The quantities F_c and F_a correspond to the F in (1), being written with respect to the appropriate plasma. Both of these quantities are approximately unity and, to a first approximation, we have assumed that the mobility ratios are the same in both plasmas. Eqs. (3) and (4) combine to give

$$\frac{J_{pc}}{J_{ec}} = \phi_p \phi_e \frac{J_{pa}}{J_{ea}}. \tag{7}$$

Thus, if ϕ_p and ϕ_e are less than unity, the inequalities (5) and (6), which require that

$$\frac{J_{pc}}{J_{ec}} < \frac{J_{pa}}{J_{ea}}, \tag{8}$$

may be satisfied. In this way the grid acts as a "matching" device between the two plasmas. An exact computation of ϕ_p and ϕ_e requires an intimate knowledge of the electric field in the grid openings and has not been accomplished. There is little doubt, however, that the transparencies are less than the optical transparency, which is obviously less than unity for any physically realizable grid.

Both J_p and J_e will vary across the grid openings and will have maximum values in the center. These maximum values, which might be comparable to the current densities present in the absence of a grid, would not satisfy both (5) and (6). These densities are, however, averaged out shortly after the particles enter the plasmas. In the analysis, the critical inequalities apply to ions and electrons flowing according to the laws of diffusion and not to particles injected at high velocity into a plasma. Thus, they do not apply to the ion and electron currents flowing through the grid until the individual particles have been scattered by collisions. By the time the injected particles have lost their incident velocity, they are spread out over a larger area than the grid holes and the maximum values of J_{pc} and J_{ea} are reduced. The degree to which this averaging action takes place depends on the ratio of the grid hole dimension to the mean free paths of the injected ions and electrons. The implications are that tacitron operation will fail if the largest grid hole dimension is greater than the mean free path of the charged particles passing through these holes. Since the mean free paths are inversely related to gas pressure, an upper limit is set on the gas pressure for a given size grid aperture. This critical limit is reasonable from the standpoint that a plasma finds it easier to exist if the channel or hole through which it passes has a lateral dimension larger than the mean free path of the plasma particles. Fetz,[5] who has considered essentially the same question, attributes the onset of the ball of fire analog to an unstable condition which arises in the sheath at the grid hole. This instability is presumably due to the ion current, arising from generation in the region near the grid hole, being too large to satisfy the mass ratio condition expressed in relation (2). The theory and experiments of Fetz show an inverse relation between gas pressure and grid hole size and, furthermore, predict magnitudes which are of the same order as those computed below from a simple relation between grid hole size and mean free paths. Thus, while the failure of the tacitron mode with increasing pressure can be interpreted in various ways,[13] all of these give approximately the same answer.

---

[12] A sheath containing a counter flow of electrons and ions is often known as a double sheath.

[13] Another reason, which may be important in certain cases, stems from the high pressure restriction noted earlier.

Using the notion of equivalence between mean free paths and grid hole size, the maximum pressure p, in millimeters of mercury, that can be tolerated by a tube with a multi-holed grid is given by

$$p = \frac{G}{d} \tag{9}$$

where d is the major dimension of a grid hole, and G[14] is taken as the electron mean free path at a pressure of one millimeter of mercury. Since relation (9) is only a rough criterion there is no real reason to use either the electron or ion mean free path in preference to the other. For convenience the values of G for the various noble gases are tabulated below in Table I.

TABLE I

GAS	G	W
Helium	0.12	1.0
Neon	0.083	1.8
Argon	0.014	13.0
Krypton	0.011	—
Xenon	0.007	25.0

The general relationship[15] that exists between tube drop, gas pressure, gas, size of grid openings, and tube geometry for experimental structures is shown in Fig. 12. In order to keep the curve general for all the noble gases the ratio of tube drop V to the ionization potential V_i is used as ordinate. The tube parameter quantity pK is used for the abscissa. The quantity p is the gas pressure in millimeters of mercury and the K is given by the semi-empirical relation

$$K = W\sqrt{a}\,b\,\phi, \tag{10}$$

where W is a gas constant whose empirically determined value is given in Table I, a is the average grid-anode distance in centimeters, b is the average cathode-grid distance in centimeters, and ϕ is the effective or empirical, mesh transparency whose values for different commonly used meshes are tabulated below in Table II.

TABLE II

Mesh Size (holes per inch)	Wire Size (mils)	Transparency	
		Optical	Effective (ϕ)
16×16	12.0	0.66	0.66
24×24	8.5	0.635	0.52
40×40	6.5	0.55	0.25
50×50	7.0	0.44	0.10

Relation (10) is based on the analysis given in the appendix and has been found to predict the voltage ratio to within about 25 per cent for the noble gases listed in Table I over the following range of geometric variables: a between 0.1 and 3 centimeters; b, between 0.1 and 1.5 centimeters; ϕ, over the range noted in Table II. The type of structure used in compiling these results is shown in Fig. 13, page 1358. No unusual precautions were taken in the construction of these tubes other than making sure that the top and bottom mica supports fitted tightly against the ends of the grid mesh cylinders.

The onset of noise at the low pressure end of the curve, where operation is in the transition range between gas and vacuum tube operation, probably originates from the low pressure restriction on the anode-glow mode mentioned earlier. This end of the curve is of little technical interest because the high tube drop causes such a severe combination of sputtering, gas cleanup, and cathode bombardment that tube life is short. Operation close to the $V/V_i = 2$ point where $pK = .02$, is advantageous for plasmatron operation.[16]

The onset of noise at the high pressure end of the curve is more reliably predicted by (9) than by the value of pK indicated on the abscissa.

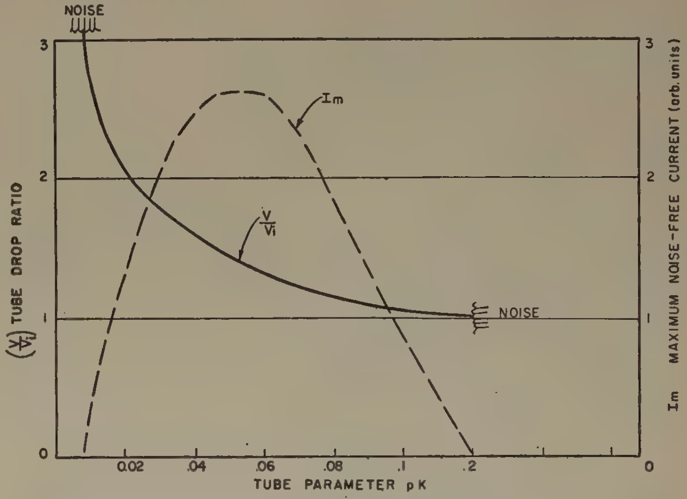

Fig. 12—Variation of tube drop and maximum noise free current with tube parameters and gas pressure.

The dotted curve in Fig. 12 is a rough indication of the behavior of the maximum noiseless current as a function of the variable pK. This current is necessarily low near the high pressure end of the curve, because here the ratio of ion to electron current density is very close[13] to the critical value given by either relation (1) or (2). Thus a small increase in anode current increases the ion losses at the cathode sufficiently for the critical value to be reached. As the value of pK is reduced the value of this current ratio is decreased. Hence larger anode currents can be tolerated before increased ion losses, due to the cathode shortcomings noted earlier, cause the critical ratio to be reached. The maximum current should start to decrease at a low value of pK because of the low pressure restriction mentioned earlier and, also, because of the additional ion losses at the cathode caused by the excessive ion mean free paths at low pressures. Here, ions falling through the drop at the grid make so few collisions with neutral atoms in the grid-cathode region that these ions retain, on the average, sufficient energy to overcome the small potential barrier at the cathode.

---

[14] Landolt-Bornstein, "Zahlenwerte und Funktionen aus Physik und Chemie," J. Springer, Berlin, 1950.

[15] For the case of zero grid bias.

[16] E. O. Johnson and W. M. Webster, "The Plasmatron, a continuously controllable gas-discharge developmental tube," Proc I.R.E., vol. 40, pp. 645–659; June, 1952.

In the design of a tube for either noiseless rectification or grid-cutoff operation the best compromise between low tube drop, maximum noiseless current, and reserve pressure occurs at a value of pK of about 0.07.

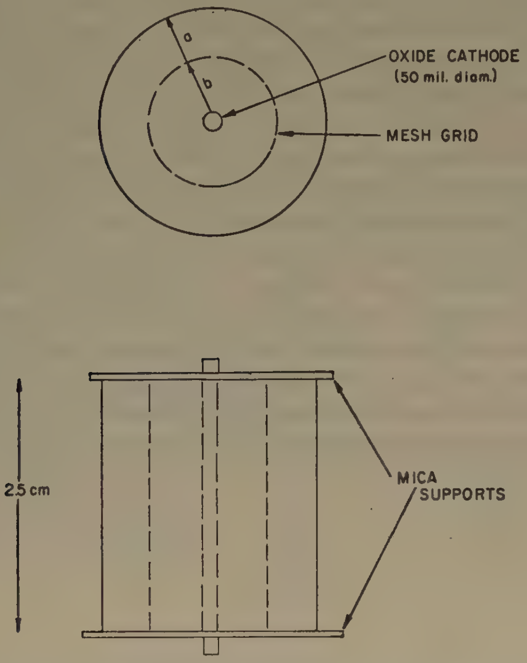

Fig. 13—Experimental structure used in arriving at results of Fig. 12.

Whereas the curve in Fig. 12 is empirically based on the cylindrical geometry shown in Fig. 13, it can be used as an effective guide for the design of structures of other geometries. For example, the tube shown in Fig. 1 has the following parameter values: $\phi = 0.3$, $a = 0.5$ cm, and $b = 0.5$ cm. Since the gas is xenon at a pressure of about 0.05 millimeter of mercury, the value of pK is 0.133 and the curve in Fig. 13 predicts a voltage ratio of about unity, a value that compares well with the actual observed value of approximately unity. In general, anything done to a tube structure to increase ion loss, or make ion generation more difficult, will inevitably tend to increase the tube-voltage drop.

As for mechanical construction, tubes with the noiseless feature are no more difficult to fabricate than other gas tubes. Care has to be taken, however, to insure that there are no holes or spaces along the edges of the mesh grid that have a major dimension larger than the mesh holes. If such openings are present, the discharge will inevitably choose these for exit and become noisy, as well as extremely difficult to interrupt by grid action.

The effect of tube deterioration on the voltage drop and the maximum noiseless current, noted above, is largely tied up with cathode behavior. Either sputter deposit on this electrode or damage by ion bombardment will act to increase the ion losses of the plasma in the cathode-grid region. This results in an increase in tube drop since there has to be a compensating increase in the rate of ion generation. Along with this, the maximum noiseless current will decrease because the ratio of ion to electron current density in relations (1) and (2) will more closely approach the critical value. Gas clean-up simply moves the operation of the tube to the left along the curve in Fig. 13 and results in an increase in tube drop. However, as can be seen from the dotted curve, it will not normally decrease the noiseless current.

2. *Cut-off Operation*

Cut-off action results from the closure of the grid holes by a space-charge sheath which is opaque to electrons attempting to move from the cathode to the anode region. The thickness of this sheath can be derived from the relation

$$j_p = 3.43 \times 10^{-7} \frac{V_g^{3/2}}{r_g B^2 M^{1/2}} \tag{11}$$

which is the familiar 3/2 power law[17] for cylindrical geometry. Here j_p is the ion current density in amperes per squre centimeter to a grid wire of radius r_g centimeters, V_g is the potential in volts across the sheath, B is a function[17] whose value depends upon the ratio of the sheath radius r_s to the grid wire radius r_g, and M is the ion mass (oxygen 16). The solution of this equation is facilitated by nomograph technique.[18] and by this means the empirical equation

$$Z = \frac{r_s}{r_g} = 1 + \frac{1}{10}\left[\frac{V_g^{3/2}}{r_g j_p}\right]^{1/2} \tag{12}$$

was derived.

The transparency ϕ_e of the mesh grid to electrons from the cathode plasma can be approximately represented in terms of geometrical considerations by the relation[19]

$$\phi_e = (1 - Znd)^2 \tag{13}$$

where d is the mesh wire diameter in inches, and n is the number of mesh openings per linear inch of a mesh with square holes.

Before (12) can be substituted into (13), to get an explicit relation for ϕ_e in terms of grid geometry and the grid bias V_g,[20] the quantity j_p has to be replaced by a more convenient parameter. It will become obvious later that j_p is a feedback term, since an increase in V_g sets up a reaction whereby j_p also increases. The ultimate behavior of ϕ_e hence depends upon the nature of this feedback process as well as upon V_g.

---

[17] I. Langmuir and K. B. Blodgett, "Currents limited by space charge between coaxial cylinders," *Phys. Rev.*, vol. 22, pp. 347–356; October, 1923.

[18] L. Malter and W. M. Webster, "Rapid determination of gas discharge constants from probe data," *RCA Review*, vol. XII, pp. 191–210; June, 1951.

[19] The transparency ϕ_e, as here defined, has a somewhat different meaning than ϕ_e as used in relation (4).

[20] Aside from a possible discrepancy of several volts due to contact potentials and several other second order effects, the voltage across the sheath can be taken as being equal to the grid bias. It is to to be noted that both V_g and j_p must be related to the cathode plasma, since the sheath conditions on the cathode side of the grid are the only ones directly operative in blocking electron flow from the cathode plasma.

Using (23) of the Appendix, along with the usual kinetic theory value for the ratio of ion and electron current densities (at the grid edge of the cathode plasma) it is found that

$$j_p = \frac{1}{A\sqrt{M/m}\sqrt{T_e/T_p}} \frac{I}{\phi_e},$$

or

$$j_p = Y\frac{I}{\phi_e}, \tag{13a}$$

where the quantity Y is introduced for convenience. Here, A is the grid mesh area facing the cathode plasma, I is the anode current in milliamperes, M/m is the ratio of ion to electron mass, and T_e/T_p is the ratio of electron to ion temperature in the cathode plasma. For the tubes considered in this paper $A \cong 1$ square centimeter, $\sqrt{M/m} = 490$ (xenon), $\sqrt{T_e/T_p} \cong 1.7$ and, therefore $Y \cong 10^{-3}$. Now, if the above value for j_p is introduced into (12) one obtains:

$$Z = 1 + \frac{1}{10}\left[\frac{V_g^{3/2}}{r_g YI}\,\phi_e\right]^{1/2}$$

or

$$Z = 1 + \frac{1}{10}\,[U\phi_e]^{1/2}. \tag{14}$$

The quantity U, which equals $[V_g^{3/2}/r_g YI]$, is introduced for convenience. By substituting (14) into (13) there is finally obtained

$$\phi_e = \frac{(1 - nd)^2}{\left(1 + \frac{nd}{10}\sqrt{U}\right)^2}. \tag{15}$$

This expression makes it clear that the mesh transparency decreases monotonically as the U increases. Thus, if the grid bias V_g is increased and I is either held constant or allowed to decrease, the mesh transparency must always decrease. The numerator of the equation will be recognized as the expression for the optical transparency of the mesh.

A plot of (15) for a tube of the form illustrated in Figs. 1 and 16 is shown in Fig. 14. The values used in the equation are as follows: $n = 50$ openings per inch, $d = 0.007$ inch, $r_g = 0.0035$ inch. The variables V_g and I are taken from Fig. 16. The plot of (15) is arbitrarily normalized so that at $v_g = 0$, ϕ_e is equal to the optical transparency, $(1 - nd)^2 = 0.44$. This is only an approximation to the true state of affairs since there can be a volt, or so, discrepancy between the actual voltage across the grid sheaths and the grid bias voltage V_g.[20] The lower curve in Fig. 14 is a plot of (13a). This plot is also normalized to the optical transparency at $V_g = 0$. The values of the variables I and j_p in this equation are taken from Fig. 16, the latter variable being simulated by its functional equivalent, the positive ion current I_p to the probe in the cathode region. The absolute values of ϕ_e, computed from (13a) with $Y = 10^{-3}$ as noted earlier, are equal to the normalized values if the ion currents I_p to the cathode probe are assumed to be about five times larger than the actual values of j_p. This deviation is not at all unreasonable since the plasma density, and hence the ion current to a probe, increases rapidly as one approaches[3] the cathode. Eq. (13a), which gives a fair approximation to the actual electron transparency of the grid mesh when used with the data as indicated, is seen from Fig. 14 to be of the same general form as the theoretical expression. This agreement is to be taken as nothing more than a rough check on the validity of the physical model of the cutoff process. It is about as close a check as can be hoped for in view of the difficulty in precisely computing or even measuring plasma and sheath conditions in the vicinity of the grid wires.

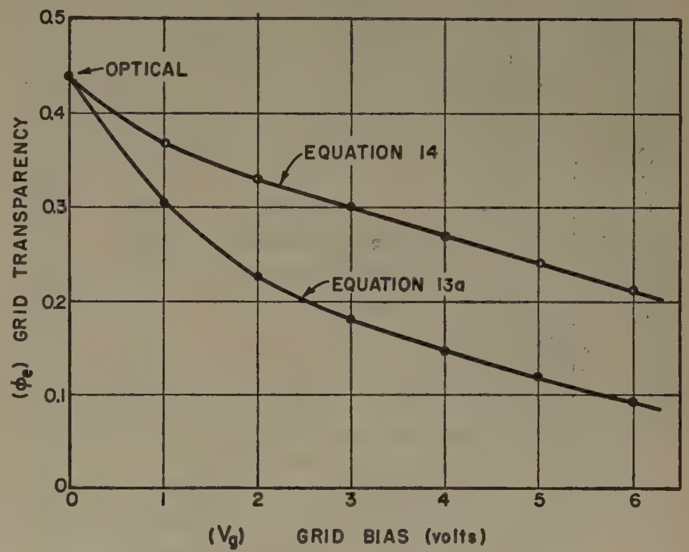

Fig. 14—Comparison between grid mesh transparency to electrons as determined from relations (12a) and (14).

If the electron transparency ϕ_e decreases the tube drop V must go up according to the relation[21]

$$\frac{V}{V_i} = 1 + \frac{1}{\left[(\alpha V_i)(f\lambda(1 - e^{-d/\lambda}))\left(\frac{AC_T}{4v\psi}\right)(\phi_p\phi_e)\right]p} \tag{16}$$

where all the terms other than ϕ_e remain roughly constant. As will be shown, the grid transparency to ions ϕ_p undergoes little change because, compared to the tenth-volt mean electron energy of the electrons in the cathode plasma, the ions falling out of the anode plasma each have about V volts of energy, and hence can pass through most of sheath even when the grid bias potential is somewhat greater than V. As the tube drop increases, the tube current decreases in the circuit of Fig. 2 according to the relation

$$I = \frac{V_b - V}{R}, \tag{17}$$

---

[21] Appendix, eq. (4).

where, as noted in figure, (see page 1351), V_b is the supply potential and R is the circuit resistance.

When V reaches some value, say about one-half of V_c, the discharge in the tube becomes unstable and the anode current suddenly falls to zero no matter how slowly the bias had been applied. In particular, this instability is found to arise when[5],[22]

$$\frac{dV}{dI} = -R. \tag{18}$$

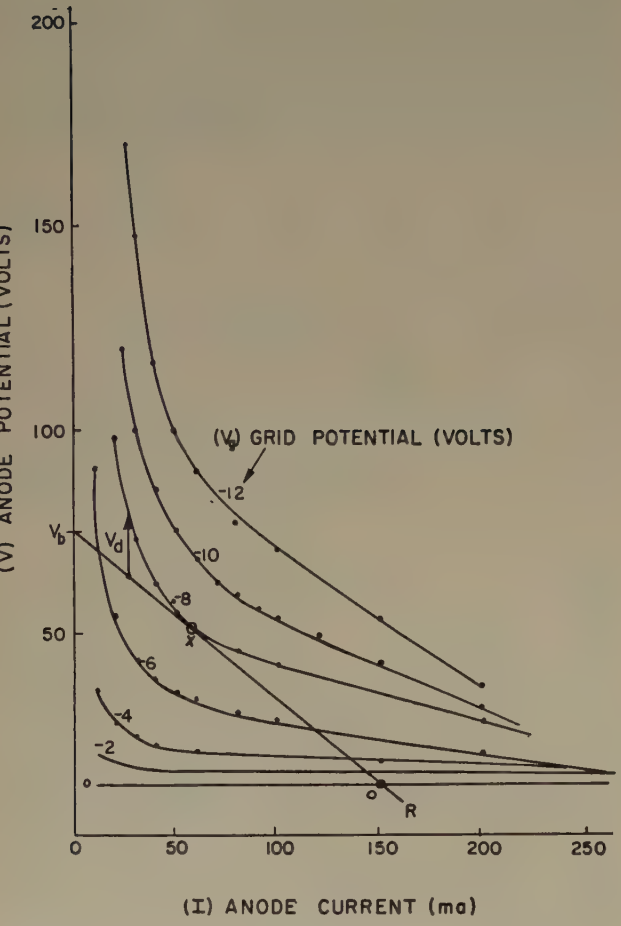

Fig. 15—Volt-ampere characteristics of an experimental tacitron for various grid potentials.

This behavior can be traced out in Fig. 15, wherein the volt-ampere characteristics are plotted for different grid bias potentials. The straight line connecting the supply potential V_b and the zero bias operating point o corresponds to the load resistance R. As the grid bias is increased the tube has current and voltage drop values which mark the intersections between the load line R and the appropriate tube curve for the grid bias potential in question. At the point x, where the grid bias potential is -8 v. and the load line is tangent to the tube curve, (18) applies and the current I suddenly and spontaneously falls to zero. The process proceeds regeneratively to the left of point x because a decreasing current causes an increase in the tube's voltage deficit (V_d in the figure) which, in turn, causes a decrease in ion generation that leads to increased sheath size, hence further current reduction, and so forth.

The negative resistance of the tube, obvious from Fig. 15, has its origin in relations (15) and (16). In these, a decreasing tube current results in a decreasing mesh transparency and, so, a higher tube drop. The process is stable as long as the circuit resistance exceeds the negative resistance of the tube. The tube curve corresponding to zero grid bias is seen to have no indication of negative resistance. This is as it should be, because if V_g is zero, the sheath parameter U is zero regardless of current, and so the tube drop cannot change with current. On the other hand, a large value of grid bias allows a large variation in U so that the tube drop can change rapidly with I.

If the cutoff criterion (18) is used in conjunction with the set of curves in Fig. 15, the cutoff characteristics displayed in Fig. 4 can be reconstructed fairly closely.

Utilization of the continuous control action of the grid, a possibility obvious from Fig. 15, is not recommended for practical operation because of the increased sputtering damage that accompanies prolonged operation at elevated anode potentials. To minimize this damage it is desirable to apply cutoff bias as rapidly as possible.

It is instructive to consider the curves shown in Fig. 16. The anode current I, the tube drop V, the positive ion current to a negative probe in the cathode region, and the positive ion current to a negative probe in the anode region are plotted as a function of grid potential. The positive ion current to these probes, in accordance with usual probe theory, is a measure of the ion density in the region surrounding the probes. Now, if the grid bias is increased, the grid becomes more opaque to electrons by virtue of (15), and the anode voltage must rise according to (16). Under the conditions presented in the figure the ion generation goes up more rapidly with tube drop than it goes down with tube current, so that the ion current measured by the probe in the anode region is seen to rise. The ion current to the probe in the cathode region is seen to rise in almost the same proportion. This indicates, as previously mentioned, that the transparency of the grid to the ions from the anode region changes very little with grid bias.

By combining (17) with the ion generation equation[23] it is easily shown that the maximum in ion generation occurs when

$$V = V_m = \frac{V_b + V_i}{2}. \tag{19}$$

The generation increases with V when V is less than V_m: it decreases when V exceeds V_m. Experiment has verified this behavior. In fact, it can be checked in Fig. 16 where the probe current, and hence ion generation, is seen to be approaching a maximum when $V=57$v. Since $V_b=110$v. and $V_i=10$v, $V_m=60$v, a value in agreement with the observed value.

---

[22] J. D. Cobine, "Gaseous Conductors," McGraw-Hill Book Co., Inc., New York, N. Y., pp. 207–209; 1941.

[23] Appendix.

The tendency for a tacitron to become noisy at high grid bias, as indicated by the wavy lines in Fig. 4, can be understood from a consideration of Fig. 16. From this latter figure it is apparent that the ion current flowing from the grid-anode plasma into the cathode-grid plasma must increase with grid bias since the ion density, as measured by the cathode probe, is increasing. The anode-electron current I, however, is seen to be decreasing. Under these conditions the current ratio J_p/J_e in relation (1) and (2) must increase and tend to reach the critical value for the onset of noise. From (3)[23] which specifies the rate of ion flow through the grid wires into the cathode plasma, there is obtained

$$\frac{I_p}{I} = f\phi_p\alpha p(V - V_i)\lambda(1 - e^{-d/\lambda}). \tag{20}$$

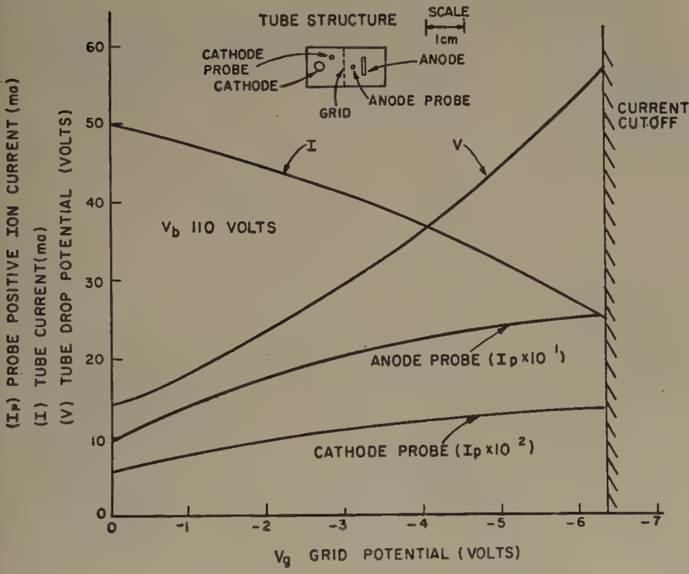

Fig. 16—Anode potential and current, and probe currents in experimental tacitron as functions of grid bias.

First of all, the appropriate parameter values[24] inserted into the right hand member of this equation show that it has a value of about 4.7×10^{-3} which is the same order of magnitude as the approximate value, $\sqrt{m/M}=2\times10^{-3}$, for the critical current ratio in xenon. Secondly, since all the factors on the right except $(V-V_i)$ remain constant for a particular tube, the onset of noise should ensue at a given value of $(V-V_i)$. This can be shown to be approximately true by making the appropriate graphical construction in Fig. 14 with the noise onset parameter values shown in Fig. 4. In making this graphical construction the curves in Fig. 15 have to be extrapolated and the current and voltage scales extended. The practical consequences of the onset of noise at a given value of $(V-V_i)$ dictate that the alterable factors in the right member of (20) should be decreased if practical operation is to be achieved at high values of V_b. The alterable factors are the mesh transparency to ions ϕ_p, the gas pressure p, and the grid anode distance d. The electron mean free path λ cancels out if it is large compared to d. Experience with tacitrons of various designs bears out the above conclusions.

We now come to the question why practical current cutoff is not observed in conventional thyratrons when operated at appreciable values of anode current. In short, this question can be answered by the statement that such tubes do not operate in the tacitron mode. Compared to the other possible discharge modes for a three-element hot-cathode gas tube, the tacitron mode possesses three important advantages with respect to current cutoff. These are: (a) the ion generation mechanism is such that the feedback action on the sheath expansion process seems to be a minimum, (b) the sheath expansion takes place in a plasma which is characterized by low particle density and low electron energies, and (c) the tube current and plasma density are distributed evenly over an interelectrode path of relatively large cross-section area.

With respect to the first feature, we always observe in a tacitron that practical cutoff ceases almost simultaneously with the onset of noise and the abrupt appearance of the luminous protuberance shown in Fig. 10. Observation of conventional thyratron operation has shown the existence of an analogous situation. As the grid bias is increased in an attempt to cut off the tube current, this protuberance is seen to increase both in brilliance and size. Accompanying probe measurements show that the ion density in the tube increases so rapidly that the factor $V^{3/2}/j_p$ in (11) stays constant, or even decreases. This implies that the mesh transparency is staying constant, or even decreasing. Apparently, then, the application of grid bias causes such an increase in ion generation, amounting to a strong negative feedback on the sheath expansion process, that cutoff is impossible with any reasonable bias. This fact could well explain the very large biases of hundreds of volts[5] required to cut off such discharges.

The second feature has to do with the fact that the cathode plasma of the tacitron is populated with free electrons having a mean energy of about a tenth volt. This is a consequence of their being in thermal equilibrium with the hot cathode. It is hard to conceive of any discharge mode where the mean electron energy, and hence case of repulsion from the grid sheath,[5] could be any less than this. On the other hand, in any plasma where ion generation is taking place there must be electrons present with energies of the order of ten volts. Accompanying this consideration of electron energy is the one involving plasma density. The density in the cathode plasma of the tacitron, and consequently the j_p term in (12), must be comparatively small because ion generation is taking place elsewhere in the tube. The probe measurements presented in Fig. 16 illustrate this point by showing how much greater the positive ion currents in the anode plasma are compared to those in the cathode plasma.

---

[24] Here $f\cong\frac{1}{6}$ from geometrical considerations, $\phi_p\cong.44$ for a 50×50 mesh, $\alpha\cong1.0$ for xenon, $p\cong.05$ mm, $(V-V_i)\cong10$ for a typical case, $\lambda\cong.25$ cm, and $d\cong.5$ cm.

When the tube current is distributed over a large cross-section area then the plasma density, hence j_p, can be relatively low at each grid hole. This obviously makes for ease of sheath closure compared to the luminous protuberance case where all of the tube current passes through one, or at best, a few grid holes. Aside from the triode mode equivalent of the Langmuir mode in the diode, which is impractical from the standpoint of the second feature mentioned above, the tacitron mode is the only one which allows this desirable spreading of the current path.

The grid input impedance of the tube can be roughly approximated by a two-branch circuit containing two resistances and one capacitor. It is not practical to generalize the values of these elements because they are a complicated function of time, tube design, and operating conditions. Accordingly, the values for one specific case are presented here to give an idea of what might be expected. Here, the tube is as shown in Fig. 1, $V_b = 200$ v, $R = 1{,}900$ ohms, and $I = 100\ \mu A$. In this case, the first branch is composed of a 620 ohm resistor R_1: the second branch is composed of an 1,800 ohm resistor R_2 in series with a 3,300 micromicrofarad capacitor C. Now, if the grid bias is applied slowly, the positive ion current from the anode plasma accounts for R_1. If the bias is applied suddenly, the sheath capacitance coupling the grid to the anode plasma gives rise to the capacitance C. The load resistance R, which connects the anode back to ground, and hence the anode plasma, is mainly responsible for R_2. To a first approximation the role played by the cathode plasma can be neglected, because it has a far smaller density than the anode plasma. This lower density obviously means that there is little effect on R_1. It also means, because of thicker sheaths between it and the grid, that the contribution to C must be small. As can be deduced from the grid current curves in Fig. 4, the resistance R_1 varies inversely as the tube current. To a first order, C is unaffected by tube current.

APPENDIX

In deriving an expression for tube-voltage drop as a function of the gas and geometrical parameters the approach in this simple analysis will be to equate ion generation to ion loss. The ion loss current I_{pl} from the cathode plasma can be expressed in terms of the mean ion lifetime τ due to ambipolar diffusion, and the total number of ions present, by the relation

$$I_{pl} = \frac{e\int_v ndv}{\tau} = \frac{en_g v\psi}{\tau} = \frac{4I}{CA\phi_e}\,\frac{v\psi}{\tau} \qquad (21)$$

where e is the electronic charge, n is plasma density, v is the total plasma volume, n_g is the average plasma density at the grid edge of the cathode plasma, I is the anode electron current, c is the mean thermal velocity of the plasma electrons, A is the total grid area facing the cathode plasma, and ϕ_e is the effective transparency of the grid to electrons from the cathode plasma. It is found convenient to introduce the plasma density distribution factor ψ, which is a dimensionless number defined by the relation

$$\psi = \frac{1}{n_g v}\int_v ndv. \qquad (22)$$

The factors A, ϕ_e, n_g, and c are introduced by means of the usual kinetic theory notion of space current by the relation

$$A\phi_e\left(\frac{n_g ec}{4}\right) = I, \qquad (23)$$

where the term in the parenthesis is the electron space current density j_e at the grid edge of the cathode plasma.

The ion loss current I_{pl} is balanced by an equal ion current I_{pg} that flows through the grid holes from the anode plasma, the site of all ion generation in the tube. The latter current can be expressed, in terms of differential ionization by the relation

$$\begin{aligned} I_{pg} &= f\phi_p I\alpha p(V - V_i)\int_0^d \epsilon^{-x/\lambda}dx \\ &= f\phi_p I\alpha p(V - V_i)\lambda(1 - \epsilon^{-d/\lambda}) \qquad (24)\end{aligned}$$

where f is the fraction of ions generated in the anode plasma that get to the grid edge of this plasma, ϕ_p is the fraction of these ions that are not lost to the grid wires and which find their way into the cathode plasma, α is the pressure normalized differential ionization coefficient, p is the gas pressure, V is the potential between the cathode and anode plasmas (which is closely equal to the tube drop) V_i is the gas ionization potential, ϵ is the base of natural logarithms, x is the distance from the grid plane to the differential distance dx, d is the effective grid-anode distance, and λ is the electron mean free path for the voltage V and the pressure p.

If relation (21) is equated to (23) one obtains:

$$\frac{V}{V_i} = 1 + \frac{1}{\left[(\alpha V_i)(f\lambda(1 - \epsilon^{-d/\lambda}))\left(\frac{AC\tau}{4v\psi}\right)(\phi_p\phi_e)\right]p}, \qquad (25)$$

which gives a curve of the form shown in Fig. 12. The factors within the brackets can be compared to the factors which compose the parameter K of (10). Thus, to a fair approximation, (αV_i) corresponds to W, $(f\lambda(1-\epsilon^{-d/\lambda})$ to $\sqrt{a}$, $(AC\tau/4v\lambda)$ to r, and $(\phi_p\phi_e)$ to ϕ. The product of the factors within the brackets is independent of pressure to the first order. The quantities f and λ depend upon the tube drop V: the quantities τ, ψ, and ϕ_e depend upon the tube current I. It should also be noted that when V exceeds about twice V_i the ionization increases less rapidly than predicted by the factor $(V - V_i)$.

IRE Standards on Receivers: Methods of Measurement of Interference Output of Television Receivers in the Range of 300 to 10,000 KC, 1954[*]

COMMITTEE PERSONNEL

Standards Committee, 1954–1955

E. WEBER, *Chairman*

M. W. BALDWIN, JR., *Vice-Chairman*
L. G. CUMMING, *Vice-Chairman*
R. F. SHEA, *Vice-Chairman*

K. E. Anspach
J. Avins
B. B. Bauer
W. R. Bennett
J. G. Brainerd
H. Burkhard
P. S. Carter
P. S. Christaldi
A. G. Clavier
W. J. Dodds
J. E. Eiselein
A. W. Friend
V. M. Graham
R. A. Hackbusch
P. J. Herbst
A. G. Jensen
J. G. Kreer
E. A. Laport
A. A. Macdonald
Warren P. Mason
Wayne Mason
D. E. Maxwell
H. R. Mimno
C. H. Page
W. J. Poch
R. Serrell
R. E. Shelby
N. Smith
P. H. Smith
W. H. Tuller
J. E. Ward

R. F. SHEA, *Measurements Coordinator*

Radio Receivers Committee, 1952–1954

J. AVINS, *Chairman*
J. D. REID, *Vice-Chairman*

K. A. Chittick
L. E. Closson
D. E. Harnett
K. W. Jarvis
J. K. Johnson
W. R. Koch
I. J. Melman
G. Mountjoy
F. R. Norton
L. Riebman
L. M. Rodgers
S. W. Seeley
W. O. Swinyard
R. F. Shea
F. B. Uphoff
R. S. Yoder

Subcommittee on Spurious Radiation, 1952–1954

R. F. SHEA, *Chairman*

A. Augustine
E. W. Chapin
K. A. Chittick
H. E. Dinger
R. J. Farber
A. B. Glenn
W. R. Koch
R. A. Maher
T. S. Loeser
F. L. Pample
L. M. Rodgers
E. H. Schrot
H. Schwarz
S. W. Seeley
C. G. Seright
W. B. Smith
J. W. Stratman
W. O. Swinyard
H. J. Tyzzer
R. S. Yoder

1. INTRODUCTION

Modern broadcast television receivers are frequently sources of interference to other services. This standard sets up methods for measuring this interference over the frequency range from 300 KC to 10 MC.

2. SOURCES AND MODES OF INTERFERENCE

2.1 The major sources of electric fields and power line interference from a television receiver are:

2.1.1 Sweep output tube elements and associated circuits.

2.1.2 High-voltage rectifier and associated circuits including picture tube.

2.1.3 Miscellaneous components such as sweep transformer, deflection yoke, etc.

2.1.4 Components of the video amplifier

---

[*] Reprints of this Standard, 54 IRE 17. S1, may be purchased while available from the Institute of Radio Engineers, 1 East 79th Street, New York 21, New York, at $0.60 per copy. A 20 per cent discount will be allowed for 100 or more copies mailed to one address.

2.1.5 Components of a color TV receiver, such as the subcarrier oscillator.

2.2 The major sources of magnetic fields in a television receiver are:

2.2.1 Deflection yoke.

2.2.2 Sweep transformer.

2.2.3 Miscellaneous sources due to connection of other components to the sweep circuits.

2.2.4 Components of a color TV receiver.

2.3 Fig. 1 illustrates a television receiver's external fields and a principal mode of coupling into the power line and antenna.

2.3.1 The magnetic field indicated in Fig. 1 is a resultant of all magnetic fields due to the sources enumerated in Section 2.2. This field may cause interference in nearby receivers employing loop antennas.

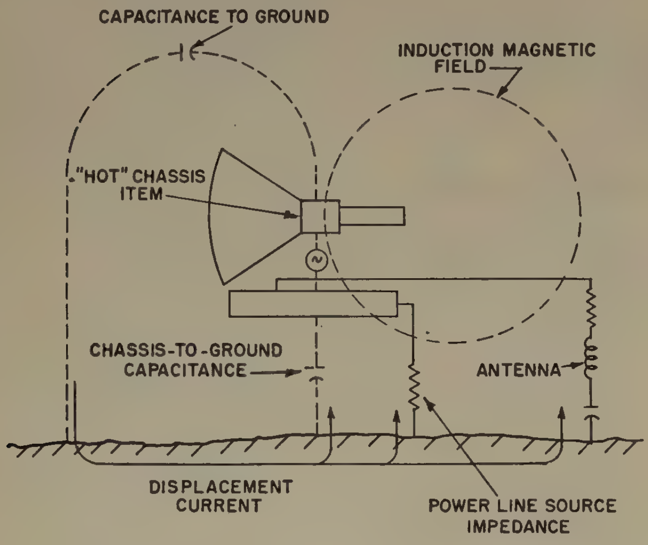
CAPACITANCE TO GROUND
INDUCTION MAGNETIC FIELD
"HOT" CHASSIS ITEM
CHASSIS-TO-GROUND CAPACITANCE
ANTENNA
DISPLACEMENT CURRENT
POWER LINE SOURCE IMPEDANCE

Fig. 1—Chassis fields and power line coupling mode.

2.3.2 An external electric field results where there is capacitance between "hot" components and ground. The displacement currents flowing through these capacitances return through the chassis-to-ground impedance consisting of the chassis-to-ground capacitance shunted by the power line impedance and by the antenna-to-ground impedance. An external electric field may also result from potential difference between chassis and power line. For specified power line source and antenna-to-ground impedances, the voltage appearing across an impedance in series with the power line provides an acceptable measure of the above electric fields and hence of the interference coupled into the power line.

2.3.3 There is also the possibility of push-pull currents flowing in the power line as a result of coupling within the receiver.

3. Methods of Measurement

3.1 General

This standard establishes a method of measurement based on the use of a typical screen room as illustrated in Fig. 2 with measurements being made of the magnetic field (at an arbitrary distance) and of the voltage between ground and each power line conductor, using the standard power line source impedance specified below.

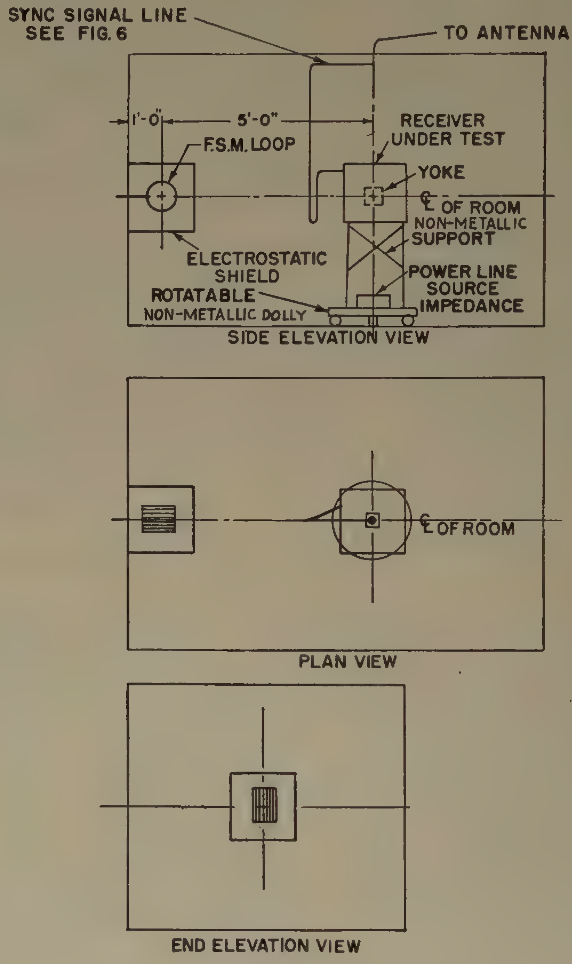
SYNC SIGNAL LINE SEE FIG. 6
TO ANTENNA
1'-0"
5'-0"
F.S.M. LOOP
RECEIVER UNDER TEST
YOKE
℄ OF ROOM
NON-METALLIC SUPPORT
ELECTROSTATIC SHIELD
POWER LINE SOURCE IMPEDANCE
ROTATABLE NON-METALLIC DOLLY
SIDE ELEVATION VIEW
℄ OF ROOM
PLAN VIEW
END ELEVATION VIEW

Fig. 2—Screen room arrangement.

3.2 Equipment Required and Setup Detail

The following equipment shall be provided:

3.2.1 A screen room of minimum inside dimensions of 7′ H×7′ W×10′ L, with adequate shielding and power line filtering to eliminate external interference.

3.2.2 A rotatable, non-metallic dolly with means for supporting the receiver under test at such height that the deflection yoke is half way between the floor and ceiling of the screen room. The dolly shall be located as shown in Fig. 2. A power outlet incorporating the standard power line impedance (specified below) shall be located at the center of the dolly and as close to the floor as possible.

3.2.3 A pickup loop for magnetic field measurement, electrostatically shielded and located as shown in Fig. 2.

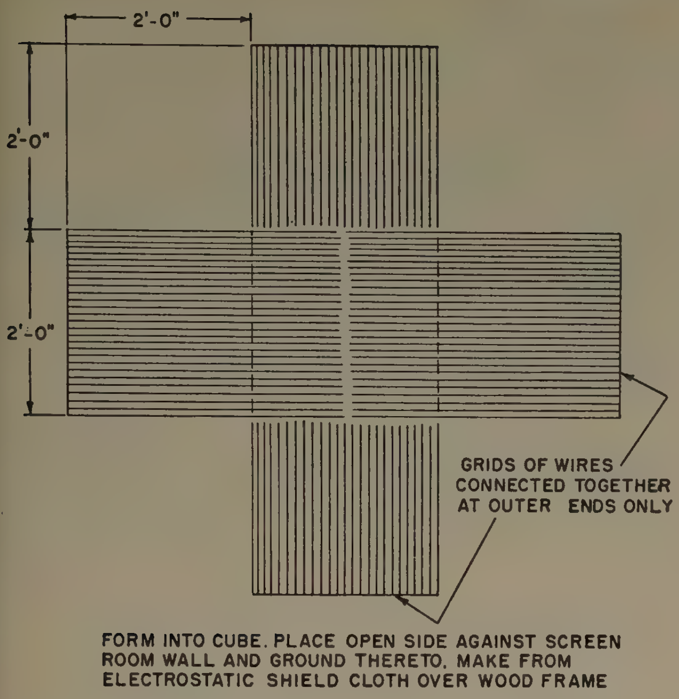
2'-0"
2'-0"
2'-0"
GRIDS OF WIRES CONNECTED TOGETHER AT OUTER ENDS ONLY
FORM INTO CUBE. PLACE OPEN SIDE AGAINST SCREEN ROOM WALL AND GROUND THERETO. MAKE FROM ELECTROSTATIC SHIELD CLOTH OVER WOOD FRAME

Fig. 3—A low capacitance loop electrostatic shield.

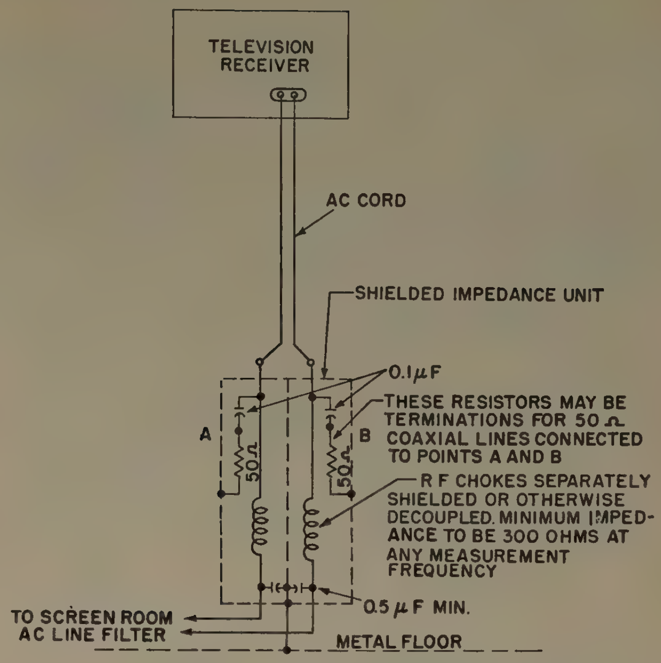
TELEVISION RECEIVER
AC CORD
SHIELDED IMPEDANCE UNIT
0.1 μF
THESE RESISTORS MAY BE TERMINATIONS FOR 50 Ω COAXIAL LINES CONNECTED TO POINTS A AND B
A
B
50 Ω
50 Ω
R F CHOKES SEPARATELY SHIELDED OR OTHERWISE DECOUPLED. MINIMUM IMPEDANCE TO BE 300 OHMS AT ANY MEASUREMENT FREQUENCY
0.5 μF MIN.
TO SCREEN ROOM AC LINE FILTER
METAL FLOOR

Fig. 4—AC line impedance unit.

A suitable electrostatic shield is shown in Fig. 3. Loop design data is given in Fig. 5.

3.2.4 A suitable field strength meter (FSM) capable of measuring both magnetic field strength and voltage with respect to ground. It shall have means for either internal or external calibration. Its nominal bandwidth shall be 10 KC or less. The FSM shall be adequately shielded and the power leads filtered to prevent spurious pick-up.

If it is practicable the receiver portion of the FSM shall be located outside the screen room, or if this cannot be done, the receiver shall be located inside the screen room so as to present a minimum effect on the field being measured without making the leads to the loop excessively long. During calibration and subsequent measurements the receiver portion of the FSM shall be maintained in this position.

3.2.5 A standard power line impedance as shown in Fig. 4 located as specified in 3.2.2. The power cord of the receiver under test shall be short and as direct as possible with any excess length bundled up as close as possible to the plug end.

The resistance values shown in Fig. 4 include the shunting effects of the input impedance of the FSM when it is connected.

3.2.6 A means of supplying a synchronizing signal, adequate to provide a substantially noise-free raster. A length of transmission line shall be connected between the antenna terminals and a pick-up loop, inductively coupled to the synchronizing signal source, which may be another loop, adequately filtered to exclude undesired broadcast signals from the screen room. The disposition of this transmission line and pick-up loop is important.

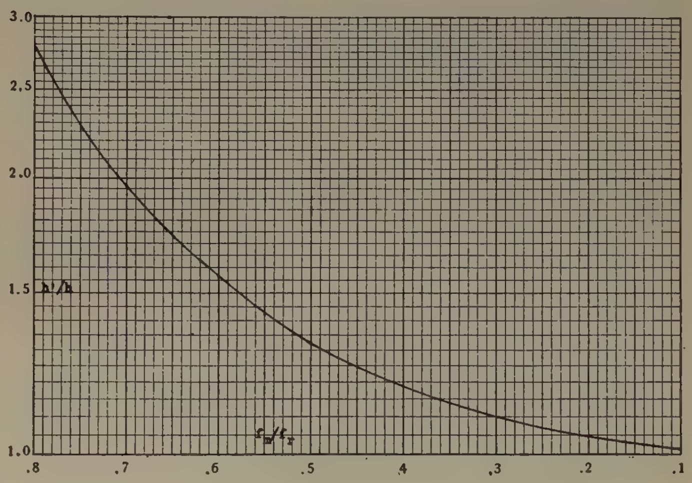

Maximum loop diameter, 12 in.
Suggested maximum axial length of winding, $\frac{2}{3}$ dia.

h = effective height of loop in meters
h' = apparent effective height
f_m = measurement frequency, megacycles
f_r = resonant frequency of untuned loop as operated into f.s.m. megacycles
C = capacity shunting loop as operated into f.s.m., $\mu\mu$fdπ.
} Shield in place
N = number of turns in loop
r = loop radius, inches
l = axial length of loop winding, inches
L = loop inductance, microhenries
h' = when loop is tuned and accurately tracked with f.s.m. $= hQ$ (Q to include loading effect of f.s.m. input circuit)
h' when loop is untuned $= hf_r^2/(f_r^2 \quad f_m^2)$ (provided f.s.m. input resistance is at least ten times loop reactance)
$h = 4.24\ N_r^2 f$ (mc.) $\times 10^{-5}$ (meters)
f_r should be at least 1.4 f_m max. for untuned operation, hence:
L max. $= 10^6/8\pi^2 f_m$ max.^{2} C microhenries

$$N = \sqrt{\frac{L(9r+10l)}{r^2}} \text{ turns (approximately)}$$

Fig. 5—F.s.m. loop design data.

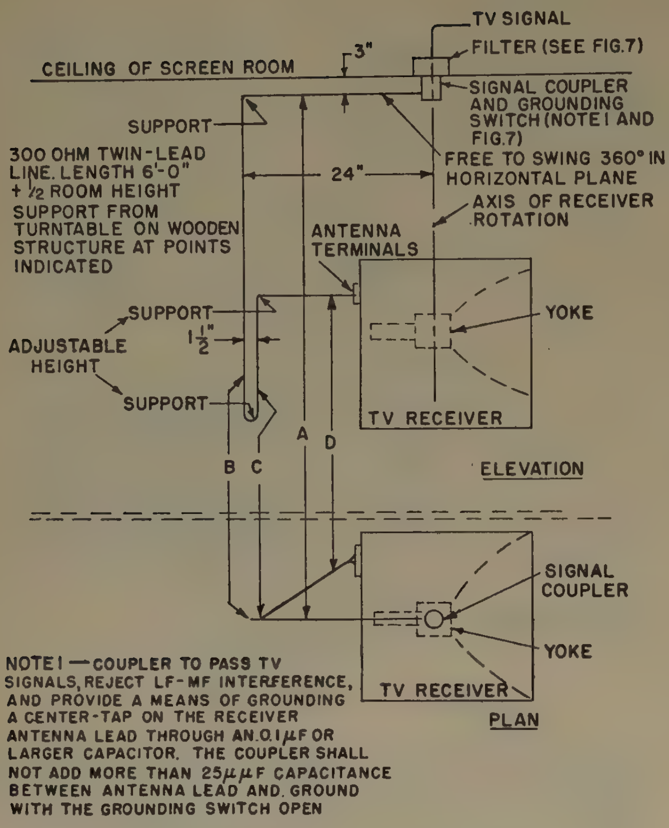
TV SIGNAL
FILTER (SEE FIG.7)
3"
CEILING OF SCREEN ROOM
SIGNAL COUPLER AND GROUNDING SWITCH (NOTE I AND FIG.7)
SUPPORT
300 OHM TWIN-LEAD LINE. LENGTH 6'-0" + ½ ROOM HEIGHT SUPPORT FROM TURNTABLE ON WOODEN STRUCTURE AT POINTS INDICATED
24"
FREE TO SWING 360° IN HORIZONTAL PLANE
AXIS OF RECEIVER ROTATION
ANTENNA TERMINALS
SUPPORT
YOKE
ADJUSTABLE HEIGHT
1½"
SUPPORT
TV RECEIVER
A
D
B
C
ELEVATION
SIGNAL COUPLER
YOKE
TV RECEIVER
PLAN
NOTE I —COUPLER TO PASS TV SIGNALS, REJECT LF-MF INTERFERENCE, AND PROVIDE A MEANS OF GROUNDING A CENTER-TAP ON THE RECEIVER ANTENNA LEAD THROUGH AN 0.1μF OR LARGER CAPACITOR. THE COUPLER SHALL NOT ADD MORE THAN 25μμF CAPACITANCE BETWEEN ANTENNA LEAD AND GROUND WITH THE GROUNDING SWITCH OPEN

Fig. 6—SYNC signal input and chassis grounding system.

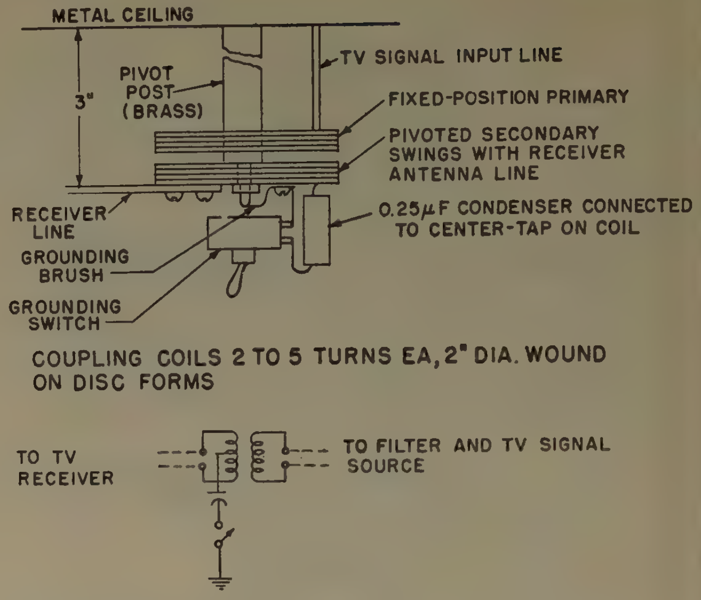
METAL CEILING
3"
PIVOT POST (BRASS)
TV SIGNAL INPUT LINE
FIXED-POSITION PRIMARY
PIVOTED SECONDARY SWINGS WITH RECEIVER ANTENNA LINE
0.25μF CONDENSER CONNECTED TO CENTER-TAP ON COIL
RECEIVER LINE
GROUNDING BRUSH
GROUNDING SWITCH
COUPLING COILS 2 TO 5 TURNS EA, 2" DIA. WOUND ON DISC FORMS
TO TV RECEIVER
TO FILTER AND TV SIGNAL SOURCE

(a) EXAMPLE OF ANTENNA COUPLER SUITABLE FOR VHF CHANNELS

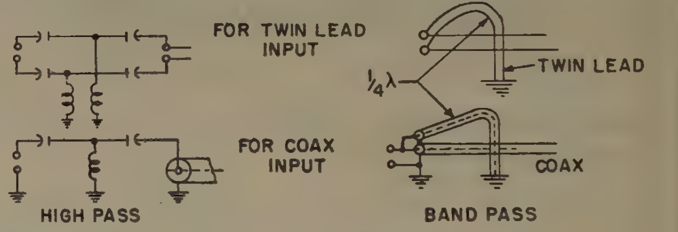
FOR TWIN LEAD INPUT
FOR COAX INPUT
HIGH PASS
¼λ
TWIN LEAD
COAX
BAND PASS

(b) FILTER CONFIGURATION EXAMPLES

Fig. 7—Antenna coupler and filters.

Figs 6. and 7 show the standard arrangement.

If the receiver has a built-in antenna it shall be disconnected from the antenna terminals during these tests.

3.2.7 The line voltage shall be maintained at 117 volts ±2 per cent unless otherwise specified.

3.2.8 All controls shall be set at their normal operating positions for the synchronizing signal specified in 3.2.6, unless otherwise specified.

3.3 Method of Measurement

3.3.1 With the antenna grounding switch in the open position and with the FSM loop oriented in the vertical plane, as shown in Fig. 2, the receiver under test shall be rotated for maximum field strength at the frequency or frequencies of interest.

3.3.2 Referring to Fig. 1 it will be seen that the left-hand displacement current loop can produce an inductive field and hence an error in the measured magnetic field. The magnitude of this error increases with frequency. An indication of this potential error is an appreciable change in the measured magnetic field with any change in the electrostatic field pattern, such as by motion of personnel within the shielded room or by electrostatic shielding of the receiver.

3.3.3 Same as 3.3.1, except with FSM loop oriented in the horizontal plane.

3.3.4 With the FSM connected between point "A" of Fig. 4 and ground measure voltage at the frequencies of interest. Repeat measurement between point "B" and ground.

3.3.5 Repeat measurement 3.3.4 with the center of the pick-up loop specified in 3.2.6 grounded to the screen room through a capacitor of 0.1 μf or larger.

3.4 Calibration of Setup

In order to convert the data obtained in the measurements described in Sections 3.3.1–3.3.5 into terms of open-field conditions at an arbitrary distance of fifteen feet, the following calibrating procedures shall be followed.

3.4.1 A standard signal generator (SSG) and a transmitting loop of not more than 10 inches diameter shall be substituted for the receiver under test, with the transmitting loop located in the position shown for the receiver yoke in Fig. 2 and aligned co-planar with the FSM loop. The SSG output is set at any value which produces a convenient indication on the FSM. The free-space value of field strength which would be produced on the transmitting loop's magnetic axis at a distance of fifteen feet with this SSG voltage applied is obtainable from data supplied in Section 4.01.03.01 of IRE "Standards on Radio Receivers: Methods of Testing Amplitude Modulation Broadcast Receivers: 1948."

The free-space field strength at a distance $x=15'$ away from a loop $10''$ in diameter is given by the equation:

$$E=0.032NI$$

where

E = equivalent electric field strength in microvolts per meter
N = number of turns
I = current in microamperes.

Note—For those frequencies where the distance, x, is comparable to the wave length, λ, a correction factor $\sqrt{1+(2\pi x)^2/\lambda^2}$ should be applied to the above expression. Thus, at $x=15$ ft (4.56 m) and $\lambda=30$ m ($f=10$ MC) the expression becomes $E=0.044\ NI$.

If the FSM reads directly in μv/m, the calculated value of free-space field strength divided by the FSM indication is the multiplying factor which must be used to convert subsequent field strength indications on receivers' fields to their free-space values.

When using a field strength indicator (FSI) calibrated in arbitrary units, the conversion factor is obtained as follows: determine the corresponding free-space field strength, as described above, for an arbitrary reading of the FSI. Substitute a standard signal generator (SSG) on the input of the FSI. Adjust the SSG output to reproduce the above arbitrary reading of the FSI. The screen room to free-space conversion factor is then the calculated free-space field strength divided by the calibrating SSG voltage. In subsequent measurements the free-space field strength is equal to this conversion factor times the calibrating voltage which reproduces the FSI indication of a receiver's field.

The foregoing calibrations must be made at each measurement frequency, or at enough frequencies to enable construction of a plot. Separate calibrations are required for horizontal and vertical loop orientations. Electrostatic shielding of the transmitting loop may be required for accurate results if its impedance is high.

A Mechanism for Water Induced Excess Reverse Dark Current on Grown Germanium *N-P* Junctions*

J. T. LAW†

Summary—**An ionic conduction process in the multilayers of water adsorbed on a germanium *n-p* junction bar is proposed to explain the increase in reverse dark current observed when the relative humidity to which the unit is exposed is increased. Experimental evidence supporting this postulate is given and discussed.**

INTRODUCTION

THE EXISTENCE of a phenomenon which produces large changes in reverse dark currents of germanium *n-p* junction units when these are exposed to water vapor has long been recognized,[1] but the mechanism of the process (or processes) involved has so far not been fully elucidated. It is the purpose of this paper to attempt such an explanation in the light of recent experimental results.

It is obvious that the excess current must be carried by either ions or electrons (or holes). A conduction process on *n-p-n* transistors exposed to water vapor has been described by Brown[2] in terms of electron conduction along an inversion layer across the *p* regions. We, however, will show that in the voltage and humidity ranges studied here on *n-p* junction units, the conduction obtained and its variation with humidity are more consistent with an ionic process. Thus both channels and ionic conduction may need to be considered in surface conduction processes in germanium devices.

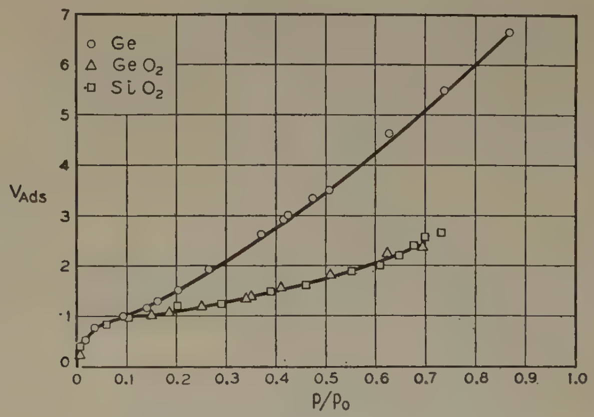

Fig. 1—Adsorption of water vapor on germanium, germanium dioxide and silica.

EXPERIMENTAL

The experimental evidence falls into three main classes:

(a) The adsorption isotherm and related thermodynamic quantities for water on germanium.

Adsorption isotherms for water on germanium and germanium dioxide have been measured volumetrically and are shown in Fig. 1, where the number of layers of water adsorbed are plotted against the relative pressure of water vapor. The germanium used was a crushed sample of high resistivity *n*-type material which had a surface area of 300 cm²/g. Oxide and adsorbed oxygen were removed from the surface by heating to 850° C in a vacuum of 10^{-6} mm. It is felt that after this treatment the surface had no more than a monolayer of oxygen left on it.

---

* Decimal classification: R282.12. Original manuscript received by the IRE, June 25, 1954.

† Bell Telephone Laboratories, Inc., Murray Hill, N. J.

[1] J. N. Shive, "Properties of the M-1740 *P-N* junction photocell," Proc. I.R.E., vol. 40, pp. 1410–1413; November, 1952.

[2] W. L. Brown, "*n*-type surface conductivity on *p*-type germanium," *Phys. Rev.*, vol. 91, p. 518; 1953.

From two or more isotherms at different temperatures it is possible to calculate heats, free energies and entropies of adsorption. It is possible to determine the mobility or immobility of the adsorbed molecules by comparing these various quantities with expected values calculated from different models.

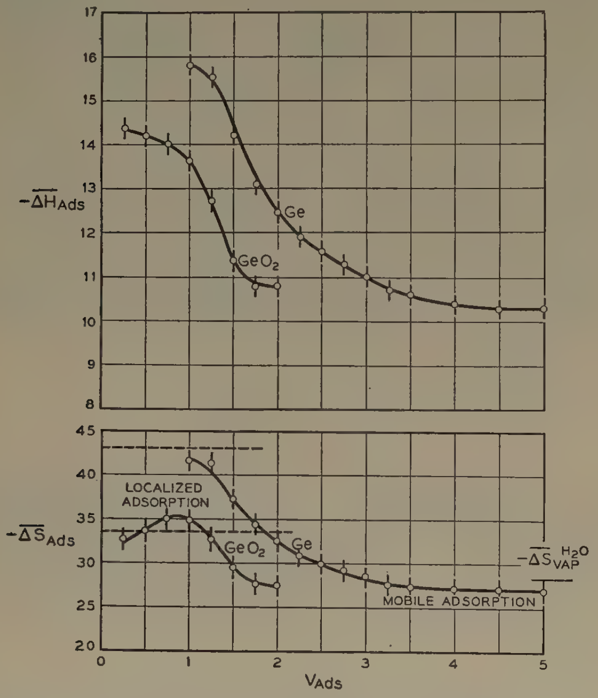

Fig. 2—Variation of heats and entropies of adsorption with amount of water adsorbed.

The differential heats of adsorption $\overline{\Delta H}$ were evaluated using the Clausius-Clapeyron equation

$$\frac{\overline{\Delta H}}{RT^2} = \left(\frac{\partial \ln p}{\partial T}\right)_V, \qquad (1)$$

where V refers to the volume of vapor adsorbed, p is the equilibrium pressure of water, R is the gas constant, and T the absolute temperature.

The difference in free energy between the three-dimensional gas standard at temperature T and the adsorbed molecules in equilibrium with p was given by

$$\Delta G = RT \ln p/p_0. \qquad (2)$$

The differential entropies were then calculated, using

$$T\overline{\Delta S} = \overline{\Delta H} - \Delta G. \qquad (3)$$

The values of $\overline{\Delta H}$ and $\overline{\Delta S}$ obtained are shown in Fig. 2 as a function of the number of layers of water adsorbed. By comparison with calculated entropy values, it can be shown that the first layer of water on germanium is fixed, while the third and succeeding layers are mobile and behave much like liquid water.

(b) The determination of the presence of appreciable numbers of foreign ions on a germanium surface.

The number of impurity ions on the germanium surface was determined by means of the solid mass spectrograph. A series of exposures were taken after a spark had passed between two germanium electrodes. The first exposure consists of lines due mainly to surface impurity atoms, while successive ones give a measure of the bulk impurities. It was found that, for an etched germanium surface, approximately 10^{14} ions/cm^2 were present. These were mainly calcium, sodium, and potassium. Because of the strong germanium lines it would be impossible to detect the anions chloride and fluoride.

(c) Reverse current measurements on germanium *n-p* junctions under various conditions.

To permit rapid measurements of reverse dark current as a function of humidity, the *n-p* junction unit was mounted on a glass stem, inserted in a tube and attached directly to a vacuum system in which the partial pressure of water could be varied from 0–1.0 by the admission of water vapor from a reservoir. By this means equilibrium current values could be obtained within a few minutes after changing the humidity conditions, rather than the several hours required when moist nitrogen is used.

Measurements were made on a number of units cut from three different grown crystals at reverse voltages between 10 and 80 volts. All samples were CP-8 etched before being measured.

Current-Humidity Variation for an Etched Surface

A typical curve showing the variation of reverse dark current with humidity is shown in Fig. 3. This is almost identical in shape with those reported by previous workers.[1]

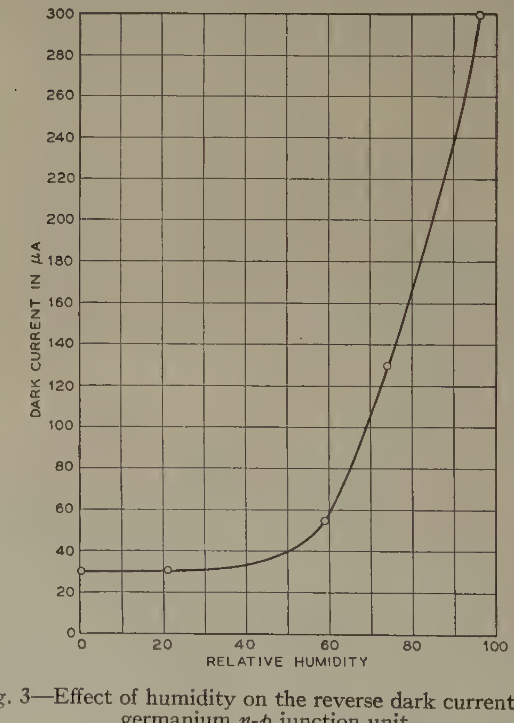

Fig. 3—Effect of humidity on the reverse dark current of a germanium *n-p* junction unit.

Time Effects

It was found also that the magnitude of the current at a fixed bias and humidity changed with time. If at a given humidity a fixed voltage was applied across the junction, the current went through a maximum value, decreasing at first rather rapidly and then more slowly.

The process causing this decrease is irreversible, and even if the bias is removed for several hours the maximum does not reappear when the bias is replaced. The current increases only to the final low value of the previous measurement.

Effect of Increasing Foreign Ion Concentration on Surface

Reverse current-humidity curves were obtained for a unit that had been washed in a dilute sodium chloride solution after etching. Another unit was exposed after etching to HCl gas before water vapor was admitted. In each case, increased conductivity occurred at lower humidities than were necessary for an etched unit without additional treatment.

Summary of Conductivity Results

(a) The reverse current begins to increase rapidly between 40 and 50 per cent relative humidity for an etched unit.

(b) The reverse current decreases with time, finally approaching a stable value.

(c) The reverse current increases at lower humidities when excess foreign ions are admitted to the surface.

DISCUSSION OF MECHANISM

Before attempting to discuss the mechanisms of conduction, we will combine the adsorption data for water on germanium shown in Fig. 1 with the conductivity data in Fig. 3. Let us assume that we are dealing with a surface impedance parallel to the bulk or junction impedance, and plot its conductance as a function of the number of layers of water adsorbed. If we assume that the width of the space charge region at the junction is 10^{-3} cm, we can calculate the conductance per square centimeter of surface. The resulting curve is shown in Fig. 4. This curve includes conductance values calculated for voltages between 10 and 80 volts. The height of the vertical lines shows the spread in data, but no monotonic change of conductance with voltage was found.

The most striking features of Fig. 4 are: (i) The conductance does not increase appreciably until two or three layers of water are adsorbed; (ii) The conductance increases as a linear function of the number of adsorbed layers beyond the fifth. If, then, conductance results are compared with the values previously calculated for the entropy of adsorption of water on germanium, as shown in Fig. 2, it is immediately obvious that the conductance begins to increase only when mobile layers of water are present on the surface, i.e., in the region of the third layer. From this one must conclude that the presence of water molecules *per se* on a germanium surface is not enough to lead to increased conductance; the water molecules present must be mobile. This is a strong indication that the conduction process is occurring through the water film itself, rather than in the surface layer of the germanium. If this is true, the conduction must be ionic in character.

It may be suggested that mobile layers of water are necessary for the migration of surface impurities under the influence of an applied field, and that these impurities then modulate the surface conductivity of the germanium in such a way as to lead to increased conductance. If this picture were true, the conductance should remain at its high value even if the water were removed, so long as the field is applied, since the water only behaves as a carrying medium for impurities and, once these are in place, the conduction is by electrons or holes. Experimentally it is found that the conductance decreases immediately the water is removed, even if the field is still applied.

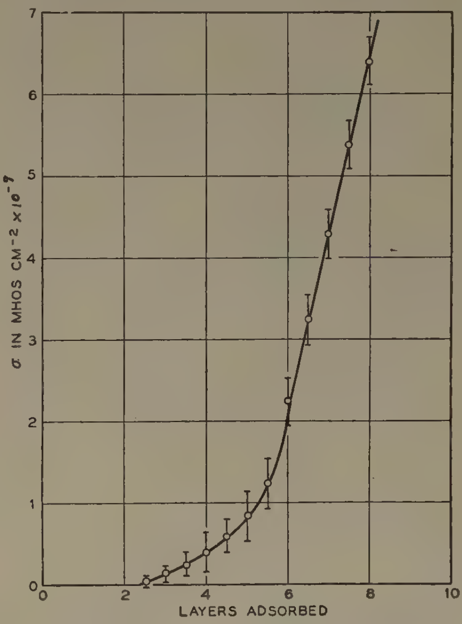

Fig. 4—Variation of surface conductivity on germanium with number of layers of water adsorbed.

It is of some interest to compare the surface conductance values shown in Fig. 4 with similar figures obtained for surface leakage on quartz. The adsorption isotherm for water on quartz has been measured by Livingston,[3] and surface conductivity values by Chirkov.[4]

If the results of these two workers are combined and we plot surface resistivity against the number of layers of water absorbed, we obtain Curve 1 in Fig. 5, page 1370. In the same figure, Curve 2 represents surface resistivity values for water on a germanium *n-p* junction. It can be seen that the two curves are almost parallel and are separated by about one layer.

Previous workers[4,5] have described the surface conductivity on quartz and other insulating materials in terms of an ionic conduction process. The close similarity of the two curves in Fig. 5 with respect to both shape and magnitude of conductivity, provides evidence in favor of the existence of ionic conduction on a germanium *n-p* junction. If one compares the entropy of adsorption of water on germanium with the corresponding values on GeO_2 (which is probably not unlike quartz), it is found that, while only the third and succeeding layers are mobile on germanium, the second adsorbed layer is mobile on GeO_2. This difference would account for the one layer separation of the curves in Fig. 5. Unfortunately, no entropy data are available for water on quartz as a function of surface coverage.

---

[3] H. K. Livingston, "Adsorption and Free Surface Energy of Solids," Ph.D. Dissertation, Univ. of Chicago; 1941.

[4] N. Chirkov, "Contribution to the problem concerning the surface conductivity of solid dielectrics," *Jour. Phys. Chem.*, U.S.S.R., vol. 21, p. 1303; 1947.

[5] H. L. Curtis, "Insulating properties of solid dielectrics," *Bull. Bur. Stands.*, vol. 11, p. 359; 1924.

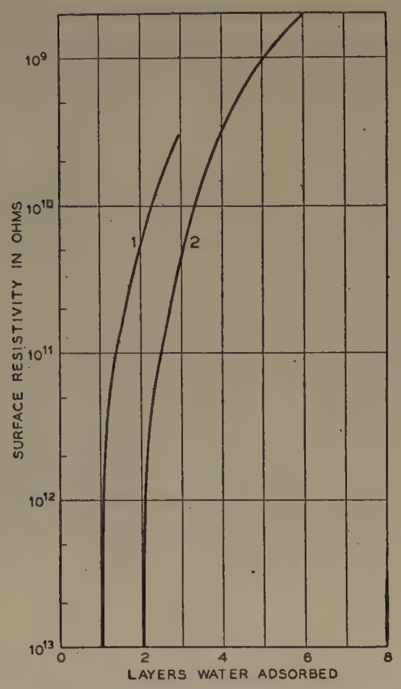

Fig. 5—Comparison of surface resistivity as a function of amount of water adsorbed for (1) quartz and (2) germanium.

It is of some interest to calculate how many ions need be present to produce the measured conductivity.

$$\text{Conductivity } \sigma = ne\mu,$$

when n is the number of ions present and μ is an average mobility. In the absence of any experimental data, we will have to assume an ionic mobility equal to that which the ion would have in the bulk medium

$$\mu \sim 10^{-4} \text{ cm}^2/\text{voltsec}. \tag{4}$$

Therefore, n has a value of 3×10^{14} ions cm^{-2} for the highest conductivity measured at eight layers of water adsorbed. This represents about one third of a monolayer. To determine whether this number of ions is actually present on the surface, an investigation was carried out using the solid mass spectrograph. It showed that foreign ions were present on the surface to an extent of about 10^{14} ions cm^{-2}. This number is great enough to account for the surface conduction actually found on a germanium junction. If the space charge region were 10^{-4} cm in width, instead of the 10^{-3} cm assumed above, only 3×10^{13} ions cm^{-2} would be required to produce the measured conductivity.

Attempts were made to increase the number of ions present on the surface by addition of NaCl or HCl. In each case the conductivity increased, but the shape of the conductivity-relative humidity curve indicated that more adsorption was occurring at low humidities than was found on a freshly etched surface. This is the same effect that was found by Chirkov[4] on a mica surface, and it prevented any quantitative deduction being made from the data, as the number of layers of water adsorbed was unknown.

Another piece of evidence that supports the ionic conduction mechanism is the change with time in reverse dark current. This appears to be some form of polarization phenomenon, the decrease probably being due to the formation of an oxide film on the n-type side of the junction. This effect is not reversible in the sense that, if the bias is removed for several hours after having been continuously applied for an extended period and is then suddenly reapplied, the current measured does not change with time after reaching its maximum value. The reason for choosing the n-side is that the junction is biased in such a way that the n-side is anodic and one would expect the discharge of oxygen at this electrode.

At the same time, however, hydrogen should be liberated at the cathodic or p-side, but so far it has not been possible to detect it. When a p-n junction is run in a closed system for some time and the water is later removed by means of a dry ice trap, there is some indication that the pressure has increased. Replacement of the dry ice by liquid nitrogen removes this material, so that it may well be germane GeH_4, which is known to be formed at a germanium cathode.[6] A mass spectrometric investigation of the gas phase is planned for the near future.

SUMMARY

The evidence in favor of ionic conductance discussed above may be summarized:

(a) The surface conductance number of layers of adsorbed water curve is very similar to those obtained for quartz.

(b) Conductance increases only when mobile water is present on the surface.

(c) The time effects are what would be expected for an electrolytic system.

(d) The number of ions required is in good agreement with the amount actually present.

It is not suggested that ionic conduction is the only process which is operative on germanium surfaces exposed to water vapor, but that, at the voltages (10–80) and humidities investigated, it is the most important.

---

[6] M. Green (Private communication).

Surface Conduction Channel Phenomena in Germanium*

H. CHRISTENSEN†

Summary—**Surface conduction channels on both the *n*-type and the *p*-type region of a *p-n* junction of germanium have been produced and investigated. Channels on the *n*-type region were produced by an oxygen rich surface environment and those on the *p*-side were produced by high humidity. At an intermediate, 75 per cent relative humidity, a condition of high surface leakage and no channel was found. A model, based on bending of energy levels at the surface to produce opposite type majority carrier conductivity than is found for the body of the germanium is used to explain the results. The particular channels studied simulate trouble conditions in transistor fabrication and in reliability problems and provide a good linkage for explanation of anomalous effects that are frequently found.**

INTRODUCTION

SEVERAL investigators[1,2] have explained the anomalously high conduction that is sometimes found between a metallic point and an *n*-type germanium surface as being due to a *p*-type surface conduction layer which results from the bending of energy levels near the surface in the direction of the conduction band.

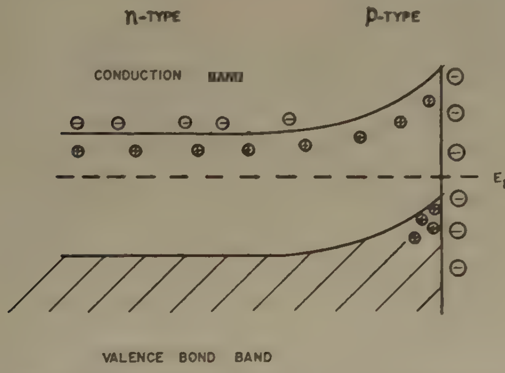

Fig. 1—Model of energy band structure at the surface, for an *n*-type sample and *p*-type surface.

A model of this condition is shown on Fig. 1. Brown[3] has used a model of this type to account for emitter floating potential in an *n-p-n* grown junction transistor for the limiting case of room temperature exposure of the transistor to high humidity and measurement at dry-ice temperature. Under these circumstances, the ionic conduction discussed in the previous paper[4] was eliminated by freezing of the absorbed water layer on the transistor surface, so that conduction in an *n*-type channel on the *p*-type base region could then be identified as the principal cause of the current flow circumventing the emitter and collector barriers, which gives rise to floating potential.

Unfortunately, this dry-ice temperature case is more of academic than general interest. The more complicated case of surface conduction, whether by a channel beneath the germanium surface or by mobile ions on the surface, is the one that must be dealt with in practical transistor design and reliability considerations. In fact when mobile ions are present on the surface, interaction of ionic and surface channel conduction makes the problem still more involved. If, for example, a channel is present initially, its action is similar to that of a high-impedance polarization layer across the surface. If on the other hand, a channel is not present initially, certain types of mobile ions may accumulate at the surface and cause a polarization layer to form just after reverse bias is applied. If this layer becomes sufficiently thick, it then gives rise to channel formation and conduction in the germanium beneath the surface. These complexities, coupled with the problem of specification of the optimum state of surface oxidation, illustrate in one way why an understanding of electrical phenomena at a transistor surface is perhaps the item that is most needed at the present time to supply information that will lead to production of reliable and stable transistors.

To make a general study of surface polarization layers as they affect junction leakage behavior and to identify surface conduction channels, an optical method has been devised and put to use for their detection. With this setup, channels can be investigated on both the *n*- and/or the *p*-type region of an *n-p* junction of germanium. The method has two attractive features: the sample can be investigated at room temperature rather than at dry-ice temperature; and a point-by-point investigation of the entire surface can be made.

This article presents the results of detailed measurements for two cases of channel formation on the *n*-type region, one, of channel formation on the *p*-type region, and the other, of cycling of the channel from the *p*- to the *n*-type region of the *n-p* junction and back again.

APPARATUS

Measurements were made with apparatus similar to that used by Goucher[5] to study the sensitivity profiles of *n-p* junction photocells. A diagram of the apparatus

---

* Decimal classification: R282.12. Original manuscript received by the IRE, June 1, 1954. This work was performed as part of a transistor reliability study under Contract No. DA-36-039 sc-5589 between the U. S. Joint Military Services and the Western Electric Company.

† Bell Telephone Labs. Inc. Murry Hill, N. J.

[1] W. H. Brattain and J. Bardeen, "Nature of the forward current in germanium point contacts," *Phys. Rev.*, vol. 74, p. 231; July 15, 1948; J. Bardeen and W. H. Brattain, "Physical principles involved in transistor action," *Phys. Rev.*, vol. 75, p. 1208; April 15, 1949.

[2] W. H. Brattain and J. Bardeen, "Surface properties of germanium," *Bell Sys. Tech. Jour.*, vol. 32, p. 1; January, 1953.

[3] W. L. Brown, "*N*-type surface conductivity on *p*-type germanium," *Phys. Rev.*, vol. 91, p. 518; August 1, 1953.

[4] J. T. Law, PROC. I.R.E., this issue, p. 1367.

[5] F. S. Goucher, "Measurement of hole diffusion in *n*-type germanium," *Phys. Rev.*, vol. 81, p. 475; February 1, 1951.

is shown in Fig. 2. Light from a lamp and pinhole source is focused in a small spot on the surface of the element. The light is chopped by a 90-cycle-per-second sector disc, and the ac photoresponse is measured by a 90-cycle amplifier-detector. Provision is made for traversing the light spot from one end of the junction bar to the other.

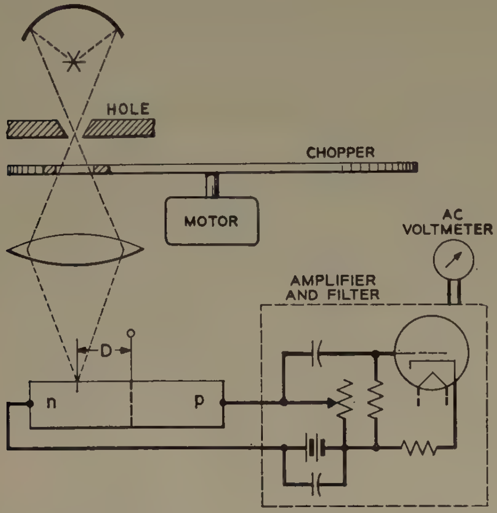

Fig. 2—Functional diagram of experimental measuring setup.

The n-p junction test bars had resistivities of about 3 and 0.3 ohm-cm respectively in the n- and p-type regions. They were sawed to a cross-section area of 0.050×0.030 inch and etched and treated as described below.

P-Type Channel Induced by Ozokerite Wax and Oxygen

The unit used in this test was given a CP4[6] etch and a coating dip in ozokerite wax. It was stored for about a month in air in a dry box. It was selected from a group of several other units, made at approximately the same time, on the basis of a saturation current of less than five microamperes. The ozokerite coat was removed in boiling CCl_4 and the unit was then dipped in a one-to-five solution of ozokerite wax in CCl_4 and allowed to drain and dry in a dry box. It is believed that the combined effects of the thin layer of ozokerite wax that is left by this solution and the oxygen exposure described below cause the channel to form. Following storage in the dry box, the unit was mounted in a glass bottle and measured for ac response to chopped light as a function of distance along the bar in a drierite desiccated air ambient.

The two dashed curves of Fig. 3 show response profiles for two different values of reverse dc bias voltage. This response is typical of the kind found for M1740 photoelements. The label "pre-channel treatment" distinguishes them from the others in the same figure which show the response profiles after exposure to oxygen.

Dry oxygen was then caused to flow through the bottle containing the unit for an overnight period, and the ac responses to chopped light for reverse biases of 0, 0.19, 0.59, 1.35, 4.58, 8.4, 18, and 23.5 volts were measured as functions of distance along the bar. These results are also shown on Fig. 3.[7] The flat portions of these curves extending to the right of the main junction (abscissa zero of the plot) indicate p-type channels extending over the surface of the n-type half of the bar. The maxima of the two curves at the 0.19-volt bias are at considerably different positions on the bar. This is hard to explain. The possibility that it may be due to an inadvertent mechanical shift of the equipment cannot be ruled out, but it is believed more likely that these positions represent an actual shift in the n-p junction region at the surface. Ionic motion in the thin wax coating might be a possible cause for this shift.

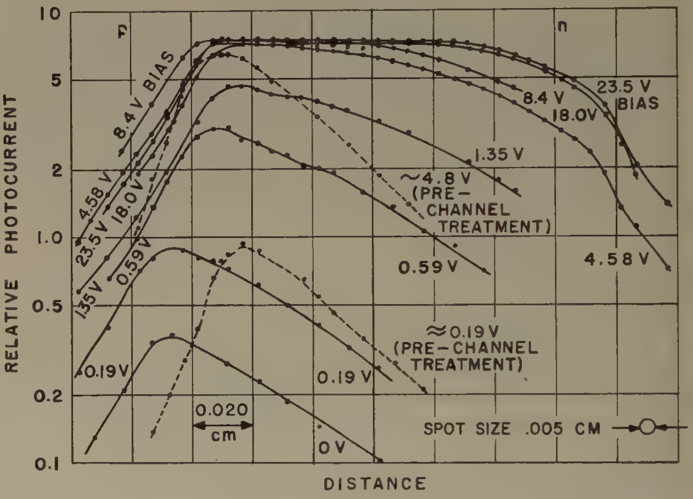

Fig. 3—Relative photocurrent versus distance in direction of the axis of the p-n bar for various reverse bias voltages.

The reverse saturation current of the bar changed during the oxygen treatment. Plots of the dc voltage-current characteristics for the "before channel," "during channel," and "residual channel" cases are shown in Fig. 4. Current saturation for the "during channel" case begins in the 0.1- to 1.0-volt range. This is about a decade higher than the normally observed and theoretically predicted[8] saturation voltage for a body junction in germanium: i.e., $I = I_s[\exp(ev/kT) - 1]$ giving saturation voltage, V, at about 25 millivolts.

---

[6] 20 cc HNO_3, 12 cc 48 per cent HF, 12 cc glacial acetic acid, 10–12 drops Bromine.

[7] The amplitudes of the curves of Figs. 3 and 7 are uncorrected data as recorded with a standardized value of 191,000 ohms for the variable load resistance shown in the amplifier of Fig. 2. At low bias voltages this resistance is comparable to or greater than the resistance of the reverse biased unit. If this mismatched coupling relationship were corrected to an equivalent high impedance photocurrent source condition, all of the curves of Figs. 3 and 7 would have a maximum relative photocurrent *about* equal to the values found in the channel portion of the high bias curves. To avoid excessive overlapping of the curves and to fix the input circuit to a standard condition, the data are presented as shown in Figs. 3 and 7, rather than in the corrected condition. The advantage of this presentation to show the shunting effect of the water vapor in Fig. 7 is obvious.

[8] W. Shockley, "Electrons and Holes in Semiconductors," D. Van Nostrand Company, Inc., New York, N. Y., p. 90; 1950.

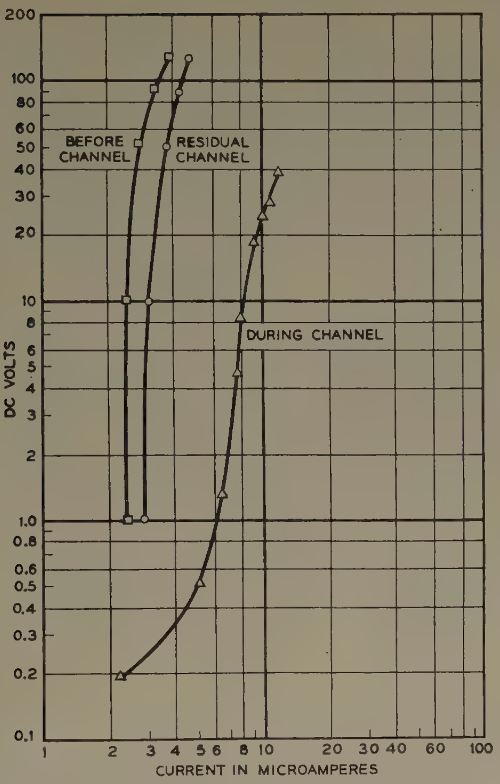

Fig. 4—Saturation current characteristics before, during, and after maximum channel formation on *n*-type germanium.

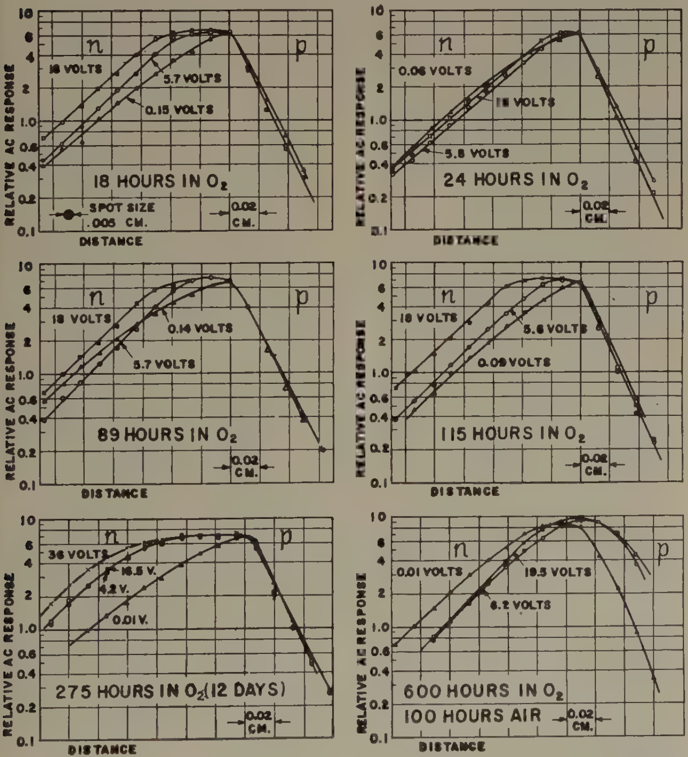

Fig. 5—Channel after superoxol dip (ac response not normalized to correct for input impedance—see footnote 7).

Channel Produced by Hydrogen Peroxide and Oxygen

The bar used in this test was given a surface conditioning treatment which consisted of a three-minute CP4 etch and a dip in hydrogen peroxide of superoxol strength. Immediately following this it was placed in a drierite desiccated test cell and oxygen gas was caused to flow through the cell. The oxygen supply was predried in a silica gel and drierite drying tower.

To follow the behavior of channel formation, curves of ac response to chopped light were taken from time to time. These are shown in Fig. 5. Intercomparison of these curves shows that *p*-type channels of somewhat varying length were found for the full 275 hours that they were observed in the oxygen gas ambient. This is the most persistent case of channel formation that has been observed to date. At about the 600-hour exposure time the oxygen supply to the cell was inadvertently shut off and the unit was exposed to an air ambient. An ac response curve was taken after the unit had remained in the air for about 100 hours. This curve is shown at the bottom of the figure. It exhibits anomalous channel tendencies on both the *n*- and *p*-regions, and demonstrates the contaminating effect that can occur by prolonged atmospheric exposure of the surface of the unit.

Voltage-Induced Photo Response in the Surface Conduction Channel

A plausible description of this phenomenon can be given by reference to Fig. 6. The shaded portion on the *n*-region surface is, in accordance with the model of Fig. 1, taken as having intrinsic conductivity due to the bending up of the energy bands near the surface as a result of the adsorption of negative charges on the surface. Application of a reverse bias field across such an intrinsic region extends the exhaustion layer down the shaded portion. This inversion layer conduction channel thus provides a means for maintaining far into the *n*-type region the high photo response such as shown for the 23.5-volt reverse bias curve in Fig. 3 because the hole-electron pairs generated by the photons in this region can pass immediately to the extended junction without recombination.

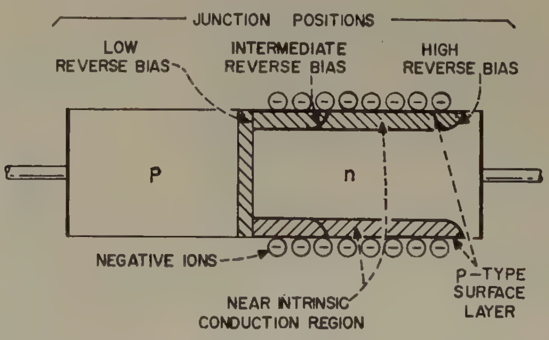

Fig. 6—Cross section of suggested model for formation of channel on *n*-region.

Water Vapor Induced Channel on *p*-Type Material

The *n*-*p* junction bar used in this test was given a surface cleaning treatment as follows: CP4 etch for a half-minute and a distilled water wash. The excess water was then removed by blotting the surface with filter paper.

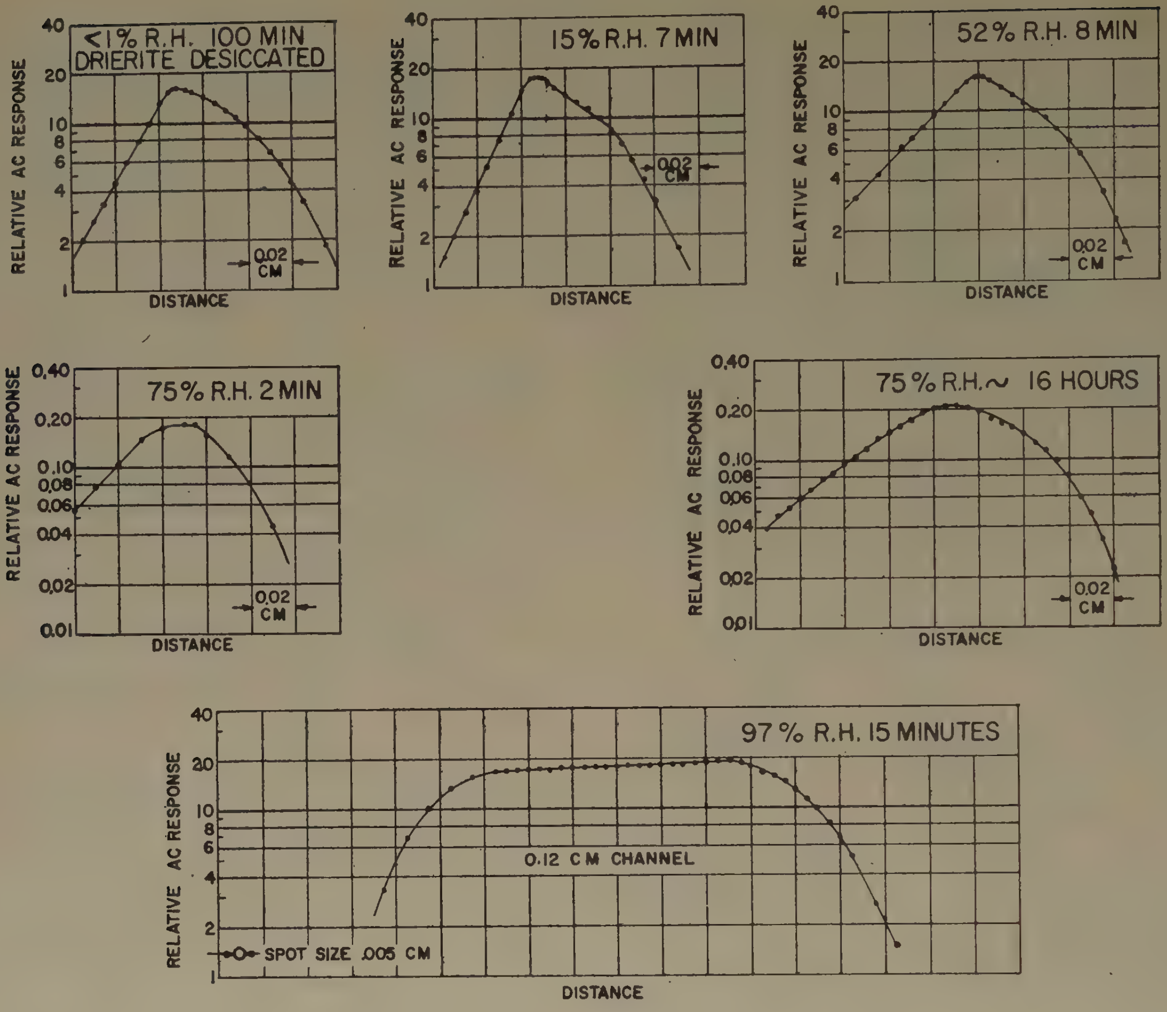

Fig. 7—Channel induced by water vapor.

Immediately following this it was given the sequence of air and water vapor ambient gas exposures shown in the first column of Table I for the times shown in the second column of this table. Near the end of each of these exposure periods an ac photo-response curve was taken for the case of a reverse bias of about one volt on the unit. These curves are shown on Fig. 7. When these curves are compared, two phenomena are of special interest: they show that a channel can be formed on the *p*-region when the relative humidity is at 97 per cent and they also show a decrease of almost a hundred to one in maximum detected photoresponse for the two exposures to 75 per cent relative humidity. For convenience the maximum relative ac photoresponses for all curves are tabulated in the right-hand column of Table I. Taken together, these two phenomena are consistent with the viewpoint that for relative humidities below 50 per cent channels did not form on this specimen, that in the 75 per cent relative humidity range enough water absorbed onto the surface to support excessive leakage across the junction, causing the specimen to present low impedance to the amplifier input and degrading the measured response, and that at 97 per cent relative humidity a channel was formed, and at the same time the polarization layer of the channel suppressed the electrolytic surface leakage and restored the higher values of measured response. In this last case minority carriers from photo-created hole-electron pairs are collected at the surface junction caused by the channel as well as in the *n-p* body junction.

TABLE I

PHOTO RESPONSE OF CURVES IN FIG. 7

Relative Humidity of Air Ambient	Exposure Time	Detected Photo Response at Body *n-p* Junction
1 per cent*	100 minutes	16.5
15 per cent	10 minutes	18.0
52 per cent	8 minutes	16.5
75 per cent	2 minutes	0.18
75 per cent	16 hours	0.21
97 per cent	15 minutes	14.0

* Drierite desiccated.

CYCLING OF CHANNEL BETWEEN *p*- AND *n*-REGIONS

It is of interest to discuss the case where a channel is first formed on the *p*-region by exposure to a gaseous ambient of air and water vapor, then suppressed when the ambient gas is changed to water vapor and oxygen, and finally formed on the *n*-region when the ambient gas is changed to dry sparked oxygen. This latter case is similar in some respects to the ambient gaseous cycle used by Brattain and Bardeen[2] in their investigation of contact potential of germanium surfaces, but it differs in the sense that air was always excluded in their cycle.

As in all of the above cases, an uncoated *n-p* photocell element was used for this test. Its surface was cleaned by a half-minute CP4 etch and a distilled water wash. Immediately following this it was placed in a drierite desiccated air ambient. This condition was taken as the reference condition. After two hours in this ambient a photoresponse curve was taken in accordance with the procedure discussed above, and no channel was found. These facts are tabulated in the first line of Table II. Similar descriptive behavior of photoresponse curves for twenty additional successive ambient conditions for this same unit are also tabulated. From this general description the following behavior pattern emerges: 97 per cent relative humidity in air gives a channel on the *p*-type region. This channel can be suppressed slowly by replacing the air by oxygen, and suppressed more rapidly by a short exposure to sparked oxygen. Sparked dry oxygen can produce a channel on the *n*-type side which goes away when the sparking is eliminated. A slightly idealized plot depicting these phenomena is shown in Fig. 8. The results are in qualitative accord with the viewpoint that sparked oxygen gives negative charge on the surface to bend the energy bands up a sufficient amount to give a *p*-type conduction surface layer on the *n*-type body material as shown in Fig. 4, and that hydrogen ions resulting from decomposition of water at the germanium surface produce a positive surface charge of sufficient magnitude to bend the energy bands down to give an *n*-type conduction surface layer on the *p*-type body material. This energy band behavior was first reported by Brattain and Bardeen,[1] later described in detail by Brown[3] for the *n*-channel on the *p*-type body region.

TABLE II

n AND *p* CHANNEL CYCLING

Test No.	Gaseous Ambient	Exposure Time	Description of Photoresponse Curve
1	Drierite air	2 hrs.	Reference condition, no channel.
2	97 per cent RH air	16 hrs.	Channel on *p*-type 0.7 mm long.
3	97 per cent RH oxygen	$\frac{1}{4}$ hr.	Channel on *p*-type 0.25 mm long.
4	97 per cent RH oxygen (sparked)	2 mins.	No channel.
5	97 per cent air	6 hrs.	Channel on *p*-type 0.75 mm long.
6	Drierite air	16 hrs.	Channel on *p*-type 0.1 mm long.
7	Drierite oxygen	$\frac{1}{2}$ hr.	No channel.
8*	Drierite oxygen	$\frac{1}{2}$ hr.	No channel.
9	Drierite oxygen (sparked)	2 mins.	Channel on *n*-type 0.3 mm long.
10	Drierite oxygen	$\frac{1}{2}$ hr.	No channel.
11	Drierite oxygen (sparked)	4 mins.	Channel on *n*-type 0.35 mm long.
12	Drierite oxygen	$\frac{1}{2}$ hr.	No channel.
13	Drierite oxygen (sparked)	4 mins.	Channel on *n*-type 0.3 mm long.
14	Drierite oxygen	1 hr.	Possible channel on *n*-type (<0.1 mm).
15	Drierite oxygen (sparked)	4 mins.	Channel on *n*-type 0.2 mm long.
16	Drierite oxygen	$\frac{2}{3}$ hrs.	Possible channel on *n*-type (<0.1 mm long).
17	Drierite oxygen (sparked)	4 mins.	No channel.†
18	Drierite oxygen	$\frac{1}{4}$ hr.	Possible channel on *n*-type (<0.1 mm long).
19	Drierite oxygen (sparked)	4 mins.	No channel.
20	97 per cent RH air	24 hrs.	Channel on *p*-type 1.0 mm long. Possible channel on *n*-type.
21	97 per cent RH oxygen	7 mins.	Possible channel on *p*-type (<0.1 mm long).

* Repeat data of Test 7.
† Oxygen cutoff during measurement.

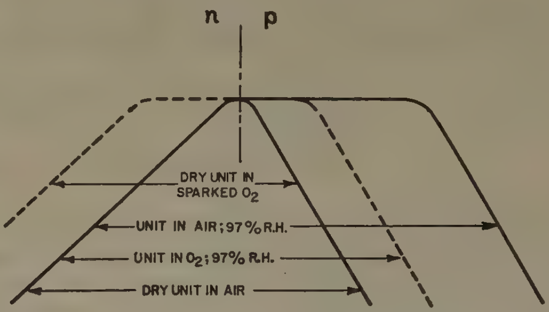

Fig. 8—Channel formation for various gas ambients on *p-n* germanium photocell.

Two minor effects are worthy of mention concerning the material given in Table II. The results of Test 17 are consistent with the viewpoint that air replaced the oxygen and somewhat altered the surface by ionic contamination. Also, with reference to Tests 11 through 15, there seems to be a trend toward decreasing length of the channel on the *n*-type material. This is consistent with the viewpoint that a surface oxide layer is building up which makes the sparking treatment less effective.

CONCLUSIONS

1. Surface conduction channels have been formed on the *n*-type regions of a germanium *n-p* photocell.
2. These channels are dependent upon reverse bias voltage.
3. A model for the formation of a channel on the *n*-type region has been developed to aid in visualizing these effects.
4. A channel on the *n*-type region has been formed and maintained for at least 275 hours (12 days) by a combination of hydrogen peroxide etching and oxygen exposure.
5. A hundred-fold decrease in the detected photoresponse of an *n-p* junction occurred when the relative humidity of its air ambient was raised to 75 per cent. This loss of sensitivity occurred in the same general humidity range as that in which mobile layers of water form on the surface.
6. The role of the electrical shunting action of a mobile water layer has been separated from the role of a channel on a *p*-type region—either one or both of these effects could cause floating potential in an *n-p-n* grown-

junction transistor. They might also be the cause of anomalous behavior of alpha for transistors in general.

7. A channel on the p-type region has been formed by exposure of a CP4-etched surface to 97 per cent relative humidity and an air ambient.

8. The alternate formation of a channel, first on the p-region, then on the n-region, and finally back on the p-region, has been accomplished on the same unit by change of gaseous ambient.

9. Contaminating action of the atmosphere has been illustrated on surfaces inclined toward n-type channels and also on surfaces inclined toward p-type channels.

Further work on the combined action of water vapor and prolonged exposure to separate components of air will need to be done before complete understanding of its role in the reliability phase of this problem can be achieved, but the above suggests that exclusion of air is desirable in cases where channel formation is considered deleterious.

ACKNOWLEDGEMENTS

The author wishes to express his appreciation to Mrs. H. Schwenker for arrangement of the tests and recording of the data presented in this paper.

Channels and Excess Reverse Current in Grown Germanium *p-n* Junction Diodes*

A. L. MCWHORTER†, AND R. H. KINGSTON‡, ASSOCIATE, IRE

Summary—**Measurements have been made on grown germanium p-n junction diodes in an attempt to correlate the excess reverse current that occurs under exposure to water vapor with the presence of an n-type surface-conductivity layer, or "channel," on the p-side of the junction. Using an optical method to measure the length of this surface layer, it has been found that (1) no channel is formed on a freshly CP4-etched surface, and that (2) for well-oxidized surfaces, large excess reverse currents occur which are directly proportional to the length of the channel for all measured values of applied voltage and humidity. By combining this observation with the known behavior of the channel conductivity with humidity and voltage, a formula for the excess current as a function of the applied bias is derived. In spite of several oversimplifications in the model, the predicted values agree reasonably well with the experimental results for biases greater than one volt.**

INTRODUCTION

IN A PRECEDING PAPER, Law[1] has discussed one possible mechanism for the occurrence of excess reverse current in grown germanium p-n junction diodes. His results indicate that when a diode with a freshly-prepared, unoxidized surface is exposed to water vapor, ion migration along the surface can produce a sizable leakage current. In the work to be described below, it has been found that much larger excess currents can occur with well-oxidized surfaces, and that in this case the current must be attributed to a completely different mechanism, namely the increase in the effective rectifying area of the diode which results from the presence of a water-induced n-type surface conduction layer on the p-side of the junction. Such surface-inversion layers, or "channels" as they are called, have been studied on n-p-n transistors by Brown[2] and were used by him to explain the high emitter floating potential often observed when a reverse bias is applied between the collector and base. Christensen has since established the existence of channels on p-n junctions by an optical detection method described in the preceding paper,[3] and has been able to produce both n-type channels on the p-side and p-type channels on the n-side of the junction by suitable surface treatments.

Since the optical technique used by Christensen allows the length of the channel to be determined as well as its existence, it provides a direct method for correlating the excess current with the channel length. Such a correlation has been carried out for different relative humidities and applied voltages, and the results, as presented below, show a direct proportionality between the two under all measured conditions. This observation is used together with other experimental results on channel conductivity to form a model of the channel behavior, which in spite of several oversimplifications is nevertheless complete enough to give a quantitative prediction of the excess current as a function of the applied voltage that agrees satisfactorily with the measured values for biases greater than one volt.

EXPERIMENTAL RESULTS

The experimental equipment was composed of three main parts: first, a sample chamber and associated apparatus for varying the humidity; second, a 900 cps chopped light source producing a line image 20 microns wide on the surface of the diode and parallel to the junc-

---

* Decimal classification: R282.12. Original manuscript received by the IRE, June 1, 1954. The research reported in this document was supported jointly by the U. S. Army, Navy, and Air Force under contract with the Massachusetts Institute of Technology.

† Research Laboratory of Electronics and Lincoln Laboratory, Mass. Inst. of Tech., Cambridge, Mass.

‡ Lincoln Laboratory, Mass. Inst. of Tech., Cambridge, Mass.

[1] J. T. Law, "Mechanism for water-induced excess reverse dark current on grown germanium n-p junctions," page 1367, this issue.

[2] W. L. Brown, "N-type surface conductivity on p-type germanium," *Phys. Rev.*, vol. 91, pp. 518–527; August 1, 1953.

[3] H. Christensen, "Surface conduction channels in germanium," page 1371, this issue.

tion; and third, a 900 cps detector and dc bias and metering instruments. The last part needs no special comment, and the only unusual feature of the optical system was the inclusion of an infrared filter to limit the light penetration to about 10^{-4} cm. This ensured that all of the minority carriers generated by the light were collected by the channel rather than by the bulk junction. Humidity was controlled by circulating the ambient gas in a closed system over different saturated salt solutions, thus obtaining the known vapor pressure associated with the particular salt.[4] This gave an easily reproducible set of relative humidities covering most of the range from 0 to 100 per cent. Furthermore, by a careful selection of the salts, nearly constant humidities could be obtained in the temperature range of 20 degrees to 30 degrees C.

The sample used throughout the experiments was a bar 0.20×0.20×2.0 cm cut from a grown germanium *p-n* junction having 1.6 ohm-cm *p*-type and 9.0 ohm-cm *n*-type resistivity. The first measurements were made immediately following a CP-4 etch and showed neither a detectable channel nor an appreciable excess current. Exposure to oxygen for several hours, however, produced both large channels and excess currents, indicating that an oxide layer is essential to channel formation, which agrees with the reported observations on transistors.[5] After this discovery all further work was confined to well-oxidized surfaces, in contrast to the work of Law[1] where the surface was prepared in vacuum and exposed only to water vapor. For greater stability of the oxide surface, only nitrogen ambients were used.

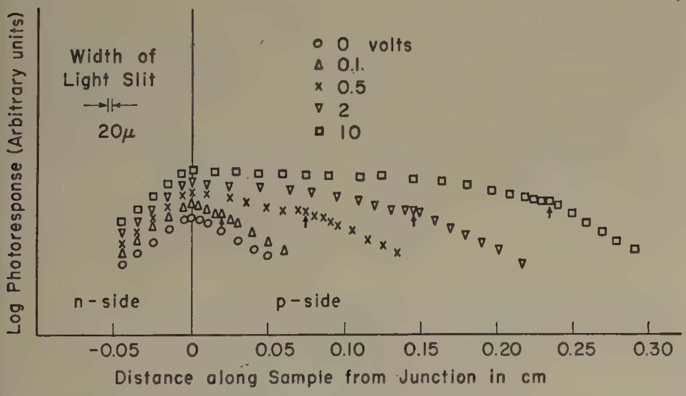

Fig. 1—Photoresponse curves at 100 per cent relative humidity, with the extent of the channel indicated by the vertical arrows. All curves were taken with a 10,000 ohm load resistor, but have been displaced vertically for clarity.

A typical set of photoresponse curves, in this case for 100 per cent relative humidity, is shown in Fig. 1. As can be seen, the end of the channel is somewhat indefinite; but if it is taken to be the point where the slope suddenly changes, as indicated by the vertical arrow, then for the entire range of applied reverse bias, 0.1 to 10 v, the excess current is found to be directly proportional to the channel length. Moreover, the constant of proportionality is independent of the relative humidity, as shown in Fig. 2. (The slope did increase slightly however over a period of weeks, presumably from slow growth of the oxide layer.) Humidities below about 30 per cent produced channels too small to be measured accurately by the light technique.

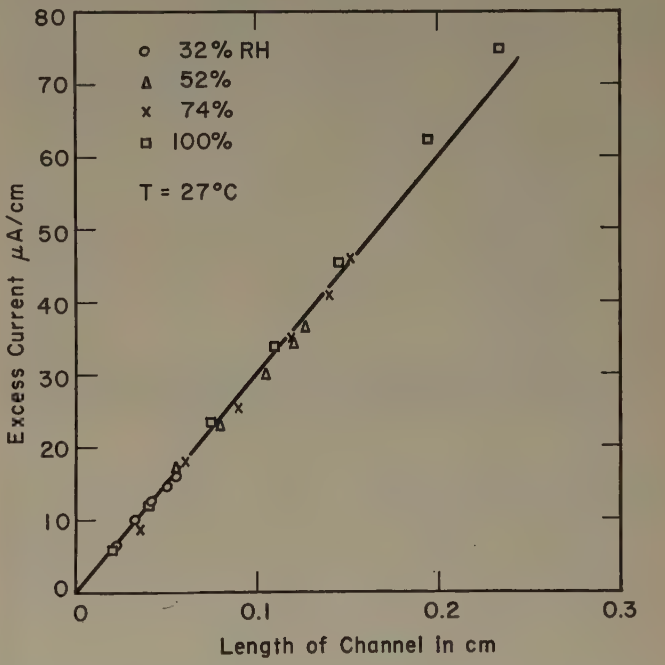

Fig. 2—Excess current per unit circumference vs channel length for several values of relative humidity.

In addition to the above results the excess reverse current vs voltage is plotted in Fig. 3 for several values of humidity. The theoretical curves also shown in this figure will be derived at the end of the next section.

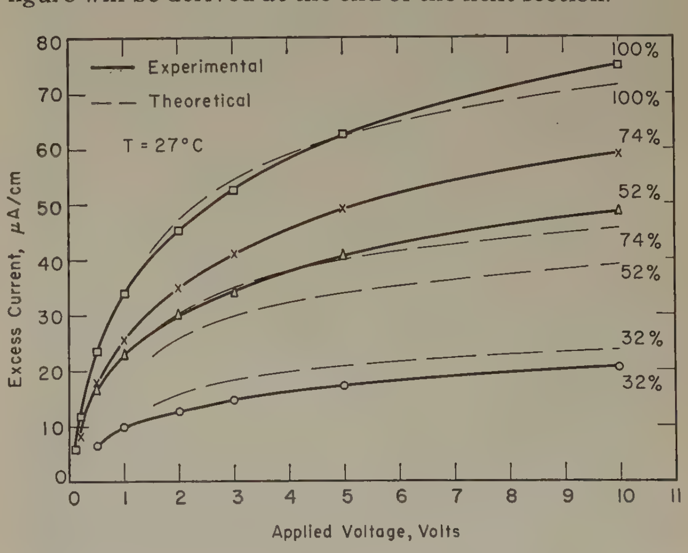

Fig. 3—Theoretical and experimental curves of excess current vs applied voltage.

---

[4] *International Critical Tables*, McGraw-Hill Book Co., Inc., New York, N. Y., vol. I, p. 67; 1926.

[5] R. H. Kingston, "Channels in *n-p-n* junction transistors: new results and a proposed model," *Bull. Amer. Phys. Soc.*, 1954 Michigan Meeting, March 18–20, 1954.

THEORY

By extending Brown's model[2] for channels in transistors to the *p-n* junction structure, a fairly complete picture of the channel behavior may be presented. As shown in Fig. 4, the channel essentially forms an extension of the normal reverse-biased junction area with an accompanying increase of current due to surface-generated holes being swept into the *p*-region and bulk-generated electrons swept into the channel. The electrons generated at the surface and those collected from the bulk combine to produce a longitudinal current in the channel which flows toward the *n*-side. The resulting voltage drop along the channel decreases the bias between the surface and the *p*-type material. Since a high field at the surface tends to pinch off the conduction path, the channel becomes wider as the distance from the junction increases. At large distances the width approaches the limiting value associated with the equilibrium inversion region.[6] Thus in one sense the channel continues indefinitely, but only over the section for which the applied voltage is much greater than kT/q will the surface barrier be acting as a perfect collector of minority carriers. As the applied bias drops through kT/q, there will be a rapid transition from full saturation current across the barrier to the equilibrium condition of zero current, giving an effective lengh l for the channel as far as excess current is concerned. Electrons generated further away than this from the junction must diffuse through the intervening distance in order to be collected, with the attending probability of recombining before the collection can take place. Thus a photoresponse curve would be expected to fall off exponentially beyond this effective end of the channel, indicating that l is the length which is measured by the curves in Fig. 1.

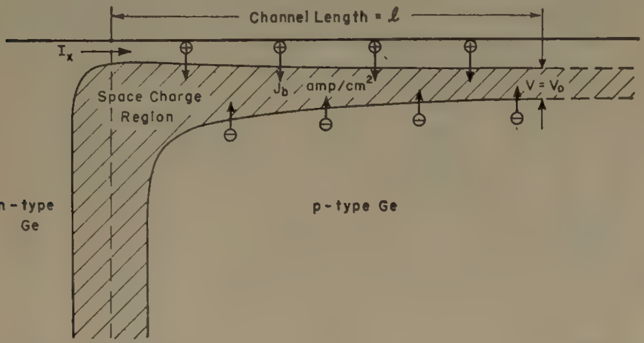

Fig. 4—Schematic diagram of channel showing the increase in the effective rectifying area of the diode produced by the space charge barrier just beneath the surface of the *p*-region.

Fig. 2 shows that the saturation current J_b flowing across the barrier is constant for this distance l, which in turn implies that the surface generation is independent of the applied bias and the relative humidity, at least for humidities above 30 per cent. The slope of the curve gives a value for J_b of about 300 μA/cm². The part due to bulk generation can be calculated from the lifetime and is about 90 μA/cm², leaving the majority to be attributed to generation at the surface.

It should be pointed out that Fig. 4 has been greatly distorted in order to show the whole channel region on one diagram. For the sample used in this experiment, the channel width is of the order of 10^{-6} cm, while the space charge barrier between the channel and the *p*-region is about 10^{-4} cm, and that at the true junction is about 10^{-3} cm because of the small doping gradient. The width of the light slit is about twice the junction barrier.

By combining the observations of Fig. 2 on the proportionality of excess current to channel length with the known behavior of channel conductance with humidity and applied bias, it is possible to derive a formula for excess current as a function of applied bias. The above discussion shows that the longitudinal current flowing in the channel at a distance x from the junction is

$$I(x) = J_b l\left(1 - \frac{x}{l}\right). \tag{1}$$

As has been reported elsewhere,[7] the surface resistance of channels as measured on the *p*-type region of an *n-p-n* transistor is proportional to the applied voltage for biases greater than about one volt, with the constant of proportionality a function of the relative humidity. Hence

$$\frac{\partial V}{\partial x} = -RI = -AVJ_b l\left(1 - \frac{x}{l}\right), \tag{2}$$

where A is a function of the relative humidity only.

If the voltage at the end of the channel is taken to be an adjustable parameter V_0, and the applied voltage at $x=0$ is denoted by V_A, then integration of (2) gives

$$\ln\frac{V_A}{V_0} = \frac{AJ_b}{2}l^2. \tag{3}$$

Therefore the excess current is

$$I_x = J_b l = \left(\frac{2J_b}{A}\ln\frac{V_A}{V_0}\right)^{1/2}. \tag{4}$$

The most recent experimental values[8] for A are given in Table I for several humidities. The values in the first column are those measured on an *n-p-n* transistor with a *p*-type resistivity of 3.3 ohm-cm. The present model[5] for the channel requires that these values be multiplied by the ratio of the resistivities, 3.3/1.6, to obtain the appropriate value for the 1.6 ohm-cm material used here. These converted values are tabulated in the second column.

---

[6] W. H. Brattain and John Bardeen, "Surface properties of germanium," *Bell Sys. Tech. Jour.*, vol. 32, pp. 1–41; January, 1953.

[7] R. H. Kingston, "Water vapor and the channel effect in *n-p-n* transistors," *Phys. Rev.*, vol. 93, p. 347; January 15, 1954. (See footnote reference 5 for revised theoretical model.)

[8] Manuscript in preparation.

The best fit between theory and experiment at the higher voltages is obtained with V_0 equal to about 0.5 v, and it is this value which is used together with the data of Table I for the theoretical curves in Fig. 3. At low voltages this of course gives a completely wrong answer; but then neither the formula for surface resistivity nor the model for the channel holds much below one volt, so that disagreement would be expected. For this reason the theoretical curves have not been continued below one volt.

TABLE I

SURFACE RESISTIVITY OF THE CHANNEL PER UNIT APPLIED VOLTAGE

Relative humidity	Experimental values for *n-p-n* transistor	Converted values for *p-n* junction
32 per cent	1.55×10^6 ohm/volt	3.2×10^6 ohm/volt
44	0.69	1.4
58	0.50	1.03
75	0.41	0.84
84	0.30	0.62
100	0.165	0.34

DISCUSSION

There are two points concerning Fig. 3 which need further comment. The first is the justification for using such a large value for V_0 when the previous discussion had indicated that the voltage at the end of the channel was of the order of kT/q, or about 0.026v at room temperature. In the last section, however, only the main features of the channel were presented for the sake of clarity. At low voltages certain refinements in the theory become quite important. For instance the complete theory predicts that the channel resistivity should be proportional not just to the applied voltage, but to the applied voltage plus the equilibrium difference in potential between the surface and the bulk. This is actually in much closer agreement with the experimental data on channels in *n-p-n* transistors. Hence V_0 in (3) and (4) should be reinterpreted as the applied voltage at the end of the channel, about kT/q as previously mentioned, plus this equilibrium difference in potential. The latter is a slowly increasing function of the relative humidity and has been found experimentally to be as large as 0.3 v. In view of this, a value of 0.5v for V_0 begins to look much more reasonable. However, even when this correction is made in the theory, (4) still does not check with the experimental curves at low voltages. The remaining discrepancy is probably just due to the use of an over-simplified model which breaks down for small channel lengths. Actually it is only for the middle section of the channel that (1) is valid. At the far end the transition between full saturation current and zero current has been completely neglected. This includes both the decrease in J_b at very low voltages and the end effects that the channel produces on the diffusion flow pattern. Near the junction, on the other hand, the problem really becomes two-dimensional because of the joining of the channel barrier to the junction barrier. Furthermore, there is the added complication of the doping gradient in this region, for the transition from *n*-type to *p*-type material takes about 0.025 cm or more in the sample used. If the channel is long enough, that is if the applied voltage is high enough, then these end regions become relatively much less important, and in fact their effect becomes more like a modification of the boundary conditions for the middle section of the channel. Therefore it is not too unreasonable to try to lump all of these corrections into the one boundary parameter V_0 and adjust that to give the best fit with experiment. Fig. 3 shows that this procedure is quite successful.

A second observation concerning Fig. 3 is the disagreement in magnitude between the theory and experiment for the two central curves despite the agreement in shape. This points out the uncertainties in experiments of this type, where the detailed effects of oxidation and surface conditions are not completely understood. It is quite possible that the *p-n* junction used here and the *n-p-n* transistor from which the values in Table I were obtained had different adsorption curves for water, or that because of the differences in the oxide layer, a given amount of adsorbed water did not have the same quantitative effect in both cases. Further investigation on the effect of the oxide layer is in progress. There could also have been trouble arising from temperature differences within the system. It has been found that the channel is relatively insensitive to a slight change of temperature for the whole system, but that only a fraction of a degree difference between the sample chamber and the salt solution gives a measurable higher or lower effective humidity for the junction. In work now in progress, steps have been taken to eliminate this possibility of error.

Several other experimental observations are of interest. One is that for about a week during the course of the investigations, a rather large *p*-type channel on the *n*-side of the junction occurred upon exposure to dry nitrogen. While it lasted, this channel was fairly stable and showed qualitatively the same behavior as the *n*-type channels discussed above. However, it then disappeared rather abruptly, and subsequent efforts to reproduce the results were unsuccessful.

As another check on the general model of the channel, the capacitance of the reverse-biased junction was measured at a frequency of 800 kc. The excess capacitance over the value without the channel was found to be of the right order of magnitude and to have qualitatively the correct dependence on voltage. No closer comparison between theory and experiment can be made since only an approximate solution was carried out. The exact calculation would be very difficult since the channel, looking from the *n*-side, is an extremely lossy transmission line whose series resistance and shunt capacitance are functions of distance.

It should be emphasized that the voltage-current characteristics discussed in this report are all taken under dc conditions. As has been reported elsewhere, the occurrence of a channel on the surface is not an instantaneous phenomenon. Studies in these laboratories indicate that for both n-p-n transistors and p-n junctions in a wet nitrogen ambient, a time of the order of 0.1 second is required for equilibrium conditions to be reached after application of bias voltage. Although the mechanism of this delay time is not completely understood, it is known that the rate of build-up of positive surface charge is the limiting factor in the establishment of the channel. Thus, in the junction discussed above, the ac current-voltage characteristics would be extremely complex, especially in the frequency range around 10 cps where the period of the applied voltage is of the order of the delay time. Since the current, in this case, will lag behind the applied bias, the impedance would be expected to be inductive; however no quantitative data is available at this time.

CONCLUSIONS

The results indicate that the behavior of junction diodes in various ambients can be treated analytically with reasonable success. Of course, the experiments described specifically apply only to a moist nitrogen ambient; however Christensen's[3] data indicates that the arguments should carry over directly to other gases. There is still a region of uncertainty as to whether the ionic conductivity discussed by Law[1] or the channel mechanism is operative in a specific case. At present there are two criteria. First, the current-voltage characteristic should be linear for ionic conduction and somewhat logarithmic for the channel case, as shown in the data above. Second, ionic conduction is most probable when the oxide layer is extremely thin, because a thick oxide seems to produce a channel, which would then greatly reduce the component of the electric field along the surface by increasing the distance over which the voltage drop occurs from the normal junction barrier width to the entire channel length.

A further mechanism of current generation in the channel is also being investigated. At much higher bias voltages or with lower resistivity p-type material, it is quite probable that there will occur some form of breakdown between the channel and the bulk material. Such a breakdown, which could be either a Zener[9] or Townsend[10] type, would produce currents much larger than those discussed above.

ACKNOWLEDGEMENT

We are indebted to J. E. Thomas, Jr. and R. B. Adler for advice and criticism, to M. Green for suggestion of the humidity apparatus, and to H. Christensen, J. T. Law, and J. N. Shive, of the Bell Telephone Laboratories, for discussion and correlation of the experimental work reported.

---

[9] K. B. McAfee, E. J. Ryder, W. Shockley, and M. Sparks, "Observations of Zener current in germanium p-n junctions," *Phys. Rev.*, vol. 83, p. 650; August 1, 1951.

[10] K. G. McKay and K. B. McAfee, "Electron multiplication in silicon and germanium," *Phys. Rev.*, vol. 91, pp. 1079–1084; September 1, 1953.

Significance of Some Receiver Errors to Color Reproduction[*]

HAROLD WEISS[†], ASSOCIATE, IRE

Summary—**A method is shown for approximating the significance of color television-receiver errors to color reproduction. For representative colors, the deviations in chromaticity caused by errors in various signals are evaluated in terms of MacAdam's unit of equal noticeability. An experimental investigation of viewer tolerances is reported.**

INTRODUCTION

THIS INVESTIGATION has grown from the need by color television receiver design engineers of a better understanding of how the typical color perception characteristics of the human eye affect their design problems. At present, very little is known about the sensitivity of various color signals to possible receiver errors. The purpose of this paper is to provide some of this information.

The problem of flesh color reproduction has been most thoroughly investigated because this involves the most televised subject and probably the most important one from the point of view of quality of color reproduction. Since the typical viewer has only memory against which to match televised scenes, those subjects which are most familiar will be most critically evaluated. The color appearance of the human complexion often becomes the most severe criterion by which reproduction is evaluated. However, while flesh color reproduction will be used as an illustrative example in this paper, results will be presented which cover a wide color gamut and which allow some broad conclusions to be drawn.

The basic procedure in evaluating analytically the significance of receiver errors is first to determine the electrical signals which should exist in a typical receiver for the color or colors one wishes to reproduce, then to introduce errors into these signals which produce deviations from the optimum color, and last to find a way of evaluating these color errors.

---

[*] Decimal classification: R583.5. Original manuscript received by the IRE, April 15, 1954; revised manuscript received, June 1, 1954. Published also in the 1954 IRE Convention Record, Part 7—Broadcasting and Television. This paper is an abstract of the thesis "Some Design Criteria for Color Television Receivers as Determined by Color Perception," to be submitted by the author to the College of Engineering of Syracuse University in partial fulfillment of the requirements for the degree of Master of Electrical Engineering.

[†] General Electric Co., Syracuse, N. Y.

RECEIVER SIGNALS

Fig. 1 shows a simplified block diagram of a color television receiver. The basic separation of the color signal into a luminance component (Y') and a chrominance component is evident. The chrominance signal may be considered to have an amplitude (A') and phase (θ). By means of a local 3.58 mc reference of proper phase, we can detect this signal along I', Q' or $R'-Y'$, $B'-Y'$ axes. From these signals, by a matrixing operation, we recover R', G', and B', the gamma-corrected voltages used to drive the picture tube.

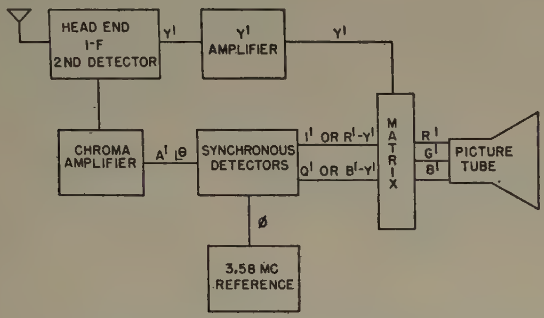

Fig. 1—Simplified block diagram of color television receiver.

To determine what these signals should be, one must go to the NTSC specifications[1] which were recently adopted by the Federal Communications Commission. These standards specify the color of the red, green, and blue reproducing primaries. A color is usually specified by a pair of chromaticity co-ordinates and its luminance. Howells[2] has given the linear transformation which allows recovery of the NTSC display primaries from the chromaticity co-ordinates and luminance of a color. The NTSC specifications may then be used to compute all the signals shown in Fig. 1. In Appendix I the necessary relationships are furnished.

The standards specify a gamma exponent of 2.2 for the display device, but do not state what the allowable tolerances are. A value of 2.0 was assumed in this study for the sake of simplicity.

SIGNAL ERRORS

It has been demonstrated how the optimum signals can be calculated for any color it is desired to reproduce. If one takes the optimum signals at any point in a typical receiver, say those corresponding to a flesh color, and increases or decreases them to simulate receiver errors, the new color produced at the receiver output can then be calculated.

In Appendix II the relationships necessary to calculate the change in chromaticity (dx, dy) produced by a chrominance signal phase or amplitude error are provided. These allow determination of the effect of changes in all the other signals save I' and Q', so a matrix which allows recovery of R', G', and B' from I', Y', and Q' is also given. It is not necessary to compute the effects of both luminance and chrominance amplitude changes, for one is the inverse of the other. Thus a 41.4 per cent increase in Y' is equivalent to $1.000-0.707$, or a 29.3 per cent decrease in chrominance amplitude.

For errors in the color difference and luminance signals and in the chrominance signal amplitude and phase, a short cut is possible by graphical methods. One can directly find the chromaticity change produced by an error by going to Howells' curve[2] "Chromaticity grid in normalized subcarrier plane" shown in Fig. 2. This graph directly relates chromaticity co-ordinates with normalized receiver signals.

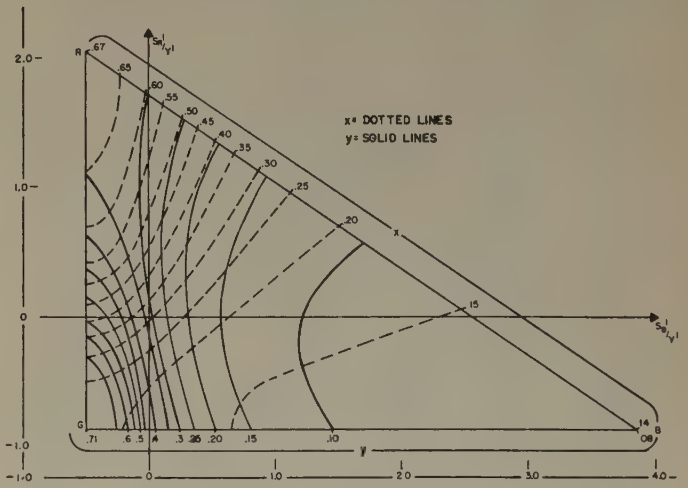

Fig. 2—Chromaticity grid in normalized subcarrier plane; $\gamma = 2.0$.

QUALITY OF COLOR REPRODUCTION

Now that a color error has been produced, the problem arises of how to evaluate the deviation from optimum color. Here we are not on such firm ground. The problem of evaluating the quality of color reproduction is under investigation in several laboratories and as yet only a beginning has been made towards its solution. The problem is quite complex, for many physical and psychological factors are involved.

So far, very little has been reported on the seriousness of deviations from optimum color reproduction. However, several studies are available on the perceptibility of color distortion. It must be realized that there is a substantial difference between the point where a color difference becomes just noticeable and the limit of acceptability.

The Maxwell color triangle and its projection, the x-y chromaticity diagram, are quite nonuniform in perceptual terms. It is not obvious from the distance between the original and reproduced chromaticity on these diagrams, how well a given color is reproduced. Several equations have been developed to evaluate color differences, equations based, either explicitly or implicitly, on the measurement of the distance between two colors when plotted in a visually uniform color space.

---

[1] "NTSC Signal Specifications," PROC. I.R.E., vol. 42, pp. 17–19; January, 1954.

[2] P. W. Howells, "Transients in color television," PROC. I.R.E., vol. 42, pp. 212–220; January, 1954.

MacAdam[3] has used another approach to the problem of the evaluation of color differences which lends itself better to graphical or analytical methods. Instead of explicitly transforming this color space, its known distortions can be compensated. An observer made numerous color matchings with a colorimeter. MacAdam plotted the results on the chromaticity diagram in terms of the standard deviation of color matching (a measure of the dispersion of equality judgments) in several directions about selected colors. The resulting 25 closed curves have the form of ellipses (Fig. 3), with the radii representing equally noticeable chromaticity differences. Under favorable conditions, color differences equal to one-tenth of these radii are just noticeably different from the color at the center of the ellipse.

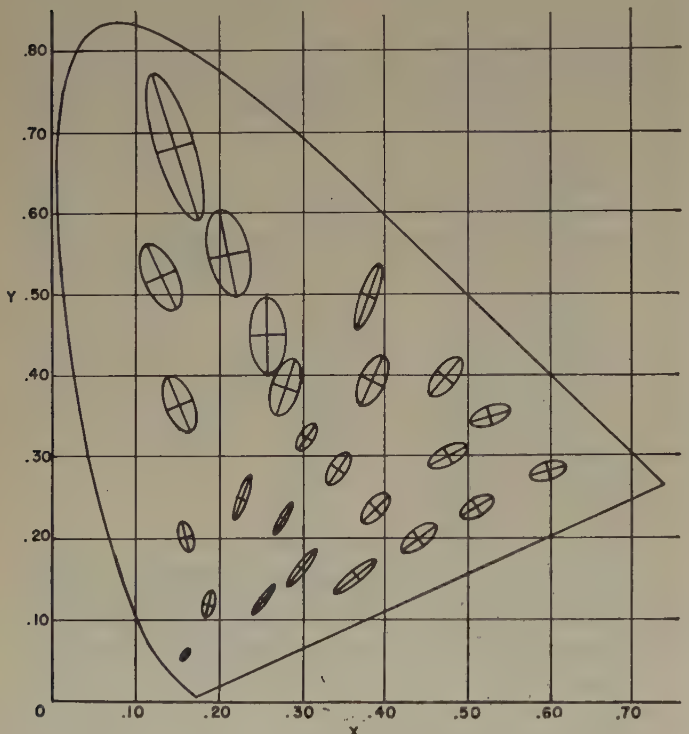

Fig. 3—Equally noticeable chromaticity differences.

MacAdam has carefully worked out a special differential geometry for the complicated surface necessary to represent such equal chromaticities, which allows color differences to be evaluated conveniently in accordance with his data. Several workers[4,5] in the field of color have indicated a preference for the specification of color tolerances in terms of multiples of MacAdam's arbitrary unit of equal noticeability. Epstein[6] has used MacAdam's data in a color television problem.

If one starts with a difference (dx, dy) between the original and reproduced chromaticity, and coefficients (g_{ik}) which MacAdam has evaluated over the chromaticity diagram, a number of just noticeable chromaticity difference (JNCD) units (ds) is arrived at for this error by means of an equation for such ellipses:

$$ds^2 = g_{11}dx^2 + 2g_{12}dxdy + g_{22}dy^2.$$

The value of ds will represent approximately the subjective reaction to the color error, the number of times that the perceived chromaticity difference is greater than the minimum difference that a normal observer can distinguish. The coefficients g_{ik} were evaluated numerically from the size and orientation of the ellipse axes at the explored centers and, at intermediate points, by interpolation. MacAdam[3] has published three contour diagrams of the values of these coefficients.

Regardless of the exact physical significance of this ds unit, we have a convenient means of evaluting the relative significance of chromaticity errors and thereby also of evaluating color television receiver errors. It is to be expected that the shape and size of acceptability boundaries will differ from one reproducing process to another and for various classes of observing conditions. In fact, slightly different noticeability data are available[7] based on different adaptive conditions of the eye. MacAdam[3] believes that to a fair first approximation the 50 per cent or greater acceptance boundaries will be similar to the ellipses of equal noticeability. Davidson[4] has done experimental work which leads him to believe too that mainly a distinction of size separates "perceptible" and "acceptable" color differences. Halsey[8] has reported an experimental investigation of the question whether large color differences can be measured in terms of a number of just noticeable differences. The results were not conclusive, but the answer is probably in the affirmative. This subject will be treated below as part of the analysis of experimental results, where an effort is made to evaluate the factor relating tolerable deviations to noticeable chromaticity differences for color television reproduction.

When any of the receiver signals are in error, both luminance and chromaticity differences will be produced. There was no effort to evaluate combined luminance and chromaticity differences, but only the latter. For the order of magnitude of the errors involved, the typical television viewer should be much more critical of chromaticity differences than luminance differences, since memory can often serve him in evaluating the former. He will probably be provided with a control for luminance level. For combined evaluations, the burden of calculation becomes prohibitive. It makes no difference to chromaticity results what initial luminance level is assumed for the color under investigation.

---

[3] D. L. MacAdam, "Quality of color reproduction," Proc. I.R.E., vol. 39, pp. 468–485; May, 1951.

[4] H. R. Davidson and E. Friede, "The size of acceptable color differences," *Jour. Opt. Soc. Amer.*, vol. 43, pp. 581–589; July, 1953.

[5] G. W. Ingle, and L. Rudick, "A comparison of the MacAdam and the Adams-Nickerson indexes of color differences," *Jour. Opt. Soc. Amer.*, vol. 43, pp. 501–504; June, 1953.

[6] D. L. Epstein, "Colorimetric analysis of RCA color television system," *RCA Review*, vol. 14, pp. 227–258; June, 1953.

[7] D. B. Judd, "Color in Business, Science, and Industry," John Wiley and Sons, Inc., New York, N. Y., pp. 238–251; 1952.

[8] R. M. Halsey, "A comparison of three methods for color scaling," *Jour. Opt. Soc. Amer.*, vol. 44, pp. 199–206; March, 1954.

Since it is necessary to consider relatively large errors in a colorimetric sense, it is important to investigate the effect of possible changes in MacAdam's coefficients for large chromaticity differences. The significance of these changes varies over the chromaticity diagram. For the range of acceptable color differences, these changes are not generally significant.

Reproduction of Flesh Color

To sum up the procedure, a typical flesh color was chosen, calculations made of the signals which should exist in different circuits for typical television receivers, these signals allowed to depart from their optimum value, and determination made of the new color produced. The deviation from the optimum flesh color chromaticity was evaluated by means of the number of MacAdam's just noticeable chromaticity difference units. The reference flesh color, along with other colors investigated, is shown plotted on the CIE chromaticity diagram in Fig. 4.

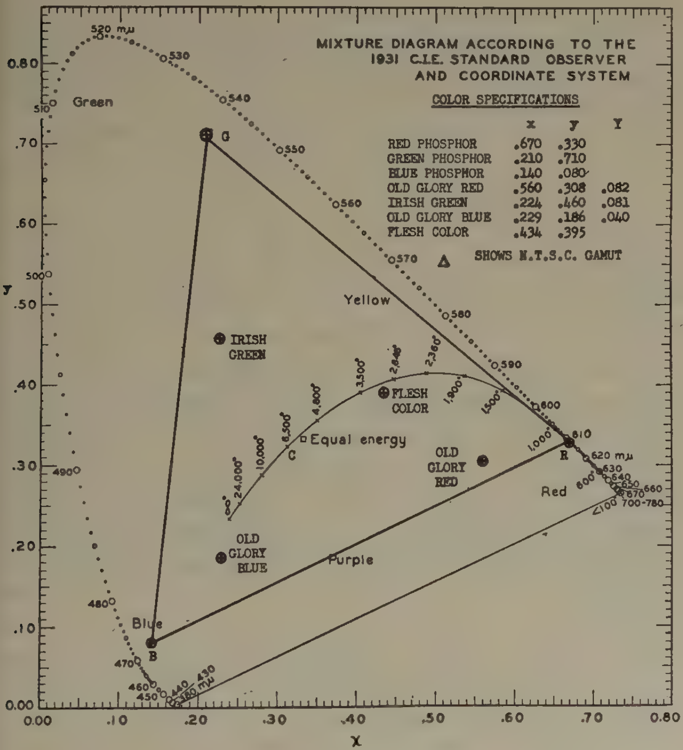

COLOR SPECIFICATIONS

	x	y	Y
RED PHOSPHOR	.670	.330	
GREEN PHOSPHOR	.210	.710	
BLUE PHOSPHOR	.140	.080	
OLD GLORY RED	.560	.308	.082
IRISH GREEN	.224	.460	.081
OLD GLORY BLUE	.229	.186	.040
FLESH COLOR	.434	.395	

Fig. 4—Color specifications.

One assumption used in this analysis is that at the antenna terminals a perfect signal is being received, for deviations are calculated from the theoretical values necessary to reproduce the chromaticity of the picture element under scan. If this is not the case, then the allowable receiver tolerances will have to be adjusted. It is further assumed that the picture tube phosphors are in accordance with NTSC specifications and that identical gammas prevail at transmitter and receiver.

In Fig. 5 can be seen the calculated results of varying the gamma-corrected red, green, or blue gun drive from the optimum value it should have for flesh color reproduction. For errors up to 40 per cent in either direction, the number of color difference units may be read off. If one decides, for example, that 25 JNCD units are the limit of acceptability, then by going horizontally across at this ordinate level until the curves are intersected, the plus and minus per cent drive changes from optimum that may be tolerated on any individual gun can be determined, given perfect signals on the other guns. This would allow, for example, a 15 per cent decrease in the G' signal from optimum. One can see that red and green are almost equally significant in the reproduction of flesh color and that each is about three times as significant as blue.

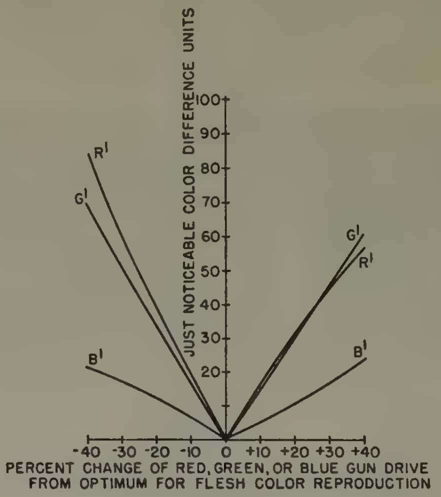

Fig. 5—Calculated effect of R', G', or B' errors on flesh color reproduction.

No matter what the source of receiver error, if it can be translated into a per cent drive change on a gun, the effect on perception in the flesh color region can be determined from Fig. 5. The results of combined drive changes have not been evaluated. If all the drives change uniformly, chromaticity will not be affected, though luminance will. If one of the drives changes relative to the other two, the effect of the unbalance can be determined by going to this figure.

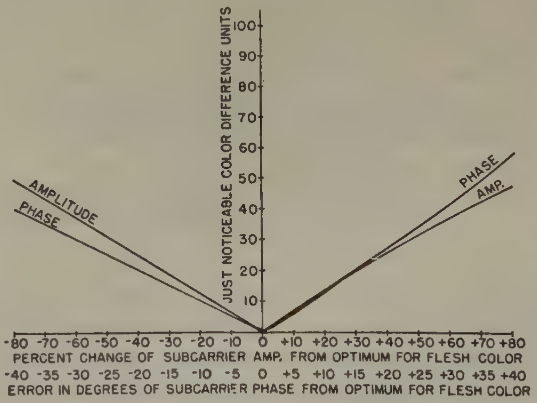

Fig. 6—Calculated effect of chrominance signal amplitude or phase errors on flesh color reproduction.

Fig. 6 shows the seriousness of deviations of phase or amplitude of the chrominance signal from the optimum value for flesh color reproduction. It may be noted that the receiver is less than half as sensitive to subcarrier amplitude errors as to red and green drive errors.

Fig. 7 applies only to a receiver detecting R'-Y' and B'-Y' gamma-corrected color-difference signals. Y' is the gamma-corrected luminance signal. It shows little sensitivity to positive errors, but a great deal to large decreases from optimum. An interesting phenomenon occurs occasionally for large signal errors. For example, once Y' is decreased over 58.5 per cent from the optimum for flesh color reproduction, the drive on the blue gun goes negative. Since there is no negative light, the contribution of that gun to the matrix relations is taken as zero. However, the negative-going component may upset the normal operation of the diode dc restorers and affect the background level produced by that gun.

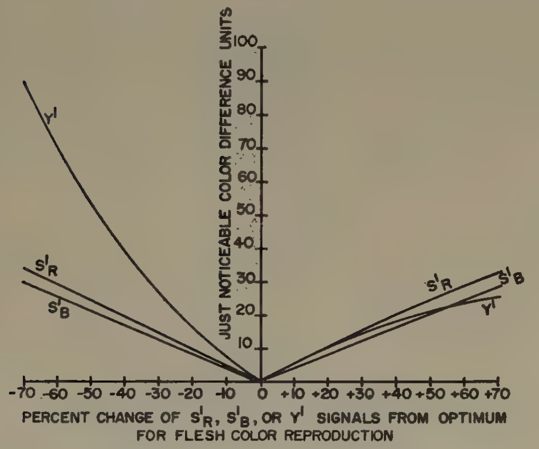

Fig. 7—Calculated effect of S'_R, S'_B or Y' signal errors on flesh color reproduction.

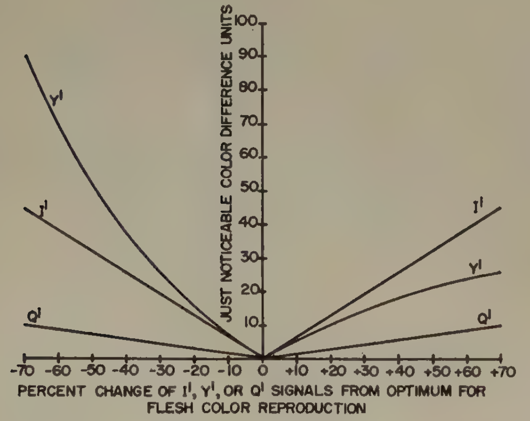

Fig. 8—Calculated effect of I', Y', or Q' signal errors on flesh color reproduction.

Fig. 8 summarizes a study of errors in a receiver where detection occurs along the I'-Q' axis. The curve for Y' errors is the same as in Fig. 7. The I' calculations indicate that this signal is approximately as sensitive as the B' signal, but much less than R' or G'. The Q' signal is of little significance for the reproduction of flesh color. This is to be expected since the I' axis falls along this region of the chromaticity diagram.

REPRODUCTION OF THREE VIVID TEXTILE COLORS

A brief treatment will be given to the problem of reproducing other colors. Three vivid textile colors (Fig. 4) were chosen as representing practical limits of the chromaticity of typical televised scenes. For R', G', and B' errors, the analytical methods of the flesh color study were used. For the other signals, use was made of Howells' "chromaticity grid" shown in Fig. 2.

Rather than presenting graphs for the individual signal errors as was done for flesh color, tables are given which compare for the various colors the errors necessary to produce the arbitrary 25 JNCD units. In Table I are shown the calculated R', G', and B' drive errors which correspond to the assumed tolerance. By going vertically under each signal, it can be seen which color sets the tolerable error limit on each gun, for example, flesh color reproduction on the green gun. By reading across, it can be seen that in reproducing blue, for example, there is greatest sensitivity to red drive changes.

TABLE I

COMPARISON OF THE PER CENT DRIVE CHANGES NEEDED TO GIVE 25 JNCD UNITS FOR FOUR COLORS

Color	R' Per Cent Error		G' Per Cent Error		B' Per Cent Error	
	+	−	+	−	+	−
Flesh Color	16	14	16	15	41	50
Old Glory Blue	13	14	30	37.5	22.5	15
Irish Green	60	>100	60	30	40	36
Old Glory Red	75	28	55	>100	47	60

Even vivid textile colors do not have high excitation purities. As a result, when reproducing the red, green, and blue, substantial signals are present on the guns representing the other primaries. Table II shows the relative gun drives for optimum reproduction of the reference colors. This table should be read across only. The strongest signal was used as a reference (unity) for each color.

TABLE II

RELATIVE GUN DRIVES FOR OPTIMUM REPRODUCTION OF REFERENCE COLORS*

Color	R'	G'	B'
Flesh Color	1.00	0.79	0.48
Old Glory Blue	0.57	0.50	1.00
Irish Green	0.37	1.00	0.59
Old Glory Red	1.00	0.26	0.36

* Note: Strongest signal used as reference (unity) for each color. Read across only.

Table III is a comparison of the chrominance signal amplitude or phase errors needed to give 25 JNCD units. Aside from the sensitivity to negative error in reproducing red, amplitude errors are limited again by flesh color reproduction, with about ±40 per cent tolerable. For phase errors, red reproduction is the most

TABLE III

COMPARISON OF AMPLITUDE AND PHASE CHANGES NEEDED TO GIVE 25 JNCD UNITS FOR FOUR COLORS

Color	Amplitude Per Cent Error		Phase Degrees	
	+	−	+	−
Flesh Color	40	40	18.5	24.5
Old Glory Blue	50	36.5	13.5	17.5
Irish Green	52	55	14	16
Old Glory Red	50	27	12.2	10.5

critical, ±10 to 12 degrees error being possible for the stated tolerance. Table IV shows comparative results for the R'-Y', B'-Y' and Y' signals. The color difference signals are generally the least sensitive ones.

TABLE IV

COMPARISON OF PER CENT ERROR OF S'_R, Y', AND S'_B NEEDED TO GIVE 25 JNCD UNITS FOR FOUR COLORS

Color	S'_R Per Cent Error		Y' Per Cent Error		S'_B Per Cent Error	
	+	−	+	−	+	−
Flesh Color	50	51	65	28	61	58
Old Glory Blue	≫100	≫100	66.7	33.3	50	40
Irish Green	80	50	125	34	100	>100
Old Glory Red	50	27	37	33.3	>100	>100

$$S'_R = \frac{R' - Y'}{1.14} \qquad S'_B = \frac{B' - Y'}{2.03}$$

EXPERIMENTAL RESULTS

It has not been possible to confront the calculated results with extensive experimental evidence. The testing problem is quite complex because of the present level of the color television art and because of the many physical and psychological variables involved. Some preliminary tests will be reported here, but the tentative nature of the conclusions should be kept in mind.

Wherever feasible, duplication of home viewing conditions was attempted. Four Kodachrome transparencies were used, two being standard NTSC subjects, the Watermelon Girl and the Fruit Bowl, and two being specially prepared, Figs. 9 and 10. One hundred conditions were imposed for each transparency. Attenuator boxes were placed in the various signal lines and errors introduced which produced color deviations from the optimum reproduction. Ten technical observers rated the quality of reproduction on a good color receiver. They were not aware of the nature of the signal errors and were instructed to judge chromaticity differences while ignoring brightness changes.

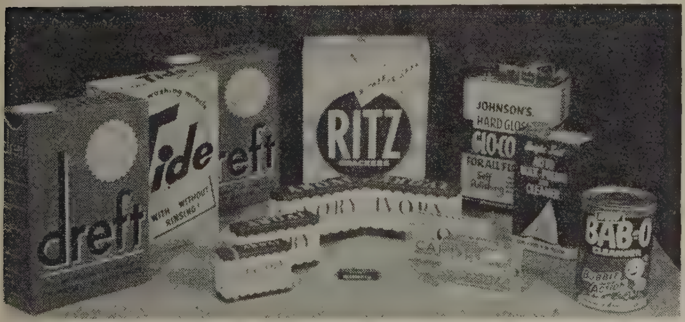

Fig. 9—Photograph of special subject.

Ratings were made in accordance with the standard NTSC scale:

1—Excellent
2—Good
3—Passable
4—Not Quite Passable
5—Poor
6—Not Usable

When requested to state the limit of acceptability on this scale, the viewers averaged a rating of 3.5.

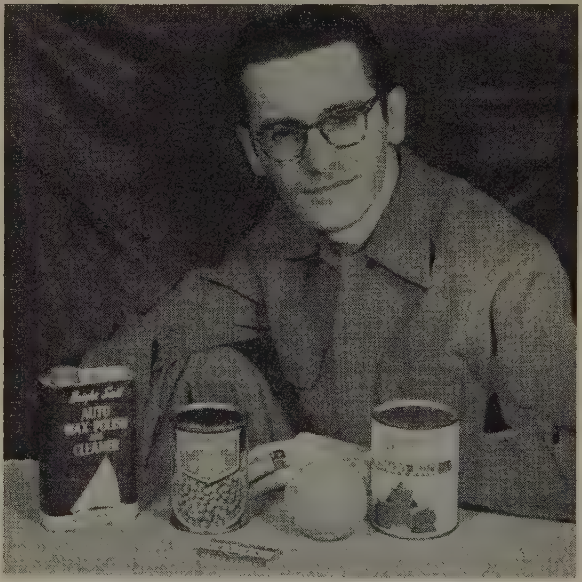
AUTO WAX POLISH AND CLEANER

Fig. 10—Photograph of special subject.

For the two NTSC slides, all the errors for each signal were made consecutively, while for the two special slides a random sequence was used. It developed that the observers were on the average 30 per cent more critical for the special slides than the NTSC ones. This may be attributed to the more sensitive subject matter of the former slides and the fact that random errors make viewers more critical, rather than gradually conditioning them to a certain type of error such as occurred with the NTSC slides.

Calculations were based on individual colors, while in the experiments a multitude of colors were present which makes direct comparison difficult. Flesh color provides some basis for comparison. In Figs. 11 to 14, on the following page, are shown average ratings for the different signals for the two transparencies with prominent flesh color. It should be noted that the scales differ from those used in Figs. 5 to 8.

The closest correlation between experimental and analytical results came from the subject shown in Fig. 10.

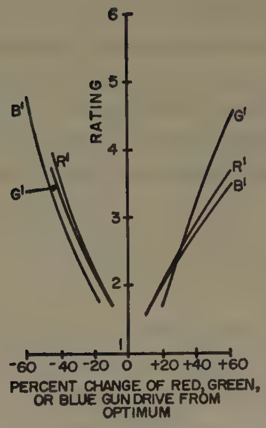

Fig. 11—R', G', B' signals. Average ratings for two transparencies with flesh color.

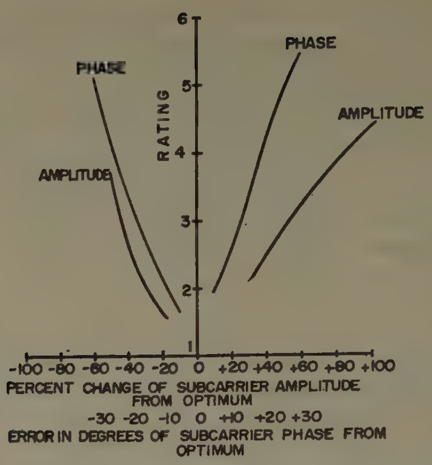

Fig. 12—Chrominance signal amplitude or phase. Average ratings for two transparencies with flesh color.

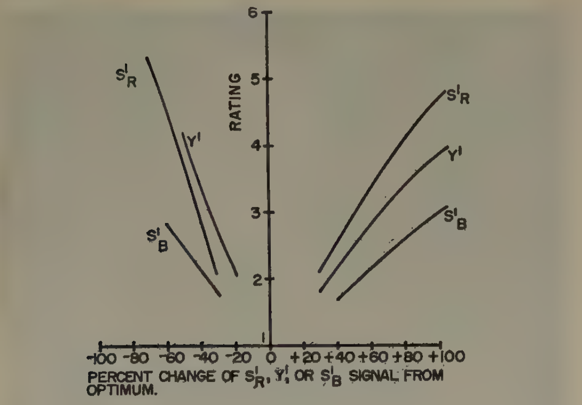

Fig. 13—S'_R, Y', or S'_B signals. Average ratings for two transparencies with flesh color.

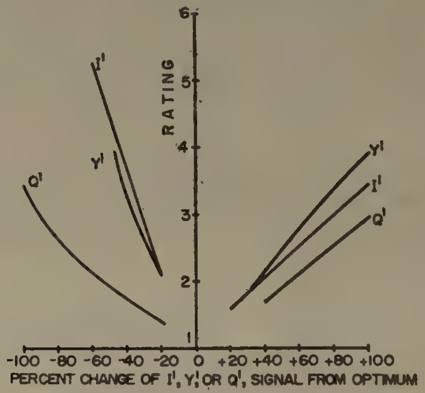

Fig. 14—I', Y', or Q' signals. Average ratings for two transparencies with flesh color.

It was noted that this transparency was very sensitive to changes in flesh color and all the observers indicated that their judgment of the quality of color reproduction for this test was based primarily on the rendition of flesh color. It must be kept in mind that results based on this transparency will be conservative, for it evoked the most critical responses from the technical observers of all the subjects used. The designer is interested primarily in such critical subject matter.

When ratings are plotted against errors for the critical transparency for each of the signals, curves such as shown in Figs. 11 to 14 result, but which are not shown here. If one moves across horizontally at the 3.5 ordinate acceptability limit, the intersections with the critical curves give the maximum tolerable errors in the positive and negative directions, for example, +32 per cent for R'. For each of these errors one can go to the appropriate flesh color theoretical curve and determine the number of just noticeably different chromaticity units which correspond to this limit of acceptability.

Table V compares for the different signals the tolerable experimental errors for the subject of Fig. 10 against flesh color calculations. In the former case the 3.5 acceptability rating is used, while for the calculated results 27.5 just noticeably different chromaticity units were found appropriate. The signals are listed in de-

TABLE V

PERMISSIBLE ERROR IN PER CENT FOR FLESH COLOR REPRODUCTION, OTHER SIGNALS BEING PERFECT

−Per Cent			
Experimental 3.5 Rating		Calculated $DS=27.5$	
G'	27	R'	15
R'	28	G'	17
Y'	30	Y'	30
I'	34	I'	43
B'	35	S.C. Ampl.	43
S.C. Ampl.	45	B'	55
$R'-Y'$	47	$R'-Y'$	56
$B'-Y'$	86	$B'-Y'$	64
Q'	94	Q'	>100
ϕ	22.5°	ϕ	27°
+Per Cent			
Experimental 3.5 Rating		Calculated $DS=27.5$	
R'	32	R'	17
G'	40	G'	17.5
S.C. Ampl.	44	I'	42
$R'-Y'$	50	S.C. Ampl.	44
B'	53	B'	47
I'	70	$R'-Y'$	56
Y'	72	$B'-Y'$	67
$B'-Y'$	98	Y'	75
Q'	135	Q'	>100
ϕ	20.5°	ϕ	20.5°

creasing order of sensitivity. It may be seen that corresponding signals are seldom more than one position out of order, which underlines the significance of perceptibility data to acceptability criteria.

This table should not give the impression that a 32 per cent increase in the R' signal from optimum can be tolerated at the same time as a 27 per cent decrease in G', for example. Remember that all signal sensitivities were determined for the condition of perfect signals in the other channels. Since an infinite combination of errors is possible, this table shows primarily the relative sensitivity of the different signals. For design purposes the indicated errors will have to be reduced.

It is useful to present the information contained in Table V in another form, which is shown in Fig. 15. The bar chart provides a more ready comparison of the allowable calculated and experimental errors for the different signals. The top group represents the per cent positive deviation from optimum for each signal, the bottom the limit of acceptable negative errors for flesh color reproduction. Under each signal label, the box on the left shows the calculated error permissible for flesh color reproduction based on a standard of 27.5 JNCD units, while the right box shows the experimental error permitted by a 3.5 rating using the critical flesh color transparency.

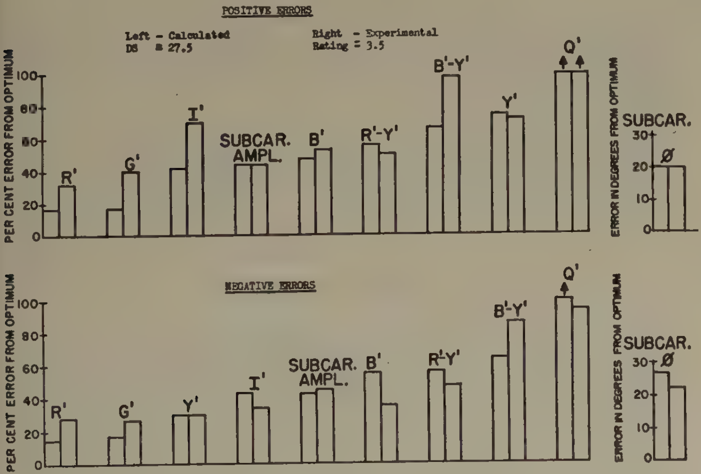

Fig. 15—Permissible calculated and experimental error for flesh color reproduction, other signals being perfect.

The smaller the height of a box, the less tolerable are the errors in that signal. The signals are arrayed from left to right in the order of decreasing sensitivity based on the calculated data. It is evident that R', G' and $-Y'$ remain the most sensitive signals, though experimental results show much less sensitivity in R' and G' than calculations indicate. Plus I' and the B'-Y' signals show more tolerance to error than calculations lead one to expect. B' decreases, on the other hand, show less tolerance. Phase errors and most of the other signals show close agreement.

The Hazeltine Corporation Research Department reported some tests on subjective evaluation of chrominance channel phase and amplitude tolerances. The point where half the observers would accept an error corresponded quite closely to the 3.5 rating point on the critical slide.

Now if acceptability judgments were based solely on a proportionality factor to perceptibility considerations, one would expect the magnitude of the proportionality factor to be consistent from signal to signal. However, there was a range of from 14 to 66 units. Some of the possible reasons for this discrepancy are the limited statistical sample, the inability of observers not to be influenced in their judgments by brightness changes, the influence of other colors besides flesh in the transparency, gamma errors, and considerations of personal taste in color rendition.

The average number of just noticeable chromaticity difference units corresponding to the critical transparency is 34. Because of the large spread, the median of 27.5 was used in the presentation of results. If the average of the two transparencies with flesh color is used to determine the proportionality factor of acceptability to perceptibility, an average of 40 and median of 32 JNCD units result.

SUMMARY AND CONCLUSIONS

A method is shown for approximating the significance of various possible errors in the signals of a color television receiver in terms of typical human color perception.

A receiver is most sensitive to errors in the R' and G' channels and beneficial results may be obtained by some form of gain stabilization of these stages. However, experimental results indicate about twice as much tolerance in these stages as do analytical results. The most sensitive remaining signals in order would then be, for the critical flesh color reproduction, Y' (for decreases), chrominance signal amplitude, I', B', R'-Y' and B'-Y', Y' increases, and Q'. The limit of acceptability on chrominance signal phase appears to range from ±15 to 25 degrees on typical subject matter, though a predominantly red picture may require closer tolerances.

Even when reproducing a deep textile red, green, or blue, substantial signals are present on the guns representing the other primaries. There actually often is greater sensitivity to error in the signals on these other guns. If the average signal on the guns does not vary very much from color to color in typical scenes, the dc restoration problem may be simplified.

The average viewer will tolerate from 25 to 40 just noticeably different chromaticity units for single-signal errors, which is a rather inferior reproduction. Because of possible error combinations and for a conservative approach, this tolerance will have to be materially reduced for design purposes.

A great deal of experimental work is still needed to make clearer why and how viewer tolerances deviate from what one should expect just on the basis of perceptibility data.

Appendix I

DETERMINATION OF RECEIVER SIGNALS

$$\begin{bmatrix} R \\ G \\ B \end{bmatrix} = Y \begin{bmatrix} 1.91 & -0.532 & -0.288 \\ -0.985 & 1.999 & -0.028 \\ 0.058 & -0.118 & 0.898 \end{bmatrix} \begin{bmatrix} \dfrac{x}{y} \\ 1 \\ \dfrac{1-x-y}{y} \end{bmatrix}$$

$$R' = R^{1/\gamma} = R^{1/2}$$

$$G' = G^{1/\gamma} = G^{1/2}$$

$$B' = B^{1/\gamma} = B^{1/2}$$

$$Y' = 0.299R' + 0.587G' + 0.114B'.$$

The signals R'-Y' and B'-Y' can be calculated by direct subtraction.

$$Q' = 0.413(B' - Y') + 0.478(R' - Y')$$

$$I' = -0.268(B' - Y') + 0.736(R' - Y').$$

Howells[2] gives the direct transformation:

$$\begin{bmatrix} I' \\ Y' \\ Q' \end{bmatrix} = \begin{bmatrix} 0.596 & -0.274 & -0.322 \\ 0.299 & 0.587 & 0.114 \\ 0.211 & -0.523 & 0.312 \end{bmatrix} \begin{bmatrix} R' \\ G' \\ B' \end{bmatrix}$$

$$S'_R = \frac{R' - Y'}{1.14} \qquad S'_B = \frac{B' - Y'}{2.03}.$$

For the chrominance signal amplitude and phase:

$$A' = \sqrt{(S'_R)^2 + (S'_B)^2}$$

$$\theta = \tan^{-1} \frac{S'_R}{S'_B}.$$

Appendix II

Chromaticity Change from Chrominance Signal Errors

For a specified color with chromaticity x_0, y_0 and luminance Y_0, one can calculate A'_0 and θ_0 from Appendix I. If the chrominance signal phase angle is in error or its amplitude changes from optimum, we have:

$$S'_R = A' \sin \theta \qquad S'_B = A' \cos \theta$$

$$\begin{bmatrix} R' \\ G' \\ B' \end{bmatrix} = \begin{bmatrix} 1.14 & 1 & 0 \\ -0.581 & 1 & -0.394 \\ 0 & 1 & 2.03 \end{bmatrix} \begin{bmatrix} S'_R \\ Y' \\ S'_B \end{bmatrix}$$

$$R = (R')^\gamma = (R')^2$$

$$G = (G')^\gamma = (G')^2$$

$$B = (B')^\gamma = (B')^2$$

$$\begin{bmatrix} X \\ Y \\ Z \end{bmatrix} = \begin{bmatrix} 0.607 & 0.174 & 0.200 \\ 0.299 & 0.587 & 0.114 \\ 0.000 & 0.066 & 1.116 \end{bmatrix} \begin{bmatrix} R \\ G \\ B \end{bmatrix}$$

where X, Y, Z are the CIE nonphysical primaries.

$$x = \frac{X}{X+Y+Z} \qquad y = \frac{Y}{X+Y+Z}.$$

The shift in chromaticity may then be represented by dx and dy where:

$$dx = x - x_0$$

$$dy = y - y_0.$$

The additional transformation needed to evaluate I' and Q' errors is:

$$\begin{bmatrix} R' \\ G' \\ B' \end{bmatrix} = \begin{bmatrix} 0.956 & 1 & 0.621 \\ -0.272 & 1 & -0.646 \\ -1.106 & 1 & 1.702 \end{bmatrix} \begin{bmatrix} I' \\ Y' \\ Q' \end{bmatrix}.$$

Acknowledgement

The author is grateful to Paul W. Howells, W. J. Gruen, W. E. Good, and J. G. Humphrey for their encouragement and advice during the course of this investigation, and to members of the Electronics Laboratory and Radio and Television Department of the General Electric Company who aided in the experimental work.

* * *

Coupling of Modes in Helixes*

J. R. PIERCE†, FELLOW, IRE AND P. K. TIEN†, ASSOCIATE, IRE

Summary—**Propagation on a helix as a function of frequency is characterized by ranges in which there is a slow wave which can be explained as very nearly a transverse electromagnetic wave traveling along the wire, and ranges in which the helix does not propagate; these are associated with "forbidden regions" of propagation constant pointed out by Sensiper. Each mode of propagation consists of an infinite number of spatial Fourier components called spatial harmonics. The complicated behavior with frequency of the modes of a helix is explained as an effect of the coupling through spatial harmonics of the slow wave which travels with about the velocity of light along the wire to fast free-space or waveguide waves which travel with about the velocity of light along the axis. The qualitative effects of such coupling agree with a tape-helix analysis of helixes in free space and helixes surrounded by a conducting tube. The case of the bifilar helix is also treated.**

INTRODUCTION

THE HELIX is of great importance as a circuit for traveling-wave tubes. No exact treatment of propagation on a helix has been given. In the papers of Pierce,[1] Phillips and Malin,[2] and others, the electromagnetic waves of a helix were investigated by assuming the helix to be an ideal cylinder with conduction in the helical direction only. The studies which idealize the actual helix as a conducting sheath are generally known as the "sheath" theory. This gives almost correct solutions for the propagating modes, although it neglects the space harmonic fields and fails to predict the forbidden regions,[3] or forbidden ranges of propagation constant. A more satisfying approach called the "tape" theory has recently been given by Sensiper,[3] following some early studies known as the "exact approach" by Phillips,[4] Sollfrey[5] and Hsu.[6] Sensiper assumed the helix to be wound of an infinitely thin conducting tape and took the electric field at the center line of the tape to be zero as one of the boundary conditions. According to his theory, the electromagnetic waves on the helix consist of various sets of propagating modes separated from each other by the forbidden regions. The details of the propagating characteristics are quite complicated and unfortunately can only be worked out by rather tedious numerical calculations. The physical picture of the propagating behavior is thus not very clear.

A study of various helix modes obtained by both the sheath and the tape theories indicates that they are made up of waves of very simple characteristics. It is the effect of the continuous coupling between these waves which complicates the propagating behavior. The primary interest of this paper is to introduce a new concept in analyzing helix waves. It will be shown that by means of the theory of the coupled waves, the somewhat obscure behavior of the helix propagation becomes clear and obvious. See Fig. 1.

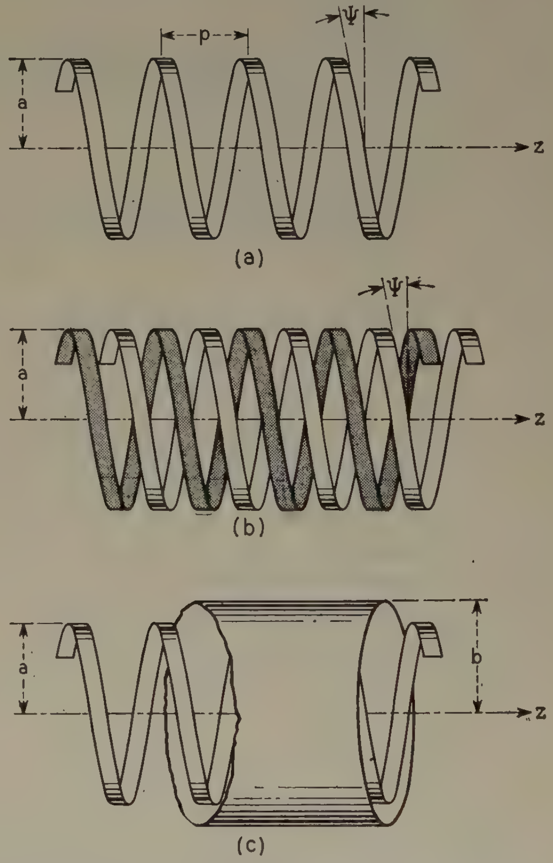

Fig. 1—(a) Single-wire helix; (b) bifilar helix; (c) helix inside a conducting pipe.

SHEATH AND TAPE THEORIES

To introduce notation necessary in later discussion, it seems advantageous to review some basic properties of the helix waves. The solution of the wave equation in the cylindrical co-ordinates (r, z, θ), and satisfying the periodicity of the helix is in the form[3]

$$A_m e^{-j(\beta_m z - m\theta)} \left\{ \begin{array}{l} I_m\left(\eta_m \dfrac{r}{a}\right) \\ \\ K_m\left(\eta_m \dfrac{r}{a}\right) \end{array} \right. \qquad (1)$$

---

* Decimal classification: R117. Original manuscript received by the IRE, April 26, 1954; revised manuscript received, May 28, 1954.

† Bell Telephone Labs., Murray Hill, N. J.

[1] J. R. Pierce, "Theory of the beam type traveling-wave tube," PROC. I.R.E., vol. 35, p. 108; February, 1947.

[2] R. S. Phillips and H. Malin, "A Helical Wave Guide II," Res. Rep. 170–3 of the N.Y.C. Math. Res. Group; August, 1947.

[3] S. Sensiper, "Electromagnetic Wave Propagation on Helical Conductors," M.I.T. Res. Lab. of Elec. Rep. No. 194; May, 1951.

[4] R. S. Phillips, "The Electromagnetic Field Produced by a Helix," Rep. TW-11 of the N.Y.U. Math. Res. Group; June, 1949.

[5] W. Sollfrey, "Propagation Along a Helical Wire," Rep. TW-10 of the N.Y.U. Math. Res. Group; June, 1949.

[6] C. P. Hsu, "Theory of Helical Waveguides and Helical Radiators," Harvard Univ. Cruft Lab. Tech. Rep. No. 93; January, 1950.

where

$$\eta_m^2 = \beta_m^2 a^2 - k^2 a^2. \tag{2}$$

A_m is the constant associated with the solution. m may be any positive or negative integer including zero. $I_m(\eta_m r/a)$ and $K_m(\eta_m r/a)$ are respectively modified Bessel functions of mth order of the first and second kinds. ω is the angular frequency, β_m, the phase constant for propagation in the axial direction, and a the radius of the helix. ka is the ratio of the circumference of the helix to the free-space wavelength, a quantity directly proportional to the operating frequency. We may thus express the electric or magnetic fields about the helix in the form of (1), with the I_m function for the fields inside the helix and the K_m function for those outside the helix.

In the sheath theory, the helix is idealized as a cylinder with conduction in the helical direction only. We are thus specifying the direction of the electric fields and that of the current density at the surface of the helical cylinder, but not the forms of their distribution. The expression (1) may be used with any value of m in satisfying the boundary conditions (the conditions at the surface of the helix), and each value of m gives an independent solution.

In the tape theory, however, the electric fields as well as the current density must be distributed properly on the helix surface. That is, the tangential electric fields on the conducting tape and the currents in the gap between tapes must be zero. It is therefore necessary to sum up the solutions with all the values of m to satisfy the field and the current distributions specified by the tape theory at the boundary of $r=a$. The solution (1) is then no more an independent solution, but only one of the Fourier components of the entire solution.

In the sheath theory the phase constant β_m is obtained from the following determinantal equation:[1,3]

$$\frac{(\eta_m^2 - m\beta_m a \cot\psi)^2}{\eta_m^2 k^2 a^2 \cot^2\psi} = -\frac{I_m'(\eta_m)K_m'(\eta_m)}{I_m(\eta_m)K_m(\eta_m)} \tag{3}$$

where the prime denotes the derivative with respect to the argument. $\cot\psi = 2\pi a/p$, where p is the pitch of the helix. The solution of (3) is not unique; each solution is a propagating mode. We may thus have many modes for each value of m.

In the tape theory,[3] the determinantal equation is

$$\sum_m \left(\left(\beta_0^2 a^2 - k^2 a^2 + k^2 a^2 \frac{m^2 \cot^2\psi}{\eta_m^2} \right) I_m(\eta_m)K_m(\eta_m) + k^2 a^2 \cot^2\psi\, I_m'(\eta_m)K_m'(\eta_m) \right) D_m \cong 0 \tag{4}$$

where D_m is a quantity determined by the distribution of the current density assumed over the conducting tape.[3] For a narrow tape helix, it is[3]

$$\frac{\sin(m\pi\delta/p)}{m\pi\delta/p} \tag{5}$$

where δ is the width of the tape. Again, the solution of (4) is not unique; each solution is considered as a propagating mode. β_0 is generally obtained from (4). Because of the periodicity of the helix, the phase constants of other Fourier components of the mode can be calculated from β_0 by the relation[3]

$$\beta_m a = \beta_0 a + m \cot\psi. \tag{6}$$

It is obvious from (6) that all the components belonging to a common mode must have a common group velocity, as it should be. Thus, in the tape theory each propagating mode consists of an infinite number of Fourier components. These component waves have the basic form of (1) and their phase constants are related to each other according to (6). As (1) varies angularly as $e^{jm\theta}$ and as each value of m corresponds to one component of the mode, the electromagnetic field distributions of the components of a propagating mode are orthogonal to each other. However, when two or more modes are present at the same frequency, two different modes may contain components having the same value of m; these components are no longer orthogonal and are consequently coupled. The effect of the coupling is strongest when phase velocities of the components of the modes are close to each other. A similar situation occurs in the sheath theory because two or more propagating modes with the same value of m always exist.

Although (3) and (4) are based on different theories, we can easily show in the following manner that they generally give similar results: When none of the η_m's in (4) or (3) approaches zero, we may substitute $I_m'(\eta_m)K_m'(\eta_m)$ by

$$-\frac{m^2 + \eta_m^2}{\eta_m^2} I_m(\eta_m)K_m(\eta_m)$$

with only a small percentage of error.[3] Both (3) and (4) then give the same solution

$$\beta_m a = (k^2a^2\cot^2\psi + k^2a^2)^{1/2} + m\cot\psi$$
$$\cong (ka + m)\cot\psi. \tag{7}$$

If one of the η_m's, say η_s, approaches zero, the terms of the sth component in (4) become rapidly changing functions, while the rest of the terms are much smaller in magnitude and vary only slightly with η_m's. Thus, we may neglect all the terms of (4) except those with $m=s$. This again reduces (4) to the form of (3).

In order to avoid confusion, we will base the following discussion on the tape theory unless otherwise specified. We will, however, frequently use (3) instead of (4) to solve for phase constants of the propagating waves, because, mathematically, (3) is much simpler, and, as argued above, gives essentially the same results as (4).

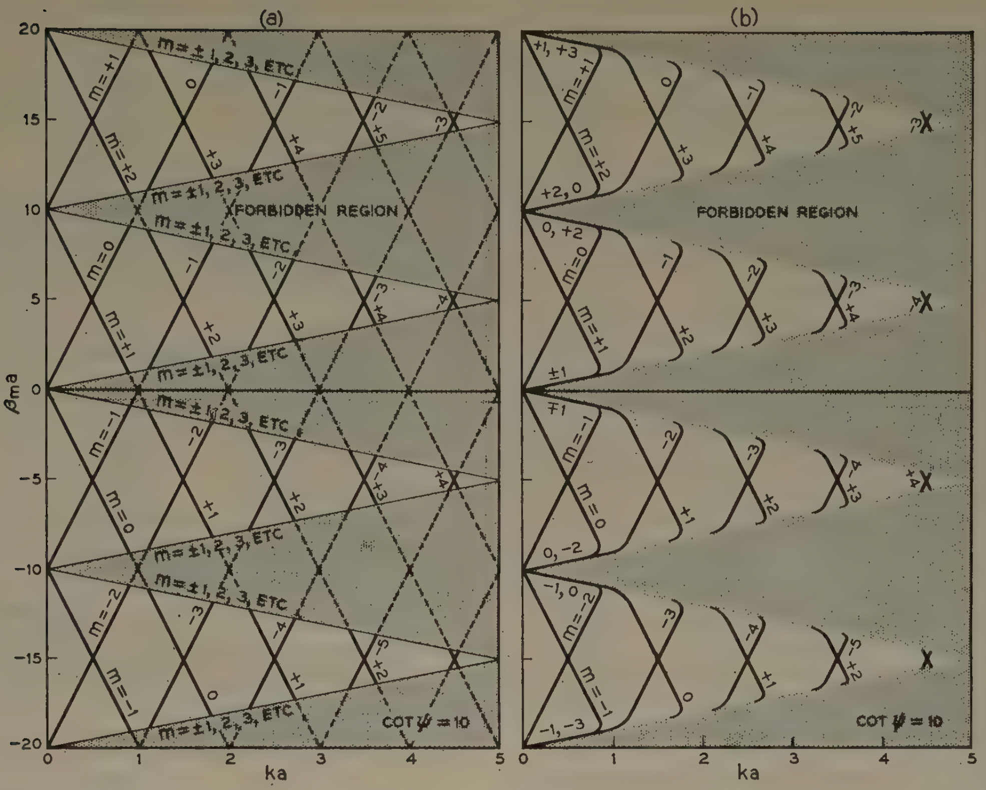

Fig. 2—(a) Approximate solutions of the determinantal equation, cot $\psi=10$; (b) Frequency characteristics of the helix waves solved by the tape theory, cot $\psi=10$.

SOLUTIONS OF THE DETERMINANTAL EQUATION

To give a general idea about the solutions of the determinantal equation, replace $I_m'(\eta_m)K_m'(\eta_m)/I_m(\eta_m)K_m(\eta_m)$ of (3) by $-(m^2+\eta_m^2)/\eta_m^2$; the approximation is good when $\eta_m>0$ and $|m|\geqq 1$. We thus have an approximate determinantal equation,

$$\eta_m^2(\eta_0^2 - k^2a^2 \cot^2 \psi) = 0$$

which gives the solutions

$$\eta_m = 0, \qquad m = \pm 1, \pm 2, \pm 3, \cdots \tag{8}$$

and

$$\eta_0 = ka \cot \psi. \tag{9}$$

From (2) and (6), and neglecting (1) as compared with $\cot^2\psi$ such that η_0 of (9) may be replaced by β_0, we have respectively from (8) and (9)

$$\beta_m a = ka, \qquad m = \pm 1, \pm 2, \pm 3, \cdots \tag{10}$$

and

$$\beta_0 a \cong ka \cot \psi. \tag{11}$$

It is seen that the helix propagation consists essentially of one "slow-wave" mode and many "fast-wave" modes. The slow-wave mode as given by (11) travels with an axially directed group velocity equal to the velocity of light divided by the value of cot ψ; and the fast-wave modes, as given by (10), have their axially directed group velocities equal to the velocity of light.

The phase constants of various components are plotted versus ka in Fig. 2(a) for the modes given by (10) and (11). Many sets of parallel lines known as the frequency characteristics are shown in the figure. In general, because of (6) the frequency characteristics (the phase constants versus ka curves) of a propagating mode consist of a family of parallel curves with one curve for each component, separated each other vertically by an interval of cot ψ. The slope of the curves is evidently the reciprocal of the group velocity. Thus, when the slope is positive, the mode carries power in the positive-z direction, and when the slope is negative, the power flows in the opposite direction.

For an open structure like the helix[3,7] η_m cannot be imaginary, for then the modified Bessel functions would be replaced by the ordinary oscillatory Bessel functions characteristic of propagation in circular waveguides. We may also express this by saying that none of the Fourier components of a propagating mode may have a phase velocity greater than the velocity of light. The situation is different when the helix is surrounded by a conducting pipe, for then the field distributions in-

---

[7] R. B. Adler, "Properties of Guided Waves on Inhomogeneous Cylindrical Structures," M.I.T. Res. Lab. Tech. Rep. No. 102; May, 1949.

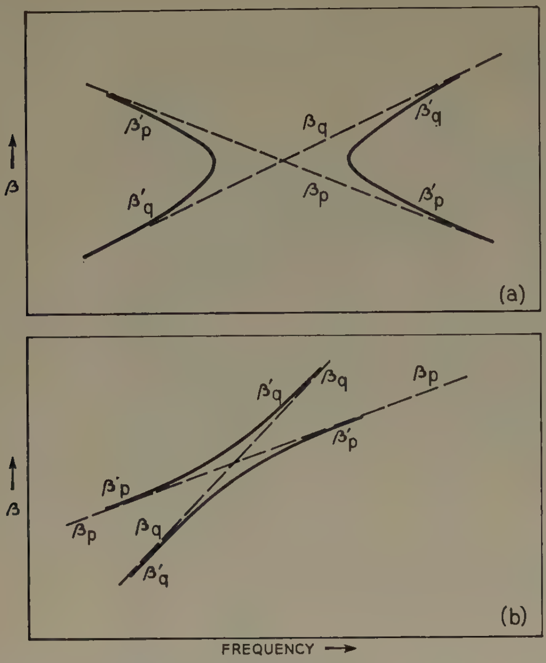

Fig. 3—General behavior of the coupling modes: (a) two modes carry power in opposite directions; (b) two modes carry power in the same direction.

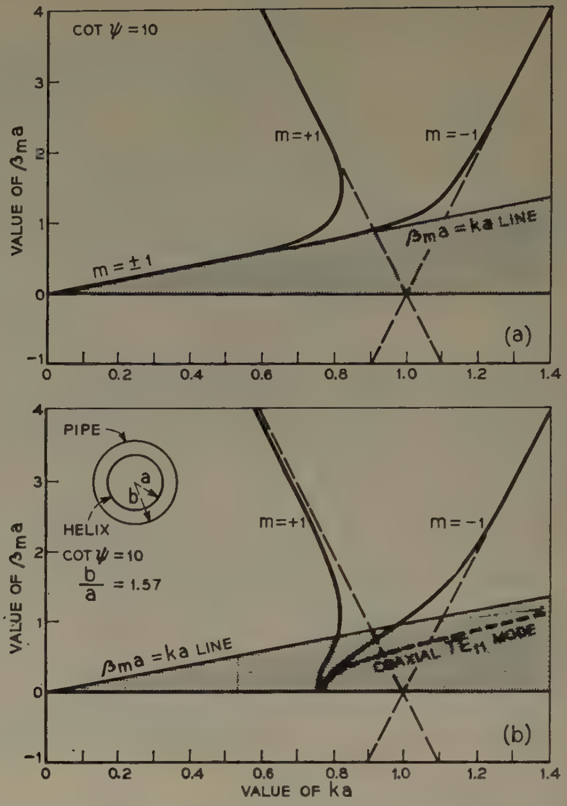

Fig. 4—Helix waves at $ka<1.5$, cot $\psi=10$: (a) for an open helix; (b) for a helix inside a conducting pipe ($b/a=1.57$).

side the conducting pipe may be expressed by the ordinary Bessel functions and the phase velocity may be greater than the velocity of light. Thus, for an open helix $\beta_m a$ may be greater or equal to, but not smaller than ka. This means that in the $\beta_m a$ versus ka diagram [Fig. 2(a)], a set of shaded regions known as the forbidden regions can be drawn. Inside these regions, $\beta_m a<ka$, propagation is impossible, and consequently the propagating characteristics should be omitted there. If the propagating mode contains all the Fourier components, as it does in general, the forbidden region will repeat according to (6) at every interval of cot ψ [Fig. 2(a) and (b)]. In the case of the bifilar helixes, some modes contain the components with m = even only, and some, with m = odd only, and the forbidden regions are then spaced by an interval of 2 cot ψ as shown in Fig. 6(a) and (b).

Exact solutions of the determinantal equation have been obtained by Sensiper[3] and are plotted in Fig. 2(b) for comparison. It may be seen that they are much more complicated in nature. Before we explain them as a result of the continuous coupling between the waves of simpler characteristics, we will study the general behavior of the coupled waves.

THEORY OF THE COUPLING MODES

General relations concerning coupling of two unattenuated modes of propagation deduced from the linearity and conservation of energy have been given in a recent paper by Pierce.[8] Suppose we have two modes of propagation which in the absence of the coupling would have waves of phase constants β_p and β_q respectively. It is shown in the appendix that if these modes are coupled continuously, they will combine to form two new modes with waves of phase constants,

$$\beta_p' = \frac{1}{2}\left[\beta_p + \beta_q + (\beta_p - \beta_q)\sqrt{1 \pm \frac{d^2}{(\beta_p - \beta_q)^2}}\right] \qquad (12)$$

$$\beta_q' = \frac{1}{2}\left[\beta_p + \beta_q - (\beta_p - \beta_q)\sqrt{1 \pm \frac{d^2}{(\beta_p - \beta_q)^2}}\right]. \qquad (13)$$

The minus sign in the radical applies if the original modes carry power in opposite directions, the plus sign, if the original modes carry power in the same direction. d is the coupling factor as defined by (19) in the Appendix.

Fig. 3(a) shows the general nature of the behavior of β versus frequency for two modes carrying power in opposite directions. The dashed lines are for the original uncoupled modes. With coupling, as β_p approaches β_q, the modes combine to give a mode with zero group velocity. Fig. 4 shows the general behavior of two modes carrying power in the same direction. Again the dashed lines indicate the original modes. As β_p approaches β_q, the modes become mixed, giving two β versus frequency curves which shear off from one another. In either Fig. 3(a) or (b), the separation between two curves increases as the coupling factor d is increased.

HELIX WAVES AT $ka<1.5$

A study of Fig. 2(b) indicates that the helix waves at $ka<1.5$ and those at higher frequencies behave differently. We will thus limit the discussion of this section to waves at $ka<1.5$. For simplicity we will analyze only the propagating characteristics in a region extended from $\beta_m a=0$ to $\beta_m a=\cot\psi$, for those outside this region can be obtained easily by means of (6).

---

[8] J. R. Pierce, "Coupling of modes of propagation," *Jour. Appl. Phys.*, vol. 25, p. 179; 1954.

Intuitively we may consider as the waves basic to the helix, those "slow waves" traveling along the helical winding with a group velocity equal to the velocity of light. Considering the helix as a coiled transmission line, we ought to expect waves of this form. Except at very low frequencies in what is known as the dispersive region, the phase velocity of the $m=0$ component increases as ka decreases, because of the fact that the electromagnetic fields extend radially further outside the helical cylinder when the wavelength becomes longer. Excluding this dispersive effect, we may naively assume, and it turns out in the later discussions to be true, that the only waves basic to the helix are the sort of transverse electromagnetic waves traveling along the helical conductor, given by (11). Here we mean by the transverse electromagnetic waves, the waves transverse in a plane normal to the helical conductor.

In addition to the basic helix mode described above, there are circularly polarized plane waves characteristic of the free space. These travel in the axial direction with the velocity of light. Their electromagnetic fields vary angularly as $e^{+j\theta}$ or as $e^{-j\theta}$ and happen to be in the same form as the $m=+1$ or the $m=-1$ component of the basic helix waves. These helix and plane waves are consequently not orthogonal, and are coupled strongly when their phase velocities are close to each other. The general behavior of the coupled waves described in the last section may therefore be applied to them.

In Fig. 4(a), the phase constants of the basic helix waves and those of the circularly polarized plane waves are plotted in dotted lines. When ka approaches 0.9, the $m=+1$ component of the basic helix mode and the $e^{+j\theta}$ component of the plane wave should combine to form a wave of zero group velocity according to Fig. 3(a), since they carry power in opposite directions. Similarly when $ka=1.1$ is approached, the $m=-1$ component of the basic helix waves and the $e^{-j\theta}$ component of the plane wave should be mixed and give according to Fig. 3(b) two sets of $\beta_m a$ versus ka curves which shear off one another, since they carry power in the same direction. Therefore because of the coupling, the actual waves turn out to be in the form shown by the solid lines [Fig. 4(a)]. Comparing Fig. 4(a) to Fig. 2(b), we find that we have obtained exactly the same picture as that given by the tape theory.

HELIX INSIDE OF A CONCENTRIC CONDUCTING PIPE

It has been argued in the last section that the only propagating mode which may be considered basic to the helix is the one of which, the $m=0$ component travels in the helical direction with a group and phase velocities equal to the velocity of light (except for the dispersive region). The actual helix waves are then shown to be a result of the continuous coupling between this basic mode and the plane waves. If now we surround the helix by a concentric conducting pipe inside which the propagation of the plane waves is eliminated, it is interesting to know what the actual helix propagation will be. We will solve this first by the tape theory and then verify the result by means of coupled waves.

In the tape theory, because of relation (6), it is impossible for a propagating mode to have simultaneously two components with $\beta_m a$'s, less than the value of ka. Suppose now that the phase constant of the sth component is less than ka, replace η_s by jq_s. The electric or magnetic fields outside the helical cylinder and inside the pipe should then be expressed by the $J_s(q_s r/a)$ and $N_s(q_s r/a)$ functions and those inside the helical cylinder by $J_s(q_s r/a)$ function, where $J_s(q_s r/a)$ and $N_s(q_s r/a)$ are respectively the ordinary Bessel functions of sth order of the first and second kinds. The determinantal equation becomes[9]

$$\begin{aligned}
\sum_m{}' \Bigg[&\left(\beta_0^2 a^2 - k^2a^2 + \frac{m^2k^2a^2\cot^2\psi}{\eta_m^2}\right)\left[1 - \frac{I_m(\eta_m)K_m\left(\eta_m \frac{b}{a}\right)}{I_m\left(\eta_m \frac{b}{a}\right)K_m(\eta_m)}\right] I_m(\eta_m)K_m(\eta_m) \\
&+ k^2a^2\cot^2\psi \left[1 - \frac{I_m'(\eta_m)K_m'\left(\eta_m \frac{b}{a}\right)}{I_m'\left(\eta_m \frac{b}{a}\right)K_m'(\eta_m)}\right] I_m'(\eta_m)K_m'(\eta_m)\Bigg] D_m \\
&+ \Bigg[\left(q_s + \frac{s\beta_s a\cos\psi}{q_s}\right)^2 \left[1 - \frac{J_s(q_s)N_s\left(q_s \frac{b}{a}\right)}{J_s\left(q_s \frac{b}{a}\right)N_s(q_s)}\right] J_s(q_s)N_s(q_s) \\
&+ k^2a^2\cot^2\psi \left[1 - \frac{J_s'(q_s)N_s'\left(q_s \frac{b}{a}\right)}{J_s\left(q_s \frac{b}{a}\right)N_s(q_s)}\right] J_s'(q_s)N_s'(q_s)\Bigg] D_s = 0 \qquad (14)
\end{aligned}$$

---

[9] L. Stark, "The Lower Modes of a Concentric Line Having a Helical Inner Conductor," M.I.T. Lincoln Lab. Tech. Rep. No. 26; July, 1953.

where b is the radius of the conducting pipe and Σ' denotes a summation over all the values of m except $m=s$. Again we find that the terms in (14) associated with the sth component are rapidly changing functions, while the rest of the terms vary only slightly with η_m's. Neglecting all the terms other than $m=s$ (14) is reduced to

$$\frac{(q_s^2 + m\beta_s a \cot\psi)^2}{q_s^2 k^2 a^2 \cot^2\psi} = -\frac{J_s'(q_s)N_s'(q_s)}{J_s(q_s)N_s(q_s)} \, \frac{\left[1 - \dfrac{J_s'(q_s)N_s'\left(q_s\dfrac{b}{a}\right)}{J_s'\left(q_s\dfrac{b}{a}\right)N'(q_s)}\right]}{\left[1 - \dfrac{J_s(q_s)N_s\left(q_s\dfrac{b}{a}\right)}{J_s\left(q_s\dfrac{b}{a}\right)N_s(q_s)}\right]} \tag{15}$$

which is again the determinantal equation of the sheath theory. The solutions of (15) are illustrated in Fig. 4(b) for $s=\pm 1$ and in Fig. 5(b) for $s=\pm 2$, with the ratio b/a equal to 1.57. Those characteristics can be easily explained by the general behavior of coupled waves. It is seen that with a surrounding pipe the basic helix waves are coupled to one of the coaxial TE waveguide modes, considering the helix as the inner conductor and the pipe, the outer conductor. The phase constants of the basic helix waves and those of the coaxial TE modes are shown in both figures as the dotted lines. It is obvious for example that in Fig. 5(a), the $m=+2$ and $m=-2$ components of the basic helix mode are coupled respectively with the $e^{+2j\theta}$ and the $e^{-2j\theta}$ components of the coaxial TE_{21} mode and the coupled waves, as described above, behave exactly like the solutions of (15).

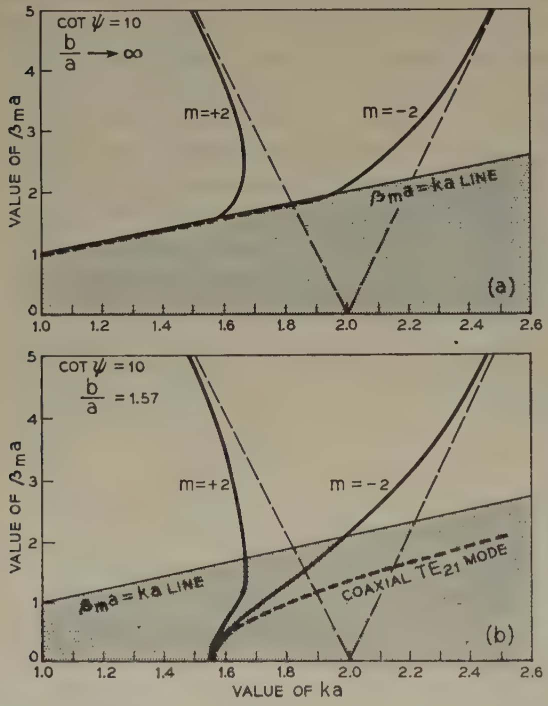

Fig. 5—Helix waves at $1.5<ka<2.5$, $\cot\psi=10$: (a) for an open helix; (b) for a helix inside a conducting pipe ($b/a=1.57$).

Helix Waves at $1.5<ka<2.5$

We will next analyze the propagation of an open helix at $1.5<ka<2.5$. In this frequency range, the $m=\pm 2$ components of the basic helix mode meet the $\beta_m a=ka$ line. The circularly polarized plane waves which vary angularly as $e^{+j2\theta}$ or $e^{-j2\theta}$ do not exist as the solutions of the free space. We may idealize the open helix as a helix surrounded by a conducting pipe and let the diameter of the pipe become infinitely large. In this case, the $m=\pm 2$ components of the basic helix mode are coupled with the $e^{+j2\theta}$ and $e^{-j2\theta}$ components of the coaxial TE_{21} waveguide mode [Fig. 5(a)]. As the diameter of the outer pipe is made infinitely large, the cut-off frequency of the coaxial waves becomes very close to zero and its phase constant versus ka curve approaches the $\beta_m a=ka$ line but always remains inside the forbidden region. Consequently the frequency characteristic of the coupled waves start following the phase constants of the basic helix waves when $\beta_m a \gg ka$, then turn toward the vertical axis because of the coupling with the coaxial mode, later cross the $\beta_m a=ka$ line and finally follow the phase constants of the coaxial TE_{21} mode [Fig. 5(a)]. If we now omit the frequency characteristics inside the forbidden region, we obtain again the same picture as that given by the tape theory [Fig. 2(b)]. It is obvious that the method of analyzing waves described above can be used for waves at higher frequencies.

We see that by means of the theory of coupled modes, the basic nature of the helix propagation becomes clear and can be better understood, even though the coaxial waveguide modes which are used in the explanation do not exist independently in the absence of an outer conductor. Physically, a theoretical open helix is impossible when $\beta_m a$ approaches ka, for then the electromagnetic fields extend far away from the helix surface, and the frequency characteristics become very sensitive to what is present in the vicinity of the helix. In general it is the propagating behavior of the surrounding structure which determines the shapes of the frequency characteristics along the forbidden regions, which again can be easily understood only by means of the theory of coupled waves. Mathematically, solutions of (3) exist both inside and outside the forbidden region, but solutions inside the forbidden region are physically meaningless for an open helix, and apply only if we assume that the helix is surrounded by a conducting pipe and use (15) instead of (3). Unfortunately the use of (3), by omitting the solutions inside the forbidden region, does not provide a complete picture of the helix propagation. This is why we have to go through (15) and let the diameter of the outer pipe be infinitely large, so that the frequency characteristics are allowed to continue inside the forbidden region. Thereby we understand the nature of the propagation.

Actually, the basic helix mode described in the previous sections can be better understood through the sheath theory. The basic mode contains many components which become independent modes in the sheath theory. With any value of m other than $m=0$, the solutions of (3) give the frequency characteristics of the coupled waves. However, with $m=0$, the frequency characteristics of the true basic helix waves are obtained, because this mode (the $m=0$ mode of the sheath theory) never has its phase constants close to ka (except at $ka \cong 0$) and is therefore not strongly coupled with any of the fast waves. It is interesting that the basic mode is actually a wave satisfying the boundary conditions of the helix, and it would be the only mode propagating on the helix if it were not coupled to the other waves.

Theory of the Bifilar Helixes

The bifilar helix is a helix wound with two wires in parallel [Fig. 1(b)]. The electromagnetic wave propagation of a bifilar helix depends upon the relative magnitudes and phases of the currents carried by two helical wires at a constant-z plane. Two special cases are particularly interesting: (1) the two currents are equal and in phase and (2) the two currents are equal and in opposite phases. The latter is important, for it offers a high impedance, useful in backward-wave oscillators.

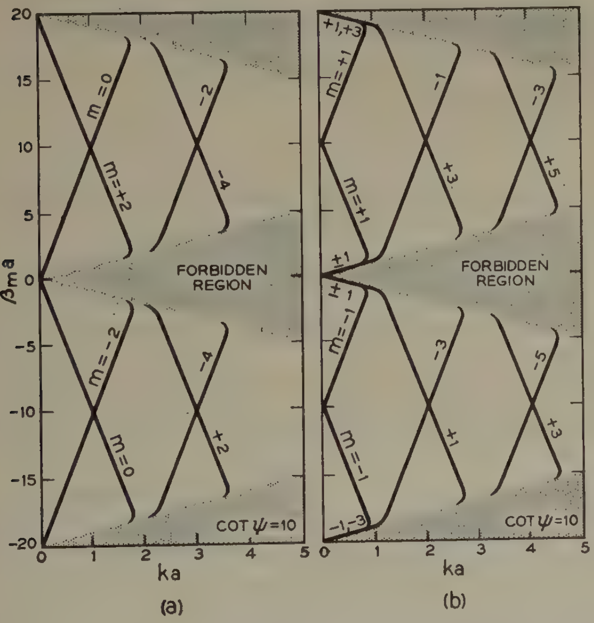

(a) (b)

Fig. 6—Frequency characteristics of a bifilar helix, cot $\psi=10$: (a) case (1); (b) case (2).

The frequency characteristics are plotted in Fig. 6(a) and (b) for the cases (1) and (2) respectively. Those characteristics become obvious when explained by means of coupled waves. In the first case, all the $m=$odd components should be omitted and in the second case none of the $m=$even components exists. The forbidden regions are therefore spaced by an interval of 2 cot ψ.

In the second case, without the $m=0$ component, the dispersive region disappears and the basic helix waves are similar to those of the coiled two-wire transmission line. The $m=+1$ and $m=-1$ components are seen to be coupled with the circularly polarized plane waves similar to the waves on a single-wire helix.

Future Studies

We have explained the behavior of helix propagation by means of the theory of the coupled waves. From the above discussions we understand that, except in the dispersive region, or near the boundaries of the forbidden regions where the effect of the coupling becomes predominant, the helix waves are essentially the sort of the transverse electromagnetic waves travelling along the helical conductor. We may thus determine the distribution in a plane normal to the helical conductor of the electromagnetic fields about the helix, and of the current density over the helical tape or wire by means of various methods used to solve Laplace's equation, or by measurements using the electrolytic tank. These problems so far as we know have not been solved exactly. It is obvious that the distribution of the current density over the conducting surface varies with the frequency and it is therefore important to know this in calculating the impedance of the helix and the ohmic loss of the conductor, which are of interest in traveling-wave tubes.

It is often interesting to know in connection with the study of the traveling-wave tubes the behavior of the electromagnetic waves of a helix surrounded by a circular or rectangular waveguide or inside some propagating structure. A direct mathematical solution is generally too complicated; the method described here, therefore, gives a better understanding and a quick solution. In general, when a complicated propagating structure involves many propagating modes and the field distribution about the structure can be expanded as a summation of the Fourier components as we have done in the tape theory, a study of coupling between the modes often gives an intuitive insight into the problem.

Appendix

From (2.4) of Reference 8, we have

$$e^{-j\beta} = m e^{j(\theta_p+\theta_q/2)}. \tag{16}$$

Here β is the phase angle in a distance of L, and θ_p and θ_q are the phase angles of the original modes in a distance L. If the coupling does not introduce any phase shift, that is $\theta_{\mathrm{I}}=\theta_{\mathrm{II}}=\theta_{\mathrm{III}}=0$, m satisfies.

$$m^2 + 2m\sqrt{1 \mp k^2}\cos\left(\frac{\theta_p - \theta_q}{2}\right) + 1 = 0. \tag{17}$$

$$m = -2\sqrt{1 \mp k^2}\cos\left(\frac{\theta_p - \theta_q}{2}\right)$$

$$\pm j\sqrt{1 - (1 \mp k^2)\cos^2\left(\frac{\theta_p - \theta_q}{2}\right)}. \tag{18}$$

Here the upper sign applies when the powers flow in the same direction for both modes and the lower sign when the powers flow in opposite directions.

If the coupling is continuous, for a small distance L, we have,

$$k \cong \frac{dL}{2}. \qquad (19)$$

Let

$$\begin{aligned} \theta &= \beta L \\ \theta_p &= \beta_p L \\ \theta_q &= \beta_q L. \end{aligned} \qquad (20)$$

Then

$$m = -\sqrt{1 \mp \left(\frac{dL}{2}\right)^2} \cos\left(\frac{(\beta_p - \beta_q)L}{2}\right) \pm j\sqrt{1 - \left(1 \mp \left(\frac{dL}{2}\right)^2\right) \cos^2\left(\frac{(\beta_p - \beta_q)L}{2}\right)}. \qquad (21)$$

If we let L approach zero, expand the cosine in power series, and neglect higher order terms in L, we obtain

$$m = -1 \pm j\left(\frac{\beta_p - \beta_q}{2}\right) L \sqrt{1 \pm \frac{d^2}{(\beta_p - \beta_q)^2}}. \qquad (22)$$

This value of m corresponds to a phase shift per unit distance

$$\left(\frac{\beta_p - \beta_q}{2}\right) \sqrt{1 \pm \frac{d^2}{(\beta_p - \beta_q)^2}}. \qquad (23)$$

Thus, from (16) we see that the phase constants of the coupled modes are reduced to the forms shown in (12) and (13) of the text.

The coupling factor d may be also expressed in the following way. If β_p and β_q are respectively the phase constants of two transmission lines p and q, without coupling, and let x_p, x_q, B_p and B_q are their respective distributed series impedances and shunt admittances, by assuming that

$$\frac{x_m^2}{x_p x_q} = \frac{B_m^2}{B_p B_q}$$

we have

$$d^2 = 4 x_m B_m$$

where x_m and B_m are respectively the distributed mutual series impedance and the distributed mutual shunt admittance of the two lines.

Detection of Television Signals in Thermal Noise*

J. E. BRIDGES†, ASSOCIATE, IRE

Summary—**This paper deals with the general problem of detecting television signals in thermal noise and with the methods of improving the performance of the second detector. A method of computing the thermal-noise spectrum and signal-to-noise ratios following the diode detector for the video and intercarrier-sound signals is described and experimentally verified. It is shown that the diode-detection process for very weak signals suppresses the desired video modulation and, in effect, creates additional noise above that introduced by the input stages. The principal factors for a given frequency component of the detected signal, are found to be the carrier-to-noise ratio, and the frequency response of the rf and IF amplifiers preceding the detector. Although the television viewpoint is emphasized, this analysis is particularly useful in analyzing the detection process of other AM transmission systems which use complex IF responses and several subcarriers.**

The theoretical and subjective aspects of improving the detection process are discussed, and a method of predicting the performance for some of the improved detection schemes is developed. Two improved detection circuits, an exalted-carrier IF and a product detector, which were constructed and tested, are described. It is found that such detection systems are capable of small improvements for very weak signals.

GENERAL ASPECTS OF DETECTING TV SIGNALS IN THE PRESENCE OF NOISE

A NUMBER of excellent papers[1–8] have been written on detecting signals in the presence of thermal noise. Most of these analyses have somewhat different objectives which emphasize the statistical aspect of the detection process or are developed for simple IF responses preceding the detector. Here the

---

* Decimal classification: R583.7×R111.6. Original manuscript received by the IRE, February 19, 1954; revised manuscript received, June 1, 1954.

† Zenith Radio Corp., Chicago, Ill.

[1] W. R. Bennett, "Response of a linear rectifier to signal and noise," *Jour. Acous. Soc. Amer.*, vol. 15, p. 164; January, 1944.

[2] E. G. Fubini, D. C. Johnson, "Signal-to-noise ratios in AM receivers," PROC. I.R.E., vol. 36, p. 1461; December, 1948.

[3] D. E. Middleton, "Rectification of a sinusoidally modulated carrier in the presence of noise," PROC. I.R.E., vol. 36, p. 1467; December, 1948.

[4] S. R. Ragazzini, "The effect of fluctuation voltages on a linear detector," PROC. I.R.E., vol. 30, p. 277; June, 1942.

[5] S. O. Rice, "Mathematical analysis of random noise," *Bell Sys. Tech. Jour.*, vol. 23, pp. 282–332; July, 1944; vol. 24, pp. 46–156; January, 1945.

[6] S. Goldman, "Frequency Analysis, Modulation and Noise," McGraw-Hill, New York, N. Y., p. 246; 1948.

[7] A. H. Schooley, S. F. George, "Input vs output signal-to-noise characteristics of linear, parabolic, and semi-cubical detectors," *NEC Proc.*, vol. 17, p. 151; 1951.

[8] D. G. Tucker, "Linear rectifier and limiters," *Wireless Eng.*, vol. 29, p. 128; May, 1952.

analysis is required not only to predict the behavior of the diode detection process preceded by a complex IF response, but also to predict the performance of the intercarrier sound as affected by the detector.

The basic method used here in the general analysis of the detection process is similar to that employed by Ragazzini.[4] In this case, because of the complex IF response, the noise is represented as the sum of a finite number of sinusoidal components. From this, the signal-plus-noise envelope preceding the detector can be obtained; and, thence, the rms noise and signal spectrum following the detector. With this basis, the signal-to-noise ratios in any channel following the detector can be computed.

The analysis will be confined to the case where the IF pass band preceding the detector is narrow compared to the center frequency of the IF response. In addition, the diode load impedance and output impedance of the last IF amplifier are assumed to be designed such that the output voltage of the detector follows the envelope of IF voltage applied to the detector. To simulate thermal noise, the IF pass band is divided into discrete channels, each b radians per second wide. Within each channel is located a sinusoidal generator of constant amplitude but randomly phased with any set of points in time. As developed in the appendix, the envelope of the IF signal presented to the diode detector is given by:

$$\left\{c^2 + 2cM \cos w_m t + 2\sum_k ca_k \cos\left[(w_k - w_c)t + \phi_{kc}\right] + \sum_k a_k^2 + 2\sum_k a_k a_{k+1} \cos\left[bt + \phi_{k1}\right] + 2\sum_k a_k a_{k+2} \cos\left[2bt + \phi_{k2}\right] + 2\sum_k a_k a_{k+3}\left[3bt + \phi_{k3}\right] + \cdots\right\}^{1/2}. \quad (1)$$

Where c is the amplitude of the carrier; M is the amplitude of a single-sideband formed by a very small percentage of modulation, and a_0, a_1, etc. are amplitudes of the various noise components. All amplitudes are taken at the output of the IF amplifier just prior to the detector.

The amplitude spectrum following the detector may be obtained by expanding this envelope expression by the binomial theorem in terms of the direct-current components $(c^2+\sum_k a_k^2)$. For most purposes, only the first two terms of the expansion need be considered. The pass band following the detector may be divided into channels similar to those of the IF pass band. The amplitude of the noise voltage in any given channel following the detector may be found by taking the square root of the sum of the squares of the various signals obtained from the binomial expansion which lie within the channel of interest. By this procedure the spectrum following the detector may be computed.

Eq. (1) appears complex, but a physical interpretation is relatively easy. The first two terms within the brackets of (1) are representative of the carrier and its modulation. The third term, a summation, is representative of the carrier-and-noise products. The remainder of the terms within the brackets are products generated by noise alone and are referred to as noise-and-noise products.

Fig. 1(a) illustrates how this procedure may be applied to the single-sideband type of transmission and detection. Only four noise generators are assumed. For the case where no carrier is present, each noise signal beats with itself to produce a dc component. Each noise signal beats with the other noise signals to produce triangular noise-and-noise spectrum illustrated by Fig 1(b).

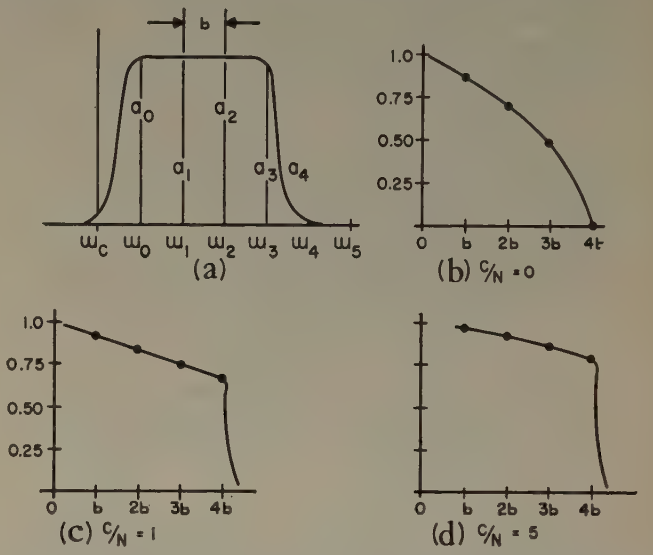

Fig. 1—(a), IF passband, assumed noise generators, single side-band system; (b), (c), and (d) approximate amplitude spectra of noise following detector, SSB system of (a) for different carrier-to-noise ratios.

Keeping the amplitude of the noise the same and adding a carrier signal at frequency of w_c produces the trapezoidal spectrum illustrated in Fig. 1(c) for a carrier-to-noise ratio of unity. In this instance, the spectrum is made up of both noise-and-noise products and carrier-and-noise products. As additional carrier is added the noise-and-noise products begin to vanish as illustrated in Fig. 1(d). For every large carrier-to-noise ratios, the noise spectrum is simply transferred from IF frequency to video frequency.

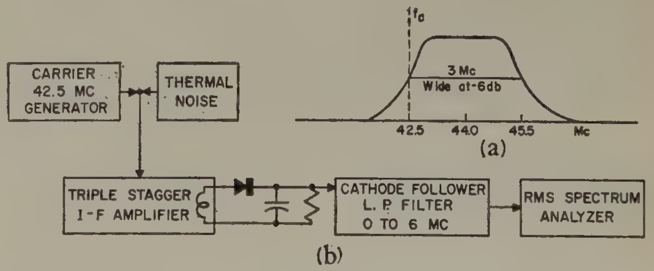
CARRIER 42.5 MC GENERATOR
THERMAL NOISE
f_0
3 Mc Wide at -6db
42.5 44.0 45.5 Mc
(a)
TRIPLE STAGGER I-F AMPLIFIER
CATHODE FOLLOWER L. P. FILTER 0 TO 6 MC
RMS SPECTRUM ANALYZER
(b)

Fig. 2—(a), Amplitude response of 44 mc amplifier; (b), equipment used to obtain noise spectrum following detector.

To verify the foregoing, the appropriate equipment was constructed and assembled as indicated in Fig. 2. As in the previous discussion, a fixed amount of thermal noise was applied to the diode detector for various carrier-to-noise ratios, and the detected amplitude spectrum was then obtained for different carrier-to-noise ratios. The accuracy of the experimental results is within ten per cent.

Fig. 3 shows the noise amplitude spectra obtained by this equipment compared with the calculated curves for the same IF pass band. The calculated curves were obtained in the manner given in the previous example, except that twelve noise channels, each 0.5 mc wide, were used to simulate thermal noise. Low-level noise, at video frequencies greater than the IF pass band cannot be accounted for by the first-order expansion of the envelope equation. This second-order noise is discussed further on.

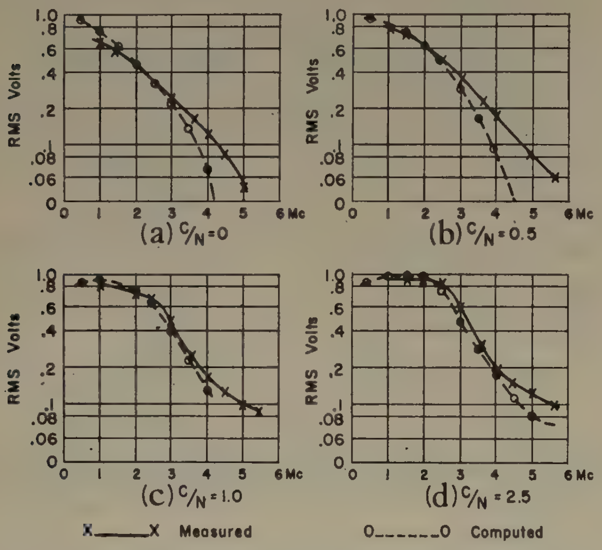

(a) C/N = 0 (b) C/N = 0.5 (c) C/N = 1.0 (d) C/N = 2.5

Fig. 3—Measured and computed noise spectra following diode detector, vestigial-side-band system of Fig. 2 for different carrier-to-noise ratios.

Of interest is a comparison of results given by the first two terms of the binomial expansion of the envelope equation with the results of others. To be compared is the ratio of the dc voltage developed at the detector by the noise alone to the dc voltage developed by a single sine wave having the same rms value as the noise voltage preceding the detector. This ratio is 1.0 as given by the methods used here. According to Goldman[6] this ratio is 0.9. Also of interest is the ratio of the rms noise following the detector when a very large carrier is present to the rms noise when the carrier is absent. By the method used here this ratio is 1.4 and by Rice's method[5] the ratio is 1.5. This ratio was measured experimentally, and it seems to be nearer 1.5.

Signal-to-Noise Ratio in Video Channel

The method used here appears to be within the usual experimental accuracy and it can be extended to something more useful, such as obtaining the signal-to-noise ratio in any channel following the detector in terms of the carrier-to-noise ratio preceding the detector. Eq. (1) can be manipulated to do this, as given in the appendix, with the following results, for small percentages of modulation:

$$S/N = \frac{s^2 p m(w_m)}{[s^2 Q^2 + R^2]^{1/2}} \qquad (2)$$

where S/N is the ratio of the rms value of a sinusoidal video signal to the rms value of the thermal noise following the detector in the channel of interest, s is the carrier-to-noise ratio prior to the detector, p, the percentage modulation, $m(w_m)$, the relative attenuation of a sideband with respect to the carrier. Q is a constant proportional to the rms value of detected noise in the channel of interest when a very large carrier is present. R is a constant proportional to the rms value of detected noise in the channel of interest when there is no carrier present.

Q and R depend on the shape of the IF response, location of the carrier within the IF response, and the particular channel following the detector. For example, the noise-and-noise products are less at the higher video frequencies. This results in slightly better signal-to-noise ratios for the color sub-carrier channel than for a comparable channel at a lower video frequency. For the vestigial sideband reception such as used in the American television system, Q and R are approximately 1.0 and 0.7 respectively over the video channel. For comparative analysis these values are used, and the normalized signal-to-noise ratios following the detector are plotted against the carrier-to-noise ratio prior to the detector as in Fig. 4.

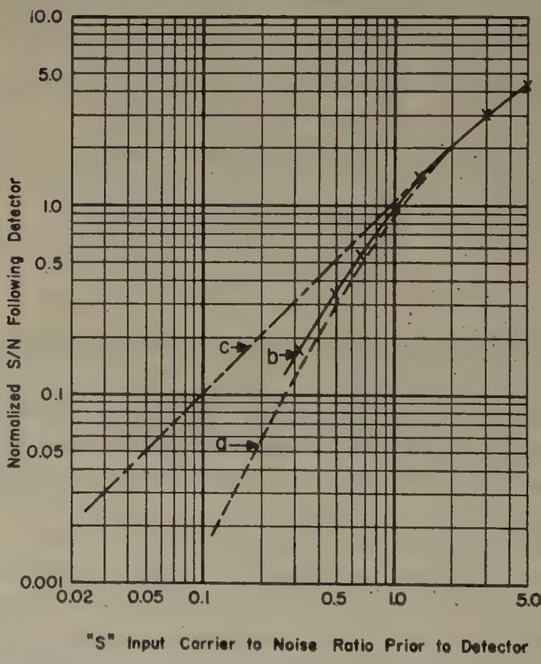

Fig. 4—Measured and computed S/N in video channel following diode detector of a typical television receiver: *a*, computed; *b*, measured; *c*, computed ideal detector.

Fig. 4 also shows the measured normalized signal-to-noise ratio channel centered at 2 mc, 50 kc wide following the diode detector. The television IF response used in this test was a typical RA (receiver-attenuation)[9] response. Fig. 5 shows a diagram of the equipment used for this experiment. The most important effect is the suppression of the carrier's modulation by thermal noise. This effect causes the detected modulation to disappear at twice the rate at which the carrier is decreased prior to the diode detector. This may be better visualized by remembering that, in the diode detection process, the largest signal dominates and reduces the modulation of any lesser signal to a second-order effect.[10]

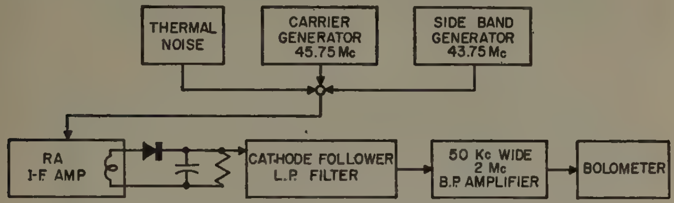
THERMAL NOISE
CARRIER GENERATOR 45.75 Mc
SIDE BAND GENERATOR 43.75 Mc
RA I-F AMP
CATHODE FOLLOWER L.P. FILTER
50 Kc WIDE 2 Mc B.P. AMPLIFIER
BOLOMETER

Fig. 5—Equipment used to measure signal-to-noise ratios in video channel.

SPECIAL PROBLEMS OF FORMING THE INTERCARRIER SOUND SIGNALS AT DETECTOR

Regarding intercarrier sound,[11] an additional effect takes place which tends to deteriorate the carrier difference signal found at the diode. This additional deterioration is caused by second-order noise. The principal reason for the importance of second-order noise is that the sound IF carrier is attenuated some thirty-two db below the peak IF response.

In analyzing the intercarrier-sound forming process, it should be noted that the objective here is to determine the signal-to-noise ratio in the 4.5 mc intercarrier sound channel. Once this ratio is known, the performance of the over-all sound system can be determined from previously published data by D. Middleton[12] on signal-to-noise ratios in FM receivers.

To account for the additional noise present in the sound channel, the higher-order terms of the binomial expansion of the envelope equation must be considered. This may be noted by observing, in Fig. 3, that the actual noise signals in the neighborhood of 4.5 mc are greater than those which are calculated from the first two terms of the binomial expansion. Section 3 of the appendix gives a simplified procedure of how the second-order noise may be computed.

For the typical RA IF mentioned previously, a complete calculation of the signal-to-noise ratio in the sound channel was made assuming a noise generator every 0.5 mc. The picture carrier and sound carrier were attenuated 6 db and 32 db respectively below the peak IF response; and the equivalent noise bandwidth of the IF was in the order of 3.5 mc. The results of this calculation and a comparison with experimental results are given in Fig. 6. Also plotted are experimental curves which show the effect of increasing or exalting the carrier-to-noise ratio while holding the IF sound carrier-to-noise ratio the same.

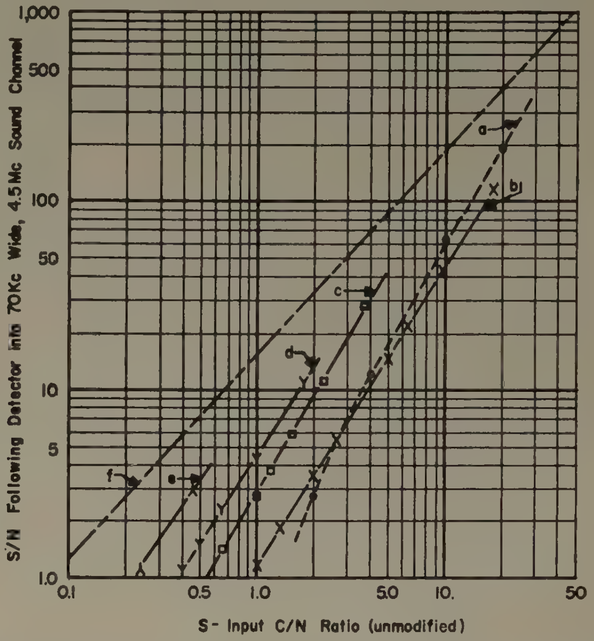

Fig. 6—Measured and computed signal-to-noise ratios in 4.5 mc intercarrier-sound channel as a function of the carrier-to-noise ratio for a typical television receiver RA IF response: *a*, computed; *b*, measured; *c*, *d*, and *e* measured for C/N enhanced, 12, 20, and 32 db over side-band-to-noise ratio; *f*, computed for ideal detector.

The most striking effect illustrated in Fig. 6 is that the signal-to-noise ratio in the sound channel may be 20 db below the signal-to-noise ratio prior to the detector. If more carrier is added while holding the sound IF carrier-to-noise ratio constant, the signal-to-noise ratio in the sound channel is correspondingly improved. This demonstrates that the basic cause for the poorer signal-to-noise ratio in the sound channel is that the picture carrier is over-ridden by noise.

For a given IF response and carrier-to-noise ratio, the noise in the sound channel arises from three sources: first, from carrier-and-noise products. These noise signals are simply transferred from the noise signals surrounding the sound carrier at IF frequency to the neighborhood of 4.5 mc following the detector.

The second contribution comes from noise-and-noise products. Noise-and-noise terms originate from IF noise frequencies having a difference in the order of 4.5 mc. These components originate from the skirts of the IF response.

The third noise contribution comes from second-order noise. Quite obviously, all noise subharmonics of 4.5 mc, such as 2.25 mc, 1.5 mc, 1.125 mc, which appear in the envelope equation, make a contribution. More important are contributions from products of terms in the envelope which have frequencies whose sums or differences are in the order 4.5 mc, such as a 1.0 mc term and a 3.5 mc term product or a 5.0 mc term and a 0.5 mc term product. In the case of intercarrier sound, only products arising from terms whose frequencies have a sum of 4.5 mc are of importance. Noise from all sectors of the IF response make a second-order noise contribution; the center sections, however, contribute the most.

---

[9] Donald Fink, "Television Standard and Practice," McGraw-Hill, New York, N. Y., p. 162; 1943.

[10] F. E. Terman, "Radio Engineers Handbook," McGraw-Hill, New York, N. Y., p. 577; 1943.

[11] R. B. Dome, "Carrier-difference reception of television sound," *Electronics*, p. 102; January, 1947.

[12] D. E. Middleton, "On theoretical signal-to-noise ratios in F-M receivers, a comparison with amplitude modulation," *Jour. Appl. Phys.*, vol. 20, p. 334; April, 1949.

Altering the IF response gives some measure of control over the signal-to-noise ratio in the 4.5 mc sound channel. The carrier-to-noise ratio may be slightly improved by decreasing the attenuation of the picture carrier by the IF response. This will tend to reduce the modulation suppression effect.

The noise-and-noise products may be decreased somewhat by narrowing the IF response. These products could also be reduced if a pure single-sideband reception system could be substituted for the wider-band vestigial-sideband system now employed.

The second-order noise in the sound channel may be minimized by decreasing the relative attenuation of the IF sound carrier with respect to the peak response. This procedure tends to elevate the intercarrier sound signal and carrier-and-noise products above the second-order noise. This is beneficial because the amplitude of the second-order noise is determined chiefly by the central sectors of the IF response and, therefore, is independent of the IF sound-carrier attenuation. Reducing the amplitude of the central portion of the IF response with respect to the two carriers also reduces second-order noise.

An IF response optimized for weak-signal intercarrier-sound reception appears to be incompatible with other requirements for the IF response. In practice, however, many receivers employ a modification of the aforementioned RA response in fringe areas to enhance intercarrier-sound reception.

THEORETICAL ASPECTS OF ELIMINATING THE SUPPRESSION OF MODULATION BY NOISE

To eliminate the modulation suppression effect of thermal noise in the detection process involves complex or unusual circuitry. The main idea of these circuits is to extract the carrier which lies buried in the thermal noise. Once the carrier is extracted, it can then be used somehow in a detection process which preserves the frequency and phase relationships of the sidebands and the carrier. By so doing, the additional noise created in the more common detection processes can be minimized.

With the present standards used for television AM receivers, the principal problem is to produce a relatively noise-free carrier at the receiver. One obvious solution is to employ passive circuits with extremely narrow pass bands to filter the carrier from the noise. Another solution would be to employ active circuits, such as locked oscillators and automatic-frequency-control systems. All of these have their own advantages and liabilities and will be discussed later.

Before discussing the theoretical aspects of reducing the added noise, a word about different types of detectors is appropriate. Detectors may be classified into two groups—heterodyne and asymmetrical. In the heterodyne-detection process an additional signal is mixed with the incoming signal to produce sum-and-difference frequency products. The heterodyne detector becomes a synchronous detector when the frequency and phase of the local oscillator is the same as that of the incoming carrier of the AM signal to be detected. The asymmetrical detectors are exemplified by the "linear diode," square-law, and infinite impedance types of detectors.

Of importance is a method to predict the performance of the different schemes which tend to reduce the modulation suppression effect. The exalted carrier IF scheme is readily handled by methods previously developed. In this scheme, the carrier-to-noise ratio is increased by a sharply peaked circuit before detection, and the proper amplitude and phase relationship of the detected signal are restored by a special de-emphasis network following the detector as indicated in Fig. 7. On this basis the performance can be predicted in terms of the increased carrier-to-noise ratio prior to the detector when compared with the IF response normally employed. If "Z" represents the ratio of the improvement in carrier-to-noise ratio over that normally associated with the IF in question, the expression for the signal-to-noise ratio following the detector becomes

$$S/N = \frac{s^2 Z p m(w_m)}{[Z^2 s^2 Q^2 + R^2]^{1/2}}. \qquad (3)$$

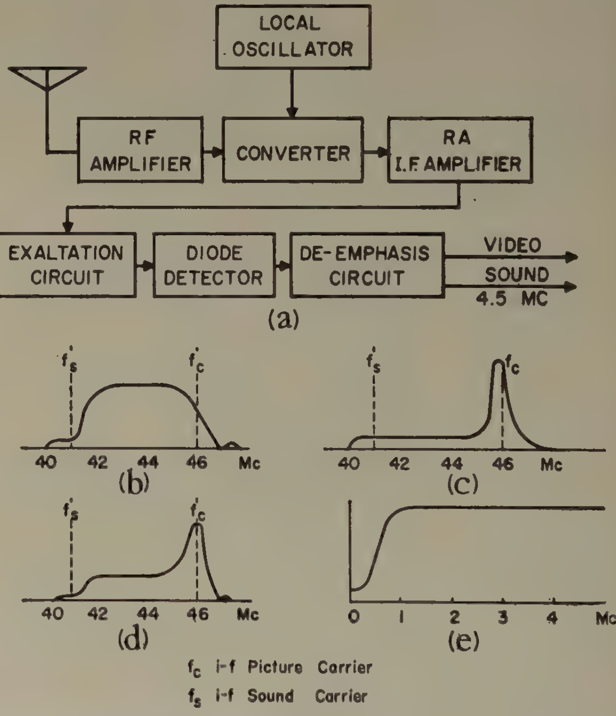

Fig. 7—(a), Exalted-carrier detection system; (b), response of RA IF Amplifier; (c), exaltation circuit response; (d), combined response: (e), response of de-emphasis circuit.

For the usual values of Q and R associated with vestigial sideband detection of the television signals, the signal-to-noise ratios following the detector are plotted for different values of increased carrier-to-noise ratios as shown in Fig. 8. All that the exaltation process does is to postpone the point at which the noise in the detection process suppresses the desired modulation.

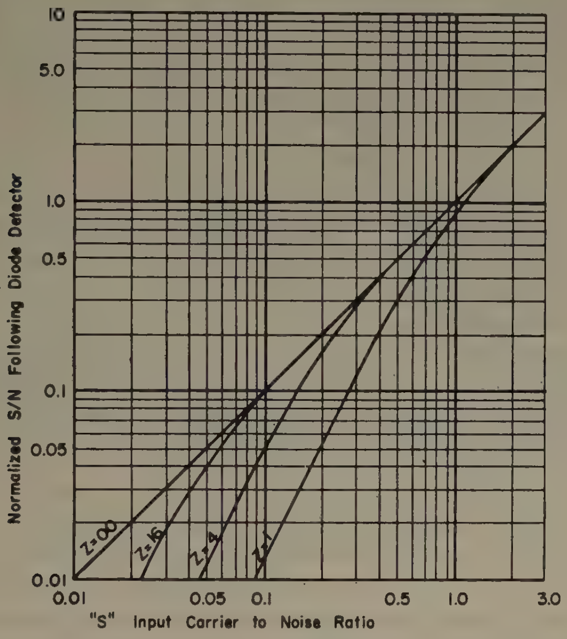

Fig. 8—Computed signal-to-noise ratios in video channel for different degrees of exaltation, Z, of the carrier-to-noise ratio.

From these curves the amount of improvement the exalted carrier system gives over the usual system can be determined. For a fixed output signal-to-noise ratio the maximum improvement possible is proportional to the square-root of "Z," the ratio of the improvement in the carrier-to-noise ratio. For a fixed input signal-to-noise ratio the maximum improvement possible is directly proportional to "Z." These maximum improvements are realizable only for extremely weak signals. The improvement for a fixed output signal-to-noise is the most meaningful and shall be used in the remainder of this paper. This definition gives the improvement in terms of added range or decreased transmitter power.

Similar procedures may be employed to predict the performance of other circuits. In the case of a product detector, the procedure is modified to the extent that the output is given in terms of product between the spectrum of signal-plus-noise and the spectrum of the extracted carrier with its associated noise. Active filters, such as locked oscillators and automatic phase or frequency control systems may be reduced to an equivalent passive filter[13–15] so far as their thermal-noise performance is concerned. On the basis of increased carrier-to-noise ratio in the equivalent passive filter, the performance of the active filter system may be computed. In general, it appears that the thermal noise performance for the circuits discussed is defined by equations similar to (3) and curves similar to Fig. 8.

Next, there are two interesting questions which arise in view of the previous discussion. First, is the modulation-suppression effect by the detection process of importance for the usual fringe area operation of TV receivers? Second, if the modulation-suppression effect by the detection process is important, are special detector circuits which eliminate this effect practical for a TV receiver?

The answer to the first question depends primarily on what the fringe-area viewer regards as a usable noisy picture. To answer this question, a conventional television set was modified such that a very large noise-free carrier could be added at will to a noisy TV signal prior to the diode detector. By such a procedure the picture representative of the best performance attained by a synchronous detector could be compared with that produced by the usual diode-detection circuit.

The results of the comparison are interesting. It was found that the minimum usable signal-to-noise ratio in the video channel is approximately 0.5. For this minimum value, it was found that the input signal-to-noise ratio could be decreased by 30 per cent when the large noise-free carrier was present, thus giving approximately a 3 db improvement over the usual detector circuit. Greater improvements were observed as the input signal-to-noise ratio was further decreased. Practically, these larger improvements were valueless because even the improved picture signal-to-noise ratio was below the minimum acceptable value. Larger improvements were observed for the intercarrier-sound signal, but, because of the second-order effects associated with diode detection, the maximum or ideal performance could not be simulated for the sound channel.

PRACTICAL CIRCUITS TO ELIMINATE MODULATION SUPPRESSION BY NOISE

The amount of improvement in both picture and sound which the ideal synchronous detector gave was deemed sufficient to investigate the possibilities of incorporating a synchronous detection circuit into a conventional mass-produced television receiver.

To this end, a number of circuits were considered to reduce the modulation-suppression effect and the second-order noise. Those constructed and tested were an exalted-carrier system and carrier extraction by filtering and limiting followed by a product detector. The locked oscillator and afc system also received attention, but none were constructed. At this point it should be mentioned that synchronous or exalted carrier detection systems are not new. This form of detection is described

---

[13] D. Richman, "Theory of synchronization applied to NTSC color television," *1953 IRE Convention Record*, part 4, p. 3; 1953.

[14] D. Richman, "APC color sync for NTSC color television," *1953 IRE Convention Record*, part 4, p. 13; 1953.

[15] W. J. Gruen, "Theory of AFC synchronization," *1953 IRE Convention Record*, part 4, p. 178; 1953.

by Tucker,[16,17] Crosby,[18–20] and Polkinghorn.[21] Most of these circuits were developed for specialized communications systems. Recent investigations of Fano[22] and Lee[23] have emphasized the thermal noise improvement produced by synchronous detectors.

The exalted-carrier system enhances the carrier-to-noise ratio by sharply peaking the video IF at the picture carrier frequency prior to detection. This process also emphasizes the lower video frequencies as well as increasing the carrier-to-noise ratio. Following a conventional diode detector, sutiable de-emphasis of the lower video frequencies can be accomplished in the video circuits following the detector. This circuit is diagrammed in Fig. 7.

For a practical circuit, the IF picture carrier must be held within 15 per cent of the peak response of the exalted IF to avoid distortion of the video and poor thermal noise performance.

It was found that considerable reduction of bandwidth prior to detection is necessary to achieve noticeable improvement. An examination of Fig. 8 shows that to approach the ideal performance of a synchronous detector in the region of interest an exaltation ratio of greater than four is necessary. This means that the equivalent noise bandwidth of the exalted carrier IF must be some sixteen times smaller than the equivalent noise bandwidth of the normal IF response.

Such a large bandwidth reduction may be impractical because of the slow drift between the peak response of the exalted IF and the IF carrier frequency, due principally to changes in the local oscillator frequency. Hence the amount of peaking is limited by the stability of the local oscillator. The exalted IF should, therefore, be sufficiently wide to accommodate the expected slow frequency shift of the IF picture carrier.

The exalted IF detection scheme which was built into a television set had an exaltation ratio in the order of 2.5. This set was compared with similar unmodified receivers and average improvements in the order of 1.5 db for the video and 3 db for the sound were observed. These improvements were realizable only for signals which were extremely noisy and which had dubious entertainment value. The unmodified receivers used in this comparison employed, as is fairly common practice, a modified IF response which enhances slightly both picture and sound carriers in weak signal areas. Somewhat larger improvements were observed when a comparison was made with a set which used a RA IF response similar to that described above.

The other circuit which was incorporated into a TV receiver was a filter-limiter carrier extractor used with a product detector. This circuit is diagrammed in Fig. 9, which illustrated the general functions of such a system.

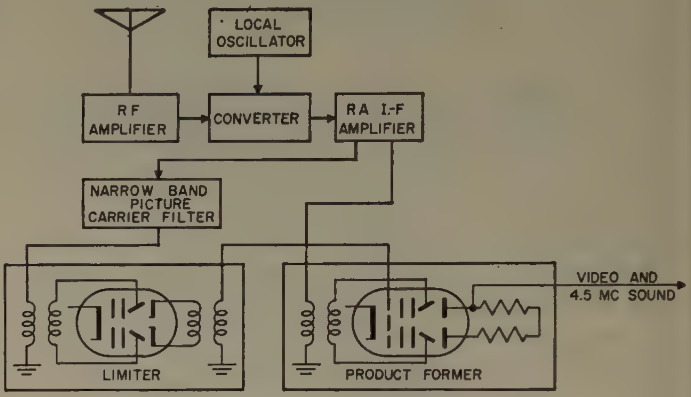

Fig. 9—Filter-limiter carrier extraction and product detector circuit.

The limiter and multiplier used to detect the 45 mc IF signal did not use conventional tubes and are, therefore, of general interest. The limiter used was an especially designed beam deflection tube in a miniature bulb as diagrammed in Fig. 9. When a signal of sufficient amplitude is applied to the deflectors, the electron beam is switched periodically between the two anodes, thereby producing a square wave current of fixed amplitude. A limiter of this type does not have a time constant and has a high input impedance at 50 mc. For these reasons it was used here.

As indicated in Fig. 9, a beam deflection tube was also used as a product detector. The tube is free from space-charge coupling effects and forms a relatively undistorted product between the two inputs. The product-former tube is similar to the limiter tube except that a control grid has been added. The tube and circuitry are so designed that the product between the inputs on grid and deflectors appears in push-pull on the two anodes. Both deflection tubes were developed by Dr. Adler (of this laboratory) and the associated circuits were devised in collaboration with him.

Experimental results with the filter-limiter-product detection process indicated that its performance was similar to that of the exalted carrier IF. No difference was observed in the performance for the same equivalent noise bandwidth prior to the limiter or detector. The filter-limiter-product detector also suffers from the same drawbacks that affect the exalted carrier scheme.

---

[16] D. G. Tucker, R. A. Seymour, "The synchrodyne as a precision demodulator," *Wireless Eng.*, vol. 27, p. 227; Aug./Sept. 1950.

[17] D. G. Tucker, "The synchrodyne," *Elec. Eng.*, vol. 19, p. 75, 1947; vol. 20, p. 49; March, 1948.

[18] M. G. Crosby, "Exalted carrier amplitude-and-phase modulation reception," PROC. I.R.E., vol. 33, p. 581; September, 1945.

[19] M. G. Crosby, "Communication by phase modulation," PROC. I.R.E., vol. 27, p. 126; February, 1939.

[20] M. G. Crosby, "Long-range communication trends," *Trans. I.R.E.*, vol. CS-1, no. 1, p. 41; July, 1953.

[21] F. A. Polkinghorn, N. F. Schlaak, "Single sideband short wave system for transatlantic telephony," PROC. I.R.E., vol. 23, p. 701; July, 1935.

[22] R. M. Fano, "Signal-to-noise ratios in correlation detectors," *M.I.T. R.L.E. Tech. Report*, No. 186, 1951.

[23] Y. W. Lee, T. P. Cheatham, J. B. Wiesner, "Application of correlation function in the detection of small signals in noise," PROC. I.R.E., vol. 38, p. 1165–1171; October, 1950.

It appears that detection circuits which use automatic frequency or phase control can be made to have an equivalent noise bandwidth sufficiently small for good thermal noise performance and yet have properties which minimize the effect of instability. In the present state of the art, however, these circuits appear to be too complex to be incorporated into an all-purpose television receiver.

In conclusion, the special detection methods which use passive circuits are capable of producing small improvements for both the sound and the picture signals. Special detection circuits which minimize the effect of instability, such as by using automatic-frequency or automatic-phase control are capable of larger improvements. It should be mentioned again that these improvements are obtained only for extremely weak signals. Aside from the fringe area performance, the special detection schemes have other useful properties, such as wider-band IF response, reduction of adjacent channel interference, reduction of beats between color and sound carriers, and reduction of any residual amplitude modulation which may be present in the intercarrier-sound signal.

ACKNOWLEDGMENT

The author wishes to thank Dr. Robert Adler of Zenith Radio Corporation for his support and encouragement of this investigation, and Mr. Karl Wossidlo for construction of test equipment and preparation of drawings and curves. Credit is due also to the author's associates at Zenith for their many valuable and practical suggestions.

APPENDIX I

The analysis will be confined to the case which is similar to that of AM detection in a TV receiver or AM radio. In this instance, the pass band of the IF preceding the detector is small compared to the center frequency of the IF response. The circuit design of the diode load impedance and of the IF output stage is such that the output of the detector follows the IF voltage envelope. To simulate thermal, noise, the IF pass band is divided into discrete channels, each "b" radians wide. Within each channel is located a sinusoidal generator of constant amplitude and randomly phased with any set of points in time. The noise voltage prior to the detector may be stated as follows:

$$f_n(t) = a_0 \cos x_0 + a_1 \cos x_1 + a_2 \cos x_2 + \cdots + a_q \cos x_q \tag{4}$$

where

$x_k = w_k t + \phi_k$

$b = w_{k+1} - w_k$, channel width radians/sec.

$a_k = a(w_k)[Pn\ b/Feq]^{1/2}$

Pn is the thermal noise power at output of IF

Feq is the equivalent noise bandwidth of IF

$a(w)$ is the frequency response (prior to detector) of IF.

These signals may be combined into the form of an amplitude modulated carrier.

$$\begin{aligned} f_n(t) &= a_0 \cos x_0 + a_1 \cos [(x_1 - x_0) + x_0] \\ &\quad + a_2 \cos [(x_2 - x_0) + x_0] + \cdots \\ &\quad + a_q \cos [(x_q - x_0) + x_0] \\ &= (A^2 + B^2)^{1/2} \cos (x_0 - \tan^{-1} B/A) \end{aligned} \tag{5}$$

where

$$\begin{aligned} A &= (1 + a_1 \cos (x_1 - x_0) + a_2 \cos (x_2 - x_0) + \cdots \\ &\qquad + a_q \cos (x_q - x_0)) \\ B &= (a_1 \sin (x_1 - x_0) + a_2 \sin (x_2 - x_0) + \cdots \\ &\qquad + a_q \sin (x_q - x_0)). \end{aligned}$$

The detected envelope is given by:

$$[A^2 + B^2]^{1/2}. \tag{6}$$

If the indicated operations are carried out the envelope for thermal noise becomes:

$$\begin{aligned} [A^2 + B^2]^{1/2} = \Bigg\{ & \sum_k a_k^2 + 2 \sum_{k=0}^{k=q-1} a_k a_{k+1} \cos [bt + \phi_{k1}] \\ & + 2 \sum_{k=0}^{k=q-2} a_k a_{k+2} \cos [2bt + \phi_{k2}] \\ & + 2 \sum_{k=0}^{k=q-3} a_k a_{k+3} \cos [3bt + \phi_{k3}] + \cdots \\ & + 2 a_0 a_q \cos [qbt + \phi_{kq}] \Bigg\}^{1/2}. \end{aligned} \tag{7}$$

If a carrier with a small percentage, p, of single side band modulation is added, the envelope expression becomes:

$$\begin{aligned} & [A^2 + B^2]^{1/2} \\ & = \Bigg\{ c^2 + 2c^2 pm(w_m) \cos w_m t \\ & \quad + 2 \sum_{k=0}^{k=q} c a_k \cos [(w_k - w_c)t + \phi_{kc}] \\ & \quad + \sum_{k=0}^{k=q} a_k^2 + 2 \sum_{k=0}^{k=q-1} a_k a_{k+1} \cos [bt + \phi_{k1}] \\ & \quad + 2 \sum_{k=0}^{k=q-2} a_k a_{k+2} \cos [2bt + \phi_{k2}] + \cdots \Bigg\}^{1/2} \end{aligned} \tag{8}$$

where c is the amplitude of the carrier prior to the detector, $cpm(w_m)$ is the amplitude, M of the sideband prior to the detector, and $m(w_m)$ is the relative attenuation of the side band with respect to the carrier.

Sample Computation of Noise-Amplitude Spectrum

Consider a small approximately rectangular bandwidth as indicated in Fig. 1(a), and that the carrier and noise to be detected is passed through this filter. Assume the thermal noise to be produced by only four sinusoidal generators of constant amplitude and randomly phased with any set of points in time. The envelope given by (8) is:

$$
\begin{aligned}
[A^2 + B^2]^{1/2} = \{ & c^2 + 2ca_0 \cos(bt + \phi_{c0}) \\
& + 2ca_1 \cos(2bt + \phi_{c1}) \\
& + 2ca_2 \cos(3bt + \phi_{c3}) \\
& + 2ca_3 \cos(4bt + \phi_{c3}) \\
& + a_0^2 + a_1^2 + a_2^2 + a_3^2 \\
& + 2a_0a_1 \cos(bt + \phi_{01}) \\
& + 2a_1a_2 \cos(bt + \phi_{12}) \\
& + 2a_2a_3 \cos(bt + \phi_{23}) \\
& + 2a_0a_2 \cos(2bt + \phi_{02}) \\
& + 2a_1a_3 \cos(2bt + \phi_{13}) \\
& + 2a_0a_3 \cos(3bt + \phi_{03}) \}^{1/2}. \qquad (9)
\end{aligned}
$$

The approximate voltage amplitudes following the detector may be determined from the first two terms of the binomial expansion of the envelope equation. Since the noise signals obtained from this expansion are incoherent, the rms amplitude of noise in any channel following the detector may be found by taking the square root of the sum of the squares of the various signals which lie within the channel of interest.

Assuming channels following the detector to be centered at b, $2b$, etc., the constants associated with detector efficiency equal to one; $a_0 = a_1 = a_2 = a_3 = 1$, $C/N = 1$, $C = 2$, the rms amplitudes of the spectrum may be computed as follows. The noise amplitude in a channel centered, say, at $2b$ is

$$\left\{ \frac{c^2a_1^2 + a_0^2a_2^2 + a_1^2a_3^2}{c^2 + \sum_k a_k^2} \right\}^{1/2} = \left(\frac{6}{8} \right)^{1/2}. \qquad (10)$$

Proceeding as above, the approximate expansion of the envelope becomes

$$
\begin{aligned}
(A^2 + B^2)^{1/2} = (8)^{1/2} & + (7/8)^{1/2} \cos(bt + \phi_1) \\
& + (6/8)^{1/2} \cos(2bt + \phi_2) \\
& + (5/8)^{1/2} \cos(3bt + \phi_3) \\
& + (4/8)^{1/2} \cos(4bt + \phi_4). \qquad (11)
\end{aligned}
$$

The above expression should be interpreted only as a method of notation to keep track of the amplitudes in the channels following the detector.

Appendix II

General Expression for S/N Following Detector

The expression for the envelope presented to the detector which includes noise plus a carrier and a single-sideband signal is:

$$
\begin{aligned}
& (A^2 + B^2)^{1/2} \\
& = \Big\{ c^2 + 2c^2pm(w_m) \cos w_mt \\
& \quad + 2\sum_{k=0} ca_k \cos(x_k - x_c) \\
& \quad + \sum_{k=0} a_k^2 + 2\sum_{i=1}\sum_{k=0} a_ka_{k+i} \cos(x_k - x_{k+i}) \Big\}^{1/2}. \qquad (12)
\end{aligned}
$$

Defining the carrier-to-noise ratio, s, as

$$s = \left[\frac{c^2}{\sum_k a_k^2} \right]^{1/2} = \left(\frac{c^2}{P_n} \right)^{1/2}$$

$$
\begin{aligned}
& (A^2 + B^2)^{1/2} \\
& = c\left(\frac{1 + s^2}{s^2} \right)^{1/2} \Big\{ 1 + 2pm \frac{s^2}{1 + s^2} \cos w_mt \\
& \quad + 2\frac{s}{1 + s^2}\left(\frac{b}{F_{\text{eq}}} \right)^{1/2} \sum_{k=0} a(w_k) \cos(x_k - x_c) \\
& \quad + 2\frac{1}{1 + s^2}\left(\frac{b}{F_{\text{eq}}} \right) \\
& \qquad \sum_{i=1}\sum_{k=0} a(w_k)a(w_{k+i}) \cos(x_k - x_{k+i}) \Big\}^{1/2}. \qquad (13)
\end{aligned}
$$

The rms noise in some specified channel following the detector is:

$$c\left[\frac{1 + s^2}{s^2} \right]^{1/2} \left\{ \left[\frac{sQ}{1 + s^2} \right]^2 + \left[\frac{R}{1 + s^2} \right]^2 \right\}^{1/2}, \qquad (14)$$

where

$$Q = \left[\sum_k a^2(w_k)(b/F_{\text{eq}}) \right]^{1/2},$$

$$R = \left[\sum_i \sum_k a^2(w_k)a^2(w_{k+i})(b/F_{\text{eq}})^2 \right]^{1/2} \qquad (15)$$

such that Q and R are obtained only from the amplitudes of signals whose frequencies lie within the specified channel. The S/N ratio following the diode would be for small precentages of modulation:

$$S/N = \frac{\dfrac{s^2pm(wm)}{1 + s^2}}{\left\{ \dfrac{s^2Q^2}{(1+s^2)^2} + \dfrac{R^2}{(1+s^2)^2} \right\}^{1/2}} = \frac{pm(w_m)s^2}{[s^2Q^2 + R^2]^{1/2}}. \qquad (16)$$

Appendix III

S/N Into Sound Channel

The number of terms involved which arise from the second order term of the binomial expansion of (1) is large. To reduce the labor, the noise-and-noise products and carrier-and-noise products of similar frequency in (8) are added together before expanding. This reduces the number of terms involved but confines the calculations to C/N ratios of two or larger and to the single sideband case. The general expression for the envelope then becomes for an example similar to Fig. 1(a).

$$
\begin{aligned}
& [A^2 + B^2]^{1/2} \\
& = \Big\{ c^2 + \sum_k a_k^2 + 2c^2pm(w_m) \cos w_mt \\
& \quad + 2\Big[\Big(a_0c + \sum_k a_ka_{k+1} \Big) \cos(bt + \phi_{k1}) \Big]
\end{aligned}
$$

$$+ 2\left[\left(a_1c + \sum_k a_ka_{k+2}\right)\cos(2bt + \phi_{k2})\right]$$

$$+ 2\left[\left(a_2c + \sum_k a_ka_{k+3}\right)\cos(3bt + \phi_{k3})\right]$$

$$+ \cdots\Big\}^{1/2}. \qquad (17)$$

This may be expanded by the binomial theorem.

$$[A^2 + B^2]^{1/2}$$

$$= \left[c^2 + \sum_k a_k^2\right]^{1/2}\{1 + A_s\cos w_mt + A_1\cos(bt + \phi_1)$$

$$+ A_2\cos(2bt + \phi_2) + \cdots\}^{1/2} \qquad (18)$$

$$= \left[c^2 + \sum_k a_k^2\right]^{1/2}\Big\{1 + \frac{A_s}{2}\cos w_mt$$

$$+ \frac{A_1}{2}\cos(bt + \phi_1) + \frac{A_2}{2}\cos(2bt + \phi_2) + \cdots$$

$$- \frac{A_1^2}{16}[1 + \cos(2bt + \phi_2')]$$

$$- \frac{A_2^2}{16}[1 + \cos(4bt + \phi_4')] - \cdots$$

$$- \frac{A_1A_2}{8}[\cos(3bt + \phi_2'') + \cos(bt + \phi_1'')]$$

$$- \frac{A_1A_3}{8}[\cos(4bt + \phi_2'') + \cos(2bt + \phi_2'')]$$

$$- \cdots\Big\} \qquad (19)$$

where

$$A_s = \frac{2c^2pm(w_m)}{c^2 + \sum_k a_k^2}, \quad A_1 = 2\frac{\left(a_0c + \sum_k a_ka_{k+1}\right)}{c^2 + \sum_k a_k^2},$$

$$A_2 = \frac{2(a_1c + \sum)}{c^2 + \sum_k a_k^2}.$$

From (19) the amplitudes of the signal and of the noise may be computed. In the event only one channel is of importance, such as the sound channel, only terms which have a frequency of 4.5 mc need be computed. Once the amplitudes of the signal and the noise are known, the signal-to-noise ratio may then be evaluated.

An Effective Ground Conductivity Map for Continental United States*

HARRY FINE†, ASSOCIATE, IRE

Summary—**The Federal Communications Commission has recently adopted a new effective ground conductivity map. The derivation of this map and its estimated accuracy are discussed in this paper.**

INTRODUCTION

A NEW EFFECTIVE ground conductivity map for continental United States is submitted in this report. This map represents estimates based on measurements over approximately 7,000 paths throughout the country which were submitted to the FCC. The previous ground conductivity map had been promulgated in 1938 and based upon relatively few measured paths plus the soil type map. Subsequent measurements had shown that the estimates of conductivity provided by this 1938 map were appreciably in error for various parts of the country. For this reason a more accurate map was considered desirable in the allocation of standard broadcast stations and the present map was adopted by the FCC for use as of April 5, 1954.

At this time it is pertinent to point out that the conductivity over a given path may vary over wide limits with location, season, weather, etc. Consequently, the effective conductivity, as used here, must be defined as that value of conductivity which will result in the overall median field strength for the path or segment of path under consideration when used in conjunction with the Commission's ground-wave field strength versus distance curves.

The Central Radio Propagation Laboratory had previously undertaken a rather comprehensive effective conductivity study based on the field strength measurements, submitted to the FCC in various proof-of-performance and in connection with the processing of application for standard broadcast facilities. These paths, most of them less than 25 miles in length, were plotted on map overlays. From these overlays with the aid of the Department of Agriculture soil maps (Atlas of American Agriculture; 1935), those paths running over one subsoil type only were analyzed for correlation between measured path conductivity and subsoil type. From this study, typical conductivity values for 144 of the 243 subsoil types were evaluated. It was found that for any given subsoil type the logarithms of the measured conductivities were distributed about the average in a normal distribution. Considering log conductivity as the basic variable, the average standard error of estimate for the 144 subsoil types was 0.266. In more familiar language, this means that approximately two-thirds of the measured path conductivities for a typical subsoil type lay within the range of 1/1.85 and 1.85 times the subsoil median conductivity. Grouping these subsoil types into parent soil groups gave so large a standard error that this approach was abandoned. With so large a standard error even for the subsoil types, the correlation of conductivity with these subsoil types was not considered very promising. CRPL has prepared a report[1] of sectional maps, showing the paths over which measurements have been made as well as their conductivities. However, no effective conductivity map was planned by CRPL. In view of proposed revision by the Commission of the Standards of Good Engineering Practice Concerning Standard Broadcast Stations, it became necessary to promulgate the new conductivity map, which is given in Fig. 1 on the opposite page.

---

* Decimal classification: R113.509. Original manuscript received by the IRE, February 2, 1954; revised manuscript received, May 18, 1954.

† Federal Communications Commission, Washington, D. C.

The following characteristics were considered desirable and incorporated into this conductivity map.

1. The indicated conductivity should not change at less than 10 mile intervals.
2. The base map should be on a scale of at least 1 to 2,500,000 and should employ Albers equal area projection to permit accurate scaling of distances.
3. The lines of demarcation between areas of different conductivities should be clearly defined in order that consistent estimates may be obtained by several different observers.

A brief study of the field strength versus distance curves revealed that the logarithm of field strength is approximately proportional to the logarithm of the conductivity for the shorter distances. Since the loudness of sound is approximately proportional to the logarithm of field strength it was decided to classify the map in steps proportional to the logarithm of conductivities. Also, it was noted that measured conductivities for paths over the same terrain often varied by more than 2 to 1, depending upon direction, frequency, interpretation, equipment, etc. Since the measured effective conductivity varies more than this amount in many cases and because of a standard error of 1.85 to 1 for subsoil types, it was decided that there was no point in having a conductivity map with classifications closer together than 2 to 1. Consequently, the following conductivity classes were established: 0.5, 1, 2, 4, 8, 15, 30, and 5,000 millimhos per meter. The 15 and 30 classes were chosen in preference to 16 and 32, respectively, because field intensity curves for 15 and 30 are already incorporated in the FCC Standards and, of course, the 5,000 class is for seawater. In line with the above system of classification the ranges of conductivity grouped into the specified classes are as given in Table I, the units being millimhos per meter.

TABLE I

Conductivity Class	Range of Conductivities
0.5	.707
1	.707– 1.414
1	1.414– 2.828
4	2.828– 5.657
8	5.657–10.95
15	10.95 –21.21
30	21.21 –45
5,000	seawater

The resulting conductivity map was drawn freehand almost entirely from data in the map overlays supplied by CRPL. These overlays, showing the locations and conductivities of all the measured radials, proved invaluable. Unfortunately, the distance scale of these overlays was not a standard size and an original map was not available, so that all the stations had to be relocated on standard maps. When there was more than one measured conductivity available for a given path or area, the geometric mean conductivity was used. Where there were no measurements available, the conductivity was estimated from those measurements in the same general area over the same subsoil type. If no measurements were available even for nearly similar subsoil types, then reference was made to the typical subsoil type conductivities computed by CRPL. Undoubtedly, had someone else drawn the lines of demarcation between the areas of different conductivity the map might have looked substantially different, especially in the region west of the Mississippi and east of the Pacific coast where comparatively few measurements were available. It is believed, however, that this map is a vast improvement over the old standard and does agree far better with the available data.

The estimation of a standard error for this effective conductivity map is not an attractive proposition in view of the variable density of the measurements throughout the country and in view of the freehand process of drawing the map. However, the writer believes that the utility of the map is greatly enhanced if its accuracy is known, even though this accuracy is only an educated guess. If there were no error of measurement or interpretation in the value of conductivity attached to each path or segment of path on the CRPL overlays, then, considering log conductivity as the basic variable, the estimated standard deviation or error in codifying the country on the conductivity map would be about 0.15—i.e. approximately two-thirds of the measured path conductivities were within 0.71 and 1.4 times the conductivities shown on the map. However, for the true over-all standard error the above standard deviation should be added in quadrature with the standard error of measurement and interpretation. The over-all standard error is then estimated to be in the order of 0.23. In other words, it is estimated, that approximately

---

[1] R. S. Kirby, J. C. Harmon, F. M. Capps, and R. H. Jones, "Effective Radio Ground Conductivity Measurements in the United States," Central Radio Propagation Lab., Boulder, Colo.; approved by the Bureau of Standards Editorial Committee and to be released in the near future.

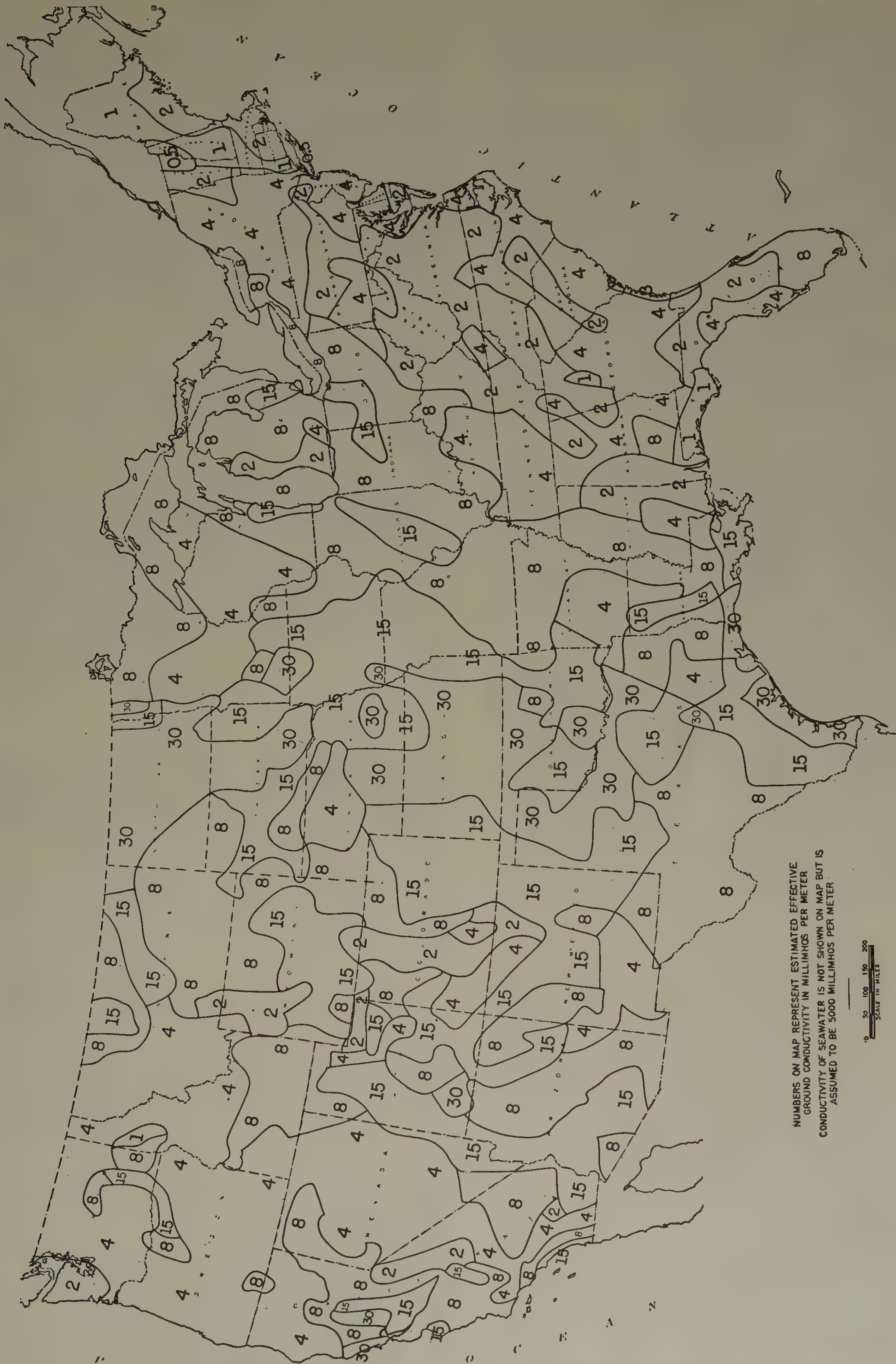
NUMBERS ON MAP REPRESENT ESTIMATED EFFECTIVE GROUND CONDUCTIVITY IN MILLIMHOS PER METER
CONDUCTIVITY OF SEAWATER IS NOT SHOWN ON MAP BUT IS ASSUMED TO BE 5000 MILLIMHOS PER METER
0 50 100 150 200
SCALE IN MILES

Fig. 1—Estimated effective ground conductivity in the United States.

two-thirds of the true effective median path conductivities for distances less than 25 miles from the transmitter were within 0.59 and 1.7 times the values which are shown on the map.

In summary, there is submitted a map of effective conductivities for the continental area of the United States. This map was based for the most part on measurements, submitted to the FCC by various standard broadcast stations. Enlarged copies of this conductivity map on a 1 to 2,500,000 scale are available for $3.50 from the Superintendent of Documents, Government Printing Office, Washington, D. C.

ACKNOWLEDGMENT

R. S. Kirby of CRPL was extremely helpful in supplying the subsoil correlation analysis data and the map overlays, which represented an enormous amount of labor by himself and other CRPL personnel. The helpful suggestions and contributions of R. Weston, H. Kassens, R. Renton, W. C. Boese, L. Light, and others, of the Commission's staff, is gratefully acknowledged. Also, acknowledgment is extended to B. Peele and B. Carpenter for their painstaking replotting of station locations and the associated drafting work involved.

On Minimum Range for Radiation Patterns*

D. R. RHODES†

Summary—**It is shown that the $2D^2/\lambda$ antenna criterion ensures a phase variation less than $\pi/8$ and an amplitude variation less than 10 per cent over D when using a paraboloidal or optimum horn antenna for illumination, providing its aperture dimensions do not exceed D. The pattern of a uniform line antenna illuminated by such a paraboloid is shown to be essentially the same as its conventional pattern (point source illumination). It is also shown that the appropriate criterion for back scattering patterns is $4D^2/\lambda$.**

INTRODUCTION

IT HAS BEEN long recognized that there is a range dependence in all radiation measurements. Serious error may result whenever long range measurements are attempted at short range. Therefore a criterion for minimum range has come into common use for antenna measurements, based on two assumptions: (1) the measurement is to be made in the field of an isotropic-point source, and (2) the maximum-phase variation over the model antenna shall not exceed $\pi/8$. The minimum-range criterion is given by

$$R = \frac{2D^2}{\lambda},$$

where D is the maximum cross-sectional dimension of the model antenna and λ is the wavelength. This criterion is actually quite arbitrary because of the arbitrariness of the assumption of the $\pi/8$ phase variation. It may be so weak as to be useless for certain types of supergain antennas, whereas it may be too restrictive for antennas with less sensitive current distributions. For the uniform line antenna, however, it has been shown[1] to be a practical criterion, and hence is probably the best single criterion available.

The assumption that the measurement is to be made in the field of an isotropic-point source does not apply strictly to either the paraboloidal or horn antennas usually used to illuminate a model. As a consequence a modified form of the minimum-range criterion is frequently used, based on the assumption that the maximum-phase difference between any point on the model and any point on the source antenna shall not exceed $\pi/8$:

$$R = \frac{2(D + d)^2}{\lambda},$$

where d is the maximum cross-sectional dimension of the source antenna. But this criterion is very weak indeed since it does not take advantage of interference resulting from radiation by the entire source aperture. The full advantage of interference is readily evident whenever the source is a portion of a plane wave (such as a paraboloid) for then the radiation on the axis of the source antenna has nearly a plane wave front at all ranges.

MINIMUM RANGE FOR ANTENNA PATTERNS

The dependence on range of the radiation pattern of a uniform line antenna in the field of a point source has been shown by Friis and Lewis[1] using wave front analysis. The dependence for antennas other than the point source cannot be shown using simple wave-front analysis but require a more advanced approach. The concept of "reaction" proposed recently by Rumsey[2] provides an exact analytical representation for the open-circuit voltage produced at the terminals of one antenna when a unit current generator is connected to the terminals of a second antenna, irrespective of the types of antennas. The induced voltage, or reaction, is the scalar product of the radiated field of one antenna by the cur-

---

* Decimal classification: R120. Original manuscript received by the IRE, October 9, 1953; revised manuscript received, May 27, 1954. The work described was supported, in part, by a contract between Wright Air Development Center and the Ohio State University Research Foundation.

† Cornell Aeronautical Lab., Buffalo, N. Y., formerly with Dept. of Elec. Eng., Ohio State University, Columbus, Ohio.

[1] H. T. Friis and W. D. Lewis, "Radar antennas," *Bell Sys. Tech. Jour.*, vol. 26, p. 270; April, 1947.

[2] V. H. Rumsey, "The Reaction Concept in Electromagnetic Theory," McGill University Symposium, June, 1953; also *Phys. Rev.*, vol. 94, p. 1483; June 15, 1954.

rent distribution in the aperture of the second antenna when the product is integrated over the aperture of the second antenna. If one of the two antennas is a point source then the pattern obtained by the reaction concept is the same as that obtained by wave-front analysis.

Before showing actual computations of the effect of the source on the pattern of an antenna it will be instructive to investigate the extent to which the field of the source antenna departs from a simple point-source field. Consider first the paraboloidal-source antenna. For purposes of analysis it will be assumed that the paraboloid can be approximated by a uniform square source of side length d. Then the maximum variation of field over the model antenna can be computed from Schelkunoff's[3] analysis of the uniform rectangular source. At minimum range, $2D^2/\lambda$, the field at the extremities of the model are functions of a single dimensionless parameter d/D. Computations of amplitude and phase deviation over the model are shown as functions of d/D in Fig. 1. Observe that the phase deviation remains nearly $\pi/8$ for $(d/D)<1$, while the amplitude falls off as $(d/D)^2$. For $d/D=1$ the amplitude drops only 0.9 decibel, or about 10 per cent. Thus the field of a uniform square source at minimum range is nearly the same as the field of a point source providing its aperture dimensions do not exceed D.

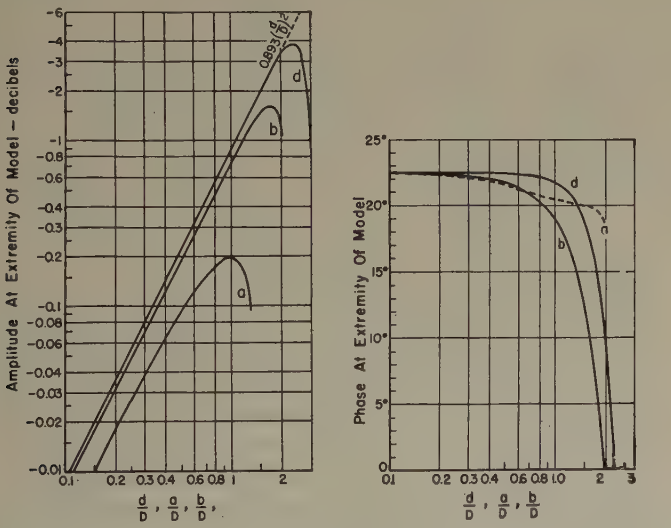

Fig. 1—Phase and amplitude at extremity of model with respect to their values at the center for models illuminated at range $2D^2/\lambda$. The illuminating antenna is a uniform square aperture of side length l, or an optimum-pyramidal horn with H-plane aperture a and E-plane aperture b.

The effect of size of a uniform square source on the pattern of a uniform line antenna can be seen in Fig. 2. The pattern for $d/D=0$, i.e. a point source, was computed from wave-front analysis; the others were computed using the reaction integral. Distortion of the far-field pattern arising from the phase and amplitude distribution of its illumination is clearly evident. Briefly, an increasing phase error causes filling in of the nulls, while an increasing amplitude taper causes broadening of the main beam and smaller side lobes. Thus it is seen that the minimum-range criterion for a point source applies nearly as well to a paraboloid, for $(d/D)\leqq 1$.

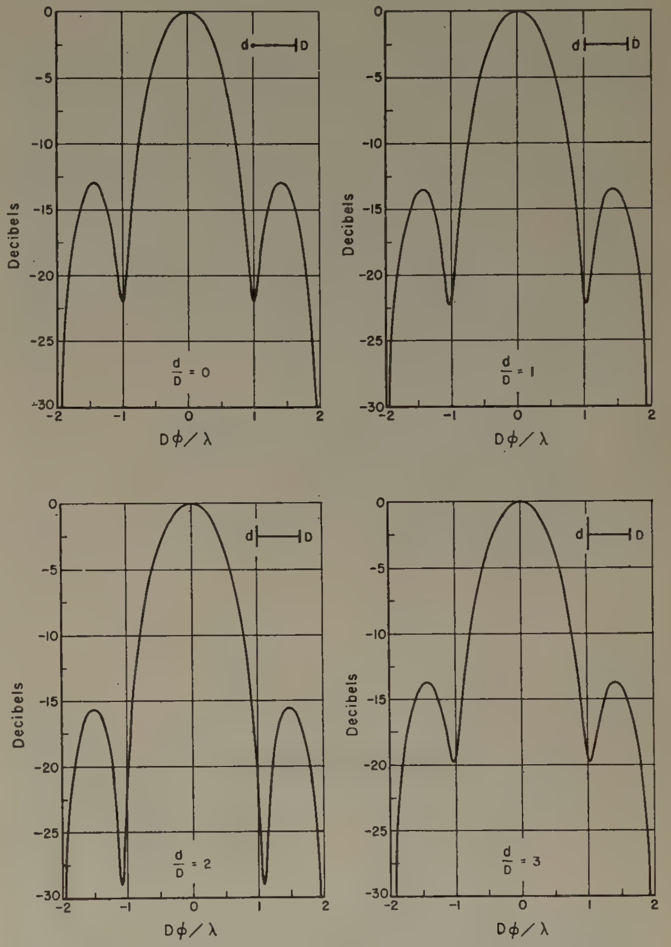

Fig. 2.—Antenna pattern of a uniform-line antenna of length D at range $2D^2/\lambda$ when illuminated by a uniform square source of length d on a side.

Consider next the pyramidal horn as a source antenna. The wave-front method can again be used to determine the illumination field over the model antenna. It is no longer possible to represent the field at the extremities of the model in terms of a single dimensionless parameter, however, because of the independent status of horn length l and aperture dimensions a and b in the H and E planes, respectively. But if we restrict our interest to optimum horns, optimum in the sense that the Fraunhofer gain is maximum, then it is possible to show that only one of these three are independent. The relationship between l, a, and b for an optimum-pyramidal horn is derived by requiring that the rate of change of its gain[4] must vanish with respect to both a and b. Differentiating with respect to a, or b, leads to an equation containing only $a/\sqrt{2\lambda l}$, or $b/\sqrt{2\lambda l}$, respectively. Graphical determination of the roots of these equations shows the following simple conditions for an optimum-pyramidal horn:

---

[3] S. A. Schelkunoff, "Electromagnetic Waves," D. Van Nostrand Co., New York, N. Y., pp. 365–368; 1943.

[4] *Ibid.*, p. 364, eqs. (23–29).

$$\frac{a}{\sqrt{2\lambda l}} = 1.02457,$$

$$\frac{b}{\sqrt{2\lambda l}} = 1.25932.$$

The field variation at minimum range in the *H* and *E* planes of the optimum pyramidal horn are shown in Fig. 1 as functions of *a/D* and *b/D*, respectively. No attempt has been made to compute the pattern of a uniform line antenna illuminated by an optimum horn because of the extreme complexity of the reaction integral. It is evident, however, that the pattern in the *E* plane of the horn should be better than for a uniform square source of the same size, and that it should be considerably better in the *H* plane.

Minimum Range for Back Scattering Patterns

A direct comparison of the effect of range on antenna and back scattering patterns can be had by comparing the pattern of a uniform line antenna with a uniform line scatterer of the same length. If a point source and receiver is used the effect of range on the pattern of a uniform line scatterer (such as a thick cylinder many wavelengths long) can be determined by including a quadratic-phase correction in the integrand of the physical optics[5] representation of radar cross section. Evaluation of the back scattering pattern then shows that the radar pattern at range 2R and angle $\phi/2$ is identical to the antenna pattern at range R and angle ϕ (in the neighborhood of broadside). Thus equivalent minimum range criterion for back scattering measurements is

$$R = \frac{4D^2}{\lambda}.$$

Radar cross section for source antennas other than a point source can be computed by application of the reaction concept.

---

[5] D. E. Kerr, "Propagation of Short Radio Waves," Rad. Lab. Series, vol. 13, McGraw-Hill Book Co., New York, N. Y., p. 463, eq. (56); 1951.

An Automatic Impedance Recorder for X-Band*

WILLIAM F. GABRIEL†, ASSOCIATE, IRE

Summary—**A broadband, low-power, automatic impedance recorder of good accuracy has been developed for the X-band frequency range. The instrument will accept any impedance which has an X-band waveguide input and will plot an ink graph of either the impedance or the admittance upon a standard Smith type impedance chart. If the test impedance is one of low mismatch, the instrument can be switched to an expanded Smith chart scale and thus provide greater plotting accuracy near the matched condition. The plane of impedance measurement, or "reference terminals," of the instrument may be located at any point desired along the waveguide transmission line leading to the test impedance and will remain fixed for all frequencies in the operating band. An rf impedance circuit utilizing broadband waveguide components extracts the amplitude and phase information which operates electromechanical servos in the amplifier-recorder unit. The components presently in use give an operating bandwidth from 8400 mc to 9900 mc, and the arrangement is such that the system will operate on any incident rf power level within the range of about 20 to 250 milliwatts. Everyday laboratory use of the instrument by both professional and nonprofessional personnel has shown it to be accurate, reliable, and a great time saver.**

Introduction

THE CONTINUOUS trend toward improved performance and broader bandwidths in rf components and antennas requires a corresponding increase in the amount of impedance information which must be obtained on these components during the research, development, and production testing stages. Point-by-point methods of impedance measurement, which usually involve either a slotted line standing-wave detector or some type of rf impedance bridge, provide the bulk of this impedance information and probably will continue to do so because of their simplicity, versatility, and relatively low cost. However, when the amount of impedance information required in a given instance becomes very large, then point-by-point methods become tedious, time-consuming, and costly, in terms of man hours, and some method for rapid, automatic presentation of the information is desired.

The instrument to be discussed herein was developed in order to fill the need for an accurate, broadband, automatic impedance recorder for the microwave frequencies. It will plot an ink graph of either impedance or admittance upon either a standard Smith chart or any

---

* Decimal classification: R244. Original manuscript received by the IRE, October 8, 1953; revised manuscript received, May 14, 1954. This paper was presented at the Joint URSI-IRE Meeting, Washington, D. C., on April 27, 1953. It is a condensation of Rep. No. 4204, Naval Res. Lab., Washington, D. C., August, 1953.

† Microwave Antennas and Components Branch, Electronics Division, Naval Research Lab., Washington 25, D. C.

expanded center portion thereof, and one may locate the "reference terminals" or plane of impedance measurement at any desired point along the waveguide transmission line leading to the test impedance. Calibration in both phase and amplitude is quick and simple and remains permanent when set. For purposes of discussion, the instrument may be divided into two major parts; the rf impedance circuit and the servo loops. These two parts are treated in Section I and Section II respectively. Section III deals with the complete system, and in Section IV the accuracy of the instrument and some of its applications are discussed.

I. RF IMPEDANCE CIRCUIT

The most convenient way of representing an impedance at the higher frequencies is to express it in terms of its reflection coefficient, ρ_z, which is related to the incident and reflected energy by the expression

$$\rho_z = \frac{E_r}{E_i} \tag{1}$$

where E_i represents the electric field vector associated with the energy incident upon the test impedance, and E_r represents the electric field vector associated with the energy reflected from the test impedance. From (1), it is evident that ρ_z can be evaluated simply by obtaining the ratio of the amplitudes of E_r and E_i and the phase difference between them. These two simple operations, then, are the ones performed by the present instrument. The rf impedance circuit permits this direct evaluation of ρ_z by obtaining the amplitudes of E_r and E_i and by comparing their phases.

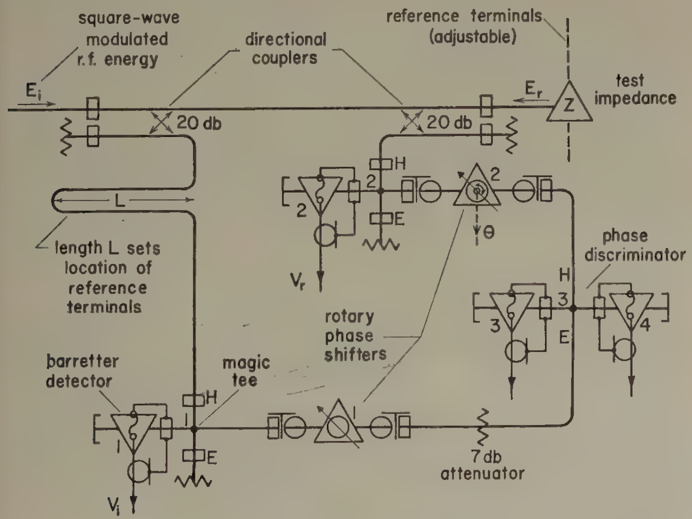

Fig. 1—Rf impedance circuit schematic.

The circuit, which is shown in schematic diagram form in Fig. 1, is an extended application of the familiar reflectometer principle. Two similar 20 db directional couplers attached to the main transmission line couple out one per cent of the energy which is incident upon and reflected from the test impedance. The sample of reflected energy enters a matched hybrid junction (No. 2 in Fig. 1) where it is divided equally, one half of it going to a square law barretter detector to give the amplitude signal, V_r, and the other half going through a rotary phase shifter to the phase discriminator. The sample of incident energy is treated similarly except for passing through an extra length of waveguide, length L in Fig. 1, the purpose of which is to make the waveguide path-length to the phase discriminator the same for the incident as for the reflected energy. This provision causes the reference plane of impedance measurement to remain constant regardless of the frequency of the incident energy. The two amplitude signals, V_r and V_i, are sent to a computer which takes the square root of their ratio, thus obtaining the amplitude of ρ_z.

At the phase discriminator, which is of a conventional magic tee type, the E_r and E_i fields are combined to give resultant amplitude signals at the two square-law barretter detectors mounted on the side arms of the magic tee. If E_r and E_i differ in phase by 90 degrees, the output signals will be equal, but if their phase difference is other than 90 degrees, the output signals will be unequal and the resulting voltage difference constitutes an error signal. Either or both of the two identical rotary phase shifters could be used to balance the discriminator outputs and indicate the phase angle between E_i and E_r, but in the present system, only the phase shifter in the E_r branch (No. 2 in Fig. 1) is used for this purpose. The other rotary phase shifter (No. 1) is used for setting the arbitrary zero phase angle position when one calibrates the system by using a short circuit for test impedance.

A 7 db attenuator is included in the E_i branch in order to help minimize the harmful effects of multiple reflections and also to permit the phase discriminator to operate over a greater range of amplitude variation in the E_r signal. The additional phase shift caused by inserting this attenuator is compensated for by inserting a similar dielectric card in the E_r branch with the resistance film removed.

The rf impedance circuit was designed primarily for those frequency ranges, particularly X-band, wherein the necessary waveguide components are of convenient size, good quality, and generally available. System performance, of course, depends primarily upon the characteristics of the individual components used. In the present X-band system, the barretter detectors and magic tees are of conventional design with a bandwidth of about 8400 to 9700 mc. The directional couplers, also commercially available, are of slightly better bandwidth with a coupling which remains flat within ±0.2 db and a directivity in excess of 40 db. Rotary phase shifters[1] were not commercially available in 1951 when this system was first assembled, but excellent laboratory models[2] with a bandwidth of 8200 to 10,000 mc were available.

---

[1] A. G. Fox, "An adjustable waveguide phase changer," PROC. I.R.E., vol. 35, pp. 1489–1498; December, 1947.

[2] R. M. Brown and A. J. Simmons, "Dielectric Quarter-Wave and Half-Wave Plates in Circular Waveguide," Rep. No. 4218, Naval Research Lab., Washington, D. C.; November, 1953.

Precision phase measurements on several of these laboratory rotary phase shifter units at 8432, 8910, 9375, and 9925 mc have shown a maximum phase deviation of about ±1 degree from perfect phase linearity (electrical phase shift versus mechanical angle of rotation). The operating frequency range of the complete impedance circuit is 8400 to 9900 mc when the above-described components are used.

An error analysis[3] of the impedance circuit shows that the principal sources of error are the reflections from the various components and junctions, the coupling between side arms of the magic tees, and the directivity of the $\boldsymbol{E}_r$ directional coupler. The first two sources give rise to terms which are independent of the magnitude of ρ_s and, for the components presently in use, these terms can add in phase to give maximum errors of as much as 20 per cent in amplitude and 13 degrees in phase at the ends of the frequency band. As would be expected, however, destructive interference effects among the various error terms keep their resultant error much smaller than maximum most of the time. The directivity term, $\boldsymbol{d}$, is a distinctive error because the effect it exerts depends upon the magnitude of ρ_z; i.e., the output of the $\boldsymbol{E}_r$ directional coupler is,

$$KE_ie^{j\phi}(\rho_z + \boldsymbol{d}) \tag{2}$$

where K is the coupling coefficient and ϕ is a phase angle. Since the directivity is in excess of 40 db, the magnitude of $\boldsymbol{d}$ is less than 0.01 over the band.

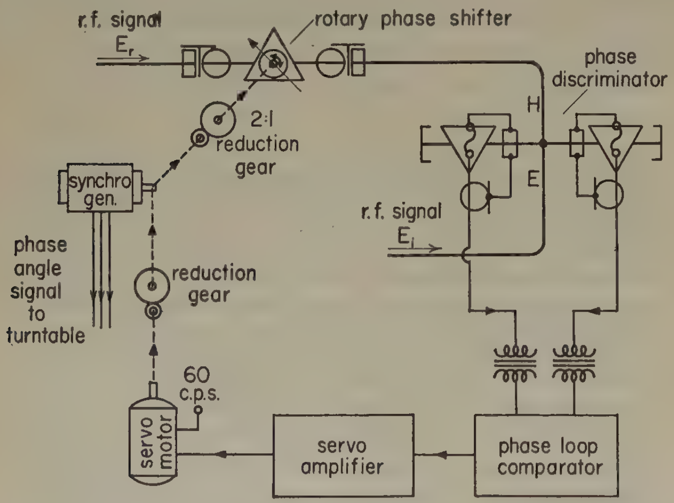
r.f. signal
E_r
rotary phase shifter
phase discriminator
H
2:1
reduction gear
synchro gen.
E
r.f. signal
E_i
phase angle signal to turntable
reduction gear
60 c.p.s.
servo motor
servo amplifier
phase loop comparator

Fig. 2—Phase servo loop.

II. Servo Loops

The phase servo loop is shown in schematic diagram form in Fig. 2. A comparator, which is of the differential amplifier type, takes the amplitude difference between the two signals of modulation frequency coming from the phase discriminator detectors and sends it to a servo amplifier which feeds the servo motor geared to the rotary phase shifter. When the signals from the discriminator detectors become unbalanced due to a shift in the phase of the $\boldsymbol{E}_r$ field, the motor receives the resultant error signal and drives the rotary phase shifter until the original shift in phase is exactly countered and balance is again restored. Thus, in keeping the discriminator balanced, the servo positions the rotary phase shifter so that the phase shift which it introduces is exactly equal to the phase angle between $\boldsymbol{E}_r$ and $\boldsymbol{E}_i$, which is the desired phase angle of the reflection coefficient.[4] A synchro generator geared 2:1 to the rotary phase shifter transmits its phase angle position to the recording turntable follow-up servo drive.

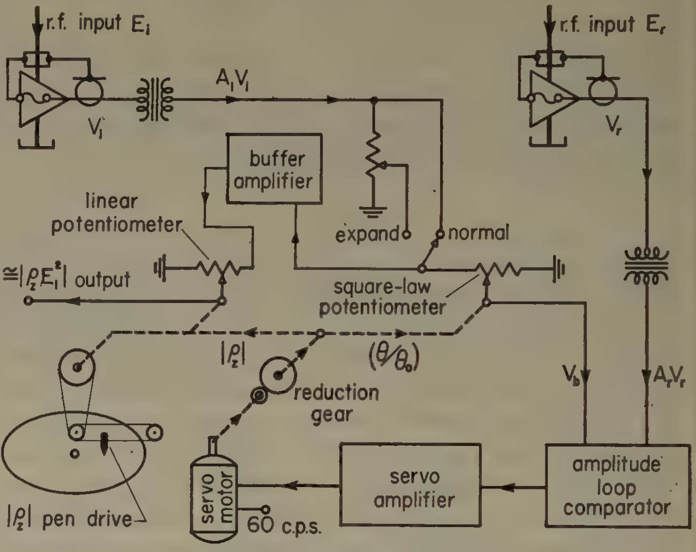
r.f. input E_i
A_iV_i
V_i
r.f. input E_r
V_r
buffer amplifier
linear potentiometer
expand
normal
$\cong|\rho_zE_i^*|$ output
square-law potentiometer
$|\rho_z|$
(θ/θ_0)
reduction gear
V_b
A_rV_r
$|\rho_z|$ pen drive
servo motor
60 c.p.s.
servo amplifier
amplitude loop comparator

Fig. 3—Amplitude servo loop.

The gear reduction ratio used between the servo motor and the rotary phase shifter must be determined rather carefully in order to arrive at a reasonable compromise between speed of response and accuracy. In the present servo, a reduction gear ratio of approximately 100 is employed. This value results in excellent accuracy and a speed of response which is better than that of the recording turntable. The maximum speed of the phase servo loop is about 120 degrees per second and its sensitivity is better than ±0.1 degree except when ρ_s approaches zero.

The complete amplitude servo, which is shown in schematic diagram form in Fig. 3, actually constitutes a square-root-ratio computer of the servo-driven-potentiometer type and operates in the following manner. The detected voltage V_i, which is proportional to the square of the amplitude of $\boldsymbol{E}_i$, is stepped-up by means of a transformer and applied across a potentiometer that has a square-law resistance winding.

$$R = R_0\left(\frac{\theta}{\theta_0}\right)^2 \tag{3}$$

where R and θ are the resistance and angle between the brush and the low end of the potentiometer winding, and R_0 and θ_0 are the total resistance and total angle of the winding. If the brush connects to a circuit of extremely high impedance compared to R_0, then the current, I, through the winding is simply (A_iV_i/R_0) where A_i is the step-up ratio of the transformer input circuit. The voltage tapped off by the brush would be

---

[3] A complete analysis of system error is contained in the NRL Rep. No. 4204.

[4] It is assumed here that the arbitrary zero phase angle position of the phase shifter has been established by using a short circuit for the test impedance.

$$V_b = RI = R_0\left(\frac{\theta}{\theta_0}\right)^2 \cdot \left(\frac{A_iV_i}{R_0}\right) = A_iV_i\left(\frac{\theta}{\theta_0}\right)^2. \tag{4}$$

V_b is then compared with A_rV_r, which is proportional to the square of the amplitude of E_r, in the amplitude loop comparator and the difference between the two is amplified and applied to a servo motor which is geared to the brush shaft of the square-law potentiometer. The servo motor drives the brush until V_b is equal to A_rV_r and we have the following relationship:

$$A_rV_r = V_b = A_iV_i\left(\frac{\theta}{\theta_0}\right)^2 \tag{5}$$

or

$$\left(\frac{\theta}{\theta_0}\right) = \sqrt{\frac{A_rV_r}{A_iV_i}}\,.$$

But since $V_r = C_r|E_r|^2$ and $V_i = C_i|E_i|^2$, where C_r and C_i are proportionality constants, then (5) becomes

$$\left(\frac{\theta}{\theta_0}\right) = \sqrt{\frac{A_rC_r|E_r|^2}{A_iC_i|E_i|^2}} = \sqrt{\frac{A_rC_r}{A_iC_i}}\cdot|\rho_z| \tag{6}$$

or

$$\left(\frac{\theta}{\theta_0}\right) = |\rho_z| \quad \text{when} \quad \sqrt{\frac{A_rC_r}{A_iC_i}} = 1.$$

Thus, the angular position of the brush is linearly related to the amplitude of the reflection coefficient. A translation of this shaft angle into corresponding radial movement of the recording pen on the turntable then permits the plotting of $|\rho_z|$ on a Smith impedance chart.

To record on an expanded Smith chart, A_iV_i is simply attenuated by the correct amount before being applied to the square-law potentiometer; that is, if we substitute (A_i/K^2) for A_i in (5), we obtain

$$\left(\frac{\theta}{\theta_0}\right) = \sqrt{\frac{A_rV_r}{\left(\dfrac{A_iV_i}{K^2}\right)}} = K\cdot\sqrt{\frac{A_rV_r}{A_iV_i}} = K|\rho_z|. \tag{7}$$

Consequently, to record on a Smith chart whose scale factor has been expanded by K times the normal size, one must reduce A_iV_i by the factor $(1/K^2)$ at the square-law potentiometer. The dropping potentiometer which is used for obtaining this reduction may be seen in Fig. 3. A switch on the present instrument enables the operator to select either the "normal" or "expand" type of impedance chart recording.

As in the case of the phase servo loop, the reduction gear ratio between the servo motor and the square-law potentiometer must be chosen with care. In the present instance, accuracy was given precedence over speed of response and resulted in a gear ratio of about 100. With this value, the speed of the servo is 0.33 units of reflection coefficient per second and the sensitivity is better than ±0.002 except when ρ_z approaches zero.

The loop gains of the phase and amplitude servo loops are a function of the incident power level and the reflection coefficient of the test impedance, the relationship[5] in each instance being

$$\text{loop gain} \simeq GE_i^2\rho_z \tag{8}$$

where G is a function containing the gain and time constant of each component in the servo loop. This being the case, it follows that optimum servo loop performance cannot be maintained over any appreciable dynamic range of impedance variation unless the above dependency is compensated for. Consequently, an AGC (Automatic Gain Control) servo is added to the system to automatically perform this function. The first step in the AGC servo loop is to obtain the product of E_i^2 and ρ_z, and this is accomplished by means of a buffer amplifier and a linear potentiometer as shown in Fig. 3. At this point it is convenient to refer to a schematic diagram of the complete system, which is shown in Fig. 4, on the following page. Picking up the AGC signal, we see that it is fed into a comparator along with a reference voltage whose amplitude is kept constant. If the $E_i^2\ \rho_z$ signal departs from the level of the reference voltage, an error signal results which is amplified and applied to a servo motor which drives a variable attenuator controlling the incident power level. Essentially, then, the AGC loop varies E_i^2 inversely as the magnitude of the reflection coefficient, thereby keeping their product constant. This action not only stabilizes the gains of the two servo loops, but it also provides some protection for the klystron oscillator against frequency and amplitude pulling caused by test impedances of high Q or high mismatch; that is, the AGC inserts attenuation in proportion to the mismatch of the test impedance.

III. COMPLETE SYSTEM

Fig. 4, page 1414, shows manner in which the rf impedance circuit, phase servo loop, amplitude servo loop, and the AGC are interconnected. Completing the system are a klystron oscillator, a cavity frequency meter, an oscilloscope, and the recording turntable.

The klystron oscillator may be any tube capable of an rf power output of about 100 to 200 milliwatts over the bandwidth of the system. Fluctuations in the power output level of the klystron oscillator have little or no effect upon the system unless they become extremely large, in which case the following two limitations may apply:

---

[5] A derivation of this relationship for each servo loop is contained in the NRL Rep. No. 4204.

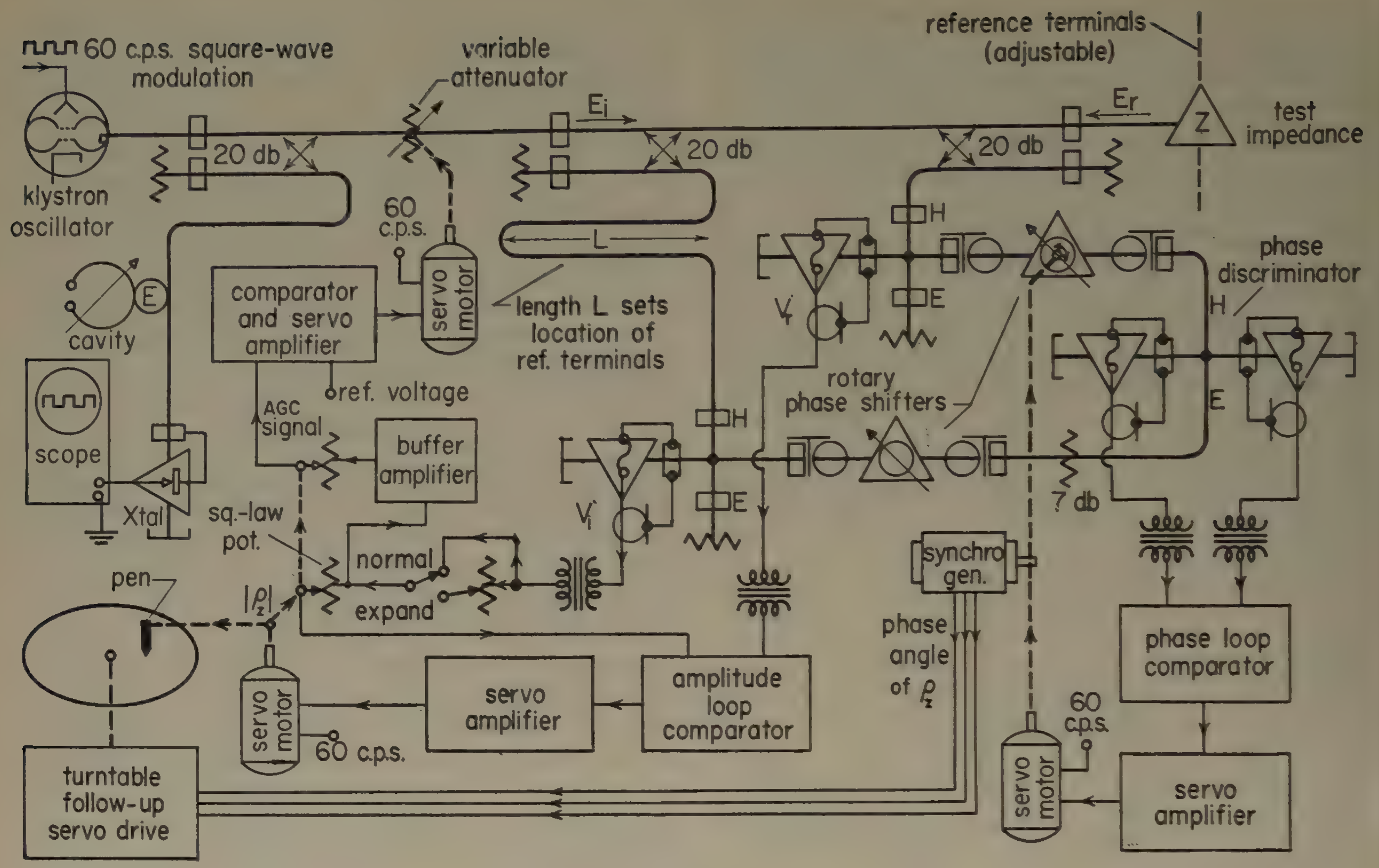
60 c.p.s. square-wave modulation
variable attenuator
reference terminals (adjustable)
klystron oscillator
20 db
Ei
20 db
Er
20 db
Z
test impedance
60 c.p.s.
servo motor
L
length L sets location of ref. terminals
cavity
E
comparator and servo amplifier
H
E
phase discriminator
H
Vi
rotary phase shifters
E
scope
AGC signal
ref. voltage
buffer amplifier
H
E
Vi
7 db
Xtal
sq.-law pot.
normal
expand
synchro gen.
pen
|ρz|
phase angle of ρz
phase loop comparator
servo motor
60 c.p.s.
servo amplifier
amplitude loop comparator
60 c.p.s.
servo motor
servo amplifier
turntable follow-up servo drive

Fig. 4—Complete system schematic.

1. There is a maximum input power level determined by the barretter detectors, which seriously depart from a square-law function for power levels in excess of a milliwatt. In the present system the attenuation ahead of the detectors is 23 db (20-db couplers and 3-db in magic tee split), which results in a maximum rf input power of 200 milliwatts average for the system. If 10-db couplers[6] had been used, it would be 20 milliwatts maximum, etc.
2. There is a minimum input power level which is determined by the minimum reflection coefficient for which an accurate measurement is desired; that is, a certain amount of reflected energy above the noise level is required to operate the servo loops, and since this is related to the input energy through the reflection coefficient, $E_r^2=\rho_z^2E_i^2$, it follows that a given minimum value of ρ_z establishes a required minimum input power level. Of course, since one usually desires to measure as close as possible to $\rho_z=0$, it is best to keep the input power level as close as possible to maximum.

The cavity frequency meter and the oscilloscope are used for monitoring the amplitude of the square-wave modulated klystron output energy and for measuring its frequency. They permit manual frequency sweeping and manual frequency indication to be performed with satisfactory rapidity in the present laboratory use of the instrument. Automatic frequency sweep and automatic frequency indication are regarded as additional features which may be added to the instrument if there is an application that warrants the additional complexity.

A photograph of the complete laboratory working model is shown in Fig. 5. Here one can distinguish the rf "plumbing" on the right, the recorder unit in the center, and the rack containing the amplifiers and power supplies on the left.

Calibration of the instrument in phase and amplitude is a fairly simple procedure and, once it is adjusted, remains permanent. Perhaps the first consideration would be the line length, L, which locates the reference terminals or impedance plane (see Fig. 1). The inverted "U"-shaped piece of waveguide seen in Fig. 5 protruding above the rest of the plumbing is a particular fixed value of L that locates the reference terminals at the exact end of the second directional coupler. This length is the one most commonly used and it is arrived at by placing a flat short-circuiting plate on the end of the directional coupler and then noting the indicated phase angle as the frequency is swept over the band. If the piece of waveguide is too long or too short, then the reference terminals will not be at the point where the short circuit is, of course, and a continuous phase shift in one direction will result. Having obtained this particular length, one may then move the reference terminals out beyond the

---

[6] The actual coupling value of the directional couplers used in the rf impedance circuit is unimportant except in regard to the relationship between the available input rf power level and the power level desired at the barretter detectors.

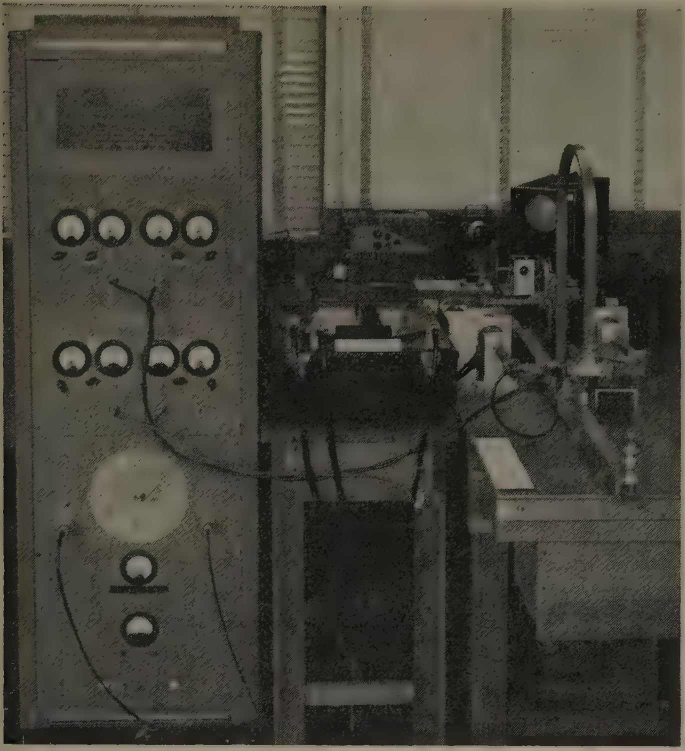

Fig. 5—Automatic impedance recorder, laboratory model.

end of the directional coupler by a distance *X* by attaching two straight pieces of waveguide of length *X* to the ends of the "U"-shaped piece.

The next calibration consists of setting the arbitrary zero phase angle position so that it coincides with the marked zero point on the recording turntable. Having placed a short circuit at the point of the reference terminals so as to give a known zero-phase angle, one positions the free rotary phase shifter (No. 1 in Fig. 1) manually until the recording turntable rotates to its marked zero-phase angle position. The phase can be advanced or retarded by any desired amount by positioning the free rotary phase shifter.

Calibration of the instrument in amplitude consists of two steps: first, the zero shaft angle position of the square-law potentiometer, ($\theta=0$), is lined up with the zero position of the recording pen on the Smith impedance chart ($\rho_z=0$); and second, using a short circuit for the test impedance, the V_i signal to the square-law potentiometer is adjusted to locate the recording pen on the outer edge of the Smith chart ($\rho_z=1$). The V_i signal adjustment is a small potentiometer in series with the square-law potentiometer and it is necessary because the reflected energy is attenuated slightly more than the incident energy due to power lost in the directional couplers. The adjustment of the expand scale potentiometer consists of attaching a variable impedance to the reference terminals and adjusting its magnitude until the normal Smith chart indicates the value which represents full-scale deflection on the expanded Smith chart. The selector switch is then shifted from the "normal" to the "expand" position and, with an expanded Smith chart placed on the recording turntable, the dropping potentiometer (see Fig. 3) is adjusted until the recording pen is positioned at full scale on the expanded chart.

If the calibration adjustments are made at a mid-band frequency, the system errors which inevitably arise over the entire bandwidth will usually tend to be evenly distributed about the true reference value. Error distribution can be checked easily by making a trial run over the entire bandwidth with a short circuit at the reference terminals. The error distribution of the present instrument for such a short circuit test is reproduced in Fig. 6 on the following page.

IV. Accuracy and Applications

The accuracy of a microwave impedance recorder is very difficult to arrive at because of the fact that there are no true impedance standards available except for the short circuit. Therefore, the most that one can do is to compare the measurements of the recorder against those taken with another impedance measuring instrument, in this case a slotted line. This has been done for five impedances which were arranged to cover the Smith Chart reasonably well.

A reproduction of one of these comparison tests is shown in Fig. 7, on page 1417. The continuous curve was traced by the impedance recorder, and added to it are frequency markers which show the exact impedance value measured at each 100 mc point over the band. The solid dots are the impedance values obtained from precision slotted line measurements on the same impedance at exactly the same frequencies as are indicated by the markers. Numerical differences between the values measured with the slotted line and those measured by the impedance recorder are listed in Table I. Another example of a comparison test between the impedance re-

TABLE I

Table of Comparison of Impedance Recorder Measurements Against Slotted Line Measurements over Frequency Range 8400 to 9900 mc

Test Impedance	Amplitude Difference in ρ_z	Phase Difference in ρ_z
Short Circuit: $\rho_z=1.00$	± 0.033 max.	± 5.2 degrees max.
Impedance No. 1: $\lvert\rho_z\rvert \cong 0.650$ (phase varies 390 degrees over band)	$+0.025$ max. ± 0.012 av.	± 4.0 degrees max. ± 2.3 degrees av.
Impedance No. 2: $\lvert\rho_z\rvert \cong 0.270$ (phase varies 390 degrees over band)	$+0.030$ max. ± 0.008 av.	$+6.0$ degrees max. ± 1.7 degrees av.
Impedance No. 3: $\lvert\rho_z\rvert \cong 0.160$ (phase varies 370 degrees over band)	$+0.017$ max. ± 0.005 av.	$+9.0$ degrees max. ± 2.4 degrees av.
Impedance No. 4: $\lvert\rho_z\rvert \cong 0.045$ (phase varies 270 degrees over band)	$+0.010$ max. ± 0.004 av.	$+30.0$ degrees max. ± 8.7 degrees av.
Impedance No. 5: $\lvert\rho_z\rvert \cong 0.018$	$+0.009$ max. ± 0.004 av.	

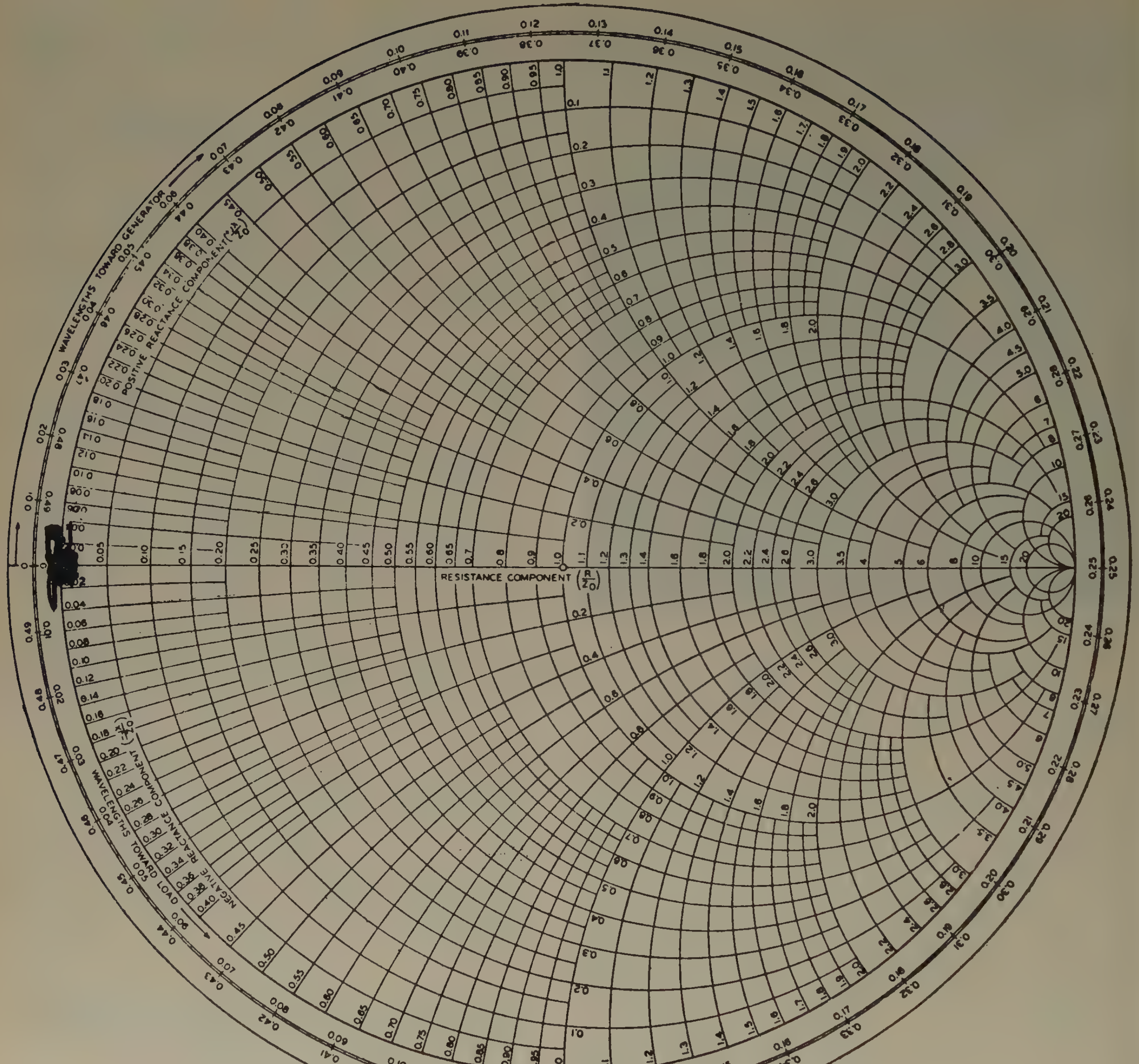

Fig. 6—Error distribution for short circuit impedance. Frequency range 8400 mc through 9900 mc.

corder and the slotted line is shown in Fig. 8, page 1418, this time on an expanded Smith impedance chart.

The foregoing two examples, plus the others in Table I, show that the accuracy attained with the present impedance recorder is sufficient for the great majority of impedance measuring applications at microwave frequencies. Another interesting fact brought out by these comparison tests was the difference in time between the two methods of measurement. Even though frequency sweep and frequency indication are performed manually on the present impedance recorder, it still took only ten or fifteen minutes to obtain an impedance plot over the band with frequency markers included, whereas the slotted line measurements on the sixteen discrete impedance values used in each comparison test always took about $2\frac{1}{2}$ hours or more to complete. The short-circuit test data are not really "comparison" data but, rather, represent absolute accuracy because the short circuit is a true impedance standard. The short circuit test is the one illustrated in Fig. 6.

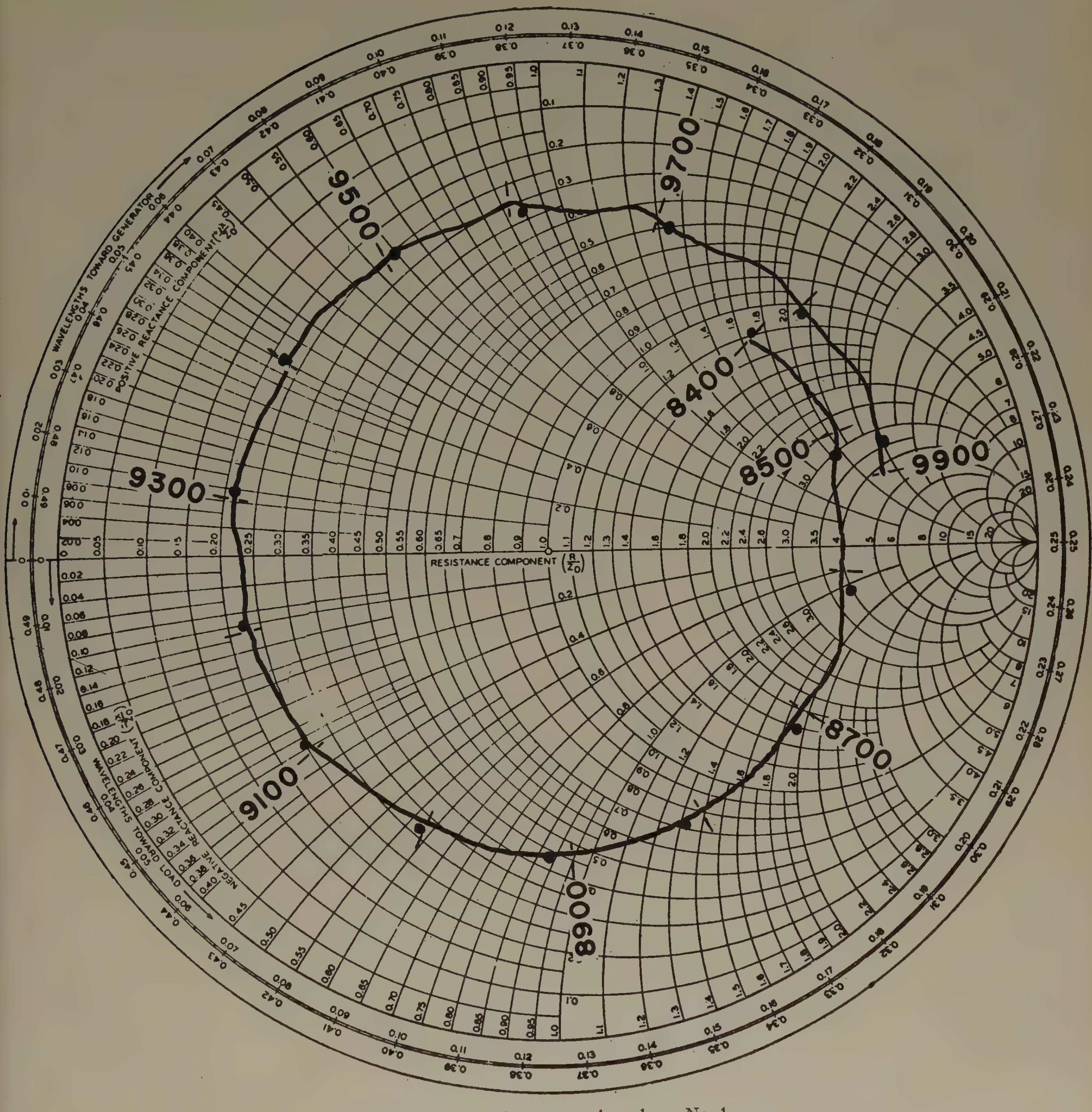

Fig. 7—Comparison test on impedance No. 1.

In Table I it will be noted that no data are listed in the phase difference column for Impedance No. 5, which happened to be an ordinary laboratory "matched load" that was chosen at random. The reason for the omission is twofold: first, the reflection from this impedance was so small at times that the phase servo loop did not have enough signal to operate on, and second, it was also too small a mismatch for obtaining an accurate phase measurement with the slotted line. Thus, since neither method was capable of measuring the phase of this small mismatch accurately, comparison was impossible. Of course, one seldom desires phase information on impedances of this magnitude. (VSWR varied between a maximum of 1.04 and a minimum of 1.015 for Impedance No. 5.)

Since the time when the instrument was first put into general laboratory use in June, 1952, it has had many applications. Most of these consist of impedance matching and/or bandwidth measurements on rf components, antennas, and antenna feeds, but occasionally a special application will arise such as impedance measurements

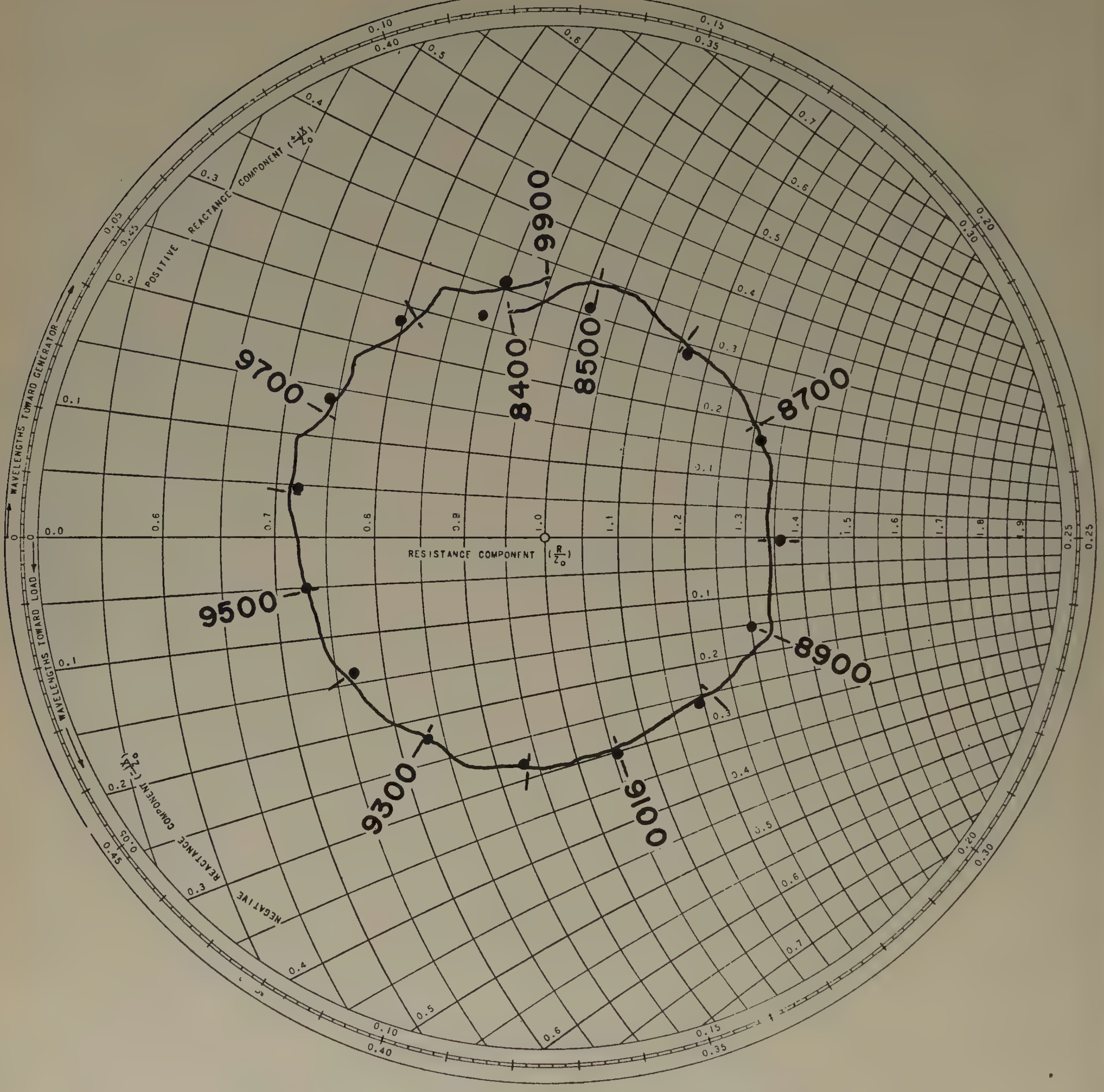

Fig. 8—Comparison test on impedance No. 3 (expand chart).

on resonant cavities of high Q, application of Deschamps method for finding the scattering matrix of a waveguide junction, impedance measurements on slots and irises, etc. Three applications have been chosen for presentation in order to give the reader a better acquaintance with the capabilities of the instrument.

The first example is a demonstration on an impedance of known impedance behavior. The impedance selected is a series "*T*" waveguide junction with a matched load on one arm and a movable short circuit in the other arm. We know that movement of the short circuit will cause an impedance variation which results in a circle of $\frac{1}{2}$ radius that passes through the center of the Smith chart. Fig. 9 shows the results obtained on the impedance recorder. This particular impedance variation covers a dynamic range of 36 db, giving an idea of performance obtained from the phase and amplitude servo loops

The second example, shown in Fig. 10 (page 1420), is an impedance-bandwidth plot on a multi-element rf component adjusted for broadband performance. This is

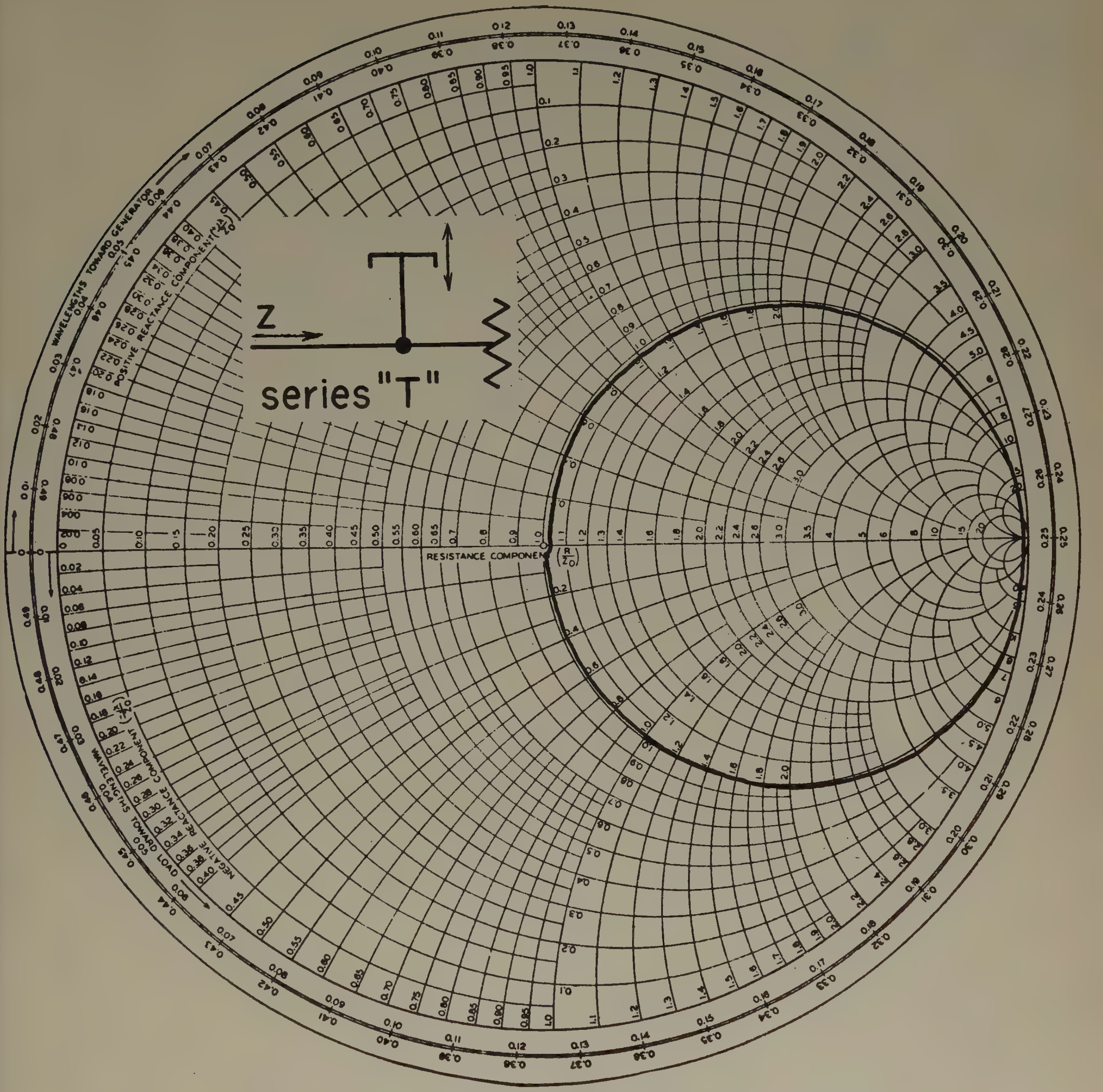

Fig. 9—Demonstration on impedance of known behavior. Frequency 9445 mc.

one of the most common uses of the instrument, but the example chosen is a little unusual in that the impedance plot contains a loop which proceeds in the counterclockwise direction with increasing frequency, a phenomenon which is ordinarily contrary to basic network theory. The reason for its occurrence here is that the reference terminals were located in the midst of the multi-element impedance structure, thus causing those elements which were distributed behind the reference terminals to have a negative waveguide phase-length term, $-4\pi l/\lambda_g$, where l is the distance between the reference terminals and a particular element.

For the third example, an application of the instrument to Deschamp's method[7] for obtaining the scattering matrix of a waveguide junction has been chosen. Deschamp's method permits rapid computation of the reflection and transmission coefficients of a junction by

---

[7] G. A. Deschamps, "Determination of reflection coefficients and insertion loss of a waveguide junction," *Jour. Appl. Phys.*, vol. 24, pp. 1046–1050; August, 1953.

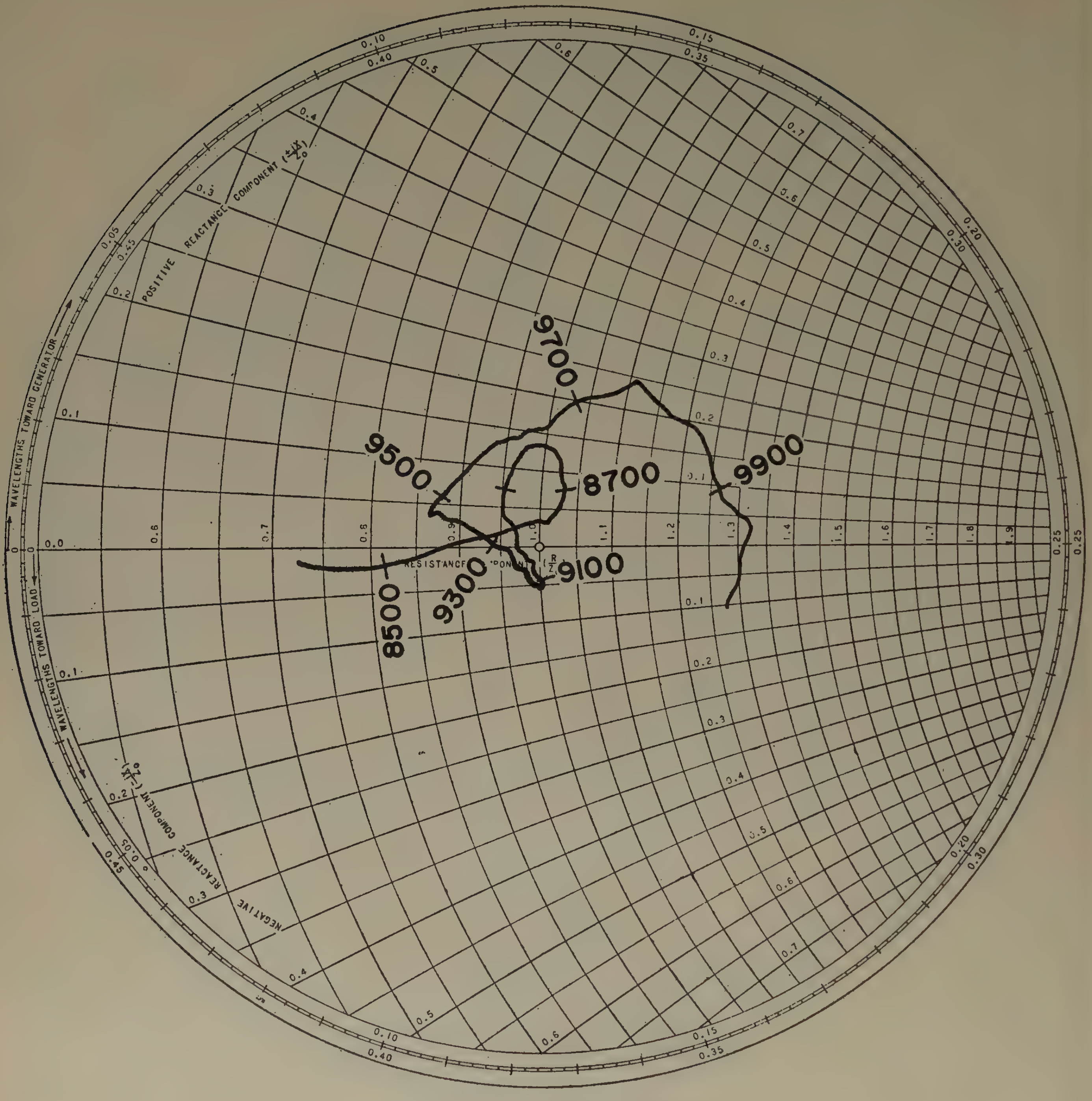

Fig. 10—Example of impedance-bandwidth plot.

means of simple graphical constructions on the Smith impedance chart. A short circuit is moved in one of the waveguides and the corresponding reflection coefficient is measured in the other waveguide. The positions of the short circuit are taken equally spaced every $\frac{1}{8}$ or 1/16 of a wavelength. When plotted on a Smith chart, these points fall on a circle and the chords joining opposite points intersect in a single point which is simply related to the desired parameters. The impedance recorder is ideally suited to the method because the necessary impedance circle can be directly plotted on the Smith chart in a matter of seconds, whereas slotted line measurements consume considerable time. Short circuit positions every $\frac{1}{8}$ or 1/16 of a wavelength are easily found by noting the amount of movement of the short circuit necessary to rotate the Smith chart a full turn (this corresponds to a half wavelength), and then dividing that movement into the desired fractions. Fig. 11 illustrates a Deschamps method circle plotted by the instrument for a lossy junction. The 1/16 wavelength positions on the circle have been joined by chords to show the point of intersection obtained in this particular instance.

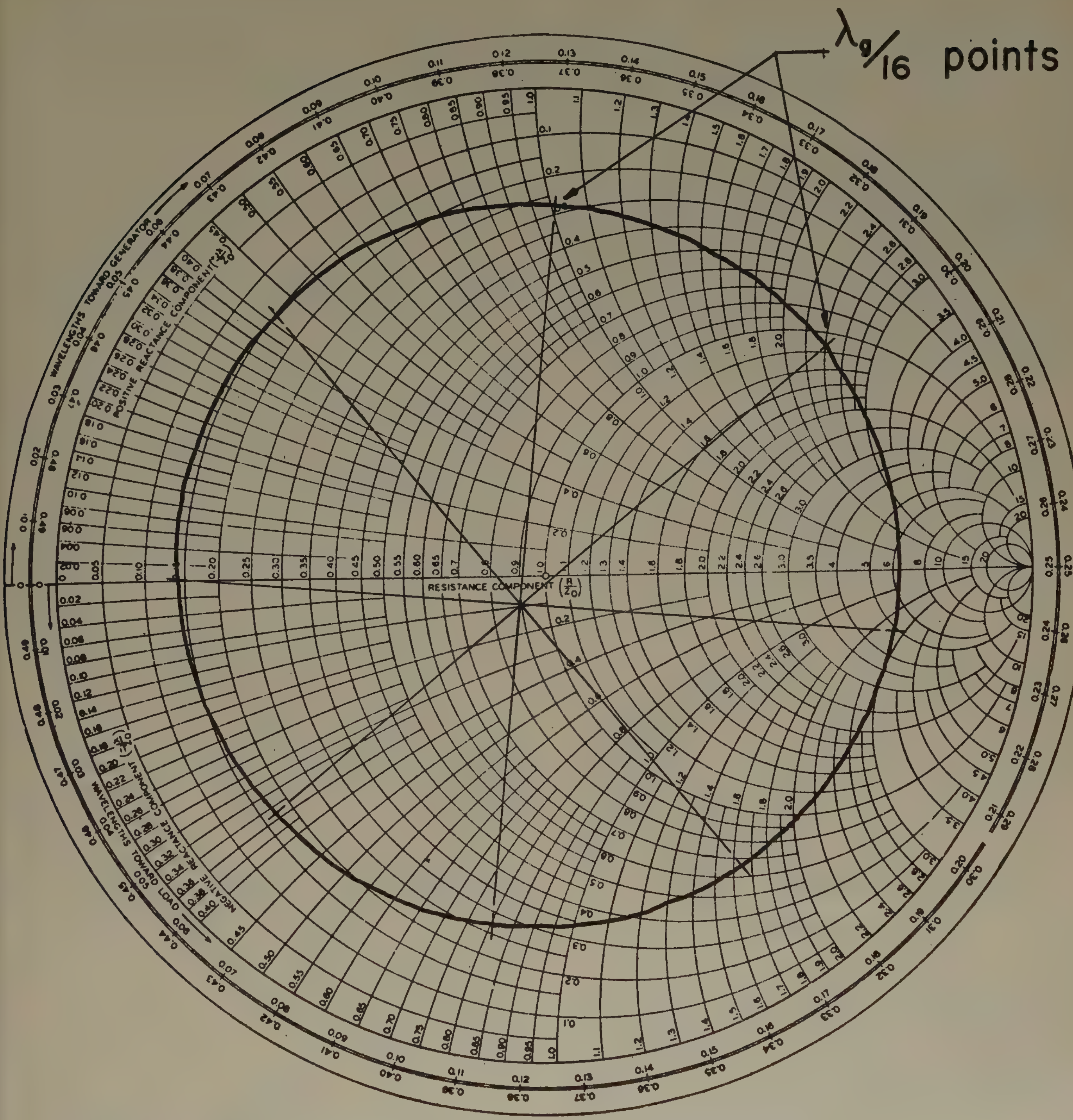

Fig. 11—Application to Deschamp's method. Frequency 8725 mc.

CONCLUSION

The present laboratory model (Fig. 5) has been in use for two years now and, during this trial period, has conclusively demonstrated its usefulness as a laboratory instrument. It has been well received and frequently used by both professional and nonprofessional personnel and is consistently accurate, reliable, and a great time-saver. The impedance curve which the instrument automatically traces on the Smith impedance chart is a form of data presentation much superior to point-by-point measurements because it is a continuous and immediately permanent record which requires no translation into other units or onto other charts. On several occasions, an impedance variation has been discovered which previous slotted line measurements had failed to reveal. In addition, the instrument has the beneficial effect of encouraging the undertaking of projects involving lengthy, broadband impedance measurements, which might otherwise be neglected.

An Investigation of the Ultimate Performance of Space-Charge Deflection Tubes*

J. T. WALLMARK, ASSOCIATE, IRE†

***Summary*—The ultimate performance of space-charge deflection tubes is investigated in several respects and a comparison is made with pentodes and multiplier tubes using essentially the same tube structure. Noise may be considerably lower than for conventional multiplier tubes and almost equal to that of pentodes. The transconductance-to-current ratio may surpass the value for conventional tubes by a factor of 2–10. The high-frequency behavior is inferior to that of pentodes. The stability of transconductance may be higher and distortion lower than for conventional multiplier tubes and even pentodes. The current drain may be lower than that of a pentode.**

INTRODUCTION

IN A previous article[1] a new principle called space-charge deflection was described for the control of the current in an electron tube. The principle, combined with one stage secondary electron multiplication, made possible the constructor of tubes with very high transconductance or, which is even more significant, with high transconductance-to-current ratio.

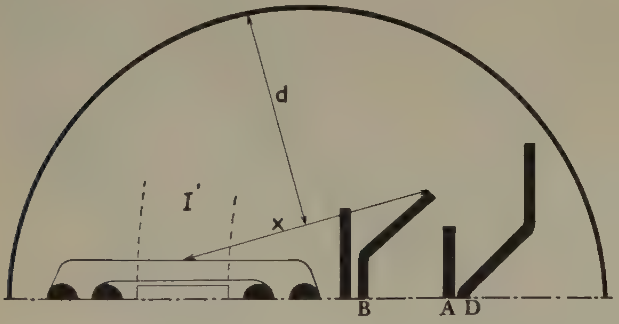

Fig. 1—Space-charge deflection tube.

The tube consists of an ordinary cathode—control grid—screen grid assembly as shown in Fig. 1, surrounded by a circular reflector on cathode potential. The electron flow passing the screen grid is turned around by the reflector and arrives at the output end where part of the flow is intercepted by an intercepting electrode *B*, and the rest passes on to the anode *A* via a secondary emission multiplying electrode *D*. By utilizing the space charge of the beam itself to influence the deflecting electric field the beam can be forced to shift its path so that for high current a large fraction of the beam arrives at the anode, for low current a very small fraction of the current arrives at the anode, which in effect means that an additive modulation has been introduced on top of the control grid modulation and resulting in increased transconductance of the tube. The secondary emission electrode is desirable to multiply the useful current and make up for the current lost to the intercepting electrode. This paper deals with some further aspects of the tube, especially noise, maximum transconductance-to-current ratio, high frequency behavior, stability and current drain. It is shown that the equivalent noise resistance of the tube compares favorably with that of a multiplier tube and is nearly the same as that of a pentode, that the maximum transconductance-to-current ratio is a combination of that of grid control and that of deflection control and consequently high, and that the high frequency behavior is poor owing to long transit times. A very interesting aspect of the tube is the possibility to achieve high stability simultaneously with high transconductance-to-current ratio in contrast to conventional principles.

TABLE I

COMPARATIVE PERFORMANCE VALUES OF DIFFERENT TUBES UTILIZING THE SAME CATHODE, CONTROL GRID ASSEMBLY

	Triode	Pentode	Multiplier	Space-Charge Deflection
Transconductance μmhos	12,000	10,000	18,000	25,000
Anode current ma	10	8	9	3
Equivalent noise resistance ohm	200	500	1,300	800
High frequency limit mc/s	300	300	300	100
Variation in transconductance for 10% variation in line voltage, no stabilizing circuits %	10	10	15	3

NOISE

The equivalent noise resistance of grid-controlled tubes is inversely proportional to the transconductance. The introduction of secondary electron multiplication to such tubes does not improve the equivalent noise resistance although the transconductance is increased by the multiplication factor, because in this case the noise is multiplied along with the signal. On the contrary the equivalent noise resistance is enlarged by the addition of extra noise from the dynode. The same reasoning can also be applied to the magnification of the transconductance by the space-charge beam deflection action. However, in that case the secondary emission noise is substantially reduced. The equivalent noise resistance can be calculated in the following way.

---

* Decimal classification: R131×R330. Original manuscript received by the IRE, October 22, 1953; revised manuscript received March 22, 1954.

† RCA Laboratories, Princeton, N. J.; formerly with Royal Institute of Technology, Stockholm, Sweden.

[1] J. T. Wallmark, "An experimental high-transconductance tube using space-charge deflection of the electron beam," PROC. I.R.E., vol. 40, pp. 41–48; January, 1952.

The beam current I' leaving the screen grid (see Fig. 1) carries the mean square fluctuations[2]

$$\bar{i}^2 = (I'/I_c)^2\Gamma^2 2eI_c\Delta f + (I_{G2}/I_c)(I'/I_c)2eI_c\Delta f$$
$$= 2eI_c\Delta f[\Gamma^2\theta^2 + \theta(1-\theta)]$$

where

I_c is the cathode current
I_{g2} is the screen grid current
e is the electron charge
Δf is the bandwidth
Γ^2 is the factor of noise reduction by space charge
θ is the fraction of current passing the screen grid ($\theta = I'/I_c$).

This is the well-known expression for the mean square fluctuations in the current in a pentode. By space-charge beam deflection action the signal and the noise are both amplified by the factor $g_m/g_m'\delta$ where

g_m is the over-all transconductance of the tube
g_m' is the transconductance of the input section looked upon as a tetrode
δ is the secondary electron multiplication factor.

The mean square fluctuations entering the multiplier are then

$$\bar{i}^2 = (g_m/g_m'\delta)^2 2eI_c\Delta f[\Gamma^2\theta^2 + \theta(1-\theta)].$$

The current distribution noise caused by the interception of part of the current by the intercepting electrode B is small and has been neglected. Also the beam is considered so short that interaction noise is insignificant. In the multiplier the signal and noise are both multiplied by the secondary electron multiplication factor δ. At the same time noise from the dynode is added. This noise has been shown to be equal to the noise from a temperature-limited primary current of the same magnitude as the multiplied current. Then the mean square fluctuations reaching the anode are

$$\bar{i}^2 = (g_m/g_m')^2 2eI_c\Delta f[\Gamma^2\theta^2 + \theta(1-\theta)] + \alpha\cdot\delta\cdot\theta 2eI_c\Delta f$$
$$= 2eI_c\Delta f\{(g_m/g_m')^2[\Gamma^2\theta^2 + \theta(1-\theta)] + \alpha\cdot\theta\cdot\delta\} \tag{1}$$

where α is the fraction of the beam current entering the multiplier. From (1) the equivalent noise resistance can be calculated in conventional manner

$$R_{eq} = (20I_c/g_m'^2)[\Gamma^2\theta^2 + \theta(1-\theta)] + (20I_c/g_m^2)\alpha\cdot\theta\cdot\delta$$
$$= \underbrace{2.2/g_m'}_{\substack{\text{shot}\\ \text{noise}}} + \underbrace{20(I'/g_m'^2)(1-\theta)}_{\substack{\text{current}\\ \text{distribution}\\ \text{noise}}} + \underbrace{20I_a/g_m^2}_{\substack{\text{secondary}\\ \text{emission}\\ \text{noise}}}. \tag{2}$$

This turns out to be the same expression that is valid for an ordinary multiplier tube. The two first terms express the noise contributed by the input section and these terms are not influenced by secondary emission or space-charge beam deflection. The third term gives the secondary emission noise, and this term is reduced compared to a conventional multiplier tube as the transconductance-to-current ratio is increased by space-charge beam deflection action. A conservative value that has been experimentally verified is a doubling of the transconductance at the same time as the anode current is cut in half, and consequently a reduction of this noise to a factor of one-eighth. As will be shown below better focusing of the electron beam can be expected to increase the transconductance and thus reduce secondary emission noise still further.

EXPERIMENTAL CHECK

The equivalent noise resistance of experimental tubes was measured with the following typical data

$$g_m' = 5{,}400\ \mu\text{mhos}$$
$$g_m = 25{,}000\ \mu\text{mhos}$$
$$I = 2.7\ \text{ma}$$
$$\theta = .75$$
$$\alpha = .41$$
$$\delta = 2.7.$$

Then (2) gives

$$R_{eq} = 305 + 465 + 95 = 865\ \text{ohm}.$$

The experimental value obtained was 800 ohm. The difference may be due to return electrons to the screen grid increasing the screen grid current and consequently giving an apparent value of θ that is too low. Under conditions when no return electrons reach the screen grid $\theta = 0.8$ which would bring the theoretical and experimental results in agreement.

CONCLUSION

The equivalent noise resistance of a space-charge beam deflection tube is less than that of an ordinary multiplier, as the high transconductance-to-current ratio reduces the secondary emission noise. The main part of the equivalent noise resistance, however, is determined by the input section.

MAXIMUM TRANSCONDUCTANCE TO CURRENT RATIO

It has been shown by Below[3] that initial velocities from the cathode set a limit to the maximum transconductance-to-current ratio that can be obtained in tubes with grid control of the current. For an oxide emitter at 1,000 degrees K this limit is 11.6 volt^{-1} (11,600 μmhos/ma). In practical tubes very rarely values above 5 volt^{-1} can be obtained while 1 volt^{-1} is a common value for high-transconductance tubes (6 AK5 0.7, WE 404 A 1.0, WE 435 A 1.0). The reason for this is the difficulty to approach an ideal grid with practical constructions.

---

[2] B. J. Thompson, D. O. North, W. A. Harris, "Fluctuations in space-charge-limited currents at moderately high frequencies," *RCA Rev.*, vol. 4, p. 251; October, 1940.

[3] E. Below, "Zur Theorie der Raumladegitterröhren," *Zeit. f. Fernmeldetechnik*, vol. 9, pp. 113–118, 136–142; 1928.

In theory an ideal equipotential plane is considered where the grid is situated, while in practice the grid wires cannot be made infinitely thin at the same time as contact potential differences on the surface cannot be avoided. Consequently a very uneven electric field is created. For maximum transconductance-to-current ratio the virtual cathode should approach the grid plane, but in practice the grid wires break up the virtual cathode in areas, with different conditions between the grid wires and behind the grid wires, with a consequent reduction in the over-all transconductance-to-current ratio.

The addition of secondary emission multiplication does not change this value of 11.6 volt^{-1} as the current is multiplied at the same time as the transconductance, and the ratio remains constant.

However, with other forms of control considerably higher ratios have been obtained. Thus with ordinary beam deflection control values as high as several hundred have been reported.[4,5]

Space-charge beam deflection can be considered as a combination of two controls in series, the first a grid control and the second a deflection control. In this case the transconductance-to-current ratio is approximately the product of the ratio for grid control and deflection control respectively.

Let us see what advantages this has and what the maximum transconductance-to-current ratio amounts to.

Transconductance of a tube, as shown in Fig. 1, is

$$g_m = g'_m\delta\left(\alpha + \frac{x\underline{I}}{d\underline{\tau}}\,\frac{\partial\underline{\tau}}{\partial\underline{I}}\right) \tag{3}$$

where

d and x are shown in Fig. 1

τ is the relative transit time as compared to space-charge free-transit time

$\underline{I}$ is the relative current as compared to space-charge limited current.

For the purpose of maximizing, α which is always <1 can be neglected compared to the second term within the parenthesis. In the case where the current density at the output, i, differs from the average current density i_0, (3) becomes

$$g_m \approx g_m'\cdot\delta\cdot\frac{i\times\underline{I}}{i_0 d\underline{\tau}}\,\frac{\partial\underline{\tau}}{\partial\underline{I}} \tag{4}$$

grid control

deflection control

which is an expression somewhat similar to expressions derived for beam deflection tubes[5] with the important difference that also a factor g_m' has entered.

The maximum value of $\underline{I}/\underline{\tau}\cdot\delta\underline{\tau}/\delta\underline{I}$ can be calculated from published data.[6] With initial velocities from the cathode considered the maximum value of this expression amounts to approximately 1.

The maximum value of x/d cannot be made much larger than 1 without violating assumptions made in deriving the expression (3). From a practical point of view large values of x/d are also of little interest as then the same difficulties would meet as with beam deflection tubes, viz. sensitivity to surface conditions of the electrodes.[4]

A theoretical upper limit for i/i_0 can be derived from calculations by Pierce[7]

$$i/i_0 = \tfrac{1}{2}2\pi^{-1/2}(eV/kT)^{1/2}\sin\theta,$$

where V is the accelerating voltage, $e/kT=10$ for a cathode temperature T of 1,160 degrees K, and θ is the focusing angle. A factor of $\frac{1}{2}$ has been inserted because i_0 is the average current.

We then have

$$g_m \approx g_m'\delta 2V^{1/2}\sin\theta. \tag{5}$$

The improvement over an ordinary multiplier tube having a transconductance

$$g_m = g_m'\cdot\delta$$

is then directly proportional to the focusing of the beam. Increasing the transconductance without increasing the voltage can then only be done by increasing the focusing angle. Considerations to practical tube design, however, limit $\sin\theta$ to 0.1–0.2.

Dividing (5) by $I_a=\delta\cdot I'\cdot\alpha$ gives

$$\frac{g_m}{I_a} = \frac{g_m'}{I'}\,\frac{2V^{1/2}\sin\theta}{\alpha}.$$

With $V=500$ volts, $\sin\theta=0.05$ and $\alpha=\frac{1}{2}$ the improvement in g_m/I-ratio over a conventional tube would amount to a factor of 4 and the improvement in g_m to a factor of 2 which correlates well with measured values on experimental tubes.

CONCLUSION

The sensitivity of a space-charge beam deflection tube, measured as transconductance-to-current ratio, can be increased over the value of a conventional tube with the same input section by a factor of 2–10. In practical tubes where not too stringent demands on alignment and exactness of dimension can be tolerated, and where the electrodes have to be simple and few, a factor of 2–4 seems reasonable.

HIGH FREQUENCY BEHAVIOR

The highest frequency at which a space-charge beam deflection tube can be used is determined by the build-up-time of the space charge in the reflection region, i.e. the transit time of the electrons. The transit time is[1]

---

[4] E. W. Herold, C. W. Mueller, "Beam-deflection mixer tubes for uhf," *Electronics*, vol. 22, pp. 76–80; May, 1949.

[5] G. R. Kilgore, "Beam-deflection control for amplifier tubes," *RCA Rev.*, vol. 8, pp. 480–505; September 1947.

[6] J. T. Wallmark, "Space-charge conditions in a reflected flow of electrons." (To be published in *Trans. of the IRE, PGED.*)

[7] J. R. Pierce, "Theory and Design of Electron Beams," D. Van Nostrand Company, Inc., New York, p. 126; 1949.

$$\tau = c4d/(2eV/m)^{1/2} \text{ sec.}$$

where c is a constant ranging from 1 to 1.5, depending upon the space-charge conditions. This gives a high frequency cut-off at

$$f \approx 10^5 \, V^{1/2}/d.$$

Fig. 2 shows two experimental curves of transconductance versus frequency, one for a relatively low voltage, the other for a relatively high voltage. For comparison the transconductance has been given in relative values. As can be seen the low voltage curve sinks below the high voltage curve and reaches its minimum at a lower frequency.

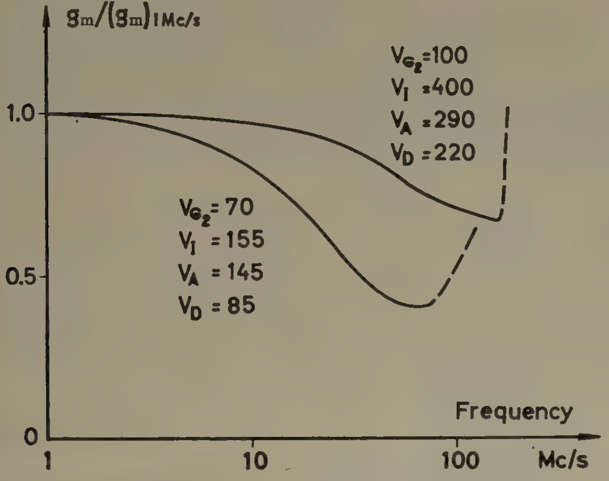

Fig. 2—Relative transconductance vs frequency.

The way to improve the upper frequency limit is then a reduction of d. A further increase of V above 400–500 volts, although feasible, is certainly not desirable and also not very efficient because of the small exponent for V. It is uncertain how far a reduction of d can be carried to advantage as other factors such as focusing, current, etc. change at the same time. However, at present a factor of 2 seems possible, pushing the upper frequency limit past the lead-in resonances which appear at approximately 300 mc[8]. Even then, however, a somewhat slumping transconductance may result above 100 mc.

STABILITY

One of the main disadvantages with all high-transconductance tubes is their sensitivity to variations in current and voltage. It has been shown by Thompson[9] that this is an inherent characteristic of such tubes, and that a large derivative of the current with respect to the control grid voltage—large transconductance—also necessarily means a by comparison large derivative of the current with respect to all other voltages. Now the transconductance-to-current ratio of grid-controlled tubes cannot exceed 11.6 volt^{-1} as mentioned above. However, even if some other means of control was employed allowing a higher limit ot the transconductance-to-current ratio, such a tube would be of doubtful value in practical applications because of the difficulties to keep its operating data constant. It will be shown in this chapter that space-charge beam deflection, although giving a transconductance-to-current ratio higher than for grid-controlled tubes, still in contrast to the general principle maintains a constant transconductance within wide limits of operating data. This is possible because the current control in the tube is a combination of two kinds of control, grid control and deflection control, and allows such a choice of operating data that variations in one form of control are mainly cancelled by opposite variations in the other.

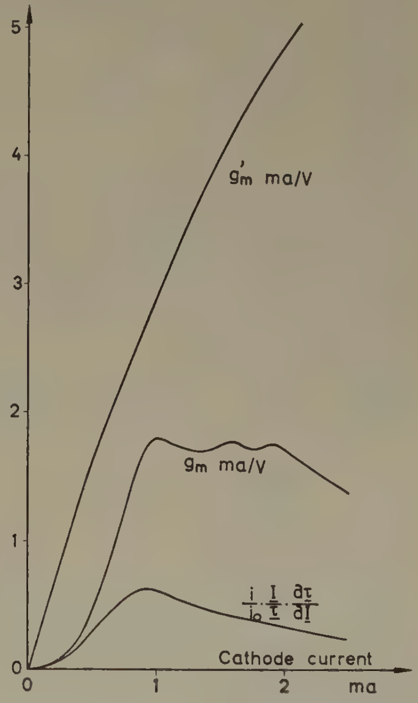

Fig. 3—Transconductance of experimental space-charge deflection tube, separated into primary transconductance and deflection-transconductance.

In verifying this principle measurements were made on experimental tubes without secondary emission, i.e. with the dynode connected to the anode. Also as the experimental tubes could not take the high power at large currents it was necessary to scale down voltages and currents. Consequently the absolute values of the transconductance measured were very small. However, the principle is still apparent.

As shown by (4) the expression for the transconductance of the tube contains two parts, the primary transconductance g_m', and the deflection transconductance

$$g_m'' = \frac{ix\underline{I}}{i_0 d\underline{\tau}} \frac{\partial \underline{\tau}}{\partial \underline{I}}.$$

Fig. 3 above shows measured values of g_m and g_m' from which g_m'' can be derived. The curve for g_m is not smooth but has a fine structure caused by inhomogeneous current density. It is to be expected that the function g_m'' should be similar to the function $\underline{I}/\underline{\tau}\cdot\partial\tau/I\underline{\partial}$ which can be computed on a theoretical basis from published results. This latter function is shown in Fig. 4 for some values of $\underline{V}=|-V_R|/V_A$. The difference between the experimental curve in Fig. 3 and these theoretical curves is explained by the experimental conditions. For high currents space-charge spread of the beam reduces current density, extending the experimental curve towards higher current. However, the general form is the one expected.

---

[8] R. P. Stone, private communication.

[9] B. J. Thompson, "Voltage-controlled electron multipliers," Proc. I.R.E., vol. 29, pp. 583–587; November, 1941.

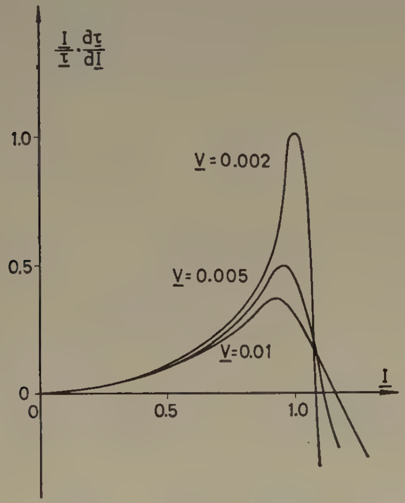

Fig. 4—The function $I/\tau\cdot\partial\tau/\partial I$ vs relative current density I.

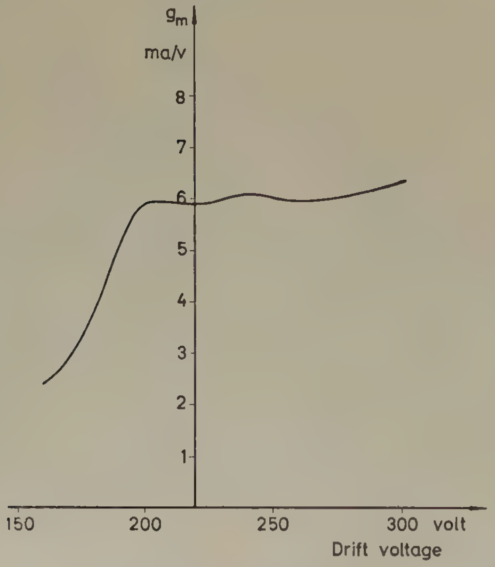

Fig. 5—Transconductance of experimental space-charge deflection tube vs drift voltage.

For changes of drift voltage it is also possible to obtain a constant value of the transconductance for the same reason: a balance of primary and deflection transconductance so that when one increases the other decreases. Fig. 5 shows a curve of transconductance versus drift voltage measured on the same tube and with the secondary electron multiplication stage in operation.

CONCLUSION

The general form of the transconductance versus current curve is a rapid rise to a high value at approximately $I=\frac{1}{2}$ and from there on either constant, slowly rising or slowly sinking, dependent upon which part of the transconductance is the dominating one. In general it is possible by a suitable choice of dimensions and voltages to obtain a balance so that the transconductance becomes approximately constant over a large current range, and also over a large voltage range.

CONSEQUENCES

Apart from the stable amplification made possible by a space-charge beam deflection tube, the stability has one more interesting feature: that of reducing distortion. This is an obvious consequence as distortion arises from variations in transconductance.

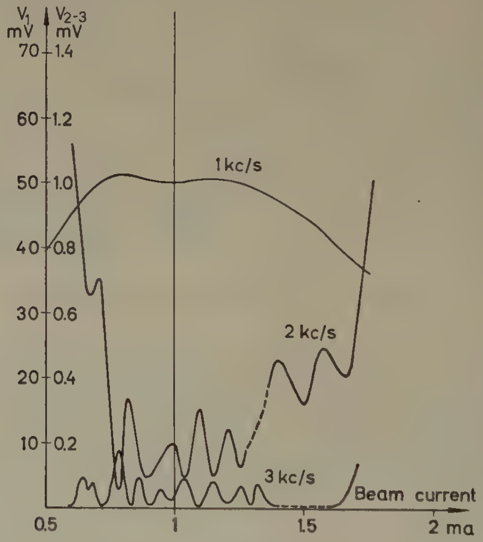

Fig. 6—Distortion of experimental space-charge deflection tube vs beam current.

Fig. 6 shows the results of measurements on an experimental tube in which the current was varied over a large range. The tube was coupled as an amplifier for 1 kc with a very small input voltage (10 mv). The output voltage was measured for 1, 2, 3 etc. kc. The curve for 1 kc is proportional to the transconductance and exhibits an approximately constant value over a current range from 0.75–1.5 ma. Within that range the second and third overtones, constituting the distortion, are very low, higher overtones being still lower. The curves show a fine structure with the natural relationship between the curves that can be expected when it is considered that they are proportional to the first, second

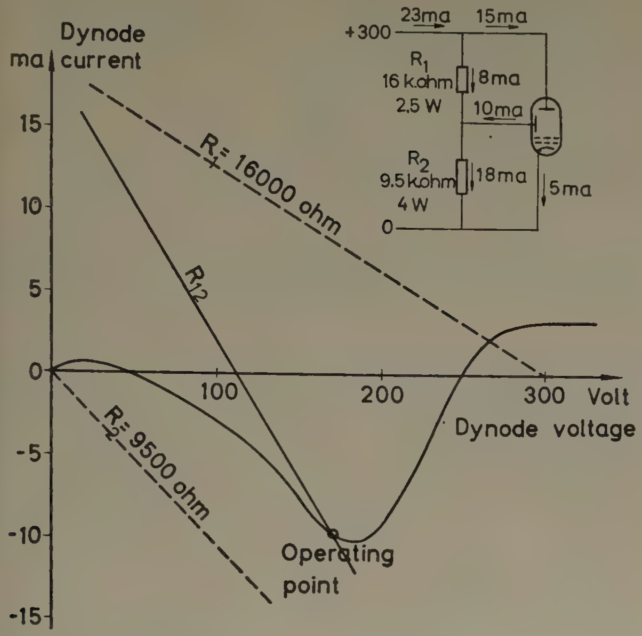

Fig. 7—Conventional bleeder arrangement for multiplier tubes.

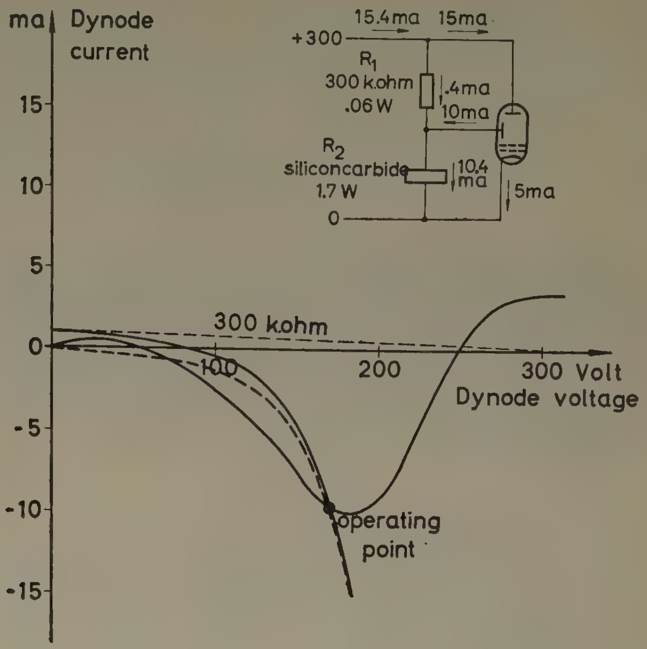

Fig. 8—Nonlinear bleeder arrangement for multiplier tubes.

and third derivative of the anode current with respect to grid voltage.

The fine structure is, of course, analogous to the fine structure found in conventional tubes.[10] It is caused by inhomogeneous current density resulting from focusing by grid wires, etc. This represents a fundamental lower limit for distortion in tubes utilizing grids for the control of the current.

Stabilizing Circuits and Power Conservation

For tubes with secondary emission multiplication, the use of stabilizing circuits has usually been recommended as a remedy for the well-known difficulties of constructing secondary emitting surfaces with high multiplication factors and stable and reproducible behavior for thousands of hours. For space-charge beam deflection tubes the addition of stabilizing circuits to the internal balancing as described above results in a still higher degree of stability. One such circuit where the decrease in secondary emission is compensated for by an automatic reduction of the control grid bias and consequent increase in primary emission has been published.[11]

Another circuit where the potential of the dynode is kept at an approximately constant value independent of the secondary emission ratio at the same time as the necessary power for driving the tube is considerably reduced, will be described.

As is well-known, a secondary emitting electrode has a negative current characteristic in the region where $\delta > 1$ as shown in Fig. 7. The common way to obtain the voltage for the dynode is by a bleeder from the anode voltage supply. In Fig. 7 the load lines for the two bleeder resistances R_1 and R_2 are shown. The combination of the two gives R_{12}. It is now easily seen that to keep the dynode voltage as stable as possible the bleeder resistances should be small. This in turn means that the current drain from the main supply is large.

Varistor Bleeder

In order to avoid this difficulty a nonlinear resistor, such as a silicon carbide varistor, may be introduced in combination with a high ohmic, low power, conventional resistor as shown in Fig. 8. The characteristics of such varistors may be chosen to match the dynode characteristic so that the load line in the operating point has a high slope thus giving a considerably improved voltage stability to the dynode. At the same time the extra current drain from the main supply is practically eliminated.

The disadvantage of silicon carbide varistors is their size and cost, especially for power exceeding 0.5 watts. However, as space-charge deflection tubes require very low currents, the size and cost of varistor bleeders may well be worth-while when the current saving is considered.

Acknowledgement

The author is indebted to E. W. Herold and R. P. Stone for discussions on noise and high frequency behavior, and O. Ekholm for measurements on distortion and high frequency behavior.

---

[10] B.v.d. Pol, T. J. Weiyers, "Fine structure of triode characteristics," *Physica*, vol. 1, pp. 481–496; 1934.

[11] J. L. H. Jonker, A. J. M. v. Overbeek, "The application of secondary emission in amplifying valves," *Wireless Eng.*, vol. 15, pp. 150–156; March, 1938.

Coding for Constant-Data-Rate Systems—Part I. A New Error-Correcting Code*

R. A. SILVERMAN†, MEMBER, IRE AND MARTIN BALSER†

Summary—**A study of coding to reduce the frequency of errors in communication systems which transmit data at a constant rate has been started. A new single-error-correcting code (the Wagner code) is described and analyzed. Its performance in a constant-data-rate system is evaluated and compared with Hamming's single-error-correcting code. The Wagner code is superior for many communication applications. Its successful implementation does not require too precise equipment.**

I. INTRODUCTION

IN THIS REPORT, we shall consider a communication system in which data consisting of sequences (known as words) of binary digits are transmitted at a predetermined constant rate. (For our purposes, a binary digit is one of two electrical signals of duration *T* and bandwidth *W*.[1]) The nature of the data and the manner in which they are translated into words are irrelevant to this discussion. For example, the data may be English letters, numbers, etc., reduced to sequences of five binary digits each for use in a teletype system, or they may be conventional symbols representing entire messages.

A basic problem of coding is to reduce the average rate of incorrectly received words as much as possible. Accordingly, additional digits are added to the word for the purposes of error detection or correction. The assumption that the words are sent at a constant rate requires that each binary digit be shortened by such an amount that the coded words (message digits plus check digits) have the same duration as the original uncoded words. This shortening of each digit increases its probability of error and, consequently, the probability of error per word. On the other hand the coding imposes constraints on the digits composing a word, so that errors may show up as inconsistencies and may in many cases be corrected. This tends to reduce the probability of error per word. The efficacy of a code depends on how much the second effect outweighs the first.

The simplest code of all consists of an extra digit selected to make the sum of all the digits in the coded word even (or odd). If the sum of the digits of the received word has the wrong parity, an odd number of errors is known to have been made. There is, however, no indication of the correct replacement for the mistaken word, unless some dependence between separate words (such as the redundancy of printed English)[2] is exploited.

Hamming[3] has devised a code that corrects all single errors. It consists of adding *k* suitably chosen check digits to the *m* message digits.[4] If another digit is added, double errors can be detected as well as single errors corrected.[3] In this paper, we describe a new single-error-correcting code (the Wagner code) and evaluate its performance in a constant-data-rate system, particularly as compared with that of the Hamming code.

Recently, multiple-error-correcting codes have been constructed.[5] An analysis of their performance in constant-data-rate systems will be given in a later paper, "Coding for Constant-Data-Rate Systems, Part II—Multiple-Error-Correcting Codes."

II. DESCRIPTION OF THE WAGNER CODE

In this study, we are concerned with communication systems that transmit words consisting of binary digits. A binary digit is one of two electrical signals $x_1(t)$ and $x_2(t)$ of duration T and bandwidth W. Let $p(x_i/y)$ be the (*a posteriori*) probability that if y is received, x_i was sent, and let Δp be $p(x_1/y)-p(x_2/y)$. In the absence of any constraints on the digits composing a word or of dependence between the words themselves, the receiver can compute only $p(x_1/y)$ and $p(x_2/y)$, and for each digit choose x_1 or x_2, depending on whether $p(x_1/y)$ or $p(x_2/y)$ is the larger (or, equivalently, whether Δp is positive or negative). The error-correcting code that we shall describe (named the Wagner code after C. A. Wagner of this laboratory, who suggested the basic idea) enables us to use some of the information presented by the magnitudes of the Δp's[6] by introducing a constraint on the digits composing a word. This information is ignored by more conventional codes.

In the Wagner code, a transmitted word consists of a sequence of m message digits and an additional digit used as a parity check. As each of the perturbed digits y arrives at the receiver, the *a posteriori* probabilities $p(x_1/y)$ and $p(x_2/y)$ are calculated. Each digit of the received sequence is tentatively identified as x_1 or x_2, de-

---

* Decimal classification: R531.1. Original manuscript received by the IRE, January 25, 1954; revised manuscript received, February 27, 1954. The research in this document was supported jointly by the Army, Navy, and Air Force under contract with the Massachusetts Institute of Technology.

† Lincoln Laboratory, Massachusetts Institute of Technology, Cambridge, Mass.

[1] These two requirements are, strictly speaking, incompatible (see Appendix).

[2] C. E. Shannon, "Prediction and entropy of printed English," *Bell Sys. Tech. Jour.*, vol. 30, pp. 50–64; January, 1951.

[3] R. W. Hamming, "Error detecting and error correcting codes," *Bell Sys. Tech. Jour.*, vol. 29, pp. 147–160; April, 1950.

[4] For $m=2$ to 4, $k=3$; for $m=5$ to 11, $k=4$; etc.

[5] I. S. Reed, "A class of multiple-error-correcting codes and the decoding scheme," Technical Report no. 44, Lincoln Laboratory, M.I.T.; October, 1953.

[6] The signs of the Δp's are used in making the tentative identification of the transmitted word.

pending on whether $p(x_1/y)$ or $p(x_2/y)$ is the larger, and the values of the *a posteriori* probabilities are stored in a memory for the duration of a word. The sequence thus obtained is checked for parity. If the parity is correct, the word is printed as received. If the parity check fails the digit for which the difference Δp between *a posteriori* probabilities is the smallest is considered the digit most in doubt, and the word is printed with this digit altered. The receiver then clears the stored values of the probability differences from the memory and proceeds to the next word.

Thus we may characterize the Wagner code as one which *probably* corrects single errors. (Multiple errors are always printed incorrectly.) However, as we shall see, it can be more effective in a constant-data-rate system than a code that corrects *all* single errors (such as the Hamming code).

The *a posteriori* probabilities $p(x_1/y)$ and $p(x_2/y)$ are functions of the random received waveform $y(t)$ and therefore are themselves random variables. The calculation of their distributions is, in general, very difficult. For simplicity, we shall consider the case where the two transmitted signals have equal energy and equal *a priori* probabilities and are perturbed by the addition of white Gaussian noise. It has been shown[7] that for this case

$$p(x_1/y) = \beta \exp\left[\gamma \int_0^T x_1(t)y(t)dt\right] \tag{1}$$

and

$$p(x_2/y) = \beta \exp\left[\gamma \int_0^T x_2(t)y(t)dt\right],$$

where β and γ are positive constants. Thus the transmitted signal with the larger correlation has the larger *a posteriori* probability. Equivalently, we may write

$$\frac{p(x_1/y)}{p(x_2/y)} = \exp\left[\gamma(z_1 - z_2)\right], \tag{2}$$

where

$$z_1 = \int_0^T x_1(t)y(t)dt \quad \text{and} \quad z_2 = \int_0^T x_2(t)y(t)dt. \tag{3}$$

From (2), we see that the smaller the difference $\Delta z = z_1 - z_2$ between the correlation integrals, the closer to unity the ratio of *a posteriori* probabilities and, consequently, the smaller the difference Δp between the two probabilities. Thus, if the parity check fails, the digit that should be changed (as the one most in doubt) is the one for which Δz is the smallest.

It is shown in the Appendix that z_1 and z_2 are normally distributed random variables (with means c_1 and c_2, and variances σ_1 and σ_2), so that calculations are especially simple for the correlation detector.[8] Moreover, under the assumptions made above, the correlation detector is equivalent to the probability detector. Therefore, it is assumed in what follows that detection is by correlation.

III. ANALYSIS OF THE WAGNER CODE

Probability of Error Per Digit

As noted above, the correlation integrals z_1 and z_2 (corresponding to the signal that was sent and the signal that was not sent, respectively) are random variables with probability densities

$$W(z_1) = \frac{1}{\sqrt{2\pi}\,\sigma_1} \exp\left[-\frac{(z_1 - c_1)^2}{2\sigma_1^2}\right], \tag{4}$$

and

$$W(z_2) = \frac{1}{\sqrt{2\pi}\,\sigma_2} \exp\left[-\frac{(z_2 - c_2)^2}{2\sigma_2^2}\right]. \tag{5}$$

It is shown in the Appendix that if x_1 and x_2 are suitably chosen, then z_1 and z_2 may be regarded as statistically independent random variables. Accordingly, the probability density of finding a separation $\Delta z = z_1 - z_2$ is

$$W(\Delta z) = \frac{1}{\sqrt{2\pi}\,\sigma} \exp\left[-\frac{(\Delta z - \Delta c)^2}{2\sigma^2}\right], \tag{6}$$

where $\Delta c = c_1 - c_2 > 0$ and $\sigma^2 = \sigma_1^2 + \sigma_2^2$. Here we make use of a well-known theorem on the distribution of the sum of independent, normally distributed random variables.[9] If Δz is negative, then selecting as the transmitted signal the signal giving the larger correlation integral will result in an error. Thus the probability of error per digit is

$$p(\alpha) = \int_{-\infty}^{0} W(\Delta z)d\Delta z = \tfrac{1}{2}(1 - \operatorname{erf} \alpha), \tag{7}$$

where $\alpha = \Delta c/\sqrt{2}\sigma$.[10] The parameter α, which is proportional to the signal-to-noise ratio of the correlator difference, is the significant parameter in the calculations that follow.

Since we do not know which digit was actually sent, we do not know the sign of Δz. From (6), the joint probability that the correlator difference lies between $|\Delta z|$ and $|\Delta z| + d|\Delta z|$, and that the larger correlation integral corresponds to the transmitted signal, is $d|\Delta z|$ times

$$W(|\Delta z|, \text{right}) = \frac{1}{\sqrt{2\pi}\,\sigma} \exp\left[-\frac{(|\Delta z| - \Delta c)^2}{2\sigma^2}\right]. \tag{8}$$

---

[7] P. M. Woodward and I. L. Davies, "Information theory and inverse probability in telecommunication," *Proc. I.E.E.*, vol. 99, p. 37; March, 1952.

[8] For simplicity of notation, we shall always use the subscript "one" for the signal that was transmitted. Thus $c_1 > c_2$, and $z_1 < z_2$ results in an error.

[9] H. Cramér, "Mathematical Methods of Statistics," Princeton University Press, Princeton, N. J., p. 212, 1946.

[10] The existence of the simple expression (7) for $p(a)$ was pointed out by Dr. I. S. Reed, who evaluated the equivalent form

$$p(\alpha) = \frac{1}{2\pi\sigma_1\sigma_2} \int_{-\infty}^{\infty} \exp\left[-\frac{(s - c_2)^2}{2\sigma_2^2}\right] \int_{-\infty}^{s} \exp\left[-\frac{(t - c_1)^2}{2\sigma_1^2}\right] dtds.$$

by a rotation of 45° in the (s, t) plane.

On the other hand, the joint probability that the correlator difference lies between $|\Delta z|$ and $|\Delta z| + d|\Delta z|$, and that the larger correlation integral does *not* correspond to the transmitted signal, is $d|\Delta z|$ times

$$W(|\Delta z|, \text{wrong}) = \frac{1}{\sqrt{2\pi}\,\sigma} \exp\left[-\frac{(|\Delta z| + \Delta c)^2}{2\sigma^2}\right]. \tag{9}$$

Probability of Correcting a Single Error

Suppose that the received word has n digits. Since the parity check fails if a single error is made, and since then the Wagner code changes the digit with the smallest $|\Delta z|$, the probability $\prod_n(\alpha)$ that a single error is made and is corrected by the Wagner code is just the probability that the digit with the smallest $|\Delta z|$ is incorrect and that the $n-1$ other digits are correct. $\prod_n(\alpha)$ can be calculated as follows.

Let $|\Delta z_i|$ be the correlator difference for the ith digit. Since the $|\Delta z_i|$ are independent random variables, the joint probability that the first digit, with correlator difference between $|\Delta z_1|$ and $|\Delta z_1| + d|\Delta z_1|$, is wrong, and that all the other digits, with correlator differences between $|\Delta z_2|$ and $|\Delta z_2| + d|\Delta z_2|, \cdots, |\Delta z_n|$ and $|\Delta z_n| + d|\Delta z_n|$ are right, is

$$W(|\Delta z_1|, \text{wrong}) \prod_{i=2}^{n} W(|\Delta z_i|, \text{right}) \prod_{i=1}^{n} d|\Delta z_i|. \tag{10}$$

Thus the joint probability that the first digit is wrong, that the $n-1$ other digits are correct, and that $|\Delta z_1| < |\Delta z_2| < \cdots < |\Delta z_n|$ is

$$\int_0^\infty W(|\Delta z_n|, \text{right})\, d|\Delta z_n| \cdot \int_0^{|\Delta z_n|} W(|\Delta z_{n-1}|, \text{right})\, d|\Delta z_{n-1}| \cdots \int_0^{|\Delta z_3|} W(|\Delta z_2|, \text{right})\, d|\Delta z_2| \cdot \int_0^{|\Delta z_2|} W(|\Delta z_1|, \text{wrong})\, d|\Delta z_1|. \tag{11}$$

Since there are in all $n!$ orderings of the n correlator differences, the joint probability $\prod_n(\alpha)$ that a single error is made in a word of n digits and that it is corrected by the Wagner code is given by

$$\begin{aligned}
\prod\nolimits_n(\alpha) = {} & n! \int_0^\infty \frac{1}{\sqrt{2\pi}\,\sigma} \cdot \exp\left[-\frac{1}{2\sigma^2}(|\Delta z_n| - \Delta c)^2\right] d|\Delta z_n| \\
& \cdot \int_0^{|\Delta z_n|} \frac{1}{\sqrt{2\pi}\,\sigma} \cdot \exp\left[-\frac{1}{2\sigma^2}(|\Delta z_{n-1}| - \Delta c)^2\right] d|\Delta z_{n-1}| \\
& \cdots \int_0^{|\Delta z_3|} \frac{1}{\sqrt{2\pi}\,\sigma} \cdot \exp\left[-\frac{1}{2\sigma^2}(|\Delta z_2| - \Delta c)^2\right] d|\Delta z_2| \\
& \cdot \int_0^{|\Delta z_2|} \frac{1}{\sqrt{2\pi}\,\sigma} \cdot \exp\left[-\frac{1}{2\sigma^2}(|\Delta z_1| + \Delta c)^2\right] d|\Delta z_1| \\
= {} & \frac{n!}{(\sqrt{\pi})^n} \int_0^\infty \exp\left[-(x_n - \alpha)^2\right] dx_n \cdot \int_0^{x_n} \exp\left[-(x_{n-1} - \alpha)^2\right] dx_{n-1} \\
& \cdots \int_0^{x_3} \exp\left[-(x_2 - \alpha)^2\right] dx_2 \cdot \int_0^{x_2} \exp\left[-(x_1 + \alpha)^2\right] dx_1,
\end{aligned} \tag{12}$$

where $\alpha = \Delta c/\sqrt{2}\sigma$ as in (7). The *conditional* probability that a single error will be corrected by the Wagner code, assuming that a single error has been made in an n-digit word, is given by

$$\frac{\prod_n(\alpha)}{nq^{n-1}(\alpha)p(\alpha)} \tag{13}$$

where $p(\alpha)$ is the probability of error per digit

$$p(\alpha) = \tfrac{1}{2}(1 - \operatorname{erf} \alpha), \tag{7}$$

and

$$q(\alpha) = 1 - p(\alpha) = \tfrac{1}{2}(1 + \operatorname{erf} \alpha). \tag{14}$$

Equation (13) follows immediately from the definition of conditional probability and the fact that $nq^{n-1}(\alpha)p(\alpha)$ is the probability of a single error in an n-digit word.

It is desirable to have $\prod_n(\alpha)$ in a form more suitable for numerical computations. Thus we reduce the n-fold multiple integral (12) to a convenient recurrence formula. Let

$$F_n(\alpha) = \frac{(\sqrt{\pi})^n}{n!} \prod\nolimits_n(\alpha), \tag{15}$$

and

$$\begin{aligned}
f_n(x, \alpha) \equiv {} & \int_0^x \exp\left[-(x_n - \alpha)^2\right] dx_n \cdot \int_0^{x_n} \exp\left[-(x_{n-1} - \alpha)^2\right] dx_{n-1} \\
& \cdots \int_0^{x_3} \exp\left[-(x_2 - \alpha)^2\right] dx_2 \cdot \int_0^{x_2} \exp\left[-(x_1 + \alpha)^2\right] dx_1.
\end{aligned} \tag{16}$$

From (15) and (16) it follows that

$$f_n(\infty, \alpha) = F_n(\alpha); \qquad f_n(0, \alpha) = 0, \tag{17}$$

and

$$F_n(\alpha) = \int_0^\infty \exp\left[-(x_n - \alpha)^2\right] f_{n-1}(x_n, \alpha)\, dx_n. \qquad (18)$$

Since

$$\frac{d}{dx} f_n(x, \alpha) = \exp\left[-(x - \alpha)^2\right] f_{n-1}(x, \alpha) \qquad (19)$$

and

$$\exp\left[-(x - \alpha)^2\right] = \frac{\sqrt{\pi}}{2} \frac{d}{dx} \operatorname{erf}(x - \alpha), \qquad (20)$$

we can reduce (18) by repeated integration by parts to

$$\begin{aligned} F_n(\alpha) = {} & \frac{\sqrt{\pi}}{2} F_{n-1}(\alpha) - \left(\frac{\sqrt{\pi}}{2}\right)^2 \frac{1}{2} F_{n-2}(\alpha) \\ & + \left(\frac{\sqrt{\pi}}{2}\right)^3 \frac{1}{3!} F_{n-3}(\alpha) + \cdots \\ & + (-1)^{n-1} \left(\frac{\sqrt{\pi}}{2}\right)^{n-2} \frac{1}{(n-2)!} F_2(\alpha) \\ & + (-1)^n \left(\frac{\sqrt{\pi}}{2}\right)^{n-1} \frac{1}{(n-1)!} \Big\{ \sqrt{\pi}\, p(\alpha) \\ & - \int_0^\infty \operatorname{erf}^{n-1}(x - \alpha) \exp\left[-(x + \alpha)^2\right] dx \Big\}. \qquad (21) \end{aligned}$$

Finally, by the definition [(15)],

$$\begin{aligned} \Pi_n(\alpha) = {} & \frac{1}{2} \binom{n}{n-1} \Pi_{n-1}(\alpha) - \frac{1}{2^2} \binom{n}{n-2} \Pi_{n-2}(\alpha) \\ & + \cdots + \frac{(-1)^{n-1}}{2^{n-2}} \binom{n}{2} \Pi_2(\alpha) \\ & + \frac{(-1)^n}{2^{n-1}} \binom{n}{1} \left(p(\alpha) - \frac{1}{2} I_n(\alpha) \right), \qquad (22) \end{aligned}$$

where

$$I_n(\alpha) = \frac{2}{\sqrt{\pi}} \int_0^\infty \operatorname{erf}^{n-1}(x - \alpha) \exp\left[-(x + \alpha)^2\right] dx. \qquad (23)$$

$I_n(\alpha)$ and $\Pi_n(\alpha)$ have been computed for values of n from 2 to 9; the results are tabulated in Tables I and II for selected values of α.

TABLE I

VALUES OF $I_n(\alpha)$ [SEE (23)]

$n \backslash \alpha$	1.0	1.5	2.0	3.0
2	−0.09943	−0.03062	−0.004604	−0.00002210
3	0.07161	0.02797	0.004533	0.00002210
4	−0.05208	−0.02571	−0.004466	−0.00002210
5	0.03932	0.02375	0.004401	0.00002210
6	−0.02979	−0.02201	−0.004339	−0.00002209
7	0.02304	0.02046	0.004279	0.00002209
8	−0.01782	−0.01906	−0.004221	−0.00002209
9	0.01400	0.01779	0.004165	0.00002209

It can be shown from the original integral forms [(23) and (12)] that

$$I_n(0) = \frac{1}{n}, \qquad (24)$$

and

$$\Pi_n(0) = \frac{1}{2^n}. \qquad (25)$$

Equation (25) may also be derived by the following argument. Since $\alpha = 0$ corresponds to a mean value of zero for the correlator differences, any digit is equally likely to be right or wrong. The probability of one incorrect digit and $n-1$ correct ones is thus $n/2^n$, and the probability that the incorrect digit has the smallest correlator difference is just $1/n$ of this, giving (25).

For large α, we obtain the asymptotic forms

$$I_n(\alpha) \sim (-1)^{n-1}(1 - \operatorname{erf} \alpha), \qquad (26)$$

and

$$\Pi_n(\alpha) \sim n \frac{1 - \operatorname{erf} \alpha}{2} = n p(\alpha). \qquad (27)$$

Equation (27) is the form to be expected. For large α, $q(\alpha) \sim 1$, so that $n p(\alpha) q^{n-1}(\alpha)$, the probability of a single error in an n-digit word, is approximately $n p(\alpha)$. Moreover, as we shall see below, for large α the wrong digit is almost certainly corrected by the Wagner code. Therefore, for large α

$$\Pi_n(\alpha) \sim n p(\alpha). \qquad (28)$$

From inspection of Tables I and II, it is seen that the asymptotic forms [(26) and (27)] are excellent approximations for $\alpha \geqq 3$.

The conditional probability that if one error is made it will be corrected by the Wagner code is given by (13). Curves of this probability as a function of α for words of 5 and 8 digits are shown in Fig. 1 on the next page. The conditional probability approaches unity for large α, i.e., for large signal-to-noise ratio of the correlator differences, almost all errors are corrected. Below values of α of about 1.5, the conditional probability drops sharply, becoming $1/n$ for $\alpha = 0$ [see (25)]. As is to be expected, the conditional probability for a given α decreases with increasing n.

TABLE II

VALUES OF $\Pi_n(\alpha)$, THE JOINT PROBABILITY THAT A SINGLE ERROR IS MADE IN AN n-DIGIT WORD AND THAT IT IS CORRECTED BY THE WAGNER CODE [SEE (22)]

$n \backslash \alpha$	1.0	1.5	2.0	3.0
2	0.128	0.0323	0.00464	0.0000221
3	0.160	0.0462	0.00691	0.0000331
4	0.181	0.0588	0.00914	0.0000442
5	0.193	0.0704	0.01134	0.0000552
6	0.199	0.0811	0.01350	0.0000663
7	0.200	0.0908	0.01564	0.0000773
8	0.199	0.0997	0.01774	0.0000884
9	0.195	0.1079	0.01982	0.0000994

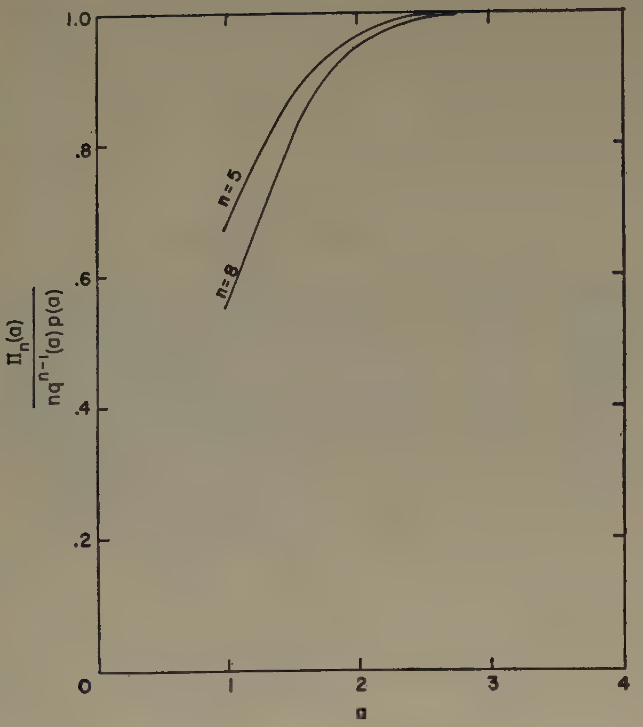

Fig. 1—Conditional probability of correction for Wagner-coded words of 5 and 8 digits.

IV. PROBABILITY OF ERROR FOR WAGNER-CODED WORDS—COMPARISON WITH UNCODED AND HAMMING-CODED WORDS

The probability of error per word for a Wagner-coded word containing m message digits ($n=m+1$ digits in all) is

$$P_W = 1 - q^{m+1}(\alpha) - \prod_{m+1}(\alpha), \tag{29}$$

that is, the probability of error is one minus the sum of the probability that the word is received correctly and the probability that a single error is made and then corrected. We wish to compare P_W with P_U the probability of error per word if no code is used, and P_H, the probability of error per word if the Hamming single-error-correcting code is used. Since we are concerned with constant-data-rate systems, the duration of the transmitted signals must be altered if coded words (message digits plus error-correcting digits) are to have the same duration as differently coded or uncoded words. Changing the signal duration changes the variance of the correlator difference and consequently the value of the parameter α and the probability of error per digit [see (7)]. For large TW (the only case we consider), it can be shown[11] that the variance of the output of any averaging device is proportional to T^{-1}. Thus σ_1, σ_2 and $\sigma=\sqrt{\sigma_1^2+\sigma_2^2}$ are all proportional to $T^{-1/2}$, so that $\alpha(=\Delta c/\sqrt{2}\sigma)$ is proportional to $T^{1/2}$.[12] Using this result, we find that, for the same value of α used in (29),

$$P_U = 1 - q^m\left(\sqrt{\frac{m+1}{m}}\,\alpha\right) \tag{30}$$

and

$$P_H = 1 - q^{m+k}\left(\sqrt{\frac{m+1}{m+k}}\,\alpha\right) - (m+k)$$
$$\cdot q^{m+k-1}\left(\sqrt{\frac{m+1}{m+k}}\,\alpha\right)p\left(\sqrt{\frac{m+1}{m+k}}\,\alpha\right), \tag{31}$$

where k is the number of check digits required by the Hamming code (see above). The three quantities [(29), (30) and (31)] have been computed for values of m from 4 to 8 and for selected values of α. The results are given in Table III.

TABLE III

PROBABILITIES OF ERROR PER WORD FOR UNCODED, HAMMING-CODED, AND WAGNER-CODED WORDS CONTAINING m MESSAGE DIGITS

m	α	P_U	P_H	P_W
4	1.0	0.209	0.191	0.143
	1.5	0.0349	0.0248	0.0115
	2.0	0.00313	0.00145	0.00030
	3.0	42×10^{-7}	6×10^{-7}	$<10^{-7}$
5	1.0	0.269	0.310	0.190
	1.5	0.0493	0.0513	0.0164
	2.0	0.00486	0.00375	0.00045
	3.0	84×10^{-7}	25×10^{-7}	$<10^{-7}$
6	1.0	0.325	0.335	0.236
	1.5	0.0641	0.0530	0.0220
	2.0	0.00673	0.00346	0.00062
	3.0	138×10^{-7}	17×10^{-7}	$<10^{-7}$
7	1.0	0.377	0.362	0.282
	1.5	0.0789	0.0552	0.0281
	2.0	0.00871	0.00330	0.00082
	3.0	201×10^{-7}	12×10^{-7}	$<10^{-7}$
8	1.0	0.425	0.388	0.326
	1.5	0.0937	0.0580	0.0347
	2.0	0.01075	0.00322	0.00103
	3.0	272×10^{-7}	9×10^{-7}	$<10^{-7}$

There is only a certain range of values of the signal-to-noise ratio of the correlator difference for which it is worth the effort to implement either of the error-correcting codes. For high signal-to-noise ratio, very few errors are made, and additional equipment is generally not justifiable. On the other hand, for low signal-to-noise ratio, multiple errors become too frequent, and single-error-correcting codes are of little use. Thus single-error-correcting codes are of considerable value for values of α from about 1.0 to 3.0.

As shown in Table III, in this range of values the probability of error of Wagner-coded words is considerably less than that of Hamming-coded words. For increasing word length, the advantage of the Wagner code diminishes from two causes: (1) the ratio k/m decreases with increasing m so that the length of the digits in the Hamming-coded word approaches that of the Wagner-coded words, thus narrowing the gap between the corresponding signal-to-noise ratios; and (2) the conditional probability of correcting a single error decreases with increasing m. Nonetheless, even for $m=8$ and $\alpha=2$, we may expect only 103 errors per 100,000 words using the Wagner code, as compared with 322 errors per 100,000 Hamming-coded words, and 1,075 errors per 100,000 uncoded words.

---

[11] W. B. Davenport, Jr., R. A. Johnson, and D. Middleton, "Statistical errors in measurements on random time functions," *Jour. Appl. Phys.*, vol. 23, pp. 377–388; April, 1952.

[12] The result that σ is proportional to $T^{-1/2}$ requires that the integrals in Eq. (3) be normalized by dividing them by T. The result that α is proportional to $T^{1/2}$ is independent of the normalization.

V. IDENTIFICATION OF THE SMALLEST CORRELATOR DIFFERENCE

Until now we have assumed that the receiver can pick out the smallest correlator difference with infinite precision. Suppose, however, that the equipment used in implementing the Wagner code is such that the smaller of two correlator differences within $\epsilon\Delta c$ of each other cannot be identified with certainty. Let $P_{W,\epsilon}$ be the revised probability of error per word, assuming that single errors remain uncorrected whenever any correlator difference lies within $\epsilon\Delta c$ of the smallest. In this notation, the P_W used above is $P_{W,0}$.[13,14]

Suppose that the first digit has the smallest correlator difference $|\Delta z_1|$ and is known to be the only one in error. Then the probability that $|\Delta z_i|$, the correlator difference of the i-th digit ($i \neq 1$), lies within $\epsilon\Delta c$ of $|\Delta z_1|$ is given by

$$\text{prob}\,(|\Delta z_1| < \Delta z_i < |\Delta z_1| + \epsilon\Delta c / \Delta z_i > |\Delta z_1|)$$
$$= \frac{1}{\text{prob}\,(\Delta z_i > |\Delta z_1|)} \int_{|\Delta z_1|}^{|\Delta z_1|+\epsilon\Delta c} W(\Delta z_i)\, d\Delta z_i$$
$$= \int_{|\Delta z_1|}^{|\Delta z_1|+\epsilon\Delta c} W(\Delta z)\, d\Delta z \Big/ \int_{|\Delta z_1|}^{\infty} W(\Delta z)\, d\Delta z, \qquad (32)$$

where $W(\Delta z)$ is given by (6). [Since the correlator difference is always positive for a correct digit, the absolute value sign is not needed on $|\Delta z_i|$. The factor prob $(\Delta z_i > |\Delta z_1|)$ in the denominator renormalizes the distribution $W(\Delta z_i)$ from one in which all values of Δz_i are possible to one which only allows values of $\Delta z_i > |\Delta z_1|$.]

The probability [(32)] is written for a given $|\Delta z_1|$. Let $J(\epsilon, \alpha)$ be the probability that Δz_i will lie within $\epsilon\Delta c$ of $|\Delta z_1|$, no matter what the value of $|\Delta z_1|$. It is clear that $J(\epsilon, \alpha)$ is independent of i. Using (6) and (9), we find

$$J(\epsilon, \alpha) = \int_0^\infty W(|\Delta z_1|, \text{wrong})\, \text{prob}\,(|\Delta z_1| < \Delta z_i < |\Delta z_1| + \epsilon\Delta c / \Delta z_i > |\Delta z_1|)\, d|\Delta z_1|$$
$$= \frac{1}{\sqrt{2\pi}\,\sigma} \int_0^\infty \exp\left[-\frac{(|\Delta z_1| + \Delta c)^2}{2\sigma^2}\right] \cdot \frac{\displaystyle\int_{|\Delta z_1|}^{|\Delta z_1|+\epsilon\Delta c} \exp\left[-\frac{(\Delta z - \Delta c)^2}{2\sigma^2}\right] d\Delta z}{\displaystyle\int_{|\Delta z_1|}^{\infty} \exp\left[-\frac{(\Delta z - \Delta c)^2}{2\sigma^2}\right] d\Delta z}\, d|\Delta z_1|$$
$$= \frac{1}{\sqrt{\pi}} \int_0^\infty \exp\,[-(x+\alpha)^2] \cdot \frac{\text{erf}\,(x - \alpha + \epsilon\alpha) - \text{erf}\,(x - \alpha)}{1 - \text{erf}\,(x - \alpha)}\, dx. \qquad (33)$$

The probability that Δz_i does *not* lie within $\epsilon\Delta c$ of $|\Delta z_1|$, assuming that $\Delta z_i > |\Delta z_1|$, is thus $1 - J(\epsilon, \alpha)$, and the probability that none of the $n-1$ correct digits has a Δz within $\epsilon\Delta c$ of $|\Delta z_1|$ is $[1 - J(\epsilon, \alpha)]^{n-1}$. Thus we find

$$P_{W,\epsilon} = 1 - q^{m+1}(\alpha) - [1 - J(\epsilon, \alpha)]^m \textstyle\prod_{m+1}(\alpha). \qquad (34)$$

Calculated values of $J(0.1, \alpha)$ for selected values of α are given in Table IV, together with a comparison of $P_{W,0.1}$ and $P_{W,0}$ for words of six message digits.

TABLE IV

SELECTED VALUES OF J(0.1, α) AND COMPARISON OF $P_{W,0}$ AND $P_{W,0.1}$ FOR WORDS OF 6 MESSAGE DIGITS

α	$J(0.1, \alpha)$	$P_{W,0}$	$P_{W,0.1}$
1.0	0.00379	0.236	0.241
1.5	0.000426	0.0220	0.0222
2.0	0.0000189	0.00062	0.00062+

From Table IV, we see that even for a rather crude receiver, which cannot distinguish correlator differences lying within 0.1 Δc of each other, the percentage change in the probability of error per word is at most about two per cent in the region of interest. Thus the advantage of the Wagner code over the Hamming code does not depend on great precision of the correlators or the memory.

VI. SUMMARY AND CONCLUSIONS

Following a suggestion of C. A. Wagner, we have constructed a code that, unlike those previously considered, makes explicit use of the *magnitude* of the difference of the *a posteriori* probabilities of the transmitted signals. The code is applied to systems transmitting sequences (words) of binary digits that are corrupted by the addition of white Gaussian noise and then detected by correlation. The simplicity of the calculations described in Sections III and IV derives from the fact that the *a posteriori* probability $p(x_i/y)$ that x_i was sent if y is received is proportional (for suitable x_i) to the exponential of the finite-time correlation

$$z_i = \int_0^T x_i y\, dt.$$

---

[13] The receiver may also have difficulty in determining the sign of small correlator differences. The percentage increases in P_U, P_H and P_W produced by this difficulty are of the order of magnitude of

$$(P_{W,\epsilon} - P_{W,0})/P_{W,0},$$

and hence, as we shall see, very small.

[14] For simplicity of calculation, we have chosen $P_{W,\epsilon}$ as the probability of error per word, assuming that single errors remain uncorrected whenever two or more correlator differences lie within $\epsilon\Delta c$ of each other. In practice, a smaller probability of error can be obtained by the simple expedient of arbitrarily changing the first digit of every set of digits with correlator differences within $\epsilon\Delta c$ of each other. In this way, we correct almost half of the errors which remain uncorrected in calculating $P_{W,\epsilon}$.

Under the assumptions made in Section II, z_i is normally distributed, and a pair of signals x_1 and x_2 can be chosen such that their correlations are statistically independent.

Unlike the Hamming code, the Wagner code has only a probability of correcting single errors. However, unless the signal-to-noise ratio of the correlator difference voltage is less than unity or the word is too long, this probability is high. The Wagner code requires only a single check digit, the burden of its operation being placed on a memory which must store the values of the *a posteriori* probabilities (or their differences) for the duration of a word. The Hamming code, on the other hand, requires several check digits (see Section I).

If the words are transmitted at a constant rate, the coded words (message digits and check digits) must have the same duration as the uncoded words (message digits only); therefore, the digits composing the word must be appropriately shortened. This increases the probability of error per digit and diminishes the advantage of the code. Since the digits of a Wagner-coded word are longer than those of the corresponding Hamming-coded word, they are less likely to be incorrectly received. Thus it is natural to ask, first, whether coding is worth the trouble in a constant-data-rate system, and second, whether the Wagner code which shortens the digits less but corrects only a certain percentage of single errors is better than the Hamming code which shortens the digits more but corrects all single errors.

These questions are answered in Section IV. It is found that both codes are valuable even for very short words, but that the Wagner code makes considerably fewer errors, depending on the length of the word and the signal-to-noise ratio of the correlator difference voltage. (No attempt is made to relate channel and output signal-to-noise ratios.)

The successful operation of the Wagner code does not require great precision of the correlators or memory, as shown in Section V.

The numerical computations reported here were done by Mrs. Elizabeth Munro.

APPENDIX ON THE DISTRIBUTION OF FINITE-TIME CORRELATIONS

Consider a transmitter sending one of two signals $x_1(t)$ and $x_2(t)$ of duration T and bandwidth W.[15] Suppose they are corrupted by the addition of white Gaussian noise. Thus, if $x_1(t)$ is sent, the received signal is

$$y(t) = x_1(t) + n(t), \tag{A-1}$$

where $n(t)$ is a representative noise waveform. Let z_1 and z_2 denote the finite-time correlations

$$z_1 = \int_0^T x_1(t)y(t)dt$$

and (A-2)

$$z_2 = \int_0^T x_2(t)y(t)dt.$$

In Section II it was stated without proof that z_1 and z_2 are normally distributed random variables. In Section III it was stated without proof that $x_1(t)$ and $x_2(t)$ can be chosen so that z_1 and z_2 are statistically independent. This appendix is devoted to a justification of these statements.

To prove the first statement, we note that z_1 and z_2 are integrals of the same Gaussian process. Linear combinations of a finite set of jointly Gaussian variables are themselves jointly Gaussian,[16] a result which may be extended to Riemann integrals to complete the proof.

To prove the second statement, it suffices to choose $x_1(t)$ and $x_2(t)$ such that $\overline{z_1 z_2} = \bar{z}_1 \bar{z}_2$ (where the averages are over the noise statistics), since linear independence implies statistical independence for two variables whose joint distribution is Gaussian.[17] The averages of z_1 and z_2 are

$$\begin{aligned} c_1 = \overline{z_1} &= \overline{\int_0^T x_1 y dt} = \overline{\int_0^T (x_1 + n) x_1 dt} \\ &= \int_0^T \overline{(x_1^2 + x_1 n)} dt \\ &= \int_0^T x_1^2 dt \text{ (since } \overline{x_1 n} = x_1 \bar{n} = 0), \end{aligned} \tag{A-3}$$

and

$$\begin{aligned} c_2 = \overline{z_2} &= \overline{\int_0^T x_2 y dt} = \overline{\int_0^T (x_1 + n) x_2 dt} \\ &= \int_0^T \overline{(x_1 x_2 + x_2 n)} dt \\ &= \int_0^T x_1 x_2 dt \text{ (since } \overline{x_2 n} = x_2 \bar{n} = 0). \end{aligned} \tag{A-4}$$

The calculation of $\overline{z_1 z_2}$ is more complicated. As a first step, write $\overline{z_1 z_2}$ as the double integral

$$\overline{z_1 z_2} = \overline{\int_0^T x_1 y dt \int_0^T x_2' y' dt'} = \int_0^T \int_0^T \overline{x_1 y x_2' y'}\, dt dt' \tag{A-5}$$

where x_1 and y are written for argument t[(A-3) and (A-4)], and x_2' and y' for argument t'. Then, substituting $y = x_1 + n$, $y' = x_1' + n'$, and expanding, we obtain

---

[15] C. E. Shannon, "Communication in the presence of noise," PROC. I.R.E., vol. 37, pp. 10–21; January, 1949. Using a well-known theorem from the above-mentioned paper, we can write a signal of bandwidth W in terms of its values at sample points $1/2W$ seconds apart, i.e.,

$$f(t) = \sum_{r=-\infty}^{\infty} f(r/2W) \frac{\sin \pi(2Wt - r)}{\pi(2Wt - r)}.$$

Even if we set $f(r/2W) = 0$ for $r < 0$ and $r > 2TW$, $f(t)$ does not vanish identically outside the interval $0 < t < T$. However, if TW is large, the amount of time $f(t)$ is significantly different from zero outside the interval $0 < t < T$ is small compared to T. This justifies the use of idealized signals of duration T and bandwidth W.

[16] H. Cramér, op. cit., pp. 312–313.

[17] H. Cramér, op. cit., pp. 310–311.

$$\overline{z_1z_2} = \int_0^T \int_0^T \overline{(x_1{}^2x_1{}'x_2{}' + nx_1x_1{}'x_2{}' + n'x_1{}^2x_2{}' + nn'x_1x_2{}')}\,dtdt'$$

$$= \int_0^T x_1{}^2dt \int_0^T x_1{}'x_2{}'dt$$

$$+ \int_0^T \int_0^T \overline{nn'}x_1x_2{}'dtdt' \text{ (using } \bar{n} = \bar{n}' = 0)$$

$$= \overline{z_1}\,\overline{z_2} + \int_0^T \int_0^T R_n(t-t')x_1(t)x_2(t')dtdt', \tag{A-6}$$

where R_n is the autocorrelation function of the noise n. Since x_1 and x_2 are negligibly small outside the interval $0 \leqq t \leqq T$, the last integral in (A-6) can be approximated by

$$\int_{-\infty}^{\infty} \int_{-\infty}^{\infty} R_n(t-t')x_1(t)x_2(t')dtdt'$$

$$= \int_{-\infty}^{\infty} R_n(\tau)R_{12}(\tau)dt, \tag{A-7}$$

where

$$R_{12}(\tau) = \int_{-\infty}^{\infty} x_1(t+\tau)x_2(t)d\tau. \tag{A-8}$$

We can choose x_1 and x_2 such that $R_{12}(\tau)$ is very small where $R_n(\tau)$ is significant, that is, for $\tau \leqq 1/W$.[18] Indeed, if x_1 and x_2 have nonoverlapping energy spectra within the band W, $R_{12}(\tau) \equiv 0$. Thus, for suitably chosen x_1 and x_2, we may neglect the integral (A-7), so that (A-6) becomes

$$\overline{z_1z_2} \approx \overline{z_1}\,\overline{z_2}. \tag{A-9}$$

Equation (A-9) states that z_1 and z_2 are (approximately) linearly independent and consequently (approximately) statistically independent.

---

[18] This means that x_1 and x_2 are approximately orthogonal and remain so when time-displaced with respect to each other by an amount $\leqq$ the correlation time of the noise.

Analysis of a Special Purpose RC Filter Incorporating a Periodically Conducting Bilinear Element*

VICTOR W. BOLIE†, MEMBER, IRE

Summary—The paper concerns the mathematical analysis of an experimentally-developed, four-terminal network consisting of a resistor-capacitor-chopper combination. The circuit is essentially a simple, low-pass rc filter, modified by the insertion of a periodically-conducting bilinear element. The circuit receives a modulated sinusoidal carrier, filters the modulation, and transmits the resulting signal as a series of amplitude-modulated rectangular pulses. The reed driving coil of the chopper is separately excited by a sinusoidal voltage of carrier frequency so that the pulse repetition rate of the output pulses is equal to the frequency of the input carrier. The analysis takes into account the "dead time" of the chopper and admits an arbitrary choice of phase difference between the input carrier voltage and the chopper-reed excitation voltage. An equivalent circuit is derived from response of circuit to an input carrier of fixed amplitude. A formula is obtained for equivalent circuit-time constant, and a condition for minimum attenuation is also derived.

INTRODUCTION

IN THE FIELD of automatic control the uses of rc filters to operate on dc-error signals are well known. If the original signal is the output of a magnetic amplifier or resolver it is usually in the form of a modulated ac carrier. While such a signal is especially easy to amplify, it is customarily demodulated in order to operate on the error signal with an rc filter. If the resultant signal requires further amplification it may be returned to the modulated carrier form by the use of a chopper.

The purpose of this paper is to investigate the operation of an experimentally-developed, four-terminal network consisting of a resistor-capacitor-chopper combination. The connections of the circuit elements are such that the circuit is essentially a simple, low pass rc filter, modified by the insertion of a periodicically-conducting bilinear element. The circuit receives an amplitude-modulated sinusoidal carrier, filters the modulation, and transmits the result as a series of amplitude-modulated rectangular pulses. The system thus described is a linear circuit which operates with periodic interruption. The circuit is analyzed by considering the stepwise accumulation of charge by the capacitor. A somewhat similar approach has appeared in a recently published paper[1] dealing with the operation of an rc memory commutator.

---

* Decimal classification: R143.2×R143.5. Original manuscript received by the IRE, September 8, 1953; revised manuscript received, May 10, 1954.

† Scientific Staff, Collins Radio Company, Cedar Rapids, Ia.

[1] C. I. Beard and E. N. Skomal, "Rc memory commutator for signal-to-noise improvement," *Rev. Sci. Instr.*, vol. 24, pp. 276–280; April, 1953.

Analysis

The circuit shown in Fig. 1 is designed for a modulated carrier input. The input carrier and the excitation of the reed-driving coil of the SPDT synchronous chopper are sinusoidal voltages, both of angular frequency ω. The motion of the switch armature is periodic with period $T=2\pi/\omega$. Choose the time origin so that terminals 2 and 3 are connected at the beginning of each cycle. For the sake of simplicity, assume that the armature motion is symmetric with respect to the input and output terminals 1 and 3. Under this assumption the closing of terminals 1 and 2 follows the closing of terminals 2 and 3 by one half-cycle, and the dwell times spent by the switch armature in each of these two contacting positions are equal. Let $t_1=\delta T$ represent the dwell time spent by the armature in each contacting position. The fraction δ is such that $0<\delta<\frac{1}{2}$. Thus, in each cycle the capacitor is first connected to the output for the dwell time $t_1=\delta T$, then disconnected from the circuit for the "dead time" $t_d=(\frac{1}{2}-\delta)T$, then connected to the input through the resistance R for the dwell time $t_1=\delta T$, and then again disconnected from the circuit for the dead time $t_d=(\frac{1}{2}-\delta)T$.

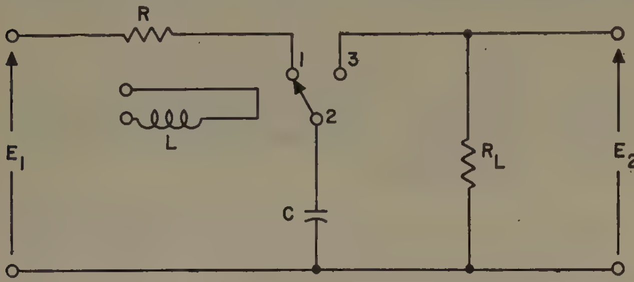

Fig. 1—Schematic of rc filter incorporating periodically conducting bilinear element. Input voltage E_1 is amplitude modulated sinewave; output voltage is a series of amplitude modulated pulses.

Assume that the load resistance R_L is large enough that no appreciable charge is lost by the capacitor during the time t_1 the switch terminals 2 and 3 are closed. Under this assumption the capacitor voltage $E(t)$ remains constant during that portion of the cycle in which the capacitor is not connected to the input. The output voltage $E_2(t)$ is then defined as

$$\left.\begin{aligned} E_2(t) &= E(mT) \quad \text{if} \quad mT \leqq t \leqq mT + t_1 \\ &= 0 \quad\quad\;\; \text{if} \quad mT + t_1 < t < (m+1)T \end{aligned}\right\}, \tag{1}$$

where $m=0, 1, 2, \cdots$, and $E(t)$ is the capacitor voltage at time t. Thus, the output voltage $E_2(t)$ consists of the series of rectangular pulses sketched in Fig. 2. These pulses commence at time $t=0$, and repeat every cycle thereafter. Each pulse has a duration $t_1=\delta T$ and an amplitude determined by the capacitor voltage $E(t)$.

According to the conditions stated above, both the input voltage $E_1(t)$ and the output voltage $E_2(t)$ are modulated carriers. The input carrier $C_1(t)$ is

$$C_1(t) = \sin(\omega t + \theta), \tag{2}$$

where θ is the phase advance of the input carrier with respect to the motion of the switch armature. The output carrier $C_2(t)$ is

$$C_2(t) = P_\delta(t), \tag{3}$$

where $P_\delta(t)$ is a nonnegative rectangular wave of unit amplitude, period T, and duty cycle δ, whose first positive excursion occurs at time $t=0$. Now, if the two nonnegative functions $F(t)$ and $G(t)$ represent the input and output modulations, respectively, then the input and output voltages $E_1(t)$ and $E_2(t)$ are

$$E_1(t) = F(t)C_1(t) \tag{4}$$

$$E_2(t) = G(t)C_2(t), \tag{5}$$

where $F(t) \geqq 0$ and $G(t) \geqq 0$. It is desired to show how $G(t)$ is related to $F(t)$.

Since the system described is linear, the relationship between the input modulation $F(t)$ and the output modulation $G(t)$ can be established by determining $G(t)$ when $F(t)$ is a step function. In a certain sense, this procedure is equivalent to finding the indicial response of the system. Taking $F(t)=V$, where V is a constant, gives the input voltage

$$E_1(t) = V \sin(\omega t + \theta). \tag{6}$$

According to (1), the corresponding output voltage $E_2(t)$ is determined by evaluating the capacitor voltage $E(t)$ at the beginning of each cycle. During the time t for which $(T/2) \leqq t \leqq (T/2)+t_1$ the capacitor voltage $E(t)$ must satisfy the differential equation,

$$RC\frac{dE}{dt} + E = V \sin(\omega t + \theta), \tag{7}$$

which has the solution

$$\begin{aligned} E(t) = {} & \left[E\left(\frac{T}{2}\right) + V\cos\phi \sin(\theta - \phi)\right] e^{-(t-T/2)/RC} \\ & + V \cos\phi \sin(\omega t + \theta - \phi), \end{aligned} \tag{8}$$

where ϕ is the acute angle determined by the equation

$$\tan\phi = \omega RC. \tag{9}$$

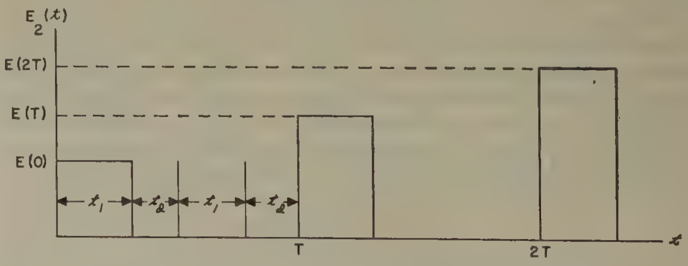

Fig. 2—Pulse-wave shape of output voltage of the circuit shown in Fig. 1.

Now, $E(T/2)=E(0)$, since R_L is assumed very large. Furthermore, $E(T)=E[(T/2)+t_1)]$, since the capacitor voltage remains constant during the dead time t_d. Eq. (8) therefore gives

$$E(T) = E(0)e^{-t_1/RC} + E_c, \tag{10}$$

where

$$E_c = V\left[e^{-t_1/RC}\sin(\theta-\phi) - \sin(\omega t_1+\theta-\phi)\right]\cos\phi. \quad (11)$$

Eq. (10) gives the capacitor voltage at the end of the first cycle in terms of its voltage at the beginning of the cycle and another quantity E_c which does not depend on the initial capacitor voltage. This formula may be applied to any subsequent cycle. Thus,

$$E(mT) = E(mT-T)e^{-t_1/RC} + E_c, \quad (12)$$

where m is any positive integer. It may be shown, by letting m successively take the values $1, 2, 3, \cdots, n$, that (12) has the equivalent form,

$$E(nT) = E(0)e^{-nt_1/RC} + E_c\sum_{k=0}^{n-1} e^{-kt_1/RC}. \quad (13)$$

It can be shown that when $t_1=\delta T \ll RC$, the above expression may be approximated as

$$E(nT) = E(0)e^{-n\delta T/RC} + \frac{RC}{\delta T}E_c\left[1-e^{-n\delta T/RC}\right]. \quad (14)$$

Consideration of (1), (4), (5), (6), and (14), shows that when $\delta T \ll RC$ the relationship between the input modulation $F(t)$ and the output modulation $G(t)$ is such that when $F(t)=V$, then $G(t)$ is very nearly

$$G(t) = E(0)e^{-\delta t/RC} + \frac{RC}{\delta T}E_c\left[1-e^{-\delta t/RC}\right], \quad (15)$$

which is the response of a simple integrating circuit of time constant RC/δ to a step voltage of magnitude $(RC/\delta T)E_c$.

It is convenient at this point to introduce a practical restriction which will simplify the quantity $(RC/\delta T)E_c$. The quantity E_c given by (11) is seen to vary sinusoidally with the input carrier phase angle θ, and may be maximized with respect to θ by equating to zero the partial derivative of E_c with respect to θ. The result of this procedure shows that the value θ_m of θ for which E_c has a maximum absolute value must satisfy, approximately, the equation,

$$\tan(\phi-\theta_m) = \tan\pi\delta, \quad (16)$$

when $\delta T \ll RC$. Substitution of a suitable solution of (16) into (11) shows that when $\delta T \ll RC$, the maximum value of E_c attainable by varying θ is approximately

$$E_{c\max} = 2V\sin\pi\delta\cos\phi. \quad (17)$$

Under the assumption that $T \ll 2RC$, which implies both that $\delta T \ll RC$ and $\omega RC \ll 1$, the above expression further reduces

$$E_{c\max} = \frac{2V}{\omega RC}\sin\pi\delta. \quad (18)$$

The substitution of (18) into (15) shows that if $T \ll 2RC$ and if $\theta=\theta_m$, the response $G(t)$ to $F(t)=V$ is approximately

$$G(t) = E(0)e^{-\delta t/RC} + V\frac{\sin\pi\delta}{\pi\delta}\left[1-e^{-\delta t/RC}\right]. \quad (19)$$

Since $0<\delta<\frac{1}{2}$, it follows that the attenuation factor $\sin\pi\delta/\pi\delta$ is such that $2/\pi < (\sin\pi\delta/\pi\delta) < 1$.

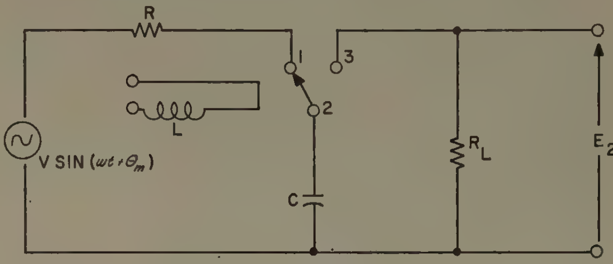

Fig. 3—Circuit with unmodulated sine-wave input. The phase angle θ_m is that required to maximize the output voltage.

Eq. (19) gives the effective indicial response of the circuit of Fig. 1, which is effectively that shown in Fig. 3 when the input voltage is $E_1(t)=V$ and the phase angle is taken as $\theta=\theta_m$. Under the conditions for which (19) is valid, the equivalent circuit of Fig. 3 is that shown in Fig. 4. The switch contacts are numbered in the equivalent circuit to correspond with those in Fig. 3. The switch-armature motions for both circuits are identical. The capacitance in Fig. 4 is taken as C/δ so that the time constant of the equivalent circuit is that indicated by (19). In both circuits the load resistance R_L is assumed so large that the loading effects are negligible.

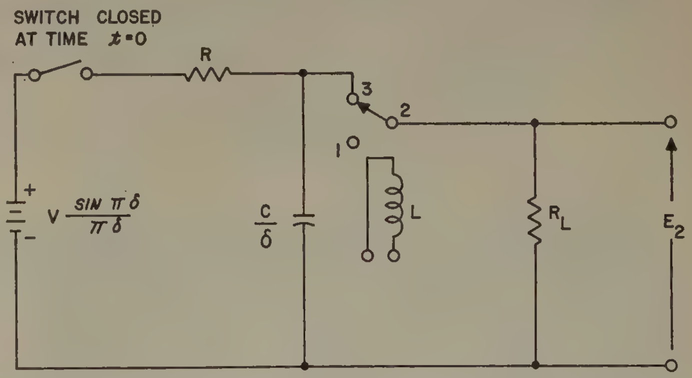
SWITCH CLOSED AT TIME $t=0$
R
3
2
1
+
−
V $\frac{\sin\pi\delta}{\pi\delta}$
$\frac{C}{\delta}$
L
R_L
E_2

Fig. 4—The equivalent circuit for Fig. 3. The switch terminals are numbered to correspond with those shown in Fig. 3.

The equivalent circuit shown in Fig. 4 has been derived from (19), which gives the output modulation $G(t)$ for the circuit of Fig. 1 when the input modulation $F(t)$ is $F(t)=V$, where V is a constant. However, since the two circuits are linear, they are also equivalent when V is any time-varying function suitable (non-negative and slowly varying with respect to the carrier frequency) for use as a modulation signal. In the latter case, of course, the voltage source in the circuit of Fig. 4 is either considered as producing a time-varying output $(\sin\pi\delta/\pi\delta)V=(\sin\pi\delta/\pi\delta)F(t)$, or is replaced by a conventional detector and smoothing filter capable of converting the input voltage $E_1(t)=F(t)\sin(\omega t+\theta_m)$ to $(\sin\pi\delta/\pi\delta)F(t)$.

As an example in which the input modulation is constant, assume that the circuit of Fig. 1 uses a 1μf capacitor, a 1-megohm resistance and a 400 cycle chopper for which $\delta=0.4$. The condition that $T \ll 2RC$ is adequately satisfied, since $RC=1$ and $T=1/400=0.0025$. When the phase angle θ of the input carrier has been adjusted for maximum output, the input voltage is given by

$$E_1(t) = V \sin(800\pi t + 1.1\pi). \qquad (20)$$

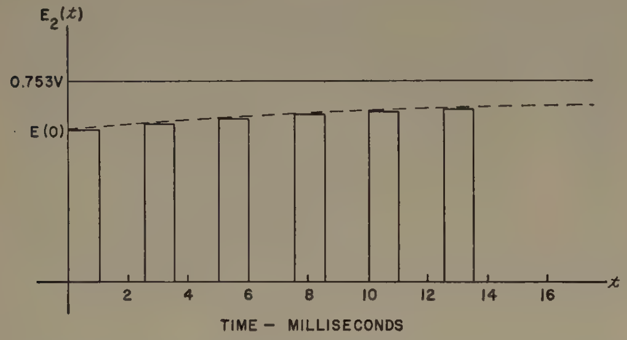

Fig. 5—Output voltage of circuit of Fig. 3. The initial capacitor-voltage is $E(0)$. The carrier frequency f, the contact-dwell constant δ, the resistance R, and the capacitance C are $f=400$ cycles, $\delta=0.4$, $R=1$ megohm, and $C=1$ microfarad.

The time-constant of the equivalent circuit is $RC/\delta = 1/0.4 = 2.5$ seconds. The attenuation factor is $(\sin \pi\delta/\pi\delta) = (\sin 0.4\pi/0.4\pi) = 0.753$. Eq. (19) then gives

$$G(t) = E(0)e^{-t/2.5} + 0.753V[1 - e^{-t/2.5}]. \qquad (21)$$

The output voltage $E_2(t)$ is the sequence of rectangular pulses, each of 1 millisecond duration, which commence $t=0$ and repeat every 2.5 milliseconds thereafter. These pulses have the peak envelope $G(t)$ defined by (21). The output voltage pulses, together with the envelope of their peaks, are sketched in Fig. 5.

ACKNOWLEDGMENT

The writer is indebted to D. C. Arnold and D. T. Pringle for their suggestion of this analysis, and their description of the circuit behavior observed in the laboratory.

Optar, a Method of Optical Automatic Ranging, as Applied to a Guidance Device for the Blind*

HEINZ E. KALLMANN†, SENIOR MEMBER, IRE

Summary—**Optical automatic devices, using ambient light only, can locate and range objects up to about 100 feet. Shallow real images of the objects are formed by a wide-aperture lens in an image space where a moving vane with minute bars and slots periodically cuts across all light rays in one image plane after another. Whenever the bars coincide with a sharp image they modulate the light received by a photocell. Range information may be read on a meter or control directly a range-following servo mechanism.**

A small hand-held guidance device for the blind is described. It is used for probing like a flashlight but operates on ambient light when that exceeds one foot-candle. Image space is explored several times per second by a helical vane with bars spaced the closer the nearer the objects whose image they intercept. A photo-multiplier and audio amplifier feed the resulting whistle-modulation to an earphone, 8 frequencies corresponding to 8 ranges from 20 inches to 20 feet. A motor turns the vane, also a chopper to supply via transformer and twentyfold voltage multiplier 1000 volts dc to the electron multiplier; total consumption is 50 ma from one 1.5v cell.

IMAGE SPACE EXPLORATION

IMAGE SPACE exploration is a method by which an automatic device can locate the presence and measure the distance of objects. It was first conceived for use in a guidance device for the blind; but it was also found useful for other applications to be mentioned briefly. It is based on less familiar aspects of simple lens optics.

The positive lens in Fig. 1 forms images in the image space[1] to the right of the exit focal plane, for all objects in the object space to the left of the entrance focal plane. The focal length b_∞ (often denoted by f which is here used for frequency) is the image distance for infinitely distant objects. The image distance b for an object distance a is

$$b = \frac{ab_\infty}{a - b_\infty}. \qquad (1)$$

---

* Decimal classification: 535.38. Original manuscript received by the IRE, June 21, 1950; revised manuscript received, April 26, 1954. Presented N. Y. Section of the IRE, January 4, 1950; briefly reported: "Optar, a new system of optical ranging," *Electronics*, vol. 23, pp. 102–105; April, 1950.

† Consulting Engineer, New York, N. Y.

[1] A. C. Hardy and F. H. Perrin, "The Principles of Optics," McGraw-Hill Book Co., Inc., New York, N. Y., ch. I, sec. 14, p. 31; 1932.

The lateral magnification

$$M = -\,i/h = -\,b/a; \tag{2}$$

the negative sign means inverted image. Expressing all distances in units of focal length b_∞ normalizes (1) as

$$\frac{b}{b_\infty} = 1 + \frac{1}{a/b_\infty - 1}\cdot \tag{3}$$

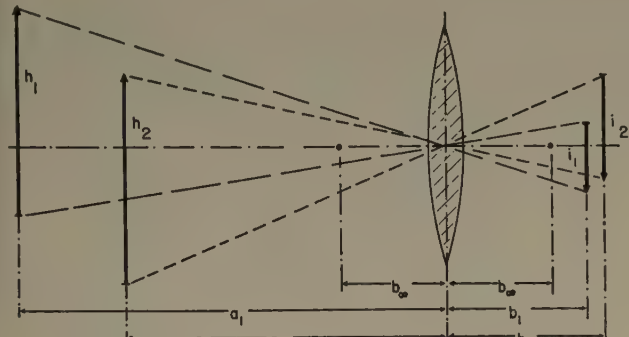

Fig. 1—Distances of objects and of real images formed by a lens.

The plot Fig. 2 shows that images of distant objects are all crowded close to the exit focal plane but that those of objects less than 100 b_∞ distant are well separated, much so for those less than 10 b_∞ away. The separation of image planes is indicated by the longitudinal magnification[2]

$$\Gamma = \frac{db}{da} = \frac{b_\infty{}^2}{(a - b_\infty)^2} = -\,M^2. \tag{4}$$

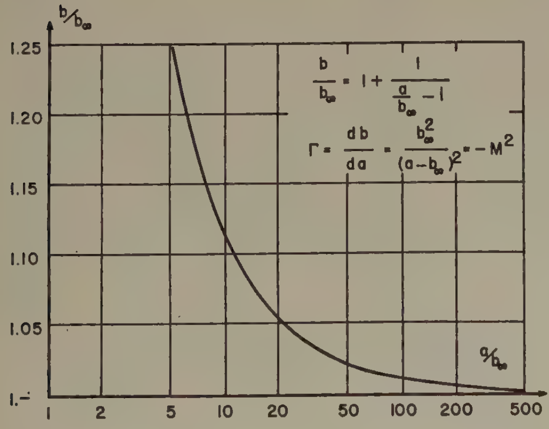

Fig. 2—Longitudinal magnification Γ vs object distance.

Γ decreases, roughly, with the square of the object distance and so does the accuracy of the ranging method here described. It cannot be improved by choice of any particular imaging system, only by increase in focal length.

How an image plane can be identified is shown in Fig. 3. The light rays from a distant point source are imaged by a wide-aperture lens to a point and then are collected on the cathode of a photocell. To locate sharp images a system of bars and slots is moved continuously across the bundle of light rays, in one image plane after another. Such comb-like interceptor with its bars seen end-on is shown in the image plane where each crossing bar will stop all light and each slot will pass it to the photocell. With f bars crossing per second the photo current will then be fully modulated with the frequency f cps. Such modulation will be called a signal. Assume next that the interceptor is shifted along the axis to another plane where the light rays have spread beyond the width of a bar or slot. For equal width of bars and slots, the light reaching the photocell will still average one-half; but the depth of the signal modulation will decrease with the distance from the sharp image as plotted as $A.C.$ vs b in Fig. 3. The peaked response curve is the narrower the wider the lens aperture; its shape depends mainly on that of the lens aperture here assumed round; a rectangular bundle of light rays would yield zeros and side lobes.

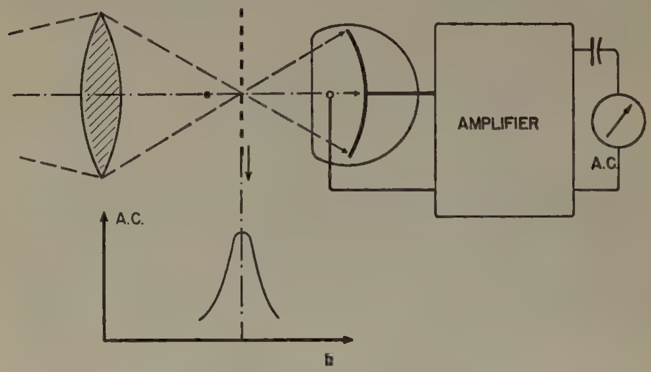

Fig. 3—Signal amplitude vs displacement of interceptor from image plane.

The "sharp" image of a point source is, due to diffraction of light, a circle of confusion[3] of diameter δ, depending on the wavelength λ of the light and the diameter D of the lens.

$$\delta = 2.44\lambda b_\infty/D. \tag{5}$$

For example for green light, $\lambda = 580\cdot 10^{-6}$ mm, and for $b_\infty/D = 1.8$, $\delta = 0.0025$ mm. For best ranging accuracy the width w of either bar or slot should be equal to, or slightly larger than, δ.

The ranging accuracy expressed by the ratio a/α of the object distance a and its possible error α (either way) is, for $a \gg b$, approximately

$$a/\alpha = bD/aw. \tag{6}$$

Thus for given object distance and focal length it increases with the lens diameter and the number of bars per inch. Although this suggests a good lens and a fine interceptor structure, other reasons may lead to choice of rather coarse bars, and a lens with correspondingly poorer resolution will then serve nearly as well.

---

[2] Hardy & Perrin, *loc. cit.*, ch. IV, sec. 40, p. 67.

[3] Hardy & Perrin, *loc. cit.*, ch. VII, sec. 60, p. 129.

SIGNALS FROM EXTENDED OBJECTS AND SIGNAL-TO-NOISE RATIO

Thus far the ranged objects had been thought of as luminous points. That the method can also be used with extended objects is far from obvious. Indeed, if the object were a detail-less surface larger than the field of view then the moving interceptor would yield no signal modulation and the device could not range the surface (nor could the human eye or other optical range finders using ambient light). But in general objects present a variety of large and small contrasting areas. In the following analysis their images will be considered as broken up into rows of n, randomly black or white, square elements, parallel to, and of width w of, a bar or slot. During each half-cycle of the signal frequency f a slot replaces the light from n elements by that of n others. A change from black to black or white to white contributes no signal, black to white counts $+1$ per element, white to black, -1. Change of n elements offers 4^n combinations, with signals s having $(2n+1)$ possible values from $-n$ to $+n$. Probabilities $p_{n,s}$ of such values each have the denominator 4^n and a numerator, for $-n \leqq s \leqq +n$,

$$\binom{2n}{s+n} = \frac{(2n)!}{(n+s)!(n-s)!} \tag{7}$$

except the first and last which are 1, as for $n=4$:— 1; 8; 28; 56; 70; 56; 28; 8; 1 with their sum equal to the denominator 256. Of any single value of s that of $s=0$ is the most likely; but it is only 0.27 for $n=4$ and less for larger n. The chance that any other particular value occurs is smaller but their collective chance $s \neq 0$ predominates. Probable total signal per half-cycle of f is

$$S_n = k \sum |s| p_{n,s}. \tag{8}$$

The factor k depends on how the indicator responds to random reversals in signal phase. Values of S computed for $k=1$ are plotted as dots in Fig. 4 for n from 1 to 10. For $n>5$ they are close to a curve that rises proportional with $\sqrt{n}$.

The noise N which the signal S has to overcome is mainly that due to fluctuations in the photoelectric emission, rising with the square root of the dc photo-current. Thus both the signal S and the noise N are found to be proportional to the root of the number n of simultaneously seen elements. It follows that the field of view may be chosen, perhaps reshaped,[4] as convenient for other reasons. This conclusion agrees with exploratory observations on models with n up to a few hundred; no significant change in signal-to-noise ratio was noted when n was varied.

The loss in total signal output due to mutual cancellation of elemental signals is severe (though it could be prevented in modified photo cathodes). The signal modulation seldom exceeds one per cent of the photo-current.

For given object and lens aperture, the signal is a fixed proportion of the photo current, thus proportional to both illumination and photo cathode efficiency. But the noise rises only with the root of the photo-current. Hence the signal-to-noise ratio improves with the root of both illumination and photo-cathode efficiency. The lowest usable signal sets the lower limit of required illumination; and the stronger the illumination, the less detail, or contrast, is needed.

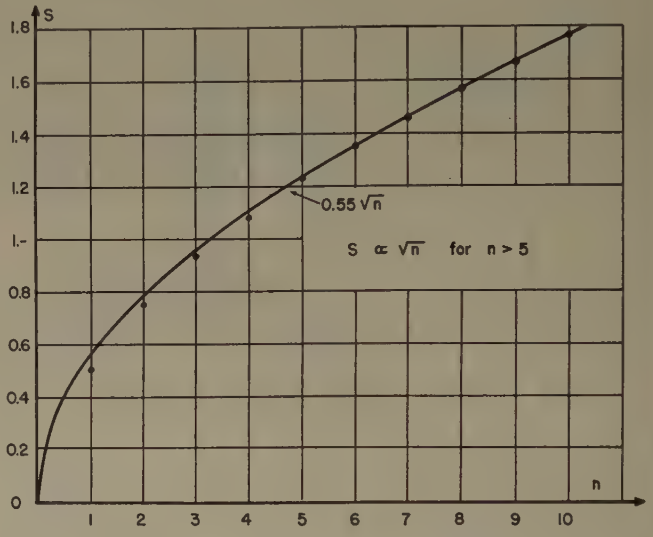

Fig. 4—Probable signal output vs number of simultaneously ranged elements.

The assumption here made that image details are purely random is, for many applications, pessimistic; outlines of objects and surface patterns are conspicuous by their strong signals.

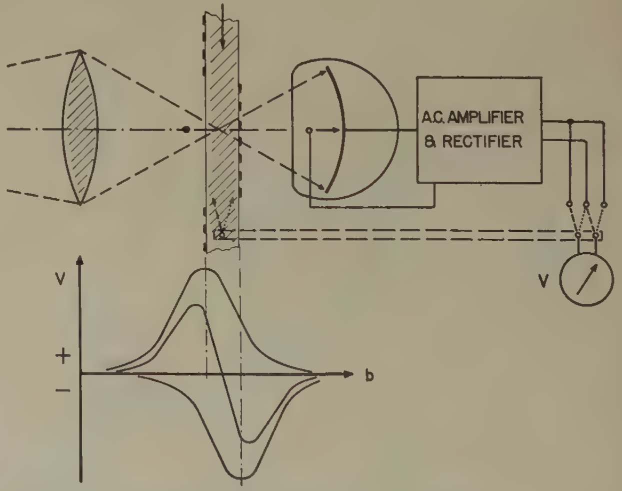

Fig. 5—Differential ranging circuit and signal.

A RANGE-FOLLOWING AND AN ABSOLUTE RANGING DEVICE

The arrangement of Fig. 3 permits an observer, perhaps remote, to search for an image plane; the differential arrangement of Fig. 5 permits a device to identify a sharp image and, via a servo system, to follow it. The modified interceptor carries groups of bars and slots alternatingly at the front and at the rear of a transparent vane; and a switch ganged with the groups reverses meter deflection. The two groups yield two signal peaks, opposite and spaced by the thickness of the vane. The differential response of an inert meter, plotted between them, changes sign when the image plane is centered, and over the range between the peaks is proportional to range displacement. Signals from a model with a lens of 5-cm focal length and 2.8-cm diameter, and an interceptor vane 0.1-cm thick, were observed on an oscilloscope. The relative strength of the two groups changed conspicuously when an object at a distance of 3 feet was moved by a fraction of an inch.

---

[4] G. W. Walton, "The stixograph," *Television*, London, Eng., vol. VII, pp. 93–96 (see Fig. 8, p. 134); March, 1934.

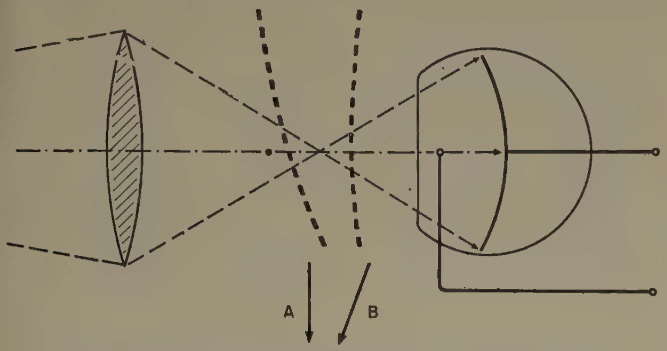

Fig. 6—Exploration of image space by (a) slanted interceptor surface, or (b) slanted motion.

Another device can find all objects within a prescribed object space by periodically exploring the image space in depth. As shown in Fig. 6 the interceptor is tilted relative to the direction of its motion indicated by the arrow. Of the two alternatives shown that at (A) permits the spindle of a rotary interceptor to be parallel to the optical axis; that at (B) is slightly more accurate since there the interceptor plane remains substantially parallel to the image planes. In either case the scans start near the photocell, where the images of the nearest objects would be located and progress towards the focal plane where the most distant objects are imaged. A suitable rotary vane, its rim twisted to a one-turn helix, is sketched in Fig. 7(a). Its radial bars and slots would detect vertical edges but yield no signals from horizontal bars. The modified interceptor Fig. 7(b) overcomes this limitation. It explores space with bars alternatingly tilted foward and back 45 degrees, the former signaling vertical, the latter, horizontal image details.

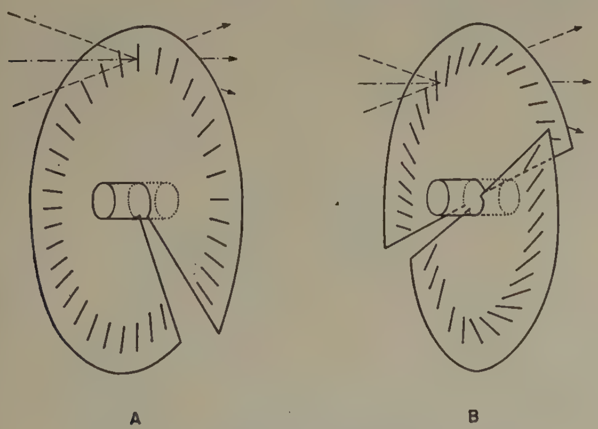

Fig. 7—Interceptor with (a) radial bars, and (b) alternatingly slanting bars.

The block diagram Fig. 8 outlines a device that explores space in depth and indicates on a calibrated meter the range of the nearest object seen. The first peak of the signal envelope permitted by the range gate (that may perhaps exclude the signal from a fence in the foreground) fires a gas triode that is quenched after each range scan.

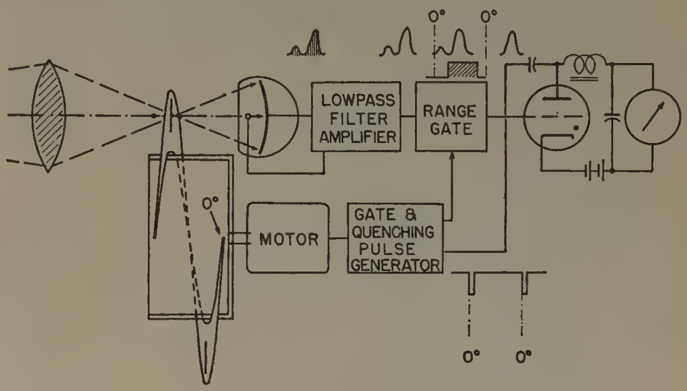

Fig. 8—Absolute ranging circuit.

A Guidance Device for the Blind

Since a single multi-purpose substitute for the human eye is beyond present reach, one may endeavor to aid the blind with a number of specific sensory devices. Among these, a device for orientation in space and for location of obstacles seems both the most needed and feasible. The device here described is intended for such use.

Any sensory device, however integrated, essentially comprises two parts, one to recognize, the other to indicate, information. In any blind-aid device the latter part is subject to a fundamental and quite severe limitation. Of all the human senses, the eye can provide by far the most information. Use of any or all of the other senses as substitute channels thus yields much less information even if all the information ordinarily provided by them could be dispensed with. Next to the eye, the ear offers the widest channel; and since the ear requires very little signal energy, most blind-aid devices proposed to date aim at audible indication, even though a blind person already strains his ear for audible clues and thus must fear additional audible signals. The next likely indicating method would be a two-dimensional display either as relief or as a pattern of electrical stimuli to be explored by fingertip. Compared with audible signals, such a display yields a more direct image, but it needs an "intelligent," thus more elaborate device, and more power.

Requirements

While methods of display depend on opinion and the state of the art, there seems to prevail agreement on the following considerations upon which the design of the device was based:

1. The range should extend from arms' reach (approximately 20 inches) to at least as far as a man walks in a second (approximately 5 feet); this range will barely give him time to avoid obstacles, particularly moving ones, and warning up to 10 or 20 feet is desirable.
2. Signals should not be more than a fraction of a second delayed so as to seem instantaneous.
3. The device should indicate range, the more accurately the closer the obstacle; in particular, it must warn of such small changes in surface distances as are signs of shallow steps, a curb, or even a rock on the road.
4. Angular accuracy need not be very good in the vertical plane; but it should yield lateral outlines to within less than a foot at five feet, i.e. better than 10 degrees azimuth.
5. Signals should not be ambiguous. Thus the device should not mistake intensity changes in the signals received for outlines of objects. For instance an optical device must not warn of a shadow on level ground.
6. The device should operate in any likely location, preferably without, or very few, adjustments.
7. The device should be inconspicuous, easy to carry, and have a minimum of tangling interconnections. Handheld units should weigh less than one pound and preferably permit ambidextrous use.
8. The device should not be too expensive to make and to maintain.

It was noted that earlier devices[5] utilize reflections of energy they themselves radiate and that for adequate range of radiation they require a large battery. If however ambient light is used as the source of signal energy, very high sensitivity can be achieved in spite of small power consumption.

BASIC DESIGN OF THE GUIDANCE DEVICE

The device employs optical recognition and yields audible signals. It can supply as much information as a blind person can receive, and it is sensitive enough for use anywhere. But to keep it small and handy, it is relieved of all work that the user can do himself. Thus it is essentially used as a probe to be pointed by hand at the space to be explored. The user does what lateral scanning is needed,[6] just as a sighted person would use a flashlight in a dark room. Besides being heavier, an automatic scanning-device with its rigid scanning pattern keeps the user waiting for the wanted information. Further, the present device does not interpret information, leaving that to the mind of the user. The language it speaks is to be learned like any other.

A modified interceptor integrates the recognition and the indicating function. As illustrated in Fig. 9, a motor-driven tilted interceptor vane moves at constant speed across the imaging light rays. Its bars and slots are wide in that part that crosses the optical axis near the exit focus, and they are the narrower the farther from the focal plane they cross the light rays. The resulting signal frequency f, the higher the closer the object of which it warns, is amplified and heard as a whistling sound in an earphone. To range distant objects more accurately than the coarse bars permit, it would be better to use fine bars throughout, moving the interceptor slowly when it operates near the focus, and increasing its speed steadily to the end of its scan; but such motion is not easily achieved.

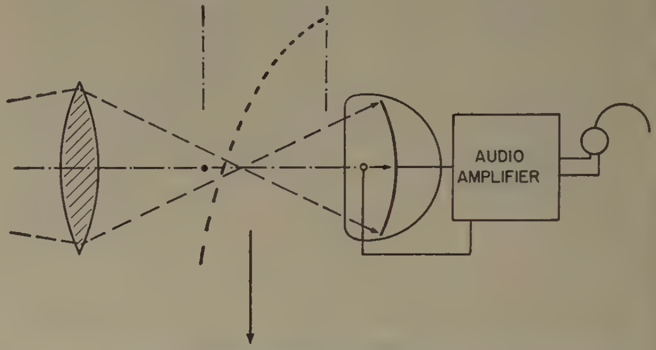

Fig. 9—Ranging with interceptor correlating signal frequency with object distance.

The device scans 2.5 (up to 10) times per second, indicating 8 (at least 4) ranges. Such (but hardly more) information can be provided by brief whistles in the frequency range from 600 to 2,000 cps, excluding lower frequencies as not very distinct and higher ones as unsuitable for older people.

Under dim light, signal currents at the photo cathode are of the order of 10^{-13} amp. An electron multiplier provides the very high gain needed yet consumes very little power. The high voltage is supplied, with automatic gain control, via an efficient 20-fold voltage multiplier from a 1.5v battery.

OPTICAL PARAMETERS AND INTERCEPTOR DIMENSIONS

The optics chosen for the model is a good projection lens system F:1.8, with 5-cm focal length. It images a point source in a spot of about 0.025 mm diameter; and that then should be the optimum width of a bar or slot. However, interceptors built to such dimensions yield very little signal, probably because one cannot hold them steadily enough. It has been found preferable to rely on much coarser details with the width of bars or slots from 1/500 to 1/200 of the focal length, here 0.1 to 0.3 mm. A modest, perhaps plastic, lens system is then adequate, perhaps oblong with F:1.4 across the direction of the slots.

Once the language of the device is mastered, fast scanning, perhaps 10 times per second, will be wanted. But a slow interceptor was built first, with 2.5 scans per second. Its circular track is 150 mm long, moving 375 mm per second; it is 3 mm wide, for an azimuthal angle of about 4 degrees, i.e. about 3 inches at 4 feet. The nearest object range begins at 20 inches, each of the other seven in steps of 33 per cent farther.

---

[5] For instance, L. Cranberg, "Sensory aid for the blind," *Electronics*, vol. 19, no. 3, pp. 116–119; March, 1946.

[6] See also Appendix II.

TABLE I

DIMENSIONS OF INTERCEPTOR, IN MM

1	2	3	4	5	6
Range	a	$b-b_\infty$	f cps	w	c/sector
Start		0			
1	4,500	0.56	625	0.30	31
2	3,400	0.75	730	0.257	37
3	2,530	1.01	855	0.219	43
4	1,900	1.31	1,000	0.187	50
5	1,430	1.81	1,170	0.16	58
6	1,070	2.45	1,370	0.137	68
7	800	3.33	1,600	0.117	80
8	600	4.55	1,875	0.10	94
End	500	5.55			

Table I gives its dimensions in mm; column 2, the object distance a; column 3, the distance $b-b_\infty$ of the track helix from the focal plane; column 4, the signal frequency f corresponding to bar width w, column 5; and column 6 gives the number of cycles if the whistle were to last the whole sector. Increments of 17 per cent in pitch between sectors can just be recognized by the average user; thus eight ranges come close to representing continuous space by a continuum of pitch. The possible ranging error α due to the coarseness of the bars can be computed from

$$\pm \alpha = \frac{awb_\infty}{D(b-b_\infty) \mp wb}. \tag{9}$$

Thus at 3 feet 5 inches in range 6 the tolerance is

$$a \pm \alpha = 1{,}070^{+120}_{-97} \text{ mm},$$

or about ±4 inches.

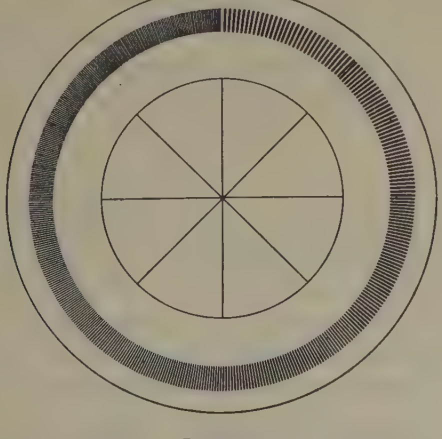

Fig. 10—Interceptor pattern.

The interceptor helix is made by photographing a large scale drawing on stiff film, all black except the "slots"; Fig. 10 is its negative, to scale. Replacing the square-wave track by a sinusoidal or other sound track changes the harmonics of the whistle signals, and can provide additional information such as azimuth.[7]

PHOTO MULTIPLIER AND VOLTAGE MULTIPLIER

Photomultiplier tubes used are of the types 1P21 or 931-A, with 70 to 120 volt acceleration to each of the 9 dynodes for over-all gains of 20,000 to 600,000. Resistive voltage dividers that can hold all dynode voltages equal in spite of varying load currents waste much power. The voltage-multiplier rectifier, used here instead, makes a particularly efficient mate to an electron multiplier. Current from a 1.5-volt cell is chopped and fed to a one-ounce step-up transformer that yields a square wave of about 80 volts p-p, with a spike of as much as 80 volts more after each current break. The shape of the spike can be controlled by shunt capacities.

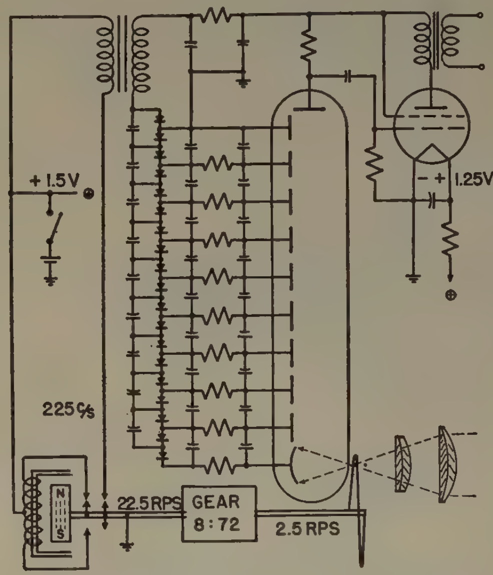

Fig. 11—Circuit of blind-aid device.

Since it is also very sensitive to resistive loading the circuit presents a rather high source impedance to a rectifier; the impedance drops appreciably with increasing load as the remainder of the spike grows blunter.

Ten equal dynode voltages are available from a chain of ten voltage-doubler rectifiers using 20 rectifiers and 20 condensers. Since the main load is drawn by the anode and dynode D_9 the chain is fed from the positive end. The other loads, most of them just the rectifier leakage, are so small that there need be little drop in dynode voltage along the chain. With 100 volts and a gain of 4 per dynode, and with 150 μa anode current, the total consumption is only 20 mw and nearly one-half of this is saved again (and some components) by feeding the anode with only about 30 volts from a half-wave rectifier, without loss in performance. The resulting circuit, with a third chain of condensers added for smoothing, will be found in the circuit diagram Fig. 11. All condensers in the chain are 0.1 μF, the tapped selenium rectifier stack has 19×6 tablets selected for small leakage current. A complete assembly of rectifiers, resistors, and condensers weighs $3\frac{1}{2}$ ounces and fits into $1\frac{1}{4} \times 1\frac{1}{8} \times 3\frac{3}{4}$ inches. The 30 condensers require $2\frac{1}{4}$ cubic inches; yet 3 condensers of each 1 μF take less than one cubic inch and weigh one-third as much. The difference is made up by the individual covers and terminations; it could largely be saved by integrating each chain in one unit with 11 leads. Two approaches are sketched in Fig. 12. In 12(a) two metalized foils are wound together, with 5 breaks in one and 4 in the other alternating, so that each half of a coating faces one half of the next. Another construction, 12(b), has no breaks, but requires simultaneous winding of 11 or more foils; C_{11} the capacity between the first and the last coating does no harm to the system.

---

[7] See Appendix II.

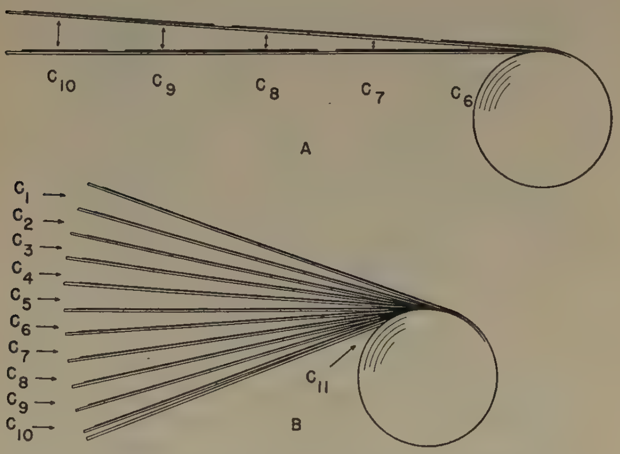

Fig. 12—Chains of ten condensers wound (a) of two interrupted foils, and (b) of eleven foils.

Of mechanical current choppers, vibrators can be shaved to operate near 200 cps on 15 ma at 1.5 volts. But then gravity affects the reed sufficiently to make the unit sensitive to tilting. Since the device already has a motor, to turn the interceptor, a ten-sector solid coin-silver chopping wheel is mounted on its 22.5 rps spindle. The filtering network is proportioned to keep the chopping frequency of 225 cps and its harmonics inaudible, yet to permit use of the device within the first second after switching on. The over-all dc-to-dc efficiency of the multiplier supply, using either a vibrator or a motor, exceeds 30 per cent.

AUTOMATIC GAIN CONTROL AND AUDIO OUTPUT STAGE

Since the device is to operate over a large range of ambient illumination its gain needs adjustment over a range of, perhaps, 40 db; yet no manual control should be needed and none is provided. Its place is taken by an automatic gain control based on an approximately logarithmic relation of output current vs light intensity.

For any given object, the response of the device consists of a modulation σ of the photo current, say 1 per cent for strong details but independent of ambient illumination I. If the over-all characteristic were linear, i.e. of "gain" k then the signal output S would be

$$S_1 = k_1[I(1 + \sigma) - I] = k_1 \sigma I, \qquad (10)$$

i.e. proportional to the illumination I. If, however, the output of the device is made to rise with the logarithm of the light received then its output will be

$$S_2 = k_2[\log I(1 + \sigma) - \log I] = k_2 \log (1 + \sigma). \qquad (11)$$

Further, for $\sigma \ll 1$, very closely $S_2 \approx k_2'\sigma$; it follows that the signal output will be, very nearly linearly, proportional to the depth of modulation and independent of ambient illumination.

The required logarithmic gain characteristic can be approximated over a wide range with the help of high source impedances for the dynode supply voltages. Rise in load current, particularly in later stages, then causes all voltages to drop. To the user, increase in ambient light is conspicuous by the receding background hiss, with signals seemingly unchanged.

Due to the very low depth of modulation, much power would be wasted on standing current if electron multiplication were continued up to adequate signal output level. A modification of the electron multiplier permits elimination of most of the standing current.[8] The model of Figs. 11 and 14 had an hearing-aid tube audio amplifier using substantial power and picking up motor interference as filament modulation. Both these schemes are superseded, since this paper was first submitted, by a stabilized[9] two-stage transistor amplifier that takes 0.2 ma from the +30-volt point, has a gain of 36 db and delivers about 1 mw.

The audio signals are heard, without obstruction to other sounds, from a plugless hearing-aid earphone that hangs on a wire hook over the ear lobe. Pushing the phone from or nearer the ear permits volume adjustment up to painfully loud. Cable and headphone can be replaced by a soft plastic tube from a built-in phone to the ear. But the attenuation was found to be 6 db per foot and much noise is heard when clothes and tubing rub.

THE MOTOR

The interceptor helix is mounted directly upon a cogwheel turning 2.5 times per second, driven by a pinion on the motor spindle. The motor was re-designed[10] to run with 22.5 rps on 13–16 ma at 1.5 volts. It occupies less than 2 cubic inches and weighs $2\frac{1}{2}$ ounces. Its operation will be understood with the help of Fig. 13. The spindle carries as rotor a transversally magnetized

---

[8] H. E. Kallmann, "Remodulation in electron multiplier cascades," PROC. I.R.E., vol. 41, no. 2, pp. 282–283; February, 1953.

[9] R. F. Shea, "Transistor power amplifiers," *Electronics*, vol. 25, no. 9, pp. 106–108; September, 1952.

[10] Parts kindly supplied by H. D. Brailsford & Co., Rye, N. Y.

Alnico disc, and one contact nose. The laminated stator is magnetized with alternating polarity by the two halves of a centertapped winding. Each of these is switched on, via an insulated contact spring, by the contact nose with such phase as to turn the rotor clockwise. Due to the tapered gaps between stator poles and the rotor, the poles of the latter always seek the narrowest gap, the position needed for instant starting. The motor speed rises with voltage from at least 1.1 volts; mechanical load has little effect on it but raises the current. In the model, the most severe load is that due to contact friction on the chopper wheel that is mounted on the spindle.

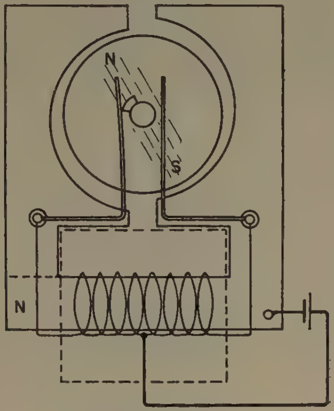

Fig. 13—Motor circuit.

The device draws about 50 ma, for over 100 hours service, from a standard flashlight cell of 1 5/16 inches diameter and $2\frac{1}{4}$ inches length, larger than needed. It is tempting to eliminate the battery and to replace the motor by a hand-powered ac generator. Hand-powered flashlights generate about 300 mw, ample energy; but besides being tiresome, such devices cannot, by far, be pointed steadily enough while being pumped.

A Model

Only a very handy device will find acceptance. The model of 1949 resembles a small box camera of $3 \times 4 \times 5$ inches, and weighs two pounds. A tight strap over the back of the hand assures consistent pointing and relieves the fingers of all work except switching. Fig. 14 shows the inside, with all parts mounted either on the front or on a spine extending from it to the rear.

Less than $\frac{1}{2}$ foot-candle illumination may be sufficient for signals from not too dark objects. In the dark, the aligned beam of a 3-volt flashlight permits ranging with the device (and uses ten times the power).

More recent and smaller components[11] would render the device even more compact, with dimensions $1\frac{1}{2} \times 2\frac{1}{2} \times 4$ inches, and about 12 ounces weight.

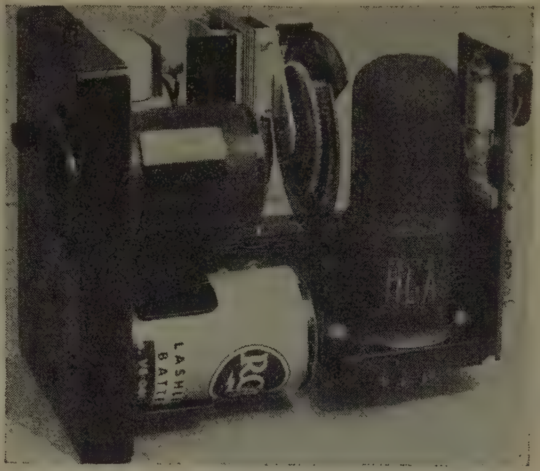

Fig. 14—Guidance device, interior.

Appendix I

False Signals from Regular Patterns—The Modulated Carrier and the Beat Frequency System

The user's confidence in the device is indispensable; thus possible sources of false signals require attention. One such source is a regular object pattern, for instance, evenly spaced black stripes as assumed in Fig. 15. Due to the finite lens diameter, the image has depth, shown as shaded regions (ignoring the penumbra around them). Whenever the spacing of such regions is equal to that of the bars (or a fraction or a multiple) there will be strong signals of a frequency other than indicates object distance correctly. While rare, they have been observed under contrived conditions. To avoid them, several refinements were worked out, should the need prove real.

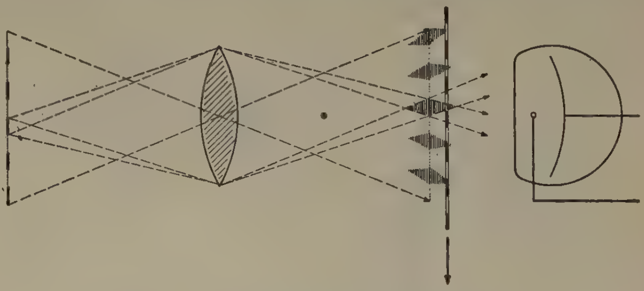

Fig. 15—Image of regular patterns as source of false signals.

One approach is the analog to a modulated-carrier transmission. Bars and slots are dimensioned for a constant carrier frequency above the audible range, and object distance is indicated by varying the transmission of the slots with an audio frequency, a different one for each sector of the interceptor. The ideally required light transmission is plotted in Fig. 16(a) for a carrier frequency of 10,000 cps and for each one audio cycle of 1666; 1250; and 1000 cps. Fig. 16(b) shows the adequate approximation when the interceptor is a photograph of a black and white drawing. Demodulation of the carrier requires a circuit modification as in Fig. 17. The loss in power much exceeds the expected factor 4 since, at such low signal levels, the rectifier efficiency is poor.

---

[11] Such as the DuMont photomultipliers types K 1193 and K 1211, with $\frac{3}{4}$ inch diameter and $2\frac{3}{4}$ inches long.

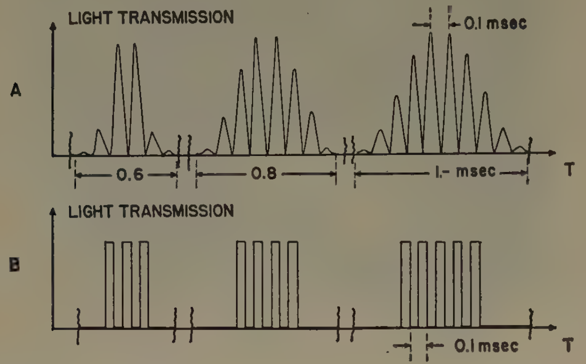

Fig. 16—Interceptor design for modulated-carrier system, (a) ideal, and (b) simplified.

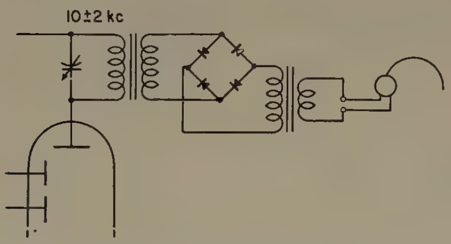

Fig. 17—Demodulator circuit for modulated-carrier system.

Another variant is nearly immune from false signals since there the range in bar spacings is relatively small. Thus the light modulation may range from 6000 to 7400 cps and then "beat" with a fixed beat frequency of 8000 cps to produce audio signals of 600 to 2000 cps.

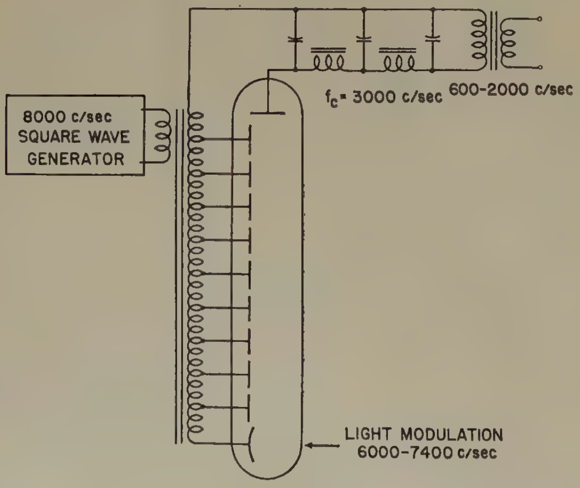
8000 c/sec SQUARE WAVE GENERATOR
f$_c$ = 3000 c/sec
600-2000 c/sec
LIGHT MODULATION 6000-7400 c/sec

Fig. 18—Electron multiplier circuit for beat-frequency system.

The circuit becomes very simple, Fig. 18, if the beat frequency is applied as square wave to all dynodes. A suitably sectionalized transformer for step-up to 1400 volts occupies less than 1 cubic inch and replaces the whole dc supply. The multiplier itself acts as the rectifier so that only a low-pass filter is needed at the output. To avoid noise modulation, the generator waveform must be very clean.

Appendix II

Wide-Angle Ranging

The present models look only in one direction at a time and require manual scanning. Scanning speed is limited by the rate the device can convey information with its limited vocabulary. With a larger vocabulary it may say more without talking faster. One may then let the device see and report a large azimuthal angle and save the manual scanning. Only moderate modifications of the basic scheme seem to be necessary, mainly of the lens system and of the sound track. Let the lens coverage be increased to at least 30 degrees as in Fig. 19. This top view assumes the interceptor to move into the plane of the paper, with three tracks side-by-side. The central track ranges forward objects as before. The one to the right ranges objects *L* around 10 degrees to the left, and the left track similarly objects *R* to the right, all simultaneously with identical spacing of "bars" and "slots." The additional information that tells from which of the tracks a signal came, may be conveyed by different harmonic content. By producing each track as a sound recording, the signals may have the same pitch yet differ from left to right, as a flute from woodwind from brass, or as a sung vowel, from *oh* to *ah* to *ee*. Indeed all sound tracks may be melted into one wide track whose harmonic content is varied gradually from one edge to the other. Except for higher audio fidelity, the remainder of the device remains unchanged.

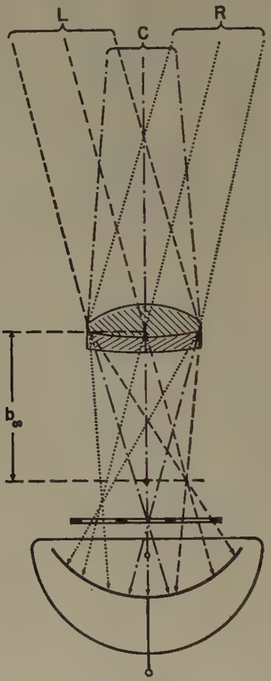

Fig. 19—Simultaneous ranging in several directions.

Correspondence

Comment on "A Simple Graphical Analysis of a Two-Port Waveguide Junction"* by J. E. Storer, L. S. Sheingold, and S. Stein[1]

In the above paper under consideration, the authors present a graphical analysis for the determination of the scattering coefficients of a two-port waveguide junction, based directly on the previous work of Deschamps (published elsewhere simultaneously).[2] In their discussion of the Deschamps procedure these authors make certain statements with regard to another method, which was developed by the present writers and was first presented at the I.R.E. National Convention in 1951.[3] A paper describing the method has recently been published in the PROCEEDINGS OF THE I.R.E.[4] We believe that a clarification of the remarks of Storer, Sheingold, and Stein concerning our method is in order.

The designation by them of our method as the "Weissfloch-tangent technique" is itself misleading. The true "Weissfloch-tangent technique" should refer to a procedure useful for *lossless* structures only; it is based on a tangent relation of Weissfloch's.[5] Our method is based on an entirely different suggestion of Weissfloch,[6] that of a network with separated lossy and lossless parts. While it is true that the lossless part of the network can be analyzed by means of the tangent procedure, this approach is not at all necessary nor even desirable in most cases. In the procedure that we recommend,[4] the tangent method is not employed, and, furthermore, the lossless part is not treated independently.

Storer, Sheingold, and Stein state that our method involves considerably more labor and requires more measurements than the Deschamps method. Presumably, their comments are based on the substance of the above-mentioned I.R.E. talk.[3] In that paper, stress was laid on a *precision method* for obtaining the equivalent circuit parameters of a lossy two-port microwave junction, by means of which the data curves are compared with known theoretical curves and the difference is minimized systematically by either analytical or graphical means. The network parameters so obtained are accurate to within definite tolerances, which depend on the randomness of the experimental data and on the limits of accuracy of the input-output measurements. We readily agree that the precision analysis involves considerable labor. However, it accomplishes much more than the graphical Deschamps method in that it leads to optimally precise parameter values. It is also our opinion that a comparable analytical analysis for the Deschamps method, if worked out (this has not been done, to our knowledge), would be at least as cumbersome as our own.

For ordinary engineering purposes, precision values for the parameters of a waveguide junction are not required. In such cases, semi-precision procedures employing data curves which are averaged by simple, nonanalytical means, are adequate. The Deschamps procedure falls in this category and provides a simple, convenient method of obtaining the scattering matrix elements of a four-terminal structure. However, we have also developed a semi-precision method which is quick and simple.[4] It yields an equivalent circuit simple in form and containing the minimum number (four) of elements between uniquely and easily determined reference planes (see Fig. 1); like the Deschamps analysis, our method applies quite naturally to asymmetrical structures.

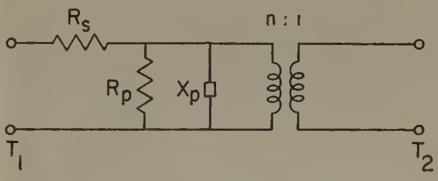

Fig. 1—Equivalent network.

The data curves required are (1) the input reflection coefficient locus; (2) the D vs S curve, which is a plot of the locations D of the voltage minima in the input guide versus the locations S of the sliding short-circuit in the output guide. In order to draw a good D vs S curve, eight or ten data points should be taken. This is no hardship, since additional input-output measurements are performed very rapidly. In addition, taking more data points improves the accuracy of the final network; this consideration applies to the Deschamps procedure as well, as is recognized by Storer, *et al.* It might be mentioned that in our method the short-circuit locations are not required to be spaced in pairs separated by a quarter wavelength, as in the Deschamps procedure. This may be of significance if a variable short-circuit is not available.

We have had both our method and that of Deschamps tried on several runs of data. It is our experience that both of these procedures take about the same length of time for a lossy, asymmetrical structure. The recommendation as to which procedure should be used therefore depends on the form in which the results are desired. If one prefers a scattering representation for the structure, the Deschamps procedure is indicated. In particular, if one requires the knowledge of only the power reflection and transmission coefficients, the Deschamps scheme is clearly the most direct. However, if a circuit picture is desired (and such a picture is frequently useful for engineering purposes), the use of the Deschamps procedure requires an additional calculational step transforming the scattering matrix elements into impedance matrix elements. In addition, unless special reference planes are sought out, the network will contain six, instead of four, parameters. The advantage of our method in this connection is that it yields directly a network in a convenient and simple form. In particular, for structures which are known to have a purely series or shunt representation at some terminal planes, such as thin transverse resistive films or thick symmetrical radiating slots, our method is especially simple. We therefore feel that its use is recommended whenever a network picture is desired as the form of the result.

L. B. FELSEN and A. A. OLINER
Microwave Research Inst.
Polytechnic Inst. of Brooklyn
Brooklyn 1, N. Y.

Rebuttal[7]

There is no basic disagreement with the remarks of Drs. Felsen and Oliner, as far as they go. Namely, we accept the fact that their method leads more naturally to an equivalent network representation for a two-port junction, whereas the Deschamps method leads most naturally to the scattering-matrix representation from which a long computation is necessary in order to go to the equivalent network. However, the basic question here is really whether the scattering matrix is not the more *natural* description of a junction, particularly since in waveguides, for example, it relates directly to the simple traveling-wave conception of the phenomena. Certainly the power of the scattering-matrix method goes beyond simply giving directly the transmission and reflection coefficients for the case when the junction is matched on its output side. Stopping at this ignores one of the most important reasons for analyzing junctions, namely, that it is so frequently necessary in microwave impedance measurements to use connectors between standard slotted-line measuring equipment, and the impedances which it is desired to measure. The graphical constructions which lead to the scattering-coefficients for the junction give also the crucial points which can be used in connection with such a measurement to give the corrected impedance by a simple construction. In fact, a connector could be "calibrated" in the sense that these critical points can be transferred from Smith Chart to Smith Chart with ease. In contrast, if only the equivalent network of the junction is known, a long computation is required each time in order to obtain the corrected impedance from the measured value.

We also question whether their semi-precision method can be accomplished as easily as they indicate. For example, although eight data points are more than adequate in

---

* Received by the IRE, January 29, 1954.

[1] PROC. I.R.E., vol. 41, pp. 1004–1013; Aug., 1953.

[2] G. A. Deschamps, "Determination of reflection coefficients and insertion loss of a waveguide junction," *Jour. Appl. Phys.*, vol. 24, p. 1046; 1953.

[3] A. A. Oliner and H. Kurss, "The precision measurement of the equivalent circuit parameters of disdipative microwave structures," paper no. 78, I.R.E. National Convention, New York, N. Y.; March, 1951. The name of L. B. Felsen was omitted inadvertently from this paper.

[4] L. B. Felsen and A. A. Oliner, "Determination of equivalent circuit parameters for dissipative microwave structures," PROC. I.R.E., vol. 42, pp. 477–483; February, 1954.

[5] A. Weissfloch, *Hochfreq. und Elektroak.*, vol. 60; 1942.

[6] A. Weissfloch, *Elek. Nach. Tech.*, vol. 19; 1942.

[7] Received by the IRE, February 18, 1954.

the graphical technique, they would seem barely enough for any accuracy in drawing the D vs S curve, as shown in Fig. 8(a) of their recent article.[4] A statement was also made regarding the precision capabilities of the Deschamps technique. The chief source of error here arises, as in their method, from the location and radius of the data circle. The techniques they suggest elsewhere for improving the data circle[3] (with known estimation of accuracy) can just as easily be applied to the Deschamps method. As a matter of preference, however, for true precision we would prefer to use standard numerical least-mean-square curve-fitting to determine the circle. In the long run it would appear to be simpler and quicker than the procedure they discuss, which seems to involve fitting a sine curve to a scatter of data.

It may be unfair to refer also to material not available to Drs. Felsen and Oliner at the time they wrote their letter, but the graphical approach seems to have potentialities over and beyond that of any methods which rely on equivalent networks. One example which may be of more than academic interest is that the data taken with an arbitrary movable impedance (instead of with the usual movable short circuit) terminating a junction can be easily corrected if only *one* measurement can be made with a true short circuit at some fixed point in the output circuit (as for example, by removing the waveguide section containing the movable impedance, and clamping a silvered plate across the opening). This could eliminate many worries about how good a short-circuit the movable pistons provide.

Also a recent letter[8] outlined a rather direct extension of the graphical method to multiport junctions, whereas it is difficult to visualize any correspondingly simple extension for an equivalent network interpretation of the data.

S. Stein, L. S. Sheingold, and J. E. Storer
Boston Engineering Lab.
per S. Stein
Sylvania Electric Products, Inc.
70 Forsyth St.
Boston, Mass.

Further Comment[9]

Our original note (above) on this paper by J. E. Storer, L. S. Sheingold, and S. Stein, had a twofold purpose: first, to clarify a remark made in the paper under discussion, and second, to present a brief but careful comparison between our semi-precision method and that of Deschamps, without elaborating on the applications of either method. We repeat our basic conclusion that both methods take about the same length of time, so that the choice between the two methods should depend upon the form in which the results are desired. We did not intend then, and do not consider it appropriate now, to delve into the dubious question of which description (scattering or equivalent circuit) of a junction is the "more natural." We suggest that the criterion for the choice of a particular representation is its utility rather than its "naturalness," where the utility depends on the application. Contrary to Mr. Stein's one-sided position, examples can be cited to support the view that an equivalent circuit approach is frequently simpler and more useful (both conceptually and for calculational purposes) for the representation of waveguide discontinuities.

We agree that the scattering formalism is of great value in many applications, but in recommending the graphical method Mr. Stein overstates his position even in his own choice of examples. Mentioned by him in some detail are the calibration of junction connectors between the slotted line and the terminating impedance, and the analysis of measurements taken with an arbitrary movable terminating impedance. While it is agreed that the Deschamps graphical procedure is well-suited to such situations, the implication that this method is *always* the simplest and most direct in these cases is not warranted. We would like to point out that we have considered and dealt with these same problems by other means. As regards the calibration of a connector or junction discontinuity between the slotted line and the terminating impedance, we have been using for this purpose for the past six years a correction scheme based on the Weissfloch tangent relation. The correction scheme applies only to lossless junctions in contrast to the above-mentioned graphical construction which is valid also for lossy junctions, but it is considerably simpler than the latter and is applicable to the majority of practical cases. Our correction procedure was issued in report form some time ago and has also recently appeared in print.[10] The example of the arbitrary movable impedance terminating a junction is also well-known to us and, in fact, forms one of a number of remarks to be made in a paper at the I.R.E. 1954 National Convention.[11] Here again we have developed simple schemes alternative, and in certain cases preferable, to Mr. Stein's graphical construction.

His extension of the Deschamps scheme to the measurement of multi-port junctions (now published[8]) also fails to justify his contentions concerning the scattering formalism. In the nature of a general remark, one recognizes that as the number of ports of a junction grows larger it becomes increasingly difficult to determine useful network pictures so that one resorts to the impedance (admittance) or scattering matrix directly; any procedure for the impedance matrix of a multi-port junction has a direct analog in terms of the scattering matrix. The well-known basic approach for the analysis of a multi-port junction proceeds in terms of successive two-ports; this analysis becomes particularly simple for both the impedance and scattering representations if the terminations on the remaining ports are chosen judiciously. Mr. Stein's specific approach, while systematic, is too restrictive in that it admits input measurements in only a single port and employs only reactive terminations. Therefore, as a result, his procedure is unnecessarily long and tedious.[12]

Concerning our measurement procedure, Mr. Stein remarks: "We also question whether their semi-precision method can be accomplished as easily as they indicate." The only reference given to support this position is the D vs S curve [Fig. 8(a)] presented in our recent paper,[4] with the remark that eight data points "seem barely enough for any accuracy" in drawing this curve. It appears clear, however, that the omission of every other data point will exercise a negligible effect on the drawing of this (smooth) curve. Even if Mr. Stein's criticism were correct, it would seem hardly sufficient to justify the above assertion concerning our entire method.

Mr. Stein's remarks on precision indicate an apparent misunderstanding. Our precision method yields *all* of the equivalent circuit parameters in a precision fashion, with estimates of error available for *each* of the parameters. Since the improvement of the data circle is only one portion of the procedure, its application to the Deschamps method, while quite valid and useful, would not at all yield a treatment of the Deschamps scheme comparable to our precision procedure for the equivalent network. While it is agreed that a standard numerical least square procedure for improving the data circle provides a criterion which, although somewhat arbitrary, will yield "true" precision, we fail to see how such a procedure can be "simpler and quicker" than our graphical scheme; in fact, the reverse is true.

L. B. FELSEN and A. A. OLINER

---

[8] S. Stein, "Graphical analysis of measurements on multiport waveguide junctions," PROC. I.R.E., vol. 42, p. 599; March, 1954

[9] Received by the IRE, March 17, 1954.

[10] A. A. Oliner, "The calibration of the slotted section for precision microwave measurements," *Rev. Sci. Instr.*, vol. 25, pp. 13–20; January, 1954.

[11] H. M. Altschuler and A. A. Oliner, "Microwave measurements with a lossy variable short circuit," paper no. 50.2, I.R.E. National Convention, New York, N. Y.; March, 1954.

[12] If input measurements are unavoidably restricted to only a single port but matched terminations are appropriately used, the number of measurements necessary in this modification of Mr. Stein's own procedure is somewhat smaller, while the number of graphical constructions is significantly reduced. This simplification is based on the recognition that, when input measurements are permitted in only one port, the measurement of an n-port can always be reduced to a succession of two- and three-port measurements by the use of appropriate terminations. Since the three-port measurements are required only to determine the mutual elements between inaccessible ports, a still shorter alternative procedure is possible under these restrictions for either the scattering or impedance matrix elements when, in addition, the only mutual element of interest in each three-port is found *via* two measurements and a single direct calculation. Such a procedure for the scattering matrix of a four-port requires only 18 measurements, with 3 Deschamps constructions and 3 direct calculations. However, the greatest simplifications occur when input measurements are performed in more than one port. For a four-port, for example, the ten independent impedance (admittance) parameters characterizing the junction can be determined from only ten input measurements (in three different ports) and computed in a *simple fashion*, if short and open circuit terminations are available for all ports. This is in contrast to the 64 measurements and an even greater number of graphical constructions required in Mr. Stein's approach. Similar simplifications apply to scattering parameters if matched terminations are employed; such a procedure requires 12 measurements with 2 Deschamps constructions and 4 extremely simple calculations. Note in the above that no simplifications follow from the use of the scattering formalism; the latter, however, permits graphical constructions which some may prefer to simple analytical calculations.

Comment on "Developments in Sintered Magnetic Materials"* by J. L. Salpeter[1]

In his instructive paper on sintered magnetic materials, Salpeter mentions the very few known ferromagnetic elements. Is not the none-too-plentiful gadolinium also ferromagnetic? At least, some of its oxides appear to be. This may not be a very practical point at the present time, but has the metal been purified yet and have its magnetic properties determined?

---

* Received by the IRE, May 5, 1954.

PROC. I.R.E., vol. 42, pp. 514–526; March, 1954.

T. Powell
Great Neck, L. I., N. Y.

Rebuttal[2]

It is true, gadolinium is the fourth ferromagnetic element. The metal has been purified, its magnetic properties determined, and its Curie point has been found to be 16 degrees C. At room temperature gadolinium is no longer ferromagnetic and this is one of the main reasons why no engineering applications have been found for the metal.

J. L. Salpeter
Philips Electrical Industries Pty., Ltd.
Sidney, South Australia

[2] Received by the IRE, May 24, 1954.

Comment on "Wien Bridge Oscillator Design"* by K. K. Clarke[1]

K. K. Clarke in his paper above analyzes the frequency errors in a Wien Bridge Oscillator by considering the full Wien bridge and the phase shift and gain of the associated amplifier, as shown in Fig. 1.

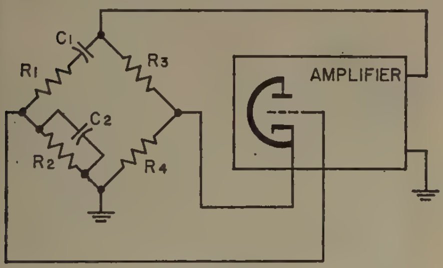

Fig. 1—Wien Bridge Oscillator, showing full Wien bridge.

There are two objections to this viewpoint. First, it attaches great importance to the ratio R_3/R_4, although this ratio is determined by operating level via a temperature sensitive element, and is in fact merely the means through which avc is obtained. It is entirely possible to dispense with R_3 and R_4 and use a conventional variable-bias avc system in the amplifier. Second, by considering R_3 and R_4 as part of the bridge, and not as simply a negative feedback loop attached to the amplifier, it overlooks the presence of reactive elements in this loop, especially of capacitance across R_4.

Fig. 2 shows the oscillator circuit when R_3 and R_4 are considered part of the amplifier, and includes several stray capacitances of importance. In the absence of C_3, C_4, C_5, and C, and letting $R_1=R_2$ and $C_1=C_2$, the rc arms of the Wien bridge have a gain of $\frac{1}{3}$ and a phase shift of zero from B to A, at $\omega=1/R_1C_1$. Therefore, to oscillate at ω, the amplifier must have a gain of 3 and zero phase shift. The first condition is met automatically by the avc system, while the second must be designed into the amplifier, using negative feedback or other wide-band techniques. When feedback is used, it is common to shunt R_4 (Fig. 1) by a capacitance to obtain high-frequency peaking, in order to extend the interval of negligible amplifier phase shift. If feedback is not used, the very low gain required (3) permits very low impedance loads, which, with inductive peaking, permit a comparable high-frequency performance. It is not my purpose, of course, to disparage the feedback arrangement, since it gives bandwidth, avc, and distortion reduction all at once (this last advantage is not obtained at all with other schemes), but only to point out the essentials of the circuit.

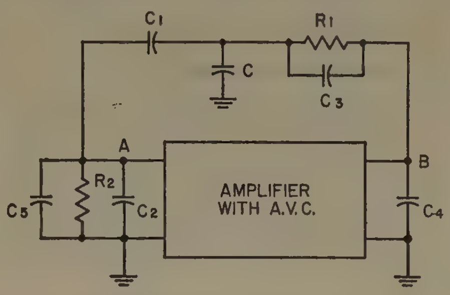

Fig. 2—Wien Bridge Oscillator, showing rc arms and stray capacitances.

It is of interest to consider the effect on frequency and output of the stray capacitances shown. C_5 can be added to C_2, giving $C_2'=C_2+C_5$. C_4 must be taken into account in designing the amplifier, but has no direct effect. (In this connection it should be remarked that the amplifier must have a low output impedance, since it must drive without phase shift a rather heavy reactive load, consisting of the Wien Bridge rc arms as seen from B, in parallel with C_4 and the negative feedback network, if any. A two-stage amplifier plus a direct-coupled cathode follower output stage, with over-all feedback, is very convenient, since it isolates the gain stages from the heavy, and variable, loading mentioned. In effect, the cathode follower adds a considerable degree of feedback to the circuit without complicating the stability problem, since its bandwidth extends from dc to far beyond the limits of the other stages. It also brings the second harmonic distortion of the output stage down to a point which allows cancellation of corresponding distortion in previous stages. This arrangement has been found useful in a number of amplifier applications.) C and C_3, however, have an important effect. It is desirable to calculate the tuning capacitors C_1 and C_2, assuming $R_1=R_2=R$, and assuming a constant Wien Bridge gain of $\frac{1}{3}$, permitting constant output independent of frequency. Let:

$$\omega=\frac{1}{RC\text{ eq.}}\ \text{(this defines } C\text{ eq.)} \tag{1}$$

$$x=\frac{C_2'}{C\text{ eq.}}=\frac{C_5}{C\text{ eq.}}+\frac{C_2}{C\text{ eq.}} \tag{2}$$

$$\alpha=\frac{C}{C\text{ eq.}} \tag{3}$$

$$\beta=\frac{C_3}{C\text{ eq.}}. \tag{4}$$

Then it can be shown that:

$$x^2+3\alpha x-1+(\alpha+\beta)(\alpha-2\beta)=0 \tag{5}$$

$$C_1=C_2'+C+C_3. \tag{6}$$

Knowing C and C_3, and C eq. as a function of ω (1), α and β can be found as functions of ω (3 and 4). Solving (5) for x and applying (2) and (6) yields C_1 and C_2 as functions of ω.

J. M. Diamond
United Transformer Co.
New York, N. Y.

* Received by the IRE, January 26, 1954.

[1] Proc. IRE, vol. 41, pp. 246–249; February, 1953.

Waveguides with Nonhomogenous Dielectric*

This correspondence is a résumé of some papers[1-6] published in Italy on waveguides with perfectly conducting walls and enclosing a nonhomogeneous dielectric.

Consider[1] a waveguide with rectangular cross section and let a and b denote the length of the two sides.

A cartesian system $0xyz$ is selected so that a lies on x, b lies on y, the cross sections of the waveguide lie in the first quadrant, and the z-axis is parallel to the axis of the guide and constitutes the inner left lower corner.

The waveguide is filled with a nonhomogeneous dielectric with a permittivity ϵ that is an (arbitrary) function of x only, and with a permeability μ that is constant. The latter assumption helps to simplify the mathematical treatment and is not a restriction in practical cases.

With these assumptions it is easy to prove that in the waveguide (and obviously in the z-direction) TE modes of propagation are possible so that the electromagnetic field in each cross section is a function of x only.

More precisely, writing E_x, E_y, E_z, H_x, H_y, H_z, for the x, y, z components of the electric field E and of the magnetic field H, and letting ω be the radiant frequency and β be the mode propagation constant (thus ω/V; with V=phase propagation velocity of the mode), then

$$E_x=E_y=H_y=0,$$

and H_y, H_z are easily shown to be functions of E_y. We may obtain E_y from the differential equation

$$\frac{d^2E_y}{dx^2}+(\epsilon\mu\omega^2-\beta^2)E_y=0 \tag{1}$$

---

* Received by the IRE, January 26, 1954. Revised, June 1, 1954.

[1] D. Graffi, "Sulla propagazione delle onde elettromagnetiche in un tubo conduttore riempito da un dielettrico eterogeneo," *Ann. di Mat.* (4), XXX, p. 233; 1949.

[2] I. Giovanardi, "Sulla propagazione delle onde elettromagnetiche in una guida riempita da dielettrico eterogeneo," *Ann. Univ. Ferrara*, Nuova serie, vol. I, p. 81; 1951.

[3] D. Graffi, "Sulla propagazione delle onde di tipo elettrico o magnetico in una guida a sezione circolare riempita con dielettrico eterogeneo," *Mem. Accademia delle Scienze di Bologna*, (10), VII, 1949–50.

[4] G. Goldoni, "Sulla propagazione delle onde elettromagnetiche di un cavo riempito con dielettrico eterogeneo," *Atti Sem. Mat. Fis. Univ. Modena*, 4, p. 105; 1949–50. "Nuove limitazioni per la frequenza delle onde elettromagnetiche in un cavo riempito da dielettrico eterogeneo," ibid. 4, p. 126; 1949–50.

[5] L. Caprioli, "Onde elettromagnetiche di tipo trasversale nelle guide d'onda rettilinee e con dielettrici eterogenei," *Atti IV Congresso Unione Matematica Italiana*, p. 478; 1951. "Onde elettromagnetiche trasversali dei tipi TE e TM nelle guide d'onda rettilinee con dielettrico eterogeneo," *Att. Acc. Scienze di Torino*, LXXXVI, p. 291; 1951–52.

[6] C. Agostinelli, "Sulla propagazione di onde elettromagnetiche guidate entro tubi cilindrici," *Rend. Sem. Mat. Univ. e Politecnico di Torino*, XI, p. 297; 1952.

with the following boundary conditions

$$E_y(0) = E_y(a) = 0.$$

From the basic theory of differential equation[7] it can be shown that an infinite number of values β_n^2 of β^2 exist for which (1) has solution not identically zero.

The β_n^2 can be placed in an orderly succession $\beta_1^2, \beta_2^2, \cdots, \beta_n^2, \cdots$, that decreases and tends to $-\infty$.

The following relations also hold:

$$\epsilon_1\mu\omega^2 - \frac{r^2\pi^2}{a^2} < \beta r^2 < \epsilon_2\mu\omega^2 - \frac{r^2\pi^2}{a^2} \qquad (2)$$

where ϵ_1 and ϵ_2 are the maximum and minimum values of ϵ.

From (2) it can be shown that $\omega > (n\pi/\sqrt{\epsilon_2\mu}a)$ is a necessary condition in order for n modes to propagate in the guide, that is, for $\beta_1^2, \beta_2^2, \cdots \beta_n^2$ to be positive. On the other hand, a sufficient condition for the propagation of n modes is $\omega > (n\pi\sqrt{\epsilon_1\mu}a)$; meaning that the cut-off frequency of the mode corresponding to β_n is between $n\pi/\sqrt{\epsilon_1\mu}a$ and $n\pi/\sqrt{\epsilon_2\mu}a$. From (2) one also obtains, if V_r is the phase velocity corresponding to $\beta_r (r \leqq n)$,

$$\frac{1}{\sqrt{\epsilon_2\mu - \frac{r^2\pi^2}{a^2\omega^2}}} \leqq V_r \leqq \frac{1}{\sqrt{\epsilon_1\mu - \frac{r^2\pi^2}{a^2\omega^2}}}, \qquad (3)$$

This means that the phase velocity of one of these TE modes lies between the values which the velocity would have if the guide were filled with homogeneous dielectrics whose dielectric constants were ϵ_1 and ϵ_2, respectively.[8]

In a previous paper[3] symmetrical modes TE and TM have been studied which exist in a circular waveguide with a dielectric whose permeability is constant and whose permitivity is a function of the distance from the axis only. The properties of these modes are similar to those discussed above for rectangular waveguides. A necessary and sufficient condition for the existence in the guide of n TM modes can be expressed by the relations

$$\omega > \frac{K_{0n}}{a\sqrt{\epsilon_2\mu}}, \qquad \omega > \frac{K_{0n}}{a\sqrt{\epsilon_1\mu}},$$

where a is the radius of the waveguide and K_{0n} is the n root of the Bessel function J_0. Similar conditions exist for TE modes provided that instead of K_{0n} one substitutes K_{1n}, the nth root, which is different from zero of the Bessel function J_1. Furthermore, the velocity of these TM and TE modes still satisfies the relation (3) above, provided that one substitutes r_π with K_{0r} or K_{1r}.

Other relations of the type just mentioned have been obtained by Goldoni[4] for a coaxial line filled with nonhomogeneous dielectric.

It has also been proved that if V_r and V_r' are the phase velocity and the group velocity of one of the TE and TM modes referred to, then the following relation holds

$$\frac{1}{\epsilon_2\mu} < V_r V_r' < \frac{1}{\epsilon_1\mu}.$$

It should finally be mentioned that Caprioli[5] and Agostinelli[6] proved that the only TE and TM modes which are possible in a nonhomogeneous dielectric waveguide are those discussed in the author's papers mentioned above.

Dario Graffi
University of Bologna
Bologna, Italy

---

[7] F. Tricomi, "Equazioni differenziali," Einaudi, Torino, chap. 3; 1948.

[8] The case of the rectangular waveguide with nonhomogeneous dielectric has been reconsidered by Miss I. Giovanardi[2] who, without limiting the discussion to the TE modes, but assuming the dielectric only slightly heterogeneous, has shown that the TE and TM modes which would propagate with an identical velocity in the same guide filled with homogeneous dieletric, change, due to the nonhomogeneity of dielectric, into two hybrid waves propagating with the different velocities: in other words, the lack of homogeneity in the dielectric renders the above mentioned TE and TM modes unstable.

A Method of Broadbanding Waveguide Windows*

A dielectric plate, of sufficient thickness to bear one atmosphere pressure difference, when placed across rectangular waveguide introduces a large shunt susceptance and a correspondingly narrow-band match if converted into a simple resonant window by means of an inductive iris. As a concrete example:

Waveguide: 2.84 inches×1.34 inches internally, at 10.2 cm.
Window: fused silica 3 mm thick (dielectric constant 3.8).
Safety factor: 8 at 1 atmosphere pressure difference.
Normalized shunt susceptance: 0.74.
Bandwidth, inductively matched: ±3 per cent to vswr of 1.05.

If all dimensions are scaled the other quantities are unchanged. There is also considerable correlation between strength and dielectric constant among other suitable materials, so that the choice of material has little effect.

Our method of broadbanding is to use inductance in series as well as in shunt, as indicated in the equivalent circuit of Fig. 1(a). For given C it is possible to choose L_1 and L_2 to make the reflection zero at center-frequency ω_0, and to first order in $\delta\omega$ near ω_0.

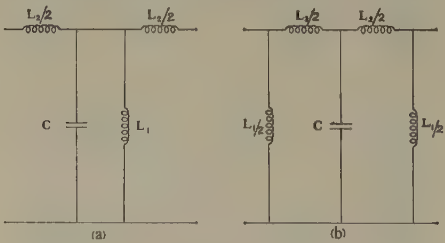

Fig. 1.

This corresponds approximately to making C, L_1, L_2 have the same proportions as in a short length of guide. The symmetrical arrangement is essential: if L_2 is not split into two equal parts then the two variable parameters are not sufficient to enable the two conditions to be satisfied simultaneously for both real and imaginary parts. The calculated performance of this circuit, for a normalized shunt susceptance, B, of 0.74, is shown in Fig. 2. It is better than 1.02 vswr over a ±20 per cent band, and near to center-frequency its behavior can be described by the formula:

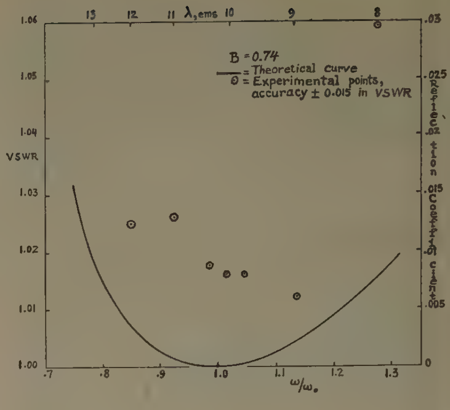

Fig. 2.

$$\text{vswr} = 1 + a_2\left(\frac{\delta\omega}{\omega}\right)^2 + \cdots$$

with

$$a_2 = 0.237.$$

For other values of shunt susceptance we give a_2 as a function of B in Fig. 3.

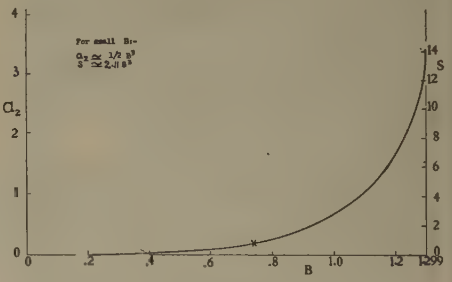

Fig. 3.

This equivalent circuit may or may not be a good approximation to any particular physical realization of a window based on these ideas, but it is worth remarking that the only reason why this model does not have exactly the same properties as a short length of guide, and consequently is not reflectionless at all frequencies, is that it consists of finite-lumped circuit elements instead of infinitesimal distributed ones. This is why the bandwidth is so broad for reasonably small B although it is only a first order match in $\delta\omega$: the a_2 coefficient is proportional to the cube of B, near $B=0$, so is very small for small B. If it were practicable to distribute C and L_1 uniformly along L_2, the window would then be a waveguide of the same characteristic impedance as the main guide, and would then be reflectionless at all frequencies in the absence of "junction effect."

The choice of L_1, L_2 to make $d/d\omega$ vanish is not, of course, the same as a choice to obtain minimum reflection in a given band. There is little point in making calculations on this point, but it means that a window broadbanded empirically could be better than Fig. 2 would indicate. One can approximately halve the reflection at the extremities at the expense of introducing a similar reflection at midband.

Received by the IRE, May 12, 1954.

* The work for this paper was done at Cambridge, England, and supported by A.E.R.E., Harwell, whom we thank for permission to publish.

The only experimental data that we have relates to the silica window shown in Fig. 4, which was adjusted to be as reflectionless as possible from 9 to 11 cm, and then measured at 8 cm and 12 cm. The equipment used for broadbanding this was only capable of measuring standing wave ratios to about $\pm 1\frac{1}{2}$ per cent, which made it impossible to accomplish the final adjustment of L_1 and L_2 that would, we believe, have made the reflection in the 9 to 11 cm region much smaller. It will be seen from Fig. 4 that the arrangement corresponds more to that of Fig. 1(b) than 1(a), and rough calculations indicate that this is by no means as good a circuit. The silica plate thickness of this window was 4.5 mm, not 3.0, but the inductive slots make it taller (parallel to E) than the waveguide so that it is about $B=0.74$ as before.

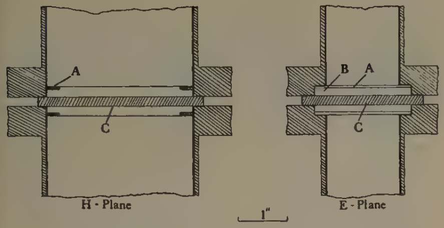

A=Inductive irises C=Silica plate
B=Inductive recesses

Fig. 4.

This window was developed as an interim, demountable, measure for use on high-power pulsed klystrons of the Stanford University type, and has been used at A.E.R.E., Harwell, and elsewhere to pass up to about 15 Mw peak power. Its broadband feature is not, of course, of great importance in this connection.

H. G. Hereward
Cavendish Nuclear Physics Lab.
Cambridge, England
M. G. N. Hine
C.E.R.N.
Geneva, Switzerland

Relationship between the Bott-Duffin and Pantell Impedance Synthesis*

In a recent letter,[1] R. H. Pantell presented a method of impedance synthesis. The author wishes to point out in this note that the network obtained by Pantell can be derived from the corresponding Bott-Duffin network by a delta-wye transformation.

Basically the network obtained by Bott and Duffin[2] ($L_0>0$) is of the form shown in Fig. 1. The impedance elements in the boxes are each other's duals. As has been pointed out by F. M. Reza,[3] this network is actually a balanced bridge and the nodes A and B can be connected together without altering the input impedance. Thus, the circuit of Fig. 2 has the same driving point impedance as that of Fig. 1, where Z_a is any impedance element whatsoever. If Z_a is chosen to be an appropriate inductance, it can be shown that the network of Fig. 2 reduces to that of Pantell's by a delta-wye transformation.

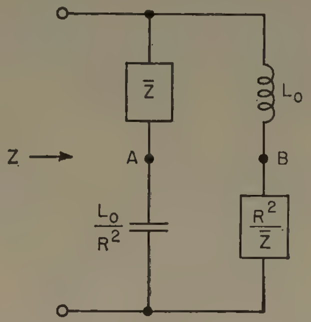

Fig. 1.

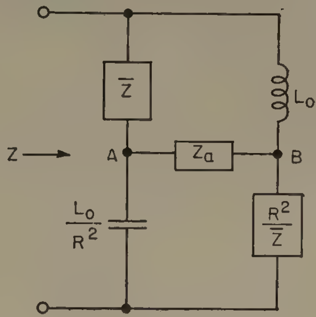

Fig. 2.

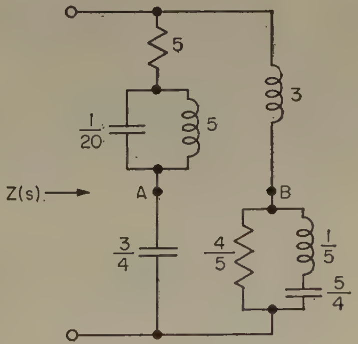

Fig. 3.

A numerical example will perhaps serve to make this clearer. For simplicity the same driving point impedance used by Pantell in his example will be chosen. This driving point impedance is

$$Z(s)=\frac{5s^2+18s+8}{s^2+s+10}.$$

Synthesizing it by the Bott-Duffin procedure one obtains the circuit of Fig. 3. Since the nodes A and B are at the same potential, they can be connected together. Using an inductance of $\frac{1}{3}$ henry for this purpose (the value of $\frac{1}{3}$ is easily obtained by noting it is the only choice which simplifies the delta-wye transformation) the circuit of Fig. 4 is obtained.

Performing a wye-delta transformation on the elements inside the dotted curve in Fig. 4 yields the network of Fig. 5. Combining the two adjacent series LC combinations

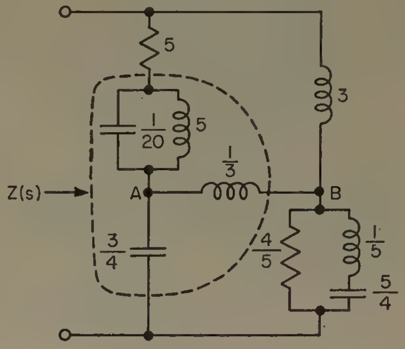

Fig. 4.

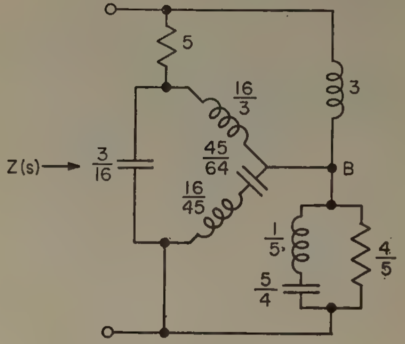

Fig. 5.

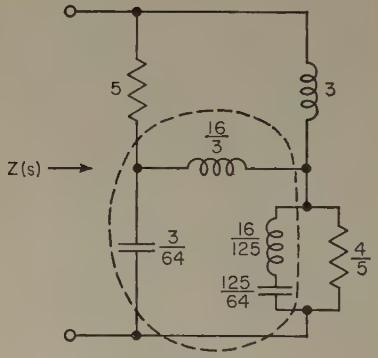

Fig. 6.

yields the circuit of Fig. 6, the same one as derived by Pantell. A delta-wye transformation on the elements in the dotted circle of Fig. 6 yields the other network of Pantell.

James E. Storer
Div. of Applied Physics
Harvard University
Cambridge, Mass.

"Rhombic Antenna Design"* by A. E. Harper

Dr. Balth. van der Pol has called our attention to an error in the above book (D. Van Nostrand Company, Inc., New

---

* Received by the IRE, May 13, 1954.

[1] R. H. Pantell, "A new method of driving point impedance synthesis," Proc. I.R.E., vol. 42, p. 861; May, 1954.

[2] R. Bott and R. J. Duffin, "Impedance synthesis without the use of transformers," *Jour. App. Phys.*, vol. 20, p. 816; August, 1949.

[3] F. M. Reza, "Conversion of a Brune cycle," *Trans. I.R.E.*, No. PGCT-1; March, 1954.

* Received by the IRE, May 18, 1954.

York, 1941) by the late author. Formulas (9) and (9A) on pages 29 and 30, which give the radiation field of a rhombic antenna over an imperfectly conducting ground, are not correct when the azimuth angle of arrival, β, is not zero.

For perfectly conducting ground the radiation intensity above ground is

$$\Phi_1 = 4 \sin^2\left(\frac{2\pi H}{\lambda} \sin \Delta\right) \times \Phi$$

where Φ is the radiation intensity in free space given by formula (7) page 27; the remaining factor is the space factor for the antenna and its image.

H. T. Friis
Holmdel Radio Lab.
Holmdel, N. J.

Bits and Binits*

Various discussions of a proper nomenclature for "binary digits" and for "one out of two" information appear to have overlooked the circumstance that these are two quite different things. The delightful expression, "bit of information," first suggested by Tukey, has been so widely used in its new dignified technical meaning that we may consider it an accepted member of the family of units, and if it has no counterpart in the decimal system, this may be ascribed to the newness of information theory, coupled with a natural preference for the binary system when treating a large class of problems.

On the other hand, the expression "binary digit" a full-fledged misnomer, continues in use in its old connotation as a place or symbol in a binary number. In occasional conversations about this with mathematicians and communication engineers during the past few years, the undersigned has gathered that the expression "binit" might receive acceptance as a logical contraction of "binary digit," and the purpose of this letter is to suggest its use as such, while retaining "bit" for its other meaning as a unit of information. Likewise, the ternary system could have "trinit" and "trit" for "ternary digit" and "one out of three" information, etc.

It does not appear at this writing whether a unit of "one out of ten" information would be pertinent, nor whether a unit of "one out of e (2.718 . . .)" would be useful, but it will be pointed out that the latter would have at least the merit that multiplication by the Boltzmann constant would reduce the entropy of information to the negentropy of thermodynamics.

M. J. E. Golay
Signal Corps Eng. Labs.
Fort Monmouth, N. J.

---

* Received by the IRE, May 13, 1954.

"High Frequency Crystal Units for Primary Frequency Standards"*

Crystal units having Q's as high as 1.2×10^6 at 9 mc and 2.6×10^6 at 5 mc were reported heretofore in my paper above.[1] Since that time the same principles of design have been used to construct a 100 mm diameter quartz crystal plate, 18 mm thick, operating at about one mc on the 11th overtone. This crystal unit has a measured Q of 12×10^6, believed to be the highest Q ever reported for room temperature operation. Other electrical characteristics are as follows:

Series resonant resistance, R_1	210 ohms
Static capacitance, C_0	4.5 mmf
Dynamic capacitance, C_1	63 mmmf
Inductance, L_1	410 henries.

The Q was determined by the equation

$$Q = \frac{1}{4\pi R_1 \Delta f[C_0 + C_t]},$$

where Δf is the measured change in series resonant frequency upon putting C_t in series with the crystal unit, and R_1 the series resonant resistance measured by the usual substitution method.

It is interesting to note that a Q of this magnitude may be measured with a stop watch, even at 1 megacycle. It was found that about 3.2 seconds were required for the voltage to decay to $1/e$ of its original value, indicating a Q of about 10×10^6.

A. W. Warner
Bell, Telephone Labs., Inc.
Murray Hill, N. J.

---

* Received by the IRE, April 16, 1954.

[1] Proc. IRE, vol. 40, pp. 1030–1033; September, 1952.

A Note on the Transfer Voltage Ratio of Passive RLC Networks*

In recent years considerable attention has been focused on the synthesis of transfer functions as the voltage ratio of a two-terminal pair, passive RLC network containing no transformers. (See Fig. 1.)

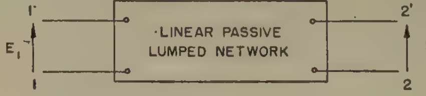

Fig. 1

$$\frac{E_2}{E_1} = A(s) = K \frac{s^m + a_{m-1}s^{m-1} + \cdots + a_1 s + a_0}{s^n + b_{n-1}s^{n-1} + \cdots + b_1 s + b_0}.$$

Fialkow and Gerst[1] seem to have been the first to point out the importance of the constant multiplier K in this problem. Their results are mainly for the rc case. The object of this note is to generalize their results to the RLC case and give an alternative method of attack on the problem, which has a certain physical significance.

Transfer Voltage Theorem

The magnitude of the voltage transfer ratio $A(s)$ of a passive RLC network containing no transformers is not greater than one for positive real values of s.

$$|A(s)| \leqq 1 \text{ for } s \text{ real and positive.}$$

Proof: For a positive real s, all the resistors, inductors, and capacitors behave as if they were positive resistors. Evidently the voltage transfer ratio for a resistive network cannot be larger than one.

Corollary I: In any two-terminal pair passive network without transformers, the voltage transfer ratio cannot equal one for a positive, real, finite, nonzero value of s (unless it does so identically).

Proof: Since, for s real and positive, all elements act as resistors, then if $|E_1| = |E_2|$, terminals 2 and 2′ must coincide with 1 and 1′; that is, there must be zero resistance paths through the network between corresponding terminals. These connections may exist identically, in which case $E_2 \equiv E_1$. If the zero resistance paths do not appear identically, then they appear because certain resistances have gone to zero, but the "resistances" considered here can only possibly go to zero for zero and infinite frequencies. Thus *Corollary I* is proved.

Corollary II: The voltage transfer ratio of a three-terminal passive network containing no transformers cannot have a positive real zero.

Proof: A zero voltage output means a short circuit between 2 and 2′. Such a short circuit cannot occur for a real positive finite nonzero value of s since no zero resistance path is possible (unless identically). Hence, one may further conclude that for three-terminal networks

$$0 < A \leqq 1 \text{ for } s \text{ real and positive.}$$

It could also be shown that in a two-terminal pair, passive RLC network containing no transformers, the voltage transfer ratio $A(s)$ may have finite positive real zeros, provided that the two pairs of terminals occupy a symmetrical position in the network graph, as in the case of a balanced bridge.

Note that the logic used in the theorem given above is independent of the lumped or finite character of the network.

F. M. Reza and
P. M. Lewis II
Massachusetts Institute of Technology
Cambridge, Mass.

---

* Received by the IRE, June 1, 1954. This work was supported in part by the Signal Corps; the Office of Scientific Research, Air Research and Development Command; and the Office of Naval Research.

[1] A Fialkow and I. Gerst, "The transfer function of general two-terminal pair rc networks." *Quart. Appl. Math.*, vol. 10, pp. 113–127; July, 1952.

IRE News and Radio Notes

JOINT COMPUTER CONFERENCE SCHEDULED

The fourth annual Eastern Joint Computer Conference & Exhibition will be held in the Bellevue-Stratford Hotel, Philadelphia, December 8–10, 1954. The theme of the conference, which is jointly sponsored by the American Institute of Electrical Engineers, the IRE, and the Association for Computing Machinery, will be "Design and Application of Small Digital Computers."

Latest products of over sixty companies in the computer field will be exhibited during the conference. Conducted tours to computer manufacturers and installations in the Philadelphia area are planned.

Proceedings of the conference will be published by the sponsoring societies and may be ordered from any one of them. Information on registration, which is open to all, may be obtained by writing Eastern Joint Computer Conference, P. O. Box 7825, Philadelphia 1, Pa.

1955 CONFERENCE ON HIGH FREQUENCY MEASUREMENTS

The fourth in a biennial series of meetings devoted to the subject of High Frequency Measurements, sponsored by the IRE AIEE, URSI, and the National Bureau of Standards, will be held on January 17, 18 and 19, 1955, in Washington, D. C. These meetings have been organized for the purpose of presenting the latest advancements in radio measurements.

Papers are solicited for the following four sessions of this meeting and one hundred word abstracts should be sent to the indicated session chairman before September 30, 1954.

1. Frequency and Time Measurements: Dr. B. M. Oliver, Hewlett-Packard Co., Palo Alto, Calif.
2. Power and Attenuation Measurements: E. W. Houghton, Bell Telephone Labs., Murray Hill, N. J.
3. Impedance Measurements: Dr. D. D. King, Johns Hopkins University, Baltimore, Md.
4. Measurements in Transmission and Reception: B. Parzen, Olympic Television and Radio Company, Long Island City, N. Y.

NATIONAL ELECTRONICS CONFERENCE MEETS IN OCTOBER

The tenth annual National Electronics Conference will convene October 4, 5 and 6, 1954, Hotel Sherman, Chicago, Illinois.

The technical program offers 88 papers on electronic research, development and industrial application, supplemented by over 160 manufacturer's exhibits.

The Conference will sponsor three luncheons featuring prominent speakers, an informal evening banquet on Tuesday, October 5, and a full three-day program for women. The Tenth Anniversary of the Conference will be celebrated at the Monday luncheon and the Tuesday evening banquet.

The Conference is sponsored by the Institute of Radio Engineers, American Institute of Electrical Engineers, Illinois Institute of Technology, Northwestern University and the University of Illinois, with Michigan State College, Purdue University, University of Michigan, University of Wisconsin, the Radio-Electronics-Television Manufacturers Association and the Society of Motion Picture and Television Engineers participating.

Advance registration may be made by writing to the NATIONAL ELECTRONICS CONFERENCE, INC., John S. Powers, Executive Secretary, 84 East Randolph Street, Chicago 1, Illinois.

Call For Papers! Deadline, November 15, 1954

1955 IRE NATIONAL CONVENTION

Prospective authors are requested to submit all of the following information:

(1) 100-word abstract in triplicate, title of paper, name and address.
(2) 500-word summary in triplicate, title of paper, name and address.
(3) Indicate the technical field in which your paper falls:

Aeronautical & Navigational Electronics
Antennas & Propagation
Audio
Broadcast & Television Receivers
Broadcast Transmission Systems
Circuit Theory
Communications Systems
Component Parts
Electron Devices
Electronic Computers
Engineering Management
Industrial Electronics
Information Theory
Instrumentation
Medical Electronics
Microwave Theory & Techniques
Nuclear Science
Production Techniques
Quality Control
Radio Telemetry & Remote Control
Ultrasonics Engineering
Vehicular Communications

Address all material to: Chairman
1955 Technical Program Committee
Institute of Radio Engineers, Inc.
1 East 79 Street, New York 21, N. Y.

Calendar of COMING EVENTS

IRE-AIEE-URSI Symposium on Information Theory, Massachusetts Institute of Technology, Cambridge, Mass., September 15–17

Cedar Rapids Conference on Communications, Cedar Rapids, Iowa, September 17–18

IRE Professional Group on Broadcast Transmission Systems Annual Broadcasting Symposium, Hotel Carter, Cleveland, Ohio, September 24–25

IRE Professional Group on Industrial Electronics Annual Conference, Mellon Institute of Industrial Research, Pittsburgh, Pa., September 29–30

IRE Professional Group on Vehicular Communications Meeting, Rice Hotel, Houston, Texas, September 30–October 1

National Electronics Conference, Hotel Sherman, Chicago, Ill., October 4–6

IRE Professional Group on Nuclear Science Annual Conference, Sherman Hotel, Chicago, Ill., October 6–7

Symposium on Marine Communication and Navigation, Hotel Somerset, Boston, Mass., October 13–15

Audio Engineering Society 1954 Annual Convention, Hotel New Yorker, New York, N. Y., October 13–17

IRE-RETMA Radio Fall Meeting, Hotel Syracuse, Syracuse, N. Y., October 18–20

IRE Baltimore Section-PGANE East Coast Conference on Airborne and Navigational Electronics, Sheraton-Belvedere Hotel, Baltimore, Md., November 4–5

IRE-PIB Microwave Symposium, Engineering Societies Auditorium, New York, N. Y., November 8–10

IRE-AIEE Conference on Electrical Techniques in Medicine and Biology, Morrison Hotel, Chicago, Ill., November 10–11

IRE Quality Control Symposium, Statler Hotel, New York, N. Y., November 12–13

Symposium on Fluctuation Phenomena in Microwave Sources, Western Union Auditorium, New York, N. Y., November 18–19

IRE Kansas City Section Annual Electronics Conference, Hotel President, Kansas City, Mo., November 18–19

IRE-AIEE-ACM Eastern Computer Conference, Bellevue-Stratford Hotel, Philadelphia, Pa., December 8–10

IRE-AIEE-NBS-URSI Conference on High Frequency Measurements, Hotel Statler, Washington, D. C., January 17–19

AIEE Winter General Meeting, Hotel Statler, New York, N. Y., January 31–February 4.

1955 Southwestern IRE Conference and Electronics Show, Baker Hotel, Dallas, Tex., February 10–12

IRE National Convention, Waldorf-Astoria Hotel and Kingsbridge Armory, New York, N. Y., March 21–24

SMPTE 77th Semiannual Convention, Hotel Drake, Chicago, Ill., April 17–22

SYMPOSIUM ON INDUSTRIAL ELECTRONICS

The I.R.E. Professional Group on Industrial Electronics and the Pittsburgh Section of the I.R.E. are co-sponsoring a symposium to be held in the Mellon Institute, Pittsburgh, Pa., September 29–30. The symposium is designed to be of interest to those in industry who find that electronics are playing an increasing role in their field. Papers on such subjects as thickness gaging, graphic arts, dielectric heating, amplifiers, power rectifiers, high-speed photography, process control, and machine tools, are scheduled among the sixteen papers to be presented.

Two sessions will be presented each day from 10 A.M. to 12:30 P.M., and 2 to 4:30 P.M., as follows:

Session I—Gaging and Process Control:
1. Industrial atom-ation.
2. Magnetic thickness gage for rubber and plastic applications.
3. Flying spot scanner for automatic process control.
4. Chemical process control.

Session II—Applications of Light:
1. Electronic flash design considerations.
2. Electronic high-speed photograph methods.
3. Automatic detection of "green-rot" in shell eggs.
4. RCA color corrector for the graphic arts.

Session III—High-Power Electronics:
1. Power oscillators for dielectric heating.
2. High-power audio amplifiers for electro-dynamic shakers.
3. What is new in power rectifiers?
4. Electronic considerations in the theory and design of electronic spark machine tools.

Session IV—Automation and Control:
1. The future of electronics in the automation of industry.
2. Digital control of machine tools.
3. A high accuracy analog to digital converter.
4. Electro-mechanically stabilized dc amplifier for telemetering small signals.

For registration information write Dr. J. B. Woodford, Jr., Electrical Engineering Dept., Carnegie Institute of Technology, Pittsburgh 13, Pa.

Technical Committee Notes

The **Circuits** Committee convened on June 25th under the chairmanship of W. R. Bennett. The Feedback definitions (54 IRE 4.7 PS2) which had been distributed to the committee members in advance of the meeting were discussed. Various modifications incorporated in this list were approved. It was decided to defer submission of this list to the Standards Committee for final approval until all the terms included in 54 IRE 4.7 R1

Continued on page 1455

TRANSACTIONS OF IRE PROFESSIONAL GROUPS

The following issues of Transactions are available from the Institute of Radio Engineers, Inc., 1 East 79 Street, New York 21, N. Y., at the prices listed below.

Sponsoring Group	Publications	Group Members	IRE Members	Non-Members*
Aeronautical & Navigational Electronics	PGAE-4; The Selectivity and Intermodulation Problem in UHF and Communication Equipment (11 pages)	$ .45	$ .65	$1.35
	PGAE-5; A Dynamic Aircraft Simulator for Study of Human Response Characteristics (6 pages)	.30	.45	.90
	PGAE-6; Ground-to-Air Cochannel Interference at 2900 MC (10 pages)	.30	.45	.90
	PGAE-8; June 1953 (25 pages)	.65	.95	1.95
	PGAE-9; September 1953 (27 pages)	.70	1.05	2.10
	Vol. ANE-1, No. 1; March 1954 (51 pages)	1.00	1.50	3.00
Antennas and Propagation	PGAP-4; IRE Western Convention, August 1952 (136 pages)	2.20	3.30	6.60
	Vol. AP-1, No. 1; July 1953 (30 pages)	1.20	1.80	3.60
	Vol. AP-1, No. 2; October 1953 (64 pages)	1.20	1.80	3.60
	Vol. AP-2, No. 1; January 1954 (39 pages)	1.35	2.00	4.05
	Vol. AP-2, No. 2; April 1954 (52 pages)	2.00	3.00	6.00
	Vol. AP-2, No. 3; July 1954 (40 pages)	1.50	2.25	4.50
Audio	PGA-5; Design Interrelations of Records and Reproducers (8 pages)	.30	.45	.90
	PGA-7; Editorials, Technical Papers and News May 1952 (48 pages)	.90	1.35	2.70
	PGA-10; November–December 1952 (28 pages)	.70	1.05	2.10
	Vol. AU-1, No. 1; January–February 1953 (26 pages)	.60	.90	1.80
	Vol. AU-1, No. 2; March–April 1953 (36 pages)	.80	1.20	2.40
	Vol. AU-1, No. 3; May–June 1953 (24 pages)	.80	1.20	2.40
	Vol. AU-1, No. 4; July–August 1953 (19 pages)	.70	1.05	2.10
	Vol. AU-1, No. 5; September–October 1953 (11 pages)	.50	.75	1.50
	Vol. AU-1, No. 6; November–December 1953 (27 pages)	.90	1.35	2.70
	Vol. AU-2, No. 1; January–Feburary 1954 (38 pages)	1.20	1.80	3.60
	Vol. AU-2, No. 2; March–April 1954 (32 pages)	.95	1.40	2.85
	Vol. AU-2, No. 3; May–June 1954 (28 pages)	.95	1.40	2.85
Broadcast and Television Receivers	PGBTR-1; Round-Table Discussion on UHF TV Receiver Considerations, 1952 IRE National Convention (12 pages)	.50	.75	1.50
	PGBTR-2; General Color-Receiver Design Considerations and Connection of UHF & Color Adaptors to UHF Receivers (21 pages)	.60	.90	1.80
	PGBTR-3; June 1953 (67 pages)	1.40	2.10	4.20
	PGBTR-5; January 1954 (96 pages)	1.80	2.70	5.40
	PGBTR-6; April 1954 (110 pages)	2.35	3.50	7.00
	PGBTR-7; July 1954 (60 pages)	1.15	1.70	3.45
Circuit Theory	PGCT-1; IRE Western Convention, August 1952 (100 pages)	1.60	2.40	4.80
	PGCT-2 Papers Presented at the Circuit Theory Sessions of the Western Electronic Show and Convention, San Francisco, California, August 19–21, 1953 (106 pages)	1.95	2.90	5.85
	Vol. CT-1, No. 1; March 1954 (80 pages)	1.30	1.95	3.90
Communications Systems	Vol. CS-1, No. 1; Includes papers presented at the Technical Conference on Communications (72 pages)	1.50	2.25	4.50
	Vol. CS-2, No. 1; January 1954 (83 pages)	1.65	2.50	4.95
	Vol. CS-2, No. 2; July 1954 (136 pages)	2.25	3.35	6.75
Component Parts	PGCP-1; March 1954 (46 pages)	1.20	1.80	3.60

* Public libraries, colleges, and subscription agencies may purchase at IRE Member rate.

have been considered. W. H. Huggins made the suggestion that the committee might air some of their questions by means of a letter to the Editor of the PGCT TRANSACTIONS or by publishing selected parts of their minutes in the TRANSACTIONS. The purpose of this suggestion is to stimulate expression of opinions by workers in the field, and thereby generate improved nomenclature; this nomenclature could then be given a trial by aggressive students of circuit theory. A number of ambiguous terms were discussed by the committee.

The **Radio Transmitters** Committee met on June 24th under the chairmanship of P. J. Herbst. Mr. Herbst read a letter from J. B. Heffelfinger, Chairman of Subcommittee 15.3, stating that he had organized a subcommittee in the Kansas City area and that the work would be done in that section. The proposed Standards on Pulses which had been sent to E. K. Gannett, Managing Editor of the IRE, for technical editing has now been referred to Subcommittee 15.4 with the revisions suggested by the Editor. After the subcommittee has approved the changes, the Standard will be sent on Grand Tour. H. R. Butler reported on the voting on "Spurious Output" definitions. It was decided that the vote was too close to constitute formal action of the committee. The committee discussed the definition of this term. It was decided that (1) the committee accept the restricted definition of "spurious output" (output outside the assigned band), (2) the committee assign to a group the responsibility with origination of terminology for the unwanted radiation within the assigned band, and (3) the committee reserve any decision on a term to describe all the unintended or unwanted output both inside and outside the assigned band until suggestions had been received from the various subcommittees. Mr. Herbst read a letter from T. M. Gluyas, Chairman of Subcommittee 15.6, stating that all the changes suggested by Committee 15 in the Proposed Standard on Television: Methods of Testing Broadcast Transmitters had been made, except the deletion of Section 4.3. The subcommittee suggested that this section be retained, as it is the one characteristic which applies to color transmitters. After some discussion H. R. Butler moved that the committee instruct subcommittee 15.6 to delete the section and to consider issuing a separate section on color characteristics at a later date. The committee voted unanimously in favor of it.

The **Standards** Committee met on July 15th with Dr. Ernst Weber presiding. Thirteen additional semiconductor definitions were added to the Semiconductor Standard approved at the June meeting which will be published in the PROCEEDINGS OF THE I.R.E. as 54 IRE 7. S2, Standards on Electron Devices: Definitions of Semiconductor Terms. The Committee authorized Dr. Weber to appoint an Ad Hoc Committee to study the problems of Spurious Radiation and to allocate responsibility to existing Technical Committees for the creation of Techniques of Measurement as requested by Mr. Hewlett, President of the IRE. The definitions prepared by the Navigation Aids Committee were considered and many were approved. Work on this proposed standard will continue at the next meeting on September 16th.

TRANSACTIONS OF IRE PROFESSIONAL GROUPS (Continued)

The following issues of Transactions are available from the Institute of Radio Engineers, Inc., 1 East 79 Street, New York 21, N.Y., at the prices listed below.

Sponsoring Group	Publications	Group Members	IRE Members	Non-Members*
Electronic Computers	Vol. EC-2, No. 2; June 1953 (27 pages)	.90	1.35	2.70
	Vol. EC-2, No. 3; September 1953 (27 pages)	.75	1.10	2.25
	Vol. EC-2, No. 4; December 1953 (47 pages)	1.25	1.85	3.75
	Vol. EC-3, No. 1; March 1954 (39 pages)	1.10	1.65	3.30
	Vol. EC-3, No. 2; June 1954 (65 pages)	1.65	2.45	4.95
Electron Devices	PGED-1; Papers from IRE Conference on Electron Tube Research and IRE-AIEE Conference on Semi-Conductor Research, June 1952 (32 pages)	.80	1.20	2.40
	PGED-2; Papers on Electron Devices presented at the IRE Conference on Electron Tube Research, Ottawa, Canada, June 16-17 1952 and IRE Western Convention, Long Beach (84 pages)	1.60	2.40	4.80
	PGED-4; December 1953 (62 pages)	1.30	1.95	3.90
	Vol. ED-1, No. 1; Feburary 1954 (75 pages)	1.40	2.10	4.20
	Vol. ED-1, No. 2; April 1954 (75 pages)	1.40	2.10	4.20
Engineering Management	PGEM-1; February 1954 (55 pages	1.15	1.70	3.45
Industrial Electronics	PGIE-1; August 1953 (40 pages)	1.00	1.50	3.00
Information Theory	PGIT-2; A Bibliography of Information Theory (Communication Theory-Cybernetics) (60 pages)	1.25	1.85	3.75
	PGIT-3; March 1954 (159 pages)	2.60	3.90	7.80
Instrumentation	PGI-2; Data Handling Systems Symposium; IRE Western Electronic Show & Convention, Long Beach, California, August 27-29, 1952 (109 pages)	1.65	2.45	4.95
	PGI-3; April 1954 (55 pages)	1.05	1.55	3.15
Medical Electronics	PGME-1; November 1953 (40 pages)	1.05	1.55	3.15
Microwave Theory and Techniques	Vol. MTT-1, No. 2; November 1953 (44 pages)	.90	1.35	2.70
	Vol. MTT-2, No. 1; Papers presented at the Microwave Radio Relay Systems Symposium, New York, N. Y.—April 1954	2.20	3.30	6.60
	Vol. MTT-2, No. 2; July 1954 (68 pages)	1.25	1.85	3.75
Quality Control	PGQC-1; Papers presented at the 1951 Radio Fall Meeting, and 1952 IRE National Convention (60 pages)	1.20	1.80	3.60
	PGQC-2; March 1953 (51 pages)	1.30	1.95	3.90
	PGQC-3; February 1954 (39 pages)	1.15	1.70	3.45
Ultrasonics Engineering	PGUE-1; June 1954 (62 pages)	1.55	2.30	4.65
Vehicular Communications	PGVC-2; Symposium on What's New in Mobile Radio (32 pages)	1.20	1.80	3.60
	PGVC-3; Theme: Spectrum Conservation, Washington, D. C., December 3-5, 1952 (140 pages)	3.00	4.50	9.00
	PGVC-4, Design, Planning and Operation of Mobile Communications Systems (June 1954) (98 pages)	2.40	3.60	7.20

---

* Public libraries, colleges, and subscription agencies may purchase at IRE Member rate.

PROFESSIONAL GROUP NEWS

PGBTS ELECTS OFFICERS

At a recent election held by the Professional Group on Broadcast Transmission Systems, the following members were elected to the Administrative Committee: C. F. Daugherty, Radio Station WSB, Atlanta, Ga.; William C. Ellis, WFAA, Dallas, Texas; W. H. Hauser, WBZ-AM-FM-TV, Boston, Mass.; Joseph B. Epperson, Scripps-Howard Radio, Inc., Cleveland, Ohio; R. K. Hellman, Hazeltine Laboratories, Little Neck, N. Y.; Scott Helt, Allen B. DuMont Laboratories, New York, N. Y.; J. G. Leitch, Radio Station WCAU, Philadelphia, Pa.; W. B. Lodge, Columbia Broadcasting System, New York, N. Y.; Frank Marx, American Broadcasting Co., New York, N. Y.; T. G. Morrissey, KFEL, Denver, Colo.; W. J. Purcell, Radio Station WGY, Schenectady, N. Y.; O. W. B. Reed, Jr., Jansky & Bailey, Washington, D. C.; Ronald J. Rockwell, Crosley Broadcasting Corp., Cincinnati, Ohio; Carl E. Smith, Consulting Radio Engineer, Cleveland, Ohio; and Lewis Winner, Bryan Davis Publishing Co., New York, N. Y.

Lewis Winner was re-elected Chairman, Scott Helt, Vice Chairman, and Clure H. Owen, Secretary-Treasurer, for 1954–55.

NEW CHAPTERS APPROVED

At a meeting held on June 29, the Executive Committee approved the establishment of the following Professional Group chapters: the Albuquerque Chapter of the Professional Group on Radio Telemetry and Remote Control; the Dallas-Ft. Worth and the St. Louis Chapters of the Professional Group on Aeronautical and Navigational Electronics; the Houston Chapters of the Professional Groups on Broadcast Transmission Systems and Instrumentation; the New York Chapter of the Professional Group on Engineering Management; and the Washington, D. C. Chapter of the Professional Group on Audio.

BROADCAST SYSTEMS MEETING SET FOR CLEVELAND

The annual meeting of the IRE Professional Group on Broadcast Transmission Systems, usually held in Philadelphia, will be held this year in Cleveland, Ohio on September 24–25. Among the subjects to be discussed at the meeting will be color television, UHF, and television antenna design.

The program is being arranged by J. B. Epperson, Scott Helt, Clure Owen, Carl E. Smith, and Lewis Winner, chairman of the PGBTS.

OBITUARIES

John L. Allison (SM'47) a senior project engineer at Federal Telecommunication Laboratories, died recently at the age of 45.

J. L. ALLISON

Mr. Allison received his B.A. degree from Columbia University in 1931 and his M.S. degree from the University of Michigan in 1933. From 1939 to 1942 he studied at the University of Colorado and was a graduate assistant in physics there.

He became affiliated with the IT&T system in 1942, joining FTL in 1946. He was a member of Sigma Pi Sigma.

❖

Herbert A. Bernreuter (SM'49) Vice President and General Manager of Simpson Electrical Company and a director of Bach-Simpson Ltd., electrical instrument firm in Canada, died recently.

H. A. BERNREUTER

Mr. Bernreuter received his B.S. degree from the University of Illinois School of Engineering in 1924. Since 1934 he had been affiliated with the Simpson Electric Company. He was recognized as one of the nation's outstanding electrical instrument engineers and held many patents for his inventions in the field. He was a member of the honorary fraternity, Eta Kappa Nu.

❖

Oliver I. Lewis (M'45–SM'45) died recently at the age of 51.

Mr. Lewis had for many years been with the Department of Defense, Engineering and Technical Division. At the time of his death, he was Chief Engineer of that Division.

He had been a member of the IRE since 1929, and was also a member of American Association for the Advancement of Science and the National Geographic Society.

Abstracts of Transactions of the I.R.E.

The following issues of "Transactions" have recently been published, and are now available from The Institute of Radio Engineers, Inc., 1 East 79 Street, New York 21, N. Y. at the following prices. The contents of each issue and, where available, abstracts of technical papers are given below.

Sponsoring Group	Publication	Group Members	IRE Members	Non-Members*
Audio	Vol. AU-2, No. 4	$0.90	$1.40	$2.85
Engineering Management	PGEM-1	1.15	1.70	3.45

*** Public libraries and colleges can purchase copies at IRE Member rates.**

AUDIO

VOL. AU-2, NO. 4, JULY–AUGUST, 1954

Comment on Flutter Standards—Edward W. Kellogg (*technical editorial*)

Now that a new IRE Standard has been adopted for methods of determining flutter content (PROC. I.R.E., March, 1954, pages 537–541), the background for further fundamental research on the subject of acceptable amounts of flutter is discussed.

"High-Fidelity" in Musical Tone Production?—Daniel W. Martin (*technical editorial*)

A distinction is drawn between musical tone production and musical sound reproduction. A brief historical account of the origin of high-fidelity is given. The paradoxical tendency for some musical instrument makers to try to adapt the term "High-Fidelity" to descriptive purposes for musical instruments is deprecated.

PGA News

IRE Technical Committee News

Natural Sound Reproduction—Howard K. Morgan

Past Columbia Broadcasting System and RCA tests of reproduction acceptability are reviewed, together with a proposal of a three-way loudspeaker system. Then each factor, such as frequency range, noise, and distortion, is related to the listener preference findings. Finally the power requirements for each range in the three-way system are discussed.

Equivalent Circuit Analysis of Mechano-Acoustic Structures—B. B. Bauer

Early electro-mechanical analogies appear to have had their beginnings with the work of Volta and Ohm over a century-and-a-half ago. Additional refinements were introduced by Rayleigh and others with the objective of using similar differential equations in the solution of acoustical, mechanical and electrical problems. Two sets of analogies are recognized; one based upon voltage-force-pressure (the EFP or "classical" analogy) and the other based upon current-force-pressure (the IFP or "mobility" analogy). Both analogies have advantages, but the EFP analogy is believed to be the more suitable for use by Audio technologists. Acoustic structures and the values of acoustical network elements are described. Certain mechanical configurations present difficulties which are resolved by transformer couplings. Diaphragm surfaces are represented by transformers. Present-day goals include the recognition of geometric and physical similarity between the networks of various types. Simplification of equivalent networks synthesis may be achieved by a device known as "Gyrator." A "Transverter" which is an approximation to this device by purely electrical means is described.

Frequency Modulation Phonograph Pickups—B. F. Miessner

The development of frequency modulation pickups is described, with particular emphasis on the historical aspects and the patent literature. A wide variety of applications of frequency modulation pickups is mentioned, and a very extensive bibliography on the subject is included.

ENGINEERING MANAGEMENT

PGEM-1, February, 1954

Message to Members of the Professional Group on Engineering Management—T. C. Rives

Message from Publications Committee—C. G. Cambridge

Management and the Engineer—T. C. Rives

The qualifications of the typical "engineer" to become a "manager" are discussed in detail and the factors favoring engineers as managers are listed. Four dominant external influences on management are spelled out: (1) increasing or multiplying technology; (2) competition; (3) big government; and (4) individual and collective public opinion. The typical engineer is analyzed to determine how well he is equipped to deal with them.

An Engineering Incentive Problem—Harold Goldberg

It is pointed out that emphasis on research has resulted in a loss of appreciation of the major engineering effort necessary to convert basic ideas to reliable hardware. The current impression is that research is 95 per cent of the job and that the conversion to hardware occurs in that mysterious process known as "production." There is a necessity for re-educating engineers to the challenging task that confronts us in making today's electronic wonders reliable. The problem of providing proper incentives is also important.

Staff Engineer's Part in Control of Design and Development Costs—Harold G. Purinton

Effective engineering cost controls can be used only if management is supplied with adequate and accurate information. The function of the Staff Engineer and the "tools" used in the control of engineering expenditures is presented. The paper discusses techniques of bid estimating, project progress reporting and scheduling.

How Design Quality Control Can Help Engineering—Charles E. Ellis

Design quality control, when properly organized and carried out, helps the engineer to design products for optimum economy by giving him information that is not ordinarily available. Moreover, it teaches him additional elements of his craft in the form of applied statistics pertinent to local conditions. Specific examples are given.

An Informational Approach to Organization and System Engineering Design—Jerome Rothstein

An informational approach is developed to the general problem of organization. It is shown by its use that system engineering design in general can be brought under the same philosophy and body of techniques now beginning to dominate the field of communication system design. The form this new theory assumes, however, being suited to quantitative treatment of any organization or system, enables it to be applied to problems encountered by management in running and improving its organization, plant or product. A brief indication is made of the potentialities of this new approach.

The Role of the Military Laboratory in Electronics Research and Development—Herbert Sherman

The role of the military laboratory in electronics research and development is examined by going through each of the phases leading to operational equipment. In each of these phases, function is examined with particular regard for the special tasks implied for the military laboratories. Some conclusions are reached, based on the premise that the military research and development program of the country is so large that it cannot be accomplished within military laboratories, but will normally be conducted under their general guidances.

Constitution of the PGEM

Bylaws of the PGEM

Professional Groups

	Chairman
Aeronautical and Navigational Electronics	K. C. Black Polytechnics Res. and Devel. Co. Brooklyn, N. Y.
Antennas and Propagation	D. C. Ports Jansky & Bailey 1339 Wisconsin Ave. N.W. Washington 7, D. C.
Audio	Vincent Salmon Stanford Research Institute Stanford, Calif.
Broadcast and Television Receivers	Earl I. Anderson RCA Labs. Div. 711-5-Ave., New York, N. Y.
Broadcast Transmission Systems	Lewis Winner 52 Vanderbilt Ave., New York, N. Y.
Circuit Theory	C. H. Page National Bureau of Standards Washington, D. C.
Communications Systems	Col. J. Z. Millar Western Union Telegraph Co. 60 Hudson St., New York 13, N. Y.
Component Parts	Floyd A. Paul Northrop Aircraft, Inc. Hawthorne, Calif.
Electron Devices	George A. Espersen Phillips Laboratories, Inc. Irvington-on-Hudson, N. Y.
Electronic Computers	Harry T. Larson Hughes Aircraft Co. Culver City, Calif.
Engineering Management	Charles J. Breitwieser RCA Victor Division Camden, N. J.

	Chairman
Industrial Electronics	George P. Bosomworth Firestone Tire & Rubber Co. Akron 17, Ohio
Information Theory	William G. Tuller Melpar, Inc., 452 Swann Ave. Alexandria, Va.
Instrumentation	R. L. Sink Consolidated Engineering Corp. 300 Sierra Madre Villa Pasadena, Calif.
Medical Electronics	J. F. Herrick Mayo Clinic Rochester, Minn.
Microwave Theory and Techniques	W. W. Mumford Bell Telephone Laboratories Whippany, N. J.
Nuclear Science	D. H. Loughbridge Northwestern Technical Institute Evanston, Ill.
Quality Control	Victor Wouk Beta Electric Co. 333 E. 103rd St., New York 29, N. Y.
Radio Telemetry and Remote Control	M. V. Kiebert, Jr. P. R. Mallory & Co., Inc. Indianapolis, Ind.
Ultrasonics Engineering	A. L. Lane 706 Chillum Road Hyattsville, Md.
Vehicular Communications	W. A. Shipman Columbia Gas. Sys. Ser. Corp. 120 E. 41 St., N. Y. 17, N. Y.

Sections*

Chairman		Secretary
K. F. Sibila 1745-13th Street Cuyahoga Falls, Ohio	AKRON (4)	C. O. Lambert 1144 Roslyn Ave. Akron 20, Ohio
T. F. Marker 3133-40th Street Sandia Base Albuquerque, N. M.	ALBUQUERQUE-LOS ALAMOS (7)	T. G. Banks, Jr. 1124 Monroe St., S.E. Albuquerque, N. M.
G. M. Howard 413 Ridgecrest Rd., N.E. Atlanta, Ga.	ATLANTA (6)	K. Winston Bugg Board of Education 14 Fl., City Hall Atlanta, Ga.
C. D. Pierson, Jr. Broadview Apts. 1126 116 West University Pkwy. Baltimore 10, Md.	BALTIMORE (3)	M. I. Jacob 1505 Tredegar Ave. Catonsville 28, Md.
L. C. Stockard 1390 Lucas Drive Beaumont, Texas	BEAUMONT-PORT ARTHUR (6)	John Petkovsek, Jr. 4390 El Paso Ave. Beaumont, Texas
N. S. Lawrence Johnson's Corners, R.D. 1 Harpursville, N. Y.	BINGHAMTON (4)	O. T. Ling 100 Henry St. Binghamton, N. Y.
A. J. Pote Lincoln Laboratory Massachusetts Inst. of Tech. Cambridge, Mass.	BOSTON (1)	T. P. Cheatham, Jr. Hosmer St. Marlborough, Mass.
P. N. Guzzi Cangallo 1286 Buenos Aires, Argentna	BUENOS AIRES	C. E. Sussenguth Gral. Urquiza 1914 Florida F.C.N.G.B.M. Argentina
J. H. Doolittle Goodrich Road Clarence, N. Y.	BUFFALO-NIAGARA (4)	W. L. Kinsell 207 Ridgewood Dr. Buffalo 21, N. Y.
J. W. Smith 1136-27 St., N.E. Cedar Rapids, Iowa	CEDAR RAPIDS (5)	R. M. Ringoen 1941 Washington Ave., SE Cedar Rapids, Iowa
H. R. Denius Box Q Melbourne, Fla.	CENTRAL FLORIDA (6)	K. A. West 1345 Indian River Dr. Eau Gallie, Fla.
J. J. Gershon De Vry Tech. Inst. 4141 Belmont Ave. Chicago 41, Ill.	CHICAGO(5)	J. S. Brown 9829 S. Hoyne Ave. Chicago 43, Illinois
R. A. Maher 6133 Sunridge Drive Cincinnati 24, Ohio	CINCINNATI (5)	W. S. Alberts 6533 Elwynne Drive Cincinnati 36, Ohio
H. R. Mull R.F.D. 3 Elyria, Ohio	CLEVELAND (4)	W. O. Piwonka 3121 Huntington Rd. Cleveland, Ohio
C. B. Sloan 568 Arden Rd. Columbus 2, Ohio	COLUMBUS (4)	P. I. Pressel 599 Northridge Rd. Columbus 14, Ohio
H. E. Rohloff Southern New England Tel. Co. 227 Church St. New Haven, Conn.	CONNECTICUT VALLEY (1)	Benjamin Kamens 45 Brooklawn Circle New Haven, Conn.
J. A. Green 6815 Oriole Drive Dallas 9, Texas	DALLAS-FORT WORTH (6)	G. K. Teal Texas Instruments Inc. 6000 Lemmon Ave. Dallas, Texas
A. B. Henderson 801 Hathaway Road Dayton 9, Ohio	DAYTON (5)	N. L. Laschever 849 N. Upland Ave. Dayton, Ohio
R. E. Swanson 1777 Kipling Street Denver 15, Colo.	DENVER (5)	Sidney Bedford, Jr. Mountain States Tel. & Tel., Room 802 Denver, Colo.
W. L. Cassell Iowa State College Ames, Iowa	DES MOINES-AMES (5)	R. E. Price 1706 Franklin Ave. Des Moines, Iowa
E. J. Love 9264 Boleyn Detroit 24, Mich.	DETROIT (4)	M. B. Scherba 270 S. Melborn Dearborn, Mich.
J. L. Sheldon 179 Dodge Ave. Corning, N. Y.	ELMIRA-CORNING (4)	J. P. Hocker Pilot Plant No. 2 Corning Glass Works Corning, N. Y.
J. F. Stuart Box 991 El Paso, Texas	EL PASO (7)	
J. B. Grund Sylvania Electric Products, Inc. Emporium, Pa.	EMPORIUM (4)	D. A. Dander 101½ W. Fourth St. Emporium, Pa.
A. P. Haase 2230 St. James Ct. Owensboro, Ky.	EVANSVILLE-OWENSBORO (5)	D. D. Mickey General Electric Co. Owensboro, Ky.
J. J. Iffland 2603 Merivale Street Fort Wayne 8, Ind.	FORT WAYNE (5)	T. L. Slater Tower Service Sta. RR6 Fort Wayne, Ind.
G. M. Cox 154 Victoria St., S. Kitchener, Ont., Canada	HAMILTON (8)	A. L. Fromanger 79 Park Row Ave. N Hamilton, Ont., Canada
G. Warren Clark Box 193 Lanikai, Oahu, T. H.	HAWAII (7)	J. R. Sanders c/o Matson Navigation Company Box 899 Honolulu, T. H.
W. J. Greer Halliburton Oil Well & Cementing Company 1628 Old Spanish Trail Houston 25, Texas	HOUSTON (6)	R. S. Bush 3818 Alberta Ave. Houston 21, Texas
J. R. Haeger 1107 Times Bldg. Huntsville, Ala.	HUNTSVILLE (7)	C. O. Brock 220 W. Rhett Ave. Huntsville, Ala.
J. T. Watson 4918 N. Kenwood Ave. Indianapolis 8, Ind.	INDIANAPOLIS (5)	M. J. Arvin 4329 Fletcher Ave. Indianapolis, Ind.
F. S. Howell 313-B Tyler St. China Lake, Calif.	INYOKERN (7)	H. A. Kirsch 528 K. Nimitz China Lake, Calif.
Ben Warriner General Electric Co. Cornell U., Ithaca, N. Y.	ITHACA (4)	R. L. Wooley 110 Cascadilla St. Ithaca, N. Y.
K. V. Newton Bendix Aviation Corp. Box 1159 Kansas City 41, Mo.	KANSAS CITY (5)	Mrs. G. L. Curtis Radio Industries, Inc. 1307 Central Ave. Kansas City 2, Kan.
Raymond Beem Route 3 Malvern, Ark.	LITTLE ROCK (5)	D. L. Winn 114 E. Capitol Little Rock, Ark.
G. A. Robitaille 19 McKinnon Pl. London, Ont., Canada	LONDON (CANADA (8))	J. D. B. Moore 27 McClary Ave. London, Ont., Canada
W. F. Bailey Hazeltine Corp. 58-25 Little Neck Pkwy. Little Neck, N. Y.	LONG ISLAND (2)	P. G. Hansel Addison Lane Greenvale, L. I., N. Y.
B. S. Angwin 3300 Colby Avenue Los Angeles 34, Calif.	LOS ANGELES (7)	C. E. Rutherford 209 S. Oakhurst Drive Beverly Hills, Calif.
R. W. Mills 1017 Eastern Pkwy. Louisville 4, Ky.	LOUISVILLE (5)	L. A. Miller 314 Republic Building Louisville 2, Ky.
A. H. Lynch Box 466 Ft. Myers, Fla.	MIAMI (6)	W. H. Epperson Box 65 Coral Gables, Fla.
H. J. Zwarra 722 N. Bdwy., Rm. 1103 Milwaukee, Wis.	MILWAUKEE (5)	Alex Paalu 1334 N. 29 St. Milwaukee, Wis.
R. W. Cooke 18 Muir Road Senneville, P.Q., Canada	MONTREAL (8)	F. H. Margolick 4601 Montclair Ave. Montreal, Que., Canada
	NEW ORLEANS (6)	J. A. Cronvich Tulane University New Orleans 18, La.
A. B. Giordano 85-99 Livingston Street Brooklyn 2, N. Y.	NEW YORK (2)	H. S. Renne 366 Madison Avenue New York 17, N. Y.
G. B. Hoadley North Carolina State College Raleigh, N. C.	NORTH CAROLINA-VIRGINIA (3)	M. J. Minor Rt. 3, York Rd. Charlotte, N. C.

---

* Numerals in parenthesis following Section designate Region number.

Sections

Chairman		Secretary
S. A. Polkinghorn 63 Monroe Pl. Bloomfield, N. J.	Northern New Jersey (2)	B. G. Griffith 127 Park Ave. Verona, N. J.
G. W. Holt 4420 N. W. 19 Blvd. Oklahoma City, Okla.	Oklahoma City (6)	W. E. Lucey 1348 Kinkaid Dr. Oklahoma City, Okla.
M. L. McGowan 5544 Mason St. Omaha 6, Neb.	Omaha-Lincoln (5)	C. W. Rook Univ. of Nebraska Lincoln 8, Neb.
W. A. Cumming National Research Council Ottawa, Ont., Canada	Ottawa (8)	Charles Pattenson Box 527 Ottawa, Ont., Canada
S. C. Spielman Philco Corp. 4700 Wissahickon Ave. Philadelphia, Pa.	Philadelphia (3)	M. S. Corrington 12 E. Cottage Ave. Haddonfield, N. J.
P. W. Sokoloff 1113 E. Oregon Ave. Phoenix, Ariz.	Phoenix (7)	Everett Eberhard 30 E. Colter St. Phoenix, Ariz.
F. C. Alexander, Jr. 2824 Mt. Royal Blvd. & Sutter Road Glenshaw, Penna.	Pittsburgh (4)	K. A. Taylor Bell Tele. Co. of Pa. 416 Seventh Ave. Pittsburgh, Pa.
Howard Vollum 1115 S.E. Lambert St. Portland 2, Ore.	Portland (7)	R. R. Pooley KPOJ, 1019 S.W. 10th Ave. Portland, Ore.
Jerome Kurshan RCA Laboratories Princeton, N. J.	Princeton (3)	J. L. Potter Rutgers University New Brunswick, N. J.
Allan Holstrom 551 Spencer Rd. Rochester, N. Y.	Rochester (4)	W. F. Bellor 186 Dorsey Rd. Rochester, N. Y.
Harry Davis 716 Cherry Street Rome, N. Y.	Rome-Utica (4)	M. V. Ratynski 205 W. Cedar Street Rome, N. Y.
I. L. Dutton 5980 N. Haven Dr. North Highlands, Calif.	Sacramento (7)	Ewald Berger 3421 58th St. Sacramento, Calif.
R. W. Benson 818 S. Kingshighway St. Louis, Mo.	St. Louis (5)	A. E. Lennert 5507 Waterman Ave. St. Louis, Mo.
Clayton Clark 710 N. First East St. Logan, Utah	Salt Lake City (7)	J. S. Hooper 1936 Hubbard Ave. Salt Lake City 5, Utah
C. M. Crain Engineering Building 149 University of Texas Austin, Texas	San Antonio (6)	W. H. Hartwig Dept. of Electrical Engineering University of Texas Austin 12, Texas
W. S. Ivans, Jr. 8669 Lemon Ave. La Mesa, Calif.	San Diego (7)	Harold Story 1068 Agate St. San Diego 9, Calif.
A. J. Morris 1827 Cordilleras Road Redwood City, Calif.	San Francisco (7)	J. S. McCullough 1791 Willow Street San Jose 25, Calif.
R. B. Russ Union College Schenectady, N. Y.	Schenectady (2)	K. N. Burnett 1317 Cresse Ave. Schenectady, N. Y.
H. M. Swarm University of Washington Seattle, Wash.	Seattle (7)	K. R. Willson 1100-17th Ave. Seattle 22, Wash.
W. H. Hall General Electric Company Syracuse, N. Y.	Syracuse (4)	M. A. Johnson R.D. 1, Totman Road East Syracuse, N. Y.
L. S. Rynder 140 Rockingham Street Toledo 10, Ohio	Toledo (4)	L. R. Klopfenstein Portage Ohio
E. L. Palin 2137 Bayview Ave. Willowdale Toronto, Ont., Canada	Toronto (8)	F. J. Heath 5 Du Maurier Blvd. Lawrence Park Toronto, Ont., Canada
C. F. Hadley 1356 E. 45th Place Tulsa 15, Okla.	Tulsa (6)	L. H. Hooker 4064 East 22nd Place Tulsa 5, Okla.
F. S. Hird Northwestern Bell Tele. Co. 224 S. Fifth St. Minneapolis, Minn.	Twin Cities (5)	J. L. Hill 25-17th Ave. N.E. North St. Paul, Minn.
Miles Green North-West Tel. Co. 2226 W. Tenth Ave. Vancouver, B.C., Canada	Vancouver (8)	J. S. Gray 4069 W. 13th Avenue Vancouver, B.C., Canada
H. P. Meisinger Hull & Old Courthouse Rds. Rt. 3, Vienna, Va.	Washington (3)	H. I. Metz Dept. of Commerce, CAA Room 2094, T-4 Bldg. Washington, D. C.
J. E. Snook 1629 Warren Avenue Williamsport, Penna.	Williamsport (4)	F. T. Henry 1345 Pennsylvania Avenue Williamsport, Penna.
H. H. Haakonsen University of Manitoba Dept. of Electrical Engineering Fort Garry, Man., Canada	Winnipeg (8)	G. R. Wallace 400 Smithfield Avenue Winnipeg, Man., Canada

Subsections

Chairman		Secretary
R. F. Lee 2704-31 St. Lubbock, Tex.	Amarillo-Lubbock (6) (Dallas-Ft.Worth)	H. A. Spuhler Texas Technological College Lubbock, Texas
S. C. Leonard Cheshire Mass.	Berkshire County (1) (Conn. Valley)	W. E. Neubert 21 Highlawn Drive Pittsfield, Mass.
W. A. Bowen, Jr. 225 E. Guava St. Oxuard, Calif.	Buenaventura (7) (Los Angeles)	E. C. Sternke Route 2, Box 122 Camarillo, Calif.
R. V. Higdon 1030 S. Atherton St. State College, Pa.	Centre County (4) (Emporium)	W. L. Baker 1184 Oneida St. State College, Pa.
W. L. Schachte 152 Grove Street Charleston 22, S. C.	Charleston (6) (Atlanta)	Arthur Jonas 21 Madden Drive Dorchester Terr. Charleston Heights, S. C.
W. W. Salisbury 910 Mountain View Dr. Lafayette, Calif.	East Bay (7)	J. M. Rosenberg 1134 Norwood Ave. Oakland 10, Calif.
Allen Davidson 3422 Argyle Ave. Erie, Pa.	Erie (4) (Buffalo-Niagara)	K. L. Hestor 2909 Tuttle Ave. Erie, Pa.
G. W. Scott, Jr. Armstrong Cork Co. Lancaster, Pa.	Lancaster (3) (Philadelphia)	G. E. Mandell RCA Lancaster, Pa.
E. J. Breiding 54 S. Grand Ave. Poughkeepsie, N. Y.	Mid-Hudson (2) (New York)	E. S. Wilson I.B.M. Corp. Poughkeepsie, N. Y.
W. M. Goodall Bell Tele. Labs., Box 107 Red Bank, N. J.	Monmouth (2) (New York)	A. H. Ross 923 Broad St. Shrewsbury, N. J.
Hugh Winter Box 374 Shalimar, Fla.	Northwest Florida (6) (Atlanta)	G. C. Jones 12 N. Okaloosa Rd. Ft. Walton Beach Fla.
B. F. Husten Naval Ordnance Laboratory Corona, Calif.	Orange Belt (7) (Los Angeles)	T. A. Mayeda 3658 Monroe Street Riverside, Calif.
J. V. Granger 320 Encinal Ave. Menlo Park, Calif.	Palo Alto (7) (San Francisco)	W. B. Wholey 342 Verano Dr. Los Altos, Calif.
	Richland (7) (Seattle) (To be Elected)	
W. V. Record 4511 E. Ninth St. Tucson, Ariz.	Tucson (1) (Phoenix)	A. J. Bersbach 5326 E. Seventh St. Tucson, Ariz.
Capt. L. A. Yarbrough 3001 USAFIT Wright-Patterson Air Force Base, Ohio	USAFIT (5) (Dayton)	
H. H. Newby 1428 Woodrow Wichita, Kan.	Wichita (Kansas City)	H. O. Byers 333 Laura Ave. Wichita, Kan.

Abstracts and References

Compiled by the Radio Research Organization of the Department of Scientific and Industrial Research, London, England, and Published by Arrangement with that Department and the *Wireless Engineer*, London, England

NOTE: The Institute of Radio Engineers does not have available copies of the publications mentioned in these pages, nor does it have reprints of the articles abstracted. Correspondence regarding these articles and requests for their procurement should be addressed to the individual publications, not to the I.R.E.

Acoustics and Audio Frequencies....... 1460
Antennas and Transmission Lines...... 1461
Automatic Computers.................. 1462
Circuits and Circuit Elements.......... 1463
General Physics...................... 1464
Geophysical and Extraterrestrial Phenomena.......................... 1465
Location and Aids to Navigation....... 1466
Materials and Subsidiary Techniques... 1467
Mathematics.......................... 1469
Measurements and Test Gear......... 1469
Other Applications of Radio and Electronics........................... 1470
Propagation of Waves................ 1471
Reception............................ 1471
Stations and Communication Systems... 1472
Subsidiary Apparatus................. 1472
Television and Phototelegraphy........ 1472
Transmission......................... 1473
Tubes and Thermionics............... 1473

The number in heavy type at the upper left of each Abstract is its Universal Decimal Classification number and is not to be confused with the Decimal Classification used by the United States National Bureau of Standards. The number in heavy type at the top right is the serial number of the Abstract. DC numbers marked with a dagger (†) must be regarded as provisional.

A new section has been introduced covering the general technique of electromagnetic waves, oscillations and pulses (i.e. transmission lines and circuits), as distinct from specific applications to telecommunications. The new section is numbered 621.37, with subdivisions. Full details of the new classification, and of the numbers which become obsolete as a result of its introduction, are given in PE Note 535, obtainable from The International Federation for Documentation, Willem Witsenplein 6, The Hague, Netherlands, or from The British Standards Institution, 2 Park Street, London, W.1., England.

Section 621.396.67, dealing with Antennas, has been modified and expanded; details of the new classification are given in PE Note 519.

Section 621.396.96, with subdivisions, has been introduced to cover Radar; details of the new classification are given in PE Note 518.

New Subject Section

A section headed Automatic Computers has been introduced.

The Index to the Abstracts and References published in the PROC. I.R.E. from February 1953 through January 1954 is published by *Wireless Engineer* and included in the March 1954 issue of that journal. Copies of this issue may be purchased for $1 (including postage) from the Institute of Radio Engineers, 1 East 79th Street, New York 21, N.Y. As supplies are limited, the publishers ask us to stress the need for early application for copies. Included with the Index is a selected list of journals scanned for abstracting with publishers' addresses.

ACOUSTICS AND AUDIO FREQUENCIES

534.13 2274

Study of the Acoustic Properties of Granular Substances excited to Shear-Mode Vibration—M. L. Exner, W. Güth, and F. Immer. (*Acustica*, vol. 4, pp. 350–358; 1954. In German.) Measurements of the mechanical impedance were made in the range 100–4000 cps on closely-packed granular carbon, using a rigid vibrometer. For small-amplitude vibrations the resonance frequencies are higher in fine-grain material and the damping less than in coarse-grain material. A decrease in velocity of propagation with increasing grain radius was observed. Results are in general agreement with those obtained by other methods.

534.2-14 2275

Wave Propagation in a Randomly Inhomogeneous Medium: Part 3—D. Mintzer. (*Jour. Acoust. Soc. Amer.*, vol. 26, pp. 186–190; March, 1954.) The assumption of a restricted pulse length made in part 1 (931 of April) is examined. The conditions necessary for the assumption to be valid are investigated. The coefficient of variation for a series of sound pulses of arbitrary length and the correlation function for successively received pulses are evaluated. Part 2: 1633 of June.

534.21-13 2276

Finite Amplitude Sound produced by a Piston in a Closed Tube—J. B. Keller. (*Jour. Acoust. Soc. Amer.*, vol. 26, pp. 253–254; March, 1954.) The one-dimensional equation of motion of a polytropic gas with adiabatic index $\gamma = -1$ is solved for an arbitrary piston motion. More detailed results are given for the case of sinusoidal motion. See also 294 of February.

534.213.4 2277

A Method of Measuring Discontinuity Effects in Ducts—W. K. R. Lippert. (*Acustica*, vol. 4, pp. 307–312; 1954.) The method is based on a transmission-line analogy. The experimental technique makes use of a nonreflecting terminal and a probe microphone for exploring the sound field on each side of the discontinuity. From the measurements the characteristic reflection and transmission factors and the equivalent impedance matrix are derived.

534.213.4 2278

The Measurement of Sound Reflection and Transmission at Right-Angled Bends in Rectangular Tubes—W. K. R. Lippert. (*Acustica*, vol. 4, pp. 313–319; 1954.) Experimental equipment is described and results are discussed for symmetrical and asymmetrical discontinuities. The measurements agree well with the theory of Miles (*Jour. Acoust. Soc. Amer.*, vol. 19, p. 572; 1947) and prove that the phase relations of the characteristic factors which have been derived theoretically for loss-free cases are valid.

534.213.4 2279

On the Theory of Sound Reflection in an Open-Ended Cylindrical Tube—H. Levine. (*Jour. Acoust. Soc. Amer.*, vol. 26, pp. 200–211; March, 1954.) Reflection coefficient R and end correction l are incorporated into a boundary-value formulation of the wave propagation problem. Two techniques are described for solving the integral equations involved: a variational procedure giving approximate results, and a method based on initial modification of an integral equation which yields exact values for R and l for a tube of circular cross-section. Results obtained by the two methods are compared.

534.232 2280

Suppression of Flexural Vibrations of Barium Titanate—C. L. Darner. (*Jour Acoust. Soc. Amer.*, vol. 26, pp. 256–257; March, 1954.) $BaTiO_3$ in thickness resonance develops an intense shear mode of vibration which sets up flexural waves and gives a directivity pattern with strong side lobes. The flexural waves are suppressed in a particular 1-mc transducer by forming square $\lambda/2$ indentations along its edges.

534.232:537.228.1 2281

Characteristics of Radiating Variable-Resonant-Frequency Crystal Systems—W. Welkowitz and W. J. Fry. (*Jour. Acoust. Soc. Amer.*, vol. 26, pp. 159–165; March, 1954.) One-dimensional theory of piezoelectric systems is applied to ADP and $BaTiO_3$ transducers with Hg backing, operating in water. Curves are presented showing (*a*) power output as a function of frequency, (*b*) resonance-frequency shift as a function of backing length, and (*c*) bandwidth as a function of frequency. A system in which half the crystals have a natural resonance frequency twice that of the others can be operated over a continuous frequency range of about 5.3:1.

534.24-14 2282

On Nonspecular Reflection at a Rough Surface—J. W. Miles. (*Jour. Acoust. Soc. Amer.*, vol. 26, pp. 191–199; March, 1954.) The reflection of a plane wave at a rough interface separating two fluid media is examined neglecting second-order terms in the magnitude of roughness. Exact solutions are obtained for the case of a sinusoidal boundary. For reflection of a pulse from a perfectly reflecting sinusoidal boundary, the boundary acts as a band-pass filter of the nonspecular components of the reflected wave; outside the pass-band, reflection is specular and distortionless. Analysis for a boundary not perfectly reflecting shows that the pass band is independent of the properties of the reflecting medium.

534.321.9 2283

An Ultrasonic Double-Reflector Concentrator—L. D. Rozenberg. (*Compt. Rend. Acad. Sci.* (*U.R.S.S.*), vol. 91, pp. 1091–1094; Aug. 11, 1953. In Russian.) Theory and description of a system consisting of a paraboloid located inside a coaxial ellipsoid and having its focus coincident with one of the foci of the ellipsoid. A plane wave incident normally on the external surface of the paraboloid is concentrated at the second focal point of the ellipsoid. The geometrical conditions for velocity- and pressure-focusing are derived and shown graphically in system-parameter form. A similar system was described by Barone (603 of 1953).

534.321.9:534.2 2284

Conditions for obtaining the Greatest Concentration of Ultrasonic Radiation—L. D. Rozenberg. (*Compt. Rend. Acad. Sci.* (*U.R.S.S.*), vol. 94, pp. 845–848; Feb. 11, 1954. In Russian.) Theoretical investigation of focusing to obtain maximum pressure or maximum velocity at the focal point of (*a*) reflected or refracted plane waves, and (*b*) waves from curved radiators such as barium titanate or quartz. The variation of the focusing factor with the aperture is shown graphically for five different systems.

534.321.9:61 2285

Ultrasound and Medicine. A Survey of Experimental Studies—J. F. Herrick and F. H. Krasen. (*Jour. Acoust. Soc. Amer.*, vol. 26, pp. 236–240; March, 1954. *Proc. NEC, Chicago*, vol. 9, pp. 235–243; 1953.) A critical review of the applications of ultrasonics in therapy, diagnosis and biological measurements. 43 references.

534.321.9-14:534.6 2286

Measurements of Sound Absorption in Aqueous Salt Solutions by a Resonator Method—O. B. Wilson, Jr. and R. W. Leonard. (*Jour. Acoust. Soc. Amer.*, vol. 26, pp. 223–226; March, 1954.) Measurements have been made in the frequency range 50–500 kc, using a modified reverberation technique. Results are presented for $MgSO_4$ solutions in particular, and for sea water.

534.6:534.321.9:537.228.1 2287

Very Small Ultrasonic Probes for Acoustic-Field Measurements in Liquids—G. Bolz. (*Z. angew. Phys.*, vol. 6, pp. 54–59; Feb., 1954.) Theoretical and experimental investigation of the performance of piezoelectric probes small compared with wavelength. Suitable crystals have only one piezoelectric axis; the best is tourmaline; $BaTiO_3$ may also have advantages. The crystal is mounted on the tip of a thin wire making contact with its metallized face. Sensitivity increases with frequency and probe surface area, and is practically independent of direction when crystal dimensions are one-eighth the wavelength in the liquid. A tourmaline probe for 1 mc was capable of measuring acoustic powers as low as 5×10^{-5} W/cm^2.

534.612:534.321.9:535.314 2288

The Study of a Sound Field by means of Optical Refraction Effects—J. Kolb and A. P. Loeber. (*Jour. Acoust. Soc. Amer.*, vol. 26, pp. 249–251; March, 1954.) The broadening of a slit image when a light beam traverses an ultrasonic field can be calculated by a method based on Wiener's theory of refraction of light in a liquid with refractive index varying continuously in one plane. The application of the principle for investigating pressure distribution in a stationary sound wave in the frequency range below 1 mc is illustrated. A simple method of measuring wavelength is outlined.

534.614-14:534.321.9 2289

The Dispersion of the Velocity of Sound in Water between 500 and 1500 kc/s.—T. K. McCubbin, Jr. (*Jour. Acoust. Soc. Amer.*, vol. 26, pp. 247–249; March, 1954.) Ultrasonic waves at 500 and 1500 kc were transmitted simultaneously by a transducer in water at 26 degrees C. Measurements were made of the change in relative phase between the two signals received by a second transducer at different distances from the first. The velocities at the two frequencies are equal to within 1 part in 290,000.

534.845 2290

Perforated Facing and Sound Absorption—U. Ingard. (*Jour. Acoust. Soc. Amer.*, vol. 26, pp. 151–154; March, 1954.) An analytical study is made of the absorption characteristics of a porous layer with perforated facing. The latter contributes to the total impedance not only a mass reactance but also an additional acoustic resistance which may be larger than that of the porous layer itself. This obtains only when the porous material is in close contact with the facing, and is due to the near-field (higher-mode) losses in the porous material around the perforations. The effect on the absorption characteristics is considerable.

534.845 2291

Propagation, Interference, Reflection, Absorption, Diffusion of Acoustic and Ultrasonic Waves rendered Visible by the Schlieren Method—F. Canac. (*Acustica*, vol. 4, pp. 320–328; 1954. In French.) A detailed description of the Schlieren method and its application to the study of absorption and reflection of various materials. Reduced-scale models of coffered ceilings and other structures were also examined. Working frequencies were normally 10 and 23 kc, but 69 kc and 4 kc have also been used.

621.395.623.7 2292

Useful Absolute Efficiencies of Typical Loudspeaker Systems—R. K. Vepa and N. K. Trivedi. (*Acustica*, vol. 4, pp. 329–332; 1954.)

An objective criterion is proposed, called the "useful absolute efficiency." This is defined as the ratio of the acoustic power output, radiated in the forward direction and contained within a 100-degree cone, to the electrical power input from a matched resistive generator. Tests were made in the open air on three types of loudspeaker at 400, 1000, and 3000 cps. Results are compared with computed axial efficiencies.

621.395.623.73 2293

Studies on the Cone-Type Loudspeakers: Part 4—On the Effects of the Surrounding Device of the Cone-Type Dynamic Loudspeakers—T. Nimura and K. Kido. (*Sci. Rep. Res. Inst. Tohoku Univ., Ser. B*, vol. 4, pp. 205–219; March, 1953.) The sound-pressure minima and cone-velocity maxima which occur in the 1–2-kc region of the frequency response of a circular conical loudspeaker are caused by the corrugated surround. By using an obliquely-cut circular cone or an elliptical cone, a nearly level frequency/pressure characteristic can be obtained over a wide frequency range. Part 3: 3328 of 1952 (Nimura and Matsui).

621.395.623.74:537.585 2294

Pressure Effects of Ionic Currents in Atmospheric Air with Various Discharge Configurations—Löb. (*See* 2365.)

621.395.624.3 2295

Magnetic Recording—M. Camras. (PROC. I.R.E., *Aust.*, vol. 15, pp. 61–69; March, 1954. 1953 I.R.E. *Convention Record*, Part 3, pp. 16–25; 1953.) Outline of principles and problems involved.

621.395.625.3:621.397.5 2296

A System for Recording and Reproducing Television Signals—Olson, Houghton, Morgan, Zenel, Artzt, Woodward, and Fischer. (*See* 2517.)

681.84/.85 2297

The Dynamic Restoring Forces on Gramophone Pickups—W. Mühe. (*Funk u. Ton*, vol. 8, pp. 147–162; March, 1954.) The factors investigated experimentally were: (*a*) effect of test-record groove characteristics on the restoring-force/frequency curve of various types of pickup, (*b*) the relation between restoring force and needle tracking and (*c*) relation between restoring force and record wear. Both the C.C.I.R. and German standard test records were used. Results show that the restoring force for the majority of pickups was too high at low frequencies, causing poor tracking or even jumping the groove at high amplitudes. An optimum needle pressure therefore exists.

ANTENNAS AND TRANSMISSION LINES

621.315.212:621.3.018.75 2298

Reduction of the Distortion of Pulses transmitted by a Perfectly Uniform Coaxial Line by Frequency Translation—R. Cazenave. (*Onde élect.*, vol. 34, pp. 147–152; Feb., 1954.) Analysis of the response of an ideal transmission line indicates the advantages of frequency translation for reducing amplitude and phase distortion, using a modulator and high-pass filter, with a phase-shift network for regrouping the transmitted frequencies at the receiving end. Unit-pulse response characteristics are compared for operation with and without the filtering and the phase-correction stages. A numerical calculation is made for transmission over 9 km of 2.6/9.4 coaxial cable with cut-off frequency 300 kc.

621.315.212(083.74) 2299

Choice of the Correct Characteristic Impedance for High-Frequency Cables—F. Gutzmann. (*Fernmeldetech. Z.*, vol. 7, pp. 136–139; March, 1954.) In fixing a standard characteristic impedance for all hf cables, considerations of maximum voltage and maximum operating temperature are inconclusive. Attenuation is the only satisfactory criterion. The relation of characteristic impedance to cable dimensions for a prescribed maximum attenuation is discussed. Comparison of different cables shows that standardization to a value of 50 or 75Ω is impracticable. About 60Ω is the only possible value.

621.372.2 2300

Some Wave Properties of Helical Conductors—J. H. Bryant. (*Elect. Commun.*, vol. 31, pp. 50–56; March, 1954.) An analysis is made of the velocity of propagation and the relation between the longitudinal field and total power flow in systems comprising a helical line with inner and/or outer coaxial cylinders. Results are shown graphically as functions of frequency.

621.372.2 2301

An Experimental Investigation of the Properties of Corrugated Cylindrical Surface Waveguides—H. E. M. Barlow and A. E. Karbowiak. (*Proc. IEE*, Part III, vol. 101, pp. 182–188; May, 1954.) Brass rods of 3/16 inch outer diameter having shallow transverse external corrugations uniformly distributed along the length of the rod were used to guide cylindrical surface waves at frequencies in the range 2.5–10 kmc. Provided there are more than two corrugations within the guide wavelength, higher-order surface waves are not present. The results of measurements of the surface reactance are shown graphically. An approximate expression for the surface reactance of a corrugated surface is derived which is in reasonable agreement with the experimental results, provided that the slot width is less than the slot depth, and that each wavelength includes several corrugations.

621.372.8 2302

Pass Band and Dispersion of Waveguides loaded with Circular Irises—R. Combe. (*Compt. Rend. Acad. Sci.* (*Paris*), vol. 238, pp. 1697–1699; April 26, 1954.) Approximate formulas are derived. Calculations are made of the permissible tolerances on the dimensions of the waveguide elements and on the frequency and temperature variations to obtain a value of λ_g within prescribed limits. Results are compared with those obtained experimentally for Al guides for $\lambda = 10$ cm with a permissible variation of 1 mm. Application is particularly relevant to linear accelerators for electrons.

621.372.8 2303

The Dimensioning of Loaded Waveguides for the H_{10} Mode—H. Weber. (*Telefunken Ztg.*, vol. 27, pp. 44–53; March, 1954.) Characteristic impedance, cut-off frequency, and propagation constant are computed for an unloaded rectangular waveguide with and without losses, using an equivalent-circuit method. The results are extended to a waveguide loaded with a longitudinal undercut section, stray capacitance at the load edges being taken into account. Equations derived are plotted, and examples illustrate their application in determining the dimensions or characteristics of waveguides for specific purposes.

621.372.8 2304

Transmission Loss of the Waveguide having Thin Dielectric Film on its Inner Wall—H. Uchida, Y. Mushiake, and S. Nishida. (*Sci. Rep. Res. Inst. Tohoku Univ., Ser. B*, vol. 4, pp. 287–298; March, 1953.) Equations are derived for the approximate transmission losses of a rectangular waveguide for an H_{10} wave, and of a circular waveguide for E and H waves. The equations are valid only at frequencies which are not near the cut-off frequency. The calculated attenuation constant of a rectangular waveguide with an 0.01-cm layer of enamel is $\sim 9.76 \times 10^{-3}$ db/m at 4 kmc, that of a circular waveguide is $\sim 3.22 \times 10^{-3}$ db/m at 4 kmc for the E_{01} wave.

621.372.8 2305

A Reflectionless Waveguide Termination—J. Smidt. (*Appl. Sci. Res.*, vol. B3, pp. 465–476; 1954.) The characteristics of an H-plane T-junction provided with a movable short-circuiting plunger and a movable dissipating element of arbitrary nature are discussed. A matrix-algebra method is used for calculating the coefficients determining the optimum positions of the plungers and the values of the reflection coefficients. Calculated and measured values for a termination for operation at about 9 kmc are in good agreement.

621.372.8:551.594.6 2306

Propagation of a Pulse in a Waveguide—M. Cotte. (*Onde élect.*, vol. 34, pp. 143–146; Feb., 1954.) Analysis of the propagation of a disturbance which can be resolved into components of similar mode but different frequency (2447 of 1948) is extended to the case of a waveguide with walls of finite conductivity. Two cases are distinguished: (*a*) H_{0n} waves in which the wavefront corresponds approximately to a pulse delay proportional to the distance travelled; (*b*) E_{mn} or H_{pn} waves suffering in addition a dispersion increasing as the square of the distance; this dispersion is the same for all E_{mn} waves. Results relating to circular waveguides may have application to the propagation of atmospherics.

621.372.8:621.385.029.64 2307

Output Windows for Tunable Magnetrons—T. S. Chen. (*Electronics*, vol. 27, pp. 170–173; May, 1954.) Design data and nomograms are given for metal diaphragms with ceramic windows used for sealing the magnetron output waveguide and for coupling power to the transmission line. Both single-frame and double-frame (sandwich) types are discussed.

621.396.67 2308

The Impedance of an Antenna above a Circular Ground Plate Laid upon a Plane Earth—G. Bekefi. (*Canad. Jour. Phys.*, vol. 32, pp. 205–222; March, 1954.) Analysis given by Storer (586 of 1952) is extended to include the case when the system is laid upon an imperfectly conducting earth. The expression for the antenna impedance is stationary with respect to small variations about its true value of the unknown radial electric field over the surface of the earth. Numerical results are given for the case of a ground plate large compared with λ. The effect of variations of the dielectric constant of the earth is shown. Results are in satisfactory agreement with those obtained using Monteath's theory (2648 of 1951). An alternative variational formula applicable to plates of smaller diameter gives the impedance in terms of radial currents flowing in the plate.

621.396.67 2309

The Theory of a Linear Antenna: Part 2—Y. Nomura and T. Hatta. (*Technol. Rep. Tohoku Univ.*, vol. 18, pp. 90–104; 1953.) The directivity and receiving quality of the linear antenna are investigated by the method developed in part 1 (3201 of 1953). The radiation field round the transmitting antenna is calculated as the sum of partial fields due to Fourier components of the antenna current; the properties of the receiving antenna follow from those of the transmitting antenna. The radiation patterns of some asymmetrically fed antennas are shown. The method is similar to, but more general than, that of Hara (*Hochfrequenztechnik und Elektroakustik*, vol. 44, pp. 185–193; Dec., 1934).

621.396.67 2310

Antenna-Scattering Measurements by Modulation of the Scatterer—H. Scharfman and D. D. King. (Proc. I.R.E., vol. 42, pp. 854–858; May, 1954.) A laboratory method is described in which scattering from an object under test is compared with that from a standard scatterer (e.g. a metal sphere) by mounting the two objects at opposite ends of a horizontal column mounted in turn on a rotating vertical shaft, and irradiating them alternately from a horn emitter. The horn is in one arm of a slightly unbalanced hybrid-T arrangement, and a fraction of the power scattered back to it is passed to the detector arm. Synchronous detection is used; because of the rotation of the objects, the phase of the backscattered signal varies rapidly with respect to that of the local signal. Curves obtained for the backscattering cross section of dipoles with lengths of 0.4 λ–1.6 λ are in good agreement with theoretical and experimental curves obtained by other workers. The method is applicable over the frequency range from about 1 to 5 kmc.

621.396.67:621.372.21 2311

Losses in Parallel-Wire Lines—J. Arsac, P. André, and R. Zaccai. (*Onde élect.*, vol. 34, pp. 170–177; Feb., 1954.) With a view to the application of open-wire feeders for radio-astronomy aerial systems, calculations are made of ohmic and radiation losses in the frequency range 150–1500 mc. For 2-wire lines 500 wavelengths long, with conductors a wavelength apart, and neglecting height factors, nonuniformities and oxidation effects, graphs are drawn showing total losses as a function of characteristic impedance for 4 wire diameters and 6 frequencies.

621.396.67:621.396.96 2312

General Theory of Plane-Wave Scattering from Finite, Conducting Obstacles with Application to the Two-Antenna Problems—J. E. Storer and J. Sevick. (*Jour. Appl. Phys.*, vol. 25, pp. 369–376; March, 1954.) The variational techniques of Levine & Schwinger (1583 of 1952) are used to obtain approximate solutions for the free-space scattering by a number of finite, perfectly conducting obstacles whose interactions are explicitly accounted for. The result gives the far-zone scattered-field distribution in terms of the obstacle currents. Variational expressions are obtained for the total scattering and for the backscattering crosssections. The complete mathematical development for the problem of the backscattering crosssection of two identical nonstaggered unloaded antennas oriented parallel to the incident field is presented, and results for the case of broadside radiation for half-wave and full-wave antennas are shown graphically.

621.396.67.029.6:621.397.62 2313

Switch-Tuned U.H.F.-V.H.F. [indoor television receiving] Antenna—G. Hills. (*Tele-Tech.*, vol. 13, pp. 93, 108; Jan., 1954.) A dipole 25 inches long with elements shaped from metal strips to form two cones attached to metal end caps is used. In the vhf band the tuning adjustment matches the antenna to the 300-Ω input lead. For the uhf band a correcting network compensates the series inductance and distributed capacitance of the standard selector switch used.

621.396.677.3 2314

The Principle and the Design of Yagi-Uda Antenna: Part 1—S. Uda and Y. Mushiake. (*Sci. Rep. Res. Inst. Tohoku Univ., Ser. B*, vol. 4, pp. 299–312; March, 1953.) Using Hallén's theory (*Nova Acta Regiae Societatis Scientiarum Upsaliensis*, Series IV, vol. 11, pp. 3–44; 1938), for the current distribution in a linear antenna, the effective lengths of the transmitting and receiving antennas are calculated. Expressions for the self and mutual impedances of the elements and the input impedance of the aerial system are given and a general expression for the radiation characteristic is derived. The effective length factors of antenna elements are also shown graphically.

621.396.677.45 2315

Wide-Frequency-Range Tuned Helical Antennas and Circuits—A. G. Kandoian and W. Sichak. (*Elect. Commun.*, vol. 31, p. 49; March, 1954.) Correction to paper abstracted in 1304 of May.

621.396.677.85 2316

Reflection of Electromagnetic Waves at Metal-Plate Media—G. Piefke. (*Arch. elekt. Übertragung*, vol. 8, pp. 101–110; March, 1954.) A theoretical investigation is made of the transmission and reflection of a plane wave incident normally on a system of infinitely thin metal plates spaced a distance a apart and aligned parallel to the electric field. A detailed analysis is made for the wavelength range $1 < 2a/\lambda_0 < 2$, considering (*a*) a plane wave incident normally on the system, and (*b*) a TE_{10} wave proceeding from the medium into free space. Reflection coefficients are equal in magnitude in the two cases, but the phase angles are different. For the transmission coefficients conditions are reversed, the phase angles being equal and the magnitudes different. Phase-angle curves obtained are used to determine the thickness and position of a dielectric plate placed behind the system for no reflection to occur. See also 1879 of 1951 (Lengyel).

AUTOMATIC COMPUTERS

681.142 2317

Arrangement of Batteries and Relays permitting the Solution by Analogy of Nonlinear Partial Differential Equations by means of a Chain of Resistances and Capacitances—A. Blanc. (*Compt. Rend. Acad. Sci.* (*Paris*), vol. 238, pp. 1377–1378; March 29, 1954.)

681.142 2318

Scale Factors for Analog Computers—J. B. Reswick. (*Product Eng.*, vol. 25, pp. 197–201; March, 1954.) Description of a design technique whereby scale factors relating analogue variables to the variables of the system investigated are first determined for true-time operation.

681.142 2319

A Time-Sharing Analog Multiplier—H. Freeman and E. Parsons. (*Trans. I.R.E.*, vol. EC-3, pp. 11–17; March, 1954.) The circuit is based on the same principle as that of Broomall and Riebman (2546 of 1952). Accuracy to within 0.2 per cent is achieved for a range of input voltages from 0 to 210v when the comparator voltage lies between 0 and 75v, depending on the circuit arrangements. 400 multiplications per second were made, indicating the suitability of the circuit for time-sharing techniques, but higher rates of operation seem possible.

681.142 2320

System Organization of the DYSEAC—A. L. Leiner and S. N. Alexander. (*Trans. I.R.E.*, vol. EC-3, pp. 1–10; March, 1954.) DYSEAC is a general-purpose high-speed digital computer incorporating the following special facilities: (*a*) external-transfer operations concurrent with internal computing, such transfers referring directly to any area of the internal storage system; (*b*) adjustment of speed of internal program so that it proceeds in step with the external program; (*c*) interruption of a program for interpolation of new orders.

681.142 2321

A Simple Analogue Divider—J. L. Douce. (*Electronic Engr.*, vol. 26, pp. 155–156; April, 1954.) A circuit is described which provides an output voltage proportional to the ratio between two input voltages, a pulse of duration inversely proportional to one input being used to gate the other input. The results are accurate to within 5 per cent over a wide range of inputs.

681.142 2322

An Operational-Digital Feedback Divider—M. A. Meyer, B. M. Gordon, and R. N. Nicola. (*Trans. I.R.E.*, vol. EC-3, pp. 17–20; March, 1954.) In this divider the input pulses operate directly on the output, the circuit forming a closed feedback loop in which the desired quotient corresponds to the only possible steady state. The accuracy of the system can be selected by using the appropriate number of significant digits from the eleven available.

CIRCUITS AND CIRCUIT ELEMENTS

621.3.011.2/.3 2323

New High-Frequency Proximity-Effect Formula—A. C. Sim. (*Elect. Commun.*, vol. 31, pp. 63–66; March, 1954.) Reprint. See 2918 of 1953.

621.314.25:621.372 2324

An R.M.S.-Sensitive Phase-Shifting Circuit—H. J. Fraser. (Proc. I.R.E., *Aust.*, vol. 15, pp. 59–60; March, 1954.) A circuit delivering an output whose phase depends on the rms value of the input uses a tungsten-filament diode as rms current detector. The diode is operated with 50-cps voltage on the anode, and a voltage derived from the ac component of anode current is added to a fixed 50-cps voltage to give the resultant variable-phase output. Applications for control purposes are mentioned.

621.314.632+621.314.7 2325

The Double-Base Diode: A Semiconductor Thyratron Analog—Aldrich & Lesk. (*See* 2535.)

621.316.842.012.3 2326

A Nomograph to Facilitate the Design of Single-Layer Resistance Windings—R. S. Read and I. Mills. (*Instrum. Practice*, vol. 8, pp. 215–217; March, 1954.)

621.316.86:537.312.6 2327

How to Use Thermistors—F. K. Bennett. (*Product Eng.*, vol. 25, pp. 182–185 and 200–204; March/April, 1954.) Review of thermistor characteristics and applications with tabulated data for rod, disk, washer, and bead types.

621.316.86:621.396.822 2328

Current-Noise in Composition Resistors—D. A. Bell and K. Y. Cheng. (*Wireless Engr.*, vol. 36, pp. 142–144; June, 1954.) Because of the inherent inhomogeneity of the resistor material, and because the noise depends on the square of the current density, modifications of the resistor structure at a few points of high current density can have a large effect on the noise without greatly affecting the dc resistance. Experimental evidence in support of this view is given. The effect may account for the observed lack of correlation between noise and dc resistance with large currents. Measurements made on resistors of the same rating but different types indicate a relation between noise coefficient and shape factor.

621.318.57 2329

A New High-Speed Bistable Device for Pulse Sharpening—Y. Druet. (*Onde élect.*, vol. 34, pp. 130–134; Feb., 1954.) Description of a triode-hexode flip-flop circuit (648 of 1953) generating 3×10^6 pulses/second and its application in switching and scaling circuits.

621.372 2330

RLC Canonic Forms—F. M. Reza. (*Jour. Appl. Phys.*, vol. 25, pp. 297–301; March, 1954.) A class of *RLC* networks is defined, which has canonic structure in the Foster sense. *LC* and *RL-RC* networks and networks with slight dissipation may belong to this class, in which case their analysis or synthesis is simplified. Examples of network synthesis illustrate the theory.

621.372 2331

Bounds Existing on the Time and Frequency Responses of Various Types of Networks—A. H. Zemanian. (Proc. I.R.E., vol. 42, pp. 835–839; May, 1954.) Six theorems are presented relating the transient and steady-state responses of linear, stable, fixed, lumped-constant networks. Fourier-transform analysis is used. Physical interpretations are discussed, rise times and settling times being considered. The overshoot or undershoot of the response to a step-current input for a *RC* driving-point impedance cannot be >100 per cent.

621.372 2332

Corner Plots—G. E. Anner. (*Radio & Telev. News, Radio-Electronic Engrg. Section*, vol. 51, pp. 14–18; March, 1954.) An approximation to the shape of the actual response curve for *RL* and *RC* circuits is obtained by suitable combinations of straight lines called corner plots. The parameters involved are defined, and rules for their determination by inspection of the circuit derived. The method is not restricted to impedances but may also be applied to network transfer functions, and is discussed in Bode's "Network Analysis and Feedback Amplifier Design," Chapter XV.

621.372:512.831 2333

Matrix Analysis of Multiterminal Transducers—J. Shekel. (Proc. I.R.E., vol. 42, pp. 840–847; May, 1954.) The multiterminal transducer is defined as a network with a set of n input terminals and a set of n output terminals. It can be represented by its impedance, admittance or transfer matrix. Special properties of networks exhibiting symmetry and/or reciprocity are discussed. The representation is classed as definite or indefinite according as the voltage reference terminals are or are not specified. Simple networks can be analyzed by inspection; more complicated networks may be treated as cascades of simple ones. The method is illustrated by deriving the transfer matrixes of some simple networks, including a distributed-amplifier section.

621.372.413 2334

Natural Vibrations of an Open Cavity—M. Jessel. (*Compt. Rend. Acad. Sci.* (*Paris*), vol. 238, pp. 1205–1206; March 15, 1954.) The field is expressed in a manner taking account of a set of oscillation modes associated with the cavity openings.

621.372.413.012.3 2335

Cavity-Resonator Design Charts—N. A. Spencer. (*Electronics*, vol. 27, pp. 186–188; May, 1954.) Charts applicable to square-section and to circular-section cavities are given.

621.372.5 2336

A Generalization of Weissfloch's Transformation Law—H. Lueg. (*Arch. elekt. Übertragung*, vol. 8, pp. 137–141; March, 1954.) The transformation law relating to a loss-free quadripole between homogeneous lines is generalized by showing that all points on the transformation curve can be correlated with corresponding positions on the input and output lines between which the quadripole acts as an ideal transformer with a reactance in parallel. See also 992 of April.

621.372.5.015.3:621.376.3 2337

Transient Response in F.M.—I. Gumowski. (Proc. I.R.E., vol. 42, pp. 819–822; May, 1954.) "The FM response to the unit impulse and the unit step function is calculated for a network whose transfer function is known. A meaning is assigned to the associated Fourier integrals, which diverge in the Riemann sense. The method is generalized to any input function which vanishes for negative t. As an illustration of the method the impulse and the step FM responses of a single tuned circuit are calculated."

621.372.54:621.315.212 2338

Filter using Coaxial Transmission Line as Elements—H. B. Yin and T. U. Foley. (*RCA Rev.*, vol. 15, pp. 62–74; March, 1954.) Exact equivalent circuits are presented for coaxial line elements with sleeve or undercut sections, taking account of capacitance or inductance effects at the discontinuities. From the corresponding equations the performance of filters comprising one or more of such elements can be predicted in terms of image impedance, cut-off frequency, attenuation and band limits. Measurements on a two-section low-pass filter confirm the theory.

621.372.54.029.62 2339

Variable U.S.W. Filters—K. H. Krambeer and F. Künemund. (*Frequenz*, vol. 8, pp. 65–77; March, 1954.) Results of an investigation of filters with distributed circuit elements and their equivalents with lumped L, C, R, indicate the circuits suitable for usw use. The filters described, which consist of adjustable cavity resonators and short lines, include separating filters for meter-band television and an adjacent-channel suppressor for transmitters and transmitter-receivers.

621.373.412 2340

Notes on a Cause of Frequency Instability of Partially Plated Piezoelectric Crystals (Proximity Effect)—W. J. 't Hart. (*Tijdschr. ned. Radiogenoot.*, vol. 19, pp. 116–117; March, 1954. In English.) External field conditions may have a marked effect on the resonance frequency of partially plated crystals. Movement of an object close to the resonator may produce a relative frequency shift of the order of 10^{-6} or even 10^{-5}. As an extreme example, a shift of about 10 cps was produced by hand effect in a 1-mc AT-cut crystal of diameter 29 mm and electrode diameter 9 mm, the equivalent resistance simultaneously increasing by 10 per cent. A qualitative explanation of the effect is given by reference to equivalent circuits.

621.373.421.1 2341

The Fluctuating Character of the Establishment of Oscillations in an Oscillator—I. S. Gonorovski. (*Compt. Rend. Acad. Sci.* (*U.R.S.S.*), vol. 94, pp. 869–872; Feb., 1954. In Russian.) The build-up of oscillations in an *LCR*-oscillator by white-noise potential fluctuations is considered theoretically.

621.373.421.11 2342

A Wide-Band Oscillator using a Conical-Helix Tuning Inductor—J. S. Chatterjee. (*Proc. IEE*, Part III, vol. 101, pp. 165–170; May, 1954.) Description of an oscillator working over a frequency range of 45:1 and using a single tank circuit between the grid and the anode of a triode. The tuning circuit consists of (*a*) a variable inductor formed by two conical helixes connected at their apices by a large capacitor, and (*b*) two variable cylindrical capacitors. For the high-frequency end the leads connecting the coils to the grid and the anode are used as transmission lines, the main tuning circuit being automatically isolated. Methods of calculating the oscillation frequency in terms of the circuit parameters are described, simplifying assumptions being made. A description is given of the design and performance of an experimental model for the range 10–450 mc.

621.373.52:621.314.7 2343

Internal Oscillations and Microwaves in Transistors—Hollmann. (*See* 2540.)

621.374:621.314.7 2344

Transistors convert Sine Waves to Pulses—R. E. McMahon, I. L. Lebow, and R. H. Baker. (*Electronics*, vol. 27, pp. 160–161; May, 1954.) A circuit using eight point-contact transistors to amplify, limit and differentiate a sine-wave input is described. The power-supply unit uses junction diodes. The frequency range is 10 cps–200 kc, minimum input is 5v, pulse output 35v maximum, pulse rise time<0.05 μs, pulse width adjustable from 0.3 to 1 μs, and output impedance 300–400 Ω.

621.375.2.024:621.317.3 2345

A Mains-Supplied Indicating D.C. Amplifier with Linear Response—W. Oesterlin and A. G. Braun. (*Arch. Tech. Messen*, pp. 41–44; Feb., 1954.) A 4-stage unit for use in conjunction with a piezoelectric transducer and a Duddell oscillograph for obtaining indicator diagrams is described. An electrometer tube is used as input to a first preamplifier stage, from which cable connection is made to the remaining amplifier stages and the oscillograph. Amplifier stability is good, and effects of value aging not apparent.

621.375.4 2346

Some Circuit Considerations of the Transistor—Y. Watanabe. (*Sci. Rep. Res. Inst. Tohoku Univ., Ser. B*, vol. 4, pp. 331–387; March, 1953.) A detailed discussion of the single-stage transistor amplifier and in particular of the "unity coupler" condition. Stability criteria are also discussed. Since four useful varieties of a single-stage amplifier exist, a two-stage amplifier can take sixteen different forms. These are divided into four groups, (*a*) high power gain, (*b*) low terminating resistance, (*c*) high terminating resistance, and (*d*) bilateral type. The latter is an emitter-base-base-emitter circuit and is suitable for obtaining high gains.

621.376.332 2347

A Triode F.M. Discriminator—I. G. Baxter. (*Electronic Eng.*, vol. 26, pp. 146–147; April, 1954.) The triode is arranged to operate as a gated rectifier, with the gating time, and hence the rectified output, dependent on the input frequency. A sine wave with the straight portion extending over about one radian can be used for the input waveform. For a particular circuit in which the rectified output should theoretically change by about 20v for a frequency change of 1 per cent, the measured change for this frequency difference was about 7.5v. The output is proportional to input amplitude as well as to frequency.

621.396.6 2348

Minimizing Contact Potential in Apparatus Design—E. C. J. Marsh. (*Electronic Eng.*, vol. 26, pp. 148–152; April, 1954.) Consideration is given particularly to the design of radio equipment required to function under adverse conditions such as exposure to humid or salt-laden atmosphere. A table reproduced from the Inter-Services document RCS/1000 gives the potentials of various metals in sea water against the saturated calomel electrode, as a guide to the choice of metal coatings; the latter may be applied by electroplating, spraying, or hot dipping.

621.396.667 2349

Signal-Operated Tone Compensation—E. C. Miller. (*Electronics*, vol. 27, pp. 184–185; May, 1954.) A triode tube is used as variable element of a circuit which boosts amplifier response at both ends of the af range to compensate for the reduced response of the ear; the amount of boost thus varies automatically with the input level.

GENERAL PHYSICS

535.42:538.566 2350

On Diffraction by a Strip—A. Erdélyi and C. H. Papas. (*Proc. Nat. Acad. Sci., Wash.*, vol. 40, pp. 128–132; Feb., 1954.) Limitations of the integral-equation and Fourier-Lamé methods of dealing with the problem of diffraction by a strip or slit are discussed. The variational technique of Levine & Schwinger (1583 of 1952) can be used to obtain an approximate value of the far-zone field in a form which is stationary with respect to small variations abouts its true value of the current induced in the strip. A calculation using this representation, and assuming as a rough approximation a uniform-density distribution of current in the strip, gives a good approximation to the value of the far-zone field. The scattering cross-section is then found by using the scattering theorem [1898 of 1950 (Papas)].

535.42:538.566 2351

Diffraction of Electromagnetic Waves, Radiated from an Arbitrarily Oriented Electric or Magnetic Dipole, at an Ideally Conducting Half-Plane—Yu. V. Vandakurov. (*Zh. eksp. teor. Fiz.*, vol. 26, pp. 3–18; Jan., 1954.) The solving of this problem is simplified by writing Maxwell's equations in a general form, so as to include the case of a conducting medium with a finite permeability, and by including a magnetic current for reasons of symmetry. The equation $\Delta P+k^2P=T$ is solved for different boundary conditions of P. In particular cases P represents components of the electric or magnetic fields or vector potentials, T is a function of position which is zero except in a small volume element surrounding the dipole, and $k^2=(\epsilon\omega-4\pi\sigma i)\mu\omega/c^2$ with the usual notation for the dielectric constant, angular frequency, electrical conductivity, permeability, velocity of light, and $\sqrt{-1}$. The solutions for various orientations of the dipole are given in the form of definite single integrals which can be evaluated.

537.122:539.23 2352

Energy Loss of Electrons in Passage through Thin Films—L. Marton and L. B. Leder. (*Phys. Rev.*, vol. 94, pp. 203–204; April 7, 1954.) Energy-loss values of 30-keV electrons passing through thin evaporated films of 21 metals and insulators are tabulated. Reasonable agreement with calculations of Pines and Bohm (1021 of April) and Pines (1376 of May) is shown.

537.2 2353

The Field $\vec{E}$ and the Induction $\vec{D}$ of a Point Electric Charge in Space—É. Durand. (*Compt. Rend. Acad. Sci.* (*Paris*), vol. 238, pp. 1478–1480; April 5, 1954.)

537.311.1 2354

Solid State Electronics—K. K. Darrow. (*Research, Lond.*, vol. 7, pp. 2–9, 46–53, 94–100, and 137–141; Jan.-April, 1954.) A general account of the mechanism of electronic conduction in solids.

537.311.31:539.234 2355

Notes on the Comparison between the Study of an Imperfect Contact and Experimental Results on Thin Metal Films—N. Nifontoff. (*Compt. Rend. Acad. Sci.* (*Paris*), vol. 238, pp. 1200–1202; March 15, 1954.) Continuation of investigation of the conduction mechanism in thin films [3258 of 1953 (Nifontoff and Perrot)].

537.52:537.533 2356

Electron Ejection by Slow Positive Ions Incident on Flashed and Gas-Covered Metallic Surfaces—J. H. Parker, Jr. (*Phys. Rev.*, vol. 93, pp. 1148–1156; March 15, 1954.)

537.52:537.533 2357

Liberation of Electrons by Positive-Ion Impact on the Cathode of a Pulsed Townsend Discharge Tube—R. N. Varney. (*Phys. Rev.*, vol. 93, pp. 1156–1160; March 15, 1954.

537.52:537.56 2358

Ionization Processes in the Electrical Breakdown of Gases—F. L. Jones. (*Brit. Jour. Appl. Phys.*, vol. 5, pp. 49–53; Feb., 1954.) A brief review.

537.525.6:537.562 2359

Diffusion Cooling of Electrons in Ionized Gases—M. A. Biondi. (*Phys. Rev.*, vol. 93, pp. 1136–1140; March 15, 1954.) Measurements made during low-pressure Ne and Ar afterglows show a reduction in ambipolar diffusion coefficient characteristic of diffusion cooling which is not observed when He is present.

537.533.8 2360

The Mechanism of Secondary Electron Emission—A. O. Barut. (*Phys. Rev.*, vol. 93, pp. 981–984; March 7, 1954.) A simple theory based on the constant energy loss per unit path length of primary electrons accounts quantitatively for the variation of secondary electron yield below its maximum value. The theory can be extended to include a Bethe-type energy loss at high primary energies. Relations between secondary electron emission and atomic structure are discussed. Secondary emission in insulators and semiconductors is also considered.

537.533.8 2361

Explanation of the Inaccuracy of Secondary-Electron Measurements—O. Beer. (*Ann. Phys., Lpz.*, vol. 14, pp. 201–214; Feb. 15, 1954.) A recording arrangement used for the measurements is described. A variation of δ, the secondary-electron ratio, with beam density was observed in several metals. This variation is probably due to the formation of positive ions at the target. When this is taken into account, the secondary-electron velocity distribution is found to be independent of temperature in the range 200–500 degrees C., contrary to several other published results.

537.533.8 2362

Threshold of Secondary Electron Emission of Nickel and Molybdenum—A. R. Shulman and E. I. Myakinin. (*Compt. Rend. Acad. Sci.* (*U.R.S.S.*), vol. 91, pp. 1075–1078; Aug. 11, 1953. In Russian.) The threshold is defined as the minimum energy of primary electrons for which the number of slow secondary electrons differs from zero. Experimental results show that it is equal to the work function, within the limits of experimental error. The velocity distribution of secondary electrons (including reflected electrons) at various primary electron energies, and the effect of pre-treatment of Mo by heating at 2500 degrees K. for a period up to 10 days, are discussed and the experimental results shown graphically.

537.533.8 2363

Effective Depth of Secondary-Electron Emission—N. D. Morgulis and N. G. Nakhodkin. (*Compt. Rend. Acad. Sci.* (*U.R.S.S.*), vol. 94, pp. 1029–1032, Feb. 21, 1954. In Russian.) An experimental investigation is reported. The principal conclusions are that the effective depth of secondary-electron emission is smaller in metals than in semiconductors, that it is independent of the primary-electron energy, and that there is no direct relation between the secondary-emission efficiency and the emission depth.

537.56:538.63 2364

Theory of Plasmas in the presence of a Constant Magnetic Field of Arbitrary Intensity superimposed on an Oscillating Electric Field—R. Jancel and T. Kahan. (*Compt. Rend. Acad. Sci.* (*Paris*), vol. 238, pp. 995–996; March 1, 1954.) Generalization of results obtained previously (2196 of July and back reference).

537.585:621.395.623.74 2365

Pressure Effects of Ionic Currents in Atmospheric Air with various Discharge Configurations—E. Löb. (*Arch. elekt. Übertragung*, vol. 8, pp. 85–90; Feb., 1954.) The mechanical pressures produced by steady and modulated ion currents were investigated theoretically for parallel-plate, concentric-sphere, and concentric-cylinder electrode systems and experimentally for a point-and-plate system. The agreement between theoretical and experimental results is good. The investigation is of interest in relation to the ionic loudspeaker.

538.114 2366

A Refinement of the Pauling Theory of Ferro-Magnetism—G. Felsenfeld. (*Proc. Nat. Acad. Sci., Wash.*, vol. 40, pp. 145–149; March, 1954.) The theory formulated by Pauling (3586 of 1953) is modified to take into account the nonuniform electron density in ferromagnetic crystals.

538.3 2367

Electrodynamics without Potentials—L. Infeld and J. Plebanski. (*Proc. Roy. Soc. A*, vol. 222, pp. 224–227; March 9, 1954.) By means of a more general approach based on the em field and not potential, field equations of a general type are derived. These contain the equations of Dirac's new theory of electrodynamics (1574 of 1952) as an important special case.

538.3 2368

Maxwell's Tensor—S. Slansky. (*Compt. Rend. Acad. Sci.* (*Paris*), vol. 238, pp. 1103–1104; March 8, 1954.) Without modifying the classical em field equations it is possible to replace Maxwell's tensor by another which gives the same expression for the Lorentz force but a different and in some ways more satisfactory expression for the distribution of energy in the field.

538.56:537.525 2369

Self-excitation of Oscillations in a Gas Discharge at High Pressures—M. E. Gertsenshtein. (*Zh. eksp. teor. Fiz.*, vol. 26, pp. 57–63; Jan, 1954.) The interaction of sound and electron waves in a gas-discharge plasma at pressures $\geqq 100$ mm Hg is considered theoretically. The possibility is shown of self-excitation of a definite range of frequencies. See also Zaitsev (2778 of 1952) for work at $\sim$/mm Hg.

538.566 2370

Group Velocity—P. Poincelot. (*Compt. Rend. Acad. Sci.* (*Paris*), vol. 238, pp. 1289–1291; March 22, 1954.) Continuation of previous work (3420 of 1952). Theory applicable to the ionosphere and to waveguides is given.

538.566:537.56 2371

The Excitation of Plasma Oscillations—D. H. Looney and S. C. Brown. (*Phys. Rev.*, vol. 93, pp. 965–969; March 1, 1954.) A beam of high-energy electrons, injected into the plasma of a dc discharge from an auxiliary electron gun, excited oscillations in the plasma, the standing-wave patterns set up for varying values of electron-beam density and thickness of the ion space-charge sheath being investigated by a movable probe. Discontinuous changes in oscillation frequency occurred as either the electron density or the sheath thickness was varied, but the frequencies were in accordance with the Tonks-Langmuir relation and Wehner's transit-time relation (2875 of 1951) in both cases. The results confirm that the mechanism of energy transfer involved is a vm process as suggested by Wehner, and indicate that the oscillation is a longitudinal pressure wave set up in the plasma electrons.

538.569.4 2372

Zeeman Effect and Line Breadth Studies of the Microwave Lines of Oxygen—R. M. Hill and W. Gordy. (*Phys. Rev.*, vol. 93, pp. 1019–1022; March 1, 1954.) Experiments with applied fields <100 gauss gave results in accordance with weak-field Zeeman theory. The two important mechanisms involved are rotational resonance interaction and quadrupole-quadrupole interaction.

538.569.4 2373

Absorption of U.H.F. Radio Waves in the Range 250–920 Mc/s by Substituted Benzenes: Part 3—D. K. Ghosh. (*Indian Jour. Phys.*, vol. 27, pp. 285–293; June, 1953.) Measurements have been made on chlorobenzene, bromobenzene, *o*-xylene and *m*-xylene at room and lower temperatures; the positions of absorption peaks are reported.

538.61 2374

Relations between Magneto-optical Phenomena in the Visible and Radio Regions of the Spectrum—A. Kastler. (*Compt. Rend. Acad. Sci.* (*Paris*), vol. 238, pp. 1007–1009; March 1, 1954.)

621.3.032.44 2375

The Distribution of Temperature along a Thin Rod Electrically Heated in Vacuo: Part 1—Theoretical—S. C. Jain and K. S. Krishnan. (*Proc. Roy. Soc. A*, vol. 222, pp. 167–180; March 9, 1954.) An integral expression derived for the temperature distribution can be expanded as a convergent power series. For evaluation two regions are defined: region *A*, in the middle of the rod, and region *B*, the portions outside *A*. In the *A* region temperature distribution is parabolic; in the *B* region it is practically the same as in the corresponding end region of an infinitely long rod. An analytical expression is obtained for the temperature at the centre of a rod as a function of its length. For a summary of the analysis see *Nature* (*London*), vol. 173, pp. 166–167; Jan. 23, 1954.

GEOPHYSICAL AND EXTRATERRESTRIAL PHENOMENA

523.7/.8:621.396.822 2376

Antenna and Receiver Measurements by Solar and Cosmic Noise—J. Aarons. (PROC. I.R.E., vol. 42, pp. 810–815; May, 1954.) The sun and various intense cosmic sources of rf radiation which have been previously measured are used as calibration sources for determining antenna patterns and receiver sensitivities for radio-astronomy investigations. Practical procedure is outlined. Inaccuracies are involved in evaluating background radiation, contours and solar energy distribution, but the technique is sufficiently accurate for checking field instruments.

523.72:621.396.822 2377

Radio Evidence of the Ejection of Very Fast Particles from the Sun—J. P. Wild, J. A. Roberts, and J. D. Murray. (*Nature* (*London*), vol. 173, pp. 532–534; March 20, 1954.) Dynamic spectra of Type-III rf bursts (fast frequency drift, duration 5–10 seconds) are discussed. The observations were made using a spectroscope with a frequency range 40–240 mc. Harmonic pairs are commonly observed, as in the case of the longer duration Type-II bursts previously studied [391 of February (Wild et al.)]; from a comparison of the profiles for the fundamental and the second harmonic it appears that a low-frequency cut-off process occurs in this case also. The observed properties of Type-III bursts can be accounted for by associating the frequency drift with motion of a disturbance such as a corpuscular stream traveling outwards through the solar atmosphere. Several possible mechanisms are considered.

532.72+523.8]:621.396.822:061.3 2378

Washington Conference on Radio Astronomy—1954—(*Jour. Geophys. Res.*, vol. 59, pp. 149–201; March, 1954.) The aim of the conference was to present a comprehensive survey of the present state of work in the field, to examine some of the most critical problems, and to indicate possible future lines of research. Summaries of some of the papers are given. For a short report see *Science*, vol. 119, pp. 588–591; April 30, 1954.

523.8:621.396.822 2379

Generation of Radio Noise by Cosmic Sources—J. H. Piddington and F. Hoyle. (*Nature* (*London*), vol. 173, pp. 482–484; March 13, 1954.) Critical comment on 125 of January and author's reply.

523.852.2:621.396.822]:523.165 2380

On the Nature of the Discrete Radio Source—R. Q. Twiss. (*Phil. Mag.*, vol. 45, pp. 249–258; March, 1954.) Investigation of results of measurements of radio noise from a source in Cassiopeia shows that the noise may be due to interaction of cosmic ray electrons with the local magnetic field if the average value of the latter is of the order of 10^{-2} gauss. The rf power received should then vary at least as rapidly as $\nu^{5/2}$ below a critical frequency in the range 10–20 mc.

550.372 2381

Effective Radio Ground-Conductivity Measurements in the United States—R. S. Kirby, J. C. Harman, F. M. Capps, and R. N. Jones. (*Nat. Bur. Stand. Circular* No. 546, 87 pp; Feb. 26, 1954.) The results of ground-conductivity determinations made at 621 broadcasting stations, at frequencies between 540 kc and 1.6 mc, are presented in a series of maps, more than 7000 radials being shown. The degree of correlation between the effective conductivity and the nature of the surface soil is insufficient for purposes of prediction.

550.381:537.12 2382

Electron Inertia and Terrestrial Magnetism—C. Darwin. (*Proc. Roy. Soc. A*, vol. 222, pp. 471–476; March 23, 1954.) Analysis shows that electron-inertia effects make no appreciable contribution to the geomagnetic field.

550.384 2383

The Areal Distribution of Geomagnetic Activity as an Aeromagnetic Survey Problem near the Auroral Zone—L. W. Morley. (*Trans. Amer. Geophys. Union*, vol. 34, pp. 836–840; Dec., 1953.)

550.384 2384

On the Dynamo Theory of Geomagnetic Field Variations—S. K. Chakrabarty and R. Pratap. (*Jour. Geophys. Res.*, vol. 59, pp. 1–14; March, 1954.) Chapman's expression for the current function is solved in the most general way, assuming that the main component in atmospheric oscillation is semidiurnal, and using the same conductivity function as Chapman. Tables of (*a*) coefficients of the current function, and (*b*) numerical equinoctial values of the coefficients deduced by the authors and by Chapman are given. The Sq variations of *H* and *V* are deduced and compared with the results of observations at Abinger and Alibag, and with Chapman's analysis. In these calculations, the phase of the atmospheric oscillations has been taken as 275 degrees, and results compare well with observations.

550.384.4 2385

The Lunar Diurnal Variations of the Earth's Magnetic Field for All Elements at Amberley, N. Z., based on Five Years' Observations—J. M. Bullen and C. H. Cummack. (*N. Z. J. Sci. Tech. B*, vol. 35, pp. 371–377; March, 1954.)

550.385 2386

Very Long Sequences of Geomagnetic Activity and its Annual Variation—B. N. Bhargava and A. M. Naqvi. (*Nature* (*London*), vol. 173, pp. 498–499; March 13, 1954.) A study was made of the recurrence tendency of geomagnetic activity for the period 1950–1953. Two long sequences of storms were identified, mainly associated with solar *M* regions. The mean recurrence period for each of the sequences was 27.05 days. Characteristic annual variation is attributed to the approach of the earth's projection on the solar disk towards the zones of maximum solar activity.

550.385:551.510.535:551.594.5 2387

Magnetic Storms, Aurorae, Ionosphere and Zodiacal Light—E. O. Hulburt. (*Sci. Mon.*, vol. 78, pp. 100–109; Feb., 1954.) General account of observed phenomena and review of theories which have been advanced in attempts to explain them.

551.510.5 2388

Study of Atmospheric Ions in a Nonequilibrium System—C. G. Stergis. (*Jour. Geophys. Res.*, vol. 59, pp. 63–66; March, 1954.) The variation with time of the concentration of small ions in the atmosphere in a nonequilibrium system has been determined theoretically and in two sets of experiments. If the atmosphere is relatively unpolluted, equilibrium conditions may not be restored after disturbance until a time of about 15 minutes has elapsed.

551.510.53 2389

The Dissociation of Oxygen in the High Atmosphere—M. Nicolet and P. Mange. (*Jour. Geophys. Res.*, vol. 59, pp. 15–45; March, 1954.) The O_2-O transition region is investigated, using recent rocket data on atmospheric transmission of solar radiation in the spectral region of the Schumann-Runge continuum of O_2. Observational data can be represented by a complete mixing of the atmosphere, which causes the vertical distribution of molecular oxygen to follow atmospheric scale height. Mixing and diffusing processes are responsible for a shift in the transition region to lower heights than given by photochemical equilibrium considerations, thus the transition region must be associated with the mesopause. Airglow, formation of ionosphere regions, and dissociation of nitrogen are briefly discussed in the light of this theory.

551.510.535 2390

Motion of the Storm-D Regions—V. Agy. (*Nature* (*London*), vol. 173, pp. 445–446; March 6, 1954.) Results of an analysis at the National Bureau of Standards of ionosphere data from 17 stations for the four years 1949–1952 do not support Piggott's hypothesis of coherent motion of storm-D regions (1672 of 1953)

551.510.535 2391

Propagation of a Plane Aerodynamic Wave of Semidiurnal Oscillation Period through a Plane Ionosphere in a Uniform Magnetic Field—I. Lucas. (*Arch. elekt. Übertragung*, vol. 8, pp. 91–95; Feb., 1954.) Analysis is based on the momentum equation for the gas and the tensor equation of electric conduction derived earlier [2085 of July (Lucas and Schlüter)]. Frequency and wavelength correspond to the atmospheric oscillations caused by tidal effects of the sun and the moon. The solution indicates that em damping of the atmospheric oscillations will occur at >300 km height. The electrical conductivity in a horizontal and in a vertical magnetic field is expressed as a function of the neutral-gas density.

551.510.535:550.38 2392

Dynamo Theory of Geomagnetic Tides—I. Lucas. (*Arch. elekt. Übertragung*, vol. 8, pp. 123–131; March, 1954.) Plasma theory and results of earlier analysis [2085 of July (Lucas and Schlüter)] are applied in deriving a differential equation expressing height-integrated ionospheric current as a function of latitude. Taking account of Coriolis forces and assuming a velocity amplitude of 60 cm/s for tidal oscillations at *E*-layer height, the calculated magnitude of geomagnetic tides is in agreement with recorded data, in particular as regards the large tidal amplitudes at the magnetic equator. The theory is consistent with the assumption that the negative particles in the *E* layer are predominantly electrons rather than ions.

551.510.535:551.55 2393

Ionospheric Wind Analysis by Meteoric Echo Techniques—L. A. Manning, A. M. Peterson, and O. G. Villard, Jr. (*Jour. Geophys. Res.*, vol. 59, pp. 47–62; March, 1954.) The procedure for finding vector average wind (3052 of 1950) is shown to be unaffected by the presence of turbulent wind components. Expressions are derived for the rms values of the horizontal and vertical wind components. Sources of errors are discussed in detail.

551.510.535:551.55:550.384 2394

Winds in the Upper Atmosphere deduced from the Dynamo Theory of Geomagnetic Disturbance—E. H. Vestine. (*Jour. Geophys. Res.*, vol. 59, pp. 93–128; March, 1954.) Simple dynamo theory of winds moving along and perpendicular to the geomagnetic field is developed, and various wind systems are discussed which might account for certain phases of magnetic storms. A possible wind system for the main phase of a magnetic storm shows some measure of agreement with diurnal atmospheric motions deduced from radio-star scintillations and auroral motions. The role of such wind systems in modifying the effective transverse conductivity of the ionosphere is uncertain. Both the flux of X rays producing ionization and the dynamo airflow in the *E* region are apparently the same on days of magnetic storms as on days prior to them.

551.510.535:551.594.5:550.384 2395

Correlation of Magnetic, Auroral, and Ionospheric Variations at Saskatoon: Part 2—J. H. Meek. (*Jour. Geophys. Res.*, vol. 59, pp. 87–92; March, 1954.) "The relations between magnetic, auroral, and ionospheric observations are summarized with reference to the occurrence of positive and negative magnetic bays. Auroral light associated with positive bays occurs at a higher geomagnetic latitude than that associated with negative bays. The magnetic and auroral light variations are compared to Martyn's theory of the aurora. If the latter is accepted, the conclusion is reached (1) that most aurora is caused by positively charged particles, and (2) that the conditions described for the early phase actually exist throughout most of a disturbance." Part 1: 1768 of June.

551.510.535:621.396.11.029.5 2396

Some Results of Sweep-Frequency Investigation in the Low-Frequency Band—J. M. Watts and J. N. Brown. (*Jour. Geophys. Res.*, vol. 59, pp. 71–86; March, 1954.) Frequency-sweep measurements in the range 50–1100 kc are reported. Day-time records show traces of three strata whose virtual heights are between 70 and 110 km, of which the lowest—not always observed—produces only a weak echo and one sometimes suggesting that scattering is taking place at randomly located clouds. Night-time records show an intermediate layer between the *E* and *F* layers, which is erratic in appearance, but seems to have continuity with the daytime *E* layer during sunset. Traces characteristic of magneto-ionic splitting are exhibited for this intermediate layer. Polarization and virtual-height records for the *F* layer at night are shown and the effects of moderate ionosphere disturbances are demonstrated.

551.510.535:[621.396.822:523.8 2397

Influence of the Ionosphere on the Reception of Galactic Radiation of Frequency 29.5 Mc/s—É. J. Blum, J. F. Denisse, and J. L. Steinberg. (*Compt. Rend. Acad. Sci.* (*Paris*), vol. 238, pp. 1695–1697; April 26, 1954.) Analysis of continuous measurements recorded at Marcoussis from May, 1949 to April, 1950 indicates that galactic radiation at 29.5 mc is attenuated by the ionosphere, the effect being due partly to the F_2 layer and partly to the *D* layer. The results agree qualitatively with those obtained by Mitra and Shain (1426 of May) using a frequency of 18.3 mc.

551.578.1:621.396.96 2398

Errors inherent in the Radar Measurement of Rainfall at Attenuating Wavelengths—Hitschfeld and Bordan. (*See* 2404.)

551.578.4:621.396.96 2399

Radar Evidence of a Generating Level for Snow—Gunn, Langleben, A. S. Dennis, and B. A. Power. (*See* 2405.)

551.594:621.396.11.029.62 2400

Atmospheric Electricity and Long-Distance Very-High-Frequency Scatter Transmissions—Isted. (*See* 2497.)

551.594.13 2401

The Electrical Conductivity of the Atmosphere over the Pacific Ocean—S. C. Coroniti and E. Heaton. (*Trans. Amer. Geophys. Union*, vol. 34, pp. 833–835; Dec. 1953.) Conductivity measurements were made at altitudes of 3.8, 5.2, and 6.4 km and between geomagnetic latitudes of 22 degrees and 45 degrees N. The rate of production of ion pairs computed from the measurements agrees well with that computed from cosmic-ray data.

551.594.6:621.372.8 2402

Propagation of a Pulse in a Waveguide—Cotte. (*See* 2306.)

LOCATION AND AIDS TO NAVIGATION

621.396.93 2403

Re-radiation from Resonant Ship's Aerials—J. H. Moon. (*Marconi Rev.*, vol. 17, pp. 61–63; 2nd Quarter, 1954.) Experiments show that it is not always necessary to isolate other antennas on board when operating the direction finder. An indication is given of the distances at which various types of antenna may be used at the same time as the direction finder without impairing its accuracy.

621.396.96:551.578.1 2404

Errors inherent in the Radar Measurement of Rainfall at Attenuating Wavelengths—W. Hitschfeld and J. Bordan. (*Jour. Met.*, vol. 11, pp. 58–67; Feb., 1954.) An equation is derived giving rainfall rate at a given range in terms of received power level; this equation takes account of attenuation due to intervening rain, and includes a calibration constant expressing the radar performance. At attenuating wavelengths (3 cm and, to a lesser extent, 5.6 cm) a small error in this constant causes a large error in the result. Correcting for attenuation is therefore not recommended unless the calibration error can be held within very narrow limits.

621.396.96:551.578.4 2405

Radar Evidence of a Generating Level for Snow—E. L. S. Gunn, M. P. Langleben, A. S. Dennis, and B. A. Power. (*Jour. Met.*, vol. 11, pp. 20–26; Feb., 1954.) An analysis is presented of precipitation patterns obtained during the winter of 1951–1952 on an AN/TPS-10A radar at Montreal Airport. Trail patterns were observed on 19 out of 22 days; on 13 stable days well defined snow trails were detected.

621.396.96:621.396.67 2406

General Theory of Plane-Wave Scattering from Finite, Conducting Obstacles with Application to the Two-Antenna Problems—Storer and Sevick. (*See* 2312.)

621.396.962.33 2407

The L.C.T. [Laboratoire Central de Télécommunications] Radar Receiver with Elimination of Fixed-Target Echoes—H. Tanter. (*Onde élect.*, vol. 34, pp. 99–109; Feb., 1954.) Description of 10-cm phase-comparison pulse radar equipment. Two types are in production: a single receiver for mobile use and a 3-receiver unit for master stations. Theoretical sensitivity and practical performance in respect of range, fixed-target echo elimination and "visibility" factor for moving targets are discussed.

621.396.963.3 2408

Information Cells on Intensity-Modulated C.R.T. Screens—D. Levine. (Proc. I.R.E., vol. 42, p. 853; May, 1954.) Correction to paper abstracted in 743 of March.

MATERIALS AND SUBSIDIARY TECHNIQUES

536.587:548.55:546.289 2409

Temperature Regulator used in Producing Germanium Crystals—G. J. Lehmann and C. A. Meuleau. (*Elect. Commun.*, vol. 31, pp. 19–26; March, 1954.) English version of paper abstracted in 1788 of June.

537.226 2410

Ferroelectricity and Crystal Structure: Part 2—H. D. Megaw. (*Acta Cryst.*, *Camb.*, vol. 7, Part 2, pp. 187–194; Feb. 10, 1954.) Part 2 of 1789 of June.

537.228.1:548.0 2411

Piezoelectric Crystals—S. Kelly. (*Wireless World*, vol. 60, pp. 275–280 and 345–348; June /July, 1954.) A survey of properties and applications. Two main classes are distinguished, for use (*a*) as resonators, (*b*) as transducers. Attention is devoted particularly to materials for gramophone pickups, viz., Rochelle salt, ADP and polycrystalline $BaTiO_3$.

537.311.33 2412

Intermetallic Semiconductors—E. W. Saker and F. A. Cunnell. (*Research* (*London*), vol. 7, pp. 114–120; March, 1954.) A simple account is given of the various types of binding forces in solid elements and binary compounds or alloys. The characteristics of the compounds between the metals and the "near-metals" of Groups IVB, VB, and VIB of the periodic table are discussed in terms of the binding forces. For transistor production, compounds from groups III and V have the important advantages of wider energy gaps than Ge and lower melting points than Si.

537.311.33 2413

Band Structure in Disordered Alloys and Impurity Semiconductors—H. M. James and A. S. Ginzbarg. (*Jour. Phys. Chem.*, vol. 57, pp. 840–847; Nov., 1953. Discussion, pp. 847–848.) The band structure is treated by a method which involves counting the number of nodes in a solution of the wave equation with energy E as a means of determining how many states of the system have energies lower than E. An illustrative example shows how the sharply defined "impurity band" of a crystal with regularly placed impurities is replaced by a broadened region of high energy-level density when the impurities are randomly arranged.

537.311.33:535.215:538.639 2414

Theory of the Photomagnetomechanical Effect—P. Aigrain and O. Garreta. (*Compt. Rend. Acad. Sci.* (*Paris*), vol. 238, pp. 1573–1575; April 12, 1954.) From theory previously given [2015 of 1953 (Aigrain and Bulliard)] it is predicted that even in a uniform magnetic field the currents produced in a semiconductor by illuminating its surface will give rise to a mechanical couple. The estimated value for a Ge cylinder of height 2 cm and diameter 0.5 cm, illuminated over a quarter of its surface at an intensity of 5×10^{17} photons/cm²/s, is 0.25 dyne.cm for a field strength of 6000 gauss.

537.311.33:535.37 2415

Luminescence of Carborundum Crystals on Passage of Current—M. Schön. (*Z. Naturf.*, vol. 8a, pp. 442–446; July, 1953.) The observed luminescence is attributed to the recombination of electrons and holes at lattice defects, the process being the inverse of that occurring in crystal phosphors. The energy diagram is established, and a formula is derived for the light yield. The relative importance of recombinations in the n, p and junction regions is examined. Luminescence intensity is proportional to current intensity for high values of the latter; there is a threshold value below which no luminescence occurs. The temperature dependence of this threshold, of the slope of the luminescence/current curve, and of the luminescence spectrum is discussed.

537.311.33:537.29 2416

Theory of the Effect of a Strong Field in Semiconductors—A. I. Gubanov. (*Zh. tekh. Fiz.*, vol. 24, pp. 308–319; Feb., 1954.) A short survey including experimental and theoretical work published in Russia up to 1953. The thermoelectron and impact ionization mechanisms of the strong-field effect are considered and relevant formulas are given. Frenkel's thermoelectron-ionization theory is generalized to include the case of an exponential dependence of the electron energy on its distance from the center binding the electron. The image forces occurring in the theory of solid rectifiers are calculated.

537.311.33:[546.28+546.289 2417

Segregation of Impurities during the Growth of Germanium and Silicon Crystals—R. N. Hall. (*Jour. Phys. Chem.*, vol. 57, pp. 836–839; Nov., 1953. Discussion, p. 839.) "The segregation factors of impurities picked up by a growing crystal of germanium or silicon have been found to depend upon the growth rate and crystal orientation as well as upon the degree of stirring in the melt. This dependence is generally much greater for donor impurities than it is for acceptors and makes possible the growth of crystals containing large numbers of p-n junctions suitable for use in rectifiers and transistors. The assumption that impurity atoms are preferentially adsorbed at the surface of the crystal leads to an expression for the growth-rate variation which is consistent with the experimental results. Calculated impurity distributions are presented for a number of periodic growth cycles of practical interest."

537.311.33:[546.28+546.289 2418

Piezoresistance Effect in Germanium and Silicon—C. S. Smith. (*Phys. Rev.*, vol. 94, pp. 42–49; April 1, 1954.) The complete tensor piezoresistance has been determined experimentally for n- and p-type Si and Ge, and expressed in terms of the pressure coefficient of resistivity and two simple shear coefficients. One of the shear coefficients for each material is exceptionally large and cannot be explained in terms of known mechanisms. An electron transfer effect due to the structure of the energy bands in Si and Ge could account for this, but for p-type Ge an additional mechanism must be envisaged.

537.311.33:[546.28+546.289 2419

Equilibrium Thermochemistry of Solid and Liquid Alloys of Germanium and of Silicon: Part 1—The Solubility of Ge and Si in Elements of Groups III, IV and V—C. D. Thurmond. (*Jour. Phys. Chem.*, vol. 57, pp. 827–830; Nov., 1953. Discussion, p. 830.)

537.311.33:[546.28+546.289 2420

Equilibrium Thermochemistry of Solid and Liquid Alloys of Germanium and of Silicon: Part 2—The Retrograde Solid Solubilities of Sb in Ge, Cu in Ge, and Cu in Si—C. D. Thurmond and J. D. Struthers. (*Jour. Phys. Chem.*, vol. 57, pp. 831–834; Nov., 1953. Discussion, pp. 834–835.)

537.311.33:546.28 2421

Drift Mobilities in Semiconductors: Part 2—Silicon—M. B. Prince. (*Phys. Rev.*, vol. 93, pp. 1204–1206; March 15, 1954.) The drift mobilities of holes in n-type and of electrons in p-type material were measured for specimens with a range of resistivities from 0.3 to 30Ω cm at 300 degrees K. For single crystals of resistivity >10Ω cm the mobility at 300 degrees K. of holes is $\mu_p=500\pm50$ cm/s per V/cm and of electrons is $\mu_n=1200\pm100$ cm/s per V/cm. The temperature dependence of mobility measured on two specimens of resistivity >10Ω cm, is given by $\mu_n=5.5\times10^6T^{-1.5}$ and $\mu_p=2.4\times10^8T^{-2.3}$. Part 1: 1462 of May.

537.311.33:546.28 2422

Optical Investigations of Impurity Levels in Silicon—E. Burstein, E. E. Bell, J. W. Davisson, and M. Lax. (*Jour. Phys. Chem.*, vol. 57, pp. 849–852; Nov., 1953. Discussion, p. 852.) Measurements were made on a number of p-type specimens, including boron-doped single crystals, over the range 2-38 μ. Ionization energies of impurities and excited states of the impurity atoms are reported.

537.311.33:546.289 2423

Directional Properties of the Cyclotron Resonance in Germanium—B. Lax, H. J. Zeiger, R. N. Dexter, and E. S. Rosenblum. (*Phys. Rev.*, vol. 93, pp. 1418–1420; March 15, 1954.) Measurements were made at 8.895 kmc at 4.2 degrees K. on n- and p-type Ge. For n-type Ge the resonance-curve shape depends on sample orientation, but not on sample shape or size. Results can be explained by a conduction-band structure in which the energy surfaces consist of eight ellipsoids of revolution lying along the [111] axes.

537.311.33:546.289 2424

Changes of Surface Conductivity of Germanium with Ambient—S. R. Morrison. (*Jour. Phys. Chem.*, vol. 57, pp. 860–863; Nov., 1953. Discussion, p. 863.) The influence of the ambient medium on the conductivity and change in contact potential on illumination was investigated experimentally. The results are compared with those obtained by Brattain and Bardeen (1698 of 1953). The conductivity changes can be correlated with changes in a space-charge layer at the free surface of the semi-conductor.

537.311.33:546.289 2425

Theory of the Galvanomagnetic Effects in n-Germanium—S. Meiboom and B. Abeles. (*Phys. Rev.*, vol. 93, p. 1121; March 1, 1954.) Calculations of magnetoresistance coefficients, based on stated assumptions, agree very well with values measured at room temperature by Pearson and Suhl (166 of 1952), but agreement is less good with measurements made at 77 degrees K.

537.311.33:546.289 2426

Infrared Absorption, Photoconductivity, and Impurity States in Germanium—W. Kaiser and H. Y. Fan. (*Phys. Rev.*, vol. 93, pp. 977–980; March 1, 1954.) "Photoconductivity in gold-doped germanium at liquid nitrogen and liquid helium temperatures shows a long wavelength tail beyond the fundamental absorption edge, which falls off sharply at about 6 microns corresponding to 0.21 ev. This value agrees well with the acceptor activation energy determined by electrical measurements. For copper-doped germanium at low temperatures both absorption and photoconductivity show a maximum at about 22 microns corresponding to 0.055 ev. This value also agrees with the acceptor activation energy given by Hall effect measurements. At room temperature more absorption is found in the region 2 to 5 microns as compared to *p*-type germanium doped with indium and aluminum. This is likely to be due to photoionization from a deeper level 0.25 ev above the valence band."

537.311.33:546.289 2427

Experimental Evidence concerning Degeneracy in Germanium—E. M. Conwell. (*Phys. Rev.*, vol. 93, p. 1118; March 1, 1954.) Comment on 1465 of May (Adams).

537.311.33:546.289 2428

Calculation of the Energy-Band Structures of the Diamond and Germanium Crystals by the Method of Orthogonalized Plane Waves—F. Herman. (*Phys. Rev.*, vol. 93, pp. 1214–1225; March 15, 1954.)

537.311.33:546.289 2429

Effect of Nickel and Copper Impurities on the Recombination of Holes and Electrons in Germanium—J. A. Burton, G. W. Hull, F. J. Morin, and J. C. Severiens. (*Jour. Phys. Chem.*, vol. 57, pp. 853–859; Nov., 1953. Discussion, p. 859.) "Nickel and copper impurities are found to increase the rate of recombination of holes and electrons in germanium single crystals. The measured dependence of lifetime on resistivity at room temperature is consistent with the Shockley-Read-Hall theory of recombination at traps near the middle of the forbidden band. The capture cross-sections for holes and electrons have been estimated for these traps produced by nickel and copper. Additional evidence for such traps is also given by conductivity, Hall effect, photoconductivity and optical absorption measurements. Nickel or copper contaminations of the order of 10^{-10} atom fraction could account for the recombination rates observed in ordinary germanium crystals at room temperature."

537.311.33:546.289 2430

Diffusivity and Solubility of Copper in Germanium—C. S. Fuller, J. D. Struthers, J. A. Ditzenberger, and K. B. Wolfstirn. (*Phys. Rev.*, vol. 93, pp. 1182–1189; March 15, 1954.) Measurements were made in the temperature range 700 degrees to 900 degrees C. both by resistivity and radioactivity methods. The average diffusivity is $2.8 \pm 0.3 \times 10^{-5}$ cm²/sec and the solubility has a maximum at about 875 degrees C. of 4.0×10^{16} atoms of Cu per cm³. Results support the conclusion that one Cu atom contributes one conducting hole at room temperature. The thermal conversion effect in Ge is explained by a temperature-dependent solution and precipitation of Cu. Acceptor and diffusion properties of Cu in Ge are accounted for by decreased electron affinity of Cu at higher temperatures.

537.311.33:546.289 2431

Transmission of Electrons and Holes across a Twin Boundary in Germanium—E. Billig and M. S. Ridout. (*Nature* (*London*), vol. 173, pp. 496–497; March 13, 1954.) The technique developed by Haynes and Shockley (2109 of 1949) for investigating the diffusion of minority carriers in an ambipolar semiconductor is used. A slice about 0.5 mm thick was cut from a single crystal of *n*-type Ge, with the twinning plane perpendicular to the surface. Graphs are presented of the variation of the signal picked up by a probe as its distance from an interrupted infrared illuminating spot is varied. The results indicate that twin boundaries do not impede the passage of electrons or holes to any appreciable extent.

537.311.33:546.561–31 2432

The Semiconductor Properties of Cu_2O: Part 8—Electrical Conductivity at 0 degrees C. as Function of Position inside Specimen—C. Fritzsche. (*Ann. Phys., Lpz.*, vol. 14, pp. 135–140; Feb. 15, 1954.) An increase of conductivity with distance from the surface of the sample was observed and was found to have been produced by the particular cooling process used in the preparation of the sample. The results are discussed. Part 7: 438 of February (Nieke).

537.311.33:546.723–31 2433

Electrical Properties of α-Fe_2O_2—F. J. Morin. (*Phys. Rev.*, vol. 93, pp. 1195–1199; March 15, 1954.) Measurements reported in 1009 of 1952 are discussed. A theoretical model giving quantitative agreement with experimental data assumes conduction to involve only electrons and holes in the *d* levels of Fe ions. Another model giving qualitative fit assumes conduction in the *sp* bands of oxygen in addition.

537.311.33:546.74–31 2434

Electrical Properties of NiO—F. J. Morin. (*Phys. Rev.*, vol. 93, pp. 1199–1204; March 15, 1954.) Measurements of the conductivity, Seebeck effect and optical transmission of NiO are reported and discussed on the basis of the two models suggested in 2433 above. NiO like αFe_2O_3 is an oxide with partially filled *d* levels, but with simpler characteristics. The first model gives quantitative agreement with experiment, the second does not.

537.311.33:546.812:539.231 2435

Transparent Semiconducting Oxide Films—R. E. Aitchison. (*Aust. Jour. Appl. Sci.*, vol. 5, pp. 10–17; March, 1954.) Highly transparent tin oxide films with a surface resistance between 50 and 10,000 Ω/square have been prepared by spraying a mixture of $SnCl_4$ and organic alcohol or acid onto heated glass. Pure SnO layers have a negative temperature coefficient of resistance; this is increased by addition of In_2O_3 and decreased by addition of Sb_2O_5. Measurements of transparency and resistance are reported; effects of impurities are discussed. Applications to electrical screening, electroluminescent panels etc. are mentioned.

537.311.33:546.817.221 2436

Further Evidence for the Energy Gap of Lead Sulfide—G. R. Mitchell and A. E. Goldberg. (*Phys. Rev.*, vol. 93, pp. 1421; March 15, 1954.) The wavelength dependence of the photovoltaic effect in a *p-n* junction in a synthetic single crystal indicates an energy gap of 0.4 ev, in agreement with measurements on the photoelectromagnetic effect in galena and the long-wavelength limit for thin films.

537.311.33:621.372.413 2437

A Resonant-Cavity Study of Semiconductors—Hsi-Teh Hsieh, J. M. Goldey, and S. C. Brown. (*Jour. Appl. Phys.*, vol. 25, pp. 302–307; March, 1954.) A solution of Maxwell's equations is obtained for a resonant cavity with an axial post of arbitrary electrical properties. This gives the dielectric coefficient and conductivity of the post in terms of the natural frequency and *Q* of the cavity. In the region of a particular value of conductivity, a relatively small change in conductivity gives rise to a transition from a cylindrical to a coaxial mode. The theory is particularly useful in the study of semiconductors.

537.311.33:621.396.822 2438

Noise in Semiconductors: Spectrum of a Two-Parameter Random Signal—S. Machlup. (*Jour. Appl. Phys.*, vol. 25, pp. 341–343; March, 1954.) The spectrum is calculated of a random signal which may be in one of two states, where the mean lives σ and τ of the two states may be different. The form of the spectrum is the same as for the case of equal lives, the single parameter occurring in that case being replaced by $2[(1/\sigma)+(1/\tau)]^{-1}$. Application of the results to a consideration of noise in semiconductors shows that the assumption that trapping and releasing of carriers are uncorrelated processes is a good approximation provided the mean time during which a carrier is trapped is long compared with the mean time during which it is free to move. Hence trapping may be the process responsible for the current-dependent noise.

537.311.33:669–492.2 2439

The Electrical Conductance of Pressed Powders, in Particular of Zinc Oxide—J. C. M. Brentano and C. Goldberg. (*Phys. Rev.*, vol. 94, pp. 56–60; April 1, 1954.) Experiments are described, mainly on ZnO, in which the dc conductance of the powder pressed between parallel plates in an evacuated chamber is determined for different pressures and temperatures. A model based on the change of the energy gaps with pressure is developed which accounts for the phenomena observed. Transient changes of conductance with time are observed for which only tentative explanations are suggested.

538.221 2440

Variation of the Permeability of Irons and Steels as a Function of Mechanical Stresses—J. Creusot. (*Compt. Rend. Acad. Sci.* (*Paris*), vol. 238, pp. 1203–1205; March 15, 1954.) Curves representing $B = f(T)$, obtained from measurements of the induction *B* of specimens subjected to a constant magnetizing field and a variable tensile stress *T*, in some cases exhibit plateaus. The occurrence of these is related to the existence of the maximum-stability equilibrium state [1102 of April (Creusot and Langevine)] in the specimen.

538.221:538.67 2441

Magnetic Domains by the Longitudinal Kerr Effect—C. A. Fowler, Jr., and E. M. Fryer. (*Phys. Rev.*, vol. 94, pp. 52–56; April 1, 1954.) Rotation of the polarization plane of obliquely incident light reflected from a polished SiFe single crystal revealed the antiparallel domains lying in the surface.

538.221:546.74 2442

Magnetic Behaviour of Thin Single-Crystal Nickel Films—L. E. Collins and O. S. Heavens. (*Phil. Mag.*, vol. 45, pp. 283–289; March, 1954.) The coercivity of monocrystalline Ni films grown epitaxially on the (100) face of rocksalt was studied as a function of thickness over the range 200–1000 Å. The high coercivity characteristic of a single-domain structure was observed and the maximum value agrees approximately with that calculated from the anisotropy-constants.

538.221:[621.318.134+621.318.134 2443

Investigation of Paramagnetism of Some Ferrites—F. Gal'perin, G. Dimtrakova, and L. Molodtsova. (*Compt. Rend. Acad. Sci.* (*U.R.S.S.*), vol. 94, pp. 833–834; Feb. 11, 1954. In Russian.) Results are given graphically of magnetic-susceptibility determinations for $MnO \cdot Fe_2O_2$, $MgO \cdot Fe_2O_3$ and $CoO \cdot Fe_2O_3$, at temperatures between about 100 degrees and 1200 degrees K.

538.221:621.318.13 2444

Dependence of the Coercivity of Magnetically Soft Materials on the Thickness of the Lamination—V. A. Zaikova and Ya. S. Shur. (*Compt. Rend. Sci.* (*U.R.S.S.*), vol. 94, pp.663–665; Feb. 1, 1954. In Russian.) Experimental investigation of the coercivity of laminations of Fe, Ni, Fe-Ni alloys with 36–87 per cent Ni, and Fe-Si alloys with 1–4 per cent Si. In all cases but one, a critical thickness between 0.03

and 0.07 mm was found, below which the coercivity increases very rapidly. The results are shown graphically and are tabulated.

538.221:621.318.134 2445

Relaxation Phenomena of Irreversible Magnetization Processes in High-Permeability Ferrites—T. Einsele. (*Z. angew. Phys.*, vol. 6, pp. 70–80; Feb., 1954.) Results of pulse measurements on ferroxcube IVB, siferrit and permenorm (1826 of June) are analyzed. Relaxation phenomena of irreversible processes can be expressed by a simple power law. Determination of the relaxation time τ of reversible magnetization by a dc pulse technique is only possible under certain conditions. The magnetization of a ferrite with a linear rising branch to the static hysteresis loop can be resolved into reversible and irreversible components; in this case τ can be determined and conforms to results of ac measurements.

538.221:621.318.134 2446

Temperature Dependence of Ferromagnetic Resonance Line Width in a Nickel Iron Ferrite: a New Loss Mechanism—J. K. Galt, W. A. Yager, and F. R. Merritt. (*Phys. Rev.*, vol. 93, pp. 1119–1120; March 1, 1954.) The ferromagnetic-resonance line width for the [111] direction was measured on two single-crystal spheres of a Ni-Fe ferrite at 24 kmc over the temperature range 4–400 degrees K. Results for temperatures below room temperature suggest that a major cause of losses in many ferrites is the relaxation associated with crystallographic transitions characterized primarily by electronic rearrangements.

546.289:548.55 2447

Recrystallization of Germanium from Indium Solution—J. I. Pankove. (*RCA Rev.*, vol. 15, pp. 75–85; March, 1954.) A detailed description, illustrated with photographs, is given of the nature of the crystal growth obtained on cooling a Ge-in-In solution in contact with a Ge single crystal. The homogeneous recrystallized *p*-type region forms a single crystal with the original *n*-type seed. The *p-n* junction appears to coincide with the alloy front, the transition between the *n* and *p* regions being very abrupt. The recrystallized region is of very low resistivity.

546.561:535.215 2448

Negative Photoconductivity of Cuprite—A. N. Krongauz and V. K. Lyapidevski. (*Zh. eksp. teor. Fiz.*, vol. 26, pp. 115–119; Jan., 1954.) The dependence of the photoconductivity on the voltage applied across the crystal and on the illumination intensity was investigated experimentally; the results are shown graphically. For every value of the illumination intensity there is a corresponding value of applied voltage above which the current variation due to the illumination changes from positive to negative. An explanation is given in terms of the number of electrons in the conduction band. The theoretical formulas are in agreement with experimental results.

546.681 2449

Gallium Purification by Single Crystal Growth—W. Zimmerman, III. (*Science*, vol. 119, pp. 411–412; March 26, 1954.) High-purity Ga required for investigations of intermetallic compounds was obtained by the recrystallization method involving zone purification and single-crystal growth, using the Kryropoulos technique.

546.719 2450

Rhenium Metal—its Properties and Future—L. W. Kates. (*Mater. & Meth.*, vol. 39, pp. 88–91; March, 1954.) Rhenium is a ductile metal resembling Mn chemically and W physically. In the field of electronics it may prove useful for the manufacture of contacts, thermocouple alloys, cathodes and cathode heaters. Its resistivity at high temperature is greater than that of W, thus permitting use of more rugged filaments. Re is still relatively rare; it does not occur as a massive mineral but is found as a minor constituent in molybdenite, and can be recovered from flue dust from molybdenum-bearing copper ore.

621.315.612 2451

Reduction in the Loss Factor of Certain Ceramics by Heat Treatment—H. Rawson. (*Nature* (*London*), vol. 173, p. 447; March 6, 1954.) Measurement of the dielectric constant and loss tangent of steatite, forsterite and other ceramics before and after treatment for 60 hr at 1000 degrees C. are reported. It is suggested that this type of heat treatment will make possible the commercial production of ceramics with reduced losses.

621.315.612.6:537.226 2452

Dielectric Losses in Silicate Glasses—V. A. Ioffe. (*Zh. tekh. Fiz.*, vol. 24, pp. 611–621; April, 1954.) The temperature dependence of the loss angle was determined experimentally at 1 mc in the range 12–420 degrees K. for K_2O-, Na_2O-, PbO-, PbO-MgO-, Na_2O-K_2O-, and PbO-TiO_2- silicate glasses. Measurements were also made at 3×10^5 and 3×10^6 cps. The relation between loss angle and composition at 8.78×10^9 cps and at room temperature was determined for the first three types of glasses. Results are shown graphically.

621.315.613.1 2453

Electrical Properties of Indian Mica: Part 5—D.C. Resistivity—S. S. Mandal and P. C. Mahanti. (*Indian Jour. Phys.*, vol. 27, pp. 294–304; June, 1953.) Report of measurements of volume and surface resistivity of various qualities of red and green muscovite micas. The influence of humidity, temperature and preheating is investigated.

621.315.616.96 2454

Epoxy Resins—R. A. Johnson. (*Electronic Eng.*, vol. 26, pp. 136–142; April, 1954.) A survey of the properties and applications of araldite casting resins, covering Type B and the more recently developed Types D, F, 33/896 (flexible), 33/912 (expanded) and 33/915 (impregnating).

666.3:621.791.3 2455

Ceramic-Metal Seals of the Tungsten-Iron Type—D. G. Burnside. (*RCA Rev.*, vol. 15, pp. 46–61; March, 1954.) Ceramic-to-metal sealing processes used in tube manufacture are briefly reviewed and desirable properties of the ceramics and sealing metals are indicated. A method is described for obtaining a firmly adherent bonding layer on the ceramic surface by brushing or spraying on a mixture of W and Fe powders and firing in a reducing atmosphere.

669.15.71 2456

16-Per cent Aluminum-Iron Alloy Cold Rolled in the Order-Disorder Temperature Range—J. F. Nachman and W. J. Buehler. (*Jour. Appl. Phys.*, vol. 25, pp. 307–313; March, 1954.) Cold rolling at 575 degrees C. of hot-rolled material gave an alloy of highly fibred structure having good resistance to oxidation and good magnetic properties.

MATHEMATICS

519.272.119 2457

Estimation of Correlation Coefficients from Scatter Diagrams—G. R. Sugar. (*Jour. Appl. Phys.*, vol. 25, pp. 354–357; March, 1954.)

517.63(083.5) 2458

Tables of Coefficients for the Numerical Calculation of Laplace Transforms. [Book Review]—H. E. Salzer. Publishers: United States Department of Commerce, Washington, 1953, 36 pp., 25 cents. (*Beama Jour.*, vol. 61, p. 96; March, 1954.) "A very useful set of tables for those working in the field of transient and nonlinear phenomena."

MEASUREMENTS AND TEST GEAR

621.317:621.383.2 2459

The Photodianode: Investigation of the Total Current and of the Differential Current in an Asymmetrical Arrangement—Deloffre, Pierre and Roig. (*See* 2543.)

621.317.3:621.315.212 2460

Coaxial Radio-Frequency Connectors and their Electrical Quality—M. C. Selby, E. C. Wolzien, and R. M. Jickling. (*Jour. Res. Nat. Bur. Stand.*, vol. 52, pp. 121–132; March, 1954.) Errors due to connectors used in impedance measurements made by the slotted-line technique are discussed. A definition is given of the connector as a component part of a connecting transformer which is completed by a supplementary line section; when the connecting transformer is short-circuited at either end a voltage node appears at the other end. The quality of the connectors is indicated by the transformation corrections needed to obtain accurate termination admittances. Node-shift methods are described for finding these corrections for various types of connector. Typical measurement results are presented for frequencies from 100 to 900 mc. The technique is also useful for determining the quality of lines.

621.317.3.029.3(083.74) 2461

I.R.E. Standards on American Recommended Practice for Volume Measurements of Electrical Speech and Program Waves, 1953—(PROC. I.R.E., vol. 42, pp. 815–817; May, 1954.) Standard 53 I.R.E. 3S2.

621.317.328.029.62:621.396.67 2462

An Experimental Field-Strength Meter for Band III—G. T. Clack. (*Jour. Telev. Soc.*, vol. 7, pp. 205–210; Jan./March, 1954.) A detailed description, with component values, is given of the circuit of a receiver for measurements of antenna gain and directivity at frequencies from 170 to 220 mc. Input sockets are provided for 80-Ω and 300-Ω termination. The design provides for interchangeable tuning units for different bands. An IF of 34 mc is used. Field tests with several types of antenna are reported, and the effect on the polar diagram of varying the spacing and length of a parasitic element is illustrated.

621.317.34.018.75:621.315.212 2463

Equipment for Measuring the Elongation of a Short-Duration Signal—J. Bendayan. (*Onde élect.*, vol. 34, pp. 153–162; Feb., 1954.) Elongation of a pulse trace due to double reflection is used to assess the over-all effect of cable discontinuities. Two sets of equipment for recording this elongation are described. For long cables a direct measurement is made of the pulse "tail" at the remote end of the cable. For cables less than about 500 m in length an echo technique is used in which two sets of pulses with different repetition rates are transmitted along the cable, which is terminated by an equalizer.

621.317.343.018.75:621.315.2 2464

New Developments in Pulse Technique for Cable Testing—J. Oudin. (*Onde élect.*, vol. 34, pp. 163–169; Feb., 1954.) The improvement in sensitivity of an echo meter attained by operating at suitably high gain with a system of amplitude and phase correction is limited ultimately, if a cr tube is used, by imperfections of vision. To maintain a fine trace and extend the range of fault location, integration techniques are necessary. The principles of (*a*) a delay-line system and (*b*) an auxiliary-pulse system with mechanical recording of the echo trace are described.

621.317.4:621.385.833 2465

Electron-Optical Shadow Method of Magnetic-Field Mapping—L. Marton, J. A. Simpson, and S. H. Lachenbruch. (*Jour. Res. Nat. Bur. Stand.*, vol. 52, pp. 97–104; Feb., 1954.)

Modifications of the method described by Marton & Lachenbruch (1211 of 1950) are indicated. Iterative analysis procedures are illustrated by the mapping of an otherwise inaccessible ferromagnetic domain field.

621.317.4:621.395.625.3 2466

Magnetic Recording Tape—H. G. M. Spratt. (*Wireless World*, vol. 60, pp. 264–267; June, 1954.) An arrangement for measuring the coercivity and remanence of recording tape is described. A large-size radio-receiver mains transformer is modified by providing a large air gap in the center limb. Two search coils arranged in series opposition are placed in the gap and the tape sample is threaded through one of them. The differential voltage obtained, proportional to dB/dt, is applied to the Y-plate amplifier of a cro while a voltage proportional to H is applied to the X-plate amplifier. By including an integrating circuit in front of the Y-plate amplifier the B/H curve can be displayed.

621.317.411.029.64 2467

Measurement of Ferromagnetic Permeability at Microwave Frequencies—G. S. Sanyal and J. S. Chatterjee. (*Indian Jour. Phys.*, vol. 27, pp. 328–339; June, 1953.) The method uses a cylindrical cavity of nonmagnetic material with a detachable end plate. Resonance frefiuency and Q are measured first with the nonmagnetic end plate in position and then with a plate of the test material substituted. Relevant theory is given, the setup is described, and results are reported for nickel and soft iron.

621.317.45 2468

Nondestructive Sensing of Magnetic Cores—D. A. Buck and W. I. Frank. (*Elect. Eng.*, vol. 73, p. 110; Feb., 1954.) Digest of paper published in *Trans. AIEE*, vol. 72, pp. 822–830; 1953. The sense of the remanent magnetic flux in a core of the type used in digital-computer storage devices is detected by applying a small pulsed quadrature field to the core, thus rotating the field vector momentarily. This change of flux induces in a sensing coil wound on the core a voltage pulse whose sign depends on that of the remanent flux.

621.317.7 2469

The Application of Counter-Rotating Fields to Electrical Measuring and Indicating Devices—R. L. Russell and N. W. Hodges. (*Proc. IEE*, Part II, vol. 101, pp. 178–182; April, 1954.) Two oppositely rotating magnetic fields which may or may not be of the same magnitude and frequency are combined to produce a resultant field of zero or low angular velocity, with which the moving element aligns itself. Various es and em applications of this principle are discussed.

621.317.7.025.001.4 2470

Alternating-Current-Instrument Testing Equipment—A. H. M. Arnold. (*Proc. IEE*, Part II, vol. 101, pp. 121–131; April, 1954. Discussion, pp. 131–133.) An account is given of the equipment and methods used at the National Physical Laboratory for calibrating ac indicating instruments by comparison with standard meters.

621.317.71 2471

Voltage Transformer for Current Measurement—A. Lutz and G. Poklekowski. (*Fernmeldetech. Z.*, vol. 7, pp. 105–110; March, 1954.) A tube voltmeter circuit is described for measurement of current in circuits at high potential with respect to earth. The effect of the tube circuit on the current to be measured and the leakage current from the high-potential circuit through the tube are compensated by (*a*) a four-terminal network in the grid circuit, or (*b*) a suitable cathode resistor automatically biasing the tube. Details of a practical circuit are given in which both methods of compensation are applied. This operates in the frequency range 30 cps–1 mc over the current range 0.01–100 ma with power consumption 0.4 μW–4 mW and error >3 per cent. It compares favorably with thermocouple and rectifier-bridge instruments.

621.317.715:621.383.4 2472

Photoelectric Measurement of the Displacement of a Luminous Spot—Å. Thulin. (*Compt. Rend. Acad. Sci.* (*Paris*), vol. 238, pp. 1210–1212; March 15, 1954.) The system uses a differential photoconductive cell arrangement to obtain a current proportional to the displacement of the spot, and is stabilized against fluctuations of illumination and sensitivity.

621.317.738 2473

Two Probe-Type Capacitance Meters—L. Medina. (*Jour. Brit. I.R.E.*, vol. 14, pp. 233–236; May, 1954.) Reprint. See 215 of January.

621.317.75 2474

A Spectrum Analyser for the Range 100 c/s to 100,000 c/s—K. R. McLachlan. (*Jour. Brit. I.R.E.*, vol. 14, pp. 217–229; May, 1954.) "The specification is given of an analyzer to measure the spectral distribution of the noise emanating from an air jet, and several methods of performing this analysis are discussed. The development of a practical instrument is described which uses a variable frequency selective amplifier with a Wien bridge as the frequency-dependent feedback network, and some details of its performance are given. Errors due to the short time available for analysis are derived and some of the less familiar aspects of the circuits used, such as a symmetrical-to-asymmetrical converter, are analyzed."

621.317.761+621.373.421.13 2475

A Quartz-Crystal-Controlled Frequency Meter and Master Oscillator of High Accuracy—E. Kettel. (*Telefunken Ztg.*, vol. 27, pp. 27–31; March, 1954.) Frequency meter Type FM 312/1 comprises a frequency analysing unit of heterodyne type, a variable-frequency oscillator with frequency regulated by the analyzing unit, and a standard-frequency generator. The frequency error is $\pm 1\times 10^{-7}\pm 0.2$ cps between 1 kc and 3 mc. The range is 1 kc–300 mc when the instrument is used as a frequency meter, and 1–32 mc for use as a master oscillator. Parasitic oscillation is 80 db below desired oscillation level. The standard-frequency generator is a 100-kc quartz crystal enclosed in a double thermostat. Provision is made for comparison with an external frequency standard.

621.372.8.001.4:621.396.96 2476

A Hybrid-Ring Method of Simulating Higher Powers than are available in Waveguides—L. Young. (*Proc. IEE*, Part III, vol. 101, pp. 189–190; May, 1954.) A radar waveguide component must be tested at powers higher than those nominally available from the magnetron generator, since operating conditions render a safety margin of 50–100 per cent or more necessary. The component is inserted in one arm of a hybrid ring in front of the plunger and the standing wave pattern is moved across the component, a second plunger maintaining a nonreflecting load to the magnetron. The effective power is then twice that of the magnetron. The method of connecting n such hybrid rings, giving a power multiplication of 2^n, is explained. It cannot be used to test high-power loads or any component that absorbs or radiates power.

621.385.029.6.001.4 2477

Magnetron Stability Tester—H. S. Bennett and A. A. Kiriloff. (*Tele-Tech.*, vol. 13, pp. 96–97, 167; March, 1954.) The main sections of the tester are (*a*) radar power supply and modulator, (*b*) measurement apparatus for valve current, voltage and magnetic field, and (*c*) slotted line and dummy terminal line with associated measurement gear. Different kinds of magnetron may be tested over different frequency bands, and all factors involved in stability of operation can be determined.

621.396.822.029.65:537.54 2478

A Gas-Discharge Noise Source for Eight-Millimeter Waves—T. J. Bridges. (Proc. I.R.E., vol. 42, pp. 818–819; May, 1954.) Noise sources of a type previously described [e.g. 185 of 1952 (Johnson and Deremer)] are adapted for operation at 8 mm λ by reducing the dimensions of the gas tube and increasing the pressure. Measured noise levels of tubes with neon and argon fillings are 18.2 db and 15.9 db respectively above room-temperature levels. These figures are in good agreement with values calculated from gas-discharge theory.

621.397.62.001.4 2479

Measurements on Television Receivers: Part 2—Measurement of Transmission Characteristics of Television Receiver Circuits—O. Macek. (*Arch. tech. Messen*, pp. 29–30; Feb., 1954.) The factors which are important in estimating performance of the rf and demodulation stages, and the suitability of square waves for testing delay characteristics are discussed. Part 1: 2397 of 1953.

OTHER APPLICATIONS OF RADIO AND ELECTRONICS

536.53:621.396.822 2480

Measurement of the Absolute Temperature of a Metallic Conductor based on the Voltage produced by Thermal Agitation of the Electrons in the Conductor—R. Aumont, J. Romand, and B. Vodar. (*Compt. Rend. Acad. Sci.* (*Paris*), vol. 238, pp. 1293–1296; March 22, 1954.) Results obtained with a modified form of the arrangement described by Garrison and Lawson (947 of 1950) are reported. Determinations are accurate to within about 1 degree at temperatures up to 780 degrees K.

621.317.083.7 2481

Optical System for the Transmission of Information—G. Cortellessa and R. Querzoli. (*Nuovo Cim.*, vol. 11, pp. 321–322; March 1, 1954.) Brief description of a telemetering system using a light beam modulated at a frequency which depends on the magnitude measured.

621.383.2:621.386 2482

Possibilities and Limitations of Image Intensification—E. Fenner and O. Schott. (*Z. angew. Phys.*, vol. 6, pp. 88–95; Feb., 1954.) The limit set by fundamental brightness fluctuations of a point image is defined. Electron-optical image converters, television pickup tubes and scanning systems for X-ray image intensification are described and their performances assessed. 46 references.

621.384.6:621.311.6 2483

An R.F. Generator for Nuclear Energy Studies—L. Kornblith, Jr. (*Electronics*, vol. 27, pp. 142–145; May, 1954.) Description of the power-supply equipment for the 450-MeV synchrocyclotron at Chicago. A 40-kw frequency-sweep oscillator is tuned between 18.2 and 28.4 mc by means of a motor-driven capacitor. The output is pulsed so as to use only the descending part of the frequency sweep; the pulsing is performed by means of a photocell circuit actuated from mirrors on the capacitor shaft.

621.384.612 2484

Orbital Instabilities due to the Coupling between Radial and Vertical Oscillations in the Cosmotron—J. Seiden. (*Compt. Rend. Acad. Sci.* (*Paris*), vol. 238, pp. 1010–1012; March 1, 1954.)

621.384.612 2485

Space-Charge Forces in Strong-Focusing Synchrotrons—S. E. Barden. (*Phys. Rev.*, vol. 93, pp. 1378–1380; March 15, 1954.) Relatively small changes in the average field gradient produced by space-charge effects may, when the number of magnet sectors is $\gg 10$, create conditions favorable to forced resonances due to imperfections in magnet alignment. This places strict limitations on the admissible space-charge forces, more particularly in the case of beams of heavy particles.

621.384.622.1 2486

Linear Accelerator for Electrons, with Preliminary Bunching—M. Papoular. (*Compt. Rend. Acad. Sci.* (*Paris*), vol. 238, pp. 1115–1117; March 8, 1954.) Use of the preliminary bunching device described with a 1-MeV accelerator gave an increase of 100 per cent in the number of electrons attaining this energy, without adversely affecting the spectral distribution of energy.

621.385.833 2487

Notes on Chromatic Aberration of Electron Lenses—H. Grümm. (*Ann. Phys., Lpz.*, vol. 14, pp. 193–200; Feb. 15, 1954.) Formulas for determining the chromatic aberration are derived using wave-mechanics theory of electron optics. The possibility of correcting the aberration in the case of a bell-shaped magnetic field is shown.

621.385.833 2488

Calculation of the Axial Potential in a Three-Electrode Electrostatic Lens—P. Ehinger. (*Compt. Rend. Acad. Sci.* (*Paris*), vol. 238, pp. 1306–1308; March 22, 1954.) The three-electrode lens with thick middle electrode is treated by applying the method previously developed for a two-cylinder lens (1877 of June) to the two halves of the system.

621.385.833 2489

A Simple Stigmator for Magnetic Electron Lenses—S. Leisegang. (*Optik, Stuttgart*, vol. 11, pp. 49–60; 1954.) Asymmetry is compensated by means of iron inserts in the pole pieces. Axial astigmatism can be reduced to about $0.1\ \mu$, and a resolving power of $1\ \mathrm{m}\mu$ can be attained.

621.387.424 2490

Operating Characteristics of Counters with External Cathode and Pure Methyl-Alcohol Filling—D. Blanc. (*Nuovo Cim.*, vol. 11, pp. 231–240; March 1, 1954. In French.)

621.387.424 2491

Response of a Pulsed Geiger Tube—H. B. Rosenstock. (*Jour. Appl. Phys.*, vol. 25, pp. 275–282; March, 1954.) The advantage of operating with pulsed rather than steady voltages on the tube is that higher radiation intensities can be measured; but if the duration of the pulse is comparable to the spread time of the discharge, the output-current/radiation-intensity relation will be nonlinear, since the resulting current surge may not reach its maximum before the end of the pulse. Using probability considerations, this relation is calculated as a function of the response of the tube under ordinary operating conditions. If the discharge initially spreads rapidly, an approximate general relation not involving the spread mechanism can be established. The response to be expected in two types of tube is discussed in detail.

PROPAGATION OF WAVES

621.396.11 2492

Ground-Wave Propagation at Ultrahigh Frequencies—(*Nature* (*London*), vol. 173, pp. 573–574; March 21, 1954.) Two papers presented at the I.E.E. are summarized. The first, by Saxton & Harden, gave results of an experimental investigation of the effects of irregular terrain on ground-wave propagation at frequencies of 102.6 and 593.6 mc. The second, by Saxton, compared results of such investigations with the corresponding conditions for transmission over a smooth earth, for propagation at frequencies between 50 and 800 mc.

621.396.11 2493

Ionospheric Propagation—R. Gea Sacasa. (*Rev. Telecomunicación, Madrid*, vol. 10, pp. 24–32; March, 1954. In Spanish and English.) Report and comment on U. S. document 224 presented at the C.C.I.R. conference, London, 1953, discussing certain optimum-working-frequency and muf predictions for 1950 and 1951. See also 1773 of 1953.

621.396.11:535.42 2494

On the Theory of Diffraction of Electric Waves by Many Parallel Screens—Y. Nomura. (*Sci. Rep. Res. Inst. Tohoku Univ., Ser. B*, vol. 4, pp. 231–248; March, 1953.) Expressions are derived for the intensity of a wave diffracted by two parallel screens, representing two mountain ranges, and the results are extended to the case of more than two parallel screens. The wave arriving by the shortest path, i.e. suffering the smallest number of diffractions, accounts for the major part of the resulting intensity. The effect of the image antenna is also considered.

621.396.11:551.510.535 2495

A Note on Sweep-Frequency Backscatter Observations—R. Silberstein. (*Jour. Geophys. Res.*, vol. 59, pp. 138–139; March, 1954.) A typical range/frequency record obtained with improved equipment is shown, and the identification of backscatter sources of particular echoes briefly discussed.

621.396.11:621.317.353.3:550.38 2496

Influence of the Earth's Magnetic Field on the Interaction of Radio Waves in the Ionosphere—I. M. Vilenski. (*Zh. eksp. teor. Fiz.*, vol. 26, pp. 42–56; Jan., 1954.) The discussion of the Luxemburg effect and cross-modulation (3095 of 1953) is extended to take account of the earth's magnetic field. A formula for the depth of cross-modulation is derived in terms of functions of the transmitter frequencies, the effective number of electron collisions and the gyromagnetic frequency. Calculations show that values of cross-modulation depths obtained by Cutolo (2617 of 1950) and Shaw (1472 of 1951) can be reconciled if the *E* layer is assumed to have been lower by 5–10 km in the former than in the latter experiments. The formulas apply to night-time conditions only.

621.396.11.029.62:551.594 2497

Atmospheric Electricity and Long-Distance Very-High-Frequency Scatter Transmissions—G. A. Isted. (*Marconi Rev.*, vol. 17, pp. 37–60; 2nd Quarter, 1954.) During an investigation of long-distance transmissions in the frequency band 30–100 mc, it was observed that signals transmitted over distances of 500 km or more arrived at the receiver in a series of bursts, many of which were grouped in trains. At the same time, electrical discharges from clouds were observed, often having the same time arrangement as the signal bursts. Theory is developed to explain how these discharges, though occurring in the lower atmosphere, can give rise to pockets of intense ionization in the *E* region. The theory indicates that ordinary clouds, rather than storm clouds, are the main generators maintaining the fine-weather vertical potential gradient. It is also suggested that when energy is transferred from discharging clouds to fine-weather areas, continuous partial ionization of the *E*-region conduction path is set up, and in extreme cases may result in the formation of sporadic *E*; and that this partial ionization together with the ionization bursts is mainly responsible for very-long-distance transmission in the vhf band. For a brief account see *Wireless World*, vol. 60, pp. 343–344; July, 1954.

621.396.81:621.396.65 2498

Reliability of U.S.W. Radio Link extending far beyond the Horizon—H. J. Fründt. (*Telefunken Ztg.*, vol. 27, pp. 41–43; March, 1954.) Field-strength recordings made at the Berlin end of a Berlin-Harz 60-mc FM link are analyzed. According as atmospheric refraction effect is or is not taken into account, the computed field strength is equalled or exceeded for 85 per cent or 99.5 per cent of the time respectively. This fact is of interest in planning. Signal/noise ratio in the individual channels is an important factor in reliability of operation; computation shows that some 14.5 db of noise is due to electrical apparatus and machines in the Berlin area. Over the period of a year, causes of service interruptions and their durations in percentage of time were (*a*) fading, 1.62 per cent, (*b*) equipment failure, 3.37 per cent, (*c*) transmission-line and cable connections, 5.82 per cent, (*d*) other causes, 1.69 per cent.

621.396.812.3 2499

Prolonged Space-Wave Fadeouts at 1046 Mc/s Observed in Cheyenne Mountain Propagation Program—B. R. Bean. (PROC. I.R.E., vol. 42, pp. 848–853; May, 1954.) The transmitter used in these propagation tests is located on the sheer face of the mountain, at a height of about 2,800 feet. Receiving sites at three different distances are used, all with standard dipoles 43 feet above the surrounding plains. Records obtained during the first year of continuous operation exhibit prolonged fades, often more than 20 db below the monthly mean level and lasting from one minute up to several hours. Their occurrence coincides with widespread superrefraction as evidenced by enhanced signals beyond the radio horizon and ground modification of the refractive-index profile. The results emphasize the need to provide sufficient transmitter power when planning uhf radio links with high-altitude transmitters and low-altitude receivers.

RECEPTION

621.396.621 2500

Radio Receiver Installations for Telegraphy and Single-Sideband Telephony in the Overseas Service. Developmental Principles and Practical Experience—K. Fischer, W. Vesper, and G. Vogt. (*Telefunken Ztg.*, vol. 27, pp. 14–26; March, 1954.) The development of Type EST 110 Kw/1 receiving equipment for telephony, and Type EST 111 Kw/1 for telegraphy is described and the technical problems involved are discussed. The equipment consists basically of a double-superheterodyne receiver with variable first IF and first local oscillator crystal-controlled. Frequency accuracy to within ±2 kc at 30 mc is achieved for ambient temperatures between 15 degrees and 25 degrees C and mains supply variations <10 per cent. Special demodulation circuits to deal with standard types of wave, and afc and avc are provided. Each installation comprises at least two receivers, so that diversity operation is possible.

621.396.621:621.376.3 2501

Mobile F.M. Broadcast Receiver Design—K. Onder. (*Electronics*, vol. 27, pp. 130–133; May, 1954.) Distortion due to multipath transmission is reduced by making the limiter and discriminator bandwidth much greater than normal [734 of 1950 (Arguimbau and Granlund)]. An experimental receiver designed on this principle was tested in a car; the results indicated that ignition interference was also eliminated.

621.396.82:621.376.33 2502

Interference in Non-idealized F.M. Receivers—H. Marko. (*Arch. elekt. Übertragung*, vol. 8, pp. 111–122; March, 1954.) The effect of imperfect demodulator performance on the level of unintelligible interference, crosstalk and noise is analyzed. Limiter, discriminator and detector characteristics are examined and design requirements for interference suppression in each stage are discussed.

STATIONS AND COMMUNICATION SYSTEMS

621.376.3:621.3.018.78:621.372.5 2503

Harmonic Distortion of Frequency-Modulated Waves by Linear Networks—R. G. Medhurst. (*Proc. IEE*, Part III, vol. 101, pp. 171–181; May, 1954.) The expression connecting the distortion of the modulating signal with the distortion of the rf spectrum when a FM carrier is passed through a linear network is used to obtain the harmonic distortion when the modulating signal is a single tone. It is assumed that departures of the phase characteristic of the network from linearity, and of the amplitude characteristic from constancy, are small. Tables of functions involved in calculating distortion by this method are provided and comparison is made with the result obtained by van der Pol (2310 of 1946) and with some measurements.

621.376.5 2504

Gaussian Pulses—J. P. Vasseur. (*Onde élect.*, vol. 34, pp. 139–142; Feb., 1954.) See 1905 of June.

621.376.56 2505

Transmission of Information by Integration of Coded Signals—H. Harmuth. (*Arch. elekt. Übertragung*, vol. 8, pp. 132–136; March, 1954.) The need for transmitting information regarding the position of individual pulses in a pcm system is eliminated if decoding is effected by suitable integrations of a pulse group. For a given channel capacity the transmitted power required is only 3 db above the theoretically required value, compared with 9 db for a pulse-amplitude detecting system. A system based on performing three integrations of a five-unit pulse group to give all but two of the 32 possible pulse sequences is outlined. The maximum possible error due to a pulse being missed can be reduced by using a suitable alphabetic code.

621.394.13 2506

Code Convertors for the Interconnection of Morse and Teleprinter Systems—R. O. Carter and L. K. Wheeler. (*Proc. IEE*, Part III, vol. 101, pp. 151–157; May, 1954. Discussion pp. 158–164.) Automatic converters for the two directions of conversion and with Morse perforated-tape storage are described.

621.394.14 2507

Telegraph Codes and Code Convertors—T. Hayton, C. J. Hughes, and R. L. Saunders. (*Proc. IEE*, Part III, vol. 101, pp. 137–150; May, 1954. Discussion, pp. 158–164.) Codes in use for submarine cable and radio circuits are reviewed from the point of view of their traffic-carrying capacity and freedom from undetectable errors. The effects of distortion and of particular methods of working on the error rate, and methods of eliminating errors are discussed. A 7-unit/5-unit electronic converter and a 5-unit/7-unit mechanical converter are described.

621.394.7+621.395.7 2508

Unit Construction Practice (UCP) applied to Line-Transmission Equipment—K. W. Harrison. (PROC. I.R.E., vol. 42, pp. 822–829; May, 1954.) By standardizing a small number of functional units a flexible method of designing complete carrier-transmission equipments is provided. Bulk is reduced by efficient use of mounting space rather than by special miniaturization techniques.

621.396.41:621.374.5 2509

Electrical Delay Networks for Time Selection in Multichannel Systems—H. Härtl and F. Rumpel. (*Fernmeldetech. Z.*, vol. 7, pp. 118–122; March, 1954.) The design and construction of a lumped-element delay network is described. Design is based on the properties of an *m*-derived filter section. A unit comprises 125 similar sections, coils being assembled coaxially on the same former. Over-all delay is 125 μs and upper cut-off frequency about 400 kc. Operating characteristics are discussed.

621.396.61+621.396.62 2510

A New Mobile Phase-Modulated Transmitter-Receiver Unit—J. Anderson and W. D. Meewezen. (PROC. I.R.E., *Aust.*, vol. 15, pp. 31–42; Feb., 1954.) The transmitter crystal oscillator circuit is noncritical in component values and has low af distortion. An af amplifier-limiter circuit prevents overloading of the oscillator. The frequency multiplication factor from crystal to antenna is 48. Power output is 24 W at 170 mc, and the units for the 70–85 mc and 156–170 mc bands differ only in the tuning circuits. Conversion from 6.3-v to 12.6-v operation is simple, and the same transmitter will give the higher output required from a base station transmitter if used with an ac hv supply unit. The double-superheterodyne receiver units for the two bands are identical apart from the rf and first mixer stages.

621.396.65:621.396.81 2511

Reliability of U.S.W. Radio Link extending far beyond the Horizon—Fründt. (*See* 2498.)

621.396.933 2512

A Single-Sideband Controlled-Carrier System for Aircraft Communication—G. W. Barnes. (*Proc. IEE*, Part III, vol. 101, pp. 121–130; May, 1954. Discussion, pp. 130–135.) A transmission system is proposed in which the carrier amplitude is made to vary inversely as the sideband amplitude. This system provides afc over a wider range than is usual and avoids the use of a very narrow carrier filter. A four-phase balanced modulator is used. The outphasing method of sideband rejection is applied in the receiver which is provided with automatic carrier-frequency control using an electromechanical system with a memory for operation on the intermittent-carrier systems. Flight trials with experimental equipment are reported.

SUBSIDIARY APPARATUS

621.3.013.783 2513

Shielding Nomograph—J. F. Sodaro. (*Electronics*, vol. 27, p. 190; May, 1954.)

621.311.69:621.362 2514

Thermoelectric Generator TGK-3—V. Daniel'-Bek, A. Voronin, and N. Roginskaya. (*Radio, Moscow*, pp. 24–26; Feb., 1954.) Description of a paraffin-lamp-driven generator for use with battery-type receivers. The outputs are 2v, 2a for the vibrator ht unit and 2v, 0.5a for heaters. A 1.2-v, 0.36-a tapping is also provided. Semiconductor-type thermoelements are mentioned as being more efficient than pure-metal thermocouples.

TELEVISION AND PHOTOTELEGRAPHY

621.397.2:621.3.018.78 2515

The Distortion of Television Signals by Attenuation and Phase Distortion in the Transmission System—F. Bath and H. Kaden. (*Arch. elekt. Übertragung*, vol. 8, pp. 55–68; Feb., 1954.) Analysis shows that for satisfactory transmission of a black/white edge the demands on the video-signal transmission system are more exacting than for satisfactory transmission of a picture element. The conditions satisfying these demands are introduced in the coefficients of the Fourier expansions of the expressions for attenuation and phase distortion of the system. Tolerance curves for the permissible distortion, as function of frequency, are deduced from statistical considerations of distortion in the sections of the transmission system.

621.397.5:535.623 2516

Colour Television on 405 Lines—(*Wireless World*, vol. 60, pp. 256–257; June, 1954.) Account of a demonstration given in London, on a closed circuit. Comparison was made between a system with color subcarrier inside the monochrome channel and one with the color channel outside the monochrome channel. Better color pictures were obtained with the latter system, but because of the extra bandwidth required use of this system in Bands I and III would involve overlap between the monochrome signal of one channel and the color signal of the adjacent channel. A camera with only two pickup tubes was used for live scenes, one tube producing a normal-definition monochrome signal and the other producing two low-definition color signals. For another account see *Elect. Jour.*, vol. 152, p. 1601; May 14, 1954.

621.397.5:621.395.625.3 2517

A System for Recording and Reproducing Television Signals—H. F. Olson, W. D. Houghton, A. R. Morgan, J. Zenel, M. Artzt, J. G. Woodward, and J. T. Fischer. (*RCA Rev.*, vol. 15, pp. 3–17; March, 1954.) Details are given of a magnetic-tape system. For monochrome television ½-inch tape is used, carrying one track for the video signal and one for the sound. For color television ½-inch tape is used carrying five tracks, for the red, green, blue, synchronization and sound signals. A servomechanism is used to provide the required constancy of tape speed. This speed is 30 feet with the equipment described, and the width of the available frequency band is >3 mc. The audio signals are modulated on to a 150-kc carrier for recording. Demonstrations of the system given at Princeton in December, 1953 are briefly reported.

621.397.61 2518

Low-Level-Modulation Vision Transmitters, with Special Reference to the Kirk O'Shotts and Wenvoe Stations—E. McP. Leyton, E. A. Nind, and W. S. Percival. (*Proc. IEE*, Part III, vol. 101, pp. 190–191; May, 1954.) Discussion on 274 of January.

621.397.611.2 2519

Vidicon Film-Reproduction Cameras—H. N. Kozanowski. (*Jour. Soc. Mot. Pict. & Telev. Engrs.*, vol. 62, pp. 153–162; Feb., 1954.) The advantages of the vidicon pickup tube for televising film are discussed, and a description is given of a complete camera unit, including deflection, video and control circuits. Equipment is under development for enabling transparent or opaque stills to be interspersed with films.

621.397.62 2520

Choice of a Television-Receiver Intermediate Frequency to suit the C.C.I.R. Standard—W. Holm and W. Werner. (*Funk u. Ton*, vol. 8, pp. 129–138; March, 1954.) Considerations of interference by other services, various transmitter harmonics, etc., show that the optimum European television sound IF is 33.4 mc and vision IF 38.9 mc. The use of these frequencies may require precautions against second-harmonic interference in channel 4 and sixth-harmonic interference in channel 8. Sound in channel 7 may be interfered with by the fifth harmonic of the vision IF if the latter is mistuned by +50 kc.

621.397.62 2521

"Leningrad" T-2—Modern Russian TV Receiver—(*Tele-Tech.*, vol. 13, pp. 90–92; Jan., 1954.) Circuit diagram and chassis photographs of this 8-inch screen receiver are shown.

621.397.62 2522

How to Handle Ringing in Television Design—L. Beiser. (*Electronics*, vol. 27, pp. 162–167; May, 1954.) A discussion of the precautions necessary in the design of the various parts of the receiver deflection system to avoid extraneous vertical-bar patterns on the raster caused by transient oscillations in the output circuits.

621.397.62 2523

A Direct-Drive Scanning Circuit—E. Jones and K. E. Martin. (*Jour. Telev. Soc.*, vol. 7, pp. 190–199; Jan./March, 1954.) A circuit based on that described in U.S.A. patent No. 2555831 (Tourshou) is discussed. The operation differs fundamentally from that of the widely used Blumlein energy-recovery circuit. The scanning coil is in series with an anode inductor whose function is to store energy during the scanning stroke and give it up during the flyback; but there is no coupling between the two coils. Dc is excluded from the scanning coil and a hv winding is provided on the anode inductor. A practical circuit is illustrated, with component values.

621.397.62:535.623:621.385.831 2524

Beam-Deflection Tube Simplifies Color Decoders—R. Adler and C. Heuer. (*Electronics*, vol. 27, pp. 148–151; May, 1954.) See 2244 of July.

621.397.62:621.314.7 2525

A Symmetrical-Transistor Phase Detector for Horizontal Synchronization—B. Harris and A. Macovski. (*RCA Rev.*, vol. 15, pp. 18–26; March, 1954.) A junction transistor with identical collector and emitter junctions is used in place of a conventional double diode as a balanced phase detector for controlling the line-deflection oscillator of a television receiver. The circuit is gated by application of synchronizing pulses to the transistor base, while the comparison sawtooth voltage is applied to the collector-emitter. Wide variations in the absolute values of the transistor parameters, in the degree of symmetry of the transistor, and in the temperature are tolerable.

621.397.62:621.385 2526

Investigation of Ultra-High-Frequency Television Amplifier Tubes—Wen Yuan Pan. (*RCA Rev.*, vol. 15, pp. 27–45; March, 1954.) An investigation is made of the possibility of improving receiver performance by including an uhf amplifier stage. Various types of available tube, including planar, pencil and miniature, are considered from the point of view of noise, gain and stability. The results indicate that no substantial advantage is obtainable with any of the available tubes, particularly when the additional cost is taken into account.

621.397.62:621.397.335 2527

A Critical Review of Synchronizing Separators with Particular Reference to Correct Interlacing—G. N. Patchett. (*Jour. Brit. I.R.E.*, vol. 14, pp. 191–214; May, 1954.) See 2918 of 1952.

621.397.62.001.4 2528

Measurements on Television Receivers: Part 2—Measurement of Transmission Characteristics of Television Receiver Circuits—Macek. (*See* 2479.)

621.397.7:628.972 2529

Television Lighting Routines—W. R. Ahern. (*Jour. Soc. Mot. Pict. & Telev. Engrs.*, vol. 62, pp. 189–196; March, 1954. Discussion, pp. 196–198.) Description of the lighting installation at N.B.C. studio 8H and account of the lighting procedure for a typical play.

621.397.828:621.396.61.013.78 2530

Screening Materials for TVI—R. Glaisher. (*Short Wave Mag.*, vol. 12, pp. 16–18; March, 1954.) The radiation from a 50-mc test transmitter screened with different materials was measured. The conductivity of mesh screens is improved by bonding with solder strips at 2-inch intervals; this greatly reduces effects of oxidation. Close-stranded copper mesh thus treated is only slightly less effective at 50 mc than copper-plated steel, the best of the solid materials tested.

TRANSMISSION

621.376.22:621.3.018.783 2531

Intermodulation Distortion in Rectifier Modulators—D. G. Tucker. (*Wireless Engr.*, vol. 36, pp. 145–152; June, 1954.) Distortion due to interference of the modulation voltage with the rectifier-switching function of the carrier is studied. Analysis previously given by Belevitch (2184 of 1949 and 1633 and 2167 of 1950) for the case of a single modulation tone is extended to deal with modulation by two or more tones. The rectifiers are assumed to be linear. For the case of two modulation tones values of all third-order distortion terms are tabulated based on first- and third-order modulation. An appendix extends this in general form to all orders of modulation and to second- as well as third-order distortion.

621.376.54 2532

Pulse Duration Modulator Circuit—F. Butler. (*Electronic Eng.*, vol. 26, pp. 153–155; April, 1954.) Adaptation of the pulse-generator circuit described by Levell (364 of 1953) for single-channel voice-communication purposes. Smooth changes of pulse duration between 12.8 and 0.7 μs are obtained on applying a direct control voltage of value between 15 and 280v via a high resistance. The pulse-duration/control-voltage characteristic has the form of a rectangular hyperbola. The circuit of a complete modulated generator is illustrated. Trigger pulses with a repetition rate adjustable to 12 kc are provided; modulation frequencies up to 6 kc are hence permissible. A method of reducing distortion is indicated.

621.396.61:621.314.22.029.51/53 2533

Tankless Low-Frequency Transmitter—P. Gomard. (*Electronics*, vol. 27, pp. 154–156; May, 1954.) Reduction of the size of a transmitter by use of iron-cored hf transformers was described by Deise and Gregory (1284 of 1950). The transmitter here described covers the frequency bands 280–330 kc and 400–510 kc, using a straight wide-band amplifier with coupling transformers wound on ferrite cores. The oscillator is coupled to the amplifier through a low-pass filter, separate filters being used for the two bands. The output stage comprises eight Type-807 tubes in push-pull parallel. The design of the output transformer is considered particularly; the measured temperature rise of 37 degrees to 39 degrees C. at the ferrite core is in fair agreement with the calculated value.

621.396.61.013.78:621.397.828 2534

Screening Materials for TVI—Glaisher. (*See* 2530.)

TUBES AND THERMIONICS

621.314.632+621.314.7 2535

The Double-Base Diode: A Semiconductor Thyratron Analog—R. W. Aldrich and I. A. Lesk. (*Trans. I.R.E.*, vol. ED-1, pp. 24–27; Feb., 1954.) The double-base diode consists of a single-crystal Ge bar with a single *p-n* junction and two base contacts. With suitable biasing current flowing between these contacts a junction-base characteristic with a stable negative-resistance region can be obtained, the order of magnitude of the junction currents being much greater than that of the emitter input characteristic of the point-contact transistor. The device is thus suitable for relaxation-oscillator and switching applications; some simple circuits are illustrated.

621.314.632 2536

Diode Theory in the Light of Hole Injection—J. A. Swanson (*Jour. Appl. Phys.*, vol. 25, pp. 314–323; March, 1954.) Classical diode theory, as applied to metal point contacts made to an *n*-type semiconductor, is adequate only for small forward voltages at which, under certain conditions, hole current may be negligible. The shape of the predicted diode characteristic is not affected by hole injection at low voltages. For voltages exceeding a critical value, dependent on the resistivity of the material, the spreading resistance is comparable to the barrier resistance, and it is the hole-injection process which accounts for continued rectification. The extent to which the spreading resistance is decreased by hole injection depends on the ratio, γ, of hole current to total current. The effect of γ on the characteristic at high voltages is considered, and a method of measuring γ is indicated.

621.314.7 2537

Frequency Variations of Junction-Transistor Parameters—R. L. Pritchard. (Proc. I.R.E., vol. 42, pp. 786–799; May, 1954.) The equivalent-*T*-network representation of the transistor is adopted in which the four independent small-signal parameters to be considered are the emitter resistance, the base resistance, the parallel combination of collector resistance and capacitance, and the effective current-amplification factor. Analysis given by Early (874 of 1953) is extended to account for observed frequency variation of collector impedance. The transistor voltage/current relations are calculated for the theoretical model using the grounded-base connection.

621.314.7 2538

High-Frequency Operation of P-Type Point-Contact Transistors—F. L. Hunter and B. N. Slade. (*RCA Rev.*, vol. 15, pp. 121–134; March, 1954.) The characteristics of *n*-type and *p*-type Ge point-contact transistors are compared. Higher operating frequencies can be attained with the *p*-type because of the greater mobility of the minority carriers, which in this case are electrons. An α-cut-off frequency as high as 50 mc with a point spacing of 0.001 inch has been attained in amplifier transistors, and an operating frequency as high as 425 mc with oscillator transistors.

621.314.7+621.314.63]:621.318.57 2539

Switching Time in Junction Diodes and Junction Transistors—R. H. Kingston. (Proc. I.R.E., vol. 42, pp. 829–834; May, 1954.) An approximate solution for the transient occurring when a junction diode is switched from forward to reverse conduction is obtained by considering the behavior of the minority carriers. Two phases are distinguished, (*a*) a constant-current phase in which the flow is limited by the external resistance, (*b*) a "collection" phase in which the current decays at a rate determined by the minority-carrier lifetime and by the diode dimensions. The duration of the two phases is determined theoretically for a planar junction, a hemispherical junction and a narrow-base diode. By considering the diode in the last of these cases as the emitter-base combination of a transistor, the corresponding collector-current transient is found.

621.314.7:621.373.52 2540

Internal Oscillations and Microwaves in Transistors—H. E. Hollmann. (*Naturwissenschaften*, vol. 41, p. 136; March, 1954.) An effect in transistors superficially similar to Barkhausen oscillations is briefly reported. The oscillation frequency is proportional to the square root of the collector current and depends on the effective electrode capacities. In the case of point contact transistors with high α-cut-off frequencies the fundamental resonance frequency is about 100 mc and the microwave harmonics are capable of exciting cavity resonators. For a fuller account, in English, see *Tele-Tech.*, vol. 13, pp. 75–77; April, 1954.

621.314.7:621.397.62 2541

A Symmetrical-Transistor Phase Detector for Horizontal Synchronization—Harris and Macovaki. (*See* 2525.)

621.314.7.012.8 2542

Transistor Characteristics—H. Beneking. (*Arch. elekt. Übertragung.*, vol. 8, pp. 69–74; Feb., 1954.) The representation of transistors by equivalent quadripoles is discussed and the advantages of one particular representation are illustrated by two numerical examples. The equivalence of various other Q and T networks is shown.

621.383.2:621.317 2543

The Photodianode: Investigation of the Total Current and of the Differential Current in an Asymmetrical Arrangement—L. Deloffre, É. Pierre, and J. Roig. (*Compt. Rend. Acad. Sci.* (*Paris*), vol. 238, pp. 1213–1215; March 15, 1954.) Modified methods of operating the photodianode (1249 of April) are described. Either gas-filled or vacuum-type photocells can be used.

621.383.5:621.396.822 2544

Shot Dependence of p-n Junction Phototransistor Noise—A. Slocum and J. N. Shive. (*Jour. Appl. Phys.*, vol. 25, p. 406; March, 1954.) Measurements of ac short-circuit noise current in a band about 400 cps wide centered at 1000 cps have been made on seven *p-n* junction phototransistors with low dc reverse saturation dark current. Results show that for bias voltages <20v, and dc bias current <300 μA, noise current is given within a factor of 2 by the theoretical shot noise current, and is independent of temperature. For bias voltages >20v, and dc bias current >300 μA, the noise current is considerably in excess of shot noise current.

621.385:621.397.62 2545

Investigation of Ultra-High-Frequency Television Amplifier Tubes—Wen Yuan Pan. (*See* 2526.)

621.385.029.6 2546

Electron-Beam Focusing with Periodic Permanent-Magnet Fields—J. T. Mendel, C. F. Quate, and W. H. Yocom. (Proc. I.R.E., vol. 42, pp. 800–810; May, 1954.) Microwave-valve beams can be focused by a system of N permanent magnets arranged periodically along the beam, having a total weight theoretically only $1/N^2$ that of a permanent magnet producing a uniform field over the same length, for comparable results. For certain combinations of beam voltage and magnetic field, "stop bands" are produced in which the beam becomes unstable and no current reaches the collector; design procedure for avoiding this effect is indicated.

621.385.029.63 2547

The Effect of Space Charge on Beam Loading in Klystrons—T. G. Mihran. (Proc. I.R.E., vol. 42, p. 862; May, 1954.) Analysis indicates that space charge can be neglected in calculating primary election beam loading but must be taken into account for secondary electron beam loading.

621.385.029.63 2548

Improvement of Power Output from Pulsed Klystrons—J. H. Jasberg. (Proc. I.R.E., vol. 42, p. 859; May, 1954.) Klystrons of the type described by Chodorow et al. (580 of February) have been modified to give considerably higher outputs and improved efficiencies.

621.385.83:621.397.62:535.623 2549

Beam-Deflection Tube Simplifies Color Decoders—R. Adler and C. Heuer. (*Electronics*, vol. 27, pp. 148–151; May, 1954.) See 2244 of July.

Raytheon – World's Largest Manufacturer of Magnetrons and Klystrons

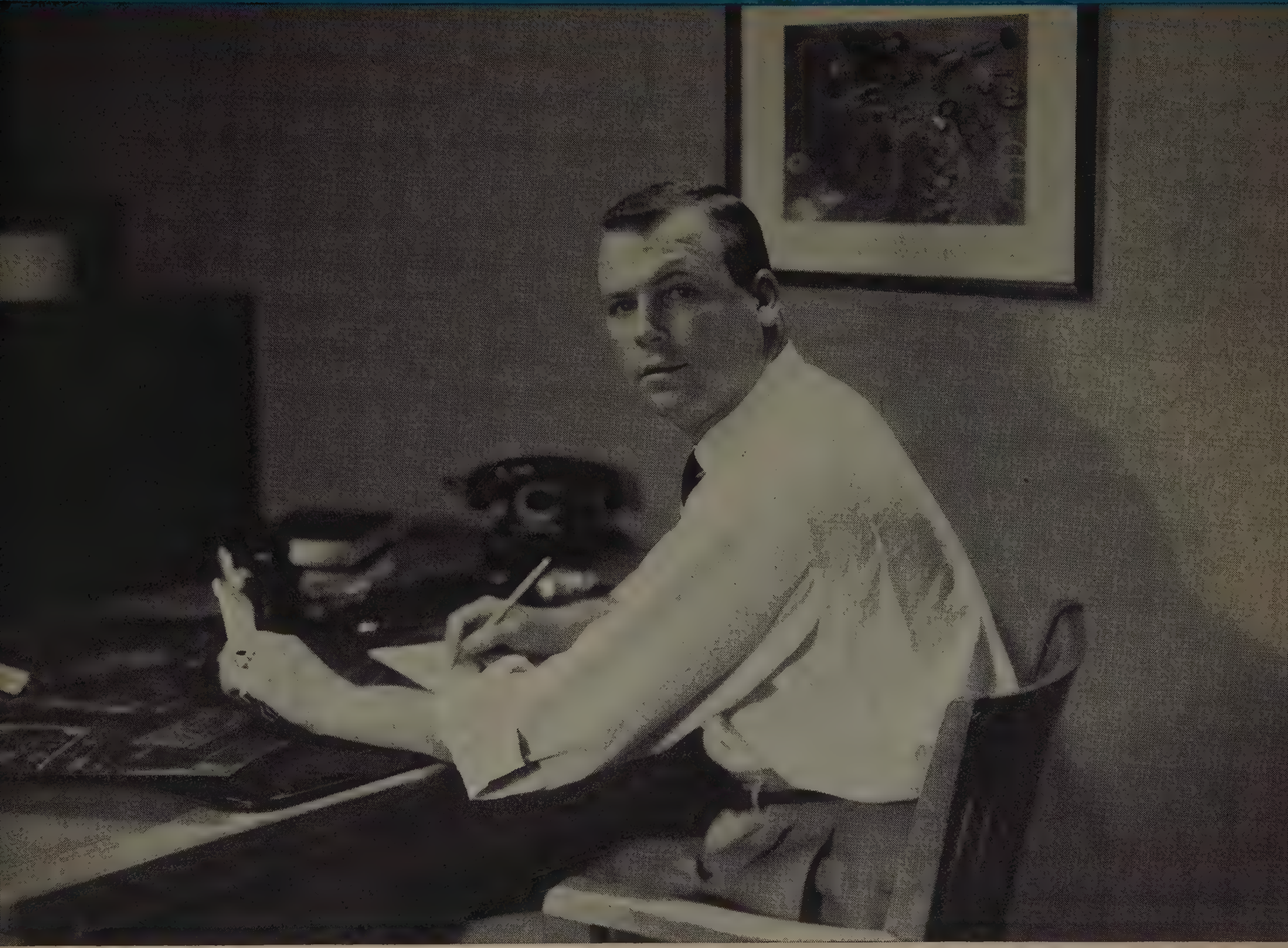

Working for You – on Raytheon's Payroll

In tackling new system design problems, what counts is to have the *right* answers at the *right* time. Here's where you can lean heavily on the help of Raytheon Application Engineers—*gratis!*

Teamed together, your engineers working with ours can determine the tube requirements of your proposed microwave system: Which Raytheon Klystron is best suited? Which Magnetron? Should an existing tube be modified? Is an entirely new design called for?

Obviously this teamwork lessens the burden on your systems engineers, lets them concentrate on equipment designs, while our engineers assist you in selecting the right tubes. Raytheon specialists help you all along the line – on design, production and quality control—without cost to you.

It pays to consult the leader about Magnetrons and Klystrons right from the start. And, wherever you are, Raytheon is ready to assist you with both military and commercial equipment plans. Write for Raytheon's valuable Tube Data Booklets—and ask for details of our free Application Engineer Consultation Service.

RAYTHEON

Excellence in Electronics

RAYTHEON MANUFACTURING COMPANY
Microwave and Power Tube Operations, Section PL 04, Waltham 54, Mass.

HUGH H. EBY INC.

ELECTRICAL AND ELECTRONIC COMPONENTS

- **SOCKETS**
  - 7- and 9-Pin Miniatures
  - Molded Lock-In and Octal
  - Battery
  - Television
  - Crystal
  - Sub-Miniature
  - UHF and Printed Circuit
- **TUBE SHIELDS**
- **CONNECTORS**
  - Speaker
  - Phono
  - Universal
  - 11-Pin (Male & Female)
  - 5-Pin (Male & Female)
- **KNOBS**
- **PLUGS**
  - Speaker
  - Molded Battery
  - Laminated Battery
  - Laminated Chassis
  - Special
- **JACKS**
  - All Molded Single & Twin
  - Metal
  - High Voltage
- **TERMINAL STRIPS**
  - Screw-Type
  - Special
- **BINDING POSTS**
  - Insulated (Single, Twin, Triple)
  - Non-Insulated Metal
  - Spring (Push-Type)
  - Panel & Telepost
  - Watertight
- **RACK and PANEL CONNECTORS**
  - 3- to 34-Pin
  - Battery Connectors
- **UHF-VHF CROSSOVER NETWORK**

FUSE HOLDER & FUSE BLOCKS
MISCELLANEOUS MECHANICAL & ELECTRICAL
COMPONENTS TO SPECIFICATION

Write for Illustrated Eby Catalog No. 51

HUGH H. EBY INC.

4703 Stenton Ave., Philadelphia 44, Pa.

Contributors

(Continued from page 72A)

Ohio State University he also accepted occasional appointments as a part time instructor in the department of electrical engineering.

Dr. Rhodes was born in Detroit, Michigan on December 31, 1923. He received the B.E.E., M.Sc., and Ph.D. degrees from Ohio State University in 1945, 1948, and 1953, respectively.

❖

R. A. Silverman (M'54) is a member of Lincoln Laboratory, Massachusetts Institute of Technology, working in the fields of radio wave propagation and communication theory. His paper appears on page 1428 of this issue.

R. A. Silverman

He was born on June 29, 1926, in Boston, Mass. He received his A.B. degree, magna cum laude, from Harvard University in 1946, his M.A. from Columbia in 1948, and his Ph.D. in theoretical physics from Harvard in 1951.

Dr. Silverman worked in solid-state physics, including a year at the Philco Corporation from 1951–1952.

He is a member of Phi Beta Kappa, Sigma Xi and the American Physical Society.

❖

P. K. Tien (S'49–A'51), since 1952, has been a member of the technical staff of the Bell Telephone Laboratories, Murray Hill, N. J., where he has been concerned with microwave tube research. His paper appears on page 1389 of this issue.

Dr. Tien was born in Checkiang, China, on August 2, 1919. He received the B.S. degree in electrical engineering from the National Central University of China in 1942, and the M.S. and Ph.D. degrees from Stanford University, Stanford, Calif., in 1948 and 1951 respectively.

From 1942 to 1947 he was an engineer at the Tien-Sun Industrial Company, Shanghai, China; from 1949 to 1952 he was research assistant and then research associate at Stanford University.

He is a member of Sigma Xi.

(Continued on page 84A)

Watch
for the
NEW, BIGGER, BETTER
IRE DIRECTORY

Designed for Application

Mu Metal Shields

The James Millen Mfg. Co. Inc. has for many years specialized in the production of magnetic metal cathode ray tube shields for the entire electronics industry, supplying magnetic metal shields to manufacturing companies, laboratories and research organizations. Stock shields are immediately available for all of the more popular sizes and types of cathode ray tubes as well as bezels for 2″, 3″ and 5″ size tubes.

Many production problems, however, make desirable special shields designed in conjunction with the specialized requirement of the basic apparatus. Herewith, are illustrated a number of such custom built shields. Our custom design and fabrication department is at the service of our customers for the development and manufacture of magnetic metal shields of either nicoloi or mumetal for such specialized applications.

JAMES MILLEN MFG. CO., INC.
MAIN OFFICE AND FACTORY
MALDEN, MASSACHUSETTS, U.S.A.

Hermetically-Sealed COILS

- ALL TYPES AND SIZES
- STANDARD STOCK ITEMS
- CUSTOM CONSTRUCTIONS

Cutaway view shows construction of the new Hermetically-Sealed coils. Metal case affords maximum protection.

Fugle-Miller hermetically-sealed coils provide positive protection against moisture and humidity. They are sealed with a true glass-to-metal technique that withstands extreme thermal and mechanical shock and vibration. Metal case provides maximum protection, is stamped and color coded as required. Units of this type meet the most rigid specifications.

ADDRESS INQUIRIES
TO DEPARTMENT P-1

FUGLE-MILLER LABORATORIES
MAIN STREET, METUCHEN, NEW JERSEY
Telephone Metuchen 6-2245

CUSTOM BUILT TRANSFORMERS

Here is an example of the type of equipment we can build to specifications for research, laboratory or experimental work. This Acme Electric custom built transformer has a primary that can be varied from 12 volts thru 115 volts, with a frequency range from 7 cycles thru 60 cycles. Nominal output voltage, 33,000 volts. This unit was built for use in connection with high voltage electrostatic separation and collection of various types of atmospheric particles.

Designing a Dry Type transformer in this voltage class that provides safe and efficient performance, is another notable example of Acme Electric transformer engineering.

ACME ELECTRIC CORPORATION
MAIN PLANT: 449 WATER ST., CUBA, NEW YORK
West Coast Engineering Laboratories: 1375 W. Jefferson Blvd. • Los Angeles, Calif.
In Canada: ACME ELECTRIC CORP. LTD. • 50 Northline Rd. • Toronto, Ontario

Acme ACME Electric

Contributors

(Continued from page 82A)

J. T. Wallmark (A'48), whose paper appears on page 1422 of this issue, is with RCA Laboratories in Princeton, N. J.

J. T. Wallmark

Dr. Wallmark was born in Stockholm, Sweden, on June 4, 1919. He received the Civilingenjordegree in electrical engineering at the Royal Institute of Technology in 1944, the Teknologie Licentiat degree in 1947, and the Teknologie Doktor degree in 1953.

From 1944 to 1945 Dr. Wallmark was a tube designer with the A B Standard Radiofabrik, and from 1945 to 1953 he was with the Royal Institute of Technology as a research engineer working on electron tubes. He was also connected part time to Statens Tekniska Forskningsrad, working on research administration, and Elektrovarmeinstitutet working on semiconductors.

In 1947 and 1948 Dr. Wallmark was a fellow of the American Scandinavian Foundation at RCA Laboratories.

❖

For a photograph and biography of W. M. Webster see page 1026 of the June issue of the Proceedings of the I.R.E. His paper appears on page 1350 of this issue.

❖

H. Weiss (S'49–A'52) has been employed by the General Electric Company since 1951, where he is engaged in development work for color television receivers. His paper appears on page 1380 of this issue.

H. Weiss

He was born on March 1, 1921 in New York, N. Y. He received a B.B.A. degree from the City College of New York in 1941. During the Second World War, he was a member of the U. S. Air Force, serving as instructor and crew chief for an instrument landing system.

From 1946 to 1949, he worked in public accounting, becoming certified, while continuing an engineering education. He received the B.E.E. degree from New York University in 1951, and is a candidate for the M.E.E. degree in August, 1954 from Syracuse University.

He is a member of Tau Beta Pi and Eta Kappa Nu.

New Simpson Core Meter Movement

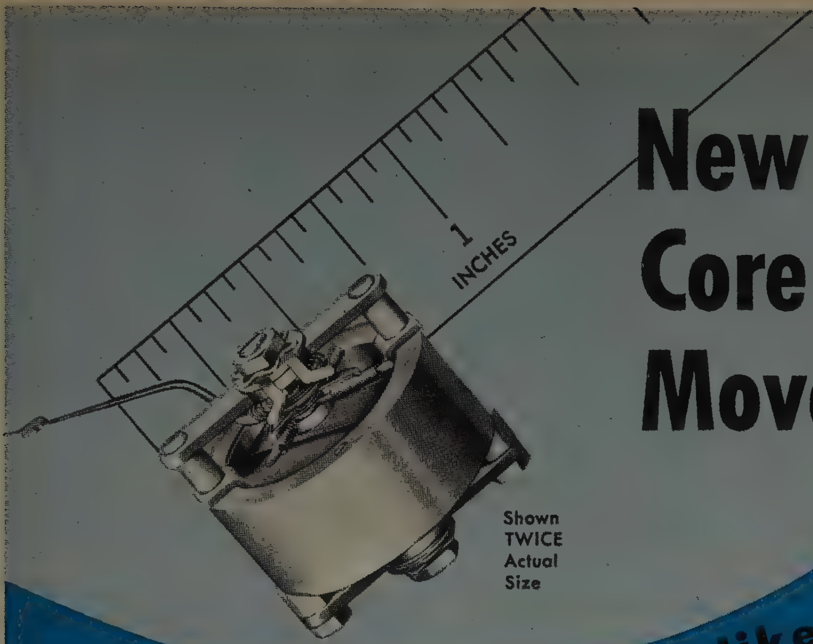

Shown
TWICE
Actual
Size

Rugged . . . yet built like a fine watch!

D.C. MILLIAMPERES
DIRECT CURRENT
MICROAMPERES
VOLTS
DC AMPERES
Simpson

Here's the new Simpson *Core-Type Meter Movement.* It's a more compact, more sensitive, ***self-shielding*** movement that gives electrical measurements with laboratory accuracy, yet has the ruggedness to withstand severe shocks. Its accuracy specifications are so rigid that Simpson engineers had to devise unusual production techniques.

Let Simpson engineers design panel meters using the new core movement to your special instrument requirements. Simpson continues to maintain its large stock of standard panel meters in over 700 sizes and ranges, available through distributors.

RUGGEDIZED METERS

Simpson's 2½″ and 3½″ Panel Meters are available in ***sealed, ruggedized*** models to meet specifications MIL-M-10304-(Sig. C). Movements are sealed against moisture and other adverse atmospheres, and are spring-mounted to absorb excessive vibration.

SEND FOR NEW CATALOG 17

INSTRUMENTS THAT STAY ACCURATE **Simpson** ELECTRIC COMPANY

5201 W. Kinzie St., Chicago 44, Illinois, Phone: EStebrook 9-1121
In Canada: Bach-Simpson, Ltd., London, Ontario

round • • oval flat ▬ ⌒ grooved ribbon ▬

SECON

precision small wire

bare • ◉ insulated plated ◉

for highly engineered applications

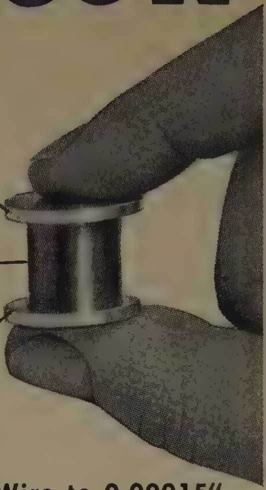

➡ all metals all alloys ⬅

Round Wire to 0.00015" diameter. Ribbon rolled to 0.0001" in thickness. Close tolerances held on all specifications.

SECON

... wherever the element calls for PRECISION

development and production metallurgists

SECON METALS CORPORATION

7 Intervale Street, White Plains, New York

WHite Plains 9-4757

Write for Pamphlet P

800 CYCLE audio frequency crystals with companion ovens

Heemco

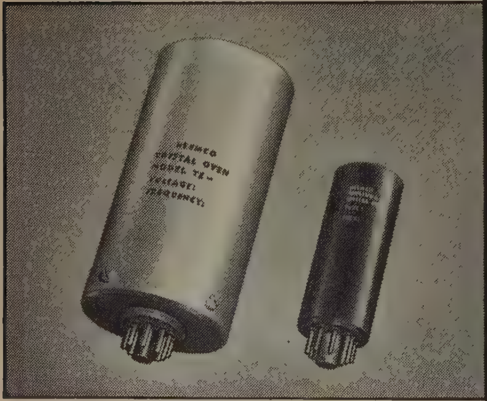

An outstanding new development of the HEEMCO Laboratories is the Heemco Audio Frequency Range Crystal Units, bringing about the extension of the fundamental crystal oscillator frequency down to 800 cycles.

Excellent application for low frequency crystals has been found in timing and marking fields where tuning fork performance does not provide the required high degree of stability and accuracy required. These units are capable of yielding stabilities better than 20 parts per 100 thousand over a temperature range of −40 to +85° C. When used with the companion oven, stabilities of one part per million or even better can be obtained.

Companion oven thermostats are hermetically sealed in glass and sensitive to 1/10° Fahrenheit. This package unit is excellent for aeronautical use, frequency being unaffected by altitude or acceleration to over 50 G. Available in octal plug-in or chassis mount. The crystal unit measures 3¼" overall, the oven, 2½" diameter × 5" high.

For complete details write for technical bulletin #j-1.

HILL ELECTRONIC ENGINEERING AND MANUFACTURING COMPANY, INC.

NEW KINGSTOWN, PA.

SECTION MEETINGS

BALTIMORE

"Home Music Systems," by C. G. McProud, Managing Editor, "Audio Engineering"; May 12, 1954.

"Tomorrow's Electronics Black Boxes Fly Higher, Faster, and Cooler," by Sidney Wald, The Glenn L. Martin Company; June 9, 1954.

DENVER

Inspection of radio and television facilities of Station KLZ, conducted by Ralph E. Sargent; election of officers; June 22, 1954.

INYOKERN

"Data Handling Equipment at AFFTC," by J. J. Dover, Air Force Flight Test Center; July 12, 1954.

KANSAS CITY

"Theory Behind Operation of Transistors: The Band Theory of Solids," by Dr. C. N. Hamtil, Faculty, Rockhurst College; election of officers; May 11, 1954.

LOS ANGELES

Film, "Project Tinkertoy"; "Today's News Today on Network T.V.," by Roy Neal, NBC, Frank La Tourette, CBS, and E. H. Schreiber, P. T. & T.; election of officers; June 1, 1954.

LOUISVILLE

Business meeting and election of officers; June 5, 1954.

MIAMI

Demonstration of de Mars loud speaker system by Paul de Mars, de Mars Engineering and Manufacturing Company; demonstration of stereophonic sound by Robert Miner, Ampex Corp.; June 25, 1954.

MILWAUKEE

"Fundamentals of Color TV," by Dr. John Jacobs, General Electric X-Ray Corp.; April 15, 1954.

Lecture series on Nuclear Power and Industry—"Basic Concepts," by Dr. David Okrent, Argonne Nat. Lab.; April 20, 1954.

Color TV demonstration by P. B. Laeser; WTMJ-TV; April 21, 1954.

Lecture series on Nuclear Power and Industry—"Reactor Design," by Dr. J. J. Grebe, Dow Chemical Company; April 27, 1954.

Lecture series on Nuclear Power and Industry—"Control of Reactors," by J. B. Reeves, Cutler-Hammer, Inc.

Lecture series on Nuclear Power and Industry—"Economic Nuclear Power Production," by Dr. J. A. Lane, Oak Ridge National Lab.; May 11, 1954.

"High Fidelity Audio Equipment," by Gene Fiebich, Heath Company; May 20, 1954.

PITTSBURGH

"A Method for Time or Frequency Compression—Expansion of Speech"—tapescript from University of Illinois (Fairbands, Everitt, Jaeger); election of officers; June 14, 1954.

PORTLAND

"How Much Distortion Can You Hear?" tapescript by Cincinnati Chapter IRE-PGA. Discussed by Ralph Hood, Tektronix; June 24, 1954.

SAN DIEGO

"Television Color Specification," by J. E. Tyler, University of California; July 6, 1954.

TOLEDO

Film, "Operation Ivy"; election of officers; June 10, 1954.

(Continued on page 88A)

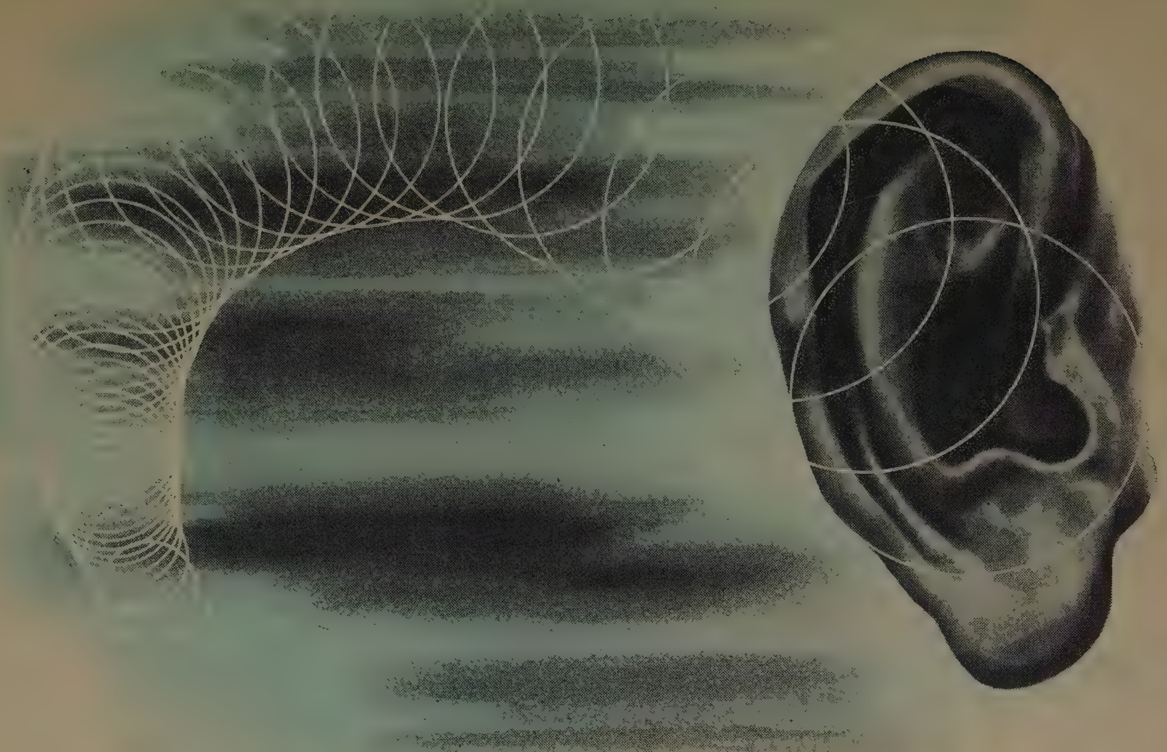

IT'S NO SECRET...

At this time our company is working on electronic projects for the defense departments of our country. Missile guidance systems . . . firing error indicators . . . and special communications equipment about which the strictest security must be maintained . . . but what we're privileged and proud to reveal *IS NO SECRET.* The competence which makes these achievements possible is in our engineering staff. Members of this group average more than ten years of experience in this complex, diverse field. Whenever you face a problem which may be solved by the use of electronic, electro-mechanical, hydraulic or pneumatic equipment, we feel sure these men can help you . . . LET'S TALK IT OVER.

WE REPRESENT OVER ONE HUNDRED TOP MANUFACTURERS OF MAJOR AVIATION PRODUCTS. A NEARBY BRANCH WILL BE HAPPY TO SERVE YOUR NEEDS. DO MORE BUSINESS . . . REALIZE MORE PROFIT WITH AIR ASSOCIATES EQUIPMENT.

J. E. Ashman
PRESIDENT

AIR ASSOCIATES, INC.
TETERBORO, NEW JERSEY

DIVISIONS: ATLANTA • CHICAGO • DALLAS • GLENDALE • HACKENSACK • MIAMI • ORANGE • TETERBORO

servo motors

the way you want 'em!

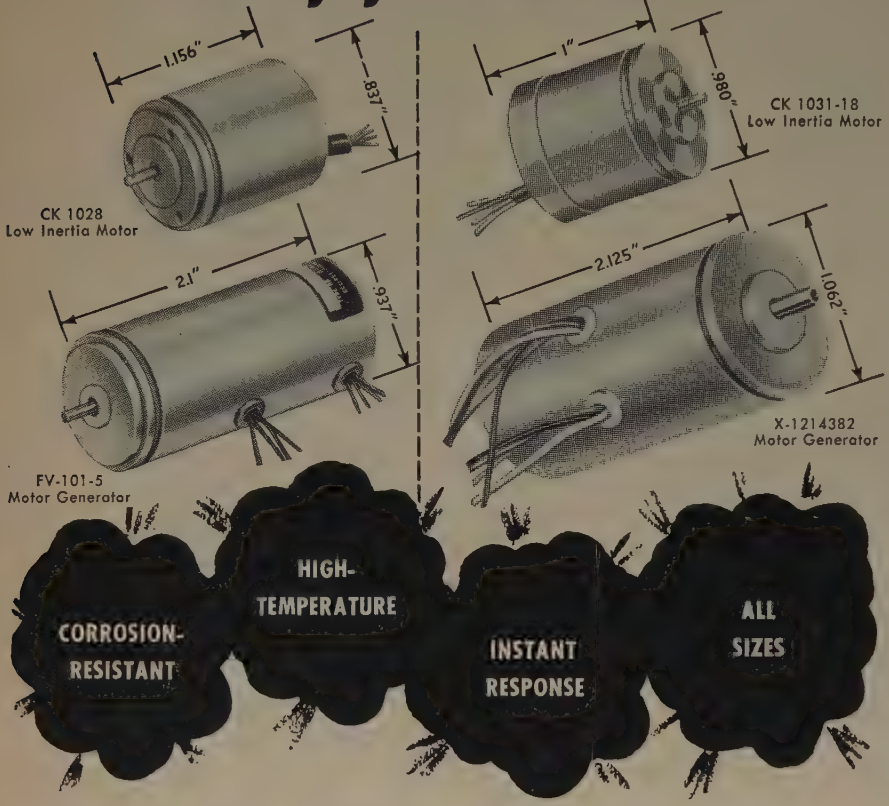

As one of the world's oldest and largest producers of servo components, we are ideally qualified to provide you with the right answer to your motor and motor generator needs. Why not take advantage of our long, practical experience? Call on us for recommendations based on your individual problem.

TYPICAL CHARACTERISTICS

Type Number	Rated Voltage		Max. Power Input Total (Watts)	No Load Speed (RPM)	Stall Torque (oz. inches)	Torque to Inertia Ratio (Radians per Sec.^{2})	Weight (oz.)
	Phase 1	Phase 2					
LOW INERTIA MOTORS							
CK-1018-7	18	18	5	10,000	0.13	13,000	1.6
CK-1022-13	115	115/57.5	12	4,800	1.45	33,800	8.0
CK-1027-14	115	115/57.5	7	6,200	0.63	41,500	4.5
CK-1028-16	26	26	6	10,000	0.28	13,000	1.6
CK-1031-18	26	55	9	6,400	0.35	10,000	2.2
CK-2006-1	64	64	30	7,200	2.6	70,000	10.0
CK-3000-1	110	220	80	3,700	14.0	3,750	30.0
MOTOR GENERATORS							
FV-101-5	26	26	9.5	10,000	0.28	10,000	2.9
FV-2001-2	115	115	30	6,600	3.0	70,000	12.6
FV-3000-1	110	220	80	3,700	14.0	3,750	30.0
X-1214382	26	26	9.7	6,000	2.6	21,000	5.5

WRITE DEPARTMENT G

ECLIPSE-PIONEER
TETERBORO, NEW JERSEY

Division of
THE NAME Bendix AVIATION CORPORATION MILLIONS TRUST

West Coast Office: 117 E. Providencia Ave., Burbank, Calif.

Export Sales: Bendix International Division, 205 E. 42nd St., New York 17, N.Y.

SECTION MEETINGS

(Continued from page 86A)

VANCOUVER

"The Development of TV Facilities in Canada," by Peter McDonald, CBUT; election of officers; May 14, 1954.

WILLIAMSPORT

"Transistor Circuit Applications," by R. F. Shea, General Electric Company; April 20, 1954.

"The Binary Number System," by Carl Volz, Pennsylvania State University; May 18, 1954.

SUBSECTIONS

BUENAVENTURA

"Stereophonic Sound," by John Mullin, Crosby Enterprises, Inc.; "The Physics of Music and Hearing," by W. E. Koch, Bell Telephone Labs.; June 10, 1954.

WICHITA

"General Design Problems of Color Television," by Kenneth Fehling, DuMont Field Engineer; July 14, 1954.

1955
Radio Engineering Show
March 21-25, 1955
Kingsbridge Armory,
New York

Crystal Temperature held to ± 0.025 °C with NEW CRYSTAL OVEN

FR-61 (Model LA-61)

Frequency Meter

(500-2000 MC)

A compact, portable, highly (0.001%) accurate instrument that will perform with utmost reliability under all conditions and in the hands of inexperienced personnel. Widely diversified application, including:

- Accurate measurement of frequency of UHF transmitters or power oscillators
- Checking narrow bandwidth and other filter characteristics . . . measurement of Hi-Q circuits.
- Checking stability and drift of UHF oscillators.
- Qualitative and quantitative evaluation of UHF oscillators with regard to frequency modulation.
- As an accurate signal source where levels of 50-100 microvolts are satisfactory.

Manufactured by Lavoie Laboratories, Inc.
Sold By
Phillip H. Harrison & Co.
Route 34, Matawan, N.J.
Matawan 1-3113, 1-4242
Write for Illustrated Descriptive Pamphlet

NEW HORIZONS IN ENGINEERING

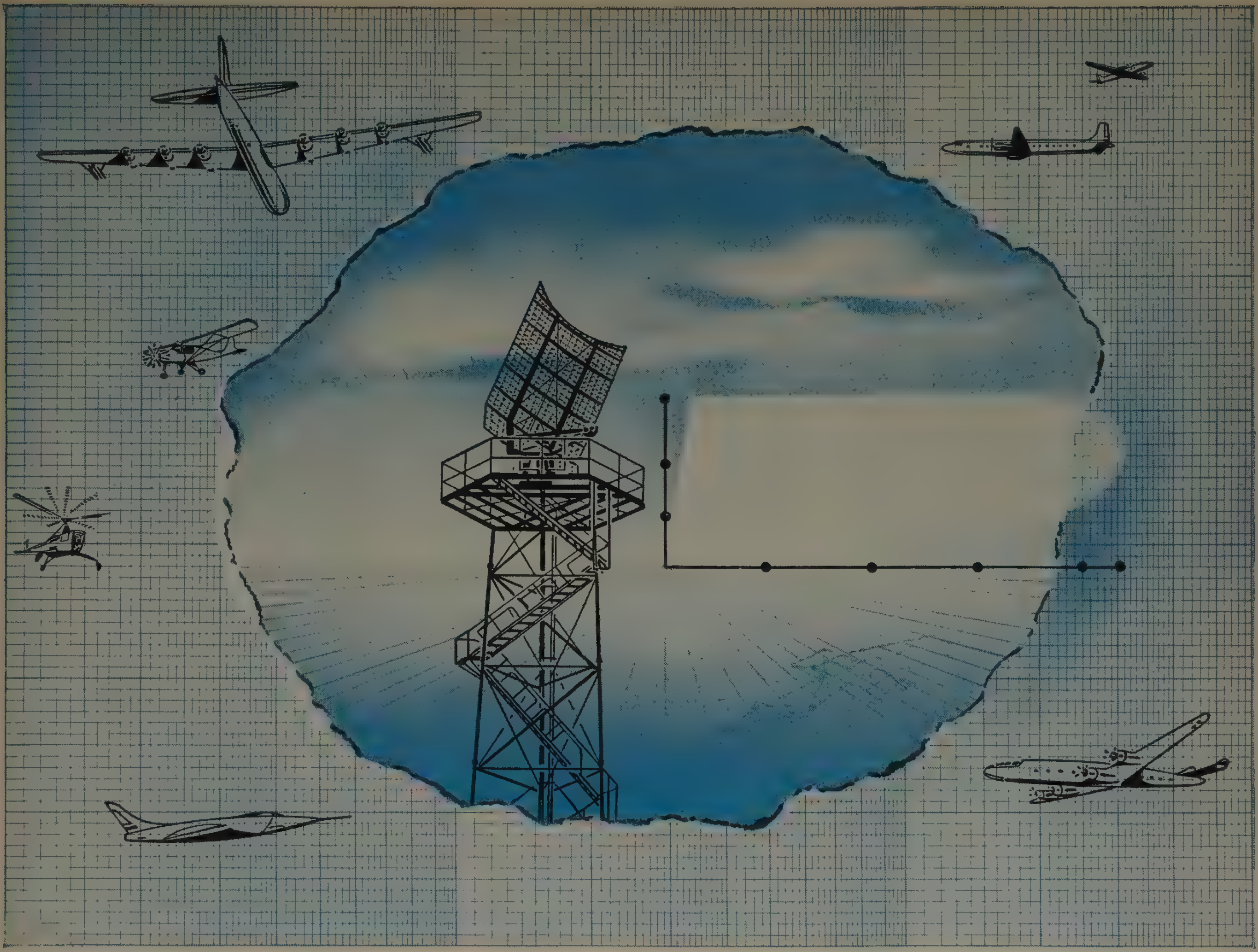

Airport "Traffic Cop"

General Electric developed this unique radar system to track, position and control plane traffic with maximum safety.

It provides many advantages over conventional systems. The special shape of the antenna radiates a beam 12,000 ft. vertically and from 30 to 60 miles horizontally, providing control of all planes in proximity to the airport. Within the pattern of this beam all aircraft are easily detected.

The Special Products Division of I-T-E was asked by General Electric to undertake the production, design and fabrication of this antenna to rigid tolerances. Although 10 feet wide and 12 feet high, the finished product deflected only ¼ inch in actual use when covered with ice and subjected to a 90 knot wind.

This is another of the many ways in which I-T-E technology and specialized fabricating background helps solve production problems for industry. Special Products has an experience in a wide variety of fields. Their engineers might have the solution to your problem.

RADAR ANTENNA SYSTEMS
design, development and fabrication

JET ENGINES
manufacture of major hot-end components

THERMODYNAMICS
design, development and fabrication of equipment to operate on advanced theories

GUIDED MISSILES
advanced fabricating techniques

TITANIUM
proven welding, forging, forming, spinning techniques with this hard-to-work metal

SPINNING
combining spinning and drawing to an almost limitless variety of designs in a wide range of metals

Why not send for Publication SP-100-PI-9 today. It shows what has been done to help others.

TECHNOLOGY
ABILITY
FACILITIES

SPECIAL PRODUCTS DIVISION
I-T-E CIRCUIT BREAKER COMPANY
601 East Erie Avenue • Philadelphia 34, Pa.
Progress through Problem Solutions

SP 10.4

No. 3198
1-1/8″ Tip
550 Watts
No. 3178
7/8″ Tip
300 Watts
No. 3158
5/8″ Tip
200 Watts
No. 3138
3/8″ Tip
100 Watts
No. 3128
1/4″ Tip
60 Watts
No. 3438
3/8″ Tip
100 Watts
No. 3128-A
1/4″ Tip
60 Watts
No. 3120
3/16″ Tip
30 Watts
"RIGHT" AT THE TIP!

THAT'S WHERE THE HEAT IS CONCENTRATED IN ALL

American Beauty

ELECTRIC SOLDERING IRONS

. . . and that's why ANY model of American Beauty Electric Soldering Iron can be chosen with the assurance that it is absolutely DEPENDABLE—DURABLE—EFFICIENT . . . from tip to attachment-plug cap.

★ ★ ★

Four new models have recently been added to our line. They are No. 3120, 3/16″ tip, and its companion iron (No. 3118, 1/8″ tip) and No. 3438, 3/8″ tip, and its companion iron (No. 3438-EP, 3/8″ Eternalloy-Plated tip).

The first two are "Bantam" irons—extremely light but ruggedly-built, small-diameter tip irons designed especially for television, radio, radar and similar precision instrument soldering.

The last two are production-line irons embodying a new type of heat application with the element permanently embedded in the tip for maximun heat-conductivity from tip to the work.

Write for descriptive literature.

AMERICAN ELECTRICAL HEATER COMPANY
DETROIT 2, MICHIGAN

American Beauty ELECTRIC IRONS 60 YEARS YOUNG 1894 1954

No. H-142

IRE People

The Boonton Radio Corporation recently announced the appointment of W. Cullen Moore (A'37–SM'44) as Manager of the company's Development Department.

Mr. Moore is a graduate of Reed College, Portland, Ore., and Boston University with degrees in physics. He was formerly associated with Tracerlabs Inc. of Boston as Chief Engineer, and with Boston University's Upper Air Research Laboratory as Project Supervisor. From 1938 to 1947, Mr. Moore was Senior Project Engineer at Motorola Inc. of Chicago, where he was active in the development of experimental television receivers. In his new post, he will direct the Development Department which is responsible for the development of new B.R.C. electronic test equipment.

International Business Machines Corporation recently announced the appointment of Donald R. Daykin (A'49) to the position of Technical Engineer in Time Equipment Engineering at the Endicott Laboratory.

A native of Cleveland, Ohio, he attended the Case Institute of Technology, graduating in 1947 with a Bachelor of Science degree in Electrical Engineering. He has also completed graduate studies in Electrical Engineering at Case Institute.

Mr. Daykin began his association with IBM in September 1951, when he was hired as a Design Engineer. In the IBM School, Mr. Daykin has completed courses of instruction in Digital Computers, Complex Variables, and Advanced Mathematics.

He is a member of the American Institute of Electrical Engineers, Tau Beta Pi, Eta Kappa Nu, and Sigma Xi.

E. Clarke Quackenbush, (A'50) has recently joined Whitney Blake Company, New Haven, Conn., manufacturers of insulated wire and cable and custom-built cord sets. Mr. Quackenbush will serve as manager of a newly formed Electronics Division which will develop, manufacture and sell electronic connectors and assemblies.

E. QUACKENBUSH

Mr. Quackenbush has specialized in communication, transmission and lighting equipment, connectors and wiring devices and the dielectrics used in their design. He holds a number of patents covering connectors and wiring devices and was one of the pioneers in the development of the AN connector line, now in general use in aircraft and many types of electronic equipment.

Before joining Whitney Blake Company, Mr. Quackenbush was Engineer in

(Continued on page 92A)

REFERENCE

GENERATOR

for remote position indication

"Sixth sense" is provided by the midget generator whose rotor is turned by scanning or tracking radar.

How many applications for these precision electro-mechanical units! Any revolving shaft can be closely monitored through reference generator output in a closed loop control system.

OSTER Avionic Products conform to military specifications for altitude, high and low temperature, life, shock, vibration, humidity, and fungicidal treatment.

You can depend on Oster quality in rotating components for automatic control.

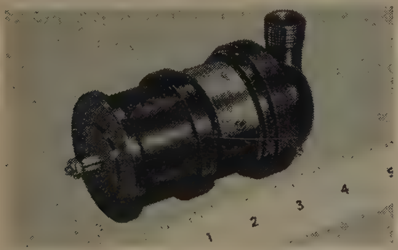

OSTER two-phase Reference Generator, Type 212055. Develops 40 volts, 35 cycles when driven 2100 rpm. Use it on rotary or rate indication applications.

Other OSTER Avionic Products include:

- Special motors: Servos, Synchros, Drive Motors, Blowers and Fans for use with D-C and A-C supply voltages in common usage on aircraft and ground equipment.
- Synchro Generators, Control Transformers, Transmitters, Differentials, Receivers, Resolvers and Two-Speed Synchros.
- Tachometer Generators and Reference Generators.
- Aircraft Actuators, both linear and rotary.

Insure dependability...specify Oster®

For your copy of our illustrated pamphlet No. 974 on Oster Avionic Products, write John Oster Manufacturing Co., Avionics Division, Dept. 489, Racine, Wisconsin, U.S.A.

JOHN OSTER
MANUFACTURING COMPANY
AVIONIC DIVISION
RACINE, WISCONSIN

NOISE

FIGURE TEST SET

Simplifies measurement of tuner noise figure of any receiver. Test set combines broad band I.F. Amplifier, built in 3db network and output indicator, and regulated power sources. Permits uniform consistent measurements of noise factor, observation of tuner R.F. selectivity.

FEATURES: **MODEL HF-20**

- Band-width 10 mc centered 20, 30, 40, or 60 mc
- Ideal for production testing or incoming inspection
- Employs most accurate NF test method
- Plate and bias voltages electronically regulated
- Provisions for accomodating variety input circuits

WRITE FOR CATALOG

LINEAR EQUIPMENT LABORATORIES INC
MASSAPEQUA, L. I., N. Y.

VHF-UHF

REFLECTION BOX

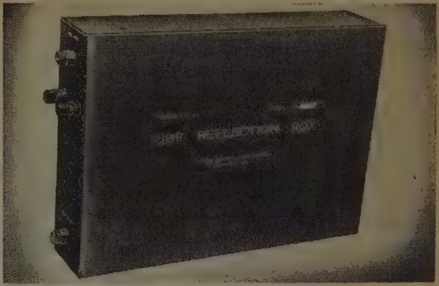

Specifically designed to facilitate the measurement of reflection coefficient of VHF and UHF tuners and converters. Enables simple visual observation of the ability of a tuner to provide a proper match to a 300 ohm transmission line over the VHF and UHF TV bands.

FEATURES:

- Aids in design of tuner input and coupling networks
- Eliminates cumbersome, unsightly transmission line installations in lab or factory.
- Increases sensitivity in measurements of impedance
- Permits accurate measurement of attenuation
- Models available 50 or 75 ohm source; VHF-50-220 mc or UHF-470-890 mc

WRITE FOR CATALOG R-9

LINEAR EQUIPMENT LABORATORIES INC
MASSAPEQUA, L. I., N. Y.

for all applications requiring exceptionally high insulation resistance and unusual stability at high temperature

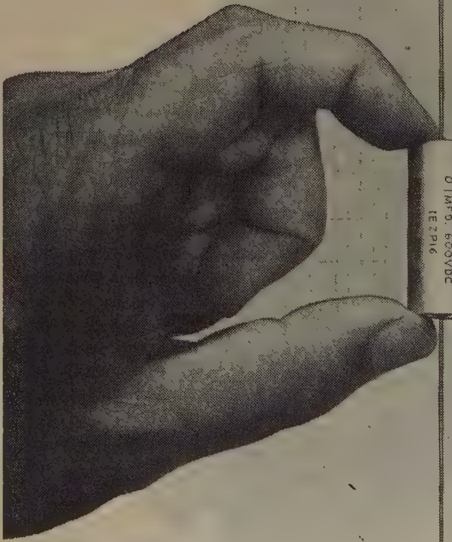

2082 Lincoln Ave.,
Altadena, Calif.
SYcamore 8-1185
Offices in
WASHINGTON, D.C.
and DETROIT

HOPKINS

"HY-THERM"

New sub-miniature high temperature

CAPACITOR

Hermetically sealed and metal encased, new HY-THERM capacitors have been designed to meet or exceed military requirements (Mil-C-25A). **Example:** At 125°C the minimum insulation resistance is 20 megohm-microfarads and maximum insulation resistance is 500 megohms. Available in all standard values and tolerances. Variety of mounting and circuit combinations. Special units designed to meet individual requirements.

HOPKINS Engineering Co.

Have a special problem? Write, wire or phone for details, TODAY! Catalog available.

HHB presents

A NEW IDEA IN Flexible Plastic TUBING CLAMPS

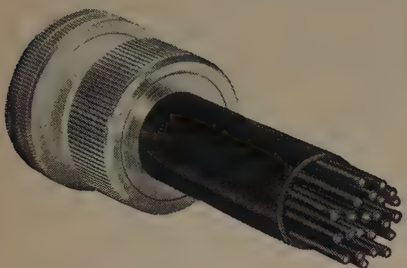

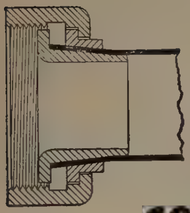

for use with AN TYPE CONNECTORS

This unique tubing clamp provides an inexpensive method to protect open wiring used in connection with a standard AN TYPE CONNECTOR.

It is an *easy* and *quick* way to attach flexible plastic tubing to a connector—*without the use of hand tools.* When used in conjunction with a gasketed adapter, a waterproof joint is provided between connector and tubing.

Material—aluminum. Sizes to accommodate tubing from ¼-in. I.D. to 2-in. I.D. AN plug sizes 12S to 48.

Write for Catalog data.

Skilled in Electronic Component Parts
RESEARCH • DESIGN
ENGINEERING
MANUFACTURING

H. H. BUGGIE, Inc.
726 STANTON STREET
TOLEDO 4, OHIO

IRE People

(Continued from page 90A)

Charge of the Eastern Division of Cannon Electric Company. He set up this company's plant in East Haven, Conn., and was in charge of its operation for several years.

He is a member of the American Society for Metals.

CBS-Hytron, a division of Columbia Broadcasting System, Inc., has recently announced the promotion of **Charles F. Stromeyer** (A'29–VA'39) to the position of executive vice-president of CBS-Hytron.

C. F. Stromeyer

Mr. Stromeyer joined CBS-Hytron in 1942 as chief engineer and assistant to the president and was later made vice-president in charge of manufacturing and engineering. He is recognized throughout the electronic industry for his abilities in both manufacturing and engineering.

Mr. Stromeyer has been awarded several patents for his developments in electronic circuits and tubes. His entire business career has been concentrated in the electronic-tube industry.

Colonel Cary J. King, Jr. (A'30, VA'39, SM'50) retired from the Regular Army on June 30, 1954, after more than 30 years commissioned service.

C. J. King, Jr.

Colonel King graduated from the United States Military Academy, B.S. 1924, received a degree of M.S. in Communication Engineering at Yale University in 1930, and the Electrical Engineer degree at Massachusetts Institute of Technology in 1949.

His Army service has been in the Signal Corps except for the period of World War II which was spent with the Air Force in communication work. He was Deputy Chief Air Signal Officer, Supreme Headquarters, Allied Expeditionary Force, during the European Operations. Prior to his assignment as Assistant Commandant of The Signal School last fall, Colonel King was Chief, Engineering and Technical Division, Office of the Chief Signal Officer in Washington, and was Assistant Chief Signal Officer for Research and Development. During his term in Washington, Colonel King was a member of the Electronics Committee, the Geophysics and Geography Committee, and the Guided Missile Committee, RDB, and of the Joint Meteorological Committee.

His military decorations include the Legion of Merit, the Bronze Star Medal, Honorary Commander of the Most Excellent Order of the British Empire, and the Medaille de l'Aeronautique (France).

A. C. Household ELECTRICITY Anywhere... IN YOUR OWN CAR!

BE PREPARED FOR ANY EMERGENCY WITH ATR INVERTERS!

THIS COULD HAPPEN!

Ideal for Emergency Lighting and Power Applications for Civil Defense, Red Cross, Rescue Work, etc. Simply Using Extension Cords.

EASY TO INSTALL
EASY TO OPERATE

Also... DICTATE REPORTS ACCURATELY-PROMPTLY!

make your car, boat or plane a "rolling office" WITH ATR INVERTERS

for changing your storage battery current to A. C. Household ELECTRICITY Anywhere . . . in your own car!

LIST PRICE $22.50 AND UP

ATR INVERTERS especially designed for operating standard 110 volt A. C.

- TAPE RECORDERS
- DICTATING MACHINES
- WIRE RECORDERS
- ELECTRIC RAZORS

See your jobber or write factory today for complete information

ATR AMERICAN TELEVISION & RADIO Co.
Quality Products Since 1931
SAINT PAUL 1, MINNESOTA—U. S. A.

PROFESSIONAL GROUP MEETINGS

AERONAUTICAL AND NAVIGATIONAL ELECTRONICS

The Los Angeles Chapter of the Professional Group on Aeronautical and Navigational Electronics met on June 8 at the University of California at Los Angeles under the chairmanship of Dr. James Marsh. A panel discussion was held on the subject of "Current Practices in Reduction and Control of Radio Interference." Panel speakers were Jules Hornung, International Electronics; Charles Weiland, Chief Engineer, Hopkins Engineering Co.; R. E. Hedges, Douglas Aircraft Co.; M. Glass, Hughes Aircraft Co.; and H. McCleece, Lockheed Aircraft Co. Following the presentation of the problem by the speakers, the panel discussion was concluded with audience participation.

The New York Chapter met on June 10 at the General Electric Auditorium under the chairmanship of R. J. Bibbero. Dr. David O. McCoy of the Engineering and Research Division, Collins Radio Company, presented a paper entitled "A Simplified Omni-Range System for Navigation." The paper was discussed by all those present. At the same meeting the following officers were elected for the coming year: Chairman, Robert J. Bibbero; Vice Chairman, Gordon McCouch; and Secretary, Philip B. Petersen. Les Glantz was appointed Membership Chairman.

ANTENNAS AND PROPAGATION

The Los Angeles Chapter of the Professional Group on Antennas and Propagation met on June 2 at the IAS Building in Los Angeles under the chairmanship of M. J. Ehrlich. Dr. Jesse L. Greenstein, Mount Wilson and Palomar Observatories, spoke on "Radio Astronomy." Officers elected for the coming year are S. M. Kerber, Chairman; R. Krausz, Vice Chairman; E. Lovick, Jr., Secretary.

AUDIO

The Boston Chapter of the Professional Group on Audio met on May 25 at Massachusetts Institute of Technology under the chairmanship of John Kessler. A paper entitled "High Fidelity: History, Objectives and Trends" was presented by Hugh S. Knowles of Industrial Research Products, Inc. The following men were elected officers for the coming year: John Kessler, Chairman; W. Wathen-Dunn, Vice Chairman; and M. W. Essigmann, Secretary-Treasurer.

The Chicago Chapter met on April 30 at the Western Society of Engineers. The presiding officer was L. Price, Vice Chairman of the Group. B. B. Vauer, Vice President of Shure Brothers, Inc., presented a paper entitled "Equivalent Circuits of Electro-Acoustics and Electro-Mechanical Devices." This meeting was held jointly with the Chicago Chapter of the Professional Group on Circuit Theory.

(Continued on page 96A)

KEARFOTT—ASKANIA ELECTRO JET

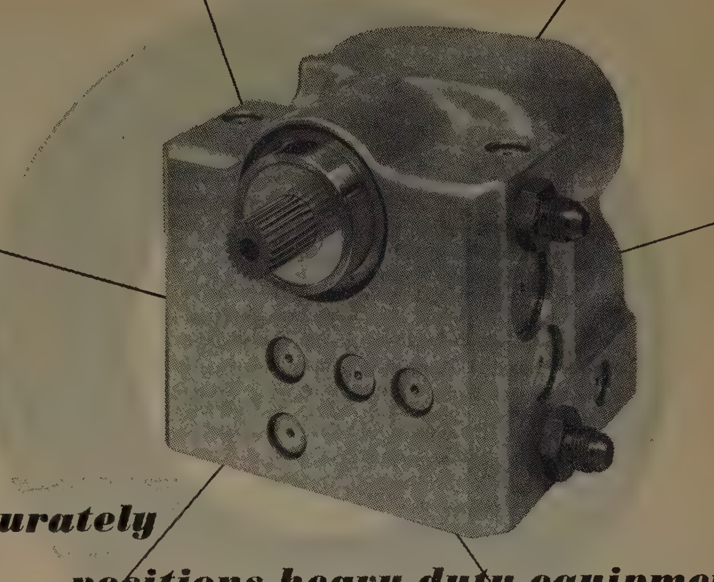

accurately positions heavy duty equipment by means of minute electrical signals

This Electro-Hydraulic Servo System is ideally suited for industrial controls to maintain flows, ratios, levels, pressures, speeds and for machine tool positioning. It is a 5¼" cube self-contained unit and weighs but 12 pounds.

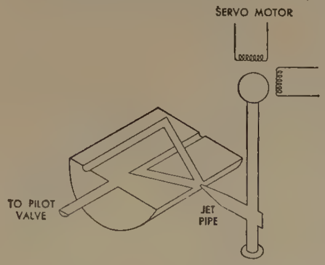

The Kearfott Electro Jet utilized the Askania jet pipe principle, characterized by high frequency response, rugged construction and highly accurate shaft positioning. Rated output is 200 inch pounds torque through ±60 degrees. Maximum torque rating is 333 inch pounds. Frequency response is flat (within 3 db) up to 25 cycles. Resolution of the output piston positions is one part in 500 or better.

Write today for full information about the Kearfott Electro Jet. It may help in the solution of your control problem.

KEARFOTT COMPONENTS INCLUDE:

Gyros, Servo Motors, Synchros, Servo and Magnetic Amplifiers, Tachometer Generators, Hermetic Rotary Seals, Aircraft Navigational Systems, and other high accuracy mechanical, electrical and electronic components.

Send for Bulletin giving data of components of interest to you.

Kearfott
SINCE 1917

KEARFOTT COMPANY, INC., LITTLE FALLS, N. J.
Sales and Engineering Offices: 1378 Main Avenue, Clifton, N. J.
Midwest Office: 188 W. Randolph Street, Chicago, Ill. South Central Office: 6115 Denton Drive, Dallas, Texas
West Coast Office: 253 N. Vinedo Avenue, Pasadena, Calif.
A GENERAL PRECISION EQUIPMENT CORPORATION SUBSIDIARY

AMPHENOL

MINIATURE AN-type CONNECTORS

SPECIAL FEATURES:

- ★ ⅓ the weight of standard AN connectors
- ★ Pressure-proof
- ★ Waterproof, mated or apart
- ★ "O" ring sealers
- ★ Spun-in sandwich construction on female connectors
- ★ Aluminum shells with *hard-cote* grey anodic finish
- ★ Gold-plated contacts
- ★ Famous AMPHENOL 1-501 blue dielectric
- ★ Unique built-in cable strain relief

Design engineers have long requested a miniature version of standard AN connectors. And here is the answer: the new AMPHENOL 165 series of miniature AN-Type connectors have the *identical electrical qualities* of standard AN's compressed into only *one-third* the weight! Now designers of electronic equipment requiring AN connectors can utilize the 165 series instead and show substantial savings in both weight and space.

The 165 series are available in two connector sizes and six contact configurations. The small size is obtainable in 5, 9 or 12 contacts; the "large" size in 11, 14 or 24 contacts—all have male or female inserts in plug or receptacle.

For more complete information about the 165 series, write and request "Amform 2397."

AMERICAN PHENOLIC CORPORATION
Chicago 50, Illinois
AMPHENOL

In Canada: AMPHENOL CANADA, LTD.

PROFESSIONAL GROUP MEETINGS

(Continued from page 95A)

Broadcast and Television Receivers

The Chicago Chapter of the Professional Group on Broadcast and Television Receivers met on April 30 at the Western Society of Engineers under the chairmanship of John T. Williams. Dr. Kurt Schlesinger, Research Director of Motorola, spoke on "Vectorscope." On May 21 the Chapter met at the Western Society of Engineers to hear Max Beier and Albert Cotsworth of Zenith Radio speak on "Noise Factor and its Measurements."

Circuit Theory

The Los Angeles Chapter of the Professional Group on Circuit Theory met on May 11 at the Institute for Numerical Analysis under the chairmanship of J. A. Aseltine. A paper entitled "Network Synthesis by Matrix Factorization Techniques," was presented by Er-Chun Ho, Engineering Department, UCLA. Arnold Rosenbloom, Department of Engineering, UCLA, presented a paper on "Randomly Time-Varying Linear Systems." The following officers were elected for the coming year: Chairman, W. R. Abbott; Secretary-Treasurer, J. E. Jacobs.

Component Parts

The Washington, D. C. Chapter of the Professional Group on Component Parts met on May 19 at the National Bureau of Standards. Philip J. Franklin, of D.O.F.L., National Bureau of Standards, spoke on "Casting Resins in Electronic Assemblies."

Electronic Computers

The Los Angeles Chapter of the Professional Group on Electronic Computers met on June 17 at the Institute for Numerical Analysis under the chairmanship of Les Kilpatrick. A panel discussion entitled "How Do You Know You Are Right," concerning diagnostic routines and procedures, was conducted under the chairmanship of John McCloud. Short summary talks were given by Wesley Melahon, Louis Fine, Donald Worthington, Monty Phister, and Frederick Holland, which were followed by general discussion and questions from the floor.

Electron Devices

A meeting of the Philadelphia Chapter of the Professional Group on Electron Devices was held on May 21, 1954, with E. I. Hawthorne, Chairman. The following officers were elected for the coming year: Chairman, B. T. Svihel, Kuljian Corp.; Vice-Chairman, W. Hasenberg, RCA; Secretary, G. R. Spencer, Philco Corp., Lansdale Division.

E. G. Nichols read his paper on "Recent Advances in Cathode Ray Tubes," presenting an interesting talk on the new monoaccelerator cathode-ray tube, which was discussed thereafter by the members present.

(Continued on page 98A)

15 Horse Power in a 7″x 11″ case!

A typical example of American Electric engineering

This 400 cycle 3 phase motor is a special custom-developed aircraft design. Rated at 15 h.p. continuous duty at 11,500 r.p.m., it actually produces 19 h.p. on intermittent duty, yet occupies less than ¼ cubic foot. Weight is 32 lbs.—approximately ½ h.p. per lb. Fungus-proof, corrosion resistant, meets AND 20002 type XIIB mounting specifications. Temperature range: −67° to +131° F. Motor length: 7″, Coupling extension 4″.

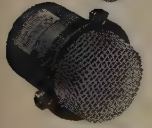

MINIATURE MOTORS for all PURPOSES!

American Electric Motors are also built in an almost unlimited range of miniatures for 60 and 400 cycle operation as well as variable frequencies. All feature low weight, compact size and meet high temperature requirements. Supplied in induction or synchronous types for motor drives, propeller fans and centrifugal blowers. Wire, write or phone for data and quotations.

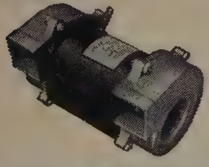

Also Manufacturers of High Cycle Motor-Alternators and A.C. Industrial Motors.

AMERICAN ELECTRIC MOTORS
TRADE MARK

4811 Telegraph Road
Los Angeles 22,
California

DIVISION OF AMERICAN ELECTRONICS, INC.
FIELD ENGINEERING REPRESENTATIVES:
Boston • Buffalo • New York City • Chicago • Dallas
Kansas City • Wright Field • Minneapolis • Seattle
Montreal • Toronto
JOE DAVIDSON & ASSOCIATES, Los Angeles

NO GUESSWORK

NO CHANCE FOR ERROR

with a
DIRECT READING

HYCON DIGITAL VTVM

MODEL 615

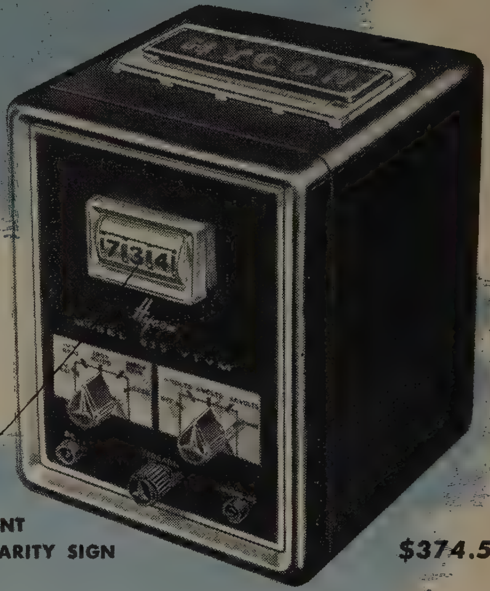

ILLUMINATED DECIMAL POINT AND POLARITY SIGN

$374.50

The Model 615 VTVM is a precision instrument — functional in design . . . professional in appearance. The direct-reading digital display eliminates most interpolation error — shortens costly "learning curve" in factory and assembly line inspection.

Other features — never before offered in an instrument of comparable price — include 1% accuracy (DC and ohms), and *1 millivolt* sensitivity. Inspect the Model 615 at your Electronic Parts Jobber's. You'll agree the new standard is Hycon . . . "where accuracy counts."

- **12 RANGES: AC, DC, OHMS** • **AC FREQUENCY RESPONSE TO 250 MC (with auxiliary probes)** • **OVERLOAD PROTECTION** • **LIGHTWEIGHT, STURDY STEEL CASE** • **PROVISIONS FOR BENCH STACKING**

The Model 615 VTVM is one of a matching set of precision test instruments, which includes the Model 617 Oscilloscope (designed for color TV) and the Model 614 Standard VTVM.

Service facilities in your area.

Hycon Mfg. Company
2961 EAST COLORADO STREET . PASADENA 8, CALIFORNIA
"Where Accuracy Counts"

for SPECIFIC microwave information on "new" components or "standard" plumbing

BALANCED
MIXERS
DIRECTIONAL
COUPLERS
Branching and Balanced
DUPLEXERS
Airtron
PRECISION CASTING FACILITIES
FOR THE MICROWAVE AND RADAR INDUSTRY

If you use microwave components . . . you can benefit from Airtron's broad range of engineering experience in designing and producing both advanced and so-called "standard" plumbing. For specific, helpful information . . . prepared *by* and *for* engineers . . . merely fill in the obligation free coupon below and send it to us.

BRANCHING AND BALANCED DUPLEXERS
Standard and special duplexers, from 6.66 x 3.41 to .360 x .220 O. D. Power, performance and packaging to meet your applications. *Bulletin T-2200.*

DIRECTIONAL COUPLERS
4 basic types in all waveguide sizes from 6.66 x 3.41 to .360 x .220 O. D. Broadband couplings and directivities to meet your needs. *Bulletin T-2400.*

BALANCED MIXERS
Mixers with waveguide crystal mounts or coaxial crystal mounts covering a frequency range from 400 to 40,000 megacycles. "Standardized" and special types. *Bulletin T-2600.*

AIRTRON PRECISION CASTING FACILITIES
Precision castings, holding tolerances of ±.002″ per inch of dimension, economically made to your own specifications. *Bulletin 6002.*

FLEXIBLE WAVEGUIDE
Available in all sizes for high power pressurized applications over wide temperature ranges. Seamless, twistable, preformed and circular. Special waveguides to meet specific problems. *Cat. 1011*

TWO-POSITION WAVEGUIDE SWITCHES
For rapid and/or cyclic switching to or from noise sources, signal generators, dummy loads, etc. Low VSWR, excellent crosstalk and high peak power performance. *Cat. 2331.*

SHORT SLOT HYBRIDS
Precision cast one piece hybrids. Low VSWR, excellent isolation and low attenuation over broad bandwidths. Used in balanced mixers, duplexers, power splitters. *Cat. 2361*

K-BAND TEST HORNS
For test purposes over the frequency range from 12,400 to 40,000 mc. One piece aluminum castings to close tolerances. Low VSWR. Low secondary lobes. *Cat. 3291.*

WAVEGUIDE MAGIC TEES
Hybrid junctions for power splitting with minimum energy loss. From 3.00 x 1.50 to all smaller standard and military sizes. Low VSWR and excellent broadband isolation. *Cat. 3330*

OTHER AIRTRON PRODUCTS

Folded Hybrids • Quick Disconnects • VSWR Standards • High Power Dummy Loads • Antenna Horns • Waveguide Bends, Twists, Elbows and Transitions • Rotating Joints • RF and Pressure Gaskets • Aircraft Junction Boxes and Cable Assemblies

Airtron INC.
Linden, New Jersey

Branch Offices
ALBUQUERQUE
CHICAGO
DALLAS
DAYTON
KANSAS CITY
LOS ANGELES
SAN FRANCISCO
SEATTLE

USE THIS HANDY COUPON

AIRTRON, INC.
1107 West Elizabeth Ave.
Linden, N.J.

Please send me without obligation information on..................
....
....
NAME..........................TITLE..................
COMPANY...
STREET..
CITY......................ZONE...........STATE.......

☐ Check here if you want Airtron representative to call.

PROFESSIONAL GROUP MEETINGS

(*Continued from page 96A*)

ENGINEERING MANAGEMENT

The Boston Chapter of the Professional Group on Engineering Management met on June 1 at the Faculty Club of Massachuetts Institute of Technology. Samuel Fishbein was the Acting Chairman. Dr. E. Bowles, Consulting Engineer Specialist at MIT spoke on "Observation on Technological Trend in Management." Officers elected for the coming year are: Samuel B. Fishbein, Chairman; Ronald McFarlan, Vice Chairman; Samuel C. Coroniti and R. L. Jones.

The Los Angeles Chapter met on May 20 at the IAS Building under the chairmanship of T. W. Jarmie. C. B. Thornton, Chairman of the Board of Electro Dynamics, Inc., presented a paper entitled "Present-Day Aspects of Management in the Electronic Industry." The Chapter also met on June 17 at the IAS Building, at which time a panel discussion on the question, "Should Engineers Be Paid Primarily for Technical Knowledge or for Leading Others." Members of the panel were C. F. Hoone, Convair; Ellis F. King, UCLA; Donald R. Blair, Electronic Engineering

(*Continued on page 100A*)

New standard of professional recording

Dynacord
PROFESSIONAL TAPE RECORDER
by PENTRON

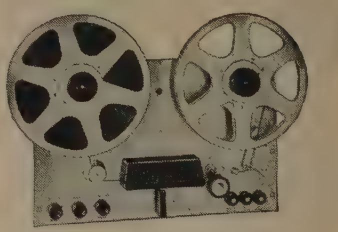

engineered throughout to NARTB standards

- Portable, may be rack mounted or installed in console.
- High inertia direct capstan drive for minimum flutter.
- New type slow speed "inside-out" hysteresis motor.
- Dynamic braking.
- Interlocked push-button control.
- 3-Head construction facilitates monitoring.
- Accommodates 10½" reels.
- Instantaneous emergency stop.
- Many more superior features.

***WRITE** for new bulletin today!*

THE PENTRON CORP. Dept. IRE-9
777 S. Tripp Ave., Chicago 24, Ill.

PENTRON
Canada:
Atlas Radio Corp., Ltd., Toronto

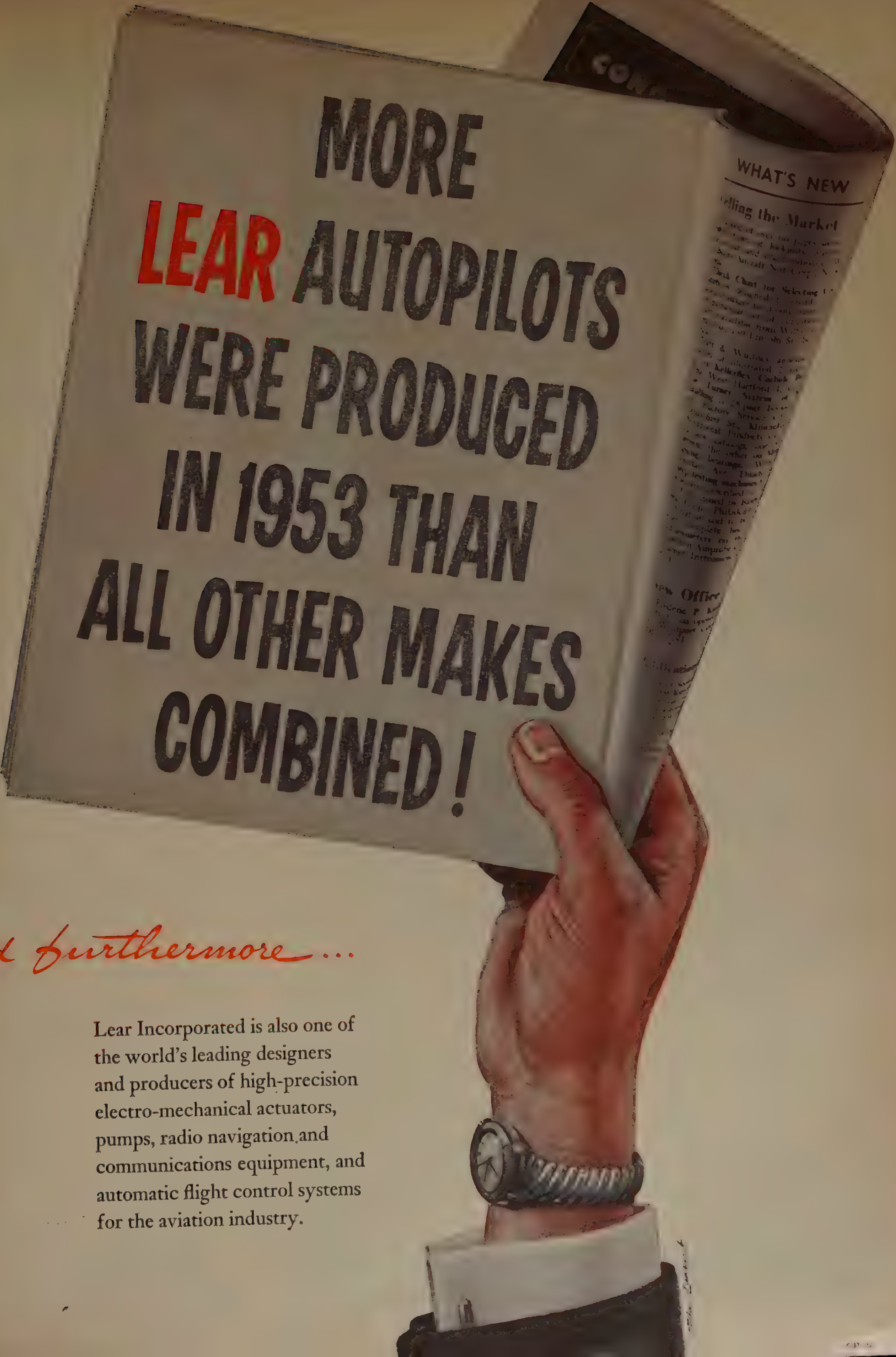
MORE LEAR AUTOPILOTS WERE PRODUCED IN 1953 THAN ALL OTHER MAKES COMBINED!
WHAT'S NEW

d furthermore ...

Lear Incorporated is also one of the world's leading designers and producers of high-precision electro-mechanical actuators, pumps, radio navigation and communications equipment, and automatic flight control systems for the aviation industry.

REGULATED HIGH VOLTAGE POWER SUPPLY

Provides Electronically Regulated, Continuously Adjustable Voltages from 150 to 1500 VDC at 0.5 Milliamperes

This unit is specially designed to supply proper power for making precise quantitative measurements with photomultiplier tubes, klystrons and similar applications.

Voltages are held to close limits even with wide line voltage and load variations.

No meter is required. Accurate voltage readings are made directly from a 15 turn vernier dial which is calibrated to read 1 volt per scale division.

Write for Literature on Other High Voltage Regulated Power Supplies

MODEL 810-P SPECIFICATIONS

- **OUTPUT VOLTAGE:** 150 to 1500 VDC at 0-5 Milliamperes.
- **REGULATION:** Output voltage varies less than .01% per volt change of line voltage and less than .1 volt with variation of output current from 0 to 5 Milliamperes.
- **RIPPLE:** Less than 5 Millivolts r.m.s.

Positive output terminal is grounded. 5 negative output connectors (type AN-3102A-18-16-s) are connected in parallel and mounted on front panel.

WRITE FOR DESCRIPTIVE BULLETIN

FURST ELECTRONICS, INC.

3326 W. Lawrence Ave., Chicago 25, Illinois

Metallurgists & Specialists in Small Wire

Serving Industry—*FOR OVER 53 YEARS*

BASE METAL WIRES
Very small diameter—for filaments, thermo-couples, resistance units.

PRECIOUS METAL WIRES
Produced in Platinum, Gold, alloys and pure metals—small diameter . . . Platinum alloy resistance wires.

COATED WIRES
Comprising an extensive range of electroplated grid wires . . . Enamel insulated wires for precision resistors and potentiometers.

. . . Write for latest List of Products.

Since 1901

SIGMUND COHN MFG. CO. INC. 121 So. Columbus Avenue, Mt. Vernon, N. Y.

PROFESSIONAL GROUP MEETINGS

(Continued from page 98A)

Co.; Maurice V. Horrell, Bendix Computer Division; and A. M. Zarem, Stanford Research Institute. Following the panel discussion the annual business meeting was held and the following newly-elected officers were installed: L. W. Baldwin, Chairman; Robert Beagles, Vice Chairman; and K. A. Giffin, Secretary-Treasurer.

INDUSTRIAL ELECTRONICS

The Chicago Chapter of the Professional Group on Industrial Electronics met on April 30 at the Western Society of Engineers. Andrew I. Wohlert, Development Engineer of the National Electronics Co., presented a paper entitled "Birth of a Tube."

NUCLEAR SCIENCE

The Chicago Chapter of the Professional Group on Nuclear Science met on April 30 at the Western Society of Engineers under the chairmanship of Theodore Fields. Movies of the 1952 Pacific tests of the H bomb, entitled "Operation Ivy," were presented.

RADIO TELEMETRY AND REMOTE CONTROL

The Los Angeles Chapter of the Professional Group on Radio Telemetry and Remote Control met on May 11 at the IAS Building. The presiding officer was R. A. Rawlins, Assistant Chairman. G. L. Larse. Lockheed Aircraft Corp,, presented a paper on "A Versatile FM Subcarrier Oscillator." Doyle F. Mattson, also of Lockheed Aircraft, presented a paper entitled "Low-level DC Input Signals in FM/FM Telemetry." The Chapter also met on June 15 at the IAS Building under the chairmanship of John Kauke. A discussion on "Crystal Controlled F.M Telemetering Transmitters" was presented by W. Chester, Bendix Aviation Corp.; Roy Murray, Raymond Rosen; A. Nuut, West Coast Electronics; R. Rawlins, Lockheed Aircraft; John Kauke, ASCOP; and R. Sherlock, R. M. Parsons Co.

VEHICULAR COMMUNICATIONS

The Chicago Chapter of the Professional Group on Vehicular Communications held a joint meeting with the Chicago Chapter of the Professional Group on Instrumentation on May 21 at the Western Society of Engineers, under the chairmanship of William J. Weisz. Gene Stiles and Philip Conway of Alfred Crossley & Associates presented a paper entitled "Field Measurement in Mobile Services." The paper was discussed by the audience.

1954
IRE DIRECTORY
COMING SOON!

MEMBERSHIP

The following transfers and admissions were approved to be effective as of August 1, 1954:

Transfer to Senior Member

Ackerman, M. J., 208 E. Browning Rd., Collingswood 7, N. J.
Alexander, F. C., Jr., 2824 Mt. Royal Blvd., Glenshaw, Pa.
Benner, A. H., 717 Cedar Ave., Haddonfield, N. J.
Bergan, K. N., 5030—41 Ave., S., Minneapolis 17, Minn.
Bergman, S. I., 3890 Orloff Ave., New York 63, N. Y.
Billingsley, F. C., 2004 Clifton Park Rd., Schenectady 9, N. Y.
Bookman, R. E., 211 Main St., Medford 55, Mass.
Bruce, G. B., 20 Maple La., c/o Brown, New Hyde Park, L. I., N. Y.
Clark, R. W., 1101 Casiano Rd., Los Angeles 49, Calif.
Cooley, A. G., 540 W. 58 St., New York 19, N. Y.
Dahlbom, C. A., Bell Telephone Laboratories, Inc., 463 West St., New York 14, N. Y.
Daniel, R. L., c/o Bendix Radio, 10500 Magnolia Blvd., N. Hollywood, Calif.
Davenport, W. B., Jr., Garfield Rd., Concord, Mass.
Dickey, D. W., 78 Park Ave., Maplewood, N. J.
Fischer, B., 1909½ Talmadge St., Hollywood 27, Calif.
Freedman, N., 57 Rowe St., Auburndale 66, Mass.
Freyman, R. W., 2255—46 St., Los Alamos, N. Mex.
Ghose, R. N., RCA Victor Division, Broadcast Engineering Section, Engineering Products Department, Bldg. 53-C1, Camden 2, N. J.
Gordon, D. I., 2711 Colston Dr., Chevy Chase 15, Md.
Graham, M. L., 333 E. Oak Ave., Moorestown, N. J.
Greenfield, A., 34 Laurel Dr., Scranton, Pa.
Harris, D. E., Boalsburg, Pa.
Harris, K. B., 65 Bala Ave., Toronto 9, Ont., Canada
Hastings, L. E., c/o Federal Communications Commission, 521 New Customhouse, Denver 2, Colo.
Hecht, B., 1430½ S. Beverly Glen Blvd., Los Angeles 24, Calif.
Hittner, C., 79-24—258 St., Floral Park, L. I., N. Y.
Hunter, W. C., 2315 Hendola Dr., N.E., Albuquerque, N. Mex.
Inderwiesen, F. H., Jr., 4105 W. 73 St., Prairie Village 15, Kan.
Jacobs, F., 8427—105 St., Richmond Hill 18, L. I., N. Y.
King, H. B., 124 Wolf Creek St., Brookville, Ohio
Kuehl, W. J., 652 Beaumond Pl., Utica, N. Y.
Lytle, A. C., Jr., 825 Calle De Arboles, Redondo Beach, Calif.
Mallinckrodt, A. J., 608 Stonehurst Ave., Altadena, Calif.
Mallory, H. R., Rock Ridge North, Greenwich, Conn.
Martin, R. E., 62-27—84 St., Rego Park 79, L. I., N. Y.
McDonald, J. F., 910 N. Seventh St., New Hyde Park, L. I., N. Y.
Merriman, H. O., 1348 Thames St., Ottawa, Ont., Canada
Neubauer, J. R., 504B Park View Apts., Collingswood 6, N. J.
Norman, S. W., 300 Buxton Rd., Falls Church, Va.
Ozone, K., 729 Holt Rd., Webster, N. Y.
Penick, D. B., Bell Telephone Laboratories, Inc., Murray Hill, N. J.
Perry, C. S., 12312 Navy St., W. Los Angeles 34, Calif.

(Continued on page 105A)

HIGH INSULATION RESISTANCE

✓ Over 500 times greater than ordinary commercial oil capacitors

Stabelex® "D" Capacitors

For Precision Circuitry in:

Diathermy Equipment
Rectifiers
Pulse Generators and Triggering Devices
Countless Other Industrial and Electronic applications

Whether your capacitor requirements are new, unusual or standard, let Industrial Condenser Corporation's specialized engineering staff recommend the *right* capacitors to meet your specific needs. For important finger-tip data on capacitor performance, characteristics and applications, send for Catalog 1117. You need this information.

Outstanding Operating Characteristics

✓ **Insulation resistance** at +20°C. after three minutes charge: 900,000 megohm microfarads

✓ **Insulation resistance** at +75°C.: 78,000 megohm microfarads

✓ **Insulation resistance** at —75°C.: In excess of one million megohm microfarads

Change in capacitance from +25°C. to —80°C.: +0.76%

Self time constant of 10 mfd. capacitor: 4800 hours

Q at 50 kilocycles: 10,000

Power Factor at 1 kc: 0.00025

INDUSTRIAL CONDENSER CORPORATION

3247 N. CALIFORNIA AVE., CHICAGO 18, ILLINOIS

Stable, Low-Noise Carbon Controls in ANY Combination You Want

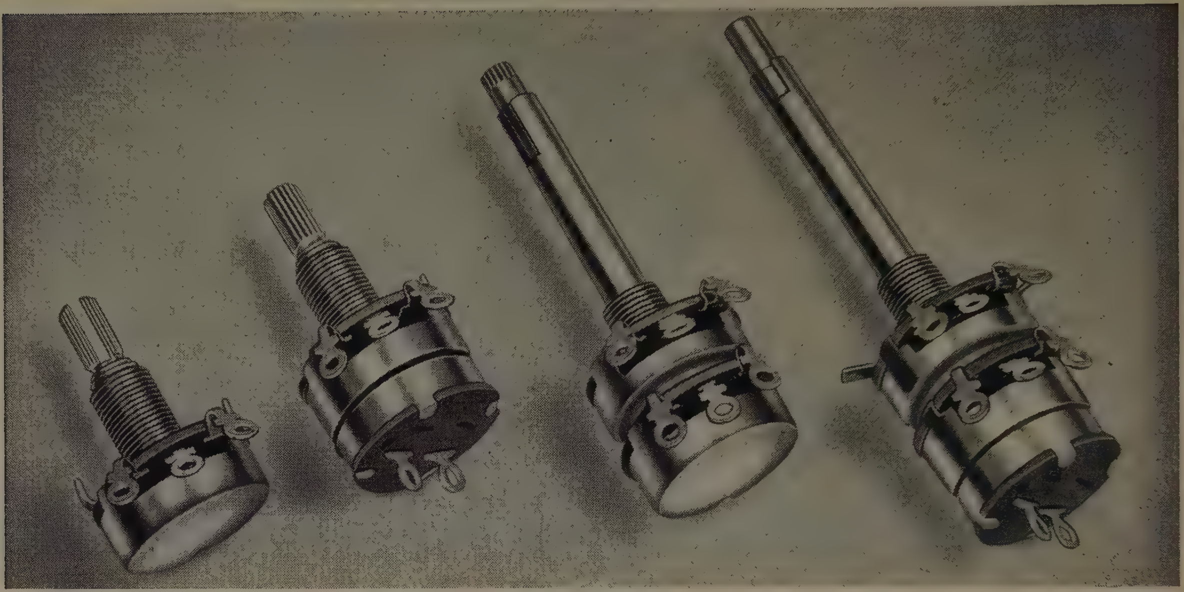

You don't have to compromise with quality to get the carbon controls your application requires. For Mallory Controls are available in a complete range of constructions, including single, dual concentric and dual tandem types . . . with or without switch.

Their noise level is unusually low, resistance values are unusually stable, and humidity drift is held to 10% . . . thanks to carbon elements with a high degree of surface smoothness and unusual density. Switches are built for long, trouble-free service, with special silver contactors and heavy gauge terminals.

Mallory Controls are built with ample ruggedness to stand any production line handling.

Expect more . . .

Get more

from **P.R. MALLORY & CO. Inc. MALLORY**

They incorporate such mechanical features as welded assembly, vibration-proof clinched terminals, and heavy gauge fastenings.

Write today for the new catalog that describes all Mallory fixed and variable resistors . . . including both carbon and wire-wound types.

CUSTOM-BUILT CONTROLS

The control illustrated is typical of the many special types which Mallory manufactures. Designed for service adjustments in television receivers, it is a tab-mounted, bushingless model with a phenolic shaft . . . for especially economical mounting.

We'll be glad to consult with you on any special adaptations to fit your individual resistor requirements . . . also, to analyze your circuits for opportunities for resistor cost reduction.

Parts distributors in all major cities stock Mallory standard components for your convenience.

Serving Industry with These Products:

Electromechanical—Resistors • Switches • Television Tuners • Vibrators

Electrochemical—Capacitors • Rectifiers • Mercury Batteries

Metallurgical—Contacts • Special Metals and Ceramics • Welding Materials

P.R. MALLORY & CO. Inc.

MALLORY

P. R. MALLORY & CO., Inc., INDIANAPOLIS 6, INDIANA

MEMBERSHIP

(*Continued from page 103A*)

Robertson, T. M., 111 Eastmoor Dr., Silver Spring, Md.
Rojo, A., Transradio Internacional, San Martin 379, Buenos Aires, Argentina
Russell, F. A., Newark College of Engineering, 367 High St., Newark 2, N. J.
Seiler, R. C., 333 W. Lemon Ave., Arcadia, Calif.
Shoemaker, H. F., Radio College of Canada, 86 Bathurst St., Toronto 2B, Ont., Canada
Stewart, J. M., 1616 N. Edgewood St., Arlington 1, Va.
Swarthout, W. M., Engineering Department, IBM Corp., Endicott, N. Y.
Turner, R. J. A., 17 Claybrooke St., Toronto 9, Ont., Canada
Williams, C. E., 60 E. 32 St., Rm. 407, Chicago 16, Ill.

Admission to Senior Member

Bailey, K. D., 154 Shrine Ave., San Antonio, Tex.
Balint, J. E., 1853 Fairmount Blvd., Eugene, Ore.
Barr, S. M., 60 Hudson St., New York 13, N. Y.
Benoit, W. E. , c/o Westinghouse Electric Corp., 2519 Wilkens Ave., Baltimore 29, Md.
Doelz, M. L., 2700 W. Olive Ave., Burbank, Calif.
Fisher, C. C., Box 327, Huntington, Ind.
Feldmann, H., 41-28—243 St., Douglaston, L. I.; N. Y.
Goldstein, L., Electrical Engineering Department, University of Illinois, Urbana, Ill
Granger, H., U. S. Marine Corps, Hq. 1st Infantry Training Regiment, Marine Corps Base, Camp Lejeune, N. C.

(*Continued on page 107A*)

Star Performers

EPCO

"QUALITY-PLUS"

TRANSFORMERS

For Industrial and Electronic Equipment

DESIGNED TO COMMERCIAL & MILITARY SPECIFICATIONS (MIL-T-27 and AN-E-19). ALSO CLASS A, B, H, AND MINIATURES.

Sample, Short and Long Runs. Let us quote on your specifications. No obligation.

Delivery as promised!

EPCO
PRODUCTS, INC.
2500 ATLANTIC AVE
BROOKLYN 7, N. Y.

Inside this housing . .

your product is safe!

You know that you have built a fine product. Your time, creative energy and accumulated years of knowledge have gone into it. Now, *protect it with the best* . . . **OLYMPIC** metal housings! **OLYMPIC** housings are designed and built to answer the specific needs of *your* product. Strength and durability are assured by using only the finest metals. A stock of over 3000 sizes and shapes means real reliance on prompt delivery.

- Mass Production Prices
- Fabrications, Drawings & Stampings: Any Size or Shape
- Complete Range of Metals And Finishes, Design, Engineering.
- Assembly & Modification Service

Let OLYMPIC experts co-operate with you on that housing problem! Write:

OLYMPIC
METAL PRODUCTS COMPANY, INC.
ALPHA, NEW JERSEY

PRECISION ANALOG COMPUTERS...
rapidly and accurately solve
complex engineering problems!

Time Saving • *Money Saving*

Electronic Associates Computation Center near Princeton, N. J.

At the EA Computation Center you may solve complex problems in Applications Engineering, Simulation, and Engineering Design by renting EA Analog Computation Equipment by the hour, week, or month.

Scientists, engineers, and mathematicians experienced in the use of analog computers are available to assist in problem solution.

PRECISION ANALOG COMPUTATION EQUIPMENT IS ALSO AVAILABLE FOR PURCHASE.

Throughout the design of this computing equipment the objective was to produce the most accurate, versatile and dependable equipment possible at a reasonable price. In achieving this end, many of the latest advances in the art have been incorporated which contribute to the superiority of this equipment.

EA Precision Analog. Computer, Type 16-31R

If you state your interest, we will be glad to send you applicable data. Write to Dept. IR.

PRECISION ANALOG COMPUTING EQUIPMENT
FOR SOLVING PROBLEMS IN DYNAMICS

ELECTRONIC ASSOCIATES
LONG BRANCH • NEW JERSEY

We Specialize in METAL STAMPING and Service

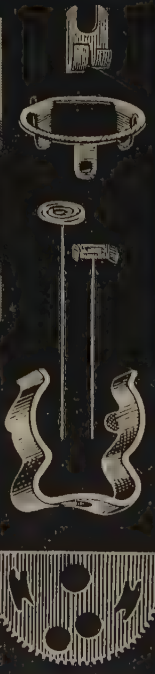

This is Stewart Stamping's modern plant . . . equipped with high-speed, electronically controlled metal working equipment of our own design. In it we produce high quality metal stampings for **ON TIME** delivery. A large inventory of raw stock is always on hand.

Bring us your hard-to-solve problems of:

• Multi-Slide forming from progressive sectional dies, steel or carbide • Metal stamping in all metals and alloys • Hot-tinning, nickel, cadmium or zinc plating • Wire forming • Welding wire to progressive stamping at high speed

Skilled craftsmen are ready to design carbide or steel dies and tooling to suit your special needs. You are assured of dependable, courteous service—and a firm delivery date. Send a sample or blueprint for a quotation. Or write for our free catalog of standard parts.

STEWART STAMPING Company, 630 Central Park Ave., Yonkers 4, N. Y.

Represented by

PHILADELPHIA 23, PA.
F. E. HARTWEG
800 N. Delaware Ave.

CHICAGO 41, ILL.
THOMAS B. HUNTER
4441 W. Irving Park Rd.

LOS ANGELES 21, CAL.
EASTMAN PACIFIC CO.
2320 East 8th St.

YOU TOO CAN HAVE THESE!

We're the source of these imported television lenses which greatly increase camera versatility. Complete the range of your TV camera lenses with these previously unavailable focal lengths. Supplement the lenses you are now using for increased versatility and performance.

ANGENIEUX RETROFOCUS

wide angle lens (35mm focal length) f2.5. Focusing mount with iris diaphragm. Highest resolution for sharpest images.

MEYER PRIMOPLAN

(75mm focal length) f1.9. Focusing mount with iris diaphragm. Longer than normal focal length for universal application.

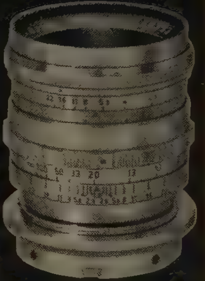

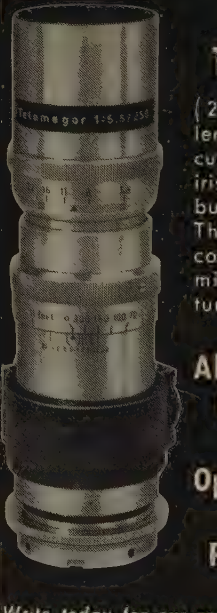

MEYER TELEPHOTO

(250mm focal length) f5.5. In focusing mount with iris diaphragm and built-in lens shade. The light weight construction permits a balanced turret action.

All Lenses Fully Guaranteed for Optical Quality and Top Performance

Write today for our complete price list of all of our special lenses for television cameras—28mm through 250mm. Samples for test purposes available on request.

PONDER & BEST
TELELENS DIVISION
Importers of Fine Photographic Equipment

814 North Cole Avenue
Hollywood 38, California

MEMBERSHIP

(Continued from page 105A)

Harrison, A. E., 2500 W. 90 St., Kansas City, Mo
Holcomb, P., Jr., Rm. 711, 60 Hudson St., New York 13, N. Y.
Johnson, J. S., School of Electrical Engineering, Purdue University, Lafayette, Ind.
Kent, R. C., 820 N. Niagara St., Burbank, Calif.
Kline, J., 46 Holden Wood Rd., Concord, Mass.
Kodis, R. D., 85 Wallis Rd., Brookline 67, Mass.
Maples, T. K., 161 Blossom St., Lexington 73, Mass.
Reinecke, B. E., 7053 Osceola Ave., Chicago 31, Ill.
Serig, H. W., Old Dutch Rd., Far Hills, N. J.
Slonczewski, T., c/o Bell Telephone Laboratories, Inc., Murray Hill, N. J.
Teich, W. W., R.F.D. Peakham Rd., S. Sudbury, Mass.
Thornton, C. G., Sylvania Electric Products, Inc., Electronics Division, Ipswich, Mass.
Weintraub, N., 9–15 Chapman Pl., Irvington 11, N. J.
Wolf, L., 1120 Prospect Ridge, Haddon Heights, N. J.

Transfer to Member

Aronson, H. A., 701 Buena Ave., Chicago 13, Ill.
Badgett, A. F., 917 Hurt Bldg., Atlanta 3, Ga.
Bellew, F. N., 605 Tompkins Ave., S. Plainfield, N. J.
Berl, S., 717 W. 177 St., New York 33, N. Y.
Bowler, D. L., Box 506, Bucknell University, Lewisburg, Pa.
Caffiiaux, J. A., 4526—49 St., Woodside 77, L. I., N. Y.
Dahse, C. A., Box 591, Tulsa, Okla.
Gamble, J. H., 35 W. Main St., Plainville, Conn.
Hartwigsen, C. K., Box 2311, Wright-Patterson AFB, Dayton, Ohio
Hodgin, D. M., Jr., 3206 Vine Ave., S.E., Cedar Rapids, Iowa
Hoffman, M., 501 W. Southgate Ave., Fullerton, Calif.
Husein, A. E., Safia Manzil, 18 Sussex Rd., Bombay 27, India
Jenkins, E. A., Box 658, Langley AFB, Va.
Kozloff, V. S., 129 W. Riverview Ave., Dayton 5, Ohio
Lester, D. R., 32 Nathan Rd., Waltham 54, Mass.
Margerum, D. L., 5024 Nagle Ave., Sherman Oaks, Calif.
Matsuoka, M. E., 335 Wadsworth Ave., New York 33, N. Y.
Matthews, E. W., Jr., 172 Colonial Ave., Williston Park, L. I., N. Y.
May, J. P., 4410 Fourth Rd., N., Arlington 3, Va.
Mitchell, W. D., 1924 Stratford, Garland, Tex.
Pugh, M. D., All America Cables, Casilla 2336, Lima, Peru
Richardson, W. R., 303 Broadmoor Rd., Baltimore 12, Md.
Rogers, R. N., U. S. Department of State, Box R, APO 239, c/o Postmaster, San Francisco, Calif.
Rothschild, L. I., 858 Church Rd., Elkins Park 17, Pa.
Sanner, G. E., 1608 E. 32 St., Baltimore 18, Md.
Schwartz, M. J., 3203 Phillips Ave., Bremerton, Wash.
Seliger, V. H., 65-35—108 St., Forest Hills 75, L. I., N. Y.
Shapin, T., Jr., 4006 N. Sheridan Rd., Chicago 13, Ill.
Sherman, S., Bell Telephone Laboratories, Whippany, N. J.
Skar, R. C., 308—38 St., N.E., Cedar Rapids, Iowa
Snook, J. E., 1629 Warren Ave., Williamsport, Pa.
Thomas, J. F., 7225 Meade St., Pittsburgh 8, Pa.
Tong, E., 533 Aurora Ave., New Orleans 20, La.

(Continued on page 108A)

FOR 15 YEARS...
High voltage,
High current
CAPACITANCE
...dependably

• The record of more than 15 years service, in thousands of installations, proves the reliability of the Lapp Gas-Filled Condenser. For duty at high voltages and high currents this unit offers the advantages of extreme compactness . . . low loss . . . high safety factor . . . constant capacitance under temperature variation . . . grounded tuning shaft . . . and rugged sturdiness. Units available in fixed or variable capacitance . . . capacitances to 60,000 mmf; current ratings to 525 amps at 1 mc; voltages to 100 Kv peak. Write for Bulletin 302 with complete description and characteristics data. Lapp Insulator Co., Inc., Radio Specialties Division, 217 Sumner St., Le Roy, N. Y.

Lapp

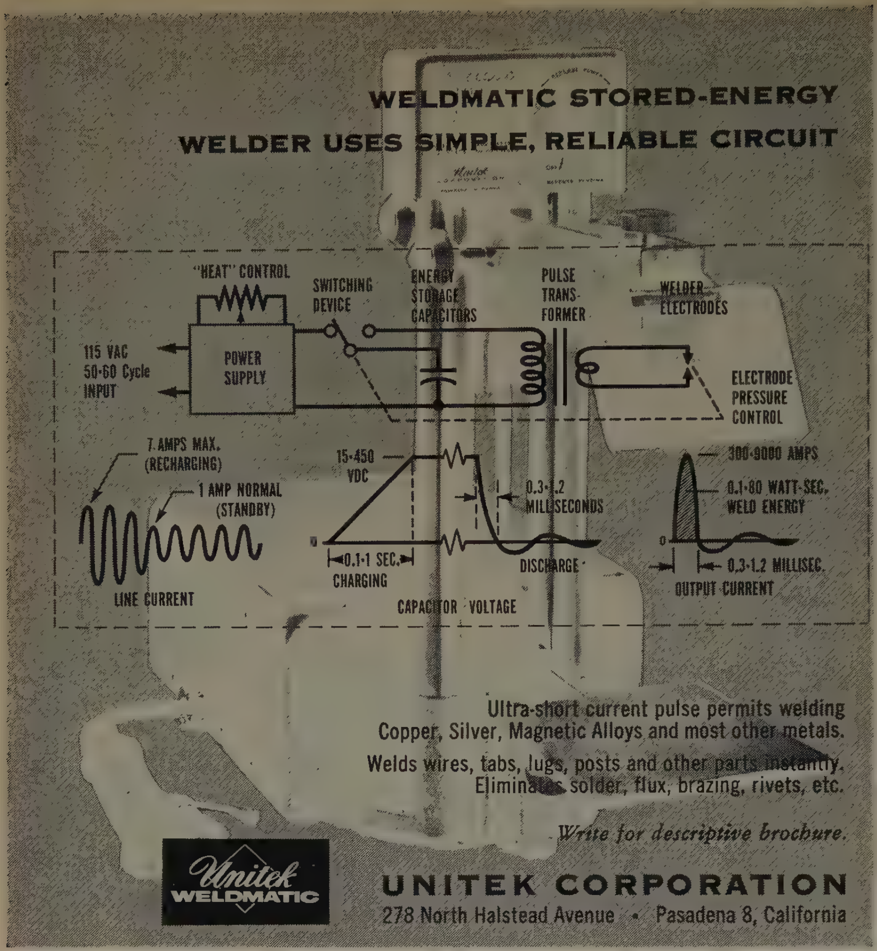
"HEAT" CONTROL
SWITCHING DEVICE
ENERGY STORAGE CAPACITORS
PULSE TRANS-FORMER
WELDER ELECTRODES
115 VAC 50-60 Cycle INPUT
POWER SUPPLY
ELECTRODE PRESSURE CONTROL
7 AMPS MAX. (RECHARGING)
1 AMP NORMAL (STANDBY)
LINE CURRENT
15-450 VDC
0
0.1-1 SEC. CHARGING
0.3-1.2 MILLISECONDS
DISCHARGE
CAPACITOR VOLTAGE
300-9000 AMPS
0.1-80 WATT-SEC. WELD ENERGY
0
0.3-1.2 MILLISEC.
OUTPUT CURRENT
Unitek WELDMATIC

WELDMATIC STORED-ENERGY WELDER USES SIMPLE, RELIABLE CIRCUIT

Ultra-short current pulse permits welding Copper, Silver, Magnetic Alloys and most other metals.

Welds wires, tabs, lugs, posts and other parts instantly. Eliminates solder, flux, brazing, rivets, etc.

Write for descriptive brochure.

UNITEK CORPORATION
278 North Halstead Avenue • Pasadena 8, California

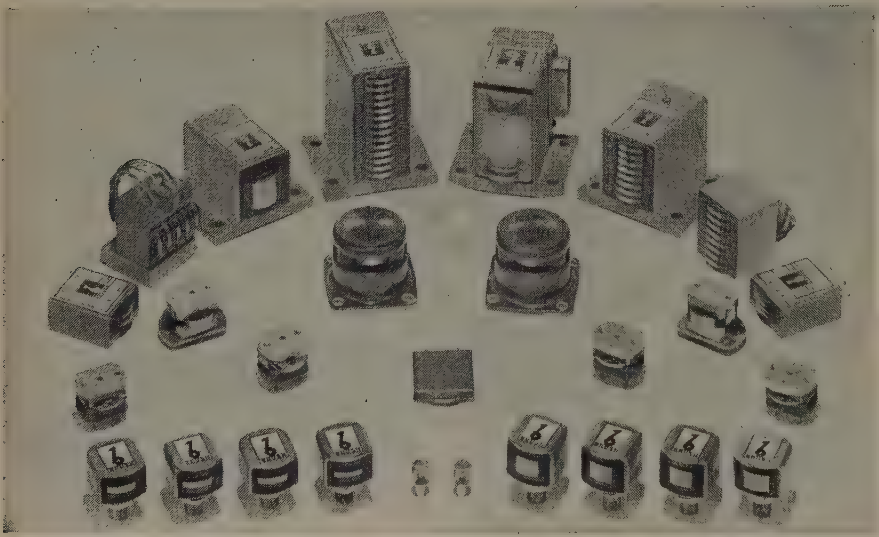

FOR ALL YOUR REQUIREMENTS IN MAGNETIC HEADS

• The performance of magnetic recording equipment depends on the quality of the magnetic head—which records, reproduces or erases. Brush offers a complete line of heads, outstanding for precision alignment and balanced magnetic construction. For assistance in application, call on Brush's unequalled experience in this field. Write Brush Electronics Company, Department F-9A, 3405 Perkins Avenue, Cleveland 14, Ohio.

BRUSH ELECTRONICS COMPANY
INDUSTRIAL AND RESEARCH INSTRUMENTS
PIEZO-ELECTRIC MATERIALS • ACOUSTIC DEVICES
MAGNETIC RECORDING EQUIPMENT
ULTRASONIC EQUIPMENT

BRUSH ELECTRONICS

formerly The Brush Development Co. Brush Electronics Company is an operating unit of Clevite Corporation.

MEMBERSHIP

(Continued from page 107A)

Townsend, G. R., 44 Lakeside St., Springfield 9, Mass.
Vreeland, R. W., 36 Magee Ave., Mill Valley, Calif.
Wilkinson, C. W., Box 268, Quaker Hill, Conn.
Winchell, A. M., Todd Rd., (Wolcott), Waterbury 12, Conn.
Yankewicz, W. W., c/o Marine Radio Station "VAP," Churchill, Man., Canada
Zakowski, L. F., Box 818, Langley AFB, Va.

Admission to Member

Allmacher, A. M., Box 215, Columbus, Neb.
Anderson, R. V., 2509—32 St., S.E., Washington 20, D. C.
Baker, D. L., 7811 Belgard St., Houston 21, Tex.
Benton, C. U., 17836 Saticoy St., Reseda, Calif.
Bruno, A., 1406 Fanshawe St., Philadelphia 11, Pa.
Chaffee, B. J., 2200 Palomas Dr., N.E., Albuquerque, N. Mex.
Chamberlin, W. C., 1643 S. 134 St., Seattle 88, Wash.
Craig, E. J., 37 Smith Ave., West Newton 65, Mass.
da Cunha, A. M. C., 131—R. S. Juliao, Lisbon, Portugal
Davis, J. K., 211 Walnut St., Elmira, N. Y.
Dennett, L. J., 11 Lanbrook Ave., Willowdale, Ont., Canada
Doherty, J. E., 6219 Menger, Dallas 27, Tex.
Dunn, W. F., 12821 Valleywood Dr., Silver Spring, Md.
Duryea, J. C., 24 Ninth St., Carle Place, L. I., N. Y.
Ervin, H. D., 3012 W. Addison, Chicago 18, Ill.
Eschner, A. H., 1448 Burmount Rd., Havertown, Pa.
Farvolden, E., 751 Godin St., Montreal 19, Que., Canada
Fritz, H. U., 363 N. St. Marys St., St. Marys, Pa.
Gale, A. J., 9 Winston Rd., Lexington 73, Mass.
Gartner, W., Evans Signal Laboratory, Belmar, N. J.
Goodman, H. L., 22 W. Fifth St., Emporium, Pa.
Hanson, R. A,, 14329 Emelita St., Van Nuys, Calif.
Harris, D. S., Staff, Comairlant, NAS, Norfolk 11, Va.
Hemmick, K. S., Box 388, R.F.D. 2, Annapolis, Md.
Inge, E. F., R.F.D. 2, Bucktail Trail, St. Marys, Pa.
Kidder, H. F., 1000 Wakefield Ave., St. Paul 6, Minn.
Lewis, J. R., 420 Crown St., Willow Grove 5, Pa.
Looney, J. M., Jr., 731 N. La Brea Ave., c/o Technology Instrument Corp., Hollywood 38, Calif.
Lowery, R. O., 310 Thompson Bldg., Tulsa, Okla.
Marshall, D. R. J., 17 Linden Ct., St. John's, Newfoundland, Canada
Melnick, H., 83-30 Kew Gardens Rd., Kew Gardens 15, L. I., N. Y.
Mika, J. I., 223 Rodney Cir., Bryn Mawr, Pa.
Mott, H., Box 5876, State College Station, Raleigh, N. C.
Newman, J. J., H 4 Cuthbert Gardens, Westmont 7, N. J.
Noakes, F., Electrical Engineering Department, University of British Columbia, Vancouver 8, B. C., Canada
Noble, R. P., 3206 D—30 Pl., Sandia Base, Albuquerque, N. Mex.
Okochi, J. A. M., Electrical Engineering Department, The Tokyo Institute of Technology, 1 Ookayama Meguro, Tokyo, Japan
Pryga, S. A., 9552 E. Rosecrans Ave., Bellflower, Calif.
Puleo, M. J., 4 E. Sixth, Emporium, Pa.
Revesz, G., 69-60—108 St., Forest Hills 75, L. I., N. Y.
Rocamora, R. L., 316 Briarwood Ave., Haddonfield, N. J.

(Continued on page 110A)

Photographic Equipment Resistor used in Photo-Flash Circuits

Bleeder Resistor for . . . Power-Line Capacitors

Heat Anticipator Resistor for Wall Thermostat

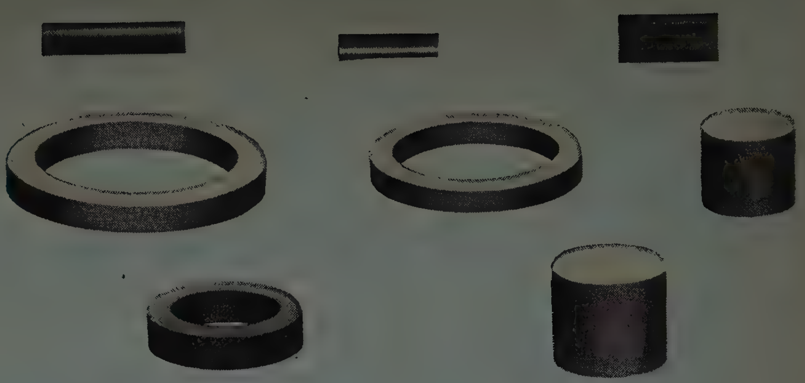

- **Film Resistors for Automatic Light Dimmers**

Where Design Calls for . . . Custom Resistance Products

Specify TRADE **ERIE** MARK RESISTOR CORP.

Resistor for Aircraft Magneto

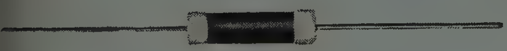

Ring Resistor for Speed Control Device

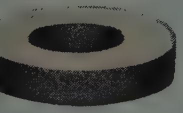

Gasoline Gage Resistor

Resistor for Electric Clock

Strain-Gage Resistor for Detecting Strain in Airplane Wings and Propellers

Voltage Dividers for TV Sets with Special Coating to Prevent Corona Discharge

- **Special and Standard Case Ignition Noise Suppressors**

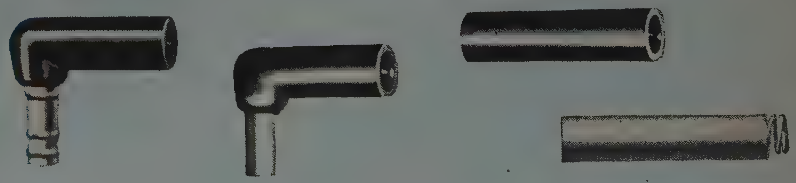

For 26 years Erie Resistor Corporation has been designing and manufacturing highest quality resistance products. That experience is at the service of every manufacturer needing individual design and application to meet product requirements.

The illustrations show a few of many custom resistance components manufactured by Erie. We also specialize in the application of resistance material on steatite plates and phenolic bases for printed circuits and special resistor applications.

You will find at Erie a ready understanding of your resistance and other electronic component problems, and an unusual skill in helping you to solve them

ERIE RESISTOR CORP.

ERIE RESISTOR CORPORATION . . . ELECTRONICS DIVISION

Main Offices and Factories: **ERIE, PA.**

Sales Offices: Cliffside, N. J. • Camden, N. J. • Chicago, Ill. • Detroit, Mich.
Cincinnati, Ohio • Fort Wayne, Ind. • Los Angeles, Calif. • Toronto, Ontario

IT'S
HARVEY
FOR PROMPT
"OFF-THE-SHELF" DELIVERY

Whether it's equipment, components or other electronic requirements, you will always find them in Harvey's extensive stocks, ready for immediate delivery to you anywhere.

Harvey's twenty-five years of service to the industry are your assurance of understanding 'know-how' and complete dependability.

WRITE
PHONE
or WIRE

Telephone
JUdson 2-1500

HARVEY
RADIO COMPANY, INC.
103 West 43rd St., New York 36, N. Y.

NEW "PARAFORMED" PAPER TUBES
MAKE YOUR COIL WINDING
EASIER! FASTER! BETTER!

FLAT SIDE WALLS
SMALL OUTSIDE CORNER RADIUS
SHARP SQUARE INSIDE CORNERS
SPIRAL WOUND
NOT DIE FORMED

ANY SIZE—SQUARE OR RECTANGULAR
Entirely new technique in tube making developed and perfected by PARAMOUNT now for the first time solves many coil winding problems, *yet costs you no more!* Hi-Dielectric. Hi-Strength. Kraft, Fish Paper, Acetate, Red Rope or any combination wound on automatic machines. Produced from stock arbors or special sizes engineered for you.
Write on Company letterhead for Stock Arbor List of over 2000 sizes

- No sharp outside edges to cut wire
- Has full rigidity and physical strength
- Permits winding coils to closer tolerances
- No need for wedges to tighten wire
- Allows faster stacking of wound coils

PARAMOUNT PAPER TUBE CORP.
617 LAFAYETTE STREET, FORT WAYNE 2, INDIANA
Manufacturers of Paper Tubing for the Electrical Industry Since 1931

MEMBERSHIP

(Continued from page 108A)

Salit, M., 1465 Townsend Ave., New York 52, N. Y.
Schnauss, E. R., ACF Electronics, 800 N. Pitt St., Alexandria, Va.
Shemanske, R., 4121 S. Clinton Ave., Berwyn, Ill.
Soldatos, G., General Greek Air Staff, 6 Amerikis St., Athens, Greece
Spencer, C. L., 1017 Quander Rd., Alexandria, Va.
Spershott, J. H., Box 472, Hamilton, Bermuda
Waugh, Jr. R., Jr., 1634 Madison Ave., Scranton, Pa.

The following admissions to the Associate grade were approved to be effective as of August 1, 1954:

Allard, G. A., 211 Pattison St., Syracuse 6, N. Y.
Anderson, D. L., Allen Bradley Co., 445 N. LaSalle St., Chicago 10, Ill.
Andreu, A. M., 383 Congreso, San Andres FCNGBM, Buenos Aires, Argentina
Arena, G., 4360 Cote des Neiges Rd., Apt. 5, Montreal, Que., Canada
Bard, R. R., Jr., 1221 Second St., Perry, Iowa
Bard, W. E., 2459 N. Walnut, Tucson, Ariz.
Beahr, A. W., SRF, Box 8, Navy 3923, c/o FPO, San Francisco, Calif.
Biel, D. T., 229 Arabella St., Pittsburgh 10, Pa.
Bokhari, T. A., 12 Kishen St., Prem Nagar, Lahore, Pakistan
Bolz, R. W., Penton Bldg., Cleveland 13, Ohio
Breen, J. M., c/o IBM, 590 Madison Ave., New York, N. Y.
Brodd, W. D., 20 Styvestandt Dr., Poughkeepsie, N. Y.
Brooke, C. E., 906 Clare St., Lansing, Mich.
Bryn, S. L., Box 235, Vails Gate, N. Y.
Carter, H. S., 43 Inf. Div., 43 Signal Co., APO 112, c/o Postmaster, New York, N. Y.
Cranshaw, R. J., Jr., Box 1102, Mather AFB, Mather Field, Calif.
Crossman, C. R., 142 Ringdahl Ct., Apt. 4, Rome, N. Y.
Dale, T. M., Box 868, Portsmouth, N. H.
Deerfield, A. J., 57 Bicknell St., Dorchester, Mass.
Diedrichs, J. K., c/o Booz, Allen and Hamilton, 135 S. LaSalle St., Chicago 3, Ill.
Dix, D. S., 43 Croft Rd., Poughkeepsie, N. Y.
Dugre, M. L., 259 Cedar St., Manchester, N. H.
Dvorak, F. J., Box 728, Langley AFB, Va.
Frigerio, N. A., 575 Ferry St., New Haven 13, Conn.
Fuks, A., 1 rue Georges Sache, Paris XIV, France
Goen, Q. F., 2110 N. 16 St., Apt. 847, Arlington 1, Va.
Goss, J. P., Jr., 87 Humboldt Ave., Boston 19, Mass.
Hager, R. E., 209 S. Birmingham Ave., Avalon, Pittsburgh 2, Pa.
Haley, D. C., 103 Olive Springs Pl., Marietta, Ga.
Hatok, W., 87 Lincoln St., Depew, N. Y.
Heinmark, H. A., 3502 S. Summit Ave., Bremerton, Wash.
Hermann, N. E., 4612 Avenue P½, Galveston, Tex.
Horst, C. W., Power House 3, Southern California Edison, Auberry, Calif.
Hovda, R. E., 11710 Lakewood Blvd., Downey, Calif.
Irvin, H. D., Box 127, Enka, N. C.
Ito, Y., c/o Koden Electronics Co., Ltd., 284-1 Chojamaru, Kamiosaki, Shinagawa-Ku, Tokyo, Japan
Janik, C. L., 346 Sound Beach Ave., Old Greenwich, Conn.
Johnston, J. J., 467 Blvd., Hasbrock Heights, N. J.
Jones, D. F., 7054 Ramsgate Ave., Los Angeles 45, Calif.
Kinberg, C., IBM: Svenska AB, Stockholm 6, Sweden
Kogan, M. A., 264 Beach 133 St., Rockaway Beach 94, N. Y.
Kundrotas, A. P., Kellogg Switchboard and Supply Co., 6650 S. Cicero Ave., Chicago 38, Ill

(Continued on page 112A)

Thinking of
SMALL RELAYS?

ADVANCE *builds 'em for heavy loads and long service!*

Cramped quarters don't cramp the style of ADVANCE midgets and miniatures. You can use them on loads up to 5 amperes continuously . . . and at three times their rating intermittently—with complete safety. They'll resist shock and vibration . . . stand up under temperature extremes. You'll find them readily adaptable to any mounting need . . . any type of duty. Here are a few examples:

"TINY MITE"

MM & MP SERIES

This ultra-small d-c relay occupies less than ½ cu. in. mounting space! It's stable under vibration and shock . . . plated to prevent corrosion. Operate time is 5 milliseconds. Contact rating: .5 amp. or 1 amp.

MINIATURE TELEPHONE TYPE

TQ SERIES

Only .94 cu. inches in size, yet this relay carries 5-amp. loads in any combination up to 4 PDT. Mechanically secured throughout, it's extremely efficient. No gassing or bubbling. Withstands 10G vibration. Temperature range: —55° to +125° C.

Hermetic enclosures on these types are impervious to varying climatic conditions . . . are sealed and carefully checked against leakage.

Write for literature on any of the above series, or the complete ADVANCE line.

ADVANCE ELECTRIC AND RELAY CO.
2435-G NORTH NAOMI STREET
BURBANK, CALIFORNIA

Sales Representatives in Principal Cities of U.S. and Canada

CORRECT COMBINATION

of Size and Power Rating—offered by Jennings Vacuum Capacitors!

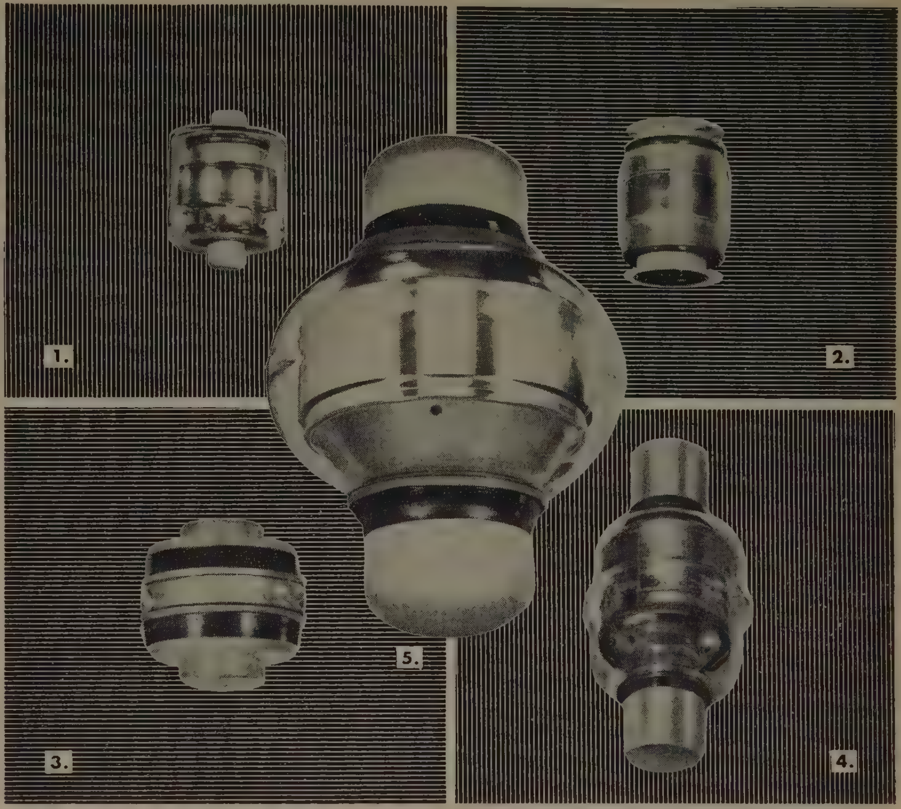

1. JCSL	1000 mmfd.; 3 KV; 42 amps rms	
2. JCS	1000 mmfd.; 7.5, 10, 12 KV; 42 amps rms	
3. MC-1	1000 mmfd.; 10, 15 KV; 75 amps rms	
4. MC	1000 mmfd.; 10, 15, 20 KV; 120 amps rms	
MLC	1000 mmfd.; 25, 30 KV; 120 amps rms	
5. MMHC	1000 mmfd.; 35, 40, 45 KV; 125 amps rms	

The wide choice of size and power ratings for a given capacity is illustrated by these five units all having capacities of 1000 mmfd. JENNINGS functional designs thus permit you to select the smallest fixed or variable vacuum capacitor that will meet your voltage and current requirements.

Send for our catalogue summary describing over 150 types and sizes of vacuum capacitors and switches.

Jennings RADIO ®
VACUUM ELECTRONIC COMPONENTS

JENNINGS RADIO MANUFACTURING CORPORATION • 970 McLAUGHLIN AVE.
P.O. BOX 1278 • SAN JOSE 8, CALIFORNIA

CO-AX
4 mmf/ft

★ ULTRA LOW capacitance & attenuation

TYPE	μμF/ft	IMPED.Ω	O.D.
C 1	7.3	150	.36"
C 11	6.3	173	.36"
C 2	6.3	171	.44"
C 22	5.5	184	.44"
C 3	5.4	197	.64"
C 33	4.8	220	.64"
C 4	4.6	229	1.03"
C 44	4.1	252	1.03"

WE ARE SPECIALLY ORGANIZED TO HANDLE DIRECT ORDERS OR ENQUIRIES FROM OVERSEAS

SPOT DELIVERIES FOR U.S.

BILLED IN DOLLARS— SETTLEMENT BY YOUR CHECK

CABLE OR AIRMAIL TODAY

TRANS T RADIO

NEW 'MX and SM' SUBMINIATURE CONNECTORS
Constant 50Ω-63Ω-70Ω impedances

TRANSRADIO LTD. 138A Cromwell Rd. London SW7 ENGLAND CABLES: TRANSRAD, LONDON

NOISE and FIELD INTENSITY METER Model NF-105
(Commercial Equivalent of AN/URM-7)

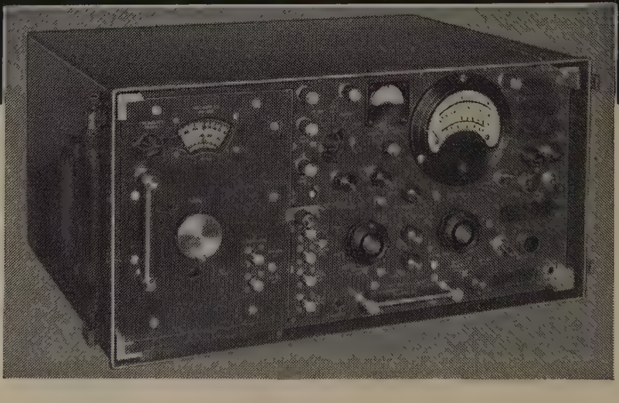

CONFORMS TO
MIL-I-6181B
MIL-I-16910

ENGINEERING DATA

- Frequency range 20 MC to 1000 MC by means of three quick-change tuning heads. At least one RF amplifier with tuned input is employed for each tuning range.
- Easy frequency scanning by means of single tuning knob.
- Built-in impulse noise calibrator flat to 1000 MC (Output externally available).
- 4½" logarithmic indicating meter reads carrier or true peak.
- Aural slideback operation.
- Input VSWR better than 1.2 to 1.
- Built-in regulated "A" and "B" supply.
- Complete line of accessories available.

Write today for additional information and our complete catalog

edp EMPIRE DEVICES PRODUCTS CORPORATION
38-15 BELL BOULEVARD • BAYSIDE 61, NEW YORK

MANUFACTURERS OF
FIELD INTENSITY METERS • DISTORTION ANALYZERS • IMPULSE GENERATORS • COAXIAL ATTENUATORS • CRYSTAL MIXERS

MEMBERSHIP

(Continued from page 110A)

Lavin, R. D., 1149A School Ave., Patrick AFB, Fla
Leone, W. C., 10739 Northgate St., Culver City, Calif.
Levin, A., 8716 Bradford Rd., Silver Spring, Md.
Loya, E., 4632 Clifton, El Paso, Tex.
Luiggi, R. H., 1507 Emory St., Asbury Park, N. J.
Maixner, F. C., 89-45—90 St., Woodhaven 21, L. I., N. Y.
Markowitz, S., 6544 Brynhurst Ave., Los Angeles 43, Calif.
Martinez, H. M., 1192 Laurel St., Berkeley 8, Calif.
Mattews, C., 4430 Gainsborough Ave., Hollywood 27, Calif.
McNabb, J. S., 1001F South AIA, Patrick AFB, Cocoa, Fla.
Meili, E. J., 138 Roosevelt Ave., Elyria, Ohio
Meredith, B. E., Bldg. 10-8, RCA, Camden, N. J.
Miller, R. W., 1501 Benedict Cyn. Dr., Beverly Hills, Calif.
Montgomerie, G. A., 7 Wood Green Rd., Quinton, Birmingham 32, England
Morris, R. B., 425 Burnett St., Lake Charles, La.
Moss, J. F., 4903 Shelby Dr., S.E., Washington 21, D. C.
Motwane, H. V., 127 Mahatma Gandhi Rd., Fort, Bombay 1, India
Neogy, S. C., RBHM Jute Mills, Ltd., P.O. Katihar Mills, Purnea (Behar), India
Nichols, N. F., 1718 N. 26 Pl., Phoenix, Ariz.
Nussbaum, O. N., 8044 Lesner Ave., Van Nuys, Calif.
Olson, C. E., 3900 N. Rockwell St., Resch. Dept., Victor Adding Machine Co., Chicago, Ill.
Pfeiffer, W. F., 5117 Shearin Ave., Los Angeles 41, Calif.
Pitrelli, F. J., 362a Hart St., Brooklyn 6, N. Y.
Pizzicara, D. J., 2528 Radcliff Ave., N. Y. 69, N. Y.
Popovich, C. D., Box 451, Downsview, Canada
Raflores, W. C., Phil Air Lines, Roxas City, Philippines
Rittenhouse, P. T., USS Conway (DDE-507), c/o FPO, New York, N. Y.
Rogers, J. H., IBM Corp., 1615 Webster St., Oakland 12, Calif.
Sassman, R. W., 1207 Dorothy Dr., Glendale 2, Calif.
St. Andre, G. O., 93 Silver St., Randolph, Mass.
Schneider, S., 4047 West Blvd., Los Angeles 8, Calif.
Scopinsky, L., 623 E. 96 St., Brooklyn 36, N. Y.
Scott, D. M., 2519 Wilkens Ave., Baltimore 3, Md.
Shapiro, H., 6936 LaTijera Blvd., Los Angeles 45, Calif.
Stephens, E. J., 56 Ximeno Ave., Apt. 4, Long Beach 3, Calif.
Stone, S. A., 243 York St., Ottawa, Ont., Canada
Stubblefield, R. L., Oyster Point, Va.
Suchanek, C. F., 223 S. Travis St., Lindenhurst, L. I., N. Y.
Sutton, W. A., 1636 W. Stadium Blvd., Ann Arbor, Mich.
ten Zeldam, H. J., 629 E. 14 Ave., Vancouver 10 B. C., Canada
Thomas, F. A., 1427 S.E. Ankeny St., Portland Ore.
Thomas, P. M., 7069½ W. Manchester Blvd., Los Angeles 45, Calif.
Tomcak, J. F., 7554 Booth Dr., Kansas City, Mo
Thomsen, R. K., 4246 Matilija Ave.,Sherman Oaks Calif
Van Hoesen, R. W., 2204 Darrow St., Silver Spring Md.
White, P. K., 905 E. Second Pl., Panama City, Fla
Wilder, E. J., 32-51—58 St., Woodside 77, N. Y
Winter, A. J., 13239 Ventura Blvd., Studio City Calif.
Wirt, M. E., 305 Stratford Rd., Jacksonville, N. C
Wolk, I. F., 4515 Prentice St., Dallas 6, Tex.
Youmans, A. B., 3404—81 Ave., S.E., Washingto 28, D. C.
Zander, C. E., 5421 Callister Ave., Sacramento 19 Calif.

News—New Products

Report on Meeting and Symposium of Cleveland Electronic Show

(Continued from page 34A)

#8. **CLEVELAND INSTRUMENT,** Cleveland; in attendance, G. E. Durham, Pres., R. E. Roeger, Sales Engr.

Products on display: Electronic microcomparator, Gaging equipment.

History: Founded in 1945 by Graham and Mintel to answer need for assuring centricity of extruded welding rod. Basic circuit was applicable to sensitive dimensional gaging. Incorporated in 1948 and name changed in 1953 to Cleveland Instrument. Their Microcomparator permits dimensional gaging in increments of one half-millionth of an inch. This type of a comparator affords a magnification factor of almost 200,000 times and repeated readings within one quarter millionth of an inch are consistently obtained. Future considerations could be in the automatic gaging of production parts.

#9. **HICKOK ELECTRICAL INSTRUMENT CO.,** Cleveland; in attendance, H. J. Greenley, A. M.

Products on display: Electrical indicating instruments laboratory type, Service testing equipment for TV, UHF, VHF and Radio.

History: Founded in 1910, developed first static tester in 1928. Versatile line of test equipment. Manufacture standard meters and special purpose meters. Future consideration is utilizing transistors in test equipment and increasing their range of test equipment to meet service and lab requirements.

#10. **BUD RADIO,** Cleveland; in attendance, A. N. Haas, Sales Mgr.

Products on display: Chassis, cabinets, TV accessories, transmitting components for amateur and communication personnel, test leads and prods for service personnel.

#11. **KEITHLEY INSTRUMENTS,** Cleveland; in attendance, Jos. F. Keithley, Pres., J. Lee Gibson, S.M. & A.M.

Products on display: Phantom Repeater utilizing high impedance input coupled with low output impedance amplifier,

(Continued on page 116A)

PROTECTED UNDER STODDART PATENTS

NOW

Precision Attenuation to 3000 mc!

TURRET ATTENUATOR featuring "PULL-TURN-PUSH" action

SINGLE "IN-THE-LINE" ATTENUATOR PADS and 50 ohm COAXIAL TERMINATION

FREQUENCY RANGE:
dc to 3000 mc.
CHARACTERISTIC IMPEDANCE:
50 ohms
CONNECTORS:
Type "N" Coaxial female fittings each end
AVAILABLE ATTENUATION:
Any value from .1 db to 60 db
VSWR:
<1.2, dc to 3000 mc., for all values from 10 to 60 db
<1.5, dc to 3000 mc., for values from .1 to 9 db
ACCURACY:
±0.5 db
POWER RATING:
One watt sine wave power dissipation

Send for free bulletin entitled "Measurement of RF Attenuation"

Inquiries invited concerning pads or turrets with different connector styles

STODDART AIRCRAFT RADIO Co., Inc.
6644-C Santa Monica Blvd., Hollywood 38, California · Hollywood 4-9294

Report on Meeting and Symposium of Cleveland Electronic Show

(Continued from page 115A)

Chopper Amplifier, Vacuum Tube Electrometers with Voltage Divider attachments.

History: Founded in 1946 by J. F. Keithley. Instruments available enable measurement of static charges, voltages with no drain, low currents and high resistances. Future consideration will be in special amplifiers and electrometers.

#12. **CLEVELAND ELECTRONICS,** Cleveland; in attendance, David Harris, Sales Mgr.

Products on display: High Fidelity speakers. Live display of audio speaker assembly, Weatherproof Radio TV Speakers, and UHF TV Antennas.

ALUMINUM
Cletron

History: Founded in 1945. Manufactures speakers for industry and replacement. Future development of a new type pickup for inexpensive phonographs and a new type speaker, and automobile vibrator power source.

#13. **THE FINNEY COMPANY,** Cleveland; in attendance, L. H. Finneburgh, Pres., R. S. Weiss, Engr.

Products on display: TV, UHF and VHF antennae with oscilloscope showing antenna reception pattern.

#14. **RAND DEVELOPMENT CORP.,** Bratennahl; in attendance, Don E. Platt, Proj. Engr.

Products on display: Warning signals for fire, theft, to be used in conjunction with telephone, automatic door, garage door opening device and conference phone attachment.

(Continued on page 119A)

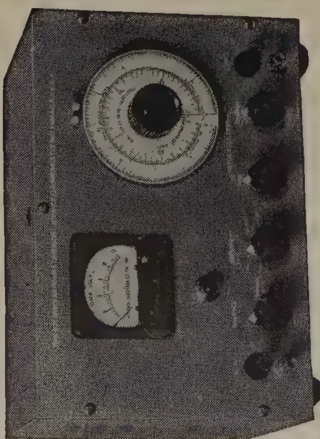

Precision Phase Detector

- MEASURES ENVELOPE DELAY WITH 1% ACCURACY
- MEASURES PHASE DELAY WITH 0.1° ACCURACY
- FREQUENCY RANGE 100 KC to 15 MC.
- 0.01 VOLT FULL SCALE SENSITIVITY

TYPE 205 PRICE $445

SPECIFICATIONS

ACCURACY: ± 0.1 degree in phase reading or ± 1% of the time delay indicated on the dial of the continuously variable delay line.
RESOLUTION TIME: 5×10^{-10} seconds or smaller; the smallest phase angle can be read on the dial is approximately equal to $5 \times 10^{-10} \times 360 \times$ frequency in degrees.
TIME DELAY: Three continuously variable delay lines are supplied with the unit, 0 to 0.45 microsecond, 0 to 0.25 microsecond and 0 to 0.05 microsecond.
PHASE RANGE: The maximum phase range is equal to the total time delay of the continuously variable delay line multiplied by the frequency of the signals and 360.
INDICATOR SENSITIVITY: Approximately 0.01 volts full scale maximum.
INPUT IMPEDANCE: Two low capacity probes with input capacitance less than 4 mmf are supplied with the unit. The panel binding posts have about 1 megohm shunted with 12 mmf on both input channels.

Continuously Variable

TIME DELAY PASSIVE NETWORK WITH 5×10^{-10} SEC. RESOLUTION TIME

TYPE 2011 PRICE $245

Type 2011 is well suited for variable time delay for pulses, phase angle measurement, or time measurement of various signals.

- Faithful reproduction of the wave form of the input signal.
- No time jitter.
- No limit on repetition rate.
- Millimicrosecond accuracy.

SPECIFICATIONS

TIME DELAY: Continuously variable from 0 to 11 microseconds.
RESOLUTION TIME: Less than 5×10^{-10} seconds from 0 up to 11 microseconds.
BANDWIDTH: 10 cps to 15 megacycles when the step variable delay line is at its off position (time delay from 0 cps to 0.5 usec), otherwise, the upper limit decreases to 2.6 megacycles.
RISE TIME: Less than 10% of the time delay at any point.
INPUT IMPEDANCE: 20 uuf shunted with 1 megohm.
OUTPUT IMPEDANCE: 300 ohms nominal.
ACCURACY OF TIME DELAY: Maximum error less than 10^{-9} second or 0.1% of the time delay at any point with correction curve, otherwise, one percent of the time delay at any point.

WRITE FOR DATA — **ADVANCE ELECTRONICS CO., INC.** — 451 HIGHLAND AVE. · PASSAIC, N.J.

News—New Products

Report on Meeting and Symposium of Cleveland Electronic Show

(Continued from page 116A)

History: Founded by James Rand of Rand Electric Shaver, developed the Bendix Economat Washing Machine, Milium Fabric. Recently incorporated to provide funds and equipment for future developments in the electronic and electrical fields.

#15. VICTOREEN INSTRUMENT, Cleveland; in attendance, Duane Mayhew, S.M., D. L. Collins, Tech. Dir.

Products on display: Proportional counters, Ion chambers, Geiger counters and Scintillation counters. Peak reading voltmeter showing "G" unit readings so that shock absorption can be measured. Adjustable VR tubes for monochrome and color TV.

History: In mid '20's, went into measurement of X-Rays with their condenser type R Meter. This instrument is accepted as the secondary standard by the Bureau of Standards. Atomic Energy Commission asked Victoreen for gamma instruments and in this development they designed and built the electrometer tube. Company is divided into Instrument Division for development, research and manufacture of medical instruments pertaining to electronics and Components Division which develops components for color TV, UHF, VR Tubes and Resistors.

Erie Components Catalog

A complete, new sixteen-page catalog has been issued by **Erie Resistor Corp.,** Erie, Pa. This catalog, "D-54," supersedes previous catalogs and includes the new line of Temperature Compensating Tubular Ceramicons and Disc Ceramicons, together with the long-time standard numbers. It is complete with up-to-date listings, illustrations, and descriptions.

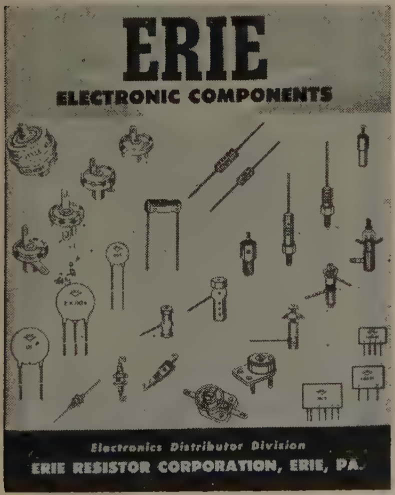

ERIE
ELECTRONIC COMPONENTS

Electronics Distributor Division
ERIE RESISTOR CORPORATION, ERIE, PA.

Copies are available at leading distributors or may be obtained by writing direct to the Erie Resistor Corp.

(Continued on page 121A)

PROVED BY USE!

In the short time the Model 1001 Regulator has been on the market, more than 300 of the instruments have been sold, mainly for meter calibration applications and for use in standards laboratories.

As a result, it can now be said — *and proved* — that the Model 1001 gives hairsplitting precision *with the rugged dependability of operation associated with voltage regulators of "ordinary" regulating accuracy!*

0.01% regulation accuracy!
1000 VA capacity!

Sorensen Model 1001
electronic AC Voltage Regulator

specifications

Input	95-130 VAC, 1Ø, 50-60∿
Output	110-120 VAC, adjustable
Load range	0-1000 VA
Regulation accuracy	±0.01% against line and ±0.01% against load guaranteed at room temperature, for a resistive load, an input variation of ±10% and over a 2-to-1 load change. For all other conditions within the specifications the 1001 has a proportionate amount of accommodation.
Distortion	3% RMS maximum
P. F. range	0.95 leading to 0.7 lagging
Time constant	0.1 second
Tube complement	6SL7GT (1), 6L6GA (1), 5Y3GT (1), 2AS15 (1)

Even greater capacity with similar accuracy will be available this fall when the Sorensen Model 2501 Regulator — ±0.01% accuracy, 2500 VA capacity — goes into production.

general catalog available

AC VOLTAGE REGULATORS — 150VA to 15000VA capacities, 115 volt and 230 volt output, 400-cycle regulators, 3-phase regulators

FREQUENCY CHANGERS — 60 cycle and 400 cycle, accuracy to ±0.01%

NOBATRONS — Regulated low-voltage, high-current DC sources

B-NOBATRONS — Regulated high-voltage, low-current B power supplies

NOBATRON-RANGERS — Wide-range variable DC sources

TUBELESS DC SUPPLIES — Magnetic amplifier supplies with various outputs and capacities

AIRBORNE FREQUENCY CHANGERS & INVERTERS, MILITARIZED REGULATORS, FILTERS, TRANSFORMERS, AND RELATED EQUIPMENT.

For your copy write Sorensen & Co., Inc., 375 Fairfield Avenue, Stamford, Conn. In Europe, Sorensen A.G., Gartenstrasse 26, Zurich 2, Switzerland.

SORENSEN
375 FAIRFIELD AVENUE, STAMFORD, CONN.

High Dielectric Bobbins
For High "Q" Coils
PRECISION

MADE TO YOUR EXACT SPECIFICATIONS
IN ANY SIZE • SHAPE • QUANTITY

Precision coil bobbins are fabricated from high dielectric materials and quality controlled to the most minute tolerances . . . Yet, because they are made on special high production equipment, they're available to you for prompt delivery at low unit cost.

Cores are spirally wound dielectric kraft, fish paper, acetate, phenol impregnated or combinations. Flanges are cut to any specification for all types of mountings.

Request illustrated bulletin. Send specifications for samples.

High Strength Low Cost Paper Tubes

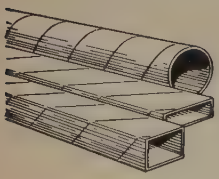

Accurately fabricated in any size, shape, ID or OD. Spirally wound from select dielectric materials. Crush resistant, with excellent dimensional stability. Subject to rigid control and inspection for tolerance and uniformity.

Ask for samples and Arbor List of over 2000 sizes.

Sales Representatives in:

New England:
Framingham, Massachusetts, Framingham 7091
Metropolitan New York, New Jersey:
Jersey City, New Jersey, Journal Square 4-3574
Upstate New York:
Syracuse, New York, Syracuse 76-8056
Northern Ohio, Western Pennsylvania:
Cleveland, Ohio, Atlantic 1-1060
Indiana, Southern Ohio:
Logansport, Indiana, Logansport 2555
Missouri, Southern Illinois, Iowa:
St. Louis, Missouri, Sterling 2318
Maryland:
Baltimore, Maryland, Plaza 2-3211
Philadelphia, Camden:
Philadelphia, Pa., Chestnut Hill 8-0282
California:
Pasadena, California, Sycamore 8-3919
Canada:
Montreal, Quebec, Canada, Walnut 2715

PRECISION

PRECISION PAPER TUBE CO.
2051 W. CHARLESTON ST. CHICAGO 47, ILL.
Plant No. 2: 79 Chapel St., Hartford, Conn.

NOW
ELIMINATE..
all types of
ANODE LEAD
RETAINERS

with
"INDUSTRIAL"
"FISH HOOK" pat. pending
ANODE CONNECTORS

Designed specifically to eliminate any supporting harnesses which were necessary in the past to prevent dangerous "Buggy Whip." This unit is absolutely slipproof once connected to the picture tube. The connector is manufactured from tempered steel, hot tinned, with vinyl insulation, and is wired to customer specifications.

Further information and samples will be sent on request. Dept. P-9.

INDUSTRIAL HARDWARE 109 PRINCE ST., NEW YORK 12, N.Y.
Manufacturing Company, Inc.

P R D

TYPE 904
VHF-UHF
NOISE
GENERATOR

FREQUENCY RANGE (mc/sec): 10 to 1000
NOISE FACTOR RANGE (db): 20
CHARACTERISTIC IMPEDANCE: 50 ohms (unbalanced)

This calibrated broadband noise source permits direct measurements of noise factors as high as 20 db for r-f amplifiers and receivers operating in the range from 10 to 1000 mc/s. Equipment is housed in an attractive metal cabinet.

Write for Catalog

Polytechnic
RESEARCH & DEVELOPMENT CO., Inc.
55 JOHNSON ST., BROOKLYN 1, N.Y.
West Coast:
741 N. Seward St., Hollywood 38, Cal.

News—New Products

These manufacturers have invited PROCEEDINGS readers to write for literature and further technical information. Please mention your I.R.E. affiliation.

(Continued from page 119A)

"The Wear and Care of Records and Styli"

"The Wear and Care of Records and Styli" is a 56-page booklet, fully illustrated, which reveals many facts about the wear of phonograph records and styli, and its effect on the quality of reproduction. It contains a great deal of information of interest to every owner of a phonograph, high fidelity or otherwise.

Harold D. Weiler, author of *"High Fidelity Simplified,"* uses as the basis of his investigations a questionnaire sent to thousands of record uses all over the world. The results of his survey prove that the vast majority of listeners are severely damaging their records by using worn styli and allowing dust and grit to wear their records.

The booklet shows, the author claims, through microphotographs, facts, figures, and charts, the effective life of diamond and sapphire styli, and why diamond styli are a "best buy" from the standpoint of performance and economy. The book is available at most record stores, or from **Climax Publishing Co.**, 19 E. 48 St., New York 17, N. Y. The price is $1.00.

Tubeless DC Voltage Standard

A new tubeless voltage standard is now being produced by **Sorensen & Co., Inc.**, 375 Fairfield Ave., Stamford, Conn. Designed primarily as a component in recording equipment, where it eliminates a power supply and a standard cell, it is also available as a laboratory standard.

The new instrument is designated as model VRS15 and features tubeless circuitry, unusual stability, and small size. Specifications are: Output, 1½ at 6 ma, not damaged by short circuit; Output impedance, 12 ohms; Accuracy, ±1 mv against line; Ripple, 350 microvolts; Stability, drift in 24 hours is well under 1 mv. DC standards up to 5 vdc at other currents can be designed and supplied. Special mechanical configurations of the model VRS15 will be designed to customer specifications.

(Continued on page 123A)

TIC
nography
of
INSTRUMENTS

Measurement of
Impedance
Inductance
Capacitance
Resistance
Dissipation Factor (D)
Storage Coefficient (Q)
Plot Impedance Functions

310A Z-Angle Meter

The type 310A Z-Angle Meter measures impedance directly in polar coordinates as an impedance magnitude in ohms and phase angle in degrees: $Z\underline{/\theta}$

Impedance Range: .5 to 100,000 ohms, covered by a single dial and a four position range switch.

Accuracy: ± 1%

Frequency Range: 30 cycles to 20 kc. for impedances below 5000 ohms, measurements can be made up to 40 kc. For frequencies from 100 kc. to 2 mc., write for specifications for the type 311A-RF Z-Angle Meter.

Phase Angle Range: 0° to 90° Direct reading on panel meter. Meter is also Calibrated in D and Q.

Phase Angle Accuracy: Within 2° of meter indication.

Internal Oscillator: 60 cycles and 400 cycles. Terminals are provided for an external, variable frequency signal generator for measurements at other frequencies.

In the field, the laboratory, the production test floor or the class room, the extreme accuracy and the simplicity of operation has proved the type 310A Z-Angle Meter to be a superb and reliable instrument.

Write now for more detailed information.

ENGINEERING REPRESENTATIVES

New York, N.Y.—Murray Hill 8-5858
Binghamton, N.Y.—Binghamton 3-1511
Rochester, N.Y.—Munroe 3143
Utica, N.Y.—Utica 2-1602
Woodridge N.J.—Webster 9-7217
Great Neck, Long Island, N.Y.—Great Neck 2-9406
Dayton, Ohio—Michigan 8721
Chicago, Ill.—Uptown 8-1141
St. Paul, Minn.—Prior 4955
Baltimore, Md.—Plaza 7694
Arnprior, Ont., Can.—Arnprior 400
Dallas, Texas—Dixon 9918
Drexel Hill, Pa.—Clearbrook 9-3031
Hollywood, Calif.—Hollywood 9-6305
Belmont, Calif.—Lytell 3-3438
Seattle, Wash.—Lander 3320
Albuquerque, N.M.—Albuquerque 3-1998

TECHNOLOGY INSTRUMENT CORP.

535 Main Street · Acton, Mass. · COlonial 3-7711
West Coast Engr'g. Facility, P.O. Box 3941 No. Hollywood, Calif., Poplar 5-8620

Rutherford makes PRECISION

PULSE FORMING and TIMING INSTRUMENTS

PULSE and SQUARE WAVE OSCILLATOR

MODEL G-1

A source of pulses with accurate, continuously variable repetition rates. 100 KC to 1 cps in 5 ranges. Positive and negative pulse output .2 μs wide, 30 V amplitude. 75 V square wave. May be frequency modulated by an external control voltage. Linear voltage to frequency transfer characteristic.

Get complete data: our Bulletin I-G-1

Rutherford ELECTRONICS CO.

Telephone: TExas 0-4362
3707 S. ROBERTSON BLVD.
CULVER CITY, CALIFORNIA

AN/APR-4 LABORATORY RECEIVERS

Complete with all five Tuning Units, covering the range 38 to 4,000 Mc.; wideband discone and other antennas, wavetraps, mobile accessories, 100 page technical manual, etc. Versatile, accurate, compact—the aristocrat of lab receivers in this range. Write for data sheet and quotations.

We have a large variety of other hard-to-get equipment, including microwave, aircraft, communications, radar; and laboratory electronics of all kinds. Quality standards maintained. Get our quotations!

NEW TS-13/AP X-BAND SIGNAL GENERATORS, with manual, $850.00 . . . TS-175/U Frequency Meters, 85-1,000 Mc., $625.00 . . . T-47A/ART-13 Transmitters, $450.00 . . . and many more!

ENGINEERING ASSOCIATES

434 PATTERSON ROAD
DAYTON 9, OHIO

CAPITOL RADIO ENGINEERING INSTITUTE

Pioneer in Radio Engineering Instruction Since 1927

An Accredited Technical Institute

Advanced Home Study and Residence Courses in Practical Radio-Electronics and Television Engineering

Request your free Home Study or Resident School Catalog by writing to: Dept. 26A9

3224 16th St., N. W. Washington 10, D. C.

Approved for Veteran Training

Wiley Books

New 2nd Edition covers latest developments, including COLOR

TELEVISION

The Electronics of Image Transmission in Color and Monochrome

By V. K. ZWORYKIN and G. A. MORTON, both of RCA Laboratories

This entirely new and greatly enlarged 2nd Edition of TELEVISION covers the great technological advances of the past 14 years and is packed with practical, up-to-date information. It is the *first* book to give adequate coverage to *color* television. Its consideration of *both* the theoretical and practical aspects is sufficiently detailed to give a sound working understanding of this important new development.

1954 1037 pages 728 illustrations $17.50

Principles of

TRANSISTOR CIRCUITS

Edited by RICHARD F. SHEA, General Electric Co.

The first full-length, integrated work on transistor characteristics and circuits. Treats both point-contact and junction transistors, with analyses applicable to both n-p-n and p-n-p units. Written by experts, it gives you the basic theory you need, plus an explanation of the various techniques used in applying them. ". . . a single source for the cream of current thinking on the subject. . . . We believe that this definitive work will soon be known as the 'bible' of the transistor engineer."—*Radio & Television News*

1953 535 pages 502 illustrations $11.00

ELECTROACOUSTICS

An Analysis of Transduction and Its Historical Background

By FREDERICK V. HUNT, Harvard University

This new monograph is the first work to provide a complete and orderly history of the evolution, growth, and modern characteristics of the major electroacoustical transducer types. Harvard Monograph in Applied Science No. 5—Co-published with Harvard University Press.

1954 260 pages $6.00

RADIO RECEIVER DESIGN

Part I

Radio Frequency Amplification and Detection
New Second Edition

By K. R. STURLEY, British Broadcasting Corporation

Up-to-the-minute data, right at your finger tips, in a book that brings you the latest information on design from antenna to detector.

1954 667 pages Illus. $10.00

ENGINEERING ANALYSIS; An Introduction to Professional Method, by D. W. Ver Planck and B. R. Teare, Jr., both of the Carnegie Institute of Technology. Shows how typical problems are solved by engineering thought processes and how the engineer arrives at the logical, most accurate and efficient course of procedure.

1954 344 pages Illus. $6.00

Introductory CIRCUIT THEORY, by Ernst A. Guillemin, The Massachusetts Institute of Technology. All the basic concepts and interpretations you need to keep up with modern approaches to advanced problems involving circuit theory.

1953 550 pages Illus. $8.50

Send for your ON-APPROVAL copies today

JOHN WILEY & SONS, Inc.

440 Fourth Avenue New York 16, N.Y.

News—New Products

(Continued from page 121A)

Audio Fair For 1954

New York—The largest assembly of high-fidelity enthusiasts ever to gather for a single event will attend the 1954 **Audio Fair,** according to Harry N. Reizes, fair manager. Scheduled for four days beginning October 14, at the Hotel New Yorker, the Fair will play host to an estimated 30,000 visitors who will come to view the latest hi-fi developments as displayed by virtually every leading manufacturer of audio equipment.

In an effort to make the Fair available to many who have not been able to attend in previous years, the 1954 event will include a Sunday in its schedule.

Although the Fair was conducted originally as an event of specific interest to music lovers, hi-fi hobbyists and professional audio engineers, it has become the principal buying mart for audio equipment on a commercial level as well.

Sponsored each year by the Audio Engineering Society, and held in conjunction with the Society's annual convention, the Audio Fair has paralleled the Society in achieving world-wide recognition.

Matching a new high in attendance will be a record-breaking number of exhibitors, many of whom have announced that they will give first public introduction to a wide selection of new amplifiers, speakers, record players, and other items so dear to the heart of the high-fidelity hobbyist. Indicative of industry growth is the fact that the 1954 Fair will occupy four floors of the hotel as compared to the two floors which sufficed two years ago.

Joining in announcement of the annual audio conclave, Jerry B. Minter, President of the Audio Engineering Society, stated that this year's Society convention will hear a greater variety of technical papers than has ever before been presented at a single gathering. The annual Society banquet will be held on the night of October 13.

Following the policy established with the first event six years ago, the 1954 Audio Fair will be open to everyone free of charge.

Shielded Differential Transformer

Control Components Co., 46 Walnut St., Brookline, Mass., announces a new long-stroke shielded differential-transformer linear-motion displacement pickoff for the industrial and military control fields.

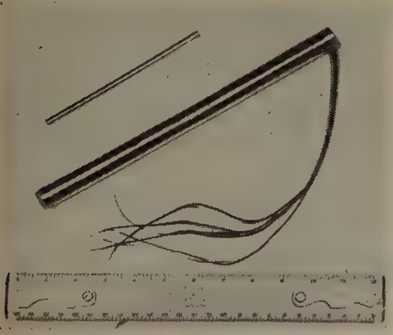

(Continued on page 125A)

BRADLEY | VACUUM PROCESSED RECTIFIERS

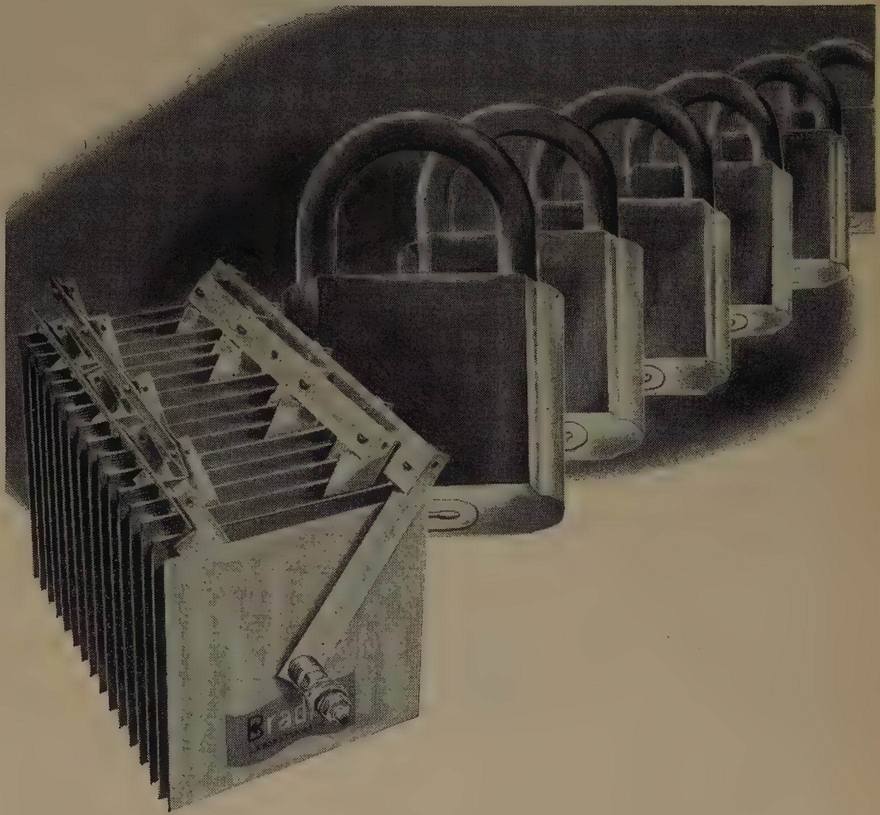

LOCKED-IN STABILITY AND LONGER LIFE

By locked-in stability and longer life, we mean this: We super-refine the selenium used in the Bradley foundation for rectifiers by vacuum distillation to achieve real control of the semi-conductor. Then we bond the selenium to plates under vacuum. The ultra-purity achieved in one step is completely protected against subsequent contamination in the second step.

Bradley rectifiers can be trusted completely. They will retain stability, last longer even under severe conditions of use, in the face of vibration, varying temperatures and sudden over-voltage surges. Your rectifier problems are over when you specify Bradley. Write us for a quotation. Let us demonstrate that Bradley rectifiers are not only highest in quality but lowest in cost.

VACUUM PROCESSED — for performance as rated

BRADLEY LABORATORIES, INCORPORATED
170P COLUMBUS AVENUE • NEW HAVEN 11, CONNECTICUT

Bradley
LABORATORIES, INC.

WELWYN

High Stability **RESISTORS**

DEPOSITED CARBON

MINIATURE POTENTIOMETERS

GLASS SEALED HIGH VALUE WELMEGS

VITREOUS ENAMEL COATED WIRE WOUND

ENCAPSULATED DEPOSITED CARBON RESISTORS

Welwyn precision products are manufactured in Canada and England. They are designed and constructed for the most exacting electronic requirements. These standards are uniformly maintained through rigid quality controls.

For complete details, write Dept. IJ-4

ROCKBAR CORPORATION
Sole U.S. Agents
215 East 37th Street, New York 16, N. Y.

There is Always One Leader in Every Field

BODNAR INDUSTRIES, Inc.

leads in the field of

PLASTIC LIGHTING PANELS AND DIALS

BECAUSE OF *Quality* • *Uniformity* • *Performance*
Design & Layout "Know-How Service"
Quantity Production Promptly

NEW YORK —19 Railroad Ave., New Rochelle (Home Office)
CALIFORNIA—4440 Lankershim Blvd., P.O. Box 264, North Hollywood
CANADA —44 Wellington St. E., Toronto

SPECIMEN PANEL MIL-P-7788 (AN-P-89) SENT ON LETTERHEAD REQUEST

HIGHEST STANDARDS
TOP QUALITY!

COSMIC

"CONDENSER SPECIALISTS SINCE 1923"

ELECTROLYTIC
AND PAPER TUBULAR
CONDENSERS
For A.C., D.C. Sets-Phonographs
etc.

COSMIC CONDENSER CO. 853 Whittier St., Bronx, N. Y.-Phone LU 9-3360

VHS* RELAY
(*Very High Sensitivity)

The VHS is a balanced armature, Alnico magnet type relay. It is internally shock mounted and resistant to vibration. The screw-on cover is gasket sealed. It can be opened and resealed.

0.2 microamperes, (3000 ohms coil) or, 0.1 millivolts, (20 ohms).

Connections: 9 pin octal style.
Dimensions: 1¾" dia. x 2¼" long.
Weight: 4 ounces.

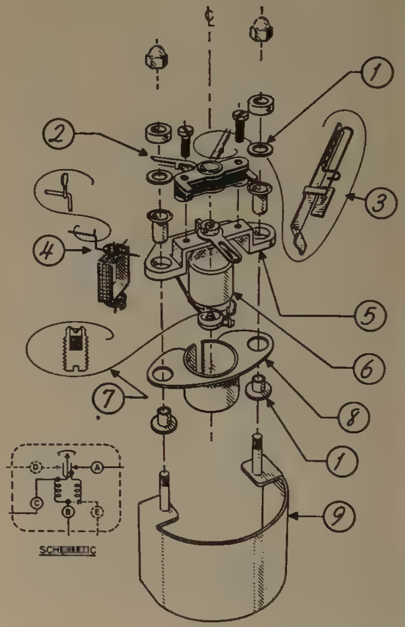

1. Shock mount
2. Contact assembly
3. Contact detail
4. Armature with contact detail
5. Cast bracket
6. Alnico magnet
7. Bearing detail
8. Yoke (steel)
9. Mounting frame

Sensitivity: Infinite variations from 0.2 Ua. to 10 Amp. or 0.1 Mv. to 500 volts, self contained. Higher volts or amps with external multipliers. A.C. rectifier types. Trip point accuracies to 1%. Differential and repeatability better than 1%.

Contacts: SPST or SPDT, 5-25 Ma. D.C. Other ratings to ½ Amp. A locking coil gives high pressure and chatter free contact even under shock and vibration. Samples 3 to 4 weeks.

ASSEMBLY PRODUCTS, Inc.
P.O. BOX 191 · CHAGRIN FALLS 2, OHIO
Ask for Bulletin 102

News—New Products

These manufacturers have invited PROCEEDINGS readers to write for literature and further technical information. Please mention your I.R.E. affiliation.

(Continued from page 123A)

The stroke range, in which the output is linear with input, is 4 inches (±2 inches about the null position) when the pickoff is excited with an ac voltage in the design range, 2 to 10 kc. This linear range is decreased somewhat when the excitation frequency is outside this range; for example, at 400 cps the linear range is 3 inches.

The unit has the designation Linearsyn model 7S2 and is designed to resist shock and mechanical abuse. To make the unit highly resistant to all possible electrical interference, and to shield the coil assembly, the moving core has been made shorter than the coil assembly.

An output impedance of less than 1,000 ohms makes it possible to use the unit with relatively long cable runs in remote control applications.

Servo Motor Features New Laminations

A new low inertia servo motor with a new and different lamination design was recently announced by **Infra Electronic Corp.**, 553 Eagle Rock Ave., Roseland, N. J. The company claims that this new design yields high motor performance at reduced manufacturing cost.

INFRA Electronic Corp.
ROSELAND N.J. U.S.A.
SERVO MOTOR
TYPE M-100
115 VOLT
400 CYCLES
MIN. NO LOAD SPEED
MIN. STALLED TORQUE
DUTY CONTINUOUS AT 6000
SER. NO
WT.

Called the type M-100 Servo Motor and built in the 1.750 OD size, this motor features: a hermetically sealed stator providing high operating stability; a high torque to inertia ratio for rapid acceleration and deceleration service encountered in servo mechanism and computing applications. The unit is designed to be inoperative under single phase conditions and a sloping speed-torque characteristic provides viscous damping in control applications.

Motor Characteristics: Voltage, 115 (fixed phase), 115/57.5 (control phase); frequency, 400 cps; phases, 2; poles, 4; no load speed 10,000 rpm; stalled torque, 2.7 ounce/inches; rotor inertia, 4.0 gr-cm; weight, 12.2 ounces.

(Continued on page 127A)

Electronic
ADVANCEMENT
with...
ELECTRONICS DIVISION
Thompson Products, Inc.
CLEVELAND 3, OHIO

THIS BOOK DOESN'T

tell all

. . . but it's full of ideas you can use

SUCCESSFUL developments in the electronics field depend mainly on three things: ideas . . . experience . . . facilities. *This book is full of all three.*

Just a short request on your letterhead . . . or the coupon below . . . will bring this valuable book in the mail to you at once.

Thompson Products, Inc.

ELECTRONICS DIVISION • 2196 CLARKWOOD ROAD, CLEVELAND 3, OHIO

Thompson Products, Inc.
Dept. PI, Electronics Division
2196 Clarkwood Road, Cleveland 3, Ohio

Please send me a copy of Electronic Advancement.

Name________________Title________
Company______________________
Address______________________
City____________Zone____State________

Victoreen
CR 50-5
TYPE
MADE IN U.S.A.
Victoreen
CR 2
TYPE
MADE IN U.S.A.
VICTOREEN
CRM 900-5
MADE IN U.S.A.

CURRENT REGULATOR TUBES

VICTOREEN OFFERS GREATER CHOICE

Of Standard Designs
Or Will Build Specials to Your Specification

Chances are Victoreen engineers have already engineered and produced in quantity a current regulator tube exactly fitted to your needs. These standard tubes are available on short notice. But, if your requirements are *special* we have the facilities, from engineering to production, to supply you with a current regulator that will help maintain high performance for your equipment.

Supply us with your specifications for quotation.

PIONEER ELECTRONICS CORP.
SUBSIDIARY OF
The Victoreen Instrument Co.
COMPONENTS DIVISION: 3813 Perkins Ave. • Cleveland 14, O.

TEKTRONIX Type 531

SAVES ENGINEERING TIME

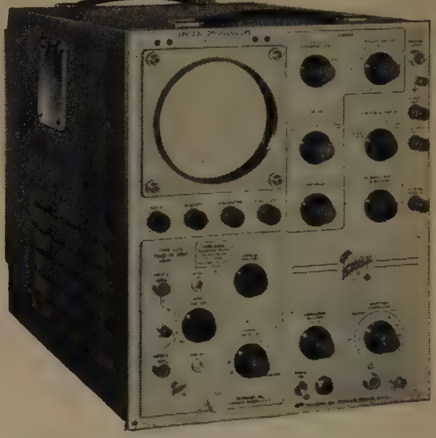

The Type 531 Oscilloscope saves engineering time two ways. It provides you with an extremely wide range of facilities. It eliminates the need to hunt up another oscilloscope when your requirements change—say from "high-gain" to "wide-band", or to "dual-trace".

Plug-in preamplifiers are used for maximum flexibility in signal handling. Sweep-speed range is 600 million to one—the widest you can get in a single oscilloscope. Accelerating potential is high enough to permit photographing a single sweep . . . even at the fastest sweep speed.

Direct-Reading in Time and Amplitude. You can read time and amplitude with accuracies comparable to indicating meters.

Sweep Range—0.02 μsec/cm to 12 sec/cm.
10KV Accelerating Potential
Versatile Triggering Circuitry
Price—$995 plus price of desired plug-in units

PLUG-IN UNITS

TYPE 53A—DC to 10 mc, 0.05 v/cm to 50 v/cm $85
TYPE 53B—Same as 53A with additional ac-sensitivity to 5 mv/cm $125
TYPE 53C—Dual-trace unit. Two identical amplifier channels, dc to 8.5 mc, 0.05 v/cm to 50 v/cm. Electronic switching triggered by oscilloscope sweep, or free-running at about 100 kc. $275
TYPE 53D—Differential input. DC to 350 kc at 1 mv/cm—passband increasing to 2 mc at 50 mv/cm. Full range—1 mv/cm to 125 v/cm. $145

Prices f.o.b. Portland (Beaverton) Oregon

See the Type 531 at the INTERNATIONAL INSTRUMENT EXPOSITION Philadelphia—and at the NATIONAL ELECTRONIC CONFERENCE, Chicago.

Tektronix, Inc.
P. O. Box 831 B
Portland 7, Oregon
Phone: CYpress 2-2611
Cable: TEKTRONIX

News—New Products

These manufacturers have invited PROCEEDINGS readers to write for literature and further technical information. Please mention your I.R.E. affiliation.

(Continued from page 125A)

Silicon Diode

The evolution of silicon diodes is shown in this photo-story prepared by **Texas Instruments Inc.,** 6000 Lemmon Ave., Dallas 9, Texas, a transistor manufacturing company.

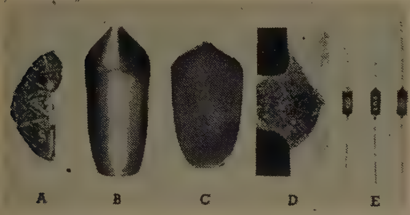

(From left to right) A. Polycrystalline silicon commonly used for point contact silicon diodes. B. Newly developed grown single crystal of high-purity silicon. C. Sectioned single crystal showing homogenous structure (contrast with A). D. Photomicrograph of new TI silicon diode showing semiconductor alloyed junction. E. Production units of Texas Instruments silicon junction diodes complete with glass-to-metal hermetic sealing. These silicon junction diodes, made from single crystal silicon, are in production and available now. They feature front-to-back current ratios as high as 10^7 (10 million to one) and safe operation up to 150°C.

Coupling Unit

Boonton Radio Corp., Boonton, N. J., announces a new Coupling Unit, Type 564-A, which will permit the coupling of an external oscillator into the new Type 260-A Q Meter for Q measurements in the audio and supersonic frequency ranges.

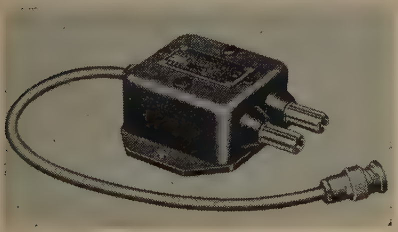

The unit is housed in a gray hammerstone case $1\frac{1}{4}\times2\frac{1}{2}\times3\frac{3}{4}$ inches, and provides binding posts for connection of the external oscillator and a coaxial cable with BNC connector for convenient connection to the Q Meter. Physical mounting is provided by means of a drilled mounting flange.

Electrical specifications are as follows: Input Impedance is 500 ohms (when output is connected to Q Meter Type 260-A); Output Impedance—0.3 ohm (provided by voltage injection circuit of Q Meter Type 260-A); Frequency Range—1 KC to 50; Input Voltage Requirements—variable up to 22 volts.

(Continued on page 143A)

COST-SAVING IDEAS FOR DESIGN ENGINEERS

S. S. WHITE FLEXIBLE SHAFTS ELIMINATE ALIGNMENT AND VIBRATION PROBLEM

By coupling the tuning knobs to variable circuit elements with S.S.White remote control flexible shafts, the designer of the radio equipment illustrated was able to eliminate all problems of alignment and thus simplify assembly. The shafts also dampen vibration, preventing it from being carried to the sensitive parts of the circuits.

WHAT ABOUT YOU?

You'll find the S.S. White remote control flexible shafts the answer to many similar design problems. It will pay you to investigate their possibilities in your own product. Our engineers stand ready to answer your questions. There's no obligation, of course.

BULLETIN 5306 has basic information and data on flexible shaft application and selection. Send for a free copy. Address Dept. G

R-2

THE S.S.White INDUSTRIAL DIVISION
DENTAL MFG. CO.
10 East 40th Street
NEW YORK 16, N. Y.

Western District Office • Times Building, Long Beach, California

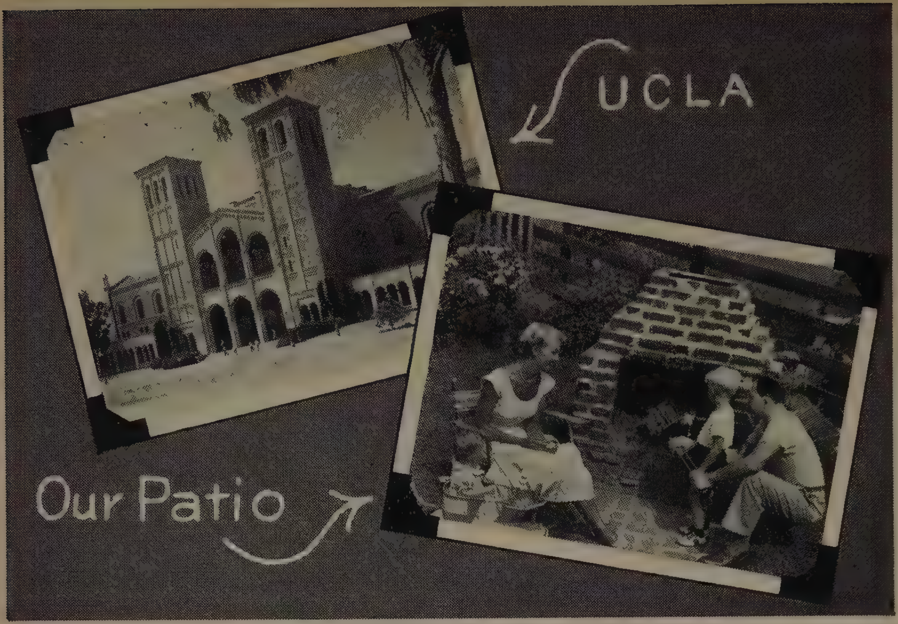

OPENING FOR ELECTRONICS ENGINEER AT GILFILLAN

Naturally, no man takes a job in California simply because living is more fun here, or because of fine educational institutions. But when these are added to everything you have been looking for in a lifelong career, including rapid advancement, interest, security and prestige—that's different.

That is what a job with Gilfillan can mean to a qualified engineer; to you, now, because Gilfillan has several openings for good men.

SECURITY

Gilfillan is a major company, with 7 plants located throughout Southern California, that has been in business more than 40 years.

SATISFACTION

Gilfillan is big enough to handle all phases of engineering research, design and production, yet not so big you get lost. You have the very real satisfaction of following through on your work, getting credit for it, and seeing its achievements in the field.

PRESTIGE

Gilfillan pioneered GCA Radar and all its major improvements, is now engaged in automatic GCA, the new lightweight Gilfillan GCA Quadradar, missile guidance, navigational systems, E. C. M.—and a series of classified projects involving advanced and unsolved techniques for all branches of the military services.

Work is interesting at Gilfillan because ideas begin here. As a Gilfillan engineer, your value increases—because of the Gilfillan reputation, and because you work in coming fields.

ADVANCEMENT

You go ahead at Gilfillan as fast as you are ready. You are paid and advanced according to ability, not seniority. If you want further formal training, Gilfillan pays your tuition at UCLA or USC. You can be sure your ability will be recognized, because every man in a supervisory capacity at Gilfillan is a qualified engineer.

WRITE:

R. E. Bell, Gilfillan Bros., Dept. 94, 1815 Venice Blvd., Los Angeles, California. Give a brief resume of your background and experience. Interview at a convenient location will be arranged for qualified men.

Gilfillan
GCA
Los Angeles

POSITIONS OPEN

The following positions of interest to I.R.E. members have been reported as open. Apply in writing, addressing reply to company mentioned or to Box No. . . . .

The Institute reserves the right to refuse any announcement without giving a reason for the refusal.

PROCEEDINGS of the I.R.E.
1 East 79th St., New York 21, N.Y.

PROFESSORS

Technion, Israel Institute of Technology, Haifa, Israel, proposes to appoint one Professor of Electrical Engineering with special qualifications in telecommunications, one Associate Professor of Electrical Power Engineering and one Professor of Mathematics. Applicant should have first-rate professional and academic qualifications, be willing to integrate themselves into the life of the country, and in due course, teach Hebrew. Applications with full details should be sent in duplicate, for transmission to Haifa, to the American Technion Society, 1000 Fifth Ave., New York 28, N.Y.

ENGINEER

Engineer with substantial experience in development of electronic instruments who is interested in administrative and operational aspects of a development laboratory. Particular field of operation is in physical measurements. Located in Chicago area. Box 778.

ELECTRONIC ENGINEERS

Several positions for graduate engineers are available in Research and Development Dept. An opening for a Project Engineer with industrial experience, who will be responsible for scheduling and co-ordinating an engineering project including fabrication of experimental and small production quantities of airborne equipment. Also openings for an engineer with experience in circuit design and in development and testing of new equipment in the 100 kc to 250 mc frequency range, and for an engineer with experience in microwave radar circuits and HF techniques. Reply to Robert L. Blanchard, Trans-Sonics, Inc., Bedford, Mass.

SENIOR ELECTRONIC ENGINEER

Physics or Electronic Engineer from a recognized university with at least 5 years' experience in electronic circuit design. British subject preferred. Salary commensurate with ability. Send resume to Chief Engineer, Cossor (Canada) Ltd., 301 Windsor St., Halifax, N.S. Canada.

ENGINEER

The English Electric Company, Ltd., Luton, England, have an interesting vacancy for work on the development of new ideas in microwave circuitry, waveguides and miniaturisation. Apply with full particulars and quoting ref. 1160c to Dept. C.P.S. 336/7 Strand, London W.C.2, England.

(Continued on page 130A)

BIGGER and BETTER
THE 1954
IRE DIRECTORY
Coming Soon!

Positions Wanted

(Continued from page 141A)

SENIOR ELECTRONICS ENGINEER

MSEE. 1949. Age 36, married. Five years varied electronic development experience, including supervision, in complex airborne systems. Desire to relocate in small community or suburban area. Box 780 W.

SENIOR ENGINEER

BEE., seven years diversified experience in circuit design, project supervision. Experience in pulse circuits, C.R.T. displays, test equipment and electromechanical design. Desires position involving commercial work only. Eta Kappa Nu. Age 37, married, one child. Northern New Jersey area preferred. Box 781 W.

ENGINEER

BSEE. 1952. Age 25, married, one child. Experience in analog and digital computer techniques. 1½ years experience maintenance CRC 102A digital computer. Desires position in computer field, preferably in design of logical circuitry in New York or vicinity. Box 782 W.

ELECTRONIC ENGINEER

BEE. Age 30. Five years audio and UHF research and development experience including supervisory, planning and contract administration assignments. Interested in operational and administrative aspects of laboratory or plant which is in need of this experience and offers opportunity to expand on supervisory ability. Present salary $7400. Box 783 W.

News—New Products

These manufacturers have invited PROCEEDINGS readers to write for literature and further technical information. Please mention your I.R.E. affiliation.

(Continued from page 127A)

Frequency Calibrator for WWV Reception

Wider application for an accurate frequency calibrator utilizing transmission from the U. S. Bureau of Standards Station WWV has prompted **Browning Laboratories, Inc.**, 750 Main St., Winchester, Mass., to make available an improved model of their frequency calibrator. Designated the RH-10, the receiver makes use of WWV's primary frequency standards for checked and setting audio frequencies, radio frequencies and timing devices.

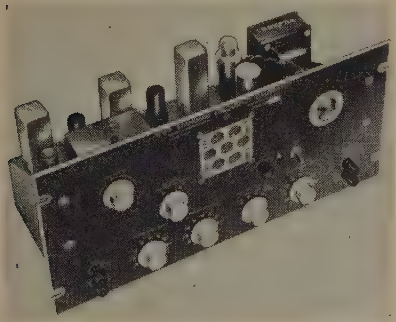

The 11-tube calibrator is pre-tuned to receive the 5 and 10 mc WWV signals. A

(Continued on page 144A)

ENGINEERS

with **EXPERIENCE**

in electronic development

with experience comes progress

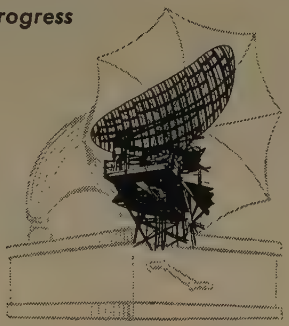

are you EXPERIENCED in

RADAR - MISSILE CONTROL
AIRBORNE COMMUNICATIONS
MOBILE COMMUNICATIONS
AUTO RADIO

. . . does an analysis of your background show that—at present—you are employed at THE HIGHEST LEVEL OF YOUR SKILL?

. . . Send us a resume of your background. We may have a higher level position open for you!

Send resume to Mr. L. H. Noggle, Dept. M-

BENDIX RADIO

Division of Bendix Aviation Corp. Baltimore-4, Md.

ENGINEERS

looking for . . .
. . . a good start?
. . . rapid development of your professional skill?

You can have both at Sperry,

PIONEERS IN A WIDE RANGE OF FIELDS, FOR MORE THAN 43 YEARS

We invite you to investigate the exceptional employment opportunities available on our unusually large research, design, and development staff, in many fields including the following:

Klystron & traveling tube research • Analogue & digital Computers • Radar • Hydraulics • Communication Equipment • Pulse Transformers • Servo Mechanisms • Electronic Circuits • Aircraft Controls • Instrumentation • Fractional H.P. Motors • Magnetic Amplifiers • Radio Frequency & Microwave Measurement.

PUBLICATIONS ENGINEERS To write manuals and engineering reports.

Advanced and challenging assignments • Association with top Engineers • Interesting, diversified work • Remuneration based on professional abilities • Modern plant—latest laboratory facilities • Adequate housing • And of course, employee benefits, and congenial surroundings, among the finest.

Please submit resume to our Engineering Personnel Section. (Personal interviews may be arranged in your city.)

SPERRY GYROSCOPE CO.
Division of the Sperry Corp.
Great Neck, Long Island, N.Y.

SPERRY

ELECTRONIC ENGRS & PHYSICISTS

You can be SURE . . .

of a lifetime opportunity,

If it's

WESTINGHOUSE

Our new aggressive and expanding Tube Division is seeking top-quality Electrical Engineers, with two or more years' experience in the following:

TUBE DESIGNERS . . .

Any of these fields: micro-wave tubes, receiving tubes, solid-state devices, image orthicon, traveling wave tubes.

APPLICATION ENGINEERS . . .

Circuit experience in one of these fields helpful: Radio, TV, VHF, semi-conductors, and sweep circuits.

PRODUCTION ENGINEERS . . .

1. For black-&-white and color TV manufacturing. Knowledge of photo-sensitized screens, silk screens or printed screens desirable.
2. For power-tube operations, including magnetrons, micro-waves and semi-conductors.
3. For quality-control. Electrical Engineering background preferred.

These positions offer: A pleasant life in Elmira, N.Y., amid New York State's resort lake-land! Good housing, excellent schools, hunting, fishing, sailing, etc. An opportunity for Professional Progress . . . stock-purchase and pension plans, tuition refund program, etc. WESTINGHOUSE will pay expenses of Engineers invited to Elmira for interview. Send Resume:

WESTINGHOUSE ELECTRIC CORP.
P. O. Box 284
Elmira, N.Y.

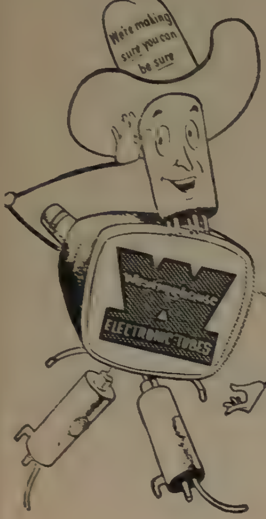
We're making sure you can be sure
ELECTRONIC TUBES

ENGINEERS
& TECHNICIANS
Insure your future in

COLOR TELEVISION

with
CBS-COLUMBIA

Positions, offering opportunity & stability, are open to men experienced in the Design and Development of TV Receivers

AS FOLLOWS:

VIDEO CIRCUITS COMPONENT DESIGN
SYNCHRONIZED CIRCUITS

You will work with a staff of engineers who are leaders in the Television field and will have at your disposal the most modern electronic equipment.

Only men with proven record of resourcefulness and technical accomplishment will be considered.

Remuneration will be high—You will enjoy a complete employee benefit program.

To help us get better acquainted write us all about yourself. Interviews with out-of-town applicants arranged.

WRITE PERSONNEL DEPARTMENT

CBS-COLUMBIA
(Division of Columbia Broadcasting System)
3400-47 Avenue
Long Island City 1, N.Y.

These manufacturers have invited PROCEEDINGS readers to write for literature and further technical information. Please mention your I.R.E. affiliation.

(Continued from page 143A)

four-position function selector switch permits receptions of standard WWV signal, 440 cps modulation, 600 cps modulation, or beat carrier (audio frequencies below 400 cps). Circuit design affords sensitivity exceeding 1.0 microvolt on any band, with high antenna input impedance for single wire or tuned doublet; selectivity 10 db at 5 kc off resonance; image rejection better than 50 db; and local oscillator voltage regulation to minimize drift. The calibrator is available in a standard rack panel with dust cover. For 105–125 volts, 50/60 cps. The price is $295.00 F.O.B. Winchester, Mass. For further information write the manufacturer.

Fractional Cycle Timer

The VTP Model F-216 Fractional Cycle Timer, designed to meet the more specialized requirements of resistance welding for timing spot, seam welders, or other timing operations in industrial service, is announced by **Vacuum Tube Products,** 506 Cleveland St., Oceanside, Calif. The fast time setting insures spatter-proof, oxide-free welds, and allows positive welding of such materials as molybdenum and tungsten. Positive adjustment in the fractional cycle range also allows reliable and uniform welding of materials less than 1.001 inches thick.

The timer unit measures $10\frac{1}{2} \times 9 \times 10\frac{1}{2}$ inches. All controls are accessible from the front panel and consist of an on-off switch with pilot indicator, a cathode protection pilot, a high-low heat range switch, and a variable time control.

The fractional cycle timer has been designed for use with the VTP Precision Spot Welder and is available installed ready for operation, or as an individual component where the excellent timing features of this unit are desired for equipment already in use.

(Continued on page 146A)

ENGINEERS

The APPLIED PHYSICS LABORATORY OF THE JOHNS HOPKINS UNIVERSITY offers an exceptional opportunity for professional advancement in a well-established laboratory with a reputation for the encouragement of individual responsibility and self-direction. Our program of

GUIDED MISSILE

RESEARCH AND DEVELOPMENT

provides such an opportunity for men qualified in:

- ELECTRONIC CIRCUIT DESIGN AND ANALYSIS
- DEVELOPMENT AND APPLICATION OF TRANSISTOR CIRCUITRY
- SERVOMECHANISMS AND CONTROL SYSTEM ANALYSIS
- ELECTRONIC EQUIPMENT PACKAGING
- INSTRUMENT DESIGN
- MISSILE SYSTEMS DEVELOPMENT
- FLIGHT TESTING

Please send your resume to

Glover B. Mayfield

APPLIED PHYSICS LABORATORY

THE JOHNS HOPKINS UNIVERSITY
8621 Georgia Avenue
Silver Spring, Maryland

TUNG-SOL 50 YEARS ACHIEVEMENT

ENGINEERS

Have you developed a "Success Perspective"?

If a year or two of practical experience has given you the youthful maturity that demands more than just a job, you may be interested in our "career opportunities" in color TV, crystal products and electronic tubes.

Submit resume or address request for personal interview to D. Bellat, Personnel Director.

TUNG-SOL ELECTRIC INC.
200 Bloomfield Avenue
Bloomfield, N.J.

UNLIMITED OPPORTUNITIES for...
Electrical Engineers and Physicists to do Digital Computer Engineering

- *All replies will be held in strict confidence.*
- *Interviews will be arranged at our expense.*

Research—Development—Design

- ✓ Automatic Data Handling
- ✓ Operational Research
- ✓ Pulse Handling Techniques
- ✓ Solid State Physics

We need qualified Electronic Engineers and Physicists. Because of the continuous growth of our electronic computer work we can offer unequaled opportunities to men with the proper education and background in the Electronics field . . . permanent positions, financial security, professional development.

HERE IS THE KEY TO YOUR FUTURE...

ENGINEERING RESEARCH ASSOCIATES
DIVISION OF **Remington Rand** INC

1902 West Minnehaha Avenue *St. Paul W4, Minnesota*

AERONAUTICAL RADIO, INC.
offers work in
RELIABILITY—KEY TO THE FUTURE OF ELECTRONICS

Growing numbers of electronics engineers are recognizing the critical importance of reliability in future expansion of the uses of electronics. ARINC, a pioneer and leader in the search for reliability, has a few select openings for well-qualified engineers of good educational background and work experience. Positions are available both in the field-investigation and headquarters-analysis phases of an important reliability project, with possibility of some overseas assignments. This work will appeal to men with a sound knowledge of electron tubes and/or circuitry, and with an interest in using engineering fundamentals and original thought to solve problems in design, application, maintenance, and many other areas of electronics.

ARINC also invites inquiries from technical writers capable of editing, rewriting, and supervising publication of narrative-type engineering reports. A clear, straightforward writing style and a meticulous regard for accuracy and integrity of the basic material are absolute essentials.

All replies will be held in confidence. Address resume of experience and education to Mr. J. W. Dunckel.

Box 786, Institute of Radio Engineers
1 East 79th St., New York 21, N.Y.

PHYSICIST

Experienced physicist or electronics engineer with Ph.D. degree for development work on electronic tubes. Minimum of five to ten years experience in this field is prerequisite. Send complete resume or apply in person to:

Research Division

NATIONAL UNION ELECTRIC CORP.
350 Scotland Rd. Orange, N.J.

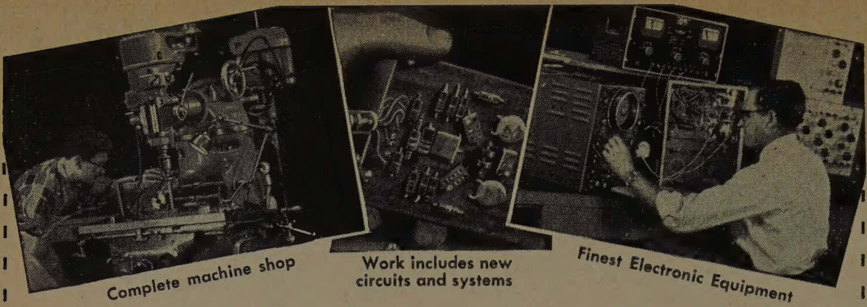

Complete machine shop

Work includes new circuits and systems

Finest Electronic Equipment

Leaders and Specialists in **"ENGINEERING"**

offered splendid opportunities in Boston Engineering Laboratory!

Men qualified to handle high level assignments in electronics are offered a challenging opportunity in Boston, under ideal working conditions divorced from production. The laboratory provides stimulating projects, an atmosphere of scientific progress and provides assistance towards your personal advancement or professional recognition. You will work with a top level technical staff possessing the finest facilities. Administrative positions are open to men qualified to guide the efforts of others.

MICROWAVE ENGINEERS

Senior engineers to handle design and development projects and provide technical direction of other top-level engineers working on microwave circuits and microwave plumbing in the development of military airborne electronic equipment. Should have 5 years' experience in such work and at least a BS degree.

RADAR SYSTEMS AND CIRCUIT ENGINEER

To assume responsibility for electronic circuit design for major elements of complex airborne electronic equipment. Should have a BS degree and about 5 years' experience.

Sylvania provides financial support for advanced education as well as a liberal insurance, pension and medical program. Investigate a career with Sylvania.

INTERVIEWS BY APPOINTMENT

Don Bradley, Personnel Manager, Boston Engineering Lab.

SYLVANIA ELECTRIC PRODUCTS INC.

70 FORSYTH STREET • BOSTON, MASSACHUSETTS • KEnmore 6-8900

EXPERIMENTAL PHYSICISTS

For the expansion of a small group of competent physicists and engineers who are concerned with the development of basically new instruments and with the solution of advanced instrumentation and measurement problems. This group is responsible for devising methods for the solution of special problems and for the experimental verification of these methods. The final engineering and packaging is normally carried out by other groups in the organization. The varied nature* of this work requires both recent graduates and experienced people capable of accepting primary responsibility for the solution of problems of varying degrees of complexity.

Excellent opportunities for advancement and advanced study. Salary commensurate with experience and educational level.

*Some of the current investigations are in the fields of mass spectrometry, light scattering, thermistors, radioactive tracers, electron and ion optics, precision electronic timing circuits, and ultrasonics.

For further information please contact:

Personnel Director

BENDIX AVIATION CORPORATION

Research Laboratories

4855 FOURTH AVENUE, DETROIT 1, MICHIGAN

Classifications with a System!

The IRE Directory Product Classifications have both a pattern and a purpose. They differ widely from most product indexes, deliberately. They aim to organize the hundreds of products and services of a complex technical industry according to the way engineers think. To this end, the product grouping follows the pattern of the IRE Professional Groups, broadly. The result is a division of all products and services into ten fundamental indexes into which 104 basic classifications have been organized.

For detailed identification, these 104 products and services, grouped in the 10 indexes, are further defined into 608 named products. We have tried to avoid oversimplification, and a tremendous amount of information is given by our product number system. But, the basic indexing adds speed. Purely alphabetical directories are as slow and cumbersome as a telephone book. IRE engineers have liked our system better! Just a little study of this system will help you get great good from this book.

The IRE DIRECTORY is 10 Indexes in one book.

News—New Products

These manufacturers have invited PROCEEDINGS readers to write for literature and further technical information. Please mention your I.R.E. affiliation.

(Continued from page 144A)

Small Stampings

High production methods now make it possible to effect cost savings on quantity runs of small stampings for radio, television and electronic use. Announcement of the "low cost" technique was made by **Malco Tool and Mfg. Co.**, Dept. MEW, 4025 Lake St., Chicago 24, Illinois.

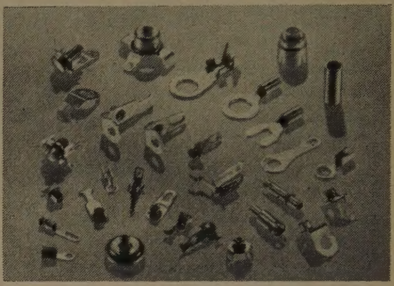

Over 1,000 different parts are available as standard items including solder lugs, terminals, contacts, corona rings and others. They are supplied to specification within minute tolerances. Base metals include brass, copper, beryllium copper, phosphorus bronze and steel.

For further information contact or send specifications to the manufacturer.

(Continued on page 148A)

ENGINEERS

SYSTEMS
RADAR
SERVO
COMPUTER

BACKGROUND: Responsible positions open for top level development and project engineers with practical and research experience in:

Advanced Electronic Circuits and Systems

Microwave Radar

Microwave Receivers and Transmitters

MAXSON

Requirements emphasize advanced analytical and/or management experience on highly complex electronic and electro-mechanical systems.

Kindly send resume and salary requirements to

The W. L. MAXSON Corp.
460 W. 34th ST., NEW YORK 1, N.Y.

COMMUNICATIONS EQUIPMENT CO.

MICROWAVE COMPONENTS

10 CM.—RG48/U Waveguide

10CM ECHO BOX: Tunable from 3200-3333 Mc. For checking out radar transmitters, for spectrum analysis, etc. Complete with pickup antenna and coupling devices. $27.50

10 CM ANTENNA ASSEMBLY: 3000-3300 Mc. Parabolic Dish, 29 inch Diam. Fed from dipole **Rotation:** 360 Deg. Azimuth at speeds of 20 and 10 RPM. **Tilt:** 20 deg. above and below horizontal. Motor-Driven by 2-28V motors, 4.5 A Total drain. Azimuth info. is fed to selsyn mechanism, and elevation data is obtained from Azimuth potentiometer. Net weight 65 lbs. $78.50

POWER SPLITTER for use with type 726 or any 10 CM Shepherd Klystron. Energy is fed from Klystron antenna through dual pick-up system to 2 type "N" connectors ....$22.50 EACH

DIRECTIONAL COUPLER. Broadband type "N" Coupling, 20 db. with std flanges, Navy #CAB-V47A-AN-2 ....$32.50

LHTR, LIGHTHOUSE ASSEMBLY. Parts of RT39 APG 5 & APG 15. Receiver and Trans. Cavities w/assoc. Tr. Cavity and Type N CPLG. To Recvr. Uses 2C40, 2C43, 1B27. Tunable APX 2400-2700 MCS. Silver Plated $22.50

BEACON LIGHTHOUSE cavity p/o UPN-2 Beacon 10 cm. Mfg. Bernard Rice, each $27.50

MAGNETRON TO WAVEGUIDE Coupler with 721-A Duplexer Cavity, gold plated $45.00

721A TR BOX complete with tube and tuning plungers $12.50

McNALLY KLYSTRON CAVITIES for 707B or 2K28. 2700-2900 Mc. $4.00

**WAVEGUIDE TO ⅞" RIGID COAX "DOOR-KNOB" ADAPTER CHOKE FLANGE SILVER PLATED BROAD BAND $32.50

AS14A AP-10 CM Pick up Dipole with "N" Cables $4.50

HOLMDELL-TO-TYPE "N" Male Adapters, W. E. #D167284 ....$2.75

I.F. AMP. STRIP: 30 MC, 30 d.b. gain, 4 MC Band-width, uses 6AC7's—with video detector, A.F.C. less tubes $24.00

BEACON ANTENNA, AS31/APN-7 in Lucite Ball. Type "N" feed $22.50

ANTENNA, AT49A/APR: Broadband Conical, 300-3300 MC Type "N" Feed $12.50

"E" PLANE BENDS, 90 deg. less flanges ...$7.50

3 CM.—RG 52/U Waveguide

3 CM ANTENNA ASSEMBLY: Uses 17" paraboloid dish, operating from 24 vdc motor. Beam pattern: 5 deg. in both Azimuth and elevation. Sector Scan: over 160 deg. at 35 scans per minute Elevation Scan: over 2 deg. Tilt: Over 24 deg. $85.00

Cross-Guide Directional Coupler, UG-40 output flange. Main Guide is 6" Long, with 90 Deg. "E" Plane bend at one end, and is fitted with Std. UG 39/UG 40 flanges. Coupling figure: 20 db Nominal $22.50

FLEX. WAVEGUIDE SECTION, 1 ft. long. With UG-40/UG-39 flanges. Attenuation is less than 0.1 db. at 9375 mc, and VSWR is less than 1.02. Rubber covered $7.50

3CM Motor-Driven Echo Box

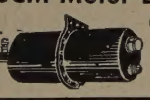

Cavity Q is 30,000. Tuning range 80 mc Motor operates from 24 VDC Type, "N" INPUT $32.50

VSWR Measuring Section. Consisting of 6" straight section, with 2 pick-up, Type "N" Output Jacks. Mounted ½ Wave apart $7.50

1" x ½" waveguide in 5' lengths, UG 39 flanges to UG40 cover. Silver plated .....**per length $5.00**

Rotating-joints supplied either with or without deck mounting. With UG40 flanges **each, $17.50**

Bulkhead Feed-thru Assembly $15.00

Pressure Gauge Section 15 lb. gauge and press nipple $10.00

Pressure Gauge, 15 lbs. $2.50

Directional Coupler, UG-40/U Take off 20db $17.50

TR-ATR Duplexer section for above $8.50

Rotary joint choke to choke with deck mounting $17.50

90 degree elbows. "E" plane 2½" radius ...$12.50

Microwave Receiver, 3 CM. Sensitivity: 10-13μ Watts. Complete with L.O. and AFC Mixer and Waveguide Input Circuits, 6 I.F. Stages give approximately 120 DV gain at a bandwidth of 1.7 MC. Video Bandwidth; 2 MC. Uses latest type AFC circuit. Complete with all tubes, including 723A/B Local Oscillator $175.00

ADAPTER, waveguide to type "N", UG 81/U, p/o TS 12. TS-13, Etc. $14.50

ADAPTER, UG-163/U round cover to special btl. Flange for TS-45, etc. ....$2.50 ea.

1¼" x ⅝" WAVEGUIDE

VSWR SECTION, 6"L. with 2-type "N" pickups mounted ½ wave apart. $7.50

GG 98B/APQ 13 12" Flex. Sect. 1¼" x ⅝" OD $7.50

Slug Tuner Attenuator W.E. guide, gold plated $6.50

Bi-Directional Coupler. Type "N" Takeoff 25 db. coupling $22.50

Bi-Directional Coupler. UG-52. Takeoff 25 db. coupling $24.95

Waveguide-to-Type "N" Adapter. Broadband $17.50

MAGNETRONS

Type	Peak Range (MC)	Peak Power Out (KW)	Duty Ratio	Price
2J21A	3345-9405	50		$ 8.75
2J22	3267-3333	265		7.50
2J26	2992-3019	275	.002	7.49
2J27	2965-2992	275	.002	19.95
2J29	2914-2939	275	.002	44.95
2J31	2820-2860	285	.002	24.50
2J32	2780-2820	285	.002	28.50
2J38*	3249-3263	5		16.50
2J39*	3267-3333	8.7		24.50
2J48	9310-9320	50	.001	24.50
2J49	9000-9160	50	.001	59.50
2J56*	9215-9275	50	.001	132.50
2J61†	3000-3100	35	.002	34.50
2J62†	2914-3010	35	.002	34.50
3J31	24-27KMC	50	.001	85.00
4J34	2740-2780	900		125.00
4J38	3550-3600	750	.001	169.45
4J42†	670-730	30	.003	169.50
5J23	1044-1056	475	.001	49.00
700B	690-700	40	.002	22.50
700D	710-720	40	.002	39.75
706EY	3038-3069	200	.001	32.50
706CY	2976-3007	200	.001	32.50
725-A	9345-9405	50	.001	Write
QK60†*	2845-3005	.100 CW		85.00
QK61†*	2975-3170	.100 CW		85.00
QK62†*	3135-3330	.100 CW		85.00
QK259†	2700-2900	800	.001	249.00

*—Packaged with magnet.
†—Tunable over indicated range.

KLYSTRONS

723A	$12.50	2K25/723A/B	$27.50
723A/B	19.50	417-A (West'Hse)	17.50

VARISTORS

D-167208	$1.35	D-171812	$1.63
D-171858	$1.42	D-172155	$1.50
D-168687	$1.35	D-167176	$1.25

THERMISTORS

D-164699 Bead Type DCR: 1525-2550 Ohms @ 75 Deg. F. Coefficient: 2% Per. Deg. Fahr. Max. Current 25 MA AC/DC $2.50

D-167332 Bead Type, DCR is 1525-2550 Ohms. Rated 25 MA at .825-1.175 VDC $1.35

D-167613 Disk Type DCR: 355 Ohms @ 75 Deg. F.P.M. 2.5%, 1 Watt $1.35

D-166228 Disk Type 7120 Ohms @ 60°F. 4220 Ohms @ 80°F. 2590 Ohms @ 100°F., 1640 Ohms @ 120°F $1.35

—IN STOCK—

AIA
APA-9
APA-10
APN-3
APN-7
APN-9*
APS-2
APS-3
APS-4
APS-6
ASD
ASH
BG
DAS†
DBS†
APT-2
APT-4
MKIV
MKX
RC145
RC148
SO-1
SO-8
SG-1
SJ-1
TAJ
TBK
TBL
SCR520*
SCR521
SCR518

* COMPONENTS. † LORAN EQUIPMENT.

—TEST SETS—

TS-10
TS-35A
TS-47
TS-12
TS-56
TS-34
TS-159
TS-268
TSX-4SE

SICKLES MODEL III RANGE CALIBRATOR $365.00

TS 98A/AP VOLTAGE DIVIDER $75.00

TS 90 DUMMY LOAD, 50 OHMS IMPEDANCE WILL HANDLE 500 WATTS AT PEAK OF 5000 VOLTS DIVIDER RATIO 50:1 ....$145.00

TS 235/UP DUMMY ANTENNA 500-1500 MC IMPEDANCE: 50 OHMS 1000 WATTS AVERAGE POWER $225.00

I. F. AMPLIFIER STRIPS

MODEL SO: 30 McGain figure is 120 db. Bandwidth: 2Mc. Uses 6 stages of 6AC7 Plus one video detector. Less Tubes $24.50

Model 15: 30 Mc center frequency, Bandwidth 2.5 Mc. gain figure: 65 db. Uses 5 stages of 6AC7's. Has D. C. Restorer and Video Detector. A.F.C. Strip included. Input impedance: 50 Ohms. Less tubes $27.50

Model APS-4: Miniature IF strip, using 6AK5's 60 Mc center Freq. Gain: 95db at Bandwidth of 2.7 Mc. Less tubes $45.00

JAN WAVEGUIDE FLANGES

UG 39/U	$1.10	UG 51/U	$1.65
UG 40/U	$1.25	UG 52/U	$3.40
UG 40A/U	$1.65	UG 52A/U	$3.40

PULSE NETWORKS

15A—1-400-50: 15 KV. "A" CKT. 1 microsec. 400 PPS. 50 ohms imp. $24.50

G.E. #3E (3-84-810) 8-2.24-405) 50P4T ; 3KV "E" CKT Dual Unit; Unit 1, 3 sections, 0.84 Microsec. 810 PPS, 50 ohms imp.; Unit 2, 8 Sections, 2.24 microsec. 405 PPS 50 ohms imp. $6.50

7-5E3-1-200-67P. 7.5 KV "E" Circuit, 1 microsec. 200 PPS, 67 ohms impedance 3 sections $7.50

7-5E4-16-60, 67P. 7.5 KV "E" Circuit, 4 sections 16 microsec, 60 PPS, 67 ohms impedance $15.00

7-5E3-3-200-67P, 7.5 KV, "E" Circuit, 3 microsec. 200 PPS. ohms imp. 3 sections $12.50

#755: 10KV. 2.2usec., 375 PPS. 50 ohms imp. ...$27.50

#754: 10KV. 0.85usec., 750 PPS. 50 ohms imp. ..$27.50

KS8865 CHARGING CHOKE: 115-150 H @ .02A, 32—40H @ .08A. 21KV Test $37.50

G.E. 25E5-1-350-50 P2T. "E" SKT, 1 Microsec. Pulse @ 350 PPS. 50 OHMS Impedance $69.50

KS9623 CHARGING CHOKE: 16H @ 75 MA, 380 Ohms DCR, 9000 Vac test $14.95

G.E. 6E3-.5-2000 50 P2T: 6 KV., "E" Circuit 0.5 usec /2000 PPS/50 ohms/2 sections $7.50

PULSE EQUIPMENT

MIT. MOD. 3 HARD TUBE PULSER: Output Pulse Power 144 KW (12 KV at 12 Amp). Duty Ratio: .001 max. Pulse duration: 5, 1.0, 2.0 microsec. Input voltage: 115 v. 400 to 2400 cps. Uses: 1-71B, 4-89-B, 3-'72's, 1-'73. New ....Less Cover—$135

ASD Modulator Units, mfd. by Sperry. Hard tube pulser delivers Pk. pulse of 144 kw. Similar to Mod. 3 unit. Brand new, less tubes $85.00

Airborne RF head, model AIA, delivers 50 Kw peak output at 9000 mc, at .001 duty. Complete with pulser unit and all tubes. Used, excel. $185.00

PULSE TRANSFORMERS

Westinghouse 4P37: Primary: 50 ohms imp, 750 v. Sec. 15 kv, 1000 ohms imp. Biflar filament trans. built in, delivers 12.6 v at 2.5 amp. (pri. 115 v, 400 cy.) $37.50

RAYTHEON WX 4298E: Primary 4KV., 1.0 USEC. SEC: 16KV-16 AMP DUTY RATIO: .001 400 CYCLE FIL. TRANS. "BUILT-IN" $42.50

WECO: KS 9948: Primary 700 ohms; Sec: 50 ohms. Plate Voltage: 18 KV. Part of APQ-13 ......$12.50

GE #K-2449A
Primary: 9.33 KV, 50 ohms Imp.
Secondary: 28 KV, 450 ohms.
Pulse length: 1.0/5 usec @ 635/120 PPS. Pk Power Out: 1,740 KW
Biflar: 1.5 amps (as shown) ...$62.50

GE #K-2748-A. 0.5 usec @ 2000 Pps. Pk. Pwr. out is 32 KW impedance 40:100 ohm output. Pri. volts 2.3 KV Pk. Sec. volts 11.5 KV Pk. Biflar rated at 1.3 Amp. Fitted with magnetron well $39.50

K-2745 Primary: 3.1/2.8 KV, 50 ohms Z. Secondary: 14/12.6 KV 1025 ohms Z. Pulse Length: 0.25/1.0 usec @ 600/600 PPS. Pk. Power 200/150 KW. Biflar: 1.3 Amp. Has "built-in" magnetron well $42.50

K-2461-A. Primary: 3.1/2.6 KV—50 ohms (line). Secondary 14/11.5 KV—1000 ohms Z. Pulse Length: 1 usec @ 600 PPS. Pk. Power Out: 200/130 KW. Biflar: 1.3 Amp. Fitted with magnetron well .$39.75

K35J45—Pulse Inversion: PRI: 5 KV PK. Pulse Negative. Sec: Pos. Pulse, 4 KV; 1 usec. and .001 DUTY RATIO $6.50

54J318-1—3 wdgs. Ratio: 1:1:1, 1.10 uh. /wdg., 2.5 ohms DCR $3.50

UTAH X-151T-1: Dual Transformer, 2 Wdgs. per section 1:1 Ratio per sec 13 MH inductance 30 ohms DCR $5.00

UTAH X-150T-1: Two sections, 3 Wdgs. per section. 1:1:1 Ratio. 3 MH. 6 ohms DCR per Wdg. $5.00

68G711: Ratio: 4:1 Pri: 200V, Sec. 53V, 1.0 usec Pulse @ 2000 PPS, 0.016 KVA $4.50

TR1049 Ratio 2:1 Pri. 220 MH, 50 Ohms, sec. 0.75 H. DCR 100 Ohms $6.75

K-904695-501: Ratio 1:1. Pri. Imp. 40 Ohm, Sec. Imp. 40 Ohms. Passes pulse 0.6 usec with 0.05 usec rise $8.95

Ray UX 7896—Pulse Output Pri, 5v sec. 41v $7.50

Ray UX 8442—Pulse inversion—40v + 40v $7.50

PHILCO 352-7250, 352-7251, 352-7287

RAYTHEON: UX8693, UX5986, UX-7307 ......$5 ea.

W.E.: D-166310, D-166638, KS9800, KD-163247.

UTAH #9262, with Cracked Beads, but will operate at full rated capacity $5.00

UX 8693 (SCS #2Z9627-54); 3 Wdgs. 32 turns #18 wire. DCR is: 362/.372/.4 ohms. Total voltage 2500 vdc. $5.00

D-166173: Input: 50 ohms Z. Output: 900 ohms 3 Wdgs. Freq. range 10 kc-2mc. P/O AN/APQ*-13 ....$12.50

K-2450: Pulse-inversion auto-transformer: primary 13 kv, 4 usec. Output: 14 kv @ 100 kw peak $34.50

TSX-4SE ANALYZER

3 cm. **Spectrum analyzer,** similar to TS 148, but with greater sensitivity. Freq. range: 8500-9600 MC. Features: Absorption wavemeter, waveguide-Beyond-cutoff attenuator, 20 mc I.F. Strip, 120 db gain. Operates from 115V/220V, 50-1200 CPS ....**Price On Request**

MAIL ORDERS PROMPTLY FILLED. ALL PRICES F.O.B. NEW YORK CITY. 25 % DEPOSIT WITH ORDER. BALANCE C.O.D. RATED CONCERNS SEND P. O.

131 Liberty St., New York 7, N. Y. Dept I-9 Chas. Rosen Phone: Digby 9-4124

PROFESSIONAL ENGINEERING CARDS

ALFRED W. BARBER LABORATORIES
Specializing in the Communications Field and in Laboratory Equipment
Offices, Laboratory and Model Shop at:
32-44 Francis Lewis Blvd., Flushing, L.I., N.Y.
Telephone: Independence 3-3306

CROSBY LABORATORIES, INC.
MURRAY G. CROSBY & STAFF
RADIO-ELECTRONIC RESEARCH
DEVELOPMENT & ENGINEERING
COMMUNICATIONS, FM & TV
ROBBINS LANE
HICKSVILLE, NEW YORK
HICKSVILLE 3-3191

INTERFERENCE MEASUREMENT SERVICES
OF
DYNAMIC ELECTRONICS—N.Y., INC.
Director—H. S. BENNETT, DR. ENG., P.E.
Specialists in determining equipment compliance with government radio interference specifications.
73-39 WOODHAVEN BLVD.
GLENDALE, L.I. IL-9-7000

ELDICO OF NEW YORK, INC.
Donald J. S. Merten and Engineering Staff
Consultants on Interference Elimination from Transmitters, Induction Heaters, Diathermy, etc.
72 East Second Street, Mineola, L.I., N.Y.
Pioneer 6-5212

RADIO INTERFERENCE MEASUREMENTS
under
MIL-I-16910 FCC, Part 18
MIL-I-17623 MIL-S-4957
MIL-I-6181B and others
ELECTRO-SEARCH
4337 N. 5th Street Philadelphia 40, Pa.
GLadstone 5-5353

TRANSISTOR ENGINEERING
S. Moskowitz D. D. Grieg N. J. Gottfried
Product Transistorization. Complete service in consulting, research, development, and production on transistor circuitry, products and instrumentation.
c/o Electronic Research Associates, Inc.
715 Main Street, N. Caldwell, N.J.
CAldwell 6-6729

ELK ELECTRONIC LABORATORIES, INC.
Jack Rosenbaum
Specializing in design and development of Test Equipment for the communications, radar and allied fields
333 West 52nd St., New York 19, PL-7-0520

FREDERICK RESEARCH CORPORATION
Carl L. Frederick, D.Sc., President
Bethesda 14, Maryland • OLiver 4-5897
Engineering Research and Development, Evaluation, Technical Writing and Publishing—Electronic and Electro-mechanical Systems, Test Equipment, Radio Interference, Instrumentation, Controls.

PAUL GODLEY CO.
Consulting Radio Engineers
P.O. Box J, Upper Montclair, N.J.
Offs & Lab.: Great Notch, N.J.
Phone: Montclair 3-3000
Established 1926

GOVERNMENT CONTRACT LIAISON AND CONSULTANTS
GORDON ASSOCIATES, INC.
Specializing in Signal Corps Electronic Requirements, Technical Manuals, Tabular List of Parts, Drawings
L. Gordon, Pres. P. Treston, Ch. Engr.
157 Broad Street Telephone
Red Bank, New Jersey Red Bank 6-2743

HOGAN LABORATORIES, INC.
John V. L. Hogan, Pres.
APPLIED RESEARCH, DEVELOPMENT, ENGINEERING
Est. 1929. Electronics, Optics, Mechanisms, Facsimile Communication, Digital Computers, Electro-sensitive recording media, Instrumentation.
155 Perry Street, New York 14 CHelsea 2-7855

LEONARD R. KAHN
Consultant in Communications and Electronics
Single-Sideband and Frequency-Shift Systems
Diversity Reception - Modulation Theory
Applications of Magnetic Tape Recording
Elizabeth Bldg., 22 Pine St., Freeport, L.I., N.Y
Freeport 9-8800

News—New Products

(Continued from page 146A)

DC Indicating Amplifier

Doelcam Corp., 1400 Soldiers Field Rd., Boston 35, Mass., has announced a DC Indicating Amplifier, Type 2HLA-3, that operates in the field of amplification and measurement of low-level dc signals. This instrument measures signals as small as 2×10^{-15} watt.

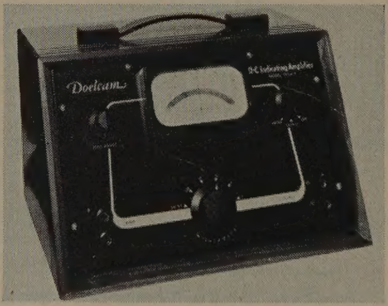

By incorporating a new design concept, utilizing the Doelcam Sound Harmonic Magnetic Converter as the input stage, the limitations of vibrator-type converters are avoided, and a higher degree of stability and reliability is achieved.

As an amplifier, the 2HLA-3 has a flat frequency response to greater than 20 cps on all five ranges and supplies sufficient power output to drive pen motor or galvanometer recorders. Its high gain, linearity, and negligible drift are unaffected by variations in line voltage of tube characteristics.

As an indicator, the 2HLA-3 provides direct readings of the magnitude and polarity of the input dc signal on a mirror-scale, zero-center meter.

This new amplifier is qualified for applications in both laboratory measurements and industrial control. Descriptive Bulletin 1A is available upon request.

Harry W. Houck Jerry B. Minter
John M. van Beuren
RESEARCH ENGINEERS
Specialists in the Design and Development of Electronic Test Instruments
c/o MEASUREMENTS CORP.
BOONTON, N.J.

L. J. CASTRIOTA M. WIND
S. W. ROSENTHAL P. G. MARIOTTI
Microwave Consultants
Radio Frequency and Microwave Components
Cable—Waveguide—Coax
Dielectric Evaluation
Telephone G.P.O. Box 844
BOulevard 3-2096 Brooklyn 1, N.Y.

EVERT M. OSTLUND
Consulting Radio Engineer
Radio—Microwave
Communication—Control
Systems and Equipment
Planning, Research, Development
ANDOVER, NEW JERSEY
Tel.: Lake Mohawk 8635

N. G. Parke S. J. O'Neil
Parke Mathematical Laboratories, Inc.
Specialists in engineering analysis and computation in the fields of electronics and aeronautics.
Independence Court • Concord, Massachusetts
Telephone Concord 827

PICKARD AND BURNS, INC.
Consulting Electronic Engineers
Analysis and Evaluation of Radio Systems
Research, Development, Design and Production of Special Electronic Equipment and Antennas
240 Highland Ave. Needham 94, Mass.

RADIO SONIC CORP.
ENGINEERS—QUALITY ASSURANCE
Testing, Processing
Electron Tubes, Semiconductors, Models, Production Test Equipment, Antennas, Analyzers, Power Supplies, Ultrasonics, Advanced Development
G. EMERSON PRAY, PRESIDENT
32 W. 22nd St., New York 10, N.Y. ORegon 5-0085

Paul Rosenberg Associates
Consulting Physicists
100 STEVENS AVE. • MOUNT VERNON, NEW YORK
CABLE: PHYSICIST MOunt vernon 7-8040

M. D. Ercolino and Associates
ANTENNA CONSULTANTS
Research and Development
Communication Arrays
Commercial and Amateur
FM and TV
c/o TELREX, INC. ASBURY PARK, N.J.
Phone Prospect 5-7252

WHEELER LABORATORIES, INC.
Radio and Electronics
Consulting — Research — Development
R-F Circuits — Lines — Antennas
Microwave Components—Test Equipment
Harold A. Wheeler and Engineering Staff
Great Neck, N.Y. HUnter 2-7876